INFORMATION TO USERS

University of Alberta

AN EXPERIMENTAL STUDY OF DILUTION AND MIXING WITH TURBULENT JETS IN CROSSFLOWS

by

Ahmed Kamal Moawad ©

A thesis submitted to the Faculty of Graduate Studies and Research

in partial fulfillment of the requirements for the degree of

Doctor of Philosophy

Department of Civil and Environmental Engineering

Edmonton, Alberta

Spring, 1998

Canada

University of Alberta

Faculty of Graduate Studies and Research
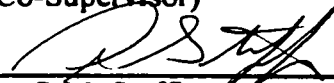
The undersigned certify that they have read, and recommended to the Faculty of Graduate Studies and Research for acceptance, a thesis entitled *"An Experimental Study of Dilution and Mixing with Turbulent Jets in Crossflows"* submitted by *Ahmed Kamal Moawad* in partial fulfillment of the requirements for the degree of *Doctor of Philosophy* in *Civil Engineering*.

Dr. N. Rajaratnam
(Supervisor)

Dr. S. J Stanley
(Co-Supervisor)

Dr. P.M. Steffler

Dr. J. Leonard

Dr. J. D. Scott

Dr. A. S. Ramamurthy
(External Examiner)

Date : 21 Jan 98

TO

MY PARENTS, MY WIFE AND MY SONS

Abstract

This thesis is written in the paper format and includes three contributions.

The first contribution presents the results of an experimental study on the dilution of circular non-buoyant turbulent surface jets of diameter d, discharged perpendicularly into relatively deep crossflows with depth D in the mixing region. The jet velocity was varied from 2.1 to 12.3 times the velocity of the crossflow. Concentration measurements were carried out as far as $x/d = 630$, where x is the distance downstream from the nozzle along the crossflow. Minimum dilutions of about 100 were attained in this mixing region. A general correlation has been developed to predict the minimum dilution in terms of the transformed distance $\alpha x/d$ where α is the ratio of the jet to crossflow velocity. The concentration profiles in the vertical and the transverse directions were found to be similar. Expressions were developed to describe the growth of the width and thickness of the deflected jets. The effect of some submergence of the jet nozzle on the minimum dilution was also investigated.

The second contribution presents the results of a laboratory study on the mixing characteristics of circular non-buoyant multiple jets discharged into relatively deep river-like crossflows. Experiments were performed for the velocity ratio α varying from 3.5 to 10 whe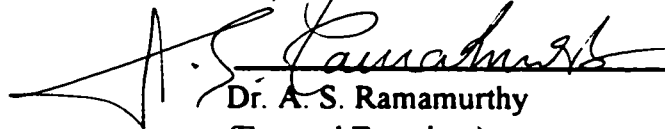re α is the ratio of the jet to that of the crossflow. Three and five ports were used and the spacing S between the ports was varied from 8d to 16 d where d is the diameter of the nozzle. The concentration measurements were carried out for a maximum relative distance of $x/d=160$ where x is the distance downstream of the diffuser. The concentration profiles in the vertical as well as the lateral directions in the planes of maximum concentration were found to be similar. A minimum dilution up to 80 was reached the mixing region. It was found that the minimum dilution decreased with the increase of the velocity ratio α and the increase of the number of ports. Increase of the spacing between ports resulted in a

considerable enhancement of the dilution. The trajectory of the multiple jets was identified based on the location of the maximum concentration. Trajectory data indicated that multiple jets rose more slowly than single jets. Finally expressions describing the growth of the width and thickness of the jets were developed. These results are believed to be useful in the design of outfalls in rivers.

The results of an experimental study on rapid mixing and dilution with multiple turbulent jets is presented in the third contribution. A diffuser with a system of ports installed in an open channel where jets could be discharged either perpendicular (jets in crossflows) or parallel (coflowing jets) to the flow. The velocity ratio α was varied from 8 to 16. The spacing between the ports was given two values of 12d and 24d. The number of ports (n) was varied from 20 to 36. Concentration measurements covered a distance of $x/d=2000$ The standard deviation of the concentration distribution was used as a measure of the degree of mixing at each section. An expression for the optimum mixing distance was developed. Also, the dilution produced by the jets arrangement was studied. The results of this study are believed to be useful in the design of an efficient mixing system which can be implemented by water treatment plants as an alternative to mechanical mixing.

Acknowledgments

List of Contents

List of Tables

List of Figures

Notations[*]

Symbol	Description
A	diffuser area ;[2]
a	costant; [2,3]
a_o	area of port; [2]
B	slot width[2]
b	constant; [2,3]
b*	length scale in the η direction; [2,3,4]
b_o	width of the jet nozzle; [2]
b_z	length scale in the z-direction; [2,3,4]
$\overline{C}$	average concentration at a section; [5]
C	concentration at any point in jet; [2,3,4,5]
$C_{1 to 4}$	constants; [2]
C_b	background concentration; [5]
C_d	drag coefficient ; [2]
C_i	concentration at a fully mixed section; [5]
C_m	maximum concentration at section; [2,3,4,5]
C_o	initial concentration at nozzle; [2,3,4,5]
C_p	pressure coefficient; [2]
D	depth of flow; [2,3,4,5]
d	jet diameter; [2,3,4,5]
F_o	densimetric Froude number; [2]
g	gravitational acceleration; [2]
g'	local apparent gravity; [2]
h_o	height of port center above the ambient bottom; [2]
J_o	buoyancy flux; [2]

---

* The number in square brackets [ ] denote relative chapter numbers.

Symbol	Description
K	dimensional diffuser parameter; [2]
k	dimensional diffuser parameter for the case of crossflow ; [2]
K1	constant; [2]
L	length of diffuser; [2,4,5]
l^*_q	discharge /buoyancy length scale; [2]
L_b	plume/ crossflow length scale; [2]
L_M	slot jet / cross-flow length scale; [2,5]
l_M	slot jet /plume transition length scale; [2]
l_m	momentum length scale; [2,3,4,5]
l_Q	discharge length scale; [2]
m	number of independent variables; [3]
mf	mass flux along the jet trajectory; [2]
mf_o	mass flux at the nozzle; [2]
M_o	momentum flux at the nozzle; [2,3,4,5]
m_o	momentum flux for diffusers; [2,5]
N	number of observation; [5]
n	number of ports; [2,4,5]
p	static pressure inside the jet with reference to the atmospheric pressure; [2]
P_L	Leakiness Parameter ; [2]
Q_o	total discharge from the nozzle(s); [2,3,4,5]
q_o	discharge per unit length of diffuser; [2]
Q_r	ratio of jets discharge to the ambient discharge; [5]
R	Reynolds number of the jet; [2,3,4,5];
Re	Result; [3]
R_{io}	Richardson number; [2]

Symbol	Description
R_m	mixing ratio; [2]
S	spacing between ports; [2,4,5]
S_c	centerline dilution for staged diffuser; [2]
S_{co}	dilution of coflowing diffuser ;[2]
S_t	dilution of tee diffuser;[2]
S_u	dilution of unidirectional diffuser;[2]
U	crossflow velocity; [2,3,4,5]
U_m	maximum velocity along the centerline of the jet; [2]
U_o	velocity at the jet nozzle; [2,3,4,5]
$V_{1\text{to }m}$	variables; [3]
W	width of the flume; [3]
$W_{1\text{to }m}$	uncertainty intervals of m independent data [3]
W_{Re}	uncertainty intervals of the result R_e; [3]
W_U	uncertainty intervals of the velocity U; [3]
W_{Uo}	uncertainty intervals of the velocity U_o; [3]
W_y	jet width;[3], jets Thickness; [4]
W_{z10}	jets width at $C/C_m=0.1$; [4]
W_{z50}	jets width at $C/C_m=0.5$; [4]
x	longitudinal distance downstream from the jet nozzle; [2,3,4,5]
x_{fm}	value of x at the start of zone III; [4]
x_m	merging distance;[2,4], mixing distance; [5]
y	distance measured in the transverse direction; [3,5], vertical distance measured from the bed;[4]
z	vertical distance below the water surface;[2], distance along the diffuser; [4], vertical distance measured from the bed [5]
α	ratio of jet velocity to ambient crossflow velocity (U_o / U); [2,3,4,5]

Symbol	Description
α_e	entrainment coefficient; [2]
β	entrainment coefficient; [2]
$\Delta\rho$	difference in densities between the effluent and the ambient flow; [2]
γ	Angle of inclination of diffuser ports; [2]
η	distance measured normal to ξ; [3,4]
ν	kinematic viscosity of fluid; [2,3,4,5]
θ	excess momentum thickness; [2]
ρ	density of water; [2,3,4,5]
σ	standard deviation; [5]
ξ	distance along axis of deflected jet; [2,3,4]

Chapter 1

Introduction

1.1 General

Wastewaters resulting from increased urbanization and industrialization have continuously increased the pollutant loading of our river systems. Pollutants may enter our river systems either through non-point sources (distributed sources) or through point sources (outfalls). Waste disposal includes discharge of municipal and industrial wastes into rivers. Generally, the discharge of these effluents requires significant dilution in a zone of limited extent. Efficient initial mixing of these effluents can substantially reduce the risk that these wastes would pose to human health and ecosystems. The initial mixing and the subsequent dilution of the pollutants is greatly influenced by the design of the outfall. One effective way of achieving maximum dilution is to discharge the effluent as circular turbulent jets perpendicular to the river flow (jets in crossflow). The interaction which occurs in a jet discharging normal to the streamflow enhances the mixing process and results in high dilutions compared to jets discharging into quiescent or coflowing ambients. One method of discharging effluents into rivers is to use single circular surface jets discharging perpendicularly into the river flow. Another way of achieving rapid dilution in the vicinity of the outfall is to use multiple circular jets in crossflows. Part of the work in this thesis investigates the dilution characteristics of non-buoyant circular surface jets and multiple non-buoyant jets in relatively deep crossflows. The general objective of these studies was to develop definitive expressions to evaluate dilution downstream of outfalls producing surface and multiple jets.

Mixing using multiple jets in confined environments has a variety of practical applications. The use of turbulent jets for mixing miscible liquids is attracting attention in chemical process industries. Jets in crossflows have been used previously to provide rapid mixing in pipes. Also, turbulent jet mixing can be used as an alternative to mechanical mixing in water treatment plants. The main challenge faced by hydraulic engineers is to come up with an efficient configuration where a rapid and thorough mixing can be achieved in a relatively short mixing distance. The optimum mixing distance is usually defined as the distance at which the variation of concentration over the cross-section is some small specified value. In this thesis, mixing using multiple turbulent jets discharged in an open channel is investigated with the intention of eventually developing efficient diffusers for use in water treatment plants.

1.2 Organization of the Thesis

Most of the research work on turbulent jets in crossflows has been directed towards examining the hydrodynamic characteristics. Investigations on the dilution characteristics of these types of jets and on rapid mixing through multiple turbulent jets, are not as numerous. In this thesis, the results of experimental studies on three practical problems dealing with the dilution and mixing with turbulent jets will be presented. Each piece of work is written as a chapter and a brief introduction to each chapter is presented below.

Chapter 2 presents a review of previous theoretical and experimental investigations that are related to the present study. These include previous studies on buoyant and non-buoyant surface jets in stagnant ambient, coflowing streams and in crossflows. Also, the studies available on the use of multiple and single jets for mixing are reviewed.

Chapter 3 introduces the results of an experimental study on the dilution of circular non-buoyant turbulent surface jets of diameter d, discharged perpendicularly into relatively deep crossflows with depth D in the mixing region. The objective of this study was to develop simple expressions for the minimum dilution produced by surface jets and for their growth in the lateral and the vertical directions. Two circular nozzles of diameters of 6.35 mm and 12.7 mm were used. The velocity ratio α varied from 2.1 to 12.3. In section 3.2, the details of the experimental plan, the experimental arrangements, the experimental procedures and the probable sources of errors are presented. Concentration measurements were carried out for a distance of x/d=630, where x is the longitudinal distance measured from the nozzle. The effect of some submergence of the jet nozzle on the minimum dilution was also investigated. The analysis of the results and the conclusions are given in sections 3.3 and 3.4 respectively.

Chapter 4 introduces the results of a laboratory study on the mixing characteristics of circular non buoyant multiple jets discharged into relatively deep river-like crossflows. The main objectives of this study were to study the effect of the velocity ratio α, the effect of increasing the number of ports and the effect of changing the spacing between the ports on the dilution characteristics of circular multiple jets in crossflows. Experiments were performed for the velocity ratio α ranging from 3.5 to 10. Three and five ports were used and the spacing between the ports was varied from 8 d to 16 d. In the introduction section (section 4.1) the general dilution characteristics of circular jets in crossflows is presented. The details of the experimental arrangements are introduced in section 4.2. In section 4.3 the experiments and the experimental arrangements are presented. Finally, the analysis of the experimental results and the conclusions are given in sections 4.4 and 4.5 respectively.

The objective of the study presented in Chapter 5 was to investigate the rapid mixing and dilution induced by multiple turbulent jets in an open channel The original inspiration of this study stems from the fact that, in water treatment plants, it is possible to use multiple turbulent jets for the mixing of chemicals, as an alternative to mechanical devices. The use of multiple jets for mixing has been studied by number of investigators. A brief review of this work is introduced in section 5.1. A system of diffusers which could discharge jets either perpendicular (crossflowing jets) or parallel (coflowing jets) to the direction of flow, was installed. The experimental setup is described in section 5.3. Several jets discharges with different α values were studied. Section 5.4 presents the details of the experiments and the experimental results. The sections that follow present the analysis and the correlation of the experimental results. The concluding remarks are made in section 5.6.

Chapter 6 contains a general discussion of the three contributions presented in chapters 3 to 5. For each of these contributions, Chapter 6 gives a brief summary and suggests recommendations for future research.

Chapter 2

Literature Review

2.1 General

Jets discharging into quiescent or flowing ambients have been investigated for many years. These jets model non-buoyant and buoyant discharges from industrial facilities into receiving streams and rivers and from power plants into water bodies like lakes. The earliest work on turbulent jets was by Young (1800) as reported by List (1982). Extensive studies have been conducted on simple axisymmetric jet discharging into stagnant ambients (see Abramovich 1963, Rajaratnam 1976). Jets discharging into crossflows are known to be effective in producing significant mixing and dilution in the vicinity of outfalls. One method of discharging effluents into rivers is to use circular surface jets discharging into crossflows. Another way of achieving rapid dilution in the vicinity of an outfall is to use multiple circular jets discharging into crossflows. In this section, the basic information on jets on crossflows will be reviewed. Previous studies on buoyant and non-buoyant surface jets in stagnant ambient, coflowing streams and in crossflows will be discussed. Jets are also used as a viable alternative to mechanical devices in mixing of chemical substances. At the end of this section, the studies available on the use of single and multiple jets for mixing will also be presented.

2.2 Jets in Crossflows

The main characteristics of jets in crossflows are defined by considering a circular jet of diameter d discharging with an initial velocity U_o perpendicular to a free stream of velocity U as shown in Fig. 2.1. The jet in a crossflow is a typical example of a free turbulent shear flow, where the curvature of the shear layer and the

5

complex turbulent flow patterns in the jet-wake region make it difficult to predict theoretically the main characteristics of such flows. Most of the experimental investigations have been directed towards examining the hydrodynamics of these jets in crossflows. This was achieved by determining the jet centerline and the jet spreading, either by photographic means or by velocity or total pressure measurements from which the velocity and pressure fields were obtained. Investigations of dilution characteristics of circular jets in cross flows are not as numerous. Conservative pollutants were used to study the dilution of circular jets in crossflows. The following section presents a discussion of previous studies performed on free circular jets in crossflows.

Gordier (1959) located the jet penetration and width from photographs of a deformed jet in a water flume. The total pressure distribution of jet discharges in a water tunnel was measured. The jet centerline was determined using the maximum pressure points and the results from this study were found to be similar to those found in previous studies of air jets.

Keffer and Baines (1963) investigated air jets discharged normal to a cross wind. The mean velocity contours and the turbulence intensities were measured using hot-wire anemometer. It was found that the entrainment coefficient depended on α which is the ratio of the velocity of the jet to that of the crossflow. It was found that as α increased, the entrainment coefficient decreased. The velocity excess in jets in cross flows decreased more rapidly than in free jets and the rate of decrease increased with distance away from the source. The reason for this was assumed to be due to the presence of the twin vortices which do not exist in the free jet. The maximum turbulence intensity along the jet axis was considerably larger in magnitude compared to that for the free jet. The variation in intensity with the jet strength indicated that similarity is not maintained in the fine structure of the flow.

Fan (1967) considered two cases; i) a round buoyant jet discharging into a cross stream of homogeneous density and ii) an inclined round buoyant jet discharging into a stagnant environment with linear density stratification . An integral technique was used to predict the jet trajectory, widths and dilution ratios. The problem of the buoyant jet in a uniform crossflow was analyzed by assuming an entrainment mechanism based upon the vector difference between the characteristic jet velocity and the ambient velocity. The experiments were carried out for the velocity ratio α varying from 4 to 12 and densimetric Froude number ranging from 10-80. The densimetric Froude number F_0 was defined as:

$$F_o = \frac{U_0}{\sqrt{gd \frac{\Delta\rho}{\rho}}} \qquad (2\text{-}1)$$

where U_0 is the velocity at the jet nozzle of diameter d, ρ is the density of the water and $\Delta\rho$ is the difference in densities between the effluent and the ambient flow. In these experiments, observations were carried out for the relative downstream distances x/d up to 250. The jet trajectories, dilution ratio and the jet half width were determined from conductivity measurements. For buoyant jets in a uniform crossflow of homogeneous density, the values of the entrainment coefficient α_e were found to vary from 0.4 to 0.5. The drag coefficient C_d of the force exerted by the crossflow on the jet defined below was found to vary from 0.1 to 1.7.

Pratte and Baines (1967) studied jets entering normally into a crosswind. From photographic observations, the edges of the jets were determined. The crossflow and the jet flow mixed rapidly in the region beyond the potential core and with increase of the entrained crossflow momentum, the jet would bend. The profiles of the jets were determined by defining the penetration of the top, centerline and the bottom of the jet into the crossflow.

Kamotani and Gerber (1972) reported the results of experiments carried out on circular air jets issuing into a crossflow. Velocities and turbulence intensities

7

were measured using a hot-wire anemometer. The measurements were performed using jets with a velocity ratio α ranging from 3.9 to 7.75. The jet velocity trajectory was defined as the locus of the maximum velocity in the plane of symmetry. It was found that the jet velocity trajectories and the turbulence intensity were affected mainly by the velocity ratio. A change of the shape of the jet was observed; the jet was deformed into a crescent shape and the crossflow created a pair of vortices behind the jet. The vortices were observed to acquire axial momentum from the jet and moved along the jet path while increasing their strength.

Chu and Goldberg (1974) carried out both theoretical and experimental investigations on the dilution of buoyant discharges in crossflows. It was found that only one entrainment coefficient determined from the experiments was sufficient to describe the plume as close as 3 to 4 times the diameter of the jets. The turbulent entrainment coefficient was found to be approximately constant and equal to 0.5 along the plume. The same constant was obtained for both non-buoyant and buoyant cases. Also an expression to define the transition point between the near-field where the momentum dominates and the far-field where the buoyancy dominates was developed.

Fearn and Weston (1974) indicated that the dominant feature of the velocity field for a jet in a crossflow is a pair of attached contrarotating vortices. The vortex pair was formed very close to the jet orifice. The vortices were deflected by the crossflow and they gradually weaken each other by the diffusion of vorticity.

Chan et al (1976) investigated the role of the pressure drag and mass entrainment in producing the expansion, deflection and the dilution of circular jets in crossflows. Analytical relations describing the global behavior of the jet were derived for each of the three flow regions (near field, curvilinear region and far field). The results indicated that the pressure distributions were somewhat similar to

8

those of the pressure field produced on a rigid circular cylinder by a free stream. With the following definition of the pressure coefficient C_p

$$C_p = \frac{p}{0.5 \rho U^2} \qquad (2\text{-}2)$$

where p is the static pressure inside the jet with reference to the atmospheric pressure and U is the ambient velocity. It was found that C_p does not reach unity at the forward stagnation point. Secondly, the magnitudes of C_p in the suction lobes of the pressure distributions are much greater than for the jet than those for a rigid cylinder. The coefficients of entrainment and drag were determined for each of the flow regions. The entrainment coefficient and the drag coefficients decreased with the increase of α in the momentum-dominated near field (MDNF), while the entrainment coefficient remained constant at the far field.

Wright (1977) considered a round turbulent buoyant jet issuing into an ambient crossflow that was either of uniform density or had a linear density stratification. The jet source was towed at a constant velocity discharging into a stagnant ambient. A photographic study was carried out to determine the jet boundaries and center line. The jet center line was also determined from concentration measurements. Rhodamine B extra dye was used as a tracer for the dilution studies. The deflected jets were analyzed in separate regions, referred to as the momentum dominated near and far fields. A length scale l_m was defined as

$$l_m = \frac{\sqrt{M_o / \rho}}{U} \qquad (2\text{-}3)$$

where M_o/ρ is the kinematic momentum flux from the nozzle and U is the ambient velocity of the crossflow. The region in which y (the vertical distance from the jet source) is much smaller than l_m is referred to as the momentum dominated near field

9

(MDNF). In this region, the jet trajectory was described by the one half-slope correlation, written as

$$\frac{y}{l_m} = C_1 \left(\frac{x}{l_m} \right)^{\frac{1}{2}}$$ (2-4)

where the coefficient C_1 was found to vary from 0.8-2.0 with α. The region in which y is larger than l_m is referred to as the momentum dominated far field (MDFF). In this region, the jet trajectory was described by the one-third slope correlation as

$$\frac{y}{l_m} = C_2 \left(\frac{x}{l_m} \right)^{\frac{1}{3}}$$ (2-5)

where C_2 was found to vary from 0.9 to 1.9 with α.

The characteristic tracer dilution defined as S_0 (the ratio between the concentration at the jet nozzle C_0 to the time averaged maximum tracer concentration measured at a jet cross-section in the vertical plane of jet symmetry C_m) was defined for different flow regions. Eq. 2-6 and 2-7 represent the dilution in the MDNF and the MDFF respectively.

$$\frac{S_0 Q_0}{U l_m^2} = C_3 \left(\frac{y}{l_m} \right)$$ (2-6)

$$\frac{S_0 Q_0}{U l_m^2} = C_4 \left(\frac{y}{l_m} \right)^2$$ (2-7)

where Q_0 is the discharge from the nozzle, C_3 and C_4 are the dilution coefficients. Wright (1977) indicated that C_3 and C_4 had values of 0.35 and 0.14 respectively.

10

Rajaratnam and Gangadhariah (1980) studied experimentally the behavior of circular jets discharging into a crossflow. The experiments were carried out for the velocity ratio α ranging from 2.73 to 23.4. The velocity and the pressure distributions were measured for the full section of the deflected jet. It was indicated that the cause of the jet deflection was a result of the pressure field exerted on the jet by the freestream and entrainment of the ambient flow further downstream. The velocity profiles were found to be similar. The entrainment velocity v_e was found to be much larger than that in a simple circular jet. Rajaratnam and Gangadhariah also quantified the relative mass flux of jets with velocity ratios α equal to 2.73, 4.52 and 7.05. The relative mass flux relationship was found to be nonlinear:

$$\frac{mf}{mf_0} = 0.54 \ (\frac{\xi}{d})^{1.22} \qquad\qquad (2\text{-}8)$$

where mf is the mass flux at distance ξ along the jet trajectory from the nozzle and mf_0 is the mass flux at the jet nozzle.

Sherif and Pletcher (1989) studied the velocity and turbulence characteristics of circular water jet discharging from the bottom of the channel into a crossflow. The study reports on the velocity and turbulence fields of an isothermal jet in a crossflow at velocity ratios of 2, 4 and 6. The jet cross-section changed to the characteristic kidney shape and the free stream fluid could be seen to be slightly accelerated in the jet wake and entrained in the jet.

Hodgson (1991) considered circular jets discharging from the bottom of a receiving stream, normal to the direction of flow. Photographic studies were carried out to observe the deflected jets. From these observations, the jet boundaries were identified. A field study was conducted to measure the dilution of the various jet discharges in the Lesser Slave River in Alberta. The field study was augmented by a laboratory investigation. The jet flow rates were varied to obtain a range of 2.32 to

11

13.05 for the velocity ratio α. The dilution studies were carried out using Rhodamine B as the tracer. Hodgson (1991) differentiated between jet discharges into deep water and shallow water using the dimensionless parameter $\alpha d/D$, where D is the depth of flow. The critical value of this parameter was found to be approximately 0.34. It was observed that the jet discharges remained unimodal (i.e. had only one point of maximum concentration) for $\alpha d/D < 0.28$ and that the transition between unimodal and bimodal jet discharges occurred between 0.28 and 0.36. A general relationship for dilution was developed as follows:

$$\frac{C_o}{C_m} = 1.09 \ (\frac{\alpha x}{d})^{0.56} \qquad (2-9)$$

From the concentration measurements, expressions were developed for the jet centerline, the width, and the thickness of the jets, as a function of the downstream distance .

Another method of maximizing the dilution near the jet nozzle is by discharging the effluent as wall jets (or bed jets, where the jet is placed at the bed of the channel and discharges perpendicular to the ambient flow.) The work of Langat (1994) considered the dilution of circular wall jets in crossflows. The deflected jets were studied for dilutions up to 100: 1 and for downstream distance (x) up to about 200 times the jet nozzle diameter. The dilution study was similar to that of Hodgson and Rajaratnam(1992). Velocity ratio was varied from 2 to 12. The results indicated that the concentration profiles are similar in both the vertical and the horizontal directions. The following equation was developed to describe the minimum dilution in the mixing region.

$$\frac{C_o}{C_m} = 0.67(\frac{\alpha x}{d})^{0.63} \qquad (2-10)$$

12

On comparing the results of the wall jet study to that of Hodgson and Rajaratnam (1992), it was found that the dilution produced by free jets was superior to that produced by wall jets.

2.3 Turbulent Surface Jets

The last three decades have seen a considerable increase in the thermal generation of electric power. This has resulted in the release of large quantities of heated water or thermal discharges into water bodies. Other types of discharges are industrial discharges into rivers. One economical method is to discharge the effluent as a surface discharge from either an open channel or pipe. In the following sections, buoyant and non buoyant surface discharges in stagnant ambients will be considered. This will be followed by consideration of the discharge of surface jets in coflowing streams and, finally, studies on surface jets in crossflows (as in river outfalls) will be presented.

2.3.1 Surface Jets in a Stagnant Ambient
Non -buoyant Surface Jets :

Let us consider a non-buoyant circular surface jet of diameter d (or plane surface jets with width b_o) discharging into a stagnant ambient with a depth D with a velocity U_o, as shown in Fig. 2.2. Rajaratnam and Humphries (1984) presented the results of an experimental study on the diffusion of plane and circular turbulent surface jets. Experimental observations showed that in the region of fully developed flow (downstream of the end of the potential core), the velocity profiles at different sections are similar for both types of jets. For the plane surface jets, the decay of the normalized velocity scale can be represented by the equation:

$$\frac{U_m}{U_o} = \frac{3.1}{\sqrt{x/b_o}}$$

(2-11)

13

It was found that the vertical spreading of the plane surface jet varied linearly with the longitudinal distance x and $db_z/dx=0.07$. For the circular jets, both the transverse length scale b_y and the vertical length scale b_z varied linearly with the distance x, such that $db_y/dx=0.09$ and $db_z/dx=0.044$.

Buoyant Surface Jets

The diffusion of buoyant surface jets in stagnant or moving surroundings has been studied by several investigators because of the importance of thermal discharges into water bodies. Harleman and Stolzenbach (1972) presented a review which outlined the state of the art in predicting the flow and temperature distribution due to heated discharges of cooling water into an adjacent water body.

Pande and Rajaratnam (1977) presented an experimental study on the behavior of bluff turbulent surface jets discharged into stagnant ambients for moderate and large source Richardson numbers Ri_0 (Ri_0 is equal to $1/F_0^2$) The values of Richardson numbers ranged from 0.15-1.14. For this range of Richardson number, the velocity and temperature profiles in the lateral and vertical directions were found to be similar. Also the surface lateral length scales for the excess temperature was about 1.9 times the corresponding velocity scale whereas, in the vertical direction, the corresponding ratio was only 1.12.

Wiuff (1978) conducted an experimental investigation of a warm surface rectangular jet discharging into a stagnant ambient. The densimetric Froude number (F_0) for the jet was 3.6. The velocity and the density measurements indicated that the longitudinal profiles were not similar for jets with small Froude numbers. The same was concluded by Rajaratnam (1985) for surface jets with densimetric Froude numbers of 1.26 and 1.58.

Jirka et al. (1981), described the distinct geometric properties and mixing characteristics within the near-field of a buoyant surface jet . A criterion for shallow

14

receiving water conditions was developed. It was found that increasing of the shallowness caused a significant reduction in dilution.

2.3.2 Surface jets in Coflowing Stream

Rajaratnam (1984) conducted an experimental study on circular non-buoyant turbulent surface jets in a coflowing channel where the jet is issuing with a uniform velocity, parallel to the surrounding flow. Photographic studies and velocity field measurements were carried out for a wide range of experiments. The velocity ratio α was varied form 1 to 44.6. It was noticed that there was a dip in the vertical velocity profiles near the surface which was attributed to the generation of waves at the water surface. The concept of the excess momentum thickness (θ) was used to analyze the decay rate of the velocity scales. The excess momentum thickness can be defined using the following equation,:

$$M_o = \pi \frac{d^2}{4}\rho(U_o(U_o - U) = \pi\theta^2\rho U^2 \qquad (2\text{-}12)$$

where M_0 is the excess momentum flux at the nozzle, ρ is the mass density, U_0 is the velocity at the jet nozzle and U is the velocity in the main stream. Based on the results of the experiments, it was found that the vertical length scale of the velocity profiles can be predicted from the equations of the submerged circular jets in coflowing streams using the excess momentum thickness as the length scale. It also appeared that the transverse length scale and width grow at a rate equal to that of circular wall jets in coflowing streams for some distance away from the nozzle.

Rajaratnam (1984) performed an experimental study on heated surface discharges into coflowing streams. The velocity ratio α varied from 1.4 to about 20 and the source Richardson number of the surface jet varied from about 0.00015 to 0.03. The results of this study showed that the vertical and the transverse velocity

profiles were similar. Similar to the non-buoyant jets in coflowing streams, the variation of the velocity and length scales were analyzed using the concept of the excess momentum thickness. The results of this study showed that even for R_{io} =0, there is hardly any growth in the vertical length scale. The effect of the shallowness of the receiving water was also investigated. The depth of the stream was only 2.8 times the jet diameter. It was found that the transverse spreading was not affected by the shallowness of the stream. Also the jet did not grow thick enough to occupy the full depth.

2.3.3 Surface Jets in Crossflows

The discharge of effluents through surface jets is a particular case of jets in crossflows. The characteristics of surface jets in crossflows are identified by considering a circular jet of diameter d discharging with a velocity U_o perpendicular to a moving free stream with a velocity U as shown in Fig. 2.3.

A number of predictive models of integral types have been proposed for predicting the behavior of warm water discharges into lakes and rivers, Motz and Bendict (1972) developed a surface jet model for heated discharges into crossflow. The main assumptions made in the development of this model are :

i) The jet is considered to be two dimensional .

ii) The velocity and the temperature normal to the jet axis are similar along the length of the jet axis.

iii) The profiles of velocity and temperature normal to the jet axis are similar along the length of the jet axis.

iv) The force exerted by the ambient flow on the jet could be represented by a drag, which could be represented by the product of a drag coefficient C_d, an appropriate dynamic pressure and an area.

v) The turbulent mixing into the jet could be represented by entrainment or an inflow velocity across the jet boundary. The inflow velocity could be expressed as a coefficient α_e multiplied by the vector difference of the jet and ambient velocities. Data from both laboratory and field studies were collected to define the zone of flow establishment as well as the empirical coefficient C_d. Values for C_d and α_e of 0.5 and 0.4 respectively were found to give reasonable results.

Several experimental studies have been carried out studying the characteristics of surface jets in crossflows. Jirka et al. (1981) used dimensional analysis and physical arguments to define distinct geometric properties and mixing characteristics within the near-field of buoyant surface jets. A criterion for shoreline attachment of surface buoyant jets in crossflowing streams was also presented. A simple trajectory relation was developed to describe the deflection of surface buoyant jets in crossflows.

The Reynolds number effects on buoyant surface jets were investigated by Kuhlman (1984). It was found that as Reynolds number increased from 2500 to 22700, for highly buoyant, attached surface jets in crossflow, the trajectory moved inwards toward the near shore line (less penetration) by approximately 30%. It was also found that the upstream or windward side of the buoyant surface jet appeared to spread less over the crossflow fluid on increasing the Reynolds number.

Habib (1987) conducted a laboratory study to determine the flow parameters of a rectangular surface jet discharging normally into a crossflow. The densimetric Froude number was 1.7 and $\alpha=1.1$. Vertical and horizontal isotherms were determined and it was found that the jet axis was strongly depth dependent. The lateral profiles of the turbulence intensity of temperature fluctuations were also measured. The maximum of the temperature fluctuation intensity occurred where the lateral gradient of the mean temperature profile was the maximum and that the turbulence intensity was appreciable at the outer edge of the jets. Even though

17

several experimental studies have been performed on the velocity field of buoyant and non-buoyant surface jets in stagnant and moving ambients, very little research appears to have been done on the dilution of surface jets in crossflows.

Abdelwahed (1981) conducted a photographic study on non-buoyant rectangular surface jets discharging into crossflows. The effect of the free water surface and the channel bottom on the spreading of surface jets in crossflows was studied. The experiments were carried out for deep and shallow crossflows. The jet thickness, the jet width and the jet trajectory were determined from top-view and side-view photographs. It was found that the overall entrainment rate for surface jets in deep crossflow was not different from that of the submerged jets in unconfined crossflow. The spreading rate parallel to the free surface was significantly larger than that in the vertical direction. For the surface jets in shallow crossflows, the spreading was unaffected by the bottom , until attachment with the bottom occurred.

McCorquodale and Abdel - Gawad (1986) and Abdel - Gawad et al (1996) studied the behavior of jets from shore based outfalls in the presence of a 3H:1V side slope. The study included both buoyant and non buoyant surface jets discharging perpendicular to the channel flow. The jet to ambient velocity ratio was varied from 2 to 5.2 while the densimetric Froude number was varied from 4.3 to ∞. Measurements were made to determine the velocity, concentration and temperature distributions downstream from the jet nozzle. Sodium fluorescent dye was used as a tracer for the dilution study. The study was limited to a longitudinal distance of 24 d downstream of the jet nozzle. Dimensional analysis together with multiple regression analysis was used to obtain expressions for the jet trajectories, the decay of the maximum velocity and the minimum dilution. The results indicated that the excess velocity, concentration and excess temperature profiles display the Guassian distribution. The lateral concentration length scale was 1.10 times the velocity scales for surface outfalls. Also, the lateral spreading of the buoyant jets of this study was

16% more than that of non buoyant jets, while the corresponding vertical spreading was 15% less. The surface jet results were compared with those of Rajaratnam (1984) for circular surface jets in coflowing streams. The lateral and vertical scales were greater than those of Rajaratnam but similar differences between the buoyant and non-buoyant jets occurred.

2.4 Multiple Jets

Submerged multiple jets from a multiport diffuser are considered to be effective for discharging effluents into water bodies. They can offer high degree of dilution in the vicinity of the outfall which is very desirable since the magnitude of the effluent concentrations would be reduced to environmentally acceptable levels. Generally, a multiport diffuser consists of several discharge ports which discharge wastewater effluent in the form of turbulent jets at a relatively high velocity into the receiving water. Even though there is a considerable body of literature on multiport diffusers, most of these studies are concerned with either sewage outfalls in the ocean, thermal discharges in lakes or thermal discharges in coflowing streams. In this section, a general review of the geometry and the dynamic behavior of these jets will be presented. Further, previous work on multiple jets discharge in shallow and deep water will also be reviewed.

2.4.1 Diffuser Geometry

The mixing characteristics of the multiport diffuser would depend to a great extent on the geometric design and its orientation in the receiving water. A variety of diffuser configurations have been proposed in terms of the orientation of the individual diffuser ports (Jirka,1982, Jirka and Akar, 1991). Fig. 2.4 shows schematically the three basic configurations which are used in coastal as well as in shallow water environments:

1) Unidirectional diffusers

In the unidirectional diffusers, the nozzles are more or less perpendicular to the diffuser line. Depending on the nature of the ambient current regime, the unidirectional diffusers can be divided into: a) Coflowing diffusers, where there is a strong non-reversing current; b) Tee diffusers, where there are weak reversing currents. The unidirectional diffusers have a net induced momentum perpendicular to the diffuser axis.

2) Staged diffusers

The nozzles point horizontally and they are more or less parallel to the diffuser line. The momentum induced is also parallel to the diffuser line.

3) Alternating diffusers

The nozzles in the alternating diffusers are arranged in an alternating fashion such that there is no net induced momentum. The mixing characteristics of these types of diffusers in a reversing current are excellent.

2.4.2 Dynamic Behavior

For a standard diffuser installation for most ocean outfalls, it is common to have the following conditions prevailing:

1) The diffuser is long compared to the water depth such that $L/D >> 1$

2) The spacing (S) between ports is small relative to the water depth $S/D << 1$

These two conditions have led to the concept of the two dimensional slot diffuser. In this concept, the details of the initial three dimensional jets from the individual ports are neglected. It is assumed that the merged two dimensional plane jets comes initially from a slot of width B where :

$$B = \frac{q_o^2}{m_o} \qquad (2\text{-}13)$$

20

where q_o is the discharge per unit length of the diffuser and $m_o = U_o q_o$

Jirka (1982) showed that the concept of the two-dimensional slot diffuser could be also applied for cases of thermal discharge in shallow water conditions. Jirka (1982) presented a comprehensive review of previous work on the various fluid mechanical problems associated with different jet group arrangements. A more recent extensive survey on diffuser research was presented by Jirka and Akar (1991). In this study, general configurations for different types of diffusers were introduced. Based on the concept of the two dimensional equivalent slot diffuser and using dimensionless analysis some length scales were defined as:

$$l_Q = \frac{q_o^2}{m_o} = \text{discharge (geometric) length scale} \qquad (2\text{-}14)$$

$$l_M = \frac{m_o}{J_o^{2/3}} = \text{slot jet /cross-flow length scale} \qquad (2\text{-}15)$$

$$L_m = \frac{m_o}{U^2} = \text{slot jet /plume transition length scale} \qquad (2\text{-}16)$$

where :

$$J_o = g_o' q_o \qquad (2\text{-}17)$$

$$g_o' = g \Delta \rho / \rho \qquad (2\text{-}18)$$

Jirka and Akar (1991) had identified different discharge classifications that had been implemented as the microcomputer-based expert system program CORMIX2 (Cornell Mixing Zone Expert System).

In the following section a summary of some of the research conducted on multiple jets in shallow and deep flowing receiving water is presented.

2.4.3 Multiple Jets in Shallow Receiving Water

For the past three decades submerged multiport diffusers have often been used to discharge thermal wastes into rivers. As thermal diffuser installations are not usually subject to high dilution requirements, they can be used in shallow rivers. Parr and Sayre (1979) investigated the jet behavior of single and multiple submerged heated jets in laterally confined, shallow, flowing ambients. The flow from the diffuser was divided into 3 different regions: the individual jet region , the transition region and the two dimensional region. Both velocity and temperature were measured in the individual region. The number of ports was varied from 1 to 3. The receiving water depth was shallow , varying from 5.5-9.9 port diameters. It was concluded from this study that the jet behavior in the confined , flowing ambients deviated dramatically from the "deep water" jet and this was due to the decrease of the ambient mixing water. The dilution of excess temperature along the jet center line varied linearly with x/d in the region where x/d was less than twice the mixing ratio R_m :

$$R_m = \frac{q_a + q_o}{q_o} \qquad (2\text{-}19)$$

where q_a is the ambient discharge per unit width of the channel. It was also found that the downstream location where a row of submerged jets became a two dimensional slot jet was proportional to $R_m^{0.89}$.

Almquist and Stolzenbach (1980) presented the results of a theoretical and experimental investigation of staged diffusers in a quiescent, unstratified water body. In this study, a theory for the volumetric dilution and the associated center-line effluent concentration was developed on the basis of a two dimensional entrainment hypothesis applied to a line source of momentum. As a result of this study, criteria

for the buoyancy and diffuser length were developed such that a vertical homogenous flow region would exist along a significant portion of the diffuser length and might be analysed as a two dimensional unstratified flow. A general formula for predicting the center line dilution S_C was presented as follows:

$$S_c = 0.82 + 0.37K \qquad (2\text{-}20)$$

where

$$K = (\frac{D}{B})^{0.5} \qquad (2\text{-}21)$$

Dominique (1980) extended the model proposed by Almquist and Stolzenbach (1980) to the case when the diffuser was in a crossflow, and the dilution in this case could be :

$$S_{cr} = S_c (k + \sqrt{k^2 + 1}) \qquad (2\text{-}22)$$

$$k = \frac{\alpha_e UD}{2q_o \sqrt{\beta} K} \qquad (2\text{-}23)$$

where α_e and β are entrainment coefficients, S_C is the dilution for the quiescent case.

Parr and Melville (1981) studied the case of unidirectional multiport diffuser discharging hot water in shallow flowing water of finite lateral extent. Using the control volume analysis, an analytical solution was developed to describe the flow field induced. In developing the mathematical model, the following assumptions were made:

1. Turbulent lateral entrainment is negligible; 2. bottom friction is negligible; 3 the hot water was completely mixed in the vertical direction; no buoyancy force. A method was also presented for estimating the near field dilution for a diffuser in a

natural channel. It was found that the near field dilution was related to the volume flux ratio (Q/Q_0); the velocity ratio α and the dimensionless diffuser length, (L/W). where W is the width of the channel. The mathematical model was compared with field data and good agreement there was between the minimum dilution measured and that predicted by the model.

Adams (1982) discussed the mixing mechanics of submerged, multiport diffusers used to discharge heated water from electric power plants into shallow receiving waters. Two types of unidirectional diffusers in shallow environments were examined, namely: 1) coflowing diffuser in which the discharge ports are oriented in the direction of the ambient current and 2) a tee diffuser in which the discharge ports are oriented at right angles to the ambient current. The flow was assumed to be incompressible and inviscid. The diffuser was sufficiently long and the water depth was sufficiently shallow such that the end effects and buoyancy could be neglected. Using both Bernoulli's equation and the momentum equation, a theoretical derivation for the dilution of the coflowing diffuser was developed. The general coflowing dilution was expressed as follows:

$$S_{co} = \frac{UA}{2Q_o} + \sqrt{\left(\frac{UA}{2Q_o}\right)^2 + \frac{A\cos\gamma}{2na_o}} \qquad (2\text{-}24)$$

in which S_{co} is the coflowing dilution; A is the area of diffuser defined as DL; n is the number of ports; a_o is the cross-sectional area of an individual port; γ is the angle of ports inclination. For the special case where U= γ=0, the dilution can be expressed as :

$$S_u = \left(\frac{A}{2na_o}\right)^{0.5} \qquad (2\text{-}25)$$

24

The same theory was then applied to the tee diffusers with weak ambient currents. An expression was then obtained comparing the dilution of the tee diffuser (S_t) with the coflowing dilution:

$$\frac{S_t}{S_{co}} = 1 - \frac{C_d UA}{nU_o^2 a_o} \qquad (2\text{-}26)$$

where C_d is an empirical drag coefficient associated with tee diffusers in crossflows.

The effect of the lateral boundaries on the mechanics of multiple shallow water jets in a coflowing current was studied by Lee (1985). Two river diffuser models were used for comparison (Parr and Melville (1981) , finite river width ; Adams (1982), infinite river width). Lee (1985) verified these models using independent experimental data. The results indicated that the differences in the predictions of the two models were small. For estimating the dilution it was found that the model of Parr and Melville(1981) gave very good results while the model of Adams (1982) could be used for the first estimations in finite width channel where the prediction errors would still be less than 20%.

2.4.4 Multiple Jets Discharge in Deep Water

Davis et al. (1978) conducted an experimental investigation to determine the dilution characteristics of single and multiple ports of buoyant discharges in stagnant ambients. The number of discharge ports (n) was varied from 1 to 7, with combinations of 1,2,3,5 and 7. The port spacing to discharge diameter ratios was 1.33. The densimetric Froude number was varied from 1.5 to infinity. It was found that the greater the number of ports, the lower the rate of dilution. This effect could be approximated by the following expressions:

$$\frac{Q}{Q_o} = 1.0 + 0.46(\frac{x}{d})^{1.1}(n)^{-0.52} \qquad (2\text{-}27)$$

25

where Q/Q_0 is defined as the ratio of the local volume flux compared to the discharge volume flux.

This was explained by the interference of the merging plumes on the entrainment mechanisms. The decrease of the available surface area upon merging lead to the decrease of the entrainment of each individual jet.

The work of Cheng et al. (1992) considered the behavior of merging buoyant discharges in an ambient current. Two discharge configurations were considered; one with the discharge in the same direction as the ambient current (coflowing) and one with the discharges in the opposite direction to the ambient current (counter flowing). The diameter of the ports used was 3.3 mm with spacing ranging between 60 to 90 mm. Results indicated that the merging buoyant flow rose more slowly than the single buoyant flow and that the profiles were similar apart from minor variations in the outer edges of the jets where there was slightly greater spread in the merged case. Concentration measurements were made using conductivity probes along the centerline of a single buoyant discharge and these were compared with measurements along the same center line where the buoyant discharges was part of an array. The port spacing to diameter ratio was effectively infinity for the single port and 27.3 for the multiple ports. For the large vertical depths the dilution was the same for both the single and multiple ports. As for small vertical depth, the dilutions for the multiple port were generally higher than those of the single port.

Mendez- Diaz and Jirka (1996) studied the discharge of buoyant plumes from multiport diffusers in deep coflowing water. The multiport diffuser had 24 ports with an internal diameter (d) of 4.72 mm. The port spacing was varied from 6.8 to 20.6d, the port densimetric Froude number (F_0) was 8 to 30 and the ambient /discharge Froude number F_a $(F_a = \dfrac{U}{J_o^{1/3}})$

The trajectories of the plumes were recorded using a video camera and the coordinates of the boundaries and centerline were then determined. The flow, after the merging of the multiple buoyant jets, was classified in to three major flow configurations depending on the ambient / discharge Froude number (F_a.) The three flow configurations ranged from a weakly - deflected plume regime with surface interaction and upstream spreading, to a complex intermediate regime with significant blocking and stagnant wedge formation, to a strongly deflected regime in which the plume reached the surface gradually. For the plane plume the discharge /buoyancy length scale l^*_q ($l^*_q = q_o/J_o^{1/3}$) was used as a dimensionless parameter that correlates the buoyancy flux (J_o) with the volume flux q_o. Two expressions were defined to evaluate the trajectory of the plumes. For the weakly deflected plume ($F_a < 0.6$), the trajectory was defined using the following equation:

$$\frac{y}{l^*_q} = \frac{C_1}{F_a} \frac{x}{l^*_q}$$

(2-28)

The trajectory constant $C_1 = 0.32$

For the strongly deflected plume ($F_a > 0.60$), the trajectory equation can be expressed as:

$$\frac{y}{l^*_q} = \frac{C_2}{F_a^{1.5}} \frac{x}{l^*_q}$$

(2-29)

The trajectory constant C_2 in Eq. 2.29 was found to be dependent on the leakiness parameter P_L defined as :

$$P_L = \frac{h_o + 1}{l^*_q}$$

(2-30)

where h_o= height of port center above the ambient bottom.

A variable trajectory relation ship was given by:

$$C_2 = 0.0017 P_L \qquad \text{for } P_L < 40 \qquad (2\text{-}31)$$

$$C_2 = 0.24 \qquad \text{for } P_L => 140 \qquad (2\text{-}32)$$

The effect of changing the port spacing (S) was also studied and it was found that it had little effect on the behavior of strongly deflected plumes. The merging distance was expressed by

$$\frac{x_m}{L_b} = K1 \left(\frac{S}{L_b}\right)^{1.5} \qquad (2\text{-}33)$$

where $L_b = J_0 / (U)^3$, $K1 = 2.5$

Density stratification plays an important role in dilution especially in ocean outfalls. Wright et al. (1982) studied the problem of horizontal discharges of buoyant fluid from submerged multiport diffusers in stagnant stratified ambient fluids. Numerical analyses based on integral methods were used to predict the maximum height of the jet rise and the associated dilution. Experiments were conducted to verify the mathematical model and the comparisons between experimental and numerical results resulted in fairly good agreement for minimum dilution

Roberts et al. (1989) investigated the dilution and the formation of wastefields resulting from the discharge into a linearly density-stratified steady current of arbitrary speed. The effect of spacing and the number of ports was also studied. The results indicated that the dilution is independent on the spacing and the number of ports while it is a function of the buoyancy flux per unit length of the diffuser.

2.5 Mixing Using Multiple Jets in Confined Environments

Mixing using multiple jets in confined environments has a variety of practical applications which have motivated a number of studies over the past decades. It is important in applications such as the mixing of chemicals in water treatment plants. It is also important in a gas turbine combustion chamber where mixing of relatively cold air jets is needed. In the next section, a review of some studies which dealt with mixing either in pipes, ducts or open channels would be reviewed.

Benzina et al. (1974) studied the mixing induced using a two dimensional plane jet that was opposed to the uniform stream (counterflowing jet). The standard deviation of the concentration about the arithmetic mean within the same cross-section and the standard deviation of the concentration distribution about the complete mixing concentration were used as a measure of the completeness of mixing through out the flume. The results indicated that the use of counterjet injection can induce rapid and thorough mixing in open channels.

Ger and Holley (1976) presented data on three single point injections in a pipe. The injections were : i) a center line source; ii) a wall source; iii) jet issuing perpendicular to the wall. The center line source and the wall source refer to situations where the injected fluid has no significant initial momentum or buoyancy. The standard deviation of the concentration distribution was used as a measure for the uniformity of mixing at a section. The mixing distance at which a low specified value of the standard deviation was achieved was found to be a function of the friction of the pipe. For the case of the jet injection, the optimum distance was found to be also dependent on the momentum flux of the jet to that of the crossflow. The results of this study showed that a wall source would give the longest mixing distance as compared to that from other sources. Analytically the mixing distance can be reduced most by a single center line source. However, practically, it was difficult to obtain a perfect axisymmetric condition and this usually causes the

29

mixing distance to be greater than that obtained from the analytical solution. As a result, it was concluded that reductions in mixing distances comparable to either a wall source or any actual centerline sources could be obtained by using jet injections.

Chao and Stone (1979) introduced a simplified approach to study initial mixing in pipes using jet injections. The empirical equations derived by Pratte and Baines (1967) for the trajectory of single jets in cross flows were used to determine the length required for the jets to reach the end of the maximum deflection zone. The total length in which rapid mixing would take place was assumed to be 3 times the maximum deflection length.

Fitzgerald and Holley (1981) investigated two types of jet injection systems in pipes to determine their mixing characteristics. The first type was a single jet placed flush with the side wall of the pipe . The arrangement of the jet was such that the jet flow would be perpendicular to the flow in the pipe (crossflowing jets) or in the opposite direction to the ambient flow (counterflowing jets). The second type consisted of two jets which originated at the pipe wall at opposite ends of the vertical diameter. Conductivity measurements were made along the pipe. The coefficient of variation of the concentration distribution was used as a measure of the degree of mixing at a given cross-section. Although the use of two jets in uniform flow did not produce significant decrease in the mixing distance compared to a single jet, the two jets would require less total power than the single jet. Experiments were also carried out on the effect on induced secondary currents in pipe flow. Results indicated that the use of two or more jets for injection would provide a factor of safety against the uncertain effects of secondary currents. The results indicated also that the assumption made by Chao and Stone(1979) in determining the rapid mixing length was not valid.

Bain et al. (1995) studied the mixing of axially opposed rows of jets injected into a rectangular duct. A CFD parametric study was conducted to determine the

influence of lateral geometric arrangement on mixing. Two lateral arrangements were analysed : 1) Inline jets (Jet centerline aligned at the top and the bottom of the duct walls); 2) Staggered Jets (Jets centerlines offset with each other on top and bottom walls). The study was carried out for velocity ratios (α) varying between 4 and 8 and ports spacing to duct height (S/H) ratios between 0.125-1.5. The mass flow ratio was kept constant for α value of 2. The results indicated that inline configurations have better initial mixing than staggered configurations. For the inline configuration it was found that at S/H ratio of 0.375 optimum mixing was achieved. The corresponding ratio for staggered configuration was 0.85. In terms of the overall downstream mixing distance, it was found that increasing α increases the downstream mixing for a staggered configuration while it had negligible effect for the inline jet.

2.6 References

Abdel Gawad, S.T., McCorquodale, J. A. and Gerges, H.(1996). "Near field mixing at an outfall. " Canadian Journal of Civil Engineering, Vol., 23, pp. 63-75.

Abdelwahed, M.S.T. (1981). Surface jets and surface plumes in crossflow: Ph.D. Thesis, Department of Civil Engineering and Applied Mechanics, McGill University, Montreal, Quebec.

Abramovich, G. N. (1963). The theory of turbulent jets. M.I.T. Press Cambridge, Mass.

Adams, E. E. (1982). "Dilution for unidirectional diffusers." Journal of the Hydraulic Division, ASCE, Vol. 108 No. HY3, pp 327-342.

Almquist, C. W. and Stolzenbach, K. D. (1980). "Staged multiport diffusers." Journal of the Hydraulic Division, ASCE, Vol. 106, No. HY2. pp 285-302.

Bain, D. B. , Smith, C. E. and Holdeman, J. D. (1995). "Mixing analysis of axially opposed of jets injected into confined crossflow." Journal of Propulsion and Power, Vol. 11, No.5 , pp 885-893.

Benzina, A. , S. Lin, and R. L. Wang (1974). "Counterjet and hydraulic blockage theory applications to mixing. " Journal WPCF, Vol. 46, No. 12. pp 2719-2731.

Chan, D. T. L., Lin, J.T., Kennedy, J. F. (1976). "Entrainment and drag forces of Deflected Jets." ASCE Journal of the Hydraulic Division, Vol. 102, No. HY5, pp 615-635.

Chao, J. L. and Stone B. G. (1979). "Initial mixing by jet injection blending." Journal AWWA, Vol. 71, pp 570-573

Cheng, C., Wood, I.R., and Davidson, M.R. (1992)."Merging buoyant discharges in an ambient current. " J. Hydr. Res., Vol. 30, No. 3 pp .361-372.

Chu, V. H. and Goldberg, M. B. (1974). "Buoyant forced plumes in a crossflow." ASCE Journal of Engineering Mechanics, Vol. 111, No. 11, pp 1343-1360.

Davis, L.R., Shirazi, M.A., Siegel, D.L. (1978). "Measurement of buoyant jet entrainment from single and multiple sources. " Journal of heat transfer, ASME, Vol. 100, pp 442-447.

Dominique, N. (1980). "Staged multiport diffusers" Discussion , Journal of the Hydraulic Division, ASCE, Vol. 106, No. HY2, pp 172-174.

Fan, L. N. (1967). "Turbulent buoyant jets into stratified or flowing ambient fluids." Report No. KH-R-15, W. M. Keck Laboratory of Hydraulics and Water Resources, California Institute of Technology. Passedena, California.

Fearn, R.L. and Weston, R.P. (1974). " Vorticity associated with a jet in a crossflow." AIAA Journal, Vol. 12, No. 12, pp 1666-1671

Fitzgerald, S., D. and Holley, E. R. (1981). "Jet Injections for Optimum Mixing in Pipe Flow." Journal of the Hydraulic Division, ASCE, Vol. 107, No. HY10, pp 1179-1195.

Ger, A., M. and Holley, E. R. (1976). "Comparison of Single Point Injections in pipe flow." Journal of the Hydraulic Division, ASCE, Vol. 102, No. HY6, pp 731-746.

Gordier, R. L. (1959). "Studies on fluid jets discharging normally into moving liquid." St. Antony Falls Hydraulic Laboratory, University of Minnesota, Technical paper.

Habib , A. (1987). "Flow of surface buoyant jet in crossflow." Journal of Hydraulic Engineering. Vol. 113, No. 7 , pp 892-904.

Hodgson, J. E. (1991). Turbulent jet discharges in rivers., Ph.D. thesis submitted to the University of Alberta, Department of Civil Engineering, Edmonton , Alberta, Canada.

Hodgson, J. E. and Rajaratnam, N. (1992) "An experimental study of jet dilution in crossflows." Canadian Journal of Civil Engineering, Vol. 19, No. 5, pp. 733-743.

Harleman, D. R. F. and Stolezenbach, K. D. (1972). "Fluid mechanics of heat disposal from power generation." Annual review of Fluid Mechanics. Vol. 4 , pp 7-32.

Isaacson, M.S., Koh, R. C. Y. and Brooks, N.H.(1983). "Plume dilution for diffusers with multiport risers. " J. Hydr. Engrg., 109(2), 199-228.

Jirka, G.H. (1982). "Multiport diffusers for heat disposal : A summary." J. Hydr. Div., ASCE, 108(12),1425-1468.

Jirka, G. H., Adams, E. E. and Stolzenbach, K. D. (1981). " Buoyant surface jets." Journal of the Hydraulic Divisions, ASCE, Vol. 107, No. HY116, pp 1467-1487.

Jirka, G. H. and Akar (1991). "Hydrodynamic classification of submerged multiport diffuser discharges." J. Hydr. Engrg., ASCE, 117(9), pp 1113-1128.

Kamotani, Y. and Gerber, I. (1972). "Experiments on a turbulent jet in a crossflow." AIAA 10th Aerospace sciences meeting. San Diego, California. paper No. 72-149.

Keffer , J. F. and Baines, W. D. (1963). "The round jet in cross-wind." Journal of Fluid Mechanics, Vol. 15, pp 481-496.

Khulman, J. (1984). "Reynolds number effects on buoyant surface jets." Journal of Hydraulic Engineering, ASCE, Vol. 110, No. 6, pp 836-840.

Langat, J. (1994). Dilution of circular wall jet in crossflow. M.Sc., thesis submitted to the University of Alberta, Department of Civil Engineering, Edmonton , Alberta, Canada.

Lee, J. H.W. (1985)."Comparison of Two River Diffuser Models." J. Hydr. Engrg. Vol. 111 pp 1069-1425.

List, E. J. (1982). Mechanics of turbulent buoyant jets and plumes. In: "Turbulent buoyant jets and plumes", W. Rodi (editor), Permagon Press, pp 1-68

McCorquodale, J. A. and Abdel-Gawad, S.T. (1986). "Non-buoyant and Buoyant jets in cross flowing streams." Proceedings of the Annual Conferences, Can. Soc. for Civil Engrg., Vol.3, Toronto, Ontario, p.24.

Mendez-Diaz, M. and Jirka, G. H. (1996)."Buoyant plumes from multiport diffuser discharge in deep coflowing water." J. Hydr. Engrg, ASCE, 122 (8), pp 428-435.

Motz, L. H. and Bendict, A. (1972). "Surface Jet Model for Heated Discharges." Journal of the Hydraulic Divisions, ASCE, Vol.98, No.HY1, pp 181-199.

Pande, B. B. Lal and Rajaratnam, N. (1977). " An experimental study of bluff jets." Journal of Hydraulic Research, IAHR, Vol. 15, No. 3, pp 261-275.

Parr, A. D. and Mellville, J.G. (1981). "Nearfield performance of river diffusers. "J. of Env. Engrg. ASCE, 107 (EE5) , 995-1008.

Parr, A.D. and Sayre, W. (1979). "Multiple jets in shallow flowing receiving waters." J. of Hydr. Engrg. ASCE, 105 (HY11), pp 1357-1374.

Pratte, B. D. and Baines, W. D.(1967). " Profiles of the round turbulent jet in crossflow. " Journal of the Hydraulic Divisions, ASCE, Vol., 93, No. HY6, pp. 53-64

Rajaratnam, N. (1976). Turbulent jets. Elsevier Scientific Publishing Co., Amesterdam, The Netherlands.

Rajaratnam, N. (1984). "Non-buoyant and buoyant circular jets in coflowing streams." Journal of Hydraulic Research, Vol. 22, No. 2, pp 117-141.

Rajaratnam, N. and Gangadhariah, T. (1980). " Circular jets in crossflow." Technical report. Dept. of Civil Engineering, University of Alberta, Edmonton, Canada.

Rajaratnam, N. and Humphries, J. A. (1984). " Turbulent non buoyant surface jets." Journal of Hydraulic Research , IAHR, Vol. 22, N0.2, pp. 103-115.

Rajaratnam, N. (1985) " An experimental study of bluff surface discharges with small Richardson number. " J. of Hydraulic Research, IAHR, Vol. 23, No. 1, pp. 47-55.

Wiuff, R. (1978). " Experiments on surface buoyant jet." Journal of the Hydraulic Divisions ASCE, Vol. 104, No. HY5, pp. 667-679.

Roberts, P.J.W., Snyder, W.H., Baumgartner, D. J. (1989)."Ocean outfalls. I Submerged wastefield formation." Journal of Hydraulic Engineering ASCE, Vol. 115, No. 1 pp 1-25.

Sherif, S. A. and Pletcher, R. H. (1989)."Measurements of the flow and turbulence characteristics of round jets in crossflow." Journal of Fluids Engineering, Vol. 111, pp. 165-171.

Wright, S. J. , Wong D. R. and Zimmerman K. E. (1982). "Outfall diffuser behavior in stratified ambient fluid." Journal of Hydraulics Divisions, ASCE, Vol. 108, No. HY4 , pp 483-501

Wright, S. J. (1977)."Effects of ambient crossflows and density stratification on the characteristic behavior of round turbulent buoyant jets." Report No. KH-R-36, W.M. Keck laboratory of Hydraulics and Water Resources Division of Engineering and Applied Science, California Institute of Technology, Passedena, California

Young, T. 1800. "Outlines of experiments and inquiries respecting sound and light." Proceedings, Physics Society, Vol. 90, pp 604-626.
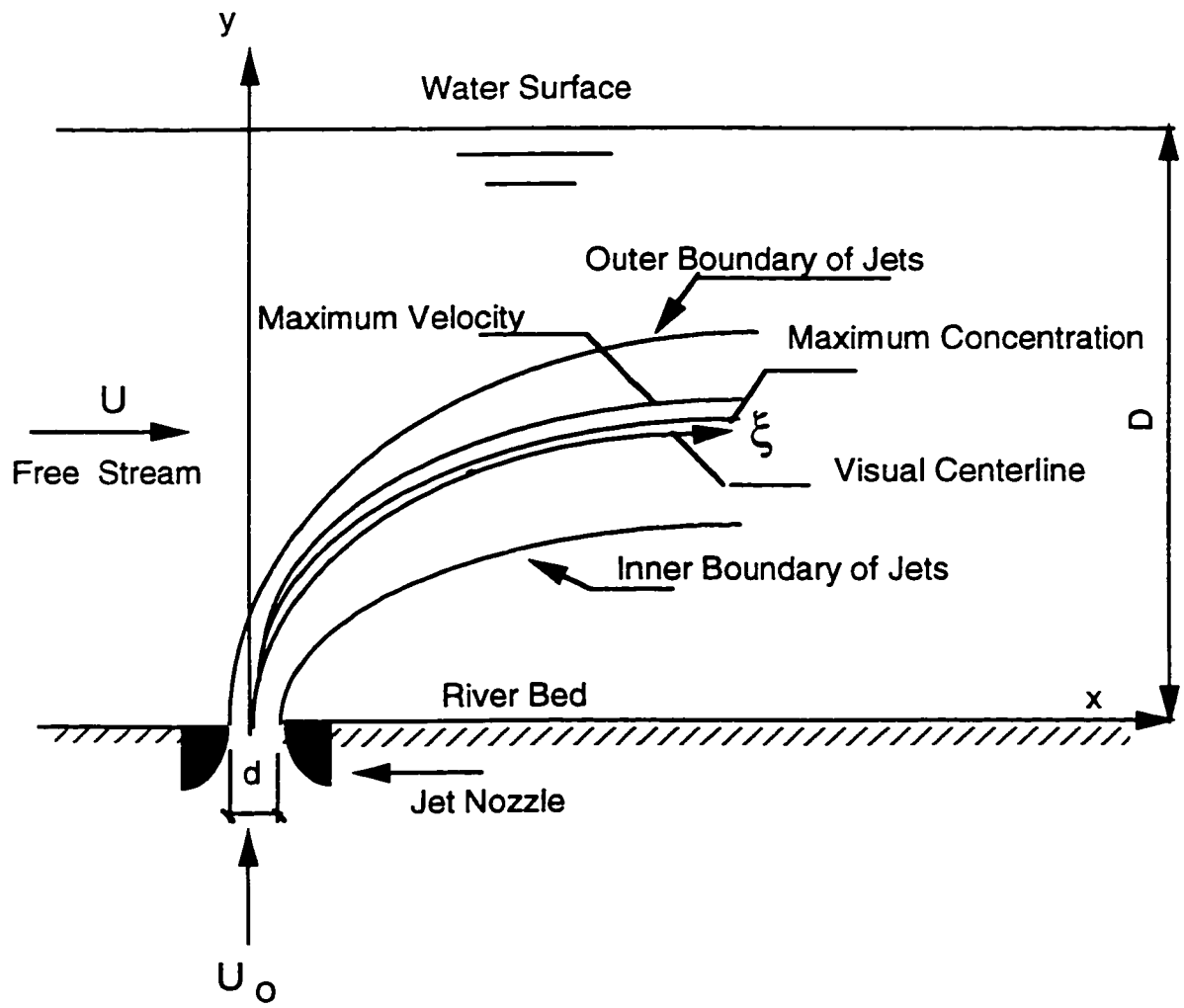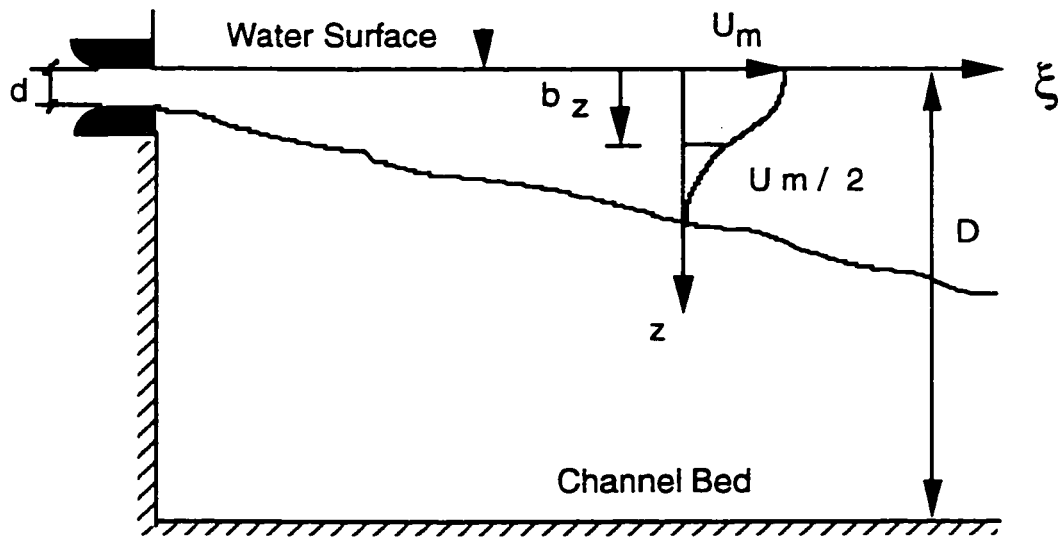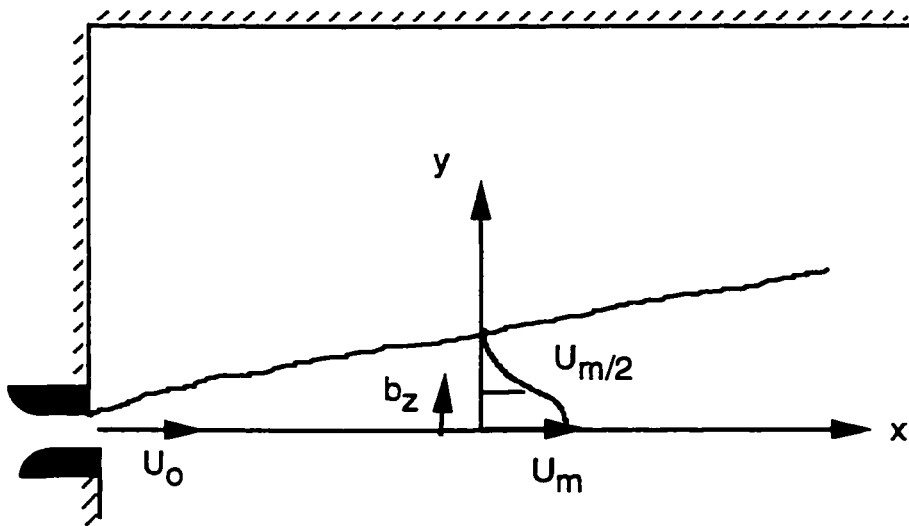
Fig. 2.1 Jet Discharge into a Crossflow

(a) Sectional View

(b) Half Plan View

Fig. 2.2 Definition Sketch for Circular Surface Jets in Stagnant Ambient

38

(a) Plan View

(b) Side View along the Jet Centreline
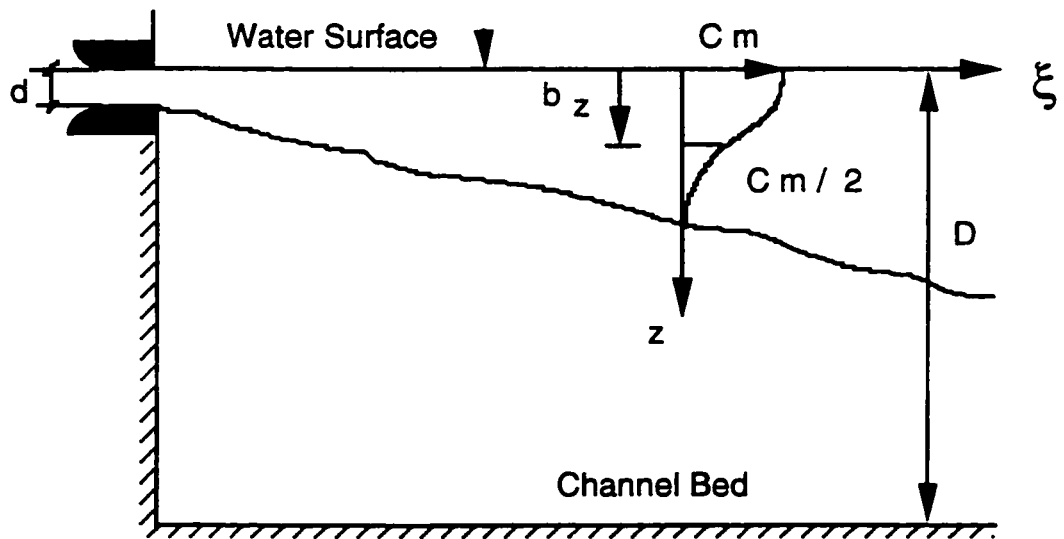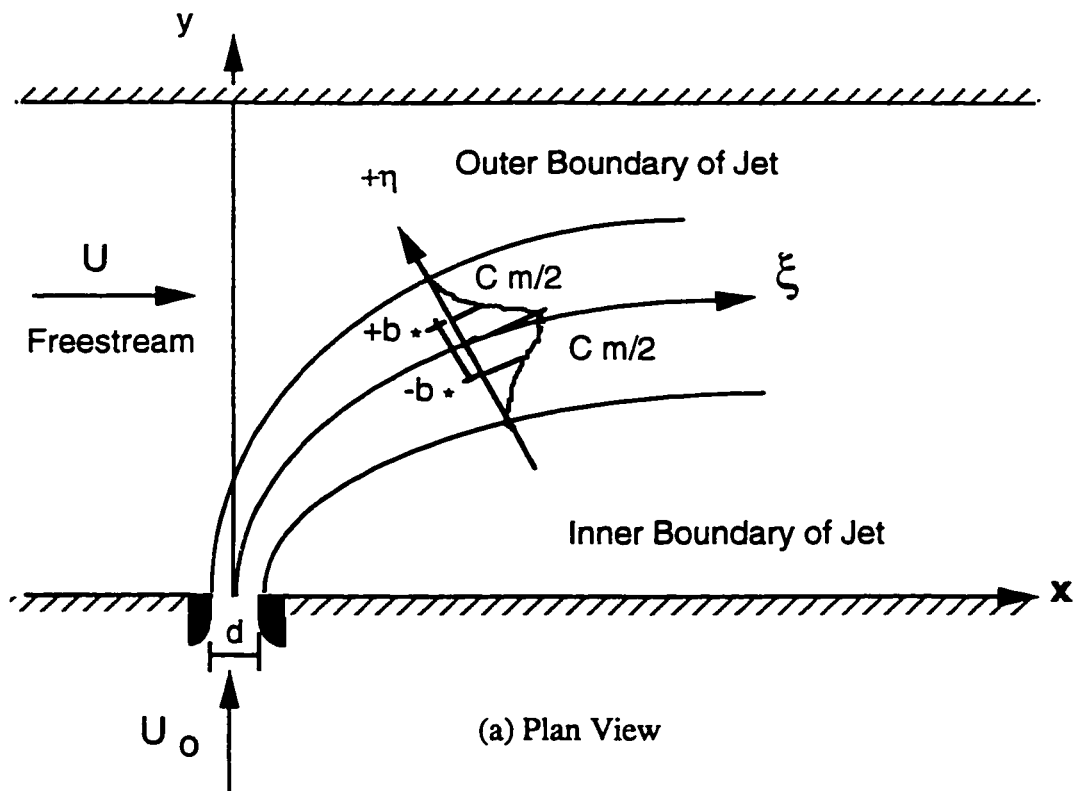
Fig. 2.3 (a-b) Definition Sketches of Surface Jet in Crossflow
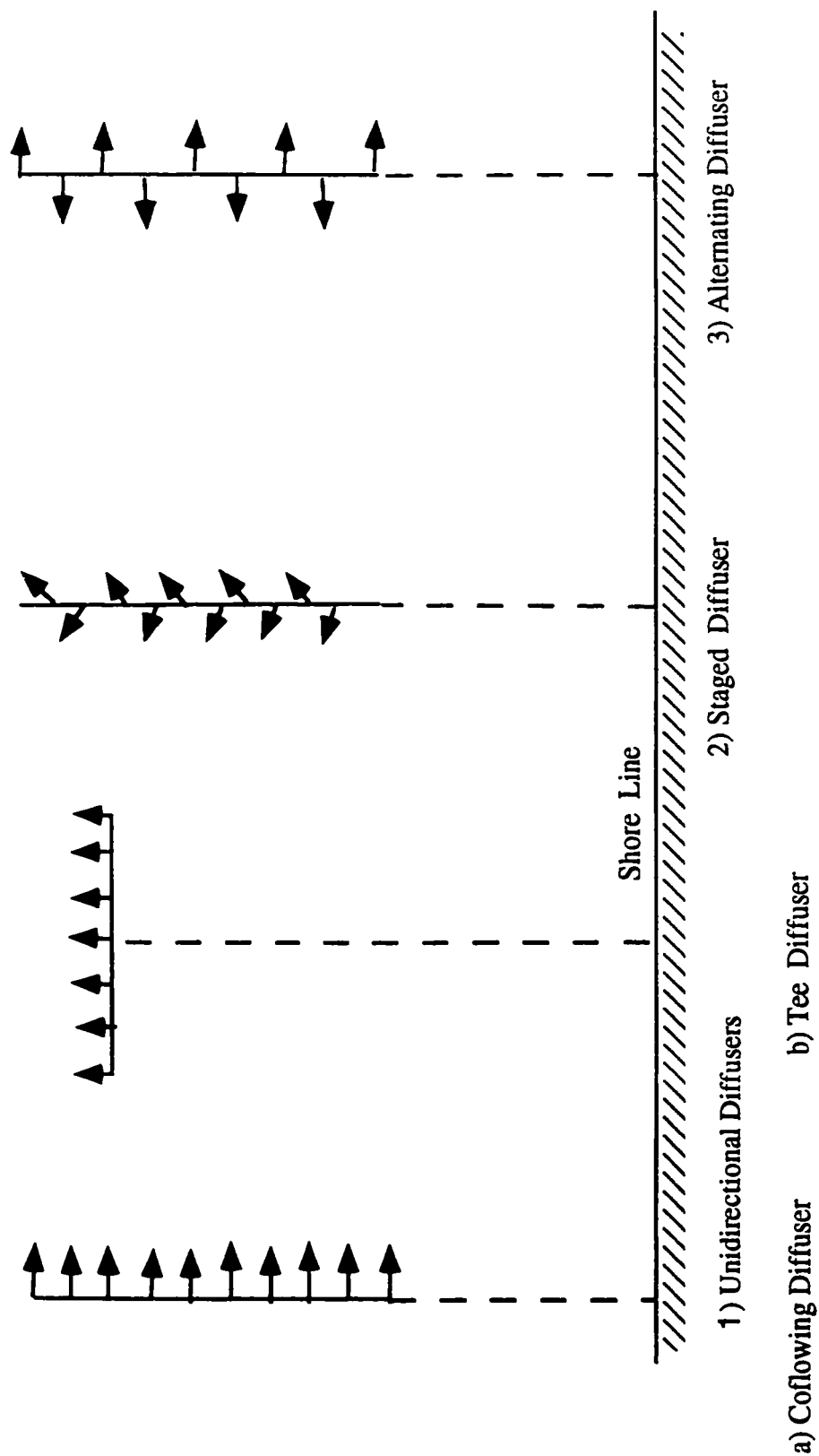
Fig. 2.4 Schematic Plan Views of Typical Multiport Diffuser Configurations

Chapter 3

Dilution of Circular Turbulent Non Buoyant

Surface Jets in Crossflows*

3.1 Introduction

The diffusion of buoyant surface jets in stagnant or moving surroundings has been studied by several investigators because of the importance of thermal discharges into water bodies (see Rajaratnam 1988 for a list of these references). A number of integral-type predictive models based on several simplifying assumptions have been developed. These have been found to have several problems (Policastro and Tokar 1972). Even though several experimental studies have been performed on the velocity field of buoyant and non-buoyant surface jets in stagnant and moving ambients (see Rajaratnam 1988 for a list of these references), very little research appears to have been done on the dilution of surface jets in crossflows except for a study by Abdel Gawad et al (1996) wherein they studied the dilution in the immediate vicinity of circular surface jets. Though buoyant surface jets in crossflows are practically more important, it was thought that a detailed study of the dilution in the mixing region of non-buoyant circular surface jets in crossflow would serve as a simpler case for future studies of the corresponding buoyant cases.

In this study, the dilution in the mixing region of circular surface jets in crossflow in an open channel is investigated. Several jet discharges, covering a wide range of α (jet velocity to ambient velocity ratio) were studied. The effect of some submergence of the jet nozzle on the minimum dilution was also investigated. These

---

results are believed to be useful in the design of outfalls discharging industrial and partially treated municipal waste waters into rivers.

3.2 Experimental Study

3.2.1 Introduction

In order to study the dilution of surface jets discharging into crossflows, an experimental study was carried out at the hydraulic laboratory at the University of Alberta. The prototype river conditions were simulated by introducing a free stream in a channel with a depth of D. A circular jet of diameter d was placed at the side of the flume such that the water surface of the free stream was just covering the top of the opening of the nozzle. The effect of some submergence of the jet nozzle on the minimum dilution was also investigated. As the sampling techniques and the concentration measurements are almost the same for the other coming chapters, more emphasis will be given to the procedure and the experimental set up in this chapter compared to that in the other two studies (chapter 4 and chapter 5). All the experiments were carried out for deep water conditions. This part describes the experimental plan, the experimental arrangements , calibration of the measuring instruments, the experimental procedure and an estimate of the errors involved in the observations.

3.2.2 Experimental Plan

A total of 10 experiments were conducted to study the dilution of the surface jets discharging into crossflows. Two circular nozzles of diameters of 6.35 mm and 12.7 mm were used. The velocity ratio (α) varied from 2.1 to 12.3. The jet Reynolds number, defined as $U_0 d / \nu$, where ν is the kinematic viscosity , was varied from 6985 to 22479. The details of the experiments are presented in Table 3.1. Concentration measurements were carried out for a distance of x/d=630, where x is the longitudinal

distance measured from the nozzle. For runs A and B, the depth to diameter ratio (D/d) was 50.4 and 25.5 respectively which ensured deep water conditions. To examine the effect of any submergence on the minimum dilution, the water level in the flume was raised to a distance of 1d, 3d and 6d above the nozzle openings (runs C1, D1, E1 respectively).

3.2.3 Experimental Arrangements

3.2.3.1 Experimental Flume

All the experiments were performed in a rectangular flume, 0.91m wide, 0.77m deep and 36.5 m long. Water was supplied to the channel by means of a pump placed in the laboratory sump. The water level in the flume was controlled by an adjustable tailgate located at the end of the channel. The discharge in the channel was measured using an in-line magnetic flow meter. The mean velocity in the channel was calculated from the measured discharge and the cross section area of flow. The vertical and the horizontal velocity profiles were measured for 3 locations across the flume at distances (y) of 100 mm, 225mm and 450mm from the inner boundary of the flume using a Prandtl tube and a pressure transducer. The velocity profiles are shown in Fig. 3.1 (a-b) . It can be seen that the effect of the wall extends at least as far as 100 mm into the stream flow.

3.2.3.2 Arrangement of Jets

The surface jets in deep cross flows were simulated in the laboratory by discharging water of the same temperature as the crossflow through circular nozzles. The nozzles were installed flush with the side wall of the flume. The nozzles were placed at a distance of 317 mm from the bottom of the channel . Figure 3.2 shows the position of the nozzles in the flume. The jet flows were produced by a 1/3 horsepower (250 watts) Jacuzzi pump. The pump raised water from a 900 L tank to a

constant head tank (placed approximately 3.5 m above the flume) which, in, turn supplied water to the jet nozzle. The flow rate through the jet nozzle was measured by a Fischer rotameter, shown in Fig. 3.3. The rotameter was volumetrically calibrated. The jet velocity was calculated from the measured flow rate and the nozzle diameter.

3.2.3.3 Sampling Rake Arrangement

Fluid samples were obtained by means of sampling tubes attached to a sampling rake. Three different sampling rakes were used through the experiments, depending on the velocity ratio (α) and the position of sampling. The sampling rakes consisted of a minimum of 8 L-shaped brass probes for the small rake up to maximum of 13 probes for the large rake. The inside diameter of the probes was 2.36 mm. The spacing between the probes varied from 10mm for the small rake to 40 mm for the larger rake. A horizontal graduated bracket was placed at the top of the flume (Fig. 3.4) on which the sample rakes were mounted. The bracket could be placed perpendicular to the jet axis which facilitated the movement of the sample rake in the lateral direction (η) (see Fig. 2.3 for definition sketch). The rakes were mounted on the horizontal bracket by means of a vertical graduated rod which allowed the movement of the rakes in the vertical direction. A protractor was mounted at the top of the rod so as to place the rake perpendicular to the jet axis (ξ). The probes were set to withdraw the samples at the same level in the η axis simultaneously. The probes were connected to a siphoning system of vinyl premium tubes of 3.175 mm internal diameter. Figure 3.4 shows the probes mounted on the horizontal bracket and connected to the vinyl tubes. The vinyl tubes were used to discharge the samples from the flume into 60 ml opaque plastic bottles (Fig. 3.5.).

3.2.4 Concentration Measurements:

Rhodamine WT was used as a tracer in these experiments. The original market concentration of the tracer is 20% by weight of the dye and its specific gravity is 1.19. The concentration of the Rhodamine dye in the jet fluid was measured by a Turner model 10 portable fluorometer (Fig. 3.6). The fluorometer uses a glass cuvette, 13 mm in diameter and 100 mm long. The sample fluid was placed in the cuvette which fitted inside a temperature control holder. The fluorometer readings are relative values of fluorescence intensity. To convert the readings to concentrations of a fluorescent solute, it was necessary to calibrate the fluorometer using standards, or prepared solutions of known concentrations. Distilled water was used in preparing the standards. The fluorometer was calibrated to diluted standards over a range of 0.1 to 80 ppb. Figure 3.7 shows the calibration curve for the fluorometer. Examination of the calibration curve indicated that the dye fluorescence is a linear function of the tracer concentration. The regression coefficient (r^2) for the best fit line is 0.999.

3.2.5 Experimental Procedure

The general procedure was to withdraw samples of the fluid in the flume at different locations downstream of the jet discharge. The procedure of sampling was more or less the same in all other experiments carried out in chapter 4 and chapter 5 The procedure followed is described below:

1) Standardized working tracer solutions were prepared and kept in dark bottles for use throughout the experiments.

2) Visual observations were carried out on the jet discharges with dye injection. To determine the location of the surface jets centerline, a 50mm square grid was placed at a distance of 25 mm above the surface of the water . Typical jet trajectories, viewed from above are shown in Fig. 3.8 (a-c).

45

3) Water from the same sump which provided the free stream flow was added to the 900 L tank . Temperature readings were taken before and after the sampling of each section.

4) For every experiment, about 10-20ml of the standard tracer solution was added and mixed thoroughly in the 900 L tank.

5) The concentration of the of the tracer mixture was checked by taking samples from the tank at different levels. Also the concentration was checked by taking samples directly from the hose connected to the nozzle.

6) Depending on the sampling position, an appropriate size of the sampling rake was chosen. The rake was placed such that the probes were perpendicular to the jet axis (ξ). The positioning of the rakes was done by adjusting the protractors placed at the top of the vertical rod or that mounted on the horizontal bracket. All the air was expelled from the vinyl tubings prior to the beginning of each run.

7) The sampling rake containing the collection bottles was positioned outside the flume such that the discharge velocity of the sample tracer coming out of the vinyl tube was approximately in the range of the crossflow velocity U .

8) The initial background fluorescence of the water from the sump was continuously monitored. If the background concentration exceeded 0.15 ppb, the sump was refilled.

9) To avoid any change in the water level in the flume, the tailgate elevation was kept constant for each experiment (A, B, C, D, E) .

10) The discharge in the flume and the jet discharges were allowed to stabilize once all settings were done. Sampling was carried out in the transverse direction along the (η) axis, starting from the water surface and moving vertically downwards.

11) The concentration measurements were carried out by transferring the contents of each the plastic bottles to the cuvette. The cuvette was carefully wiped

before placing it in the fluorometer. The results were then adjusted to account for the background concentration.

3.2.6 Experimental Errors

The difference between the observed value of any physical quantity and the accurate value is called the "error of observation". Errors of observations are usually grouped as accidental errors , fixed errors or mistakes . Usually it is assumed that all the fixed errors and mistakes have been detected and eliminated. Hence, accidental (random) errors would be considered. In most engineering problems, it is difficult to evaluate the reliability of the results by repetition. Kline and McClintock (1953) and Kline (1985) suggested a method to analyze the uncertainties for these types of problems as follows:

Assume that a certain result Re is a function of m independent variables $(V_1, V_2, V_3, ... V_m.)$. The variables have uncertainity intervals $(W_1, W_2, W_3, ... W_m)$ with the same confidence levels. The uncertainty interval of the result, W_{Re} can be expressed by:

$$W_{Re} = \left[\left(\frac{\partial Re}{\partial V_1} W_1 \right)^2 + \left(\frac{\partial Re}{\partial V_2} W_2 \right)^2 + ...\left(\frac{\partial Re}{\partial V_m} W_m \right)^2 \right]^{0.5} \qquad (3\text{-}1)$$

Estimate of Uncertainty

The possible sources of errors for the measured variables in the experiments carried out in the whole thesis would be presented in this section. The uncertainty of the results would be computed using Eq.3-1.

The depth of flow, the vertical and the transverse location of the rake were measured with point and transverse gauges to the nearest 0.1 mm. An estimated error in the depth of flow was 2mm which is about 1% of the lowest depth used, for the

location of the rake the error was estimated as 0.5 mm. The dimensions of the flumes used were measured with instruments that provide an uncertainty of 0.5 mm which is about 0.8% of the width of the channel. The nozzles used were machined to a precision of 0.025 mm, this would yield to an error of 0.8%.for the lowest diameter used (3.2mm). The discharge in the channels was measured using a magnetic flowmeter and the discharge through the nozzles was measured using rotameters which were volumetrically calibrated. The estimated errors for the discharge values are 2%.

In calculating the average crossflow velocity, three variables are involved ; the Discharge Q, the depth of flow D and the width of the channel W (U=Q/DW). Equation 3.1 can be used to find the uncertainity of the velocity W_u so that

$$\frac{W_U}{U} = [(\frac{\partial Q}{Q})^2 + (-\frac{\partial W}{W})^2 + (-\frac{\partial D}{D})^2]^{0.5}$$ (3-2)

From Eq. 3.2 the value of $\frac{W_U}{U} = 0.023$

The error in the jet velocity (U_O) resulted from the errors in jets discharge measurements Q_O (estimated error of 2%) and the errors resulting from the machining of the nozzles diameter (estimated error of 0.8%). Using Eq. 3.2 the value of $\frac{W_{U_o}}{U_o}$. was equal to 2%.

One of the main sources of errors in these types of dilution studies is the concentration measurements. The concentration was measured using a manual flourometer which was used for the studies on surface jets and multiple jets (chapter 3, 4). The magnitude of the error associated with the use of the fluorometer to measure the concentrations was evaluated by preparing several samples of the standard solutions. Each sample from a certain dilution was analyzed in the fluorometer, the average and the standard deviation of each sample was computed.

The standard deviations varied from 3-10% of the average reading for the different samples which indicated probable errors in the order of 2% to 6%. For the last study (chapter 5), a digital flourometer was used. The calibration of the flourometer was set to give the direct reading of the concentration and hence the errors were estimated to be much less than the manual one. Also, to have an estimate of the possible errors in the experiments, certain experiments were replicated and the standard deviations for these readings ranged from 1.5 to 3% which corresponded to 2 to 4% probable errors.

3.3 Results and Analysis

3.3.1 Introduction

In this section, experimental observations on the concentration distribution are presented. The concentration profiles in the vertical $(z-\xi)$ and the lateral $(\eta-\xi)$ planes are analysed in a dimensionless form, and are tested for similarity. The data are analyzed for the maximum concentration (or minimum dilution) and a general equation for the minimum dilution (C_0/C_m) in terms of the non dimensional distance $(\alpha x/d)$ is suggested. The effect of the nozzle submergence is also investigated. Finally the growth of the length scales of the surface jets in the vertical and the lateral directions are considered.

3.3.2 Conditions Investigated

Concentrations were measured along the jet axis ξ in both the vertical plane and the transverse direction η. Fig. 2.3 (a-b) shows a sketch of the surface jet discharges into a cross flow. The sketch defines the planes considered in the presentation of the results. An average of eight sections were measured for each run. On the average, a total of 5000 concentration measurements were made. Two jet nozzles of diameters 6.35mm and 12.7 mm were used in this study. For runs C, D

and E (Table 3.1), the jet nozzle was covered to distances of 1d, 3d and 6d respectively. The velocity ratio α was varied from 2.1 to 12. The concentration measurements were carried out as far as x/d=630 downstream the jet nozzle. In terms of the transformed distance αx/d, the measurements were carried out for a range of 4 to 5000.

3.3.3 Analysis of the Results

Turbulent jets in stagnant as well as coflowing surroundings have been studied both theoretically and experimentally for many years (see Abramovich 1963 and Rajaratnam 1976 for a list of references). But for jets issuing at right angles into a moving ambient, commonly referred to as jets in crossflows, the investigations have been generally empirical. The earlier studies were of the integral type (see Abramovich 1963 and Rajaratnam 1976) with the later studies leaning more on dimensional considerations along with simplified models, made popular by Wright (1977). Using a length scale l_m equal to $\sqrt{(M_0 / \rho)} / U$ where M_0 is the momentum flux from the nozzle, ρ is the mass density of the fluid and U is the velocity of the crossflow, the region in which the distance y along the initial direction of the jet is less than l_m was called the momentum dominated near field (MDNF). In this MDNF, the crossflow simply pushes the jet downwind, with the jet diffusing essentially as in a stagnant environment. The region where y is larger than l_m was called the momentum dominated far field (MDFF). In this region, the deflected jet is replaced by a series of momentum puffs issuing from a line source into the ambient fluid. From these considerations, it has been possible to predict theoretically the trajectory as well as the average dilution of the deflected jets, at least partially (See Wright 1977). Hodgson and Rajaratnam (1992), found an expression for the trajectories constants in the MDNF and MDFF zones. The above two regimes are followed by what can be termed as the passive plume region (PPR), in this region the

50

mixing and dilution is due to the turbulence in the ambient flow. The transition from the MDFF region to the PPR was assumed (Langat,1994) to occur where the excess velocity in the jet above that of the ambient flow falls to about 1% of the initial velocity, i.e. $(U_m-U)/(U_0-U)=0.01$. This was found (Rajaratnam and Gangadhariah 1980) to occur approximately at $\xi/\xi_*=10$, where ξ_* is defined as the axial distance of the deflected jet from the virtual origin to the end of the potential core. The results from Wright (1977) and Hodgson (1991) for the MDNF and MDFF regions and from that of Rajaratnam and Gangadhariah (1980) for the PPR were combined together and analyzed (Langat, 1994). The results were then categorized graphically and a dimensionless plot of $\alpha x/d$ against α was produced as given in Fig (3.9). This figure shows the three regions defined as the MDNF, MDFF and the PPR. For this study, Fig. (3.9) will be used as the basis for identifying the different mixing regions.

3.3.3.1 Transverse Concentration Profiles

The concentration (C) at any point was normalized by the concentration at the nozzle (C_0) and the concentration profiles in the $(z-\xi)$, and $(\eta-\xi)$ planes were plotted. The concentration distributions in the transverse direction ($\eta - \xi$ plane) were investigated at different locations downstream the nozzle. For all the runs, the jets were not affected by the side walls of the flume except for the weak jets with $\alpha=2.1$. Figure 3.10 (a-f) shows the transverse concentration profiles for different jet discharges at the maximum concentration planes. The concentration at each point (C) was normalized by the concentration at the nozzle (C_0) and plotted against the lateral distance η. The center of the jet was taken at the point of maximum concentration. The concentration measurements were also carried out at different elevations in the vertical direction z and for various distances x from the outfall. Figures 3.11 to 3.17 show typical transverse profiles in several horizontal planes from the water surface for several values of α and at different longitudinal distances.

On examining the transverse concentration profiles, it can be noticed that the lateral concentration profiles were not symmetrical around the maximum concentration center line. Also, the maximum concentration is not symmetrically located on the visual centerline of the jet trajectory as observed in axisymmetric jets, but occur generally on the outer half-section of the jet width. In other words, the concentration centerline seems to be more deflected towards the outer boundary of the jet. Similar observations have been made earlier for rectangular buoyant surface jets in crossflows (Habib, 1987) and wall jets in crossflows (Langat, 1995). It is also interesting to notice the shift of the maximum concentration centerline towards the inner boundary as z increases, which shows that the location of the jet centerline is depth dependent. The decay of the jet velocity in the vertical direction combined with the nearly uniform velocity of the crossflow near the surface can cause the jet axis deflection towards the inner boundary as z increases. Run A2 (α=8.25, Fig. 3.15) was chosen as a typical run to quantify the significance of the jet axis deflection. Figure 3.18a shows a normalized plot of the jet centerline deflection at distances 5, 10, 20, 25 and 40 mm below the water surface. It was found that the jet centerline can be described by the equation:

$$\frac{y}{d} = a \left(\frac{x}{d}\right)^b \qquad\qquad (3\text{-}3)$$

where a and b are dimensionless constants.

The values for a and b are given in Table 3.2 with the corresponding coefficient of determination (r^2). It can be noticed that the b values approach the 1/3 value suggested by Wright (1977). The a values do not exhibit a definite trend. Similar observations have been made earlier for rectangular buoyant surface jets in crossflows (Habib, 1987). An average estimate for the jet deflection at the five elevations is given by :

$$\frac{y}{d} = 9.5(\frac{x}{d})^{0.33}$$
(3-4)

with a coefficient of determination $r^2 = 0.90$.

Equation 3.4 is plotted and shown in Fig. 3.18 (a-b).

The concentration field in the jet cross section is best described by examining concentration contours at a number of downstream stations. The concentration at any point (C) is expressed in terms of the maximum concentration at that section (C_m). Typical concentration contours are shown in Fig. 3-19. While the concentration plots are unimodal for the jets with the velocity ratio $\alpha=2.1$ to 10.3, the jet with $\alpha=12.3$ had bimodal (i.e. twin peaks) concentration distributions as shown in Figs.3-19 (d-f). For high velocity jets ($\alpha=12.3$), double peaked concentration profiles appeared for the sections investigated in the PPR as shown in Fig.3-19(e-f) ($\alpha x/d=1000$ to about 2000), the jet effects weaken and give way to vortex mixing to occur. The biomodal peak concentrations were not identical, with the maximum peak always located at the outer boundary of the jet. The ratio between the concentration at the maximum peak to the concentration at the second lower peak is about 1.6.

3.3.3.2 Similarity of Transverse Concentration Profiles

The concentration profiles in the center plane were tested for similarity by using the maximum concentration C_m as the concentration scale and b* as the length scale. The length scale b* is defined as the distance where the concentration is half the maximum concentration (C_m) on either side of the jet axis. The outer scale is conventionally considered positive (+b*) and the inner scale negative (-b*) (see Fig. 2.3). Figure 3-20 (a-f) shows a typical set of normalized transverse concentration profiles for different values of α for several sections. A consolidated set is shown in Fig.3-21 for several values of α from 2.1 to 12.3 for x/d=630. It can be seen that the

53

profiles are similar with limited scatter occurring for data points sampled in the MDNF near the edges of the jets on the inner side in the wake region near the nozzle (x/d=3). For α=12.3, scatter is appreciable due to the occurrence of the double peak in the concentration profile for the sections in the passive plume regions at distances x/d=82 to x/d=157. We can also notice the skeweness which is due to the unsymmetrical concentration distribution in the lateral direction. The growth of the transverse length scales on the outside (+b*) and the inside (-b*) regions of the deflected jet were considered separately. Figure 3.22 shows typical variation of the positive and the negative length scales normalized by the diameter of the jet with the dimensionless distance x/d downstream the nozzle. It can be noticed that near the nozzle, both length scales are approximately equal but as we go further downstream, the negative length scale (-b*) tends to be larger than the positive length scale (+b*). This observation indicates that the jet centerline tends to shift more towards the outer half of the jet as discussed earlier. It is believed that this is due to the enhanced entrainment on the leeward side of the jet due to the circulation caused by the component of the crossflow velocity perpendicular to the deflected jet. The ratio between (-b*) and (+b*) varies from about 1.5 to 2 except for jets with high velocity ratios (α=10.3 and 12.3) where the negative length scale (-b*) increases dramatically due to the double peak concentration profiles. The ratio between (-b*) and (+b*) may reach an approximate value of 4.

3.3.3.3 Vertical Concentration Profiles

The vertical concentration profiles in the z-ξ plane are studied in this section. For Runs A and B, the maximum value of C/C_0 was plotted against the vertical distance z measured from the surface of the water surface. Fig. 3.23 shows typical vertical concentration profiles for different values of α. All the runs were carried out for deep conditions and the spreading of the jet in the vertical direction was not

affected by the bottom of the channel. For experiments in series A, the maximum concentration C_m, for almost all the runs occurred at the surface of the water. As for runs in series B, it was noticed that for some of the sections, the maximum concentration was located below the free surface. The dip in the concentration profiles near the surface was more pronounced in Expts. with $\alpha=2.1$ and $\alpha=4.2$. The jet trajectories for these discharges tend to be closer to the inner boundary of the channel. As noticed in Fig. 3.1 the effect of the wall extends to about 100 mm in the channel causing a dip in the crossflow velocity near the surface which in turn may have caused the dip in the concentration profiles. A similar dip in the velocity profiles was observed for non buoyant circular surface jets in a stagnant flow (Rajaratnam and Humphries 1984) and for circular surface jets in a coflowing stream (Rajaratnam, 1984). The dip of the velocity was attributed to the high jet velocities which generated waves at the surface of the free stream.

3.3.3.4 Similarity of Vertical Concentration Profiles

The vertical concentration profiles were tested for similarity by normalizing the concentration with C_m and the vertical distance z by b_z which is equal to z where $C/C_m=0.5$. Figure 3.24 shows the non dimensional concentration profiles for the six jet discharges ($\alpha=2.1,4.2,6.8,8.3,10.3,12.3$). These profiles were generally found to be similar and were described well by the exponential equation

$$\frac{C}{C_m} = \exp(-0.693(\frac{z}{b_z})^2) \qquad (3-5)$$

A consolidated plot is given for all the concentration profiles in Fig. 3-25. It may be noticed that near the water surface, there is some dispersion of the data because of the occurrence of a concentration dip for some experiments near the water surface.

Also, some scatter can be noticed near the lower part of the jet especially for the high velocity cases (α=10.3 and 12.3).

3.3.3.5 Minimum Dilution

The concentration C_O at the nozzle and the maximum concentration at each section C_m are used to define the minimum dilution ratio (C_O/C_m). As indicated by previous work (Patrick, 1967 and Rajaratnam and Gangadhariah, 1980), the jet dilution could be quantified by a power law relationship :

$$\frac{C_o}{C_m} = a(\frac{\xi}{d})^b \qquad\qquad (3\text{-}6)$$

where C_O is the concentration at the jet nozzle, C_m is the maximum concentration ,ξ is the distance to the section along the curvilinear axis, d is the diameter of the jet nozzle, a is the dilution coefficient, and b is a dilution exponent.

Wright (1977), developed the dilution equation as a function of the vertical distance (y) (distance from the flume boundary to the jet centerline). Hodgson and Rajaratnam (1992), expressed the dilution ratio (C_O/C_m) in terms of the transformed distance $\alpha x/d$ (see Eq.2.9). The same approach was adopted for the dilution of circular wall jets (Langat, 1994). The dimensionless distance $\alpha x/d$ will be also considered for the present analysis. The results of this study will be compared to these of Hodgson, (1992) and Langat, (1994).

Variation of the minimum dilution C_O/C_m with the dimensionless distance $\alpha x/d$ was studied for all the experiments (including the submergence cases, Expt. C1, D1, E1). Some typical results showing the variation of C_O/C_m with $\alpha x/d$ are shown in Fig. 3-26 (a-j) for several values of α. The measurements covered a range of $\alpha x/d$ from 4 to 5000. Based on the work carried out by Wright (1977) and the analysis of Hodgson (1991), It was found that in the MDNF, the exponent in a power

law relation ship (similar to Eq.2.10) was equal to 1/2 whereas the corresponding value for the MDFF was 2/3. For the present study, though fewer data points were available in the MDNF region than those for the far field region, yet based on a regression analysis carried on all the points at the MDNF region ($\alpha x/d < 100$), the exponent in the power law relation was approximately equal to 0.5. Hence, it is reasonable to say that the data in the MDNF and MDFF can be described by straight lines with slopes of 1/2 and the 2/3 respectively on log-log plots of C_0/C_m versus $\alpha x/d$ as shown in Fig. 3.26 (a-j). The transition between the MDNF and MDFF fields is identified by the intersection of the two sloping lines. It was found that this transition occurs for $\alpha x/d < 100$ for the range of velocity ratio (α) considered in this study. The MDNF was found to increase with the increase of the velocity ratio α. The minimum dilution at the end of the MDNF ranged from approximately 2 for $\alpha = 4.2$ to about 6 for $\alpha = 12.3$.

Following the work of Hodgson and Rajaratnam (1992) for free jets in crossflow and Rajaratnam and Langat (1995) for wall jets in crossflow, all the results from the present study on surface jets in crossflow are plotted with C_0/C_m against $\alpha x/d$ in Fig.3.27. All the observations for the experiments with $\alpha = 4.2$ to 12.3 (except Expt. D1 and Expt. E1) fall together and can be described by the equation

$$\frac{C_o}{C_m} = 0.5 \left(\frac{\alpha x}{d}\right)^{0.63} \tag{3-7}$$

with a correlation coefficient of 0.98. Fig. 3.27 shows that the minimum dilution for the case of (1d) submergence (Expt.C1) can be well represented by Eq.3-7. On increasing the nozzle submergence (Expt. D1 and E1), the data seemed to follow Eq. 3.7 up to a distance $\alpha x/d=600$ after which the observations tend to fall lower. It is believed that more experiments should be carried out to quantify the effect of the nozzle submergence beyond this distance ($\alpha x/d=600$). For the weaker jet with $\alpha = 2.1$, the dilution is larger than that produced by jets with larger values of α.

Similar observation had been made earlier for free jets and wall jets in crossflow. Fig. 3.27 shows minimum dilutions to 100 with $\alpha x/d$ varying from 4 to about 5000. The exponent in Eq. 3-7 is closer to 2/3 as most of the observations were in the MDFF region. The results from this study on minimum dilution are compared with those for circular jets in cross flows (Hodgson and Rajaratnam, 1992) and wall jets in crossflows (Rajaratnam and Langat, 1995) in Fig. 3.28. It can be seen that in general free jets in crossflows provide more dilution than the other two cases with the surface jet providing the least dilution. A minimum dilution of 50 is achieved at $\alpha x/d$ equal to about 900 for both free and wall jets whereas the corresponding distance is about 1500 for surface jets. For a minimum dilution of 100, the corresponding value of $\alpha x/d$ is about 3000 for the first two cases and 4000 for the surface jet.

3.3.3.4 Jet Thickness:

The thickness of the jet b_z is defined as the vertical distance from the water surface at which the concentration at any vertical section is one-half the maximum concentration at that section (see Fig.2.3). In all the experiments the jet growth was not affected by the channel bottom. The growth of b_z/d with the distance x/d for different values of α is shown in Fig. 3.29a. It can be seen that for the wide range of experiments the vertical growth of the jet is curvilinear and can be expressed by the following equation.

$$\frac{b_z}{d} = (\frac{x}{d})^{0.32} \qquad (3\text{-}8)$$

The coefficient of determination (r^2) is equal to 0.92. The power in Eq. 3-8 indicates that the overall vertical growth for the jets is relatively small. Equation 3-8 seems to represent the data well except for the weakest and the strongest jets (α=2.1

58

and $\alpha=12.3$). For $\alpha=2.1$, the spreading of the jet seems to be less than that for the other runs especially at the passive plume regions. For the high velocity jets ($\alpha=12.3$) it was observed that the water as it goes out of the jet nozzle tends to expand the surrounding water (crossflow) and hence the jet thickness decreases as shown in Fig. 3.29b for the points near the jet nozzle.

Neglecting the MDNF and the PP regions, the observations for $x/d=10$ to about 160, were replotted in Fig. (3.29b). This represents the MDFF regions for all the experiments. Figure 3.29b shows the growth of the jet thickness in this region. It is found that in the MDFF, the jet growth can be approximately expressed with a linear relation ship as follows.

$$\frac{b_z}{d} = 0.045 * \frac{x}{d} + 4.15 \qquad (3-9)$$

The coefficient of determination r^2 is 0.90. In Fig. 3.29b , the rate of growth of the deflected jet db_z/dx is approximately equal to 0.045 From previous experiments (Rajaratnam and Pani, 1974 and Rajaratnam, 1984), the corresponding expansion rate for circular surface and wall jets in stagnant flow using velocity measurements was approximately equal to 0.04 . The jet thickness predicted by Eq. 3.9 is about four times that for both surface and wall jets in stagnant flow. This is due to the effect of the crossflow which enhances the vertical spreading.

3.3.3.6 Jet Width

The jet width is defined as the distance measured along the η axis where the concentration on either side of the jet centerline is 50% of the maximum concentration and hence equal to (l -b* l+b*). The jet width Wy is first normalized by the diameter of the nozzle and Fig. 3-30a shows the variation of this normalized jet width with x/d . For the case with $\alpha=12.3$ the width of the jet tends to increase

59

rapidly when the transverse concentration profiles become biomodal. If these bimodal distributions are excluded, the variation of the normalized width with x/d may be described by the equation:

$$\frac{W_y}{d} = 2.29(\frac{x}{d})^{0.49}$$
(3-10)

with a determination coefficient (r^2=0.87). Also the jet width can be expressed in term of the dimensionless distance $x/\alpha d$ using the following equation:

$$\frac{W_y}{\alpha d} = 0.93(\frac{x}{\alpha d})^{0.49}$$
(3-11)

with a determination coefficient (r^2=0.93)

Equation 3-11 is shown in Fig. 3.30b. The results for the surface jets were compared with the results of bottom discharges in crossflows (Hodgson and Rajaratnam, 1992). Fig. 3.30b shows the comparison of jet width for surface jet and free jet in crossflows. From Fig. 3.30b, it can be seen that the widths were essentially the same for $x/\alpha d$ up to about 10. For $x/\alpha d$ greater than 10, $W_y/\alpha d$ was larger for the surface jet and was equal to about 7.8 for $x/\alpha d$=100 where as the corresponding value for the free jet was about 4.6. It should be noted that the experiments for the free jets were carried out for a downstream distance $x/\alpha d$ ranging from about 1 to 30.

The effect of the free surface on the lateral spread was previously observed by Rajaratnam and Pani (1974) for wall jets and Hodgson (1991) for circular jets in cross flows. Abdelwahed (1981) reported that the ratio between the spreading of rectangular surface jets in crossflows to the jet vertical growth varies from 1.47 for weak jets to 5.4 for high α values.

On comparing the results of the jet width (Eq. 3-8) to that of the jet thickness (Eq. 3-10). It can be concluded that the transverse growth of the surface circular jet is much larger than the spreading in the vertical direction. Figure 3.31 shows the

variation of the jet growth in both the lateral and the vertical direction. It can be noticed that the ratio between the jet width W_y and the jet thickness b_z increases as we go further downstream from the outfall. This ratio varies from about 1.2 in the MDNF(x/d=1) to 1.8 at x/d =10 ; 2.8 at x/d = 100 (MDFF) and 3.6 at x/d=700 (PPR). The water surface seems to restrict the vertical growth of the jet and enhances the lateral growth.

3.4 Conclusions

Based on the experimental results from this investigation the following conclusions may be drawn:

1) The mixing zone can be defined as the region in which minimum dilution of about 100 is achieved. This zone extends through the MDNF, MDFF into the PPR.

2) The concentration field in the lateral and the vertical directions in the planes of the maximum concentration were found to be fairly similar with limited scatter near the nozzle. This indicated that the concentration distributions for a circular jet in crossflows are preserved from one section to another.

3) The location of the jet centerline, as defined by the point of maximum concentration, was found to be dependent on the distance measured from the water surface in the vertical direction (z). The jet centerline was found to move towards the inner boundary of the deflected jet as the distance from the water surface increased.

4) For large velocity ratios (α), the vortices may partially separate and the concentration profiles become bimodal.

5) The minimum dilution (C_0/C_m) results indicated that the data can be represented by the 1/2 and 2/3 slopes on a log-log plot in the momentum dominated near field (MDNF) and the momentum dominated far field (MDFF) respectively. The results showed that the minimum dilution attained in the MDNF ranges from 2:1

to 6:1. Beyond the MDFF, dilutions up to 100:1 was achieved for $\alpha x/d$ approximately equal to 4500. The variation of the minimum dilution C_0 / C_m with the transformed longitudinal distance $\alpha x/d$ was described by a relatively simple equation for the entire mixing region.

7) The results of the minimum dilutions for this study were compared with that of the free circular jets and wall circular jets in crossflows. It is found that the minimum dilution for the free jets is superior to that of the wall jets and surface jets.

8) Expressions were developed to describe the growth of the width and the thickness of surface jets in crossflows. It was found that the ratio of the jet width to thickness was about 1.2 to 3.6 in the MDNF and the PPR respectively.

3.5 References

Abdel Gawad, S.T., McCorquodale, J.A. and Gerges, H. (1996). "Near field mixing at an outfall." Canadian Journal of Civil Engineering, Vol. 23 No. 2 pp 63-75.

Abdelwahed, M.S.T. (1981). Surface jets and surface plumes in crossflow: Ph.D. Thesis, Department of Civil Engineering and Applied Mechanics, McGill University, Montreal, Quebec.

Abramovich, G. N. (1963). The Theory of Turbulent Jets. English Translation, M.I.T. Press, Cambridge, Mass., USA, 671p.

Habib O. (1987). "Flow of surface buoyant jet in crossflow." Journal of Hydraulic Engineering, Vol. 113 No. 7, pp 892-904.

Hodgson, J. E. (1991). Turbulent jet discharges in rivers., Ph.D. thesis submitted to the University of Alberta, Department of Civil Engineering, Edmonton , Alberta, Canada.

Hodgson, J. E. and Rajaratnam, N. (1992). "An experimental study of jet dilution in crossflows." Canadian Journal of Civil Engineering, Vol. 19, No. 5, pp 733-743.

Kline, S. J. (1953). "The purposes of uncertainty analysis." ASME Journal of Fluid Engineering, Vol.107, pp 153-160.

Kline, S. J. and McClintock, F. A. (1953). "Describing uncertainties in single-sample experiments." Mechanical Engineering, Vol.75, pp 3-8.

Langat, J (1994). Dilution of circular wall jet in crossflow. M.Sc., thesis submitted to the University of Alberta, Department of Civil Engineering, Edmonton , Alberta, Canada.

Patrick, M. A. (1967). "Mixing and penetration of a round turbulent jet injected perpendicularly into a transverse stream." Transaction, Institute of Chemical Engineers, Vol. 45, pp T16-T31.

Policastro, A. J and Tokar, J. V. (1972). "Heated effluent dispersion in large lakes; State of the art of analytical modeling: Critique of model formulations." Argonne National Lab. Report No ES-11.

Rajaratnam, N. (1976). Turbulent Jets. Elsevier Publishing Co., The Netherlands, 304p.

Rajaratnam, N. (1984). " Non -Buoyant and Buoyant circular jets in coflowing streams." Journal of Hydraulic Research , IAHAR, Vol. 22, No.2. pp. 117-140.

Rajaratnam, N. (1988). "Turbulent surface jets in stagnant and moving ambients". In Vol. 2 of Civil Engineering Practice Ed. by Cheremisinoff, P. N., Cheremisinoff, N. P and Cheng, S. L., Technomic Publishing Co., Pennsylvania, USA, 629-658.

Rajaratnam, N. , Gangadhariah, T., 1980. " Circular jets in crossflow", Technical report, Dept. of Civil Engineering, University of Alberta, Edmonton, Canada.

Rajaratnam, N. and B.S. Pani.(1974). " Three dimensional turbulent wall jets." Journal of Hydraulic Division, ASCE, Vol. 100, pp 69-83.

Rajaratnam, N. and Humphries, J.A. (1984). " Turbulent non buoyant surface jets." Journal of Hydraulic Research , IAHR, Vol. 22, NO.2, pp. 103-115.

Rajaratnam, N. and Langat, J. K (1995)."Mixing of circular turbulent wall jets in crossflows." Journal of the Hydraulic Engineering, ASCE, Vol. 121,No., 10, pp 694-698.

Wright, S. J. (1977). "Effects of ambient crossflows and density stratification on the characteristic behavior of round turbulent buoyant jets". Report No. KH-R-36, W.M. Keck laboratory of Hydraulics and Water Resources. California Institute of Technology, California, USA, 254 p.

Table 3.1 Details of Experiments of Turbulent Circular Surface Jets in Crossflow

Experiment No.	Diameter d(mm)	Water Level	Jet Velocity Uo (m/s)	Channel Velocity U (m/s)	$\alpha=Uo/U$	Jet Reynolds No. $R=Uod/v$
A1	6.35	just covering nozzle	1.84	0.27	6.8	11684
A2	6.35	//	2.23	0.27	8.25	14160
A3	6.35	//	2.78	0.27	10.3	17652
A4	6.35	//	3.32	0.27	12.3	21081
B1	12.7	//	0.55	0.26	2.1	6985
B2	12.7	//	1.09	0.26	4.2	13843
B3	12.7	//	1.77	0.26	6.8	22479
C1	12.7	(1d) above nozzle	1.77	0.26	6.8	22479
D1	6.35	(3d) above nozzle	3.32	0.27	12.3	21081
E1	6.35	(6d) above nozzle	3.32	0.27	12.3	21081

Table 3.2 Coefficients for the Variation of Surface Jet Centreline in the Vertacl Direction

z(mm)	a	b	r^2
5	9.35	0.35	0.96
10	9.71	0.35	0.90
20	8.00	0.36	0.93
25	10	0.31	0.92
40	9.5	0.32	0.91
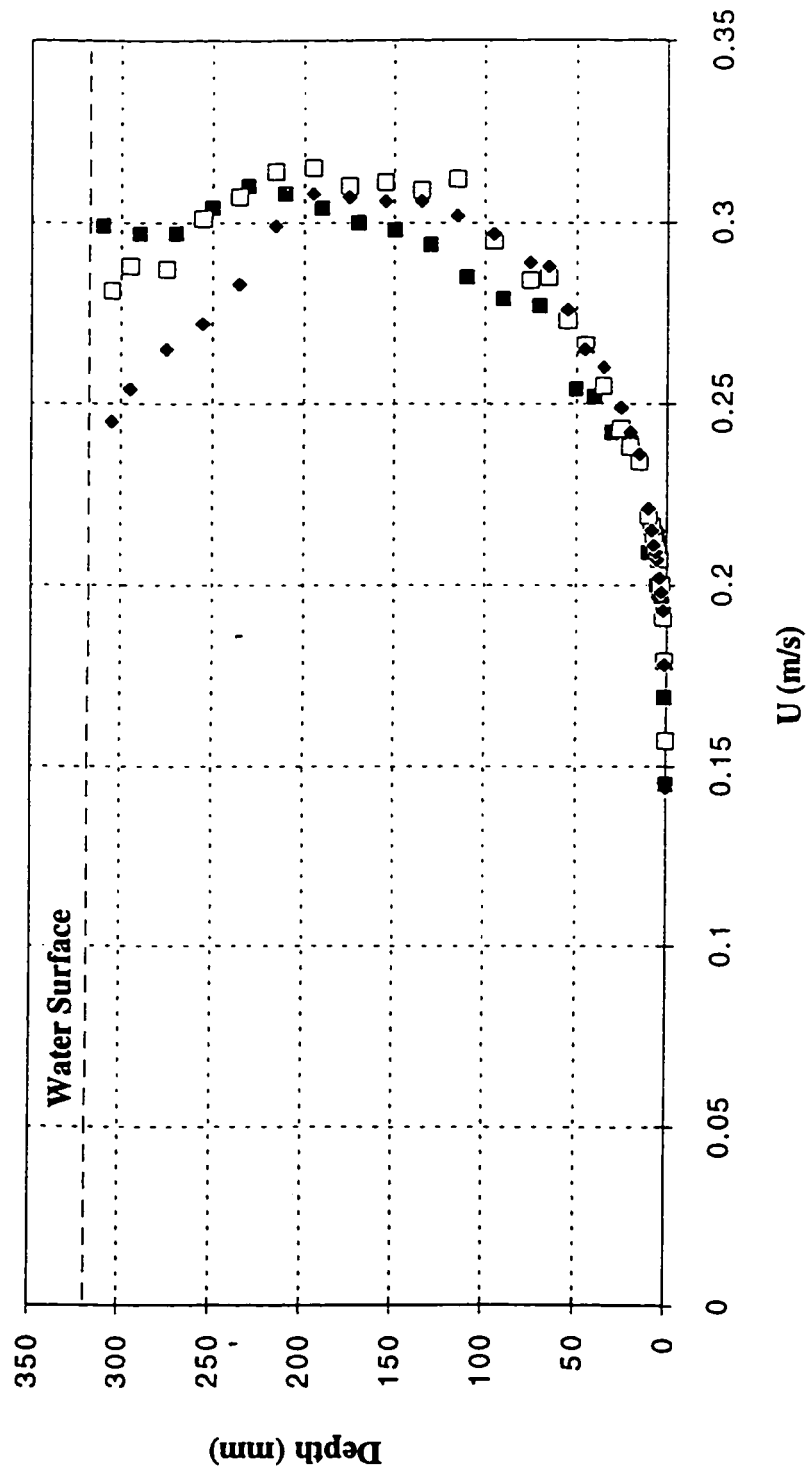
Fig. 3.1a Vertical Velocity Profiles
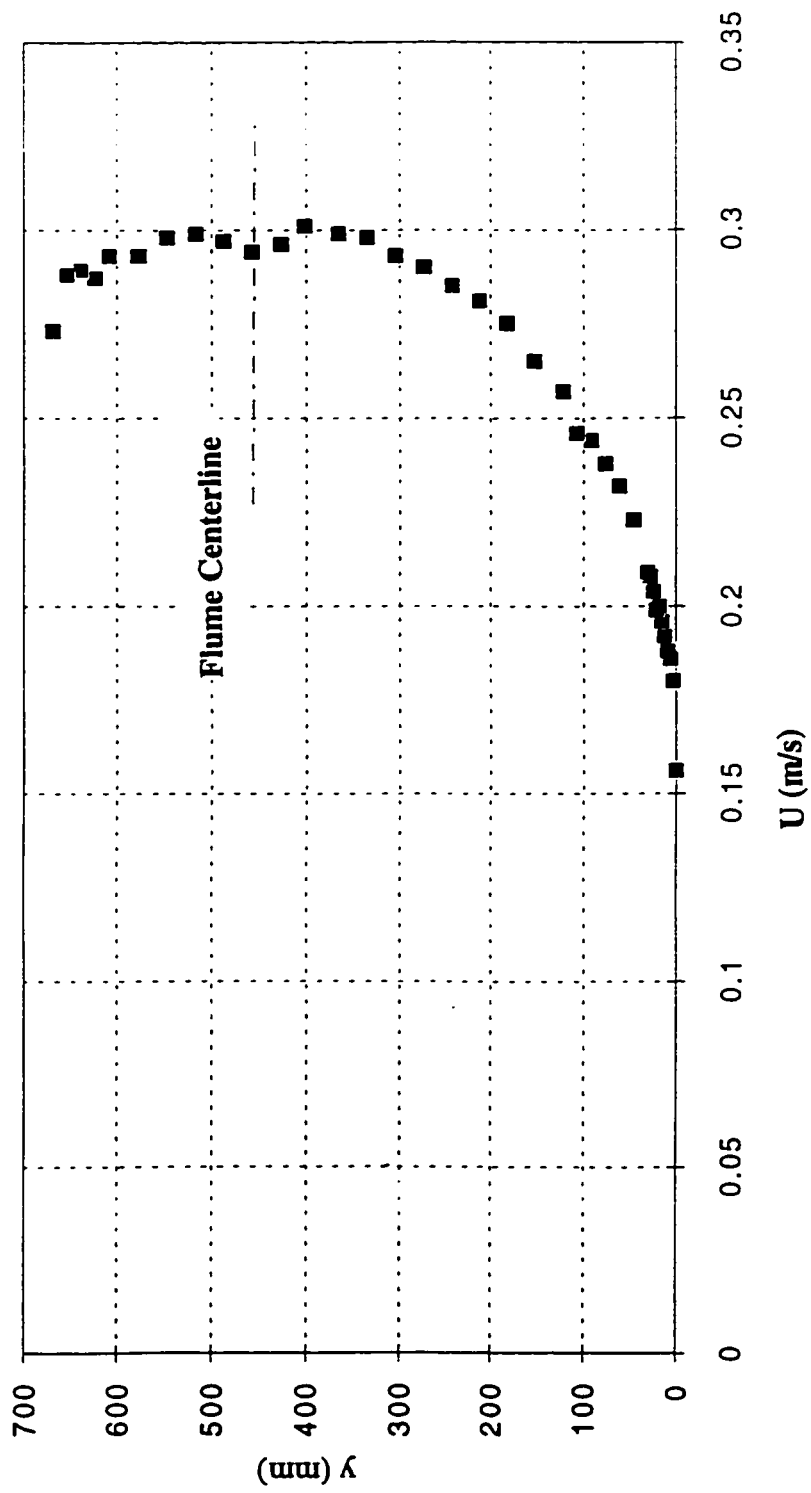
Fig. 3.1b Lateral Surface Velocity Profile
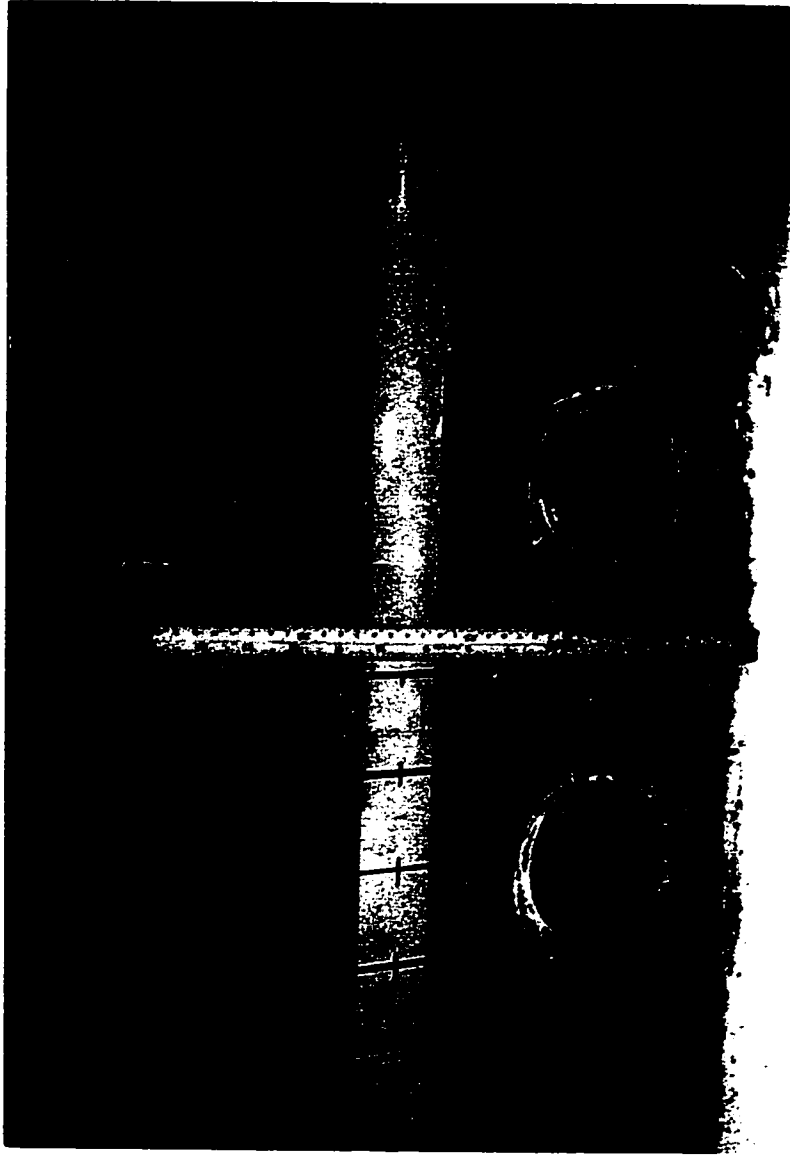
Fig. 3.2 Jet Nozzle on the Sidewall

Fig. 3.3 Fischer Rotameter
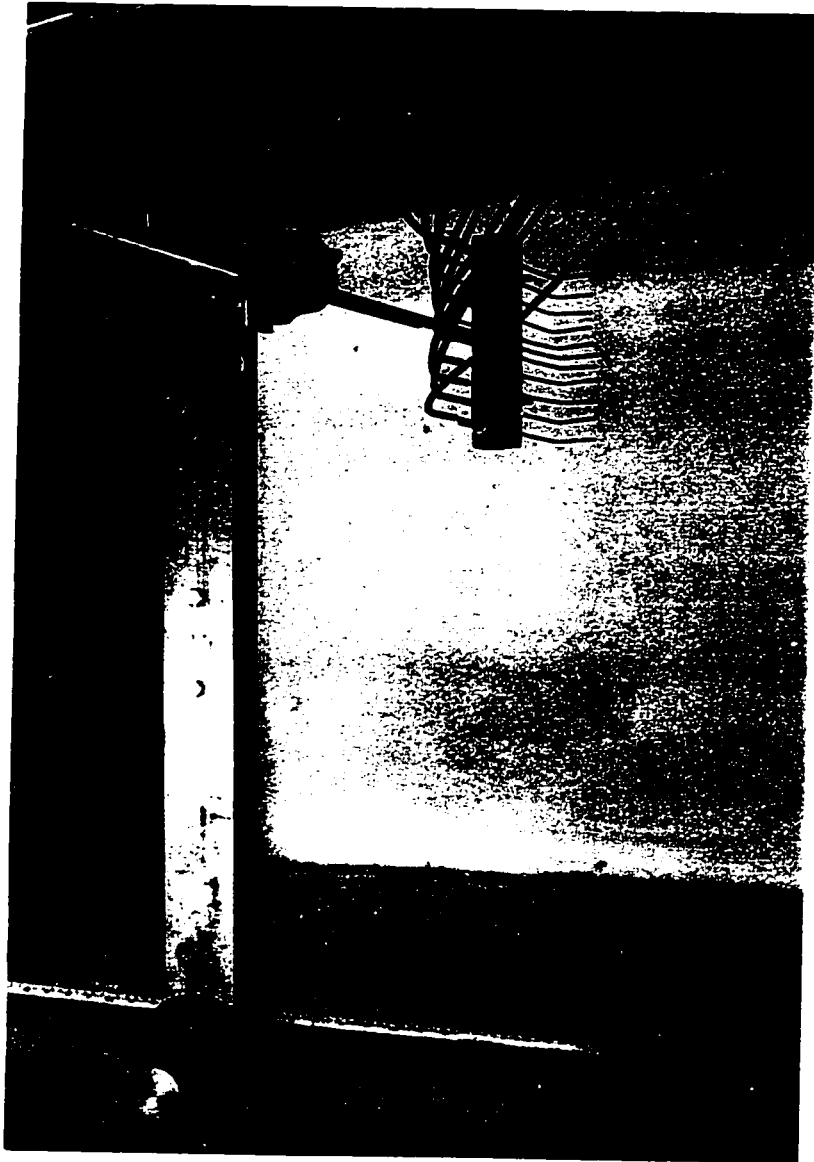
Fig. 3.4 Sampling Rake
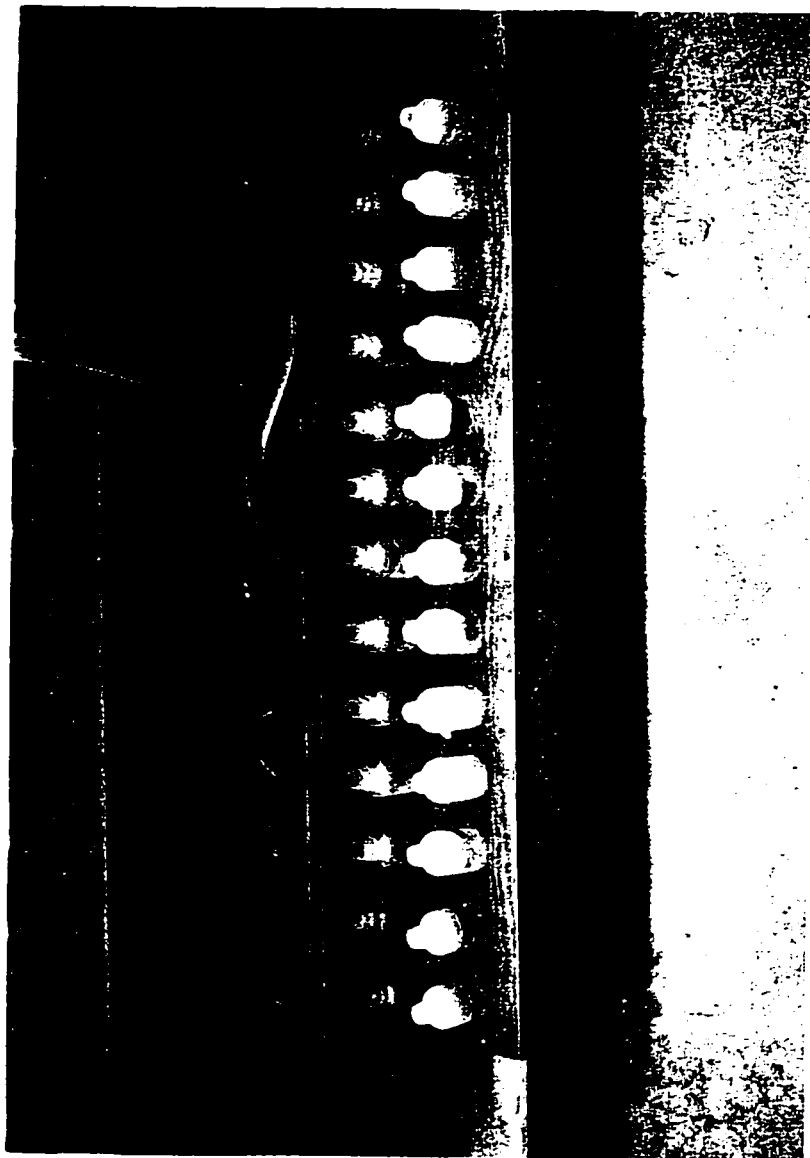
Fig. 3.5 Sampling Rack (showing 60 mL bottles and delivery tubes)
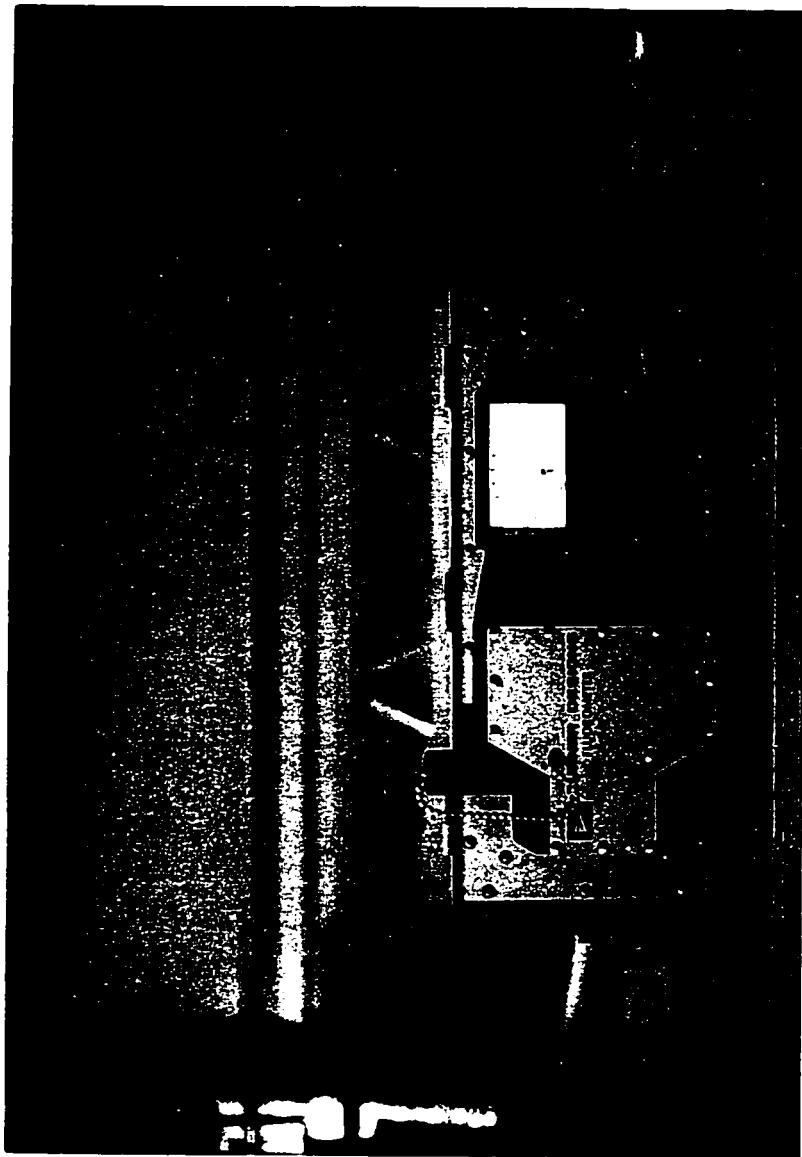
Fig. 3.6 Turner Fluorometer
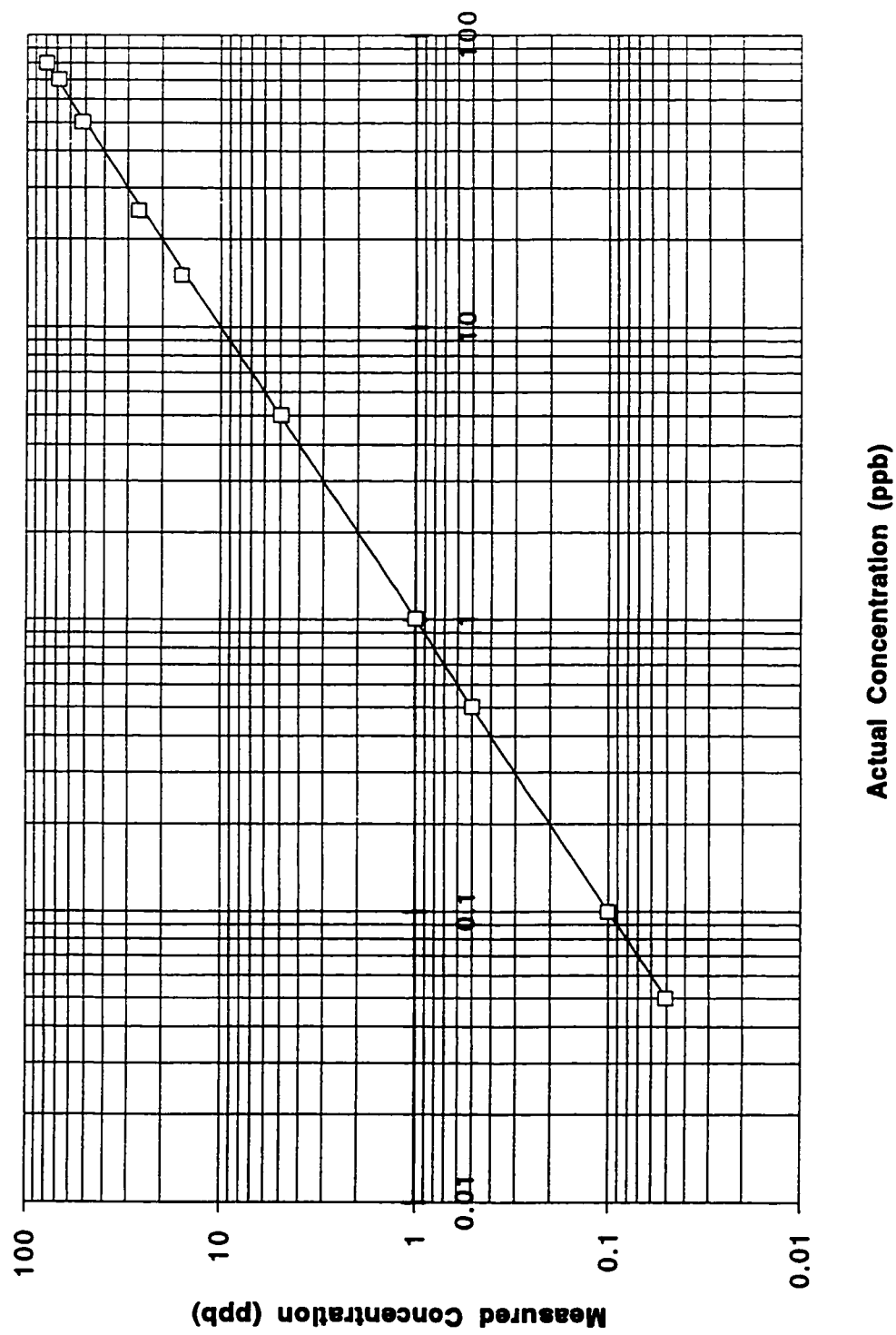
Fig. 3.7 Calibration of the Fluorometer
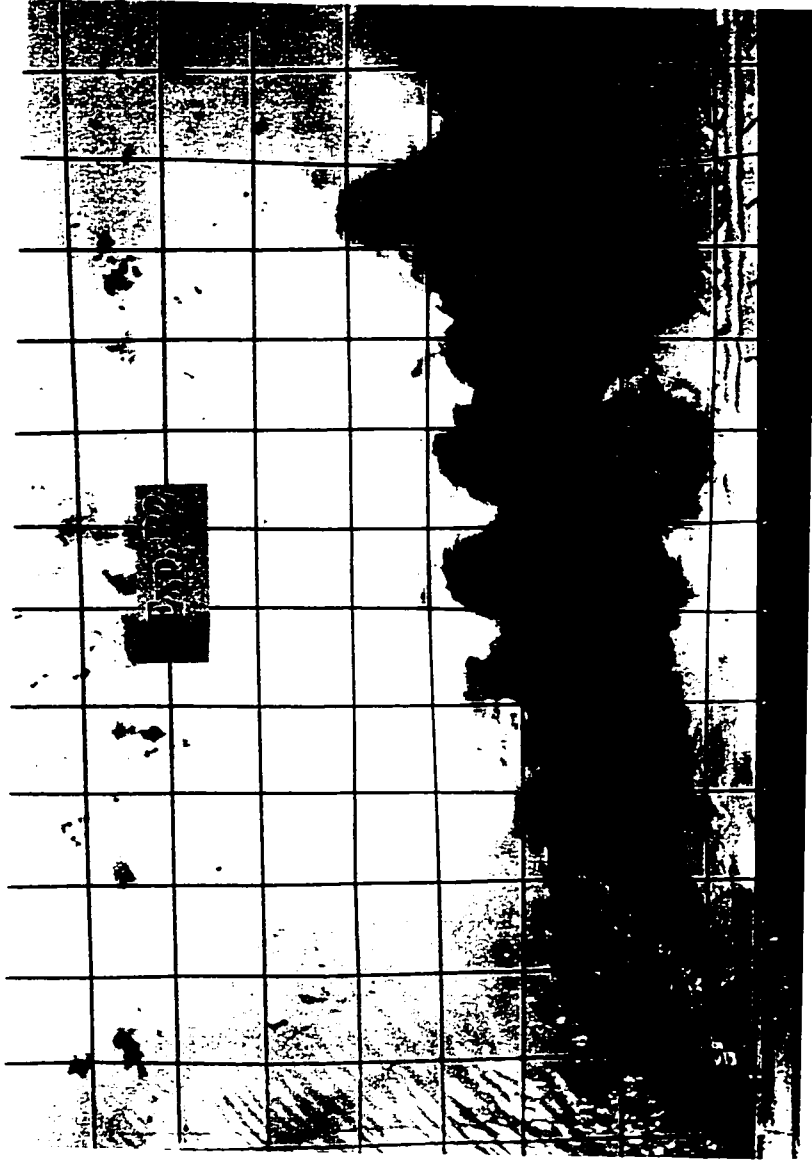
Fig. 3.8a Typical Plan View Photograph for Experiment (B2), Velocity Ratio $(U_0/U) = 4.2$ d=12.7 (grid size=50 mm)

74
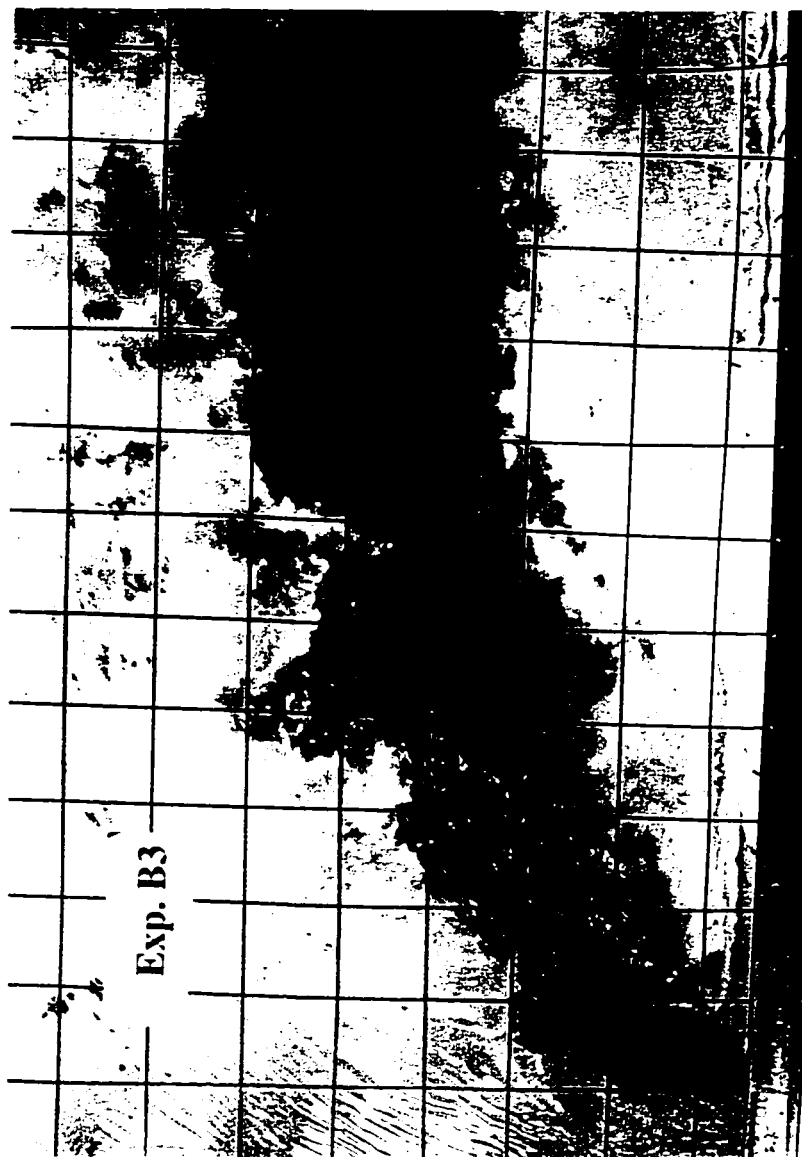
Fig. 3.8b Typical Plan View Photograph for Experiment (B3), Velocity Ratio $(U_0/U) = 6.8$
d=12.7 (grid size = 50 mm)

Exp. B3

Fig. 3.8c Typical Plan View Photograph for Experiment (D1), Velocity Ratio $(U_0/U) = 12.3$
d=6.35 (grid size = 50 mm)
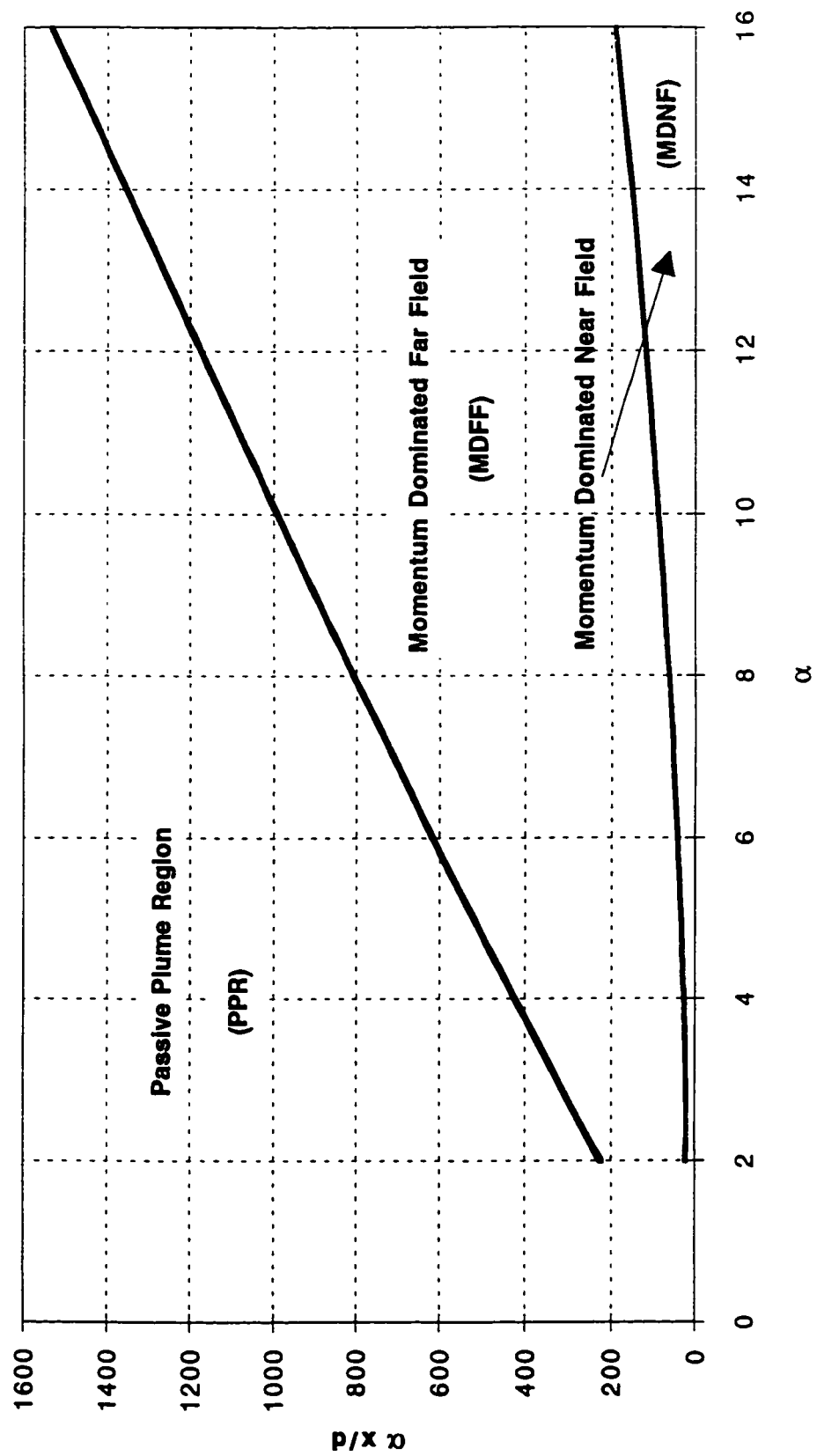
Fig. 3.9 Boundaries of Momentum Dominated Regions for Circular Jets
in Crossflows (adapted from Langat, 1994)
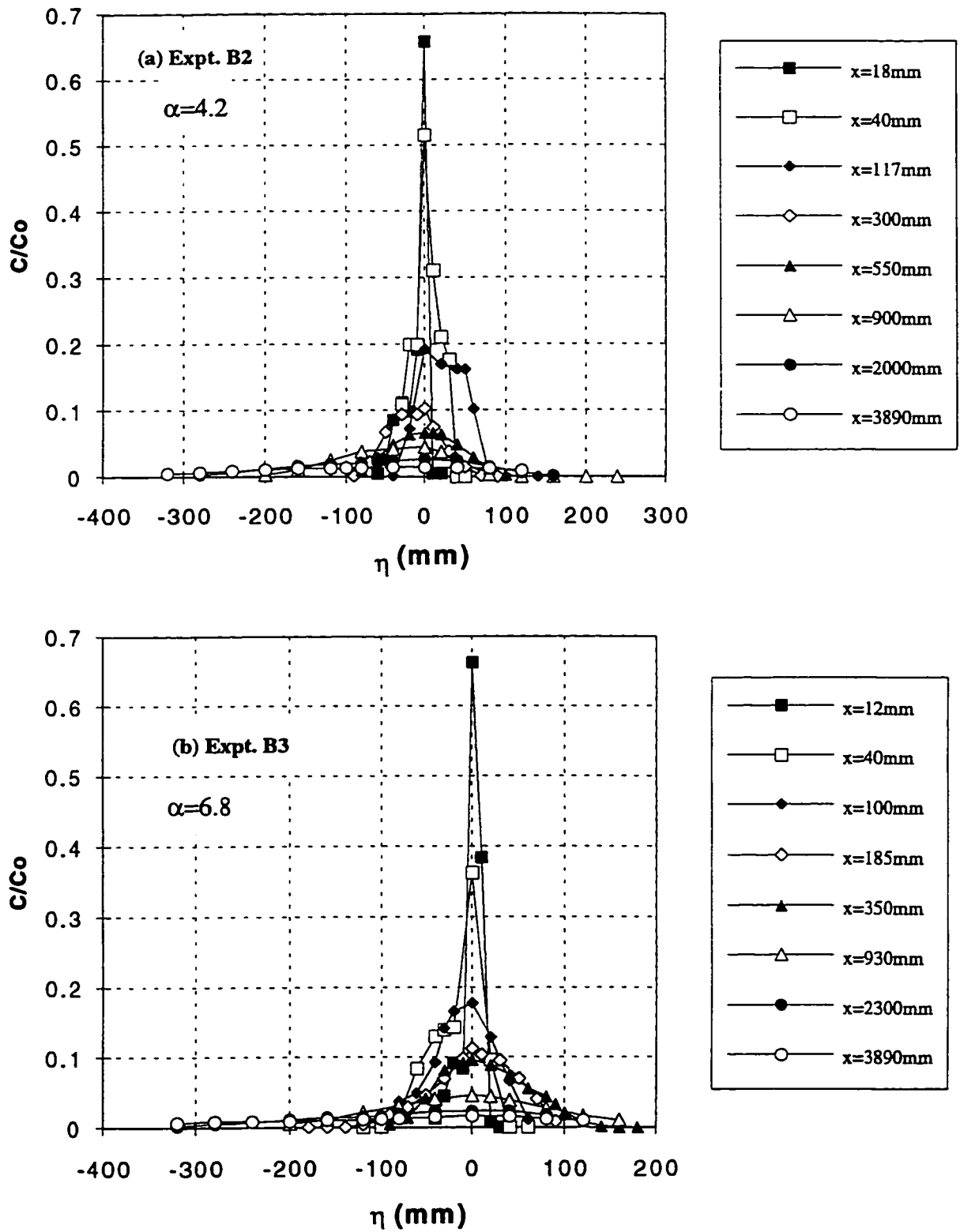
Fig. 3.10 (a-b) Typical Transverse Concentration Profiles near the Water Surface
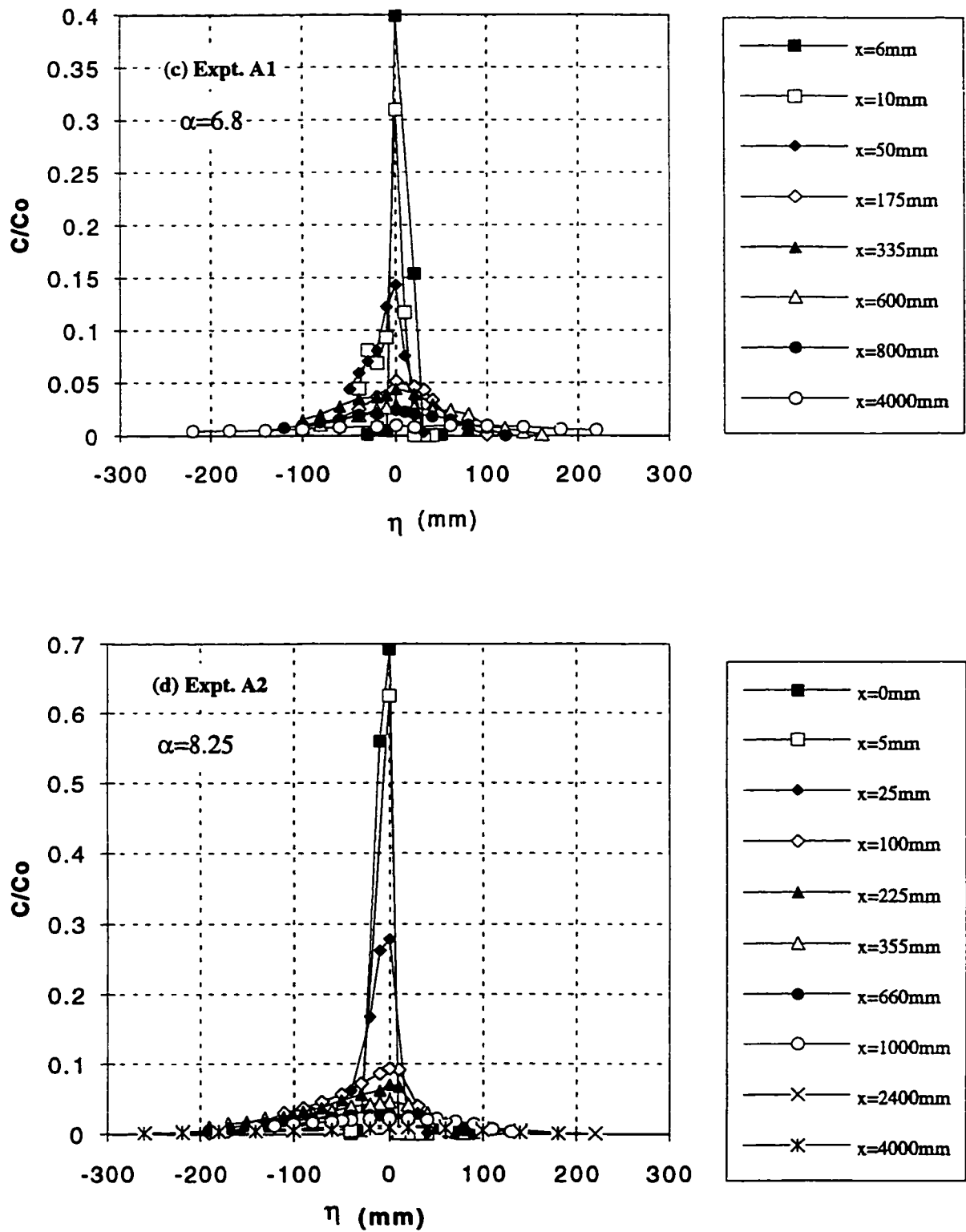
Fig.3.10 (c-d) Typical Transverse Concentration Profiles near the Water Surface
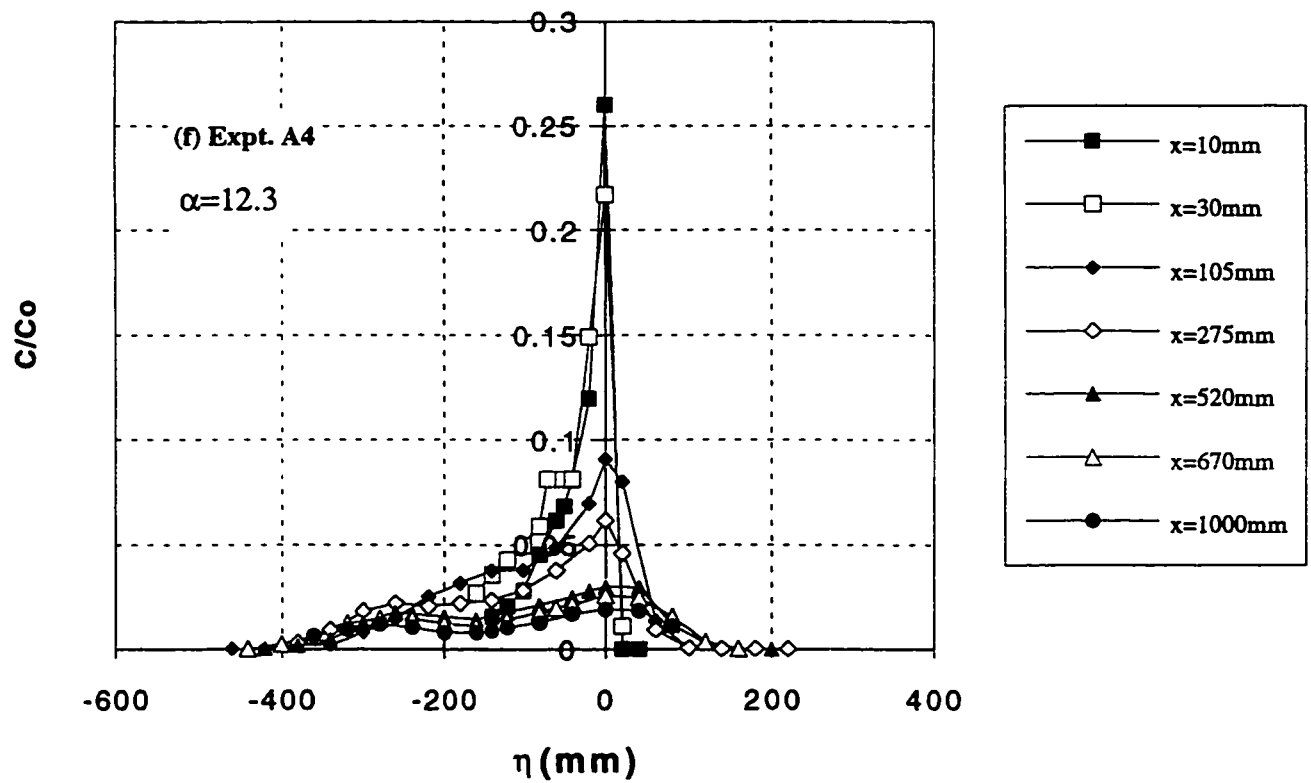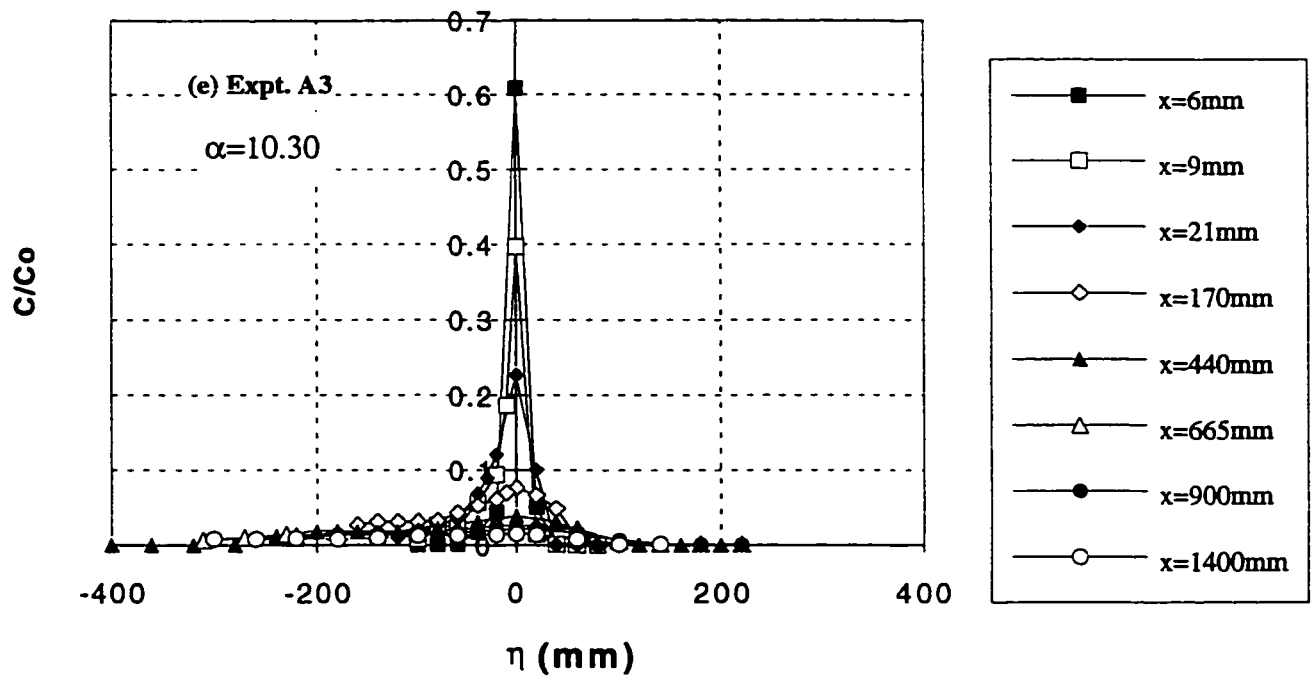
Fig. 3.10 (e-f) Typical Transverse Concentration Profiles near the Water Surface
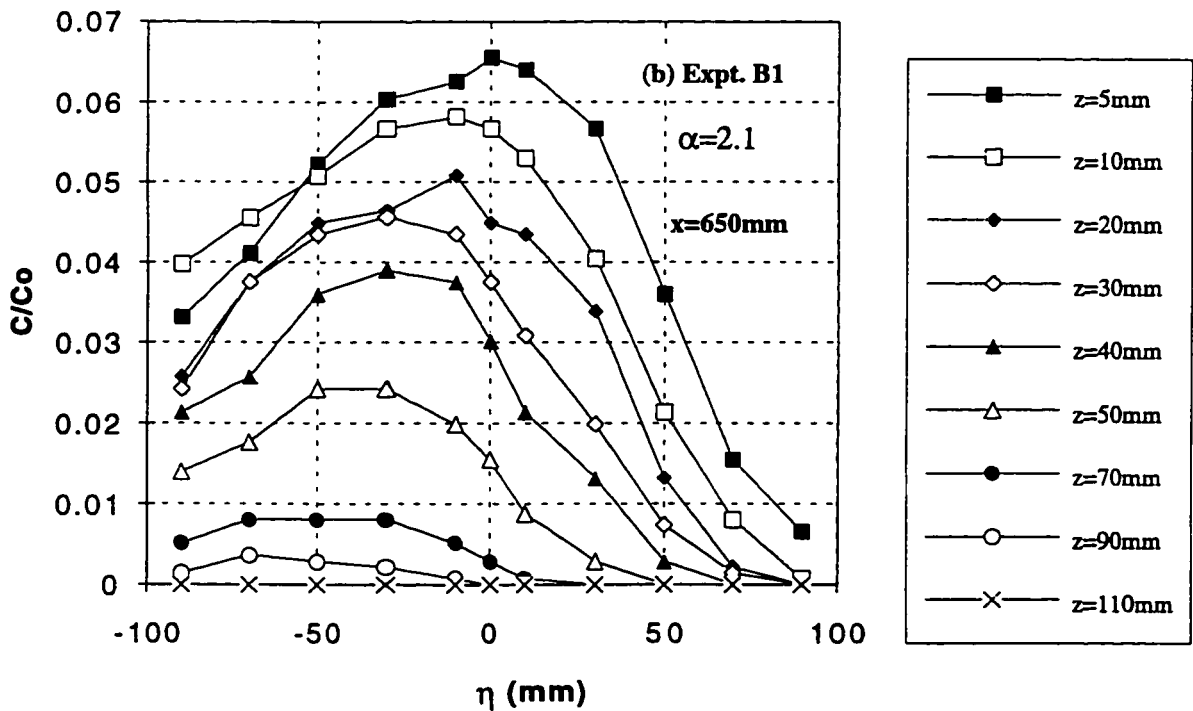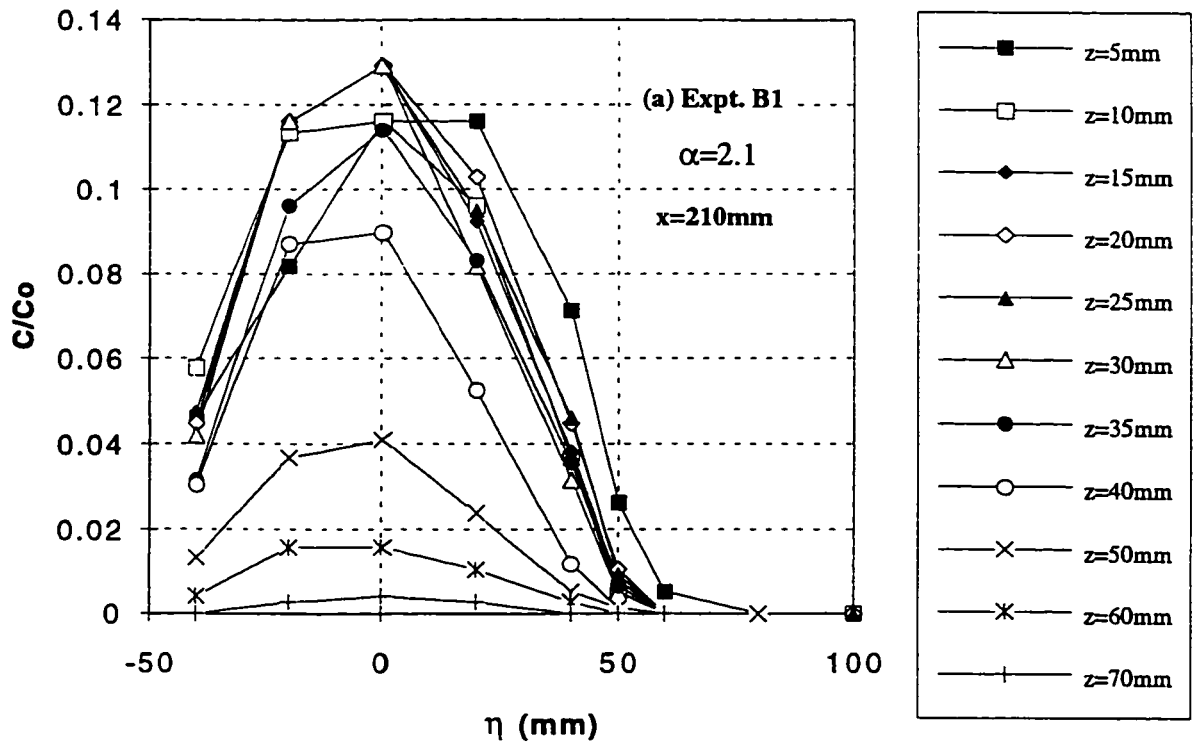
Fig. 3.11 (a-b) Typical Transverse Concentration Profiles at Different Levels for
Expt. B1
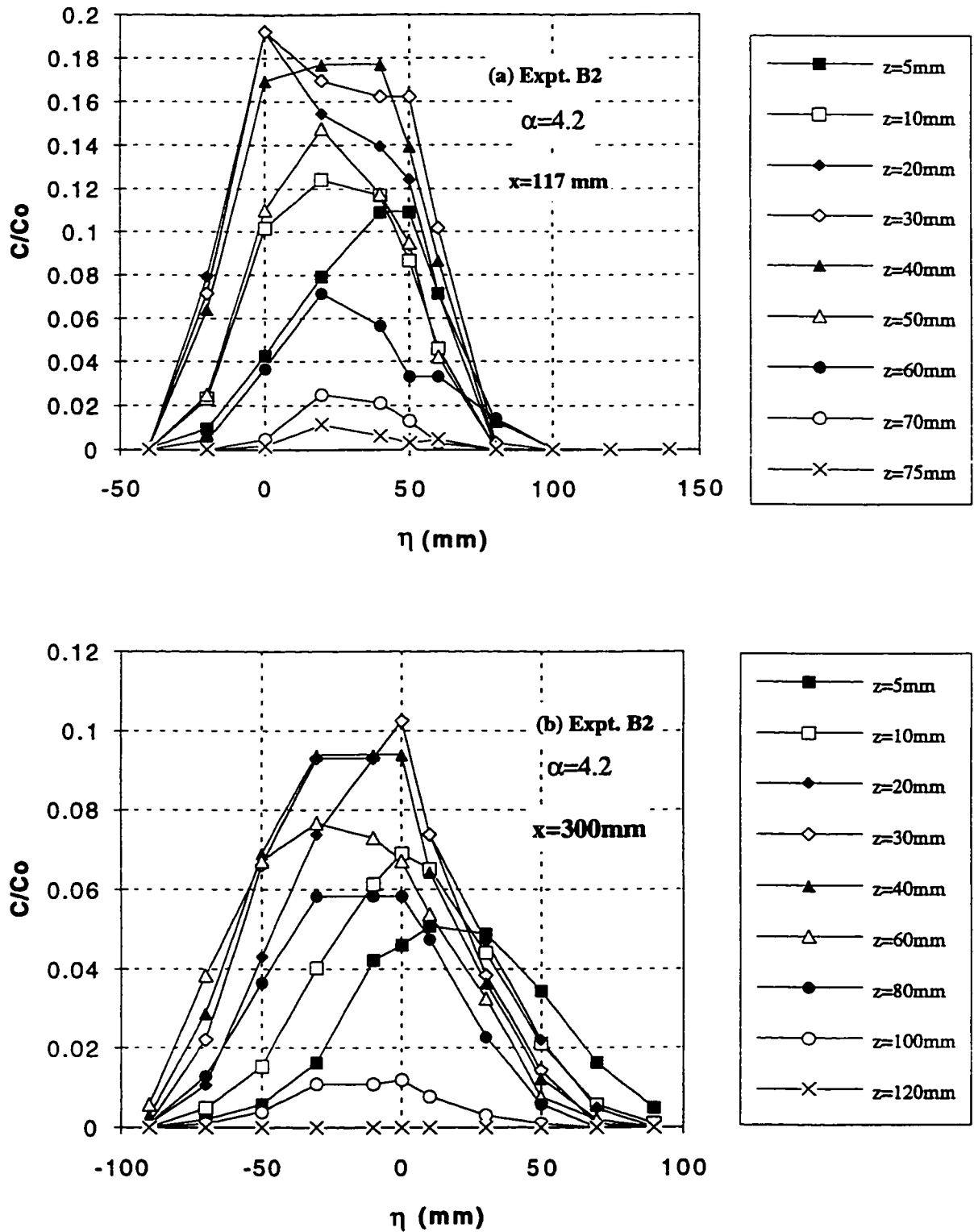
Fig. 3.12 (a-b) Typical Transverse Concentration Profiles at Different Levels for Expt. B2
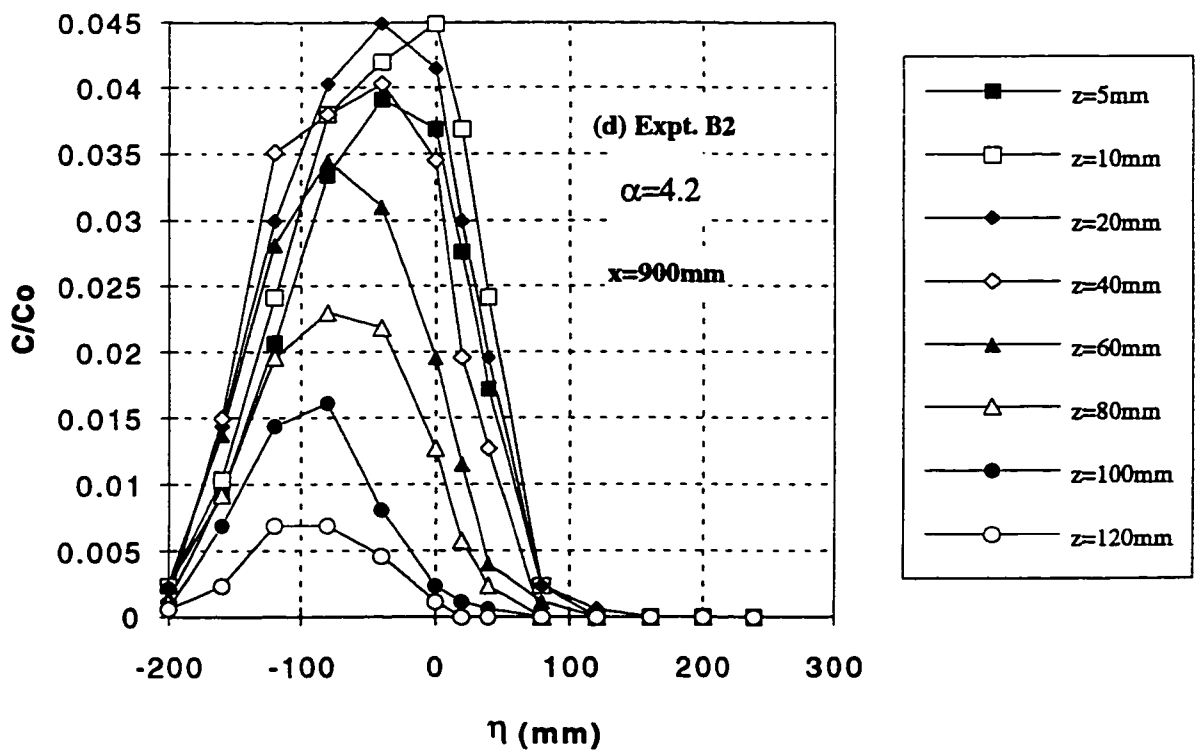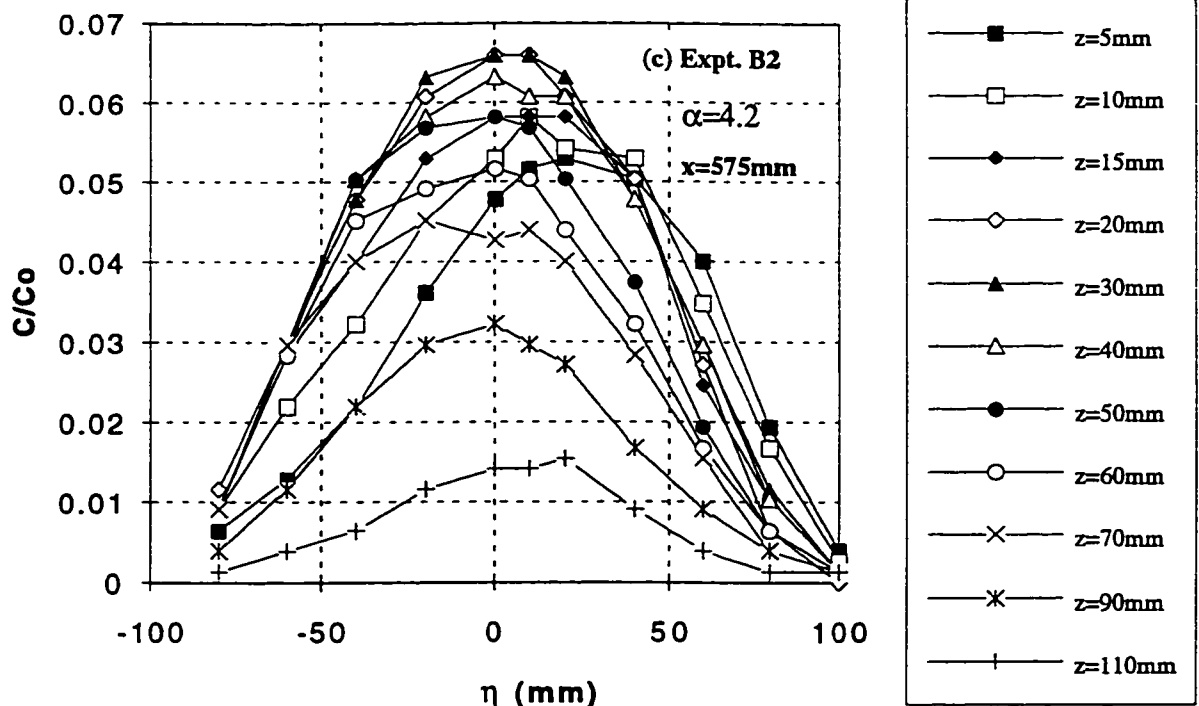
Fig. 3.12 (c-d) Typical Transverse Concentration Profiles at Different Levels for
Expt. B2
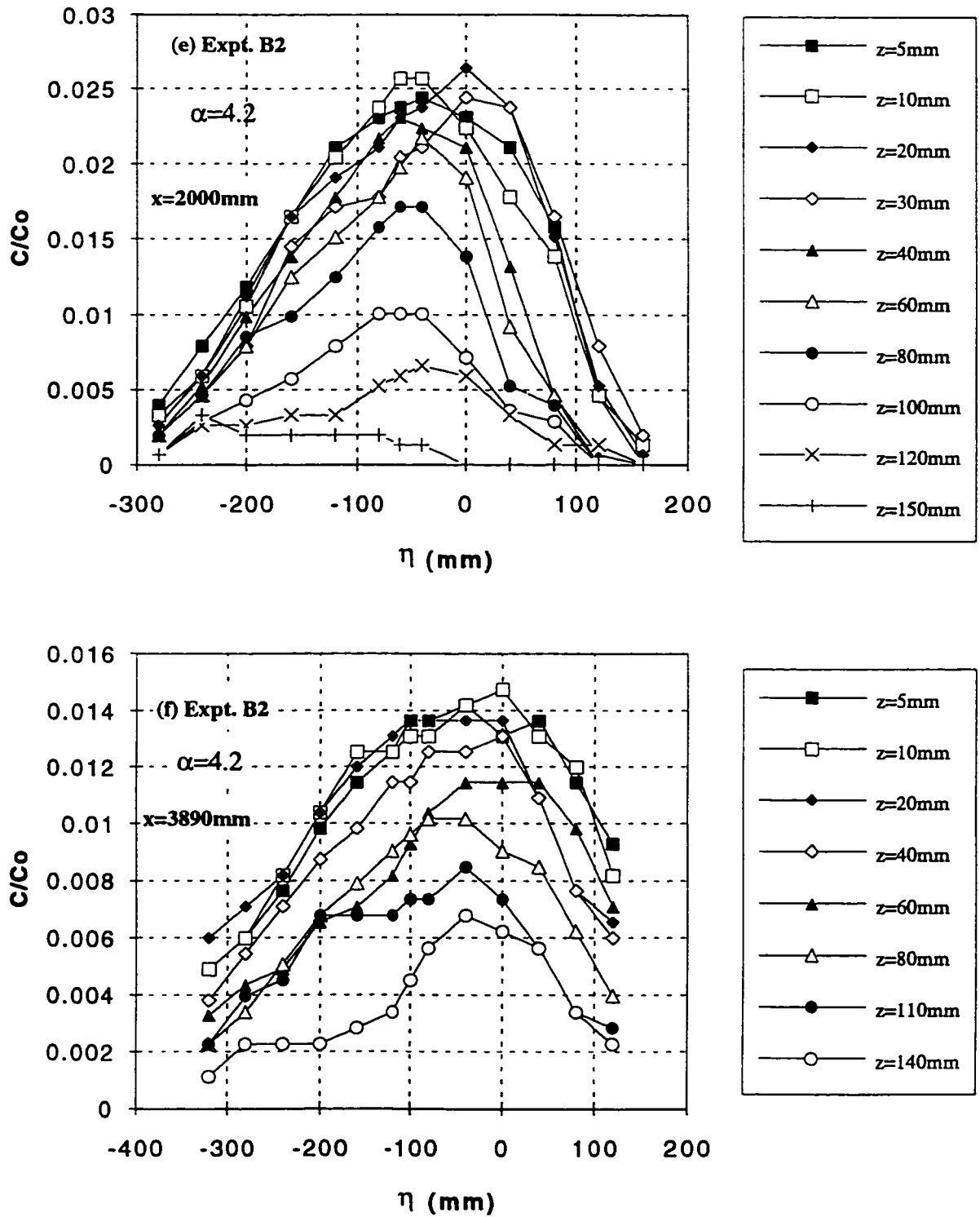
Fig. 3.12 (e-f) Typical Transverse Concentration Profiles at Different Levels for
Expt. B2

84
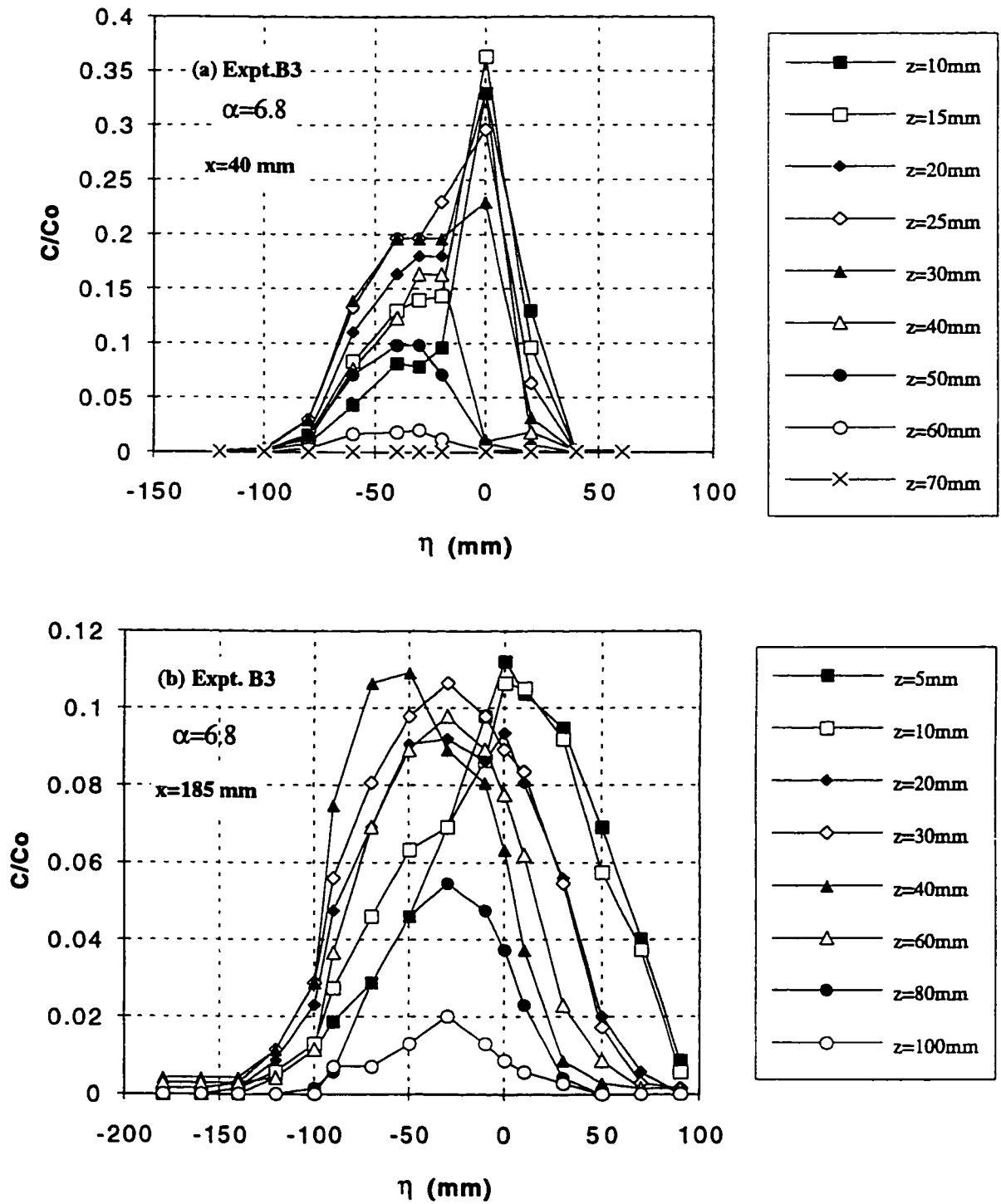
Fig. 3.13 (a-b) Typical Transverse Concentration Profiles at Different Levels for Expt. B3
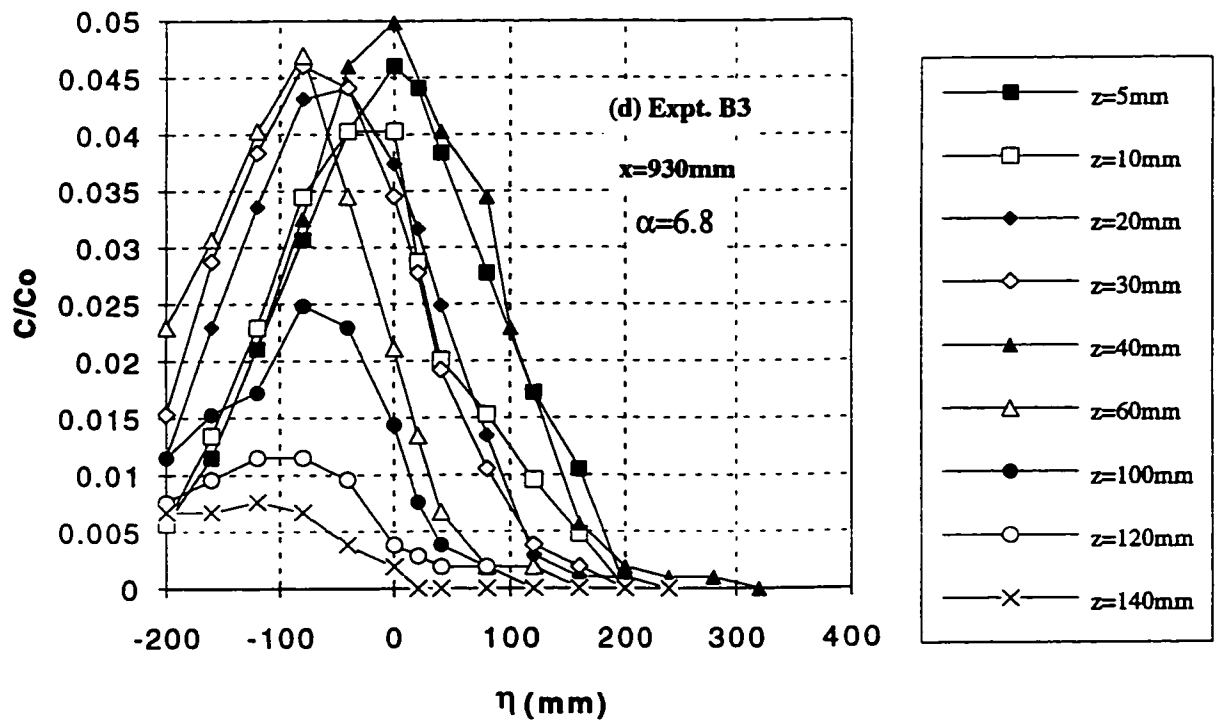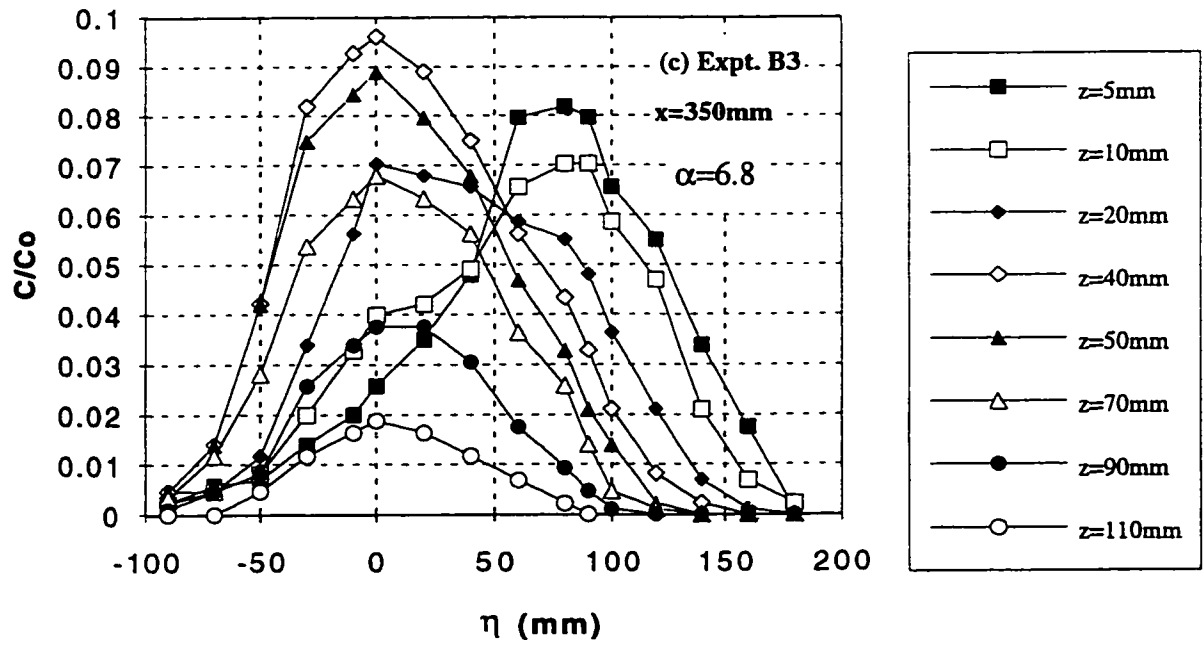
Fig. 3.13 (c-d) Typical Transverse Concentration Profiles at Different Levels for Expt. B3
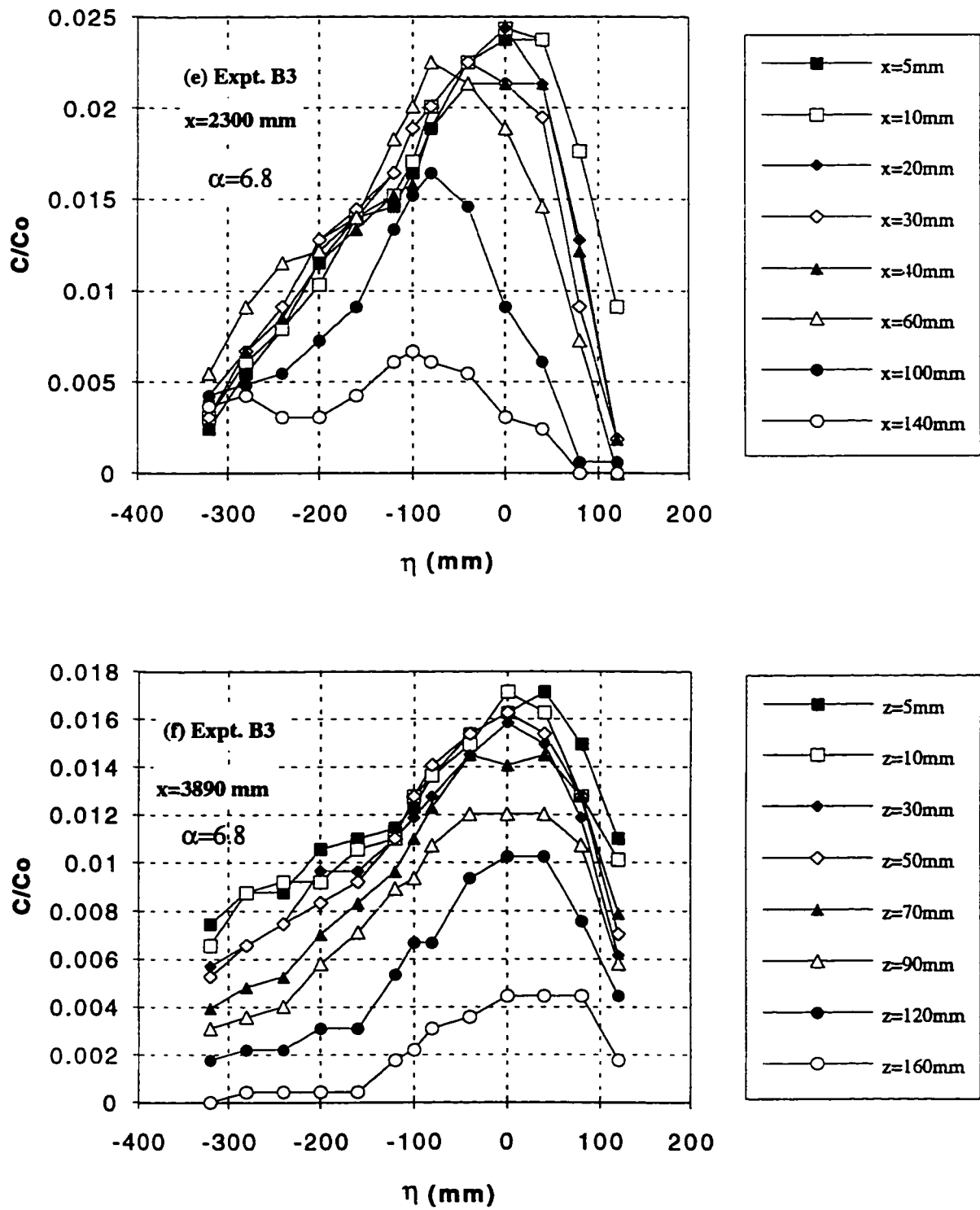
Fig. 3.13 (e-f) Typical Transverse Concentration Profiles at Different Levels for Expt. B3
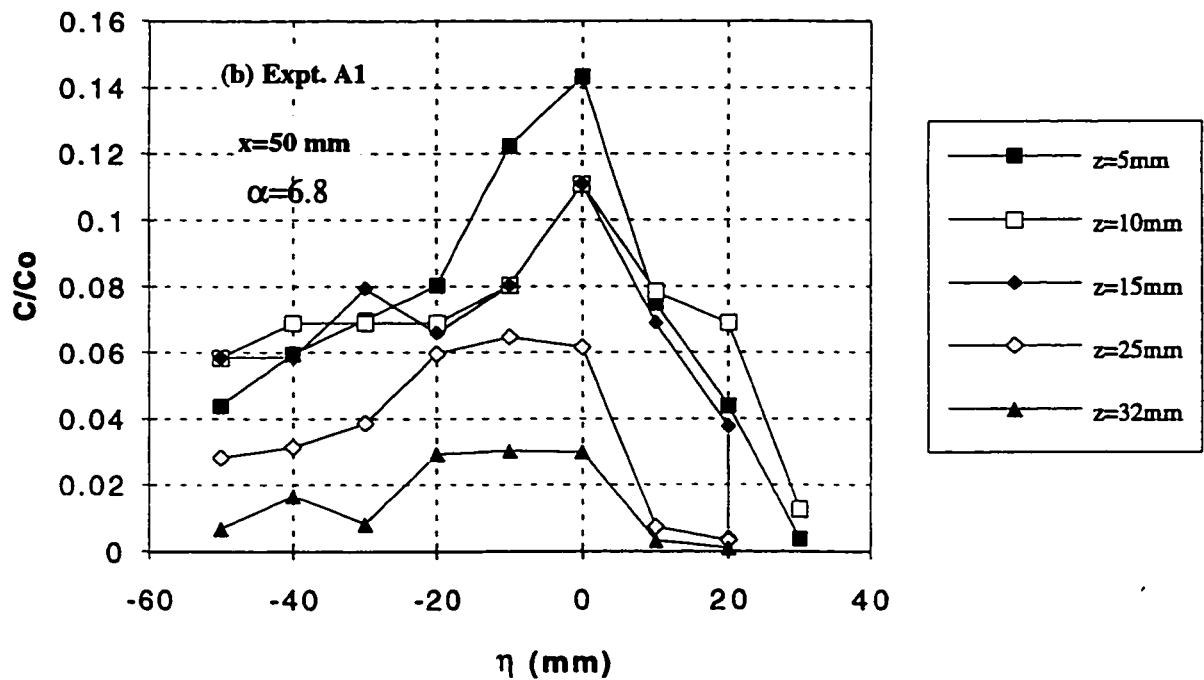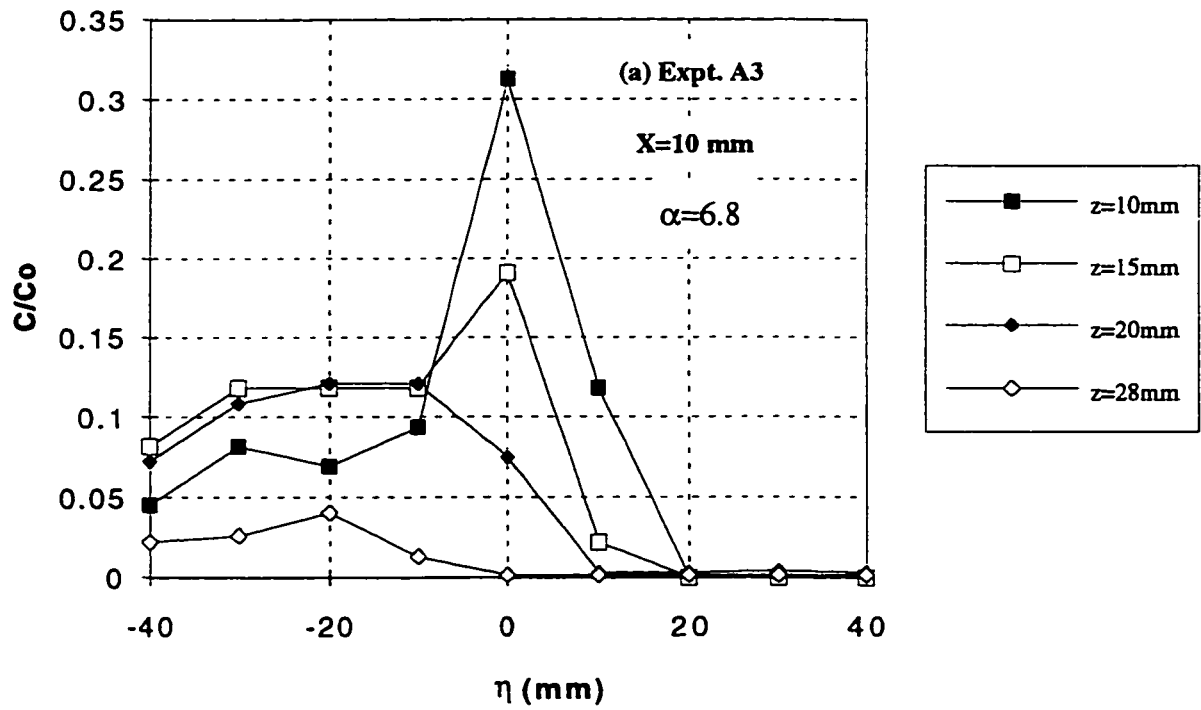
Fig. 3.14 (a-b) Typical Transverse Concentration Profiles at Different Levels for Expt. A1
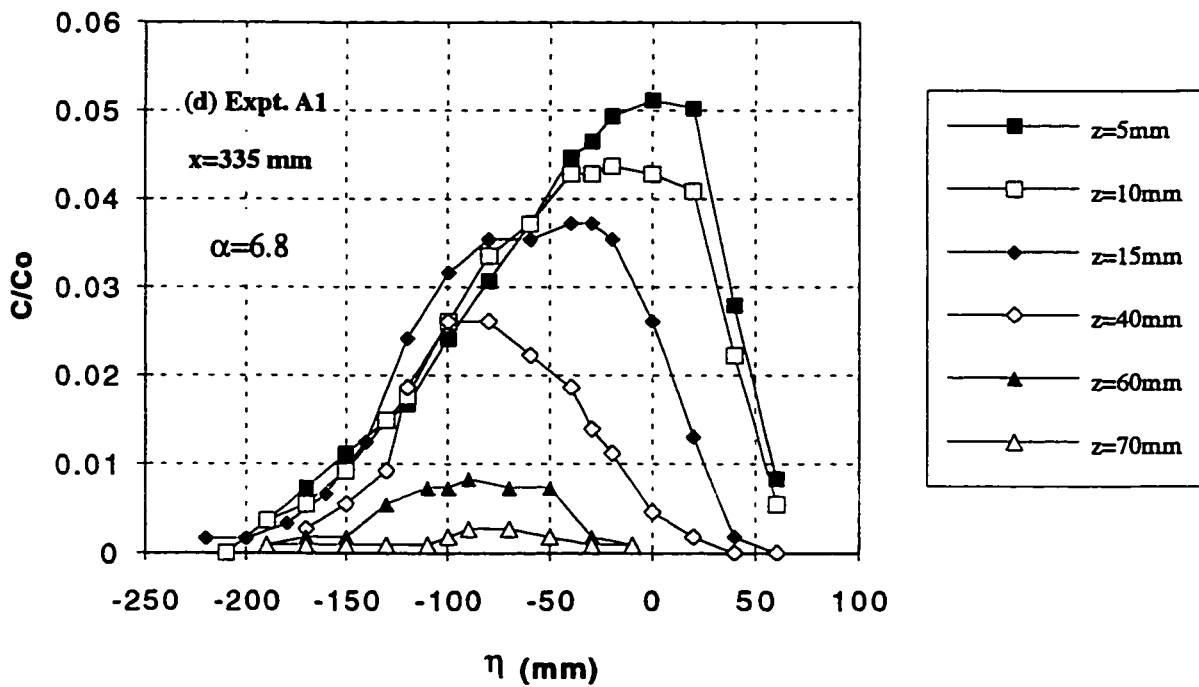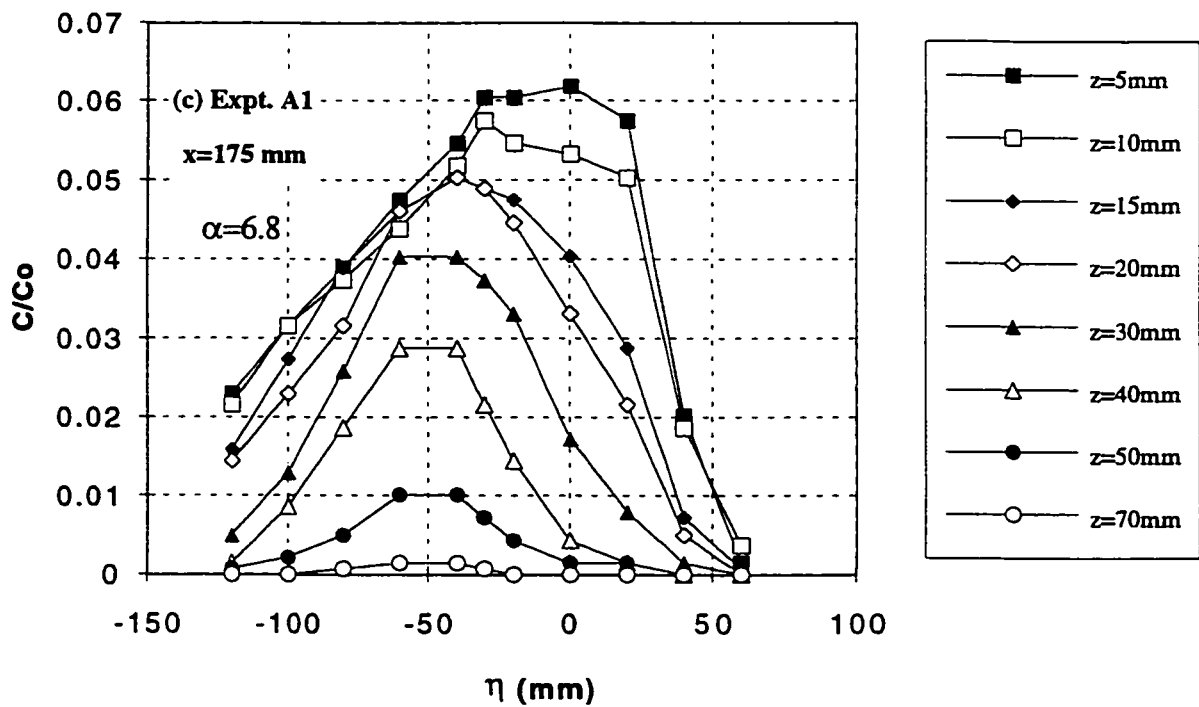
Fig. 3.14 (c-d) Typical Transverse Concentration Profiles at Different Levels for Expt. A1

89
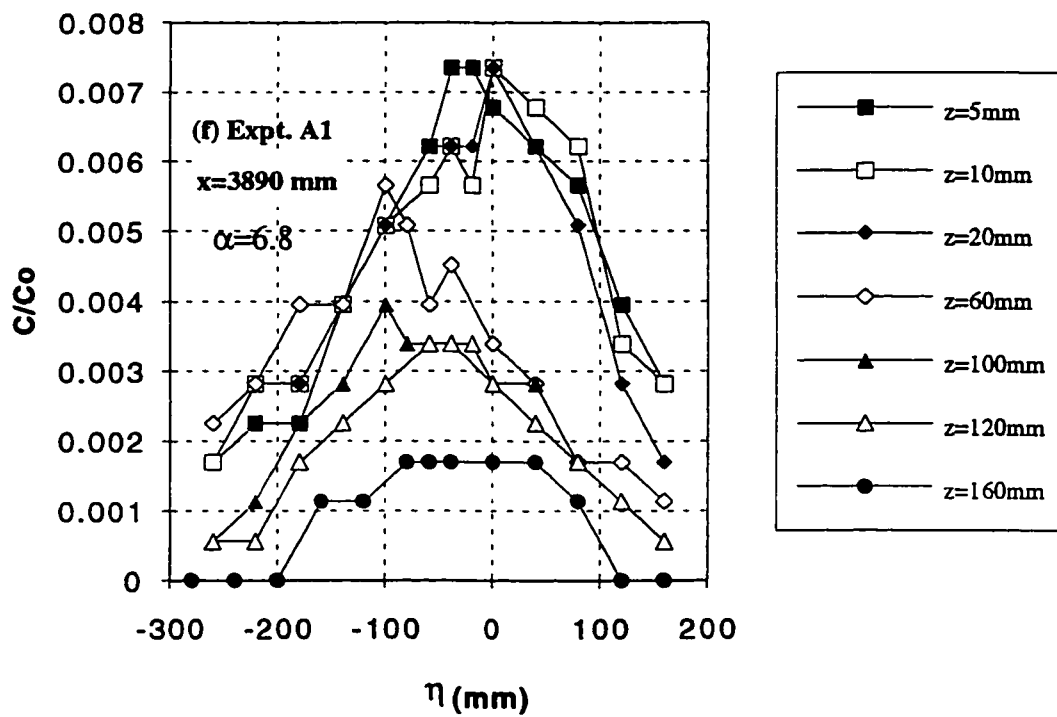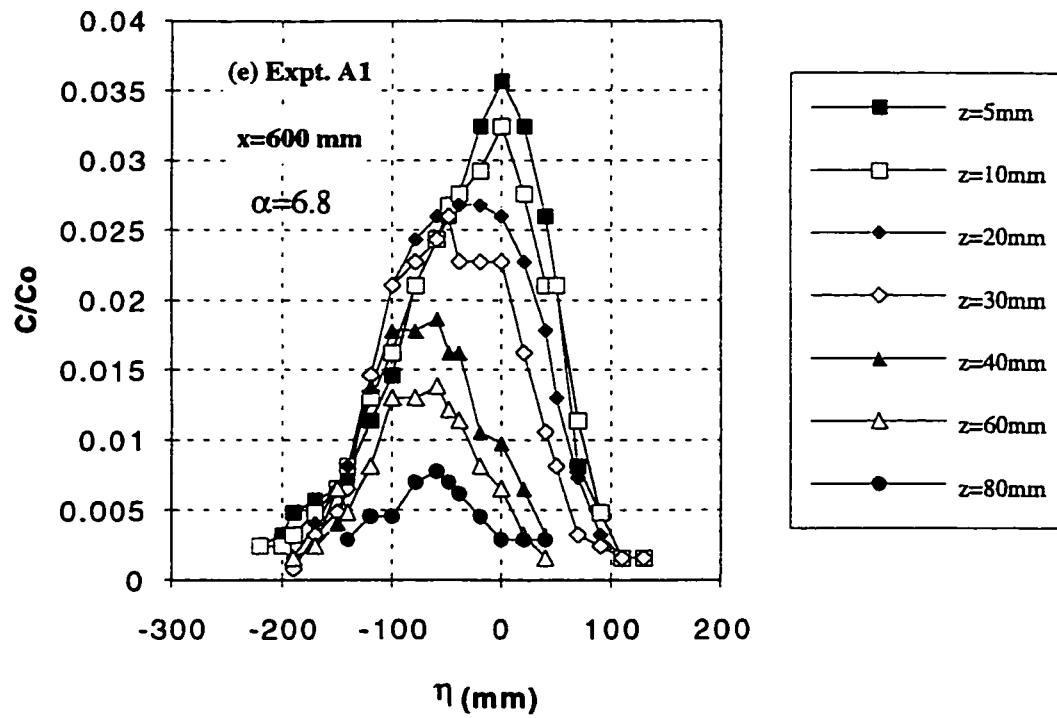
Fig. 3.14 (e-f) Typical Transverse Concentration Profiles at Different Levels for Expt. A1
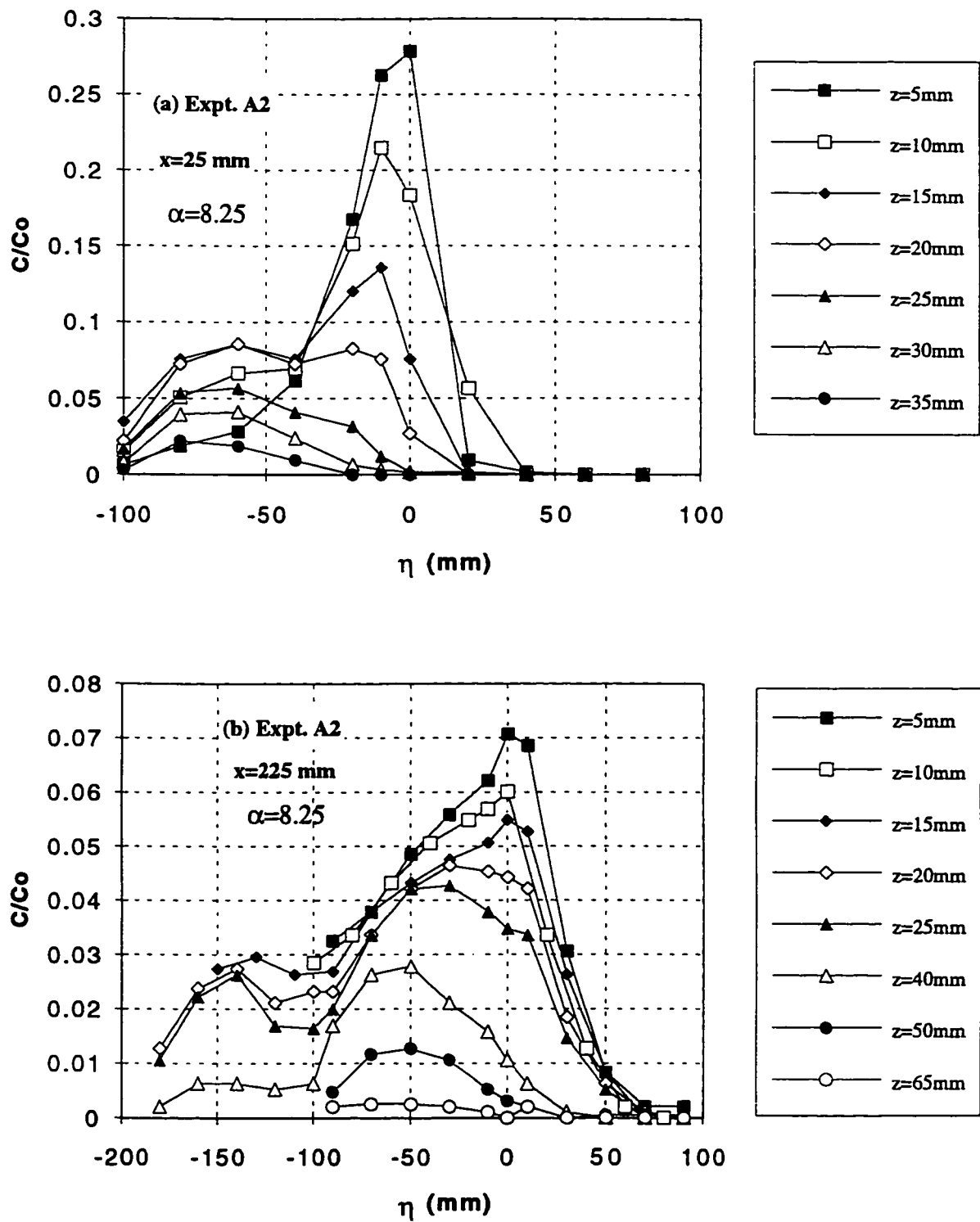
Fig. 3.15 (a-b) Typical Transverse Concentration Profiles at Different Levels for Expt. A2
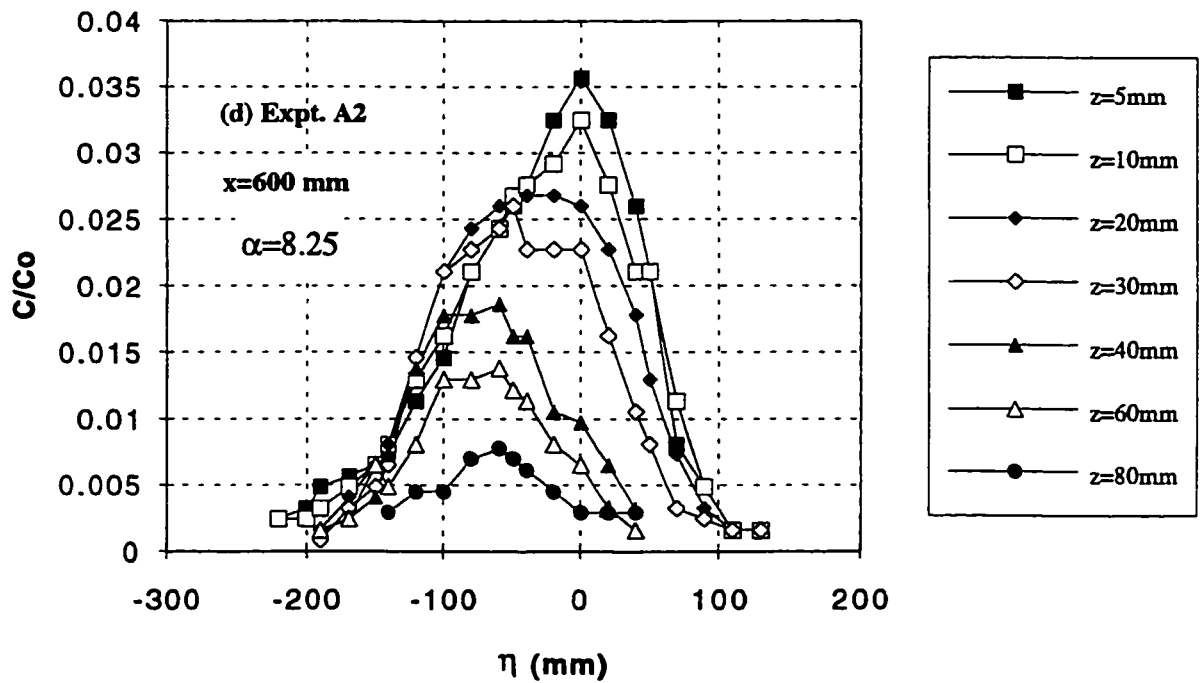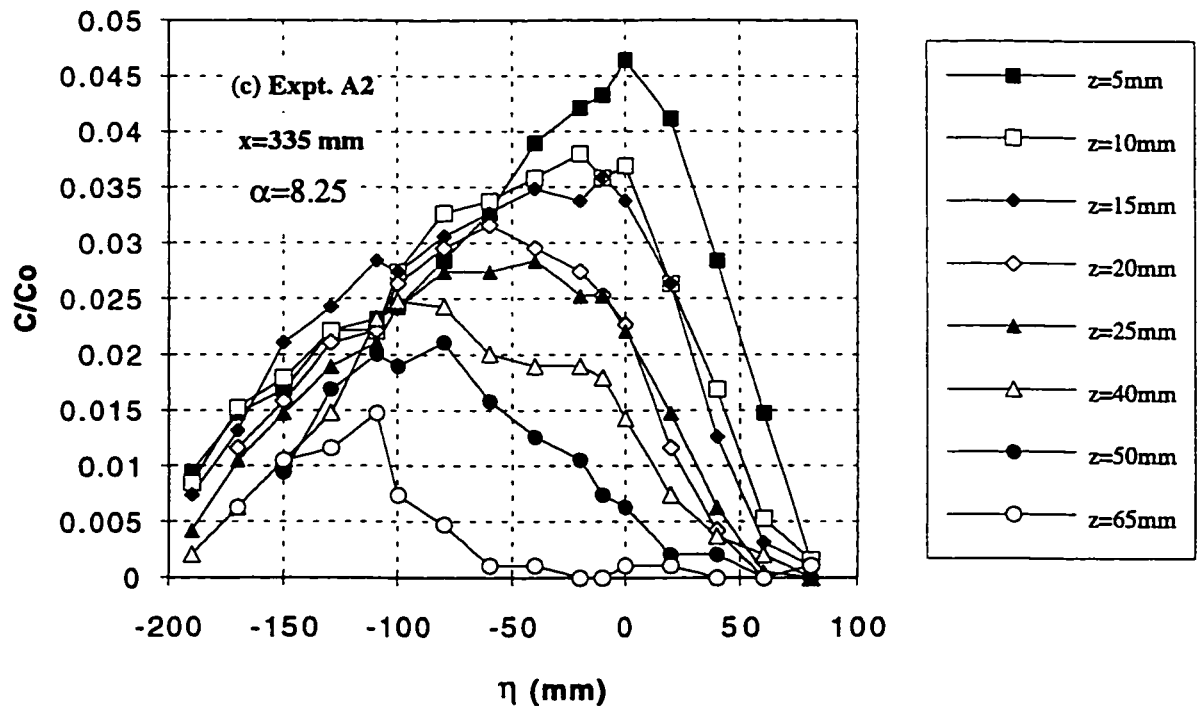
Fig. 3.15 (c-d) Typical Transverse Concentration Profiles at Different Levels for Expt. A2
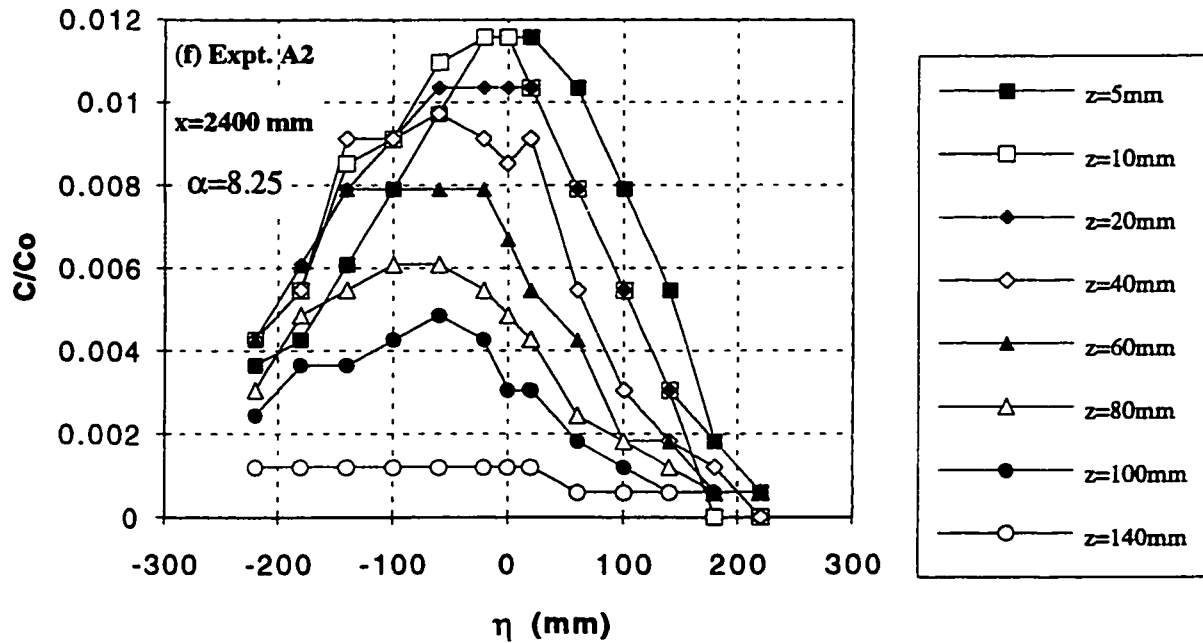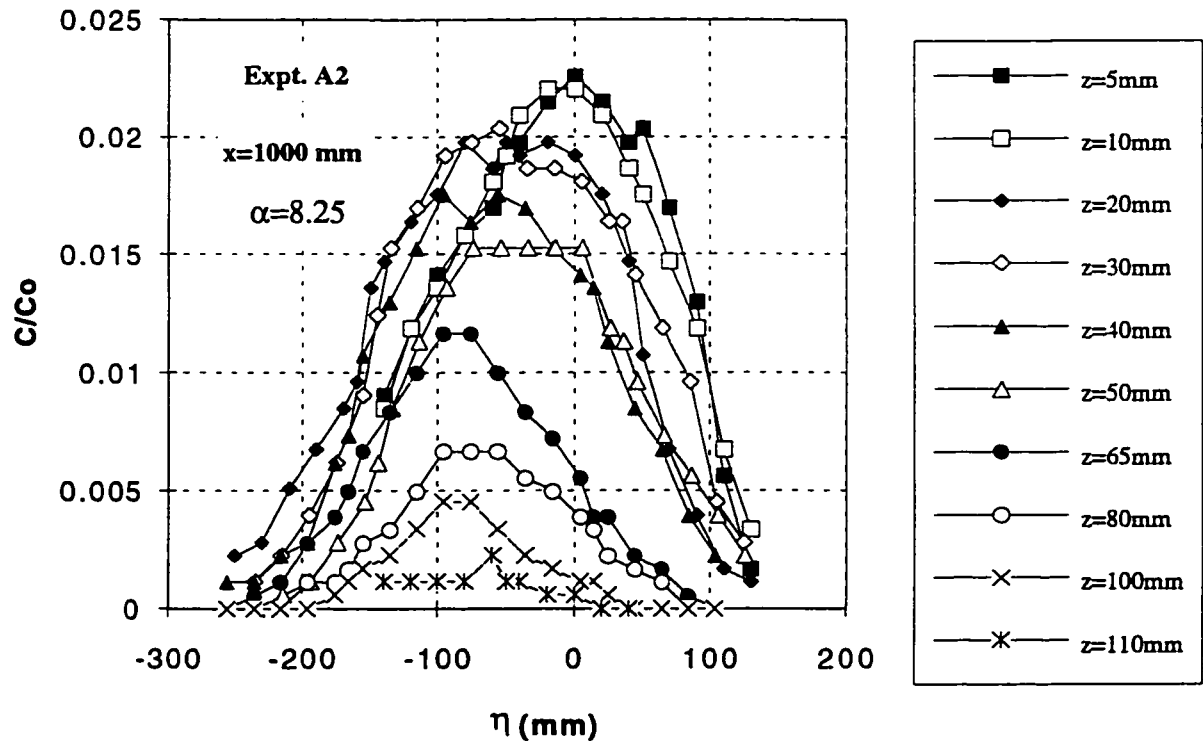
Fig. 3.15 (e-f) Typical Transverse Concentration Profiles at Different Levels for Expt. A2
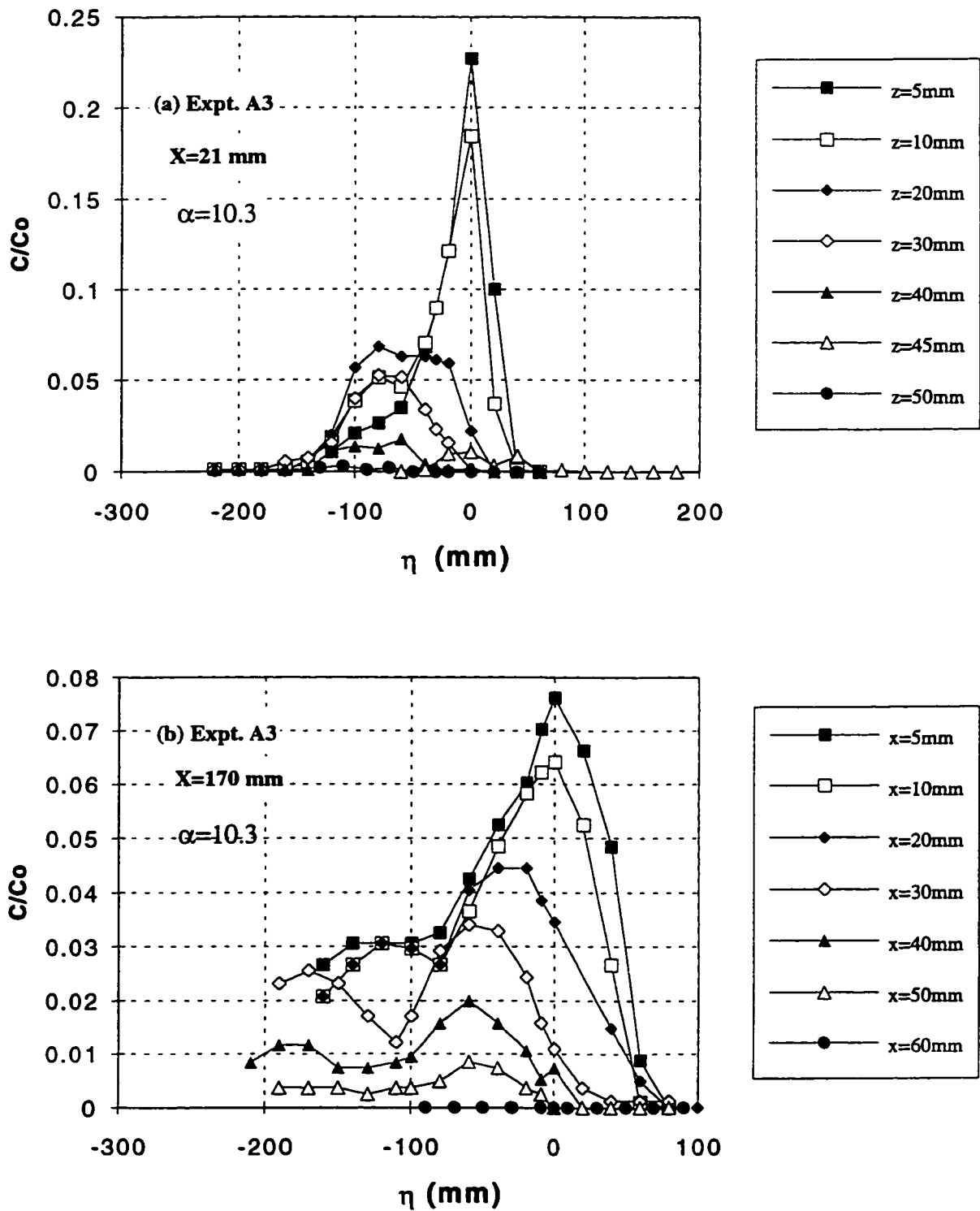
Fig. 3.16 (a-b) Typical Transverse Concentration Profiles at Different Levels for Expt. A3
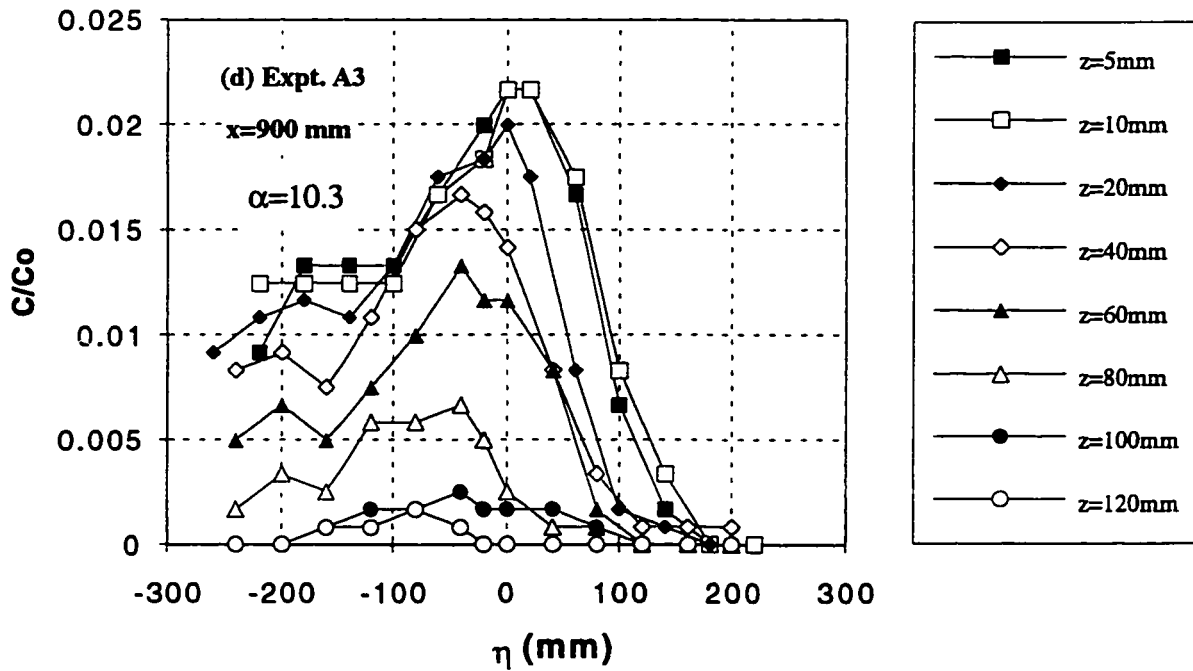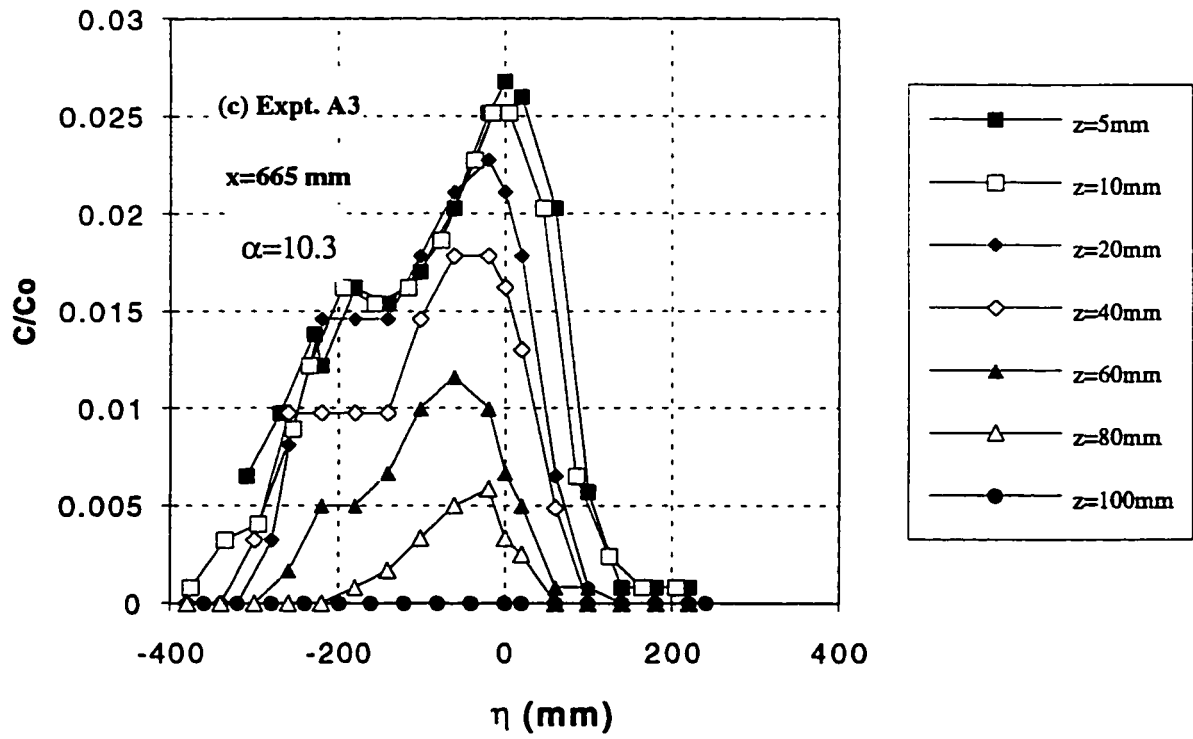
Fig. 3.16 (c-d) Typical Transverse Concentration Profiles at Different Levels for
Expt. A3
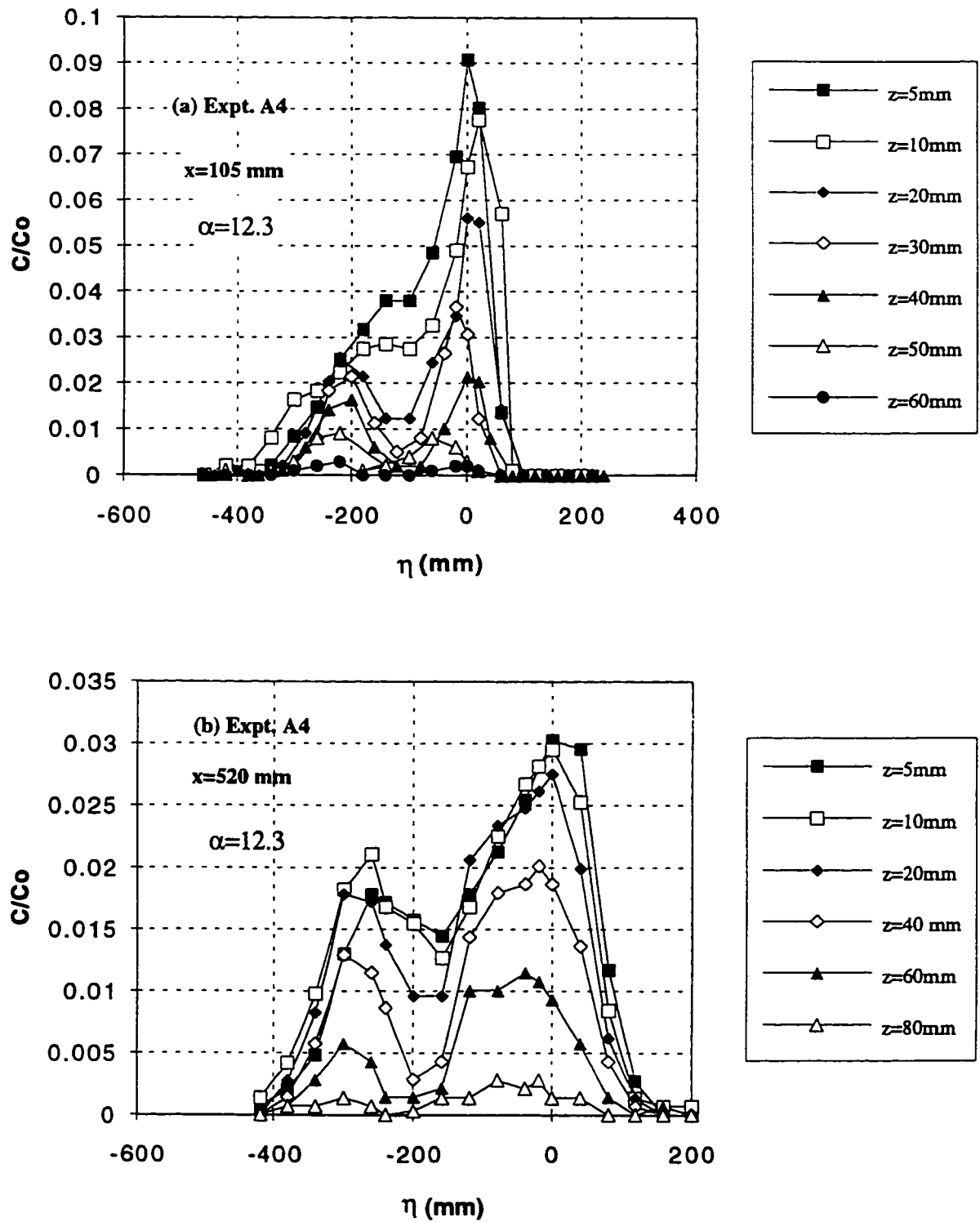
Fig. 3.17 (a-b) Typical Transverse Concentration Profiles at Different Levels for Expt. A4
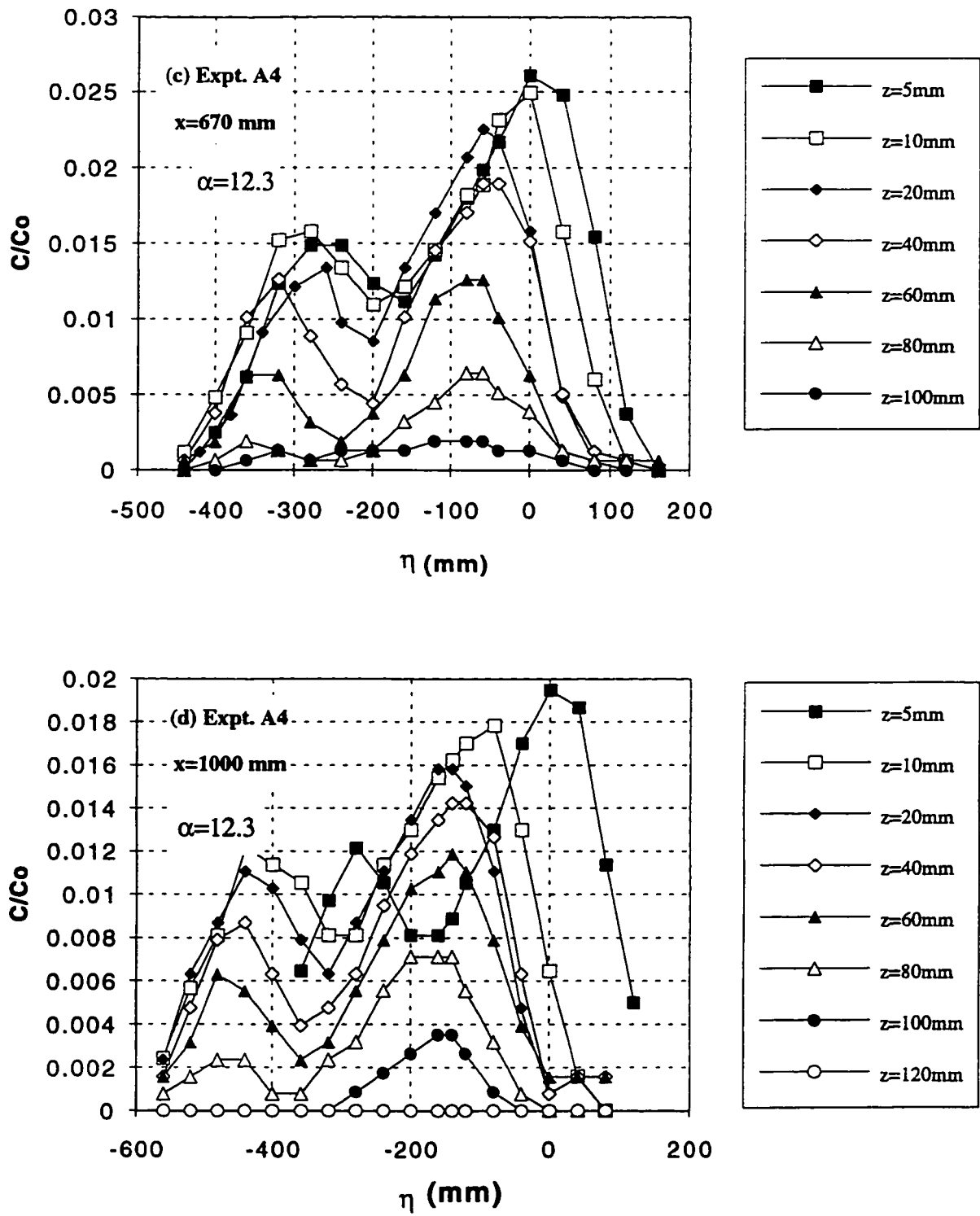
Fig. 3.17 (c-d) Typical Transverse Concentration Profiles at Different Levels for Expt. A4
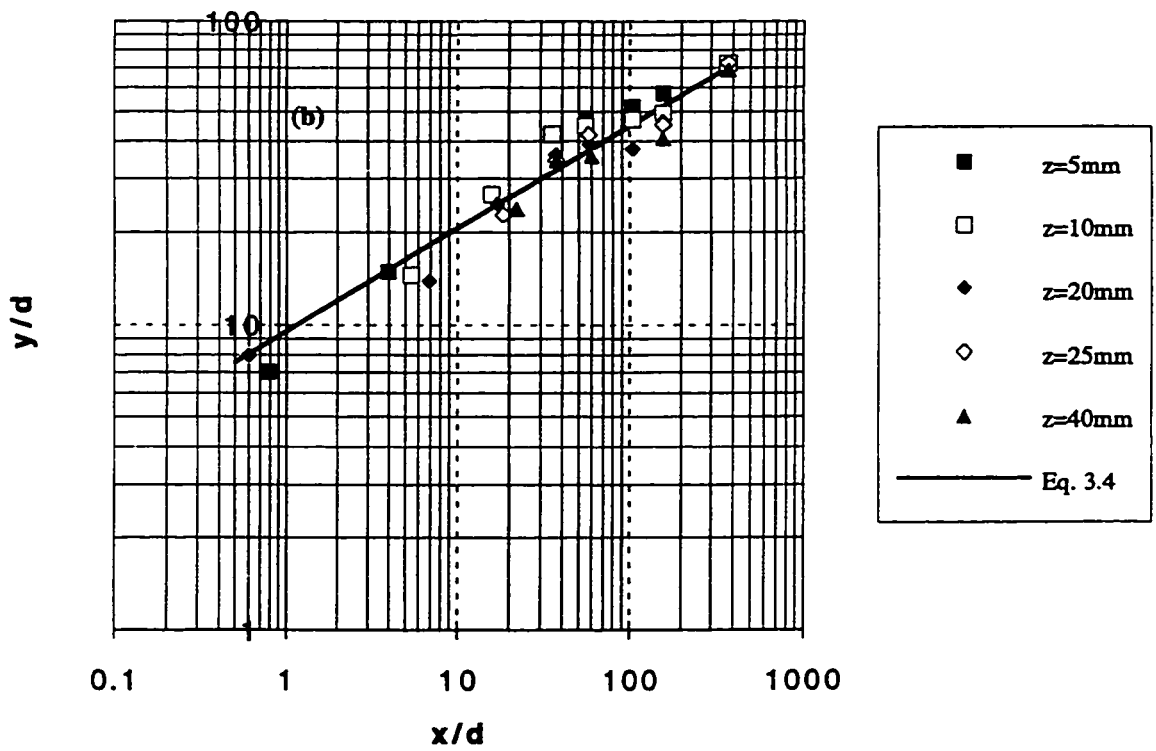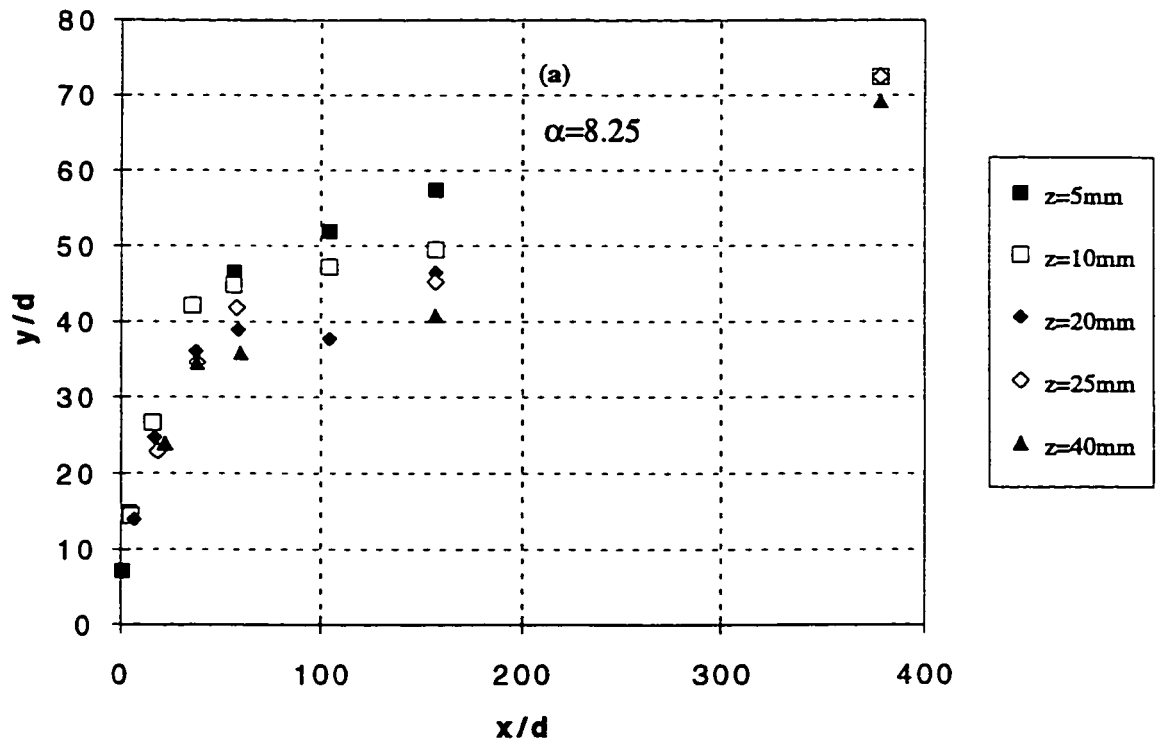
Fig. 3.18 (a-b) Variation of the Jet Centerline with the Vertical Distance for α=8.25
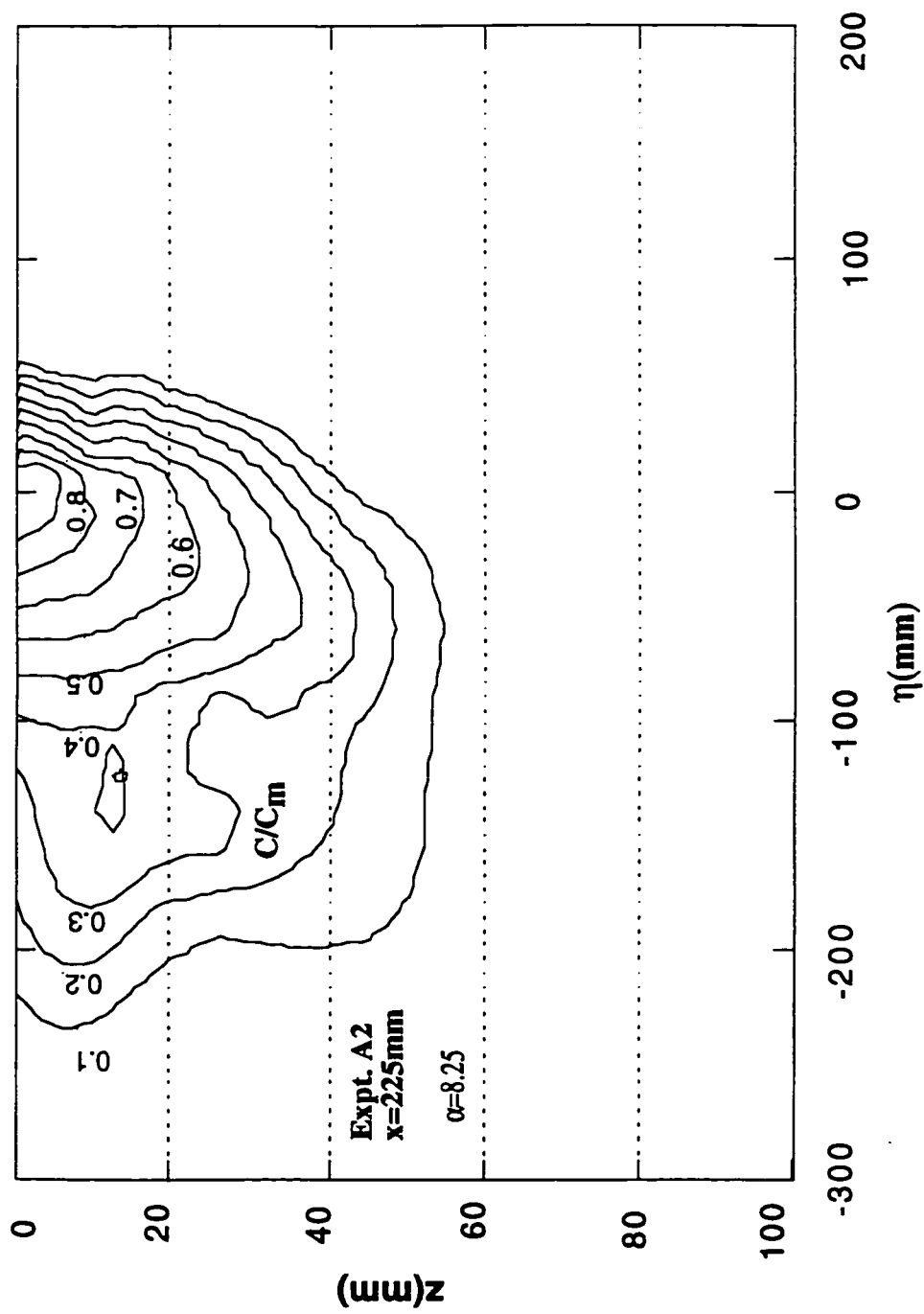
Fig. 3.19a Typical Concentration Contours for Expt. A2
α=8.25, x=225mm
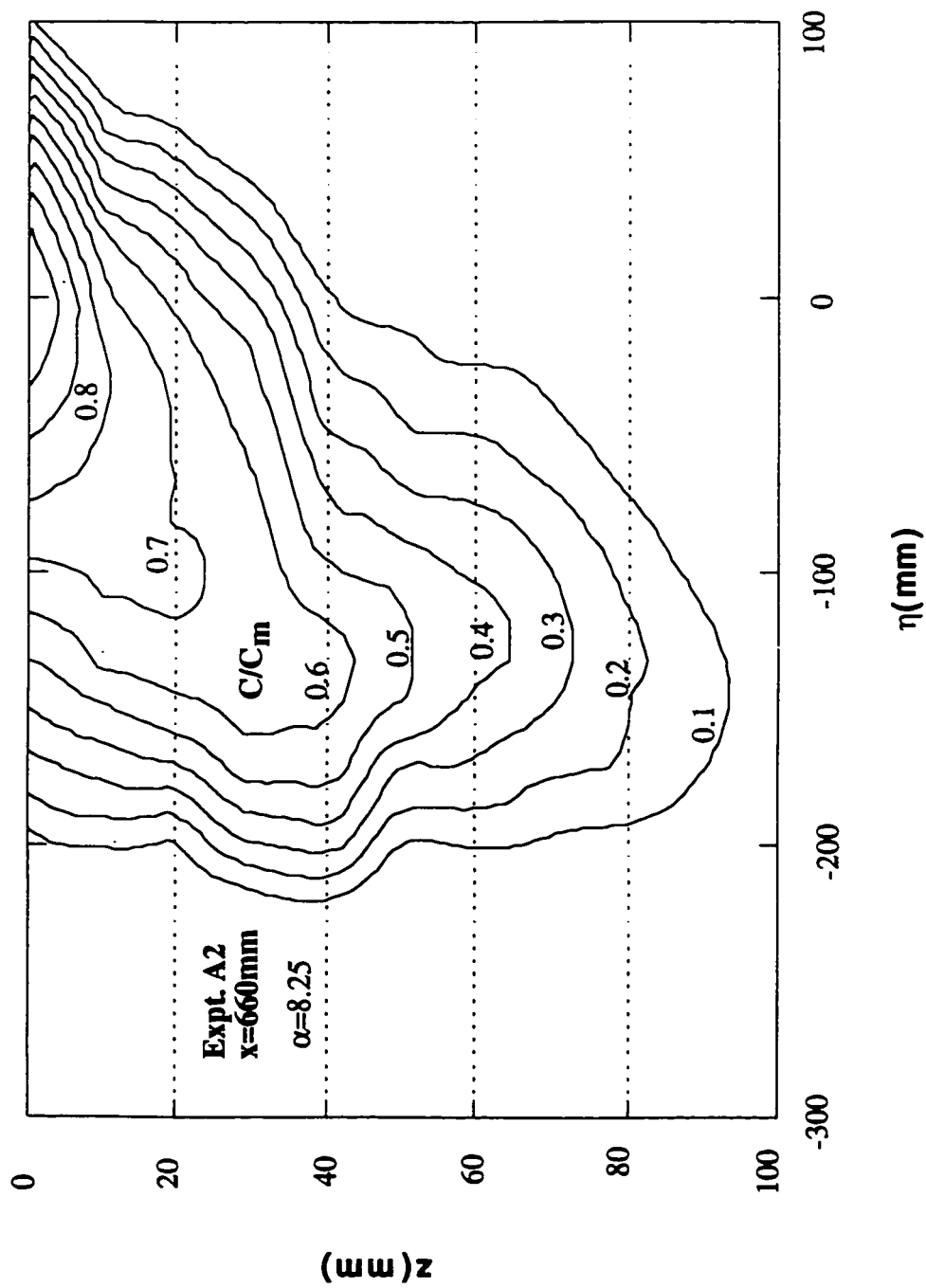
Fig. 3.19b Typical Concentration Contours for Expt. A2
$\alpha=8.25$, x=660mm
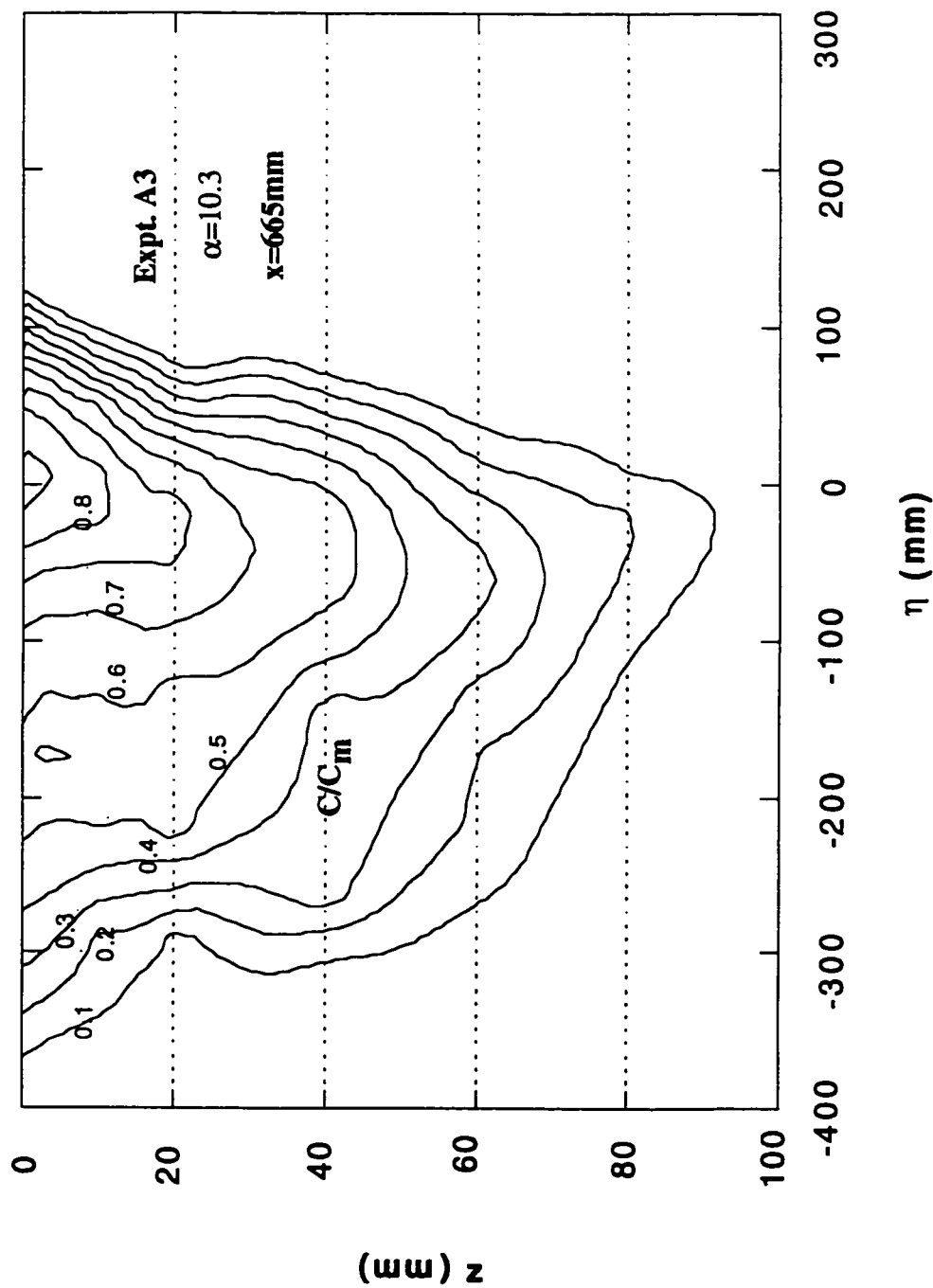
Fig. 3.19c Typical Concentration Contours for Expt. A3
α=10.3, x=665mm
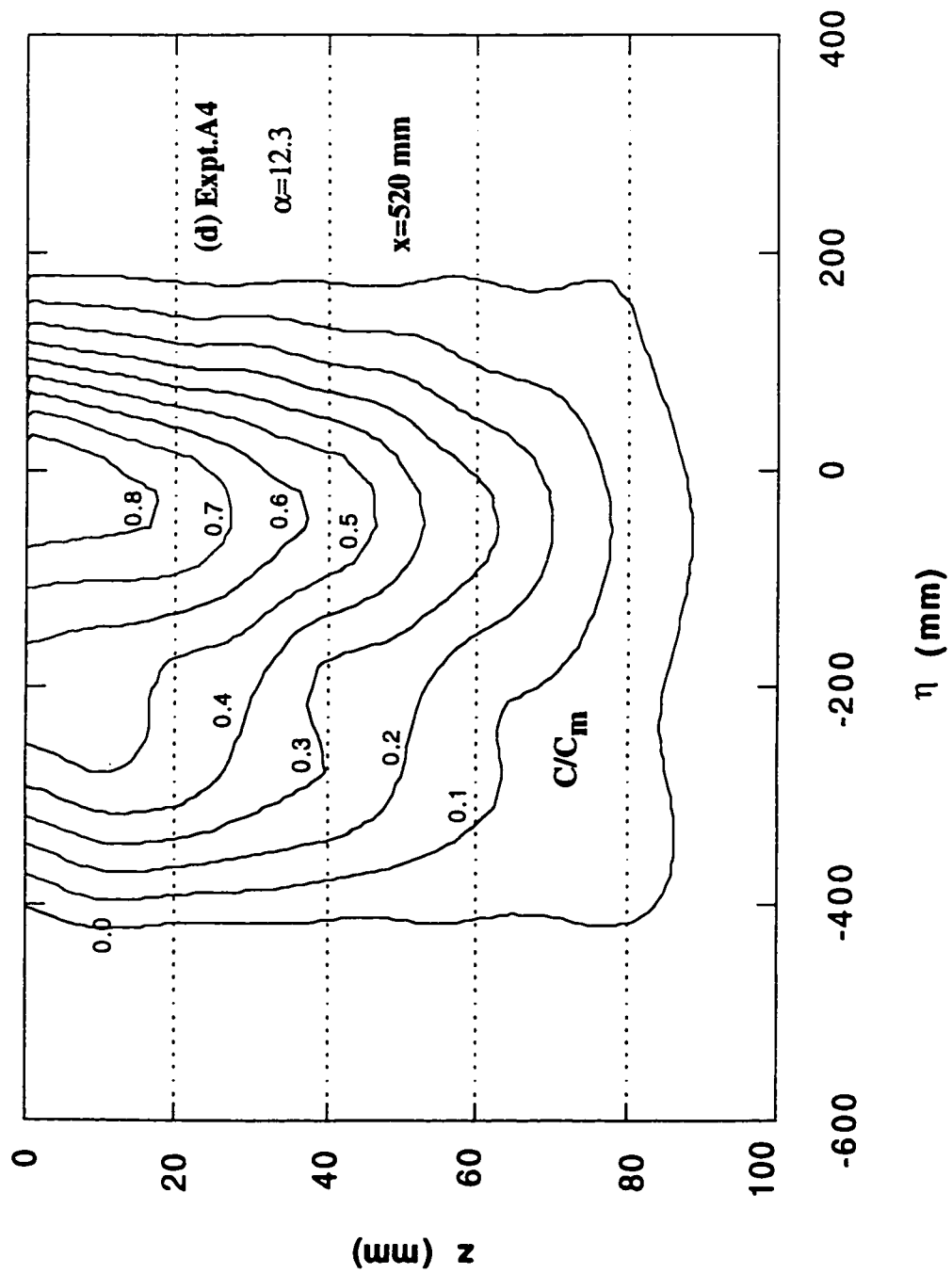
Fig. 3.19d Typical Concentration Contours for Expt. A4
α=12.3, x=520mm
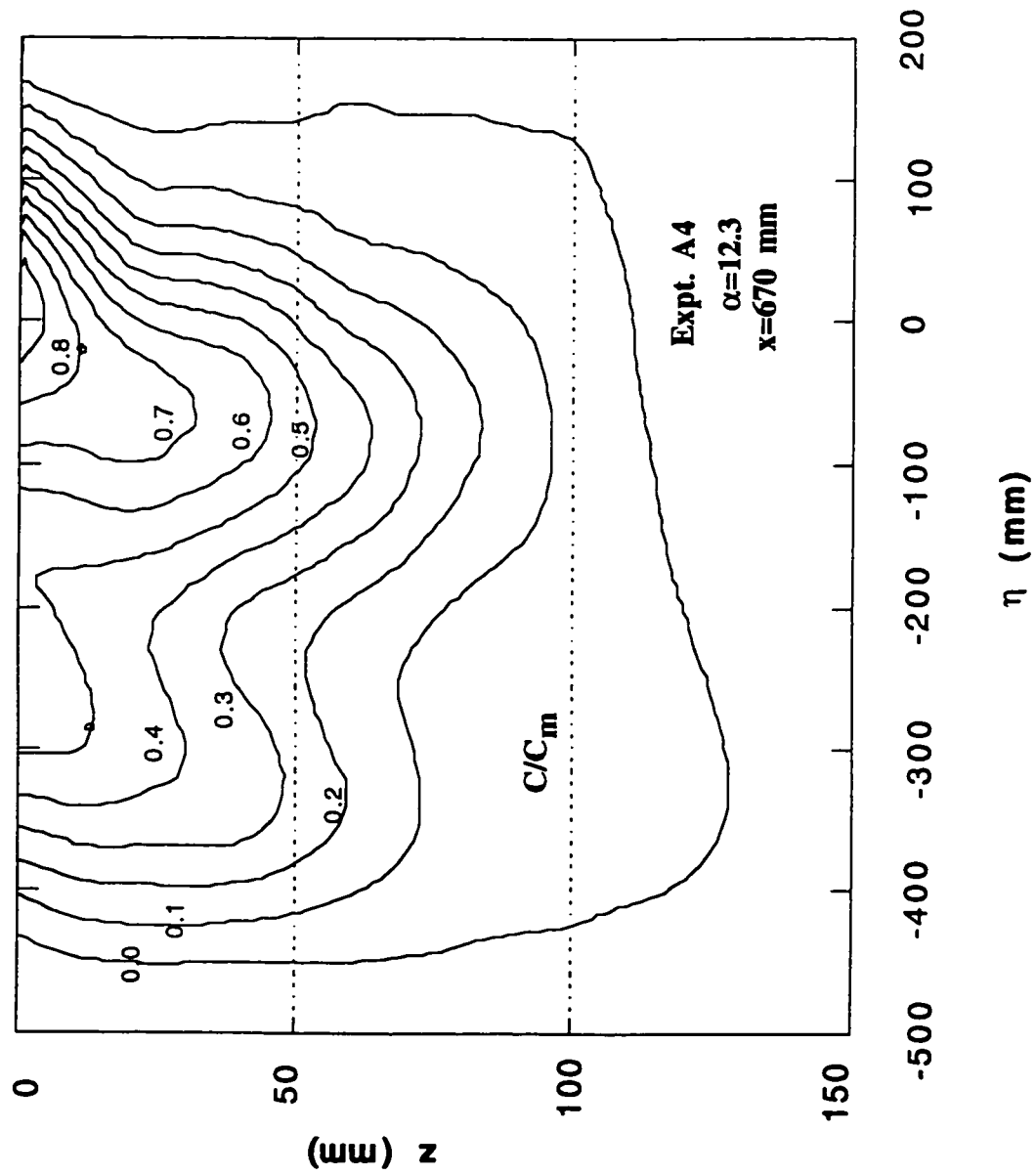
Fig. 3.19e Typical Concentration Contours for Expt. A4
$\alpha = 12.3$, x=670mm

103
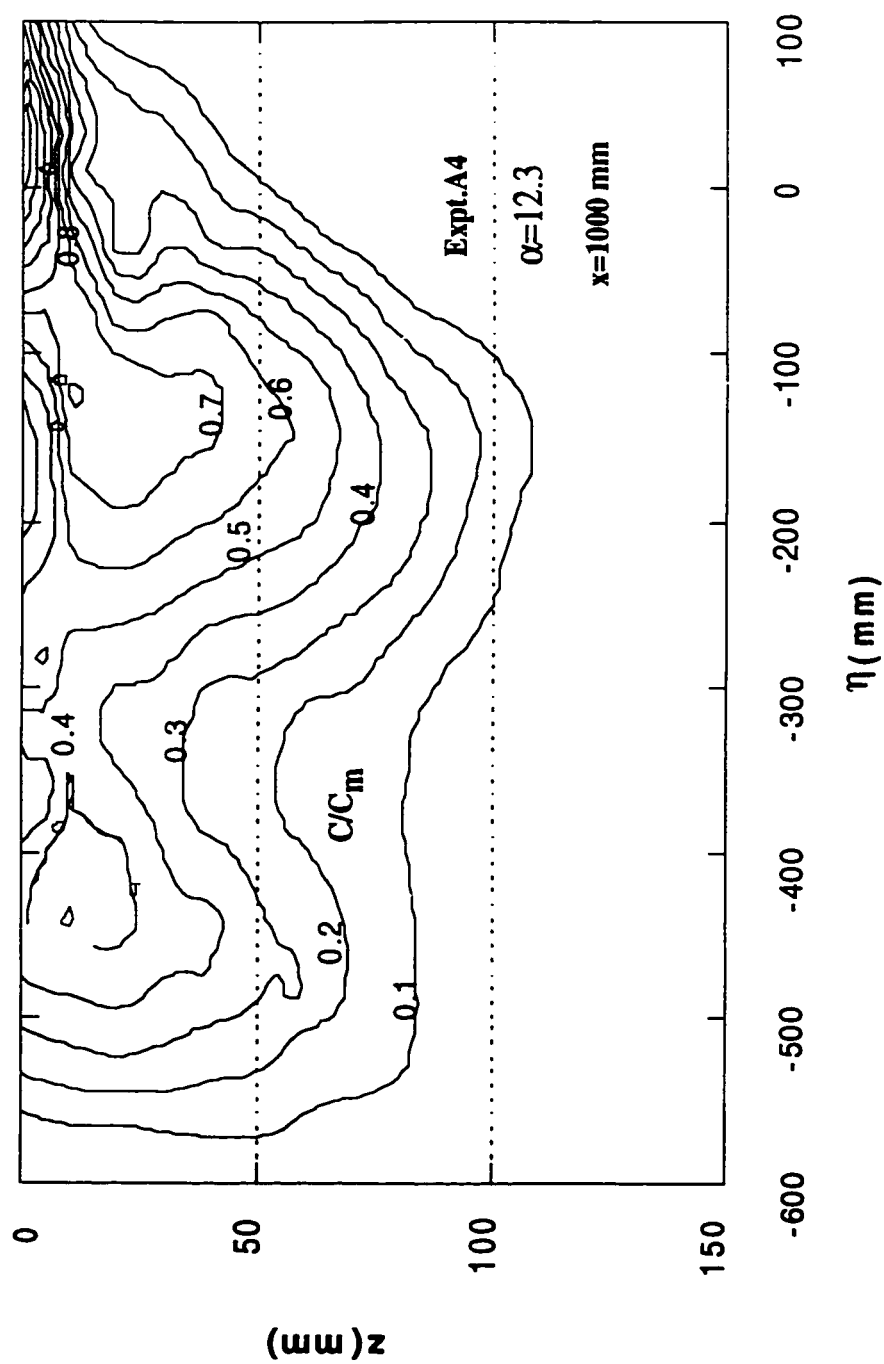
Fig. 3.19f Typical Concentration Contours for Expt. A4
$\alpha=12.3$, x=1000mm
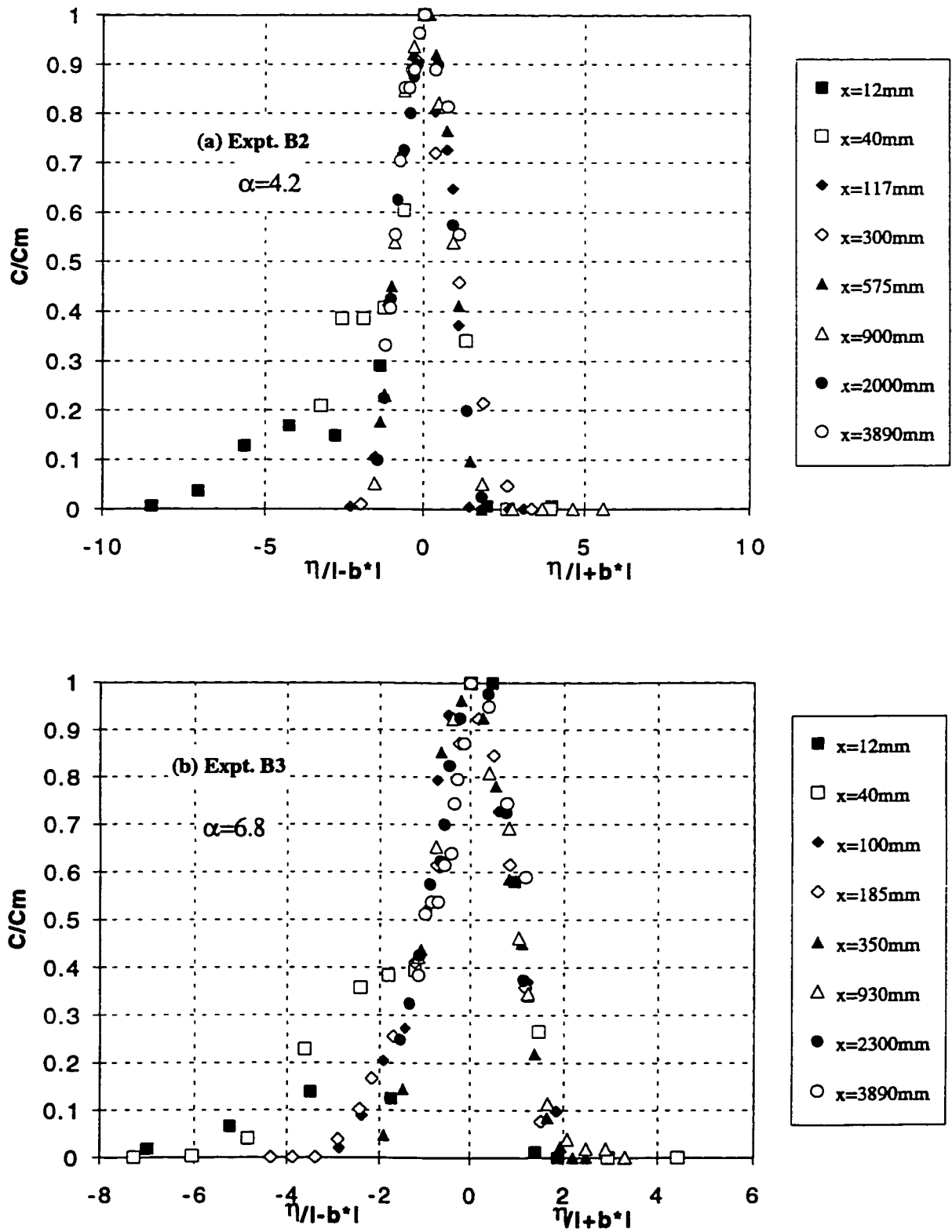
Fig. 3.20 (a-b) Similarity of Transverse Concentration Profiles
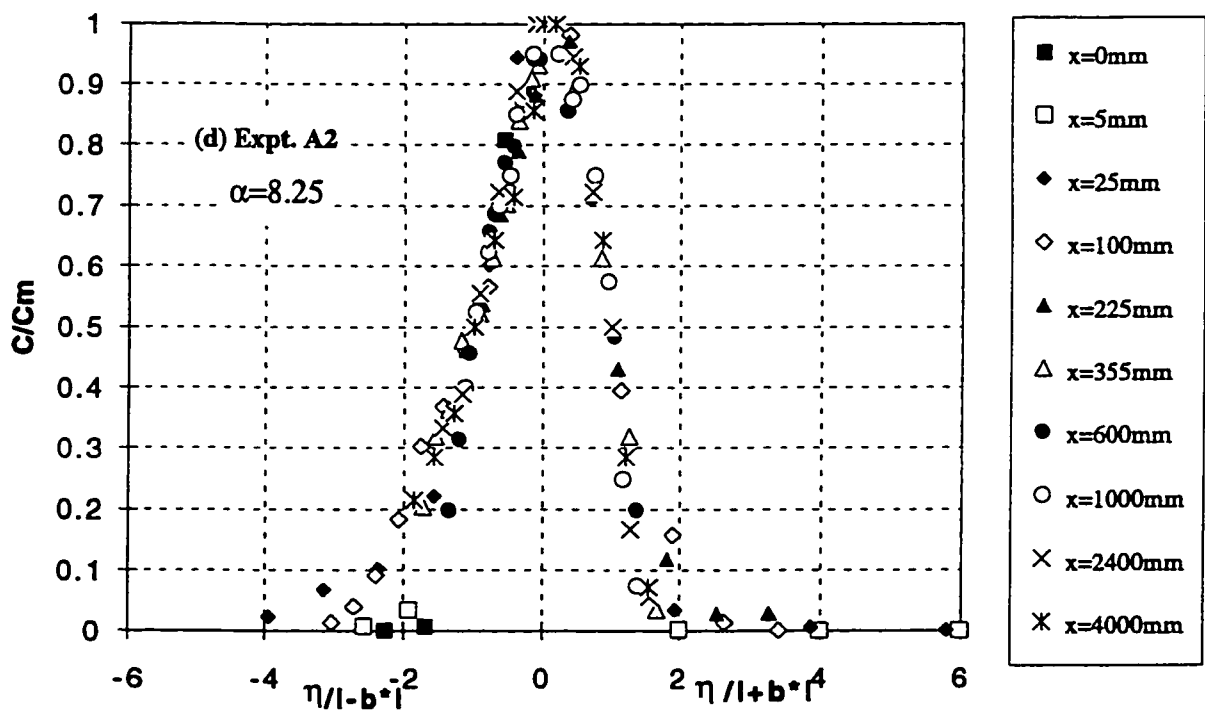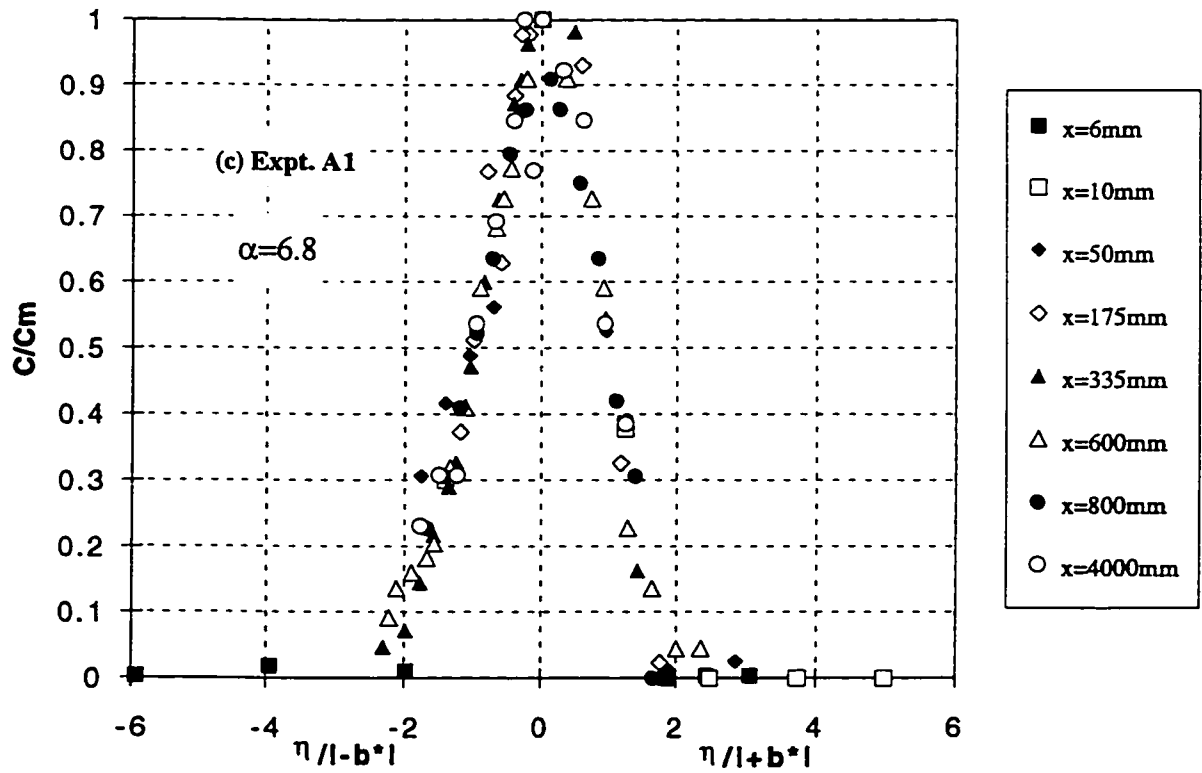
Fig. 3.20 (c-d) Similarity of Transverse Concentration Profiles
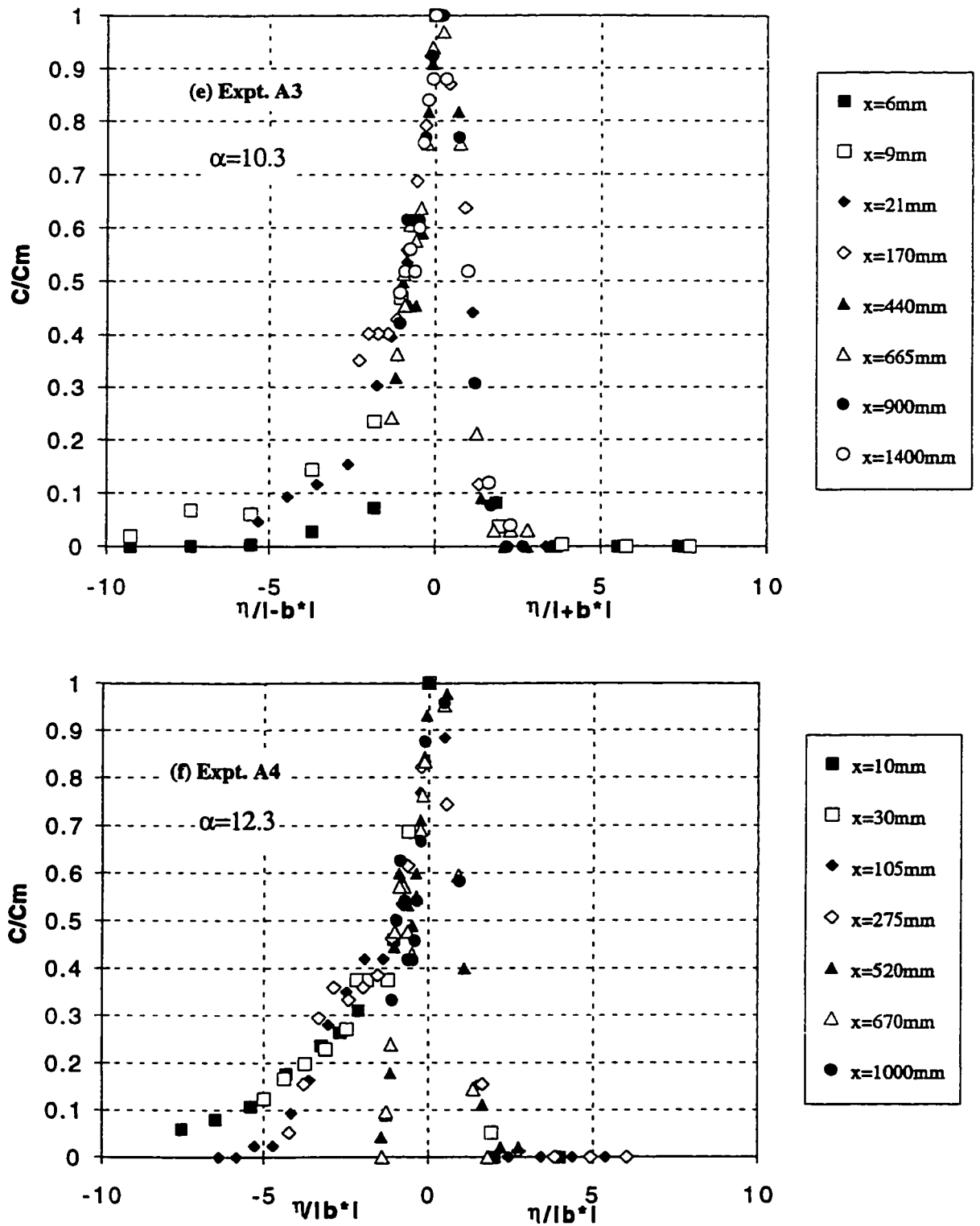
Fig. 3.20 (e-f) Similarity of Transverse Concentration Profiles
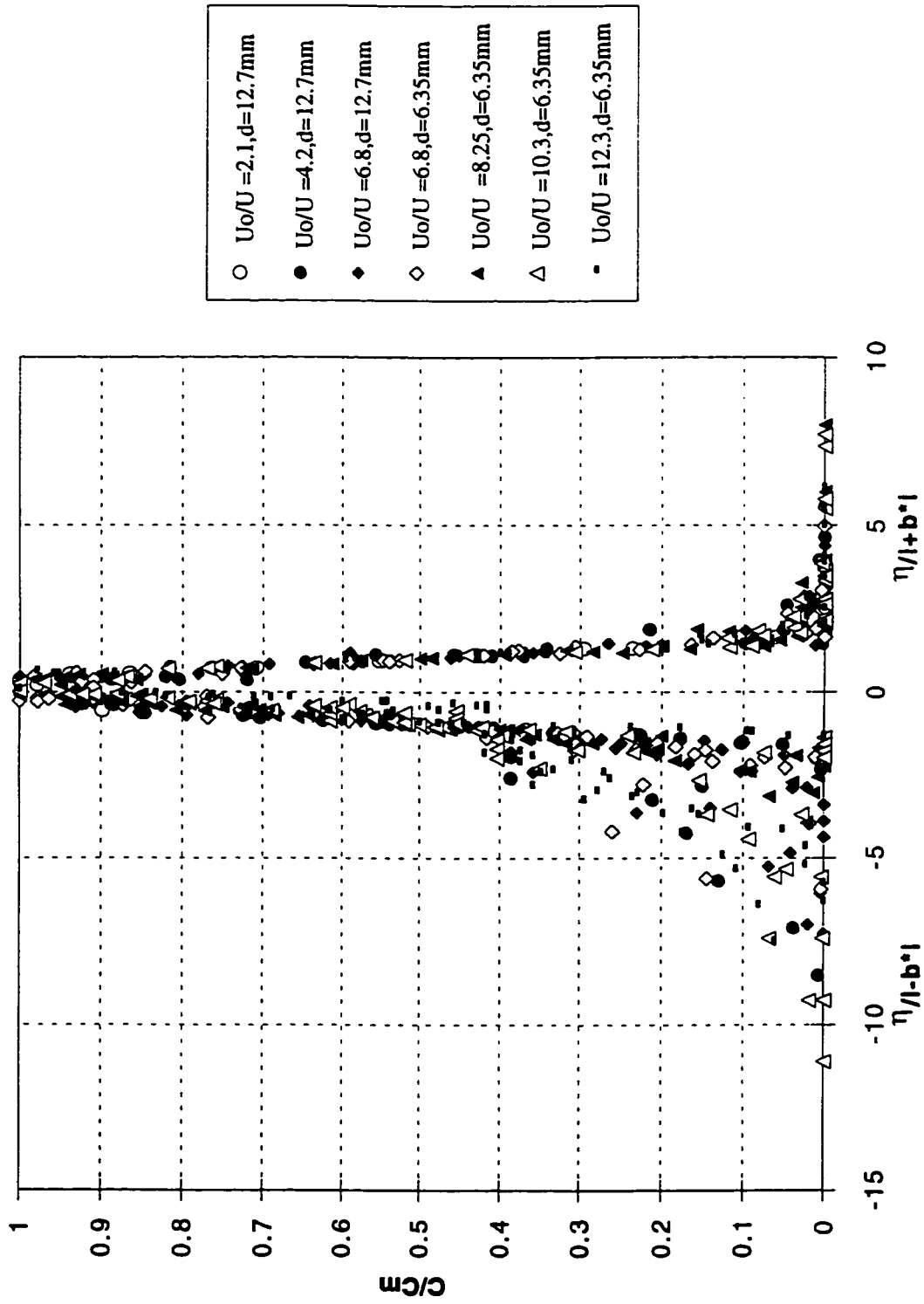
Fig. 3.21 Consolidated Plot for all the Transverse Concentration Profiles

108
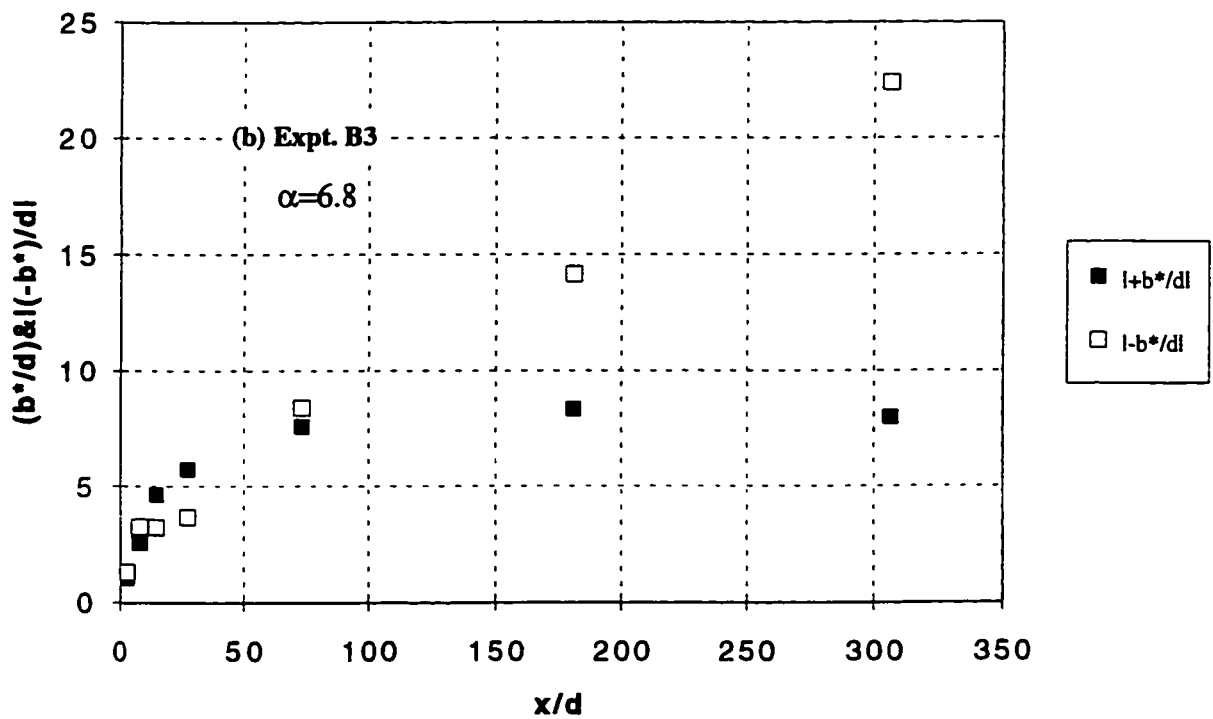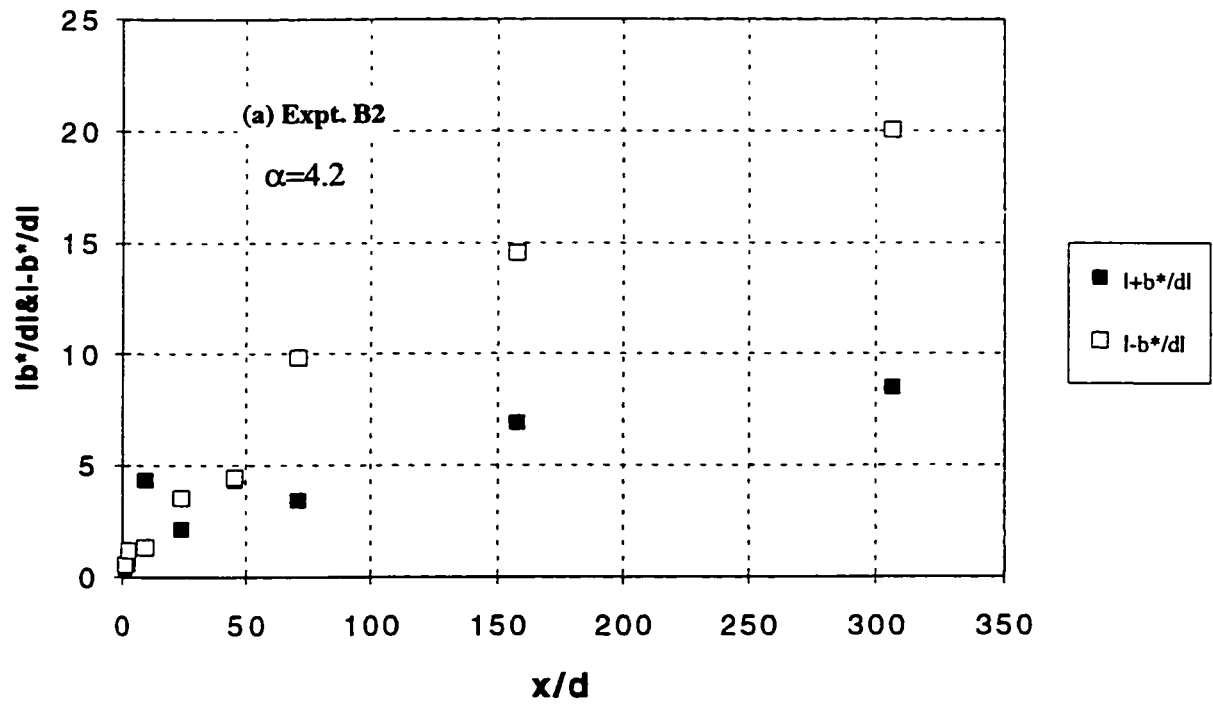
Fig. 3.22 (a-b) Typical Transverse Length Scales
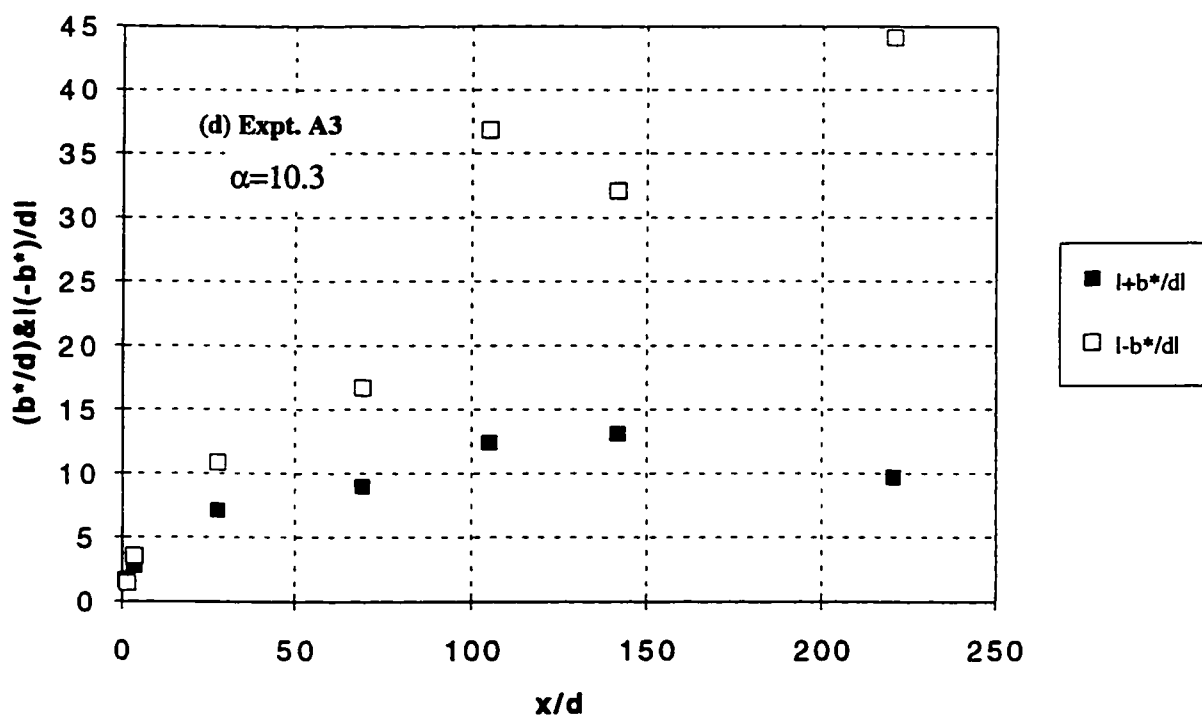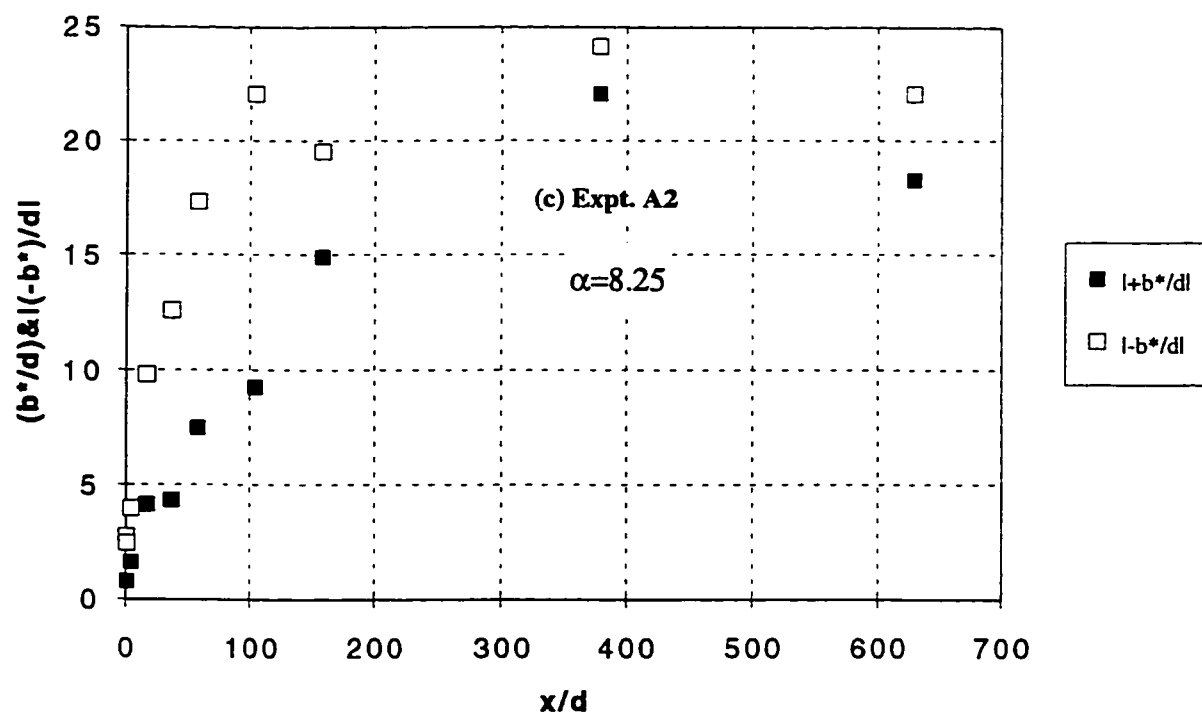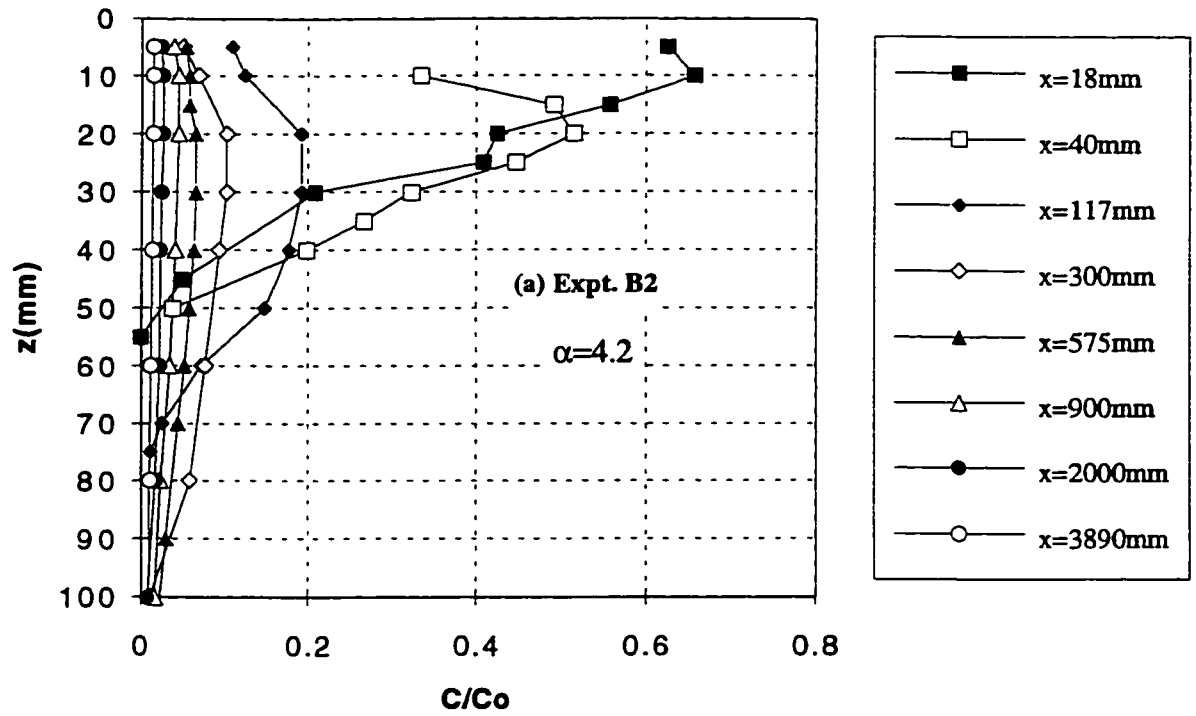
Fig. 3.22 (c-d) Transverse Length Scales
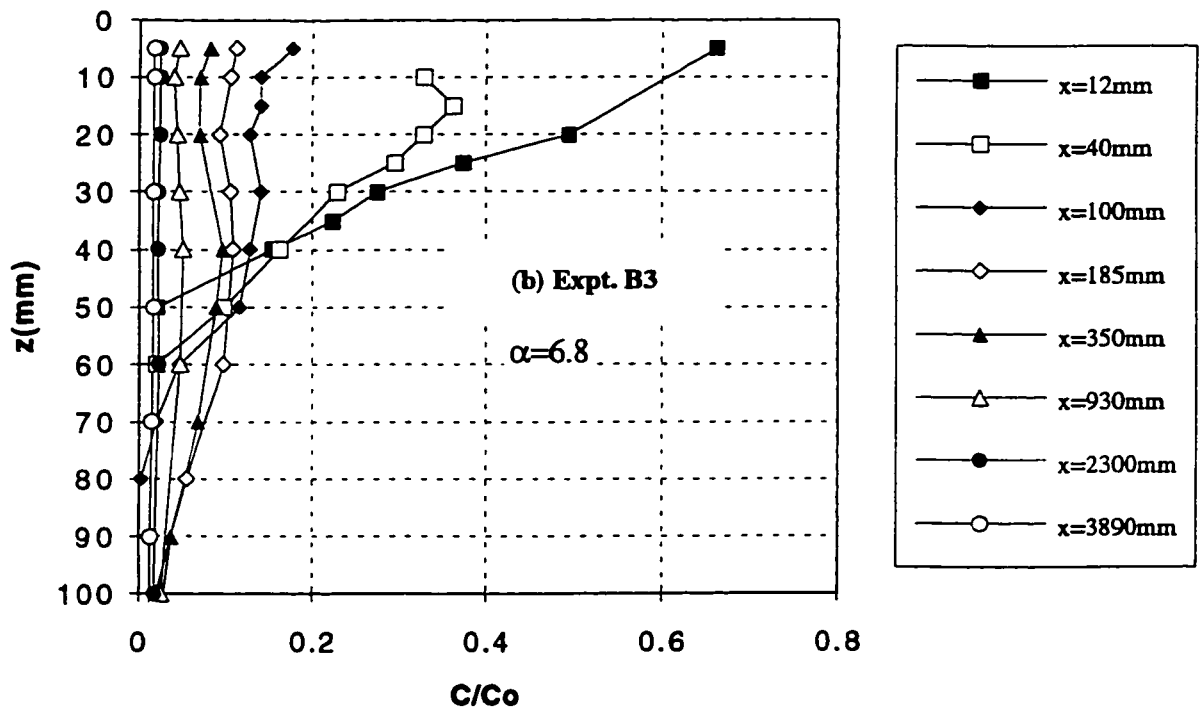
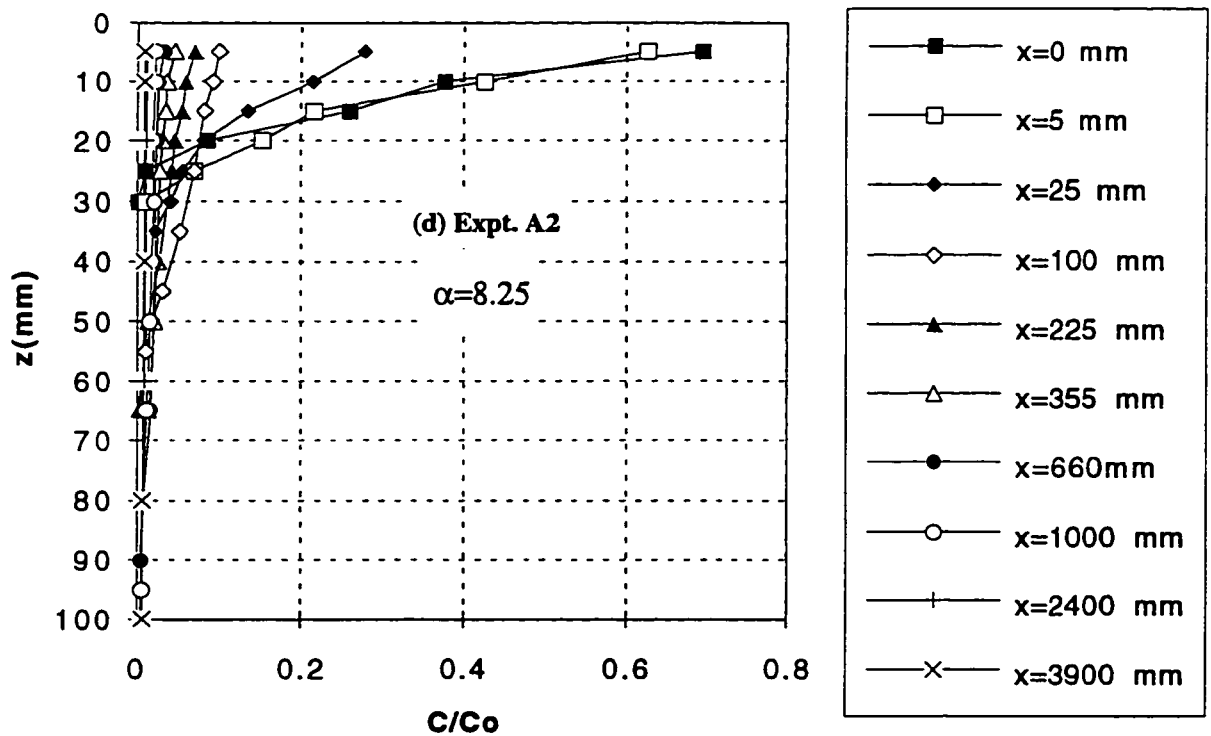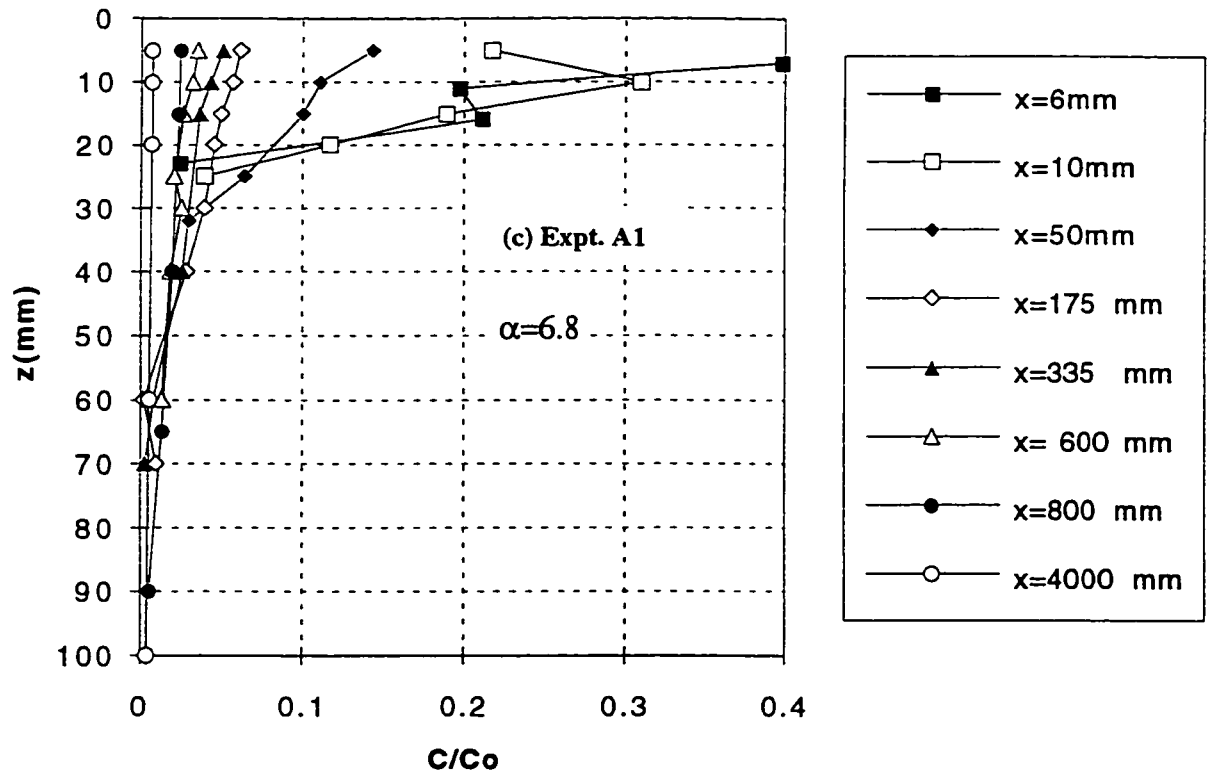**Fig. 3.23 (a-b) Typical Vertical Concentration Profiles**

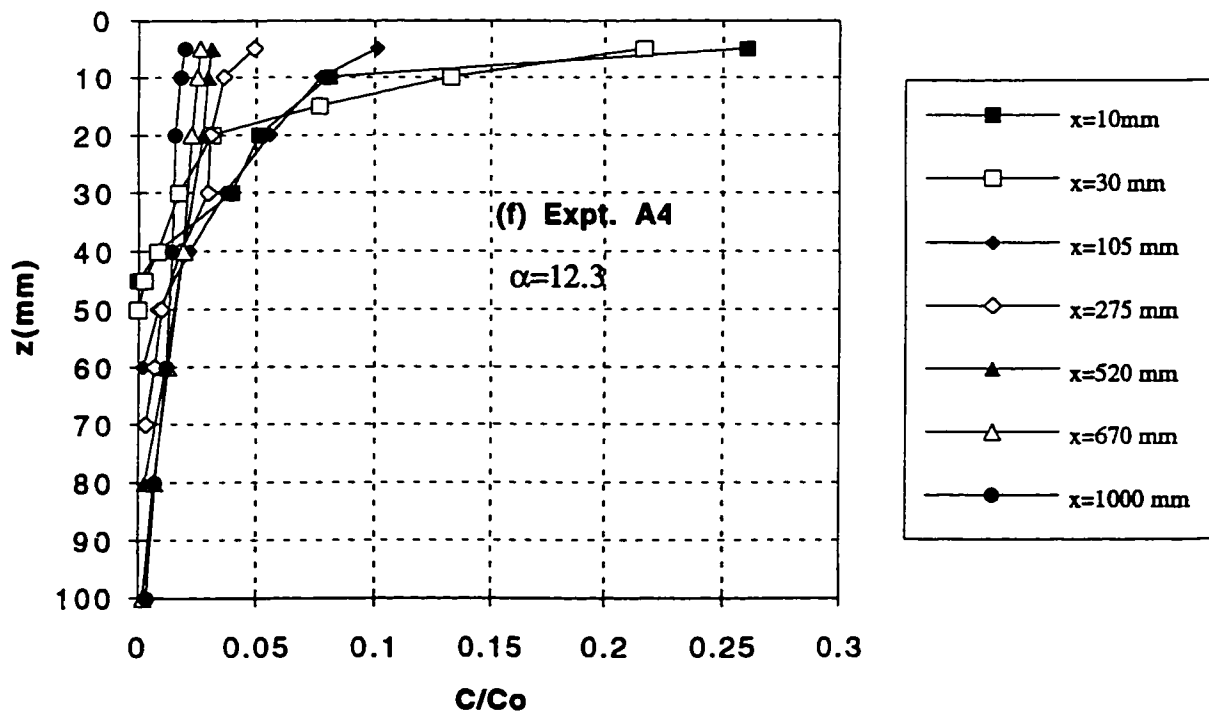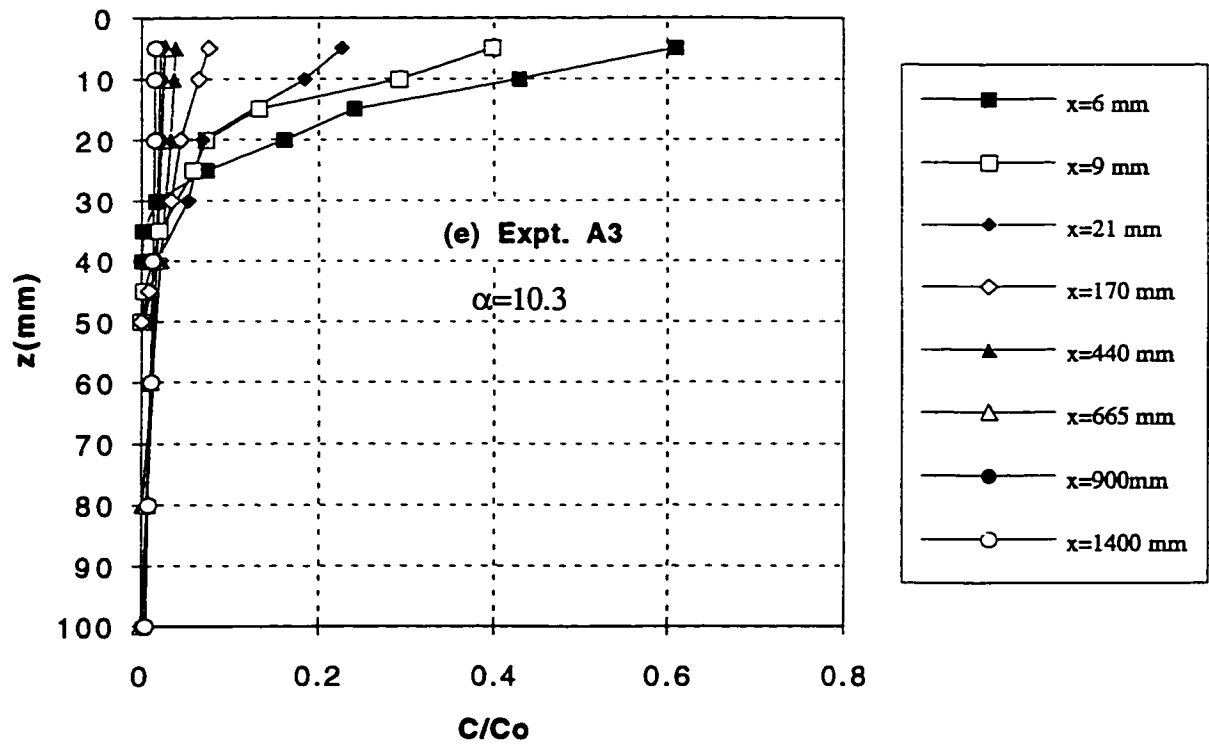**Fig. 3.23 (c-d) Typical Vertical Concentration Profiles**

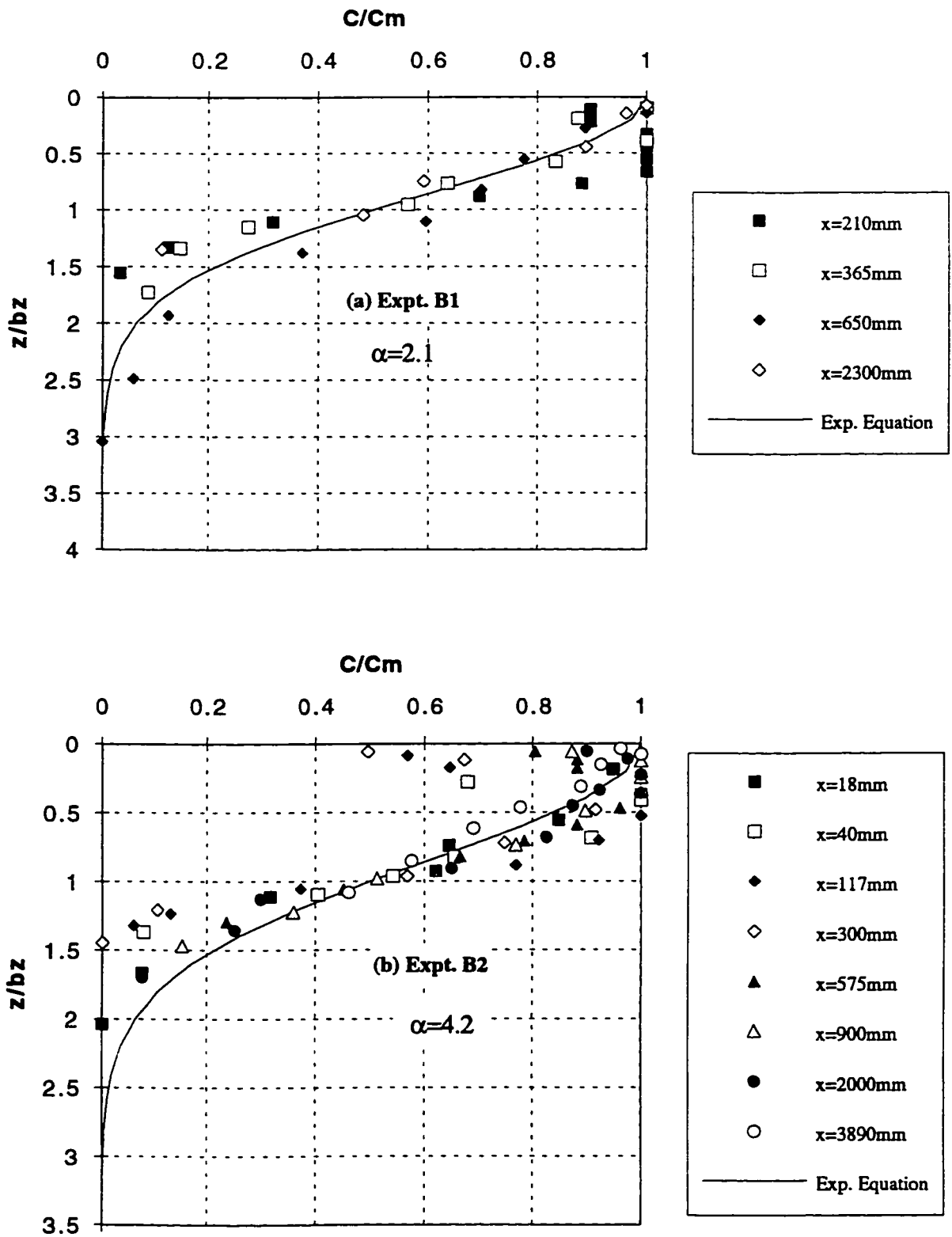**Fig. 3.23 (e-f) Typical Vertical Concentration Profiles**

113

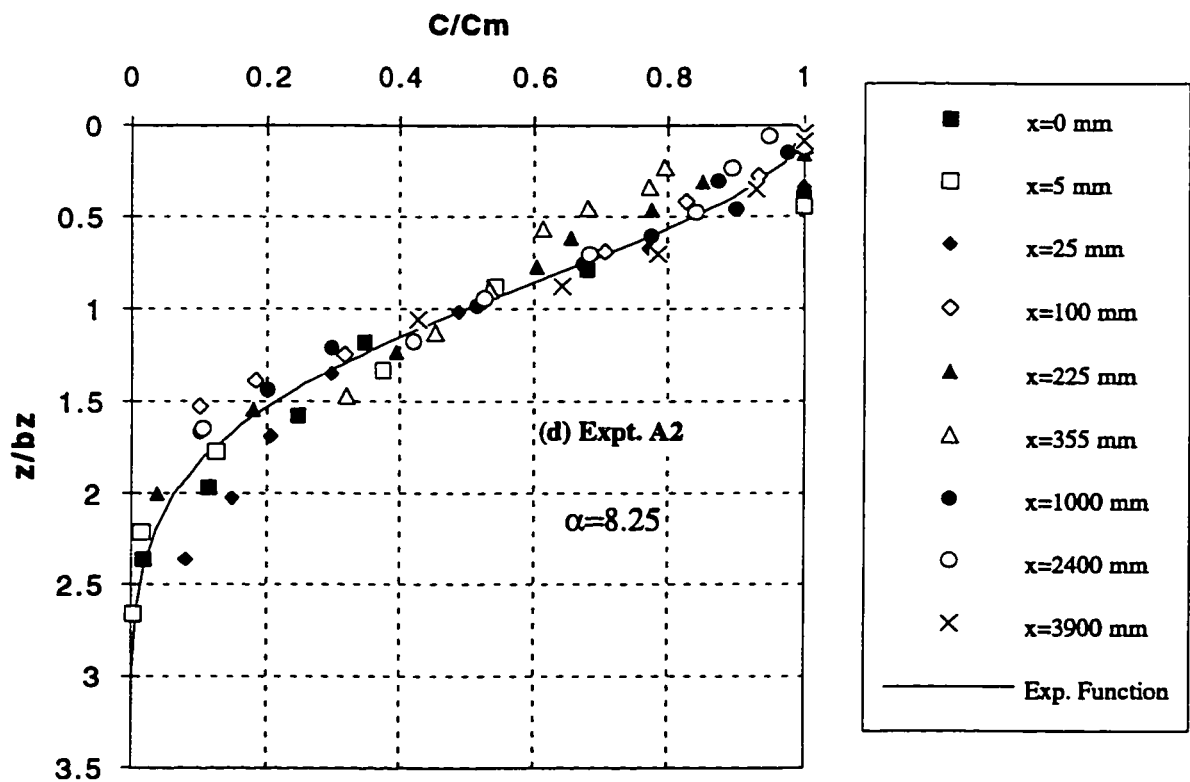Fig. 3.24 (a-b) Similarity of Vertical Concentration Profiles

114
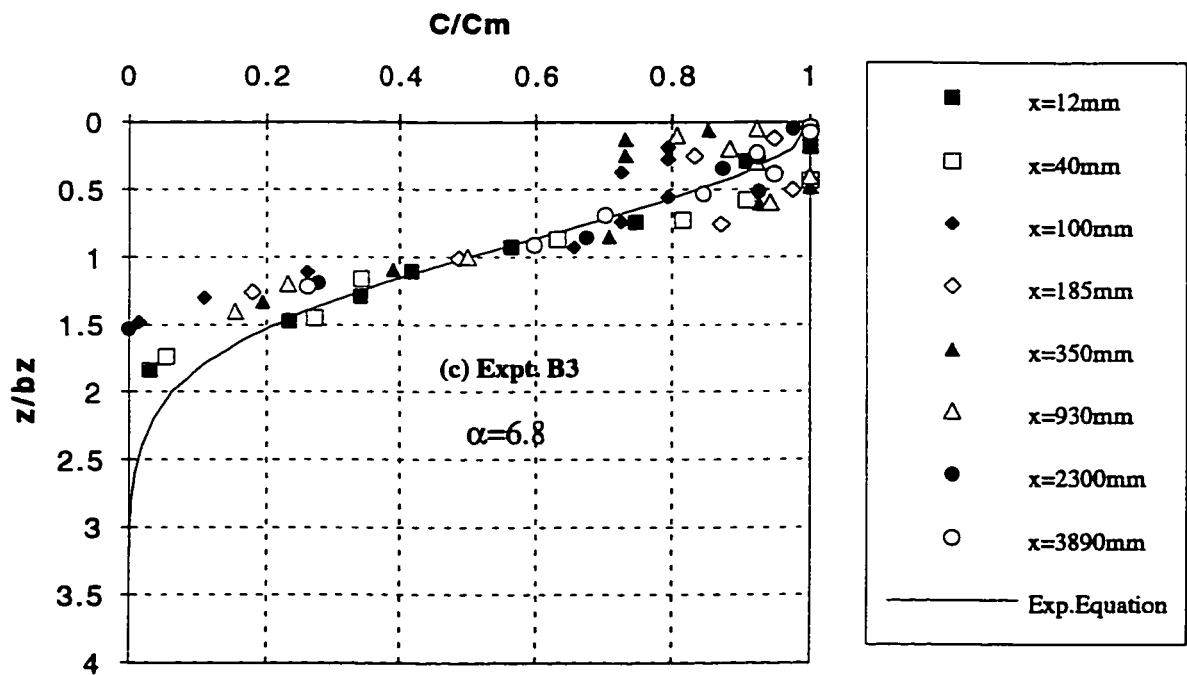
Fig. 3.24 (c-d) Similarity of Vertical Concentration Profiles
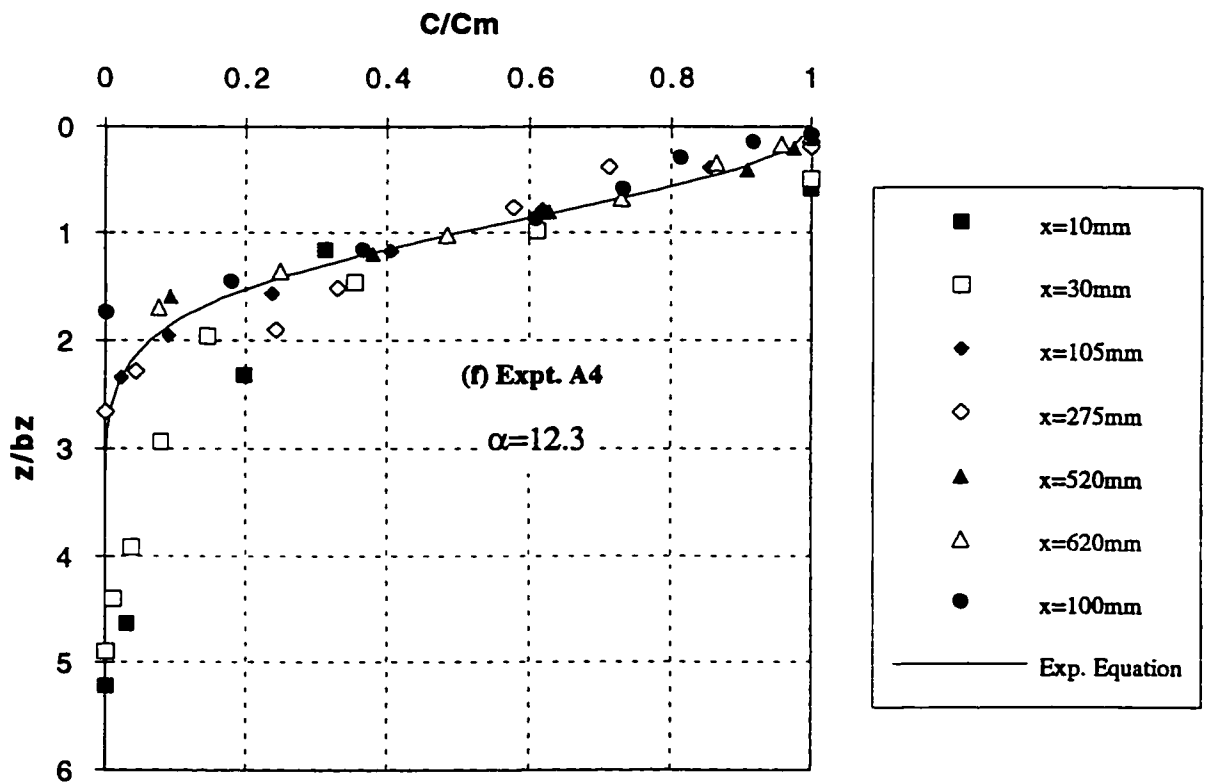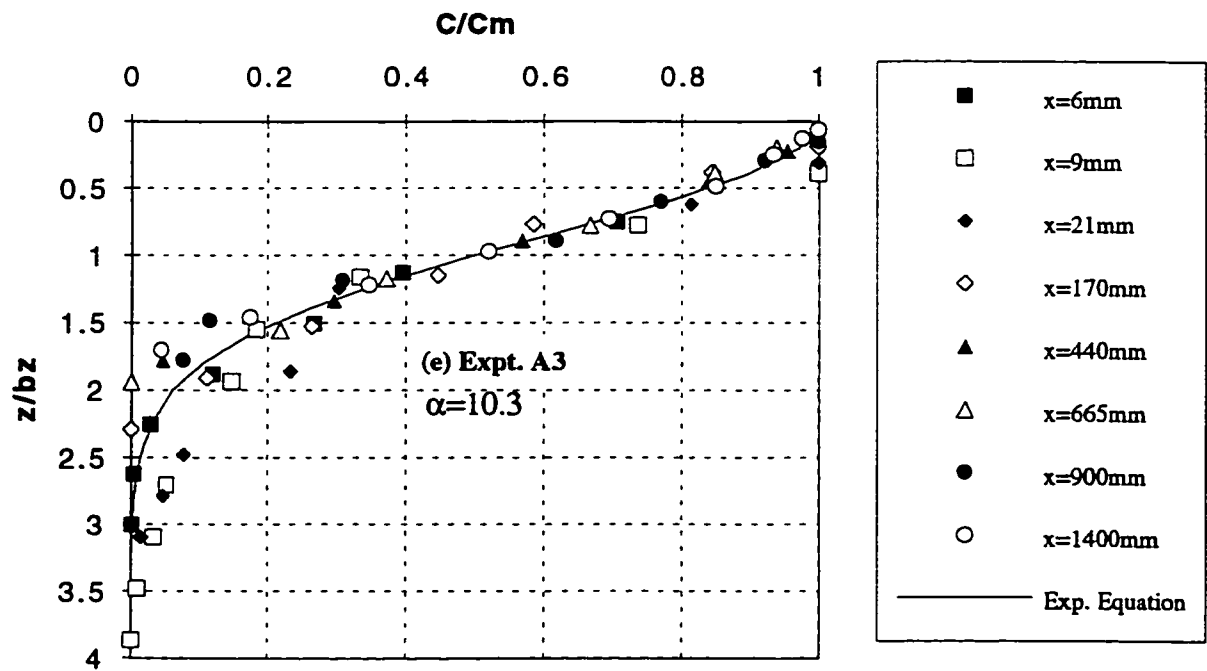
Fig. 3.24 (e-f) Similarity of Transverse Concentration Profiles
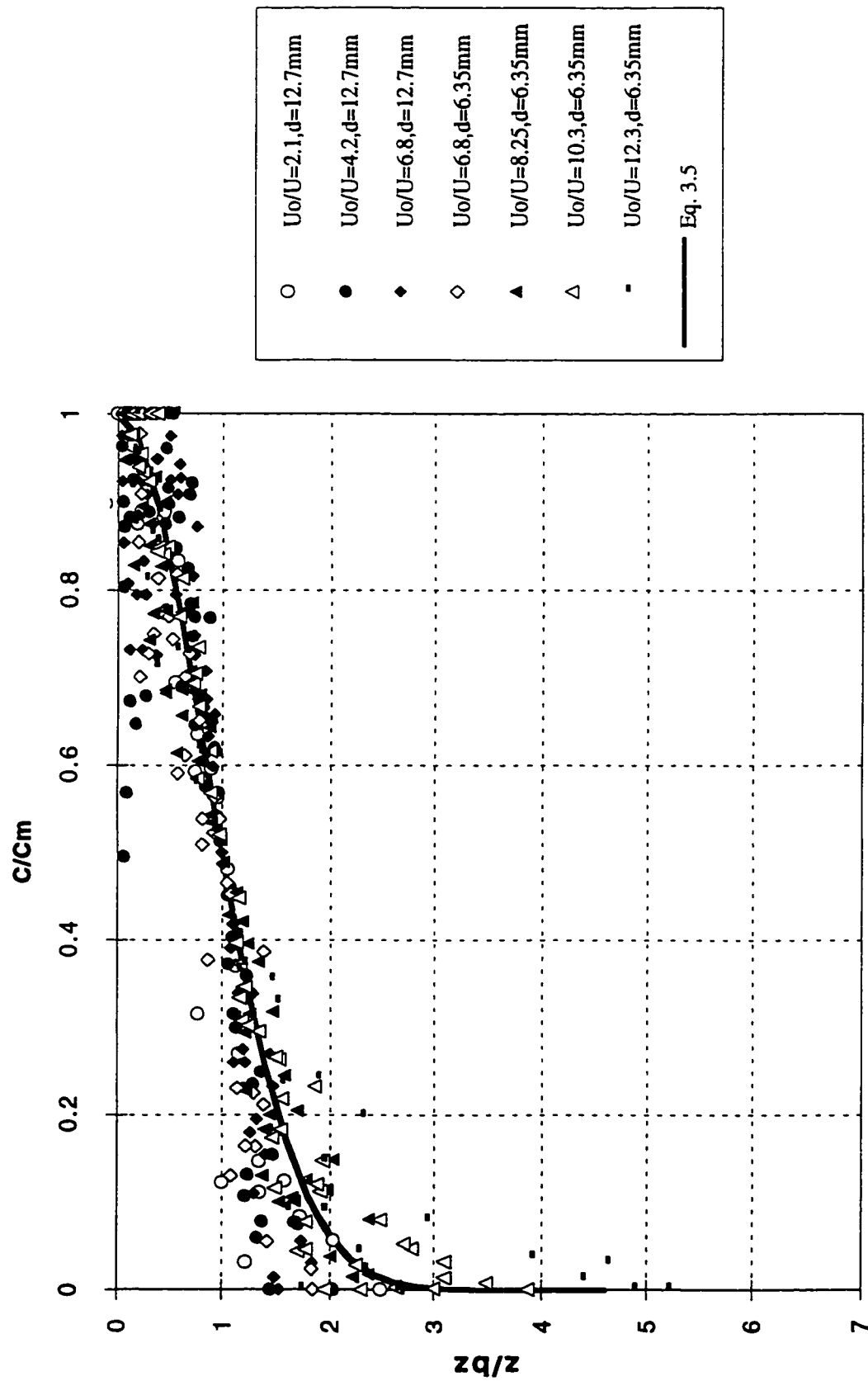
Fig. 3.25 Consolidated Plot for all the Vertical Concentration Profiles

Legend:
- ○ Uo/U=2.1,d=12.7mm
- ● Uo/U=4.2,d=12.7mm
- ◆ Uo/U=6.8,d=12.7mm
- ◇ Uo/U=6.8,d=6.35mm
- ▲ Uo/U=8.25,d=6.35mm
- △ Uo/U=10.3,d=6.35mm
- ▪ Uo/U=12.3,d=6.35mm
- —— Eq. 3.5

117

Fig. 3.26 (a-b) Variation of Minimum Dilution (C_0/C_m) with ($\alpha x/d$)
for Several Values of α
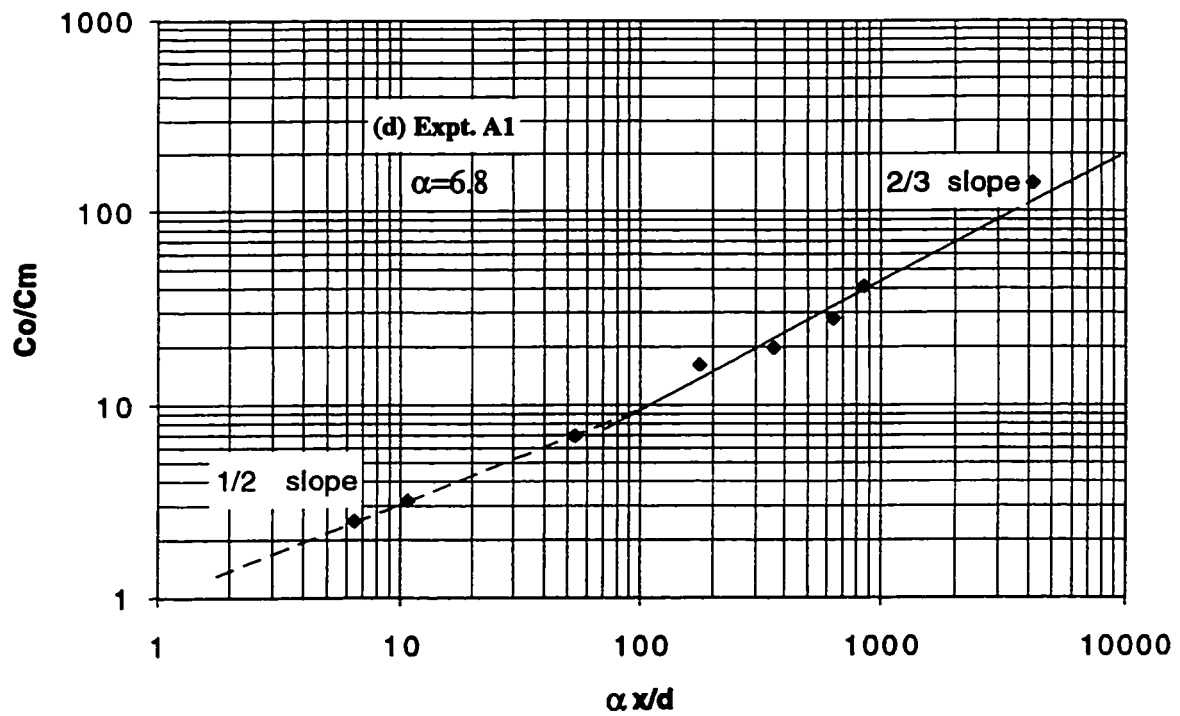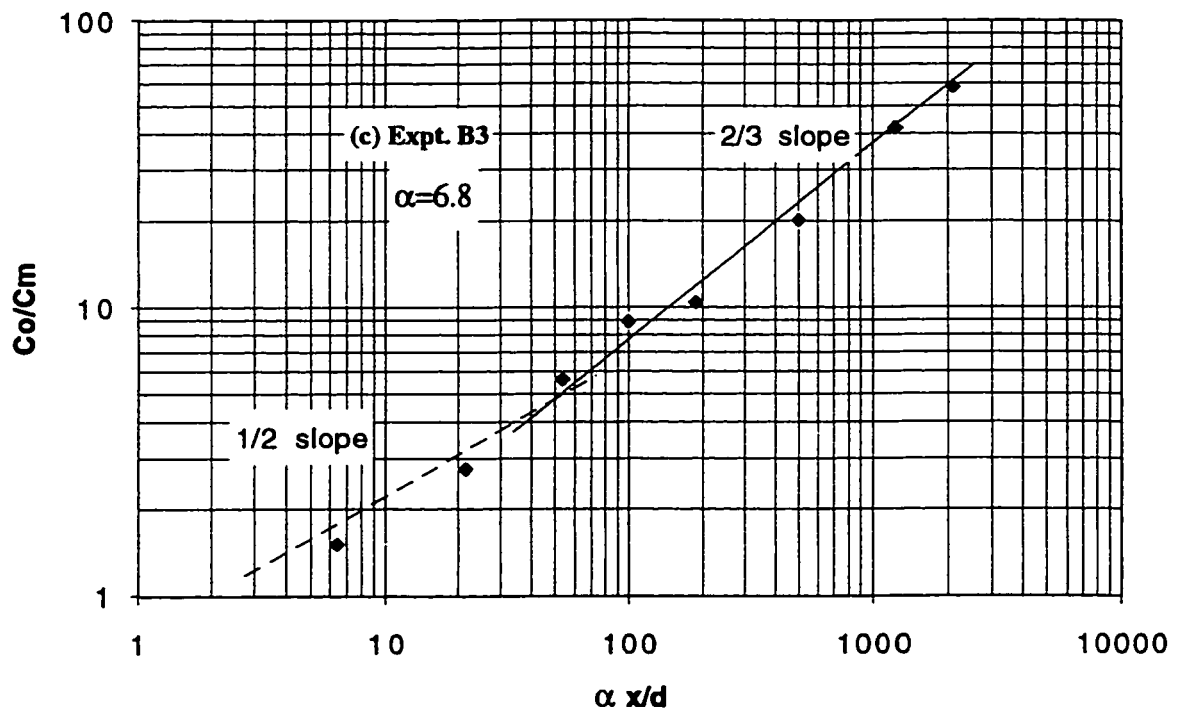
Fig. 3.26 (c-d) Variation of Minimum Dilution (C_0/C_m) with ($\alpha x/d$) for Several Values of α
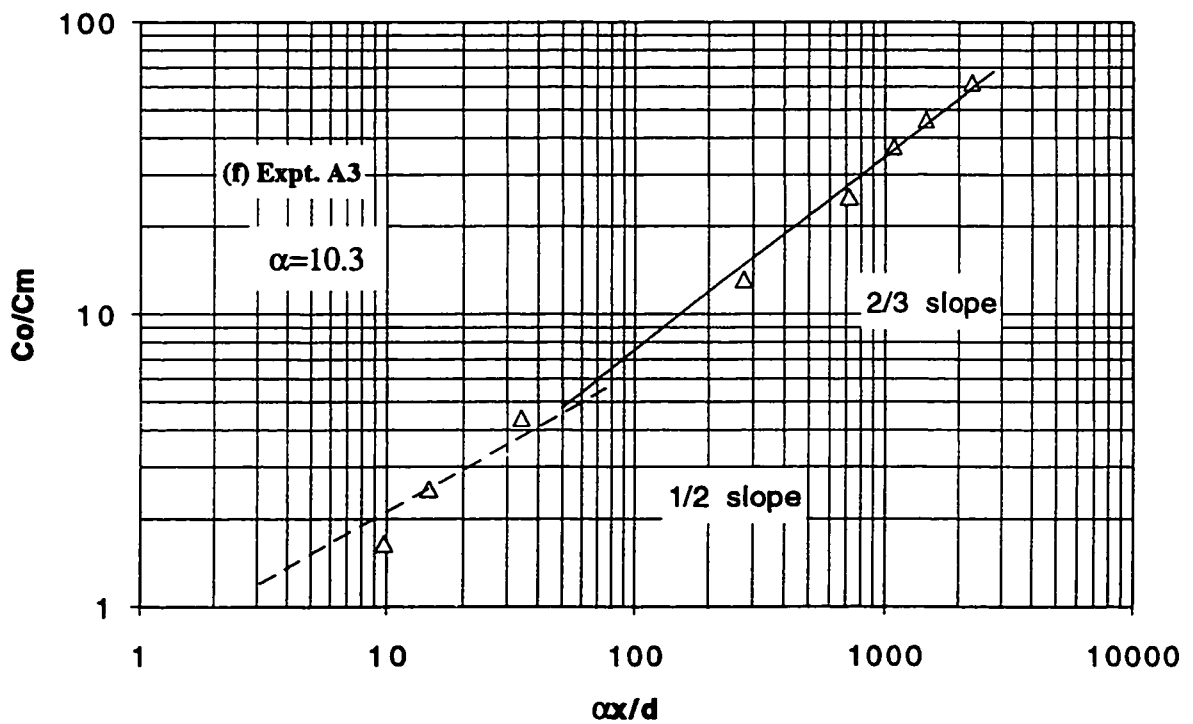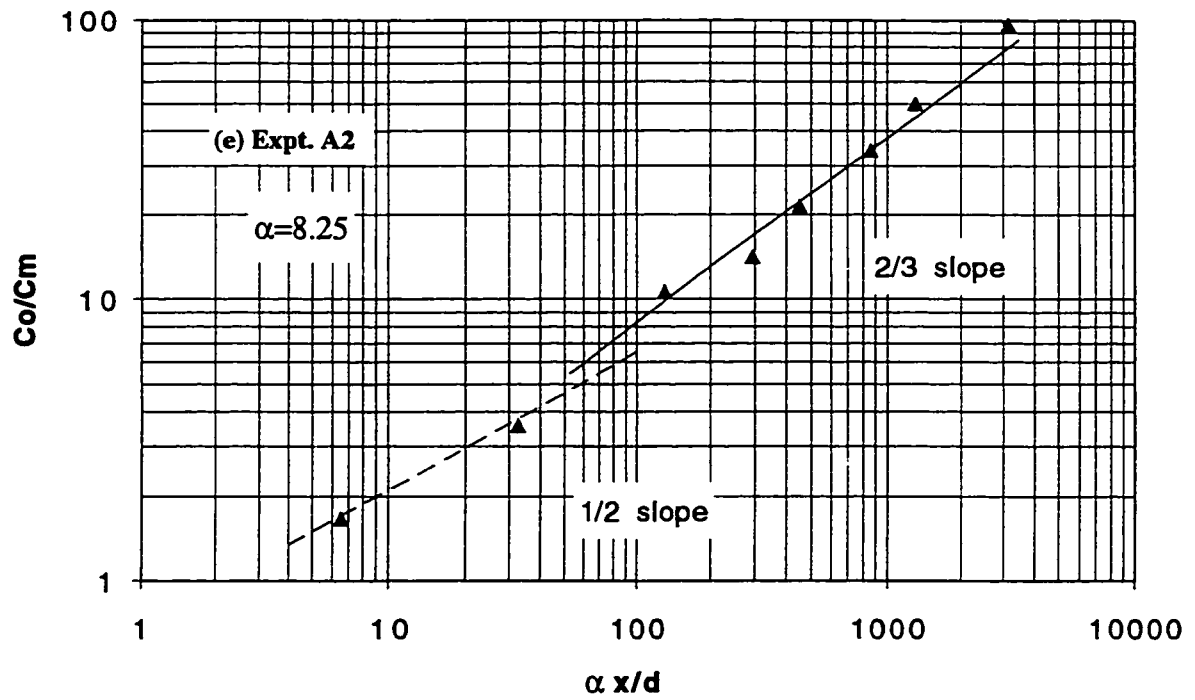
Fig. 3.26 (e-f) Variation of Minimum Dilution (C_0/C_m) with ($\alpha x/d$) for Several Values of α

120
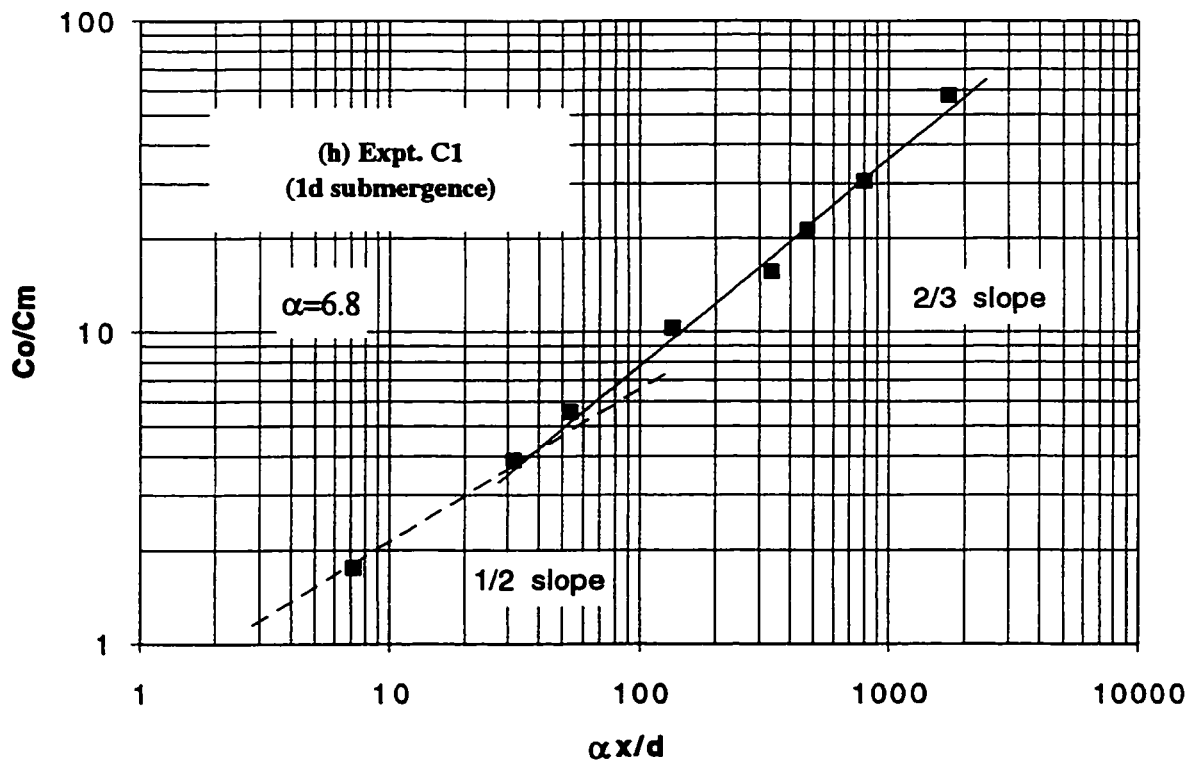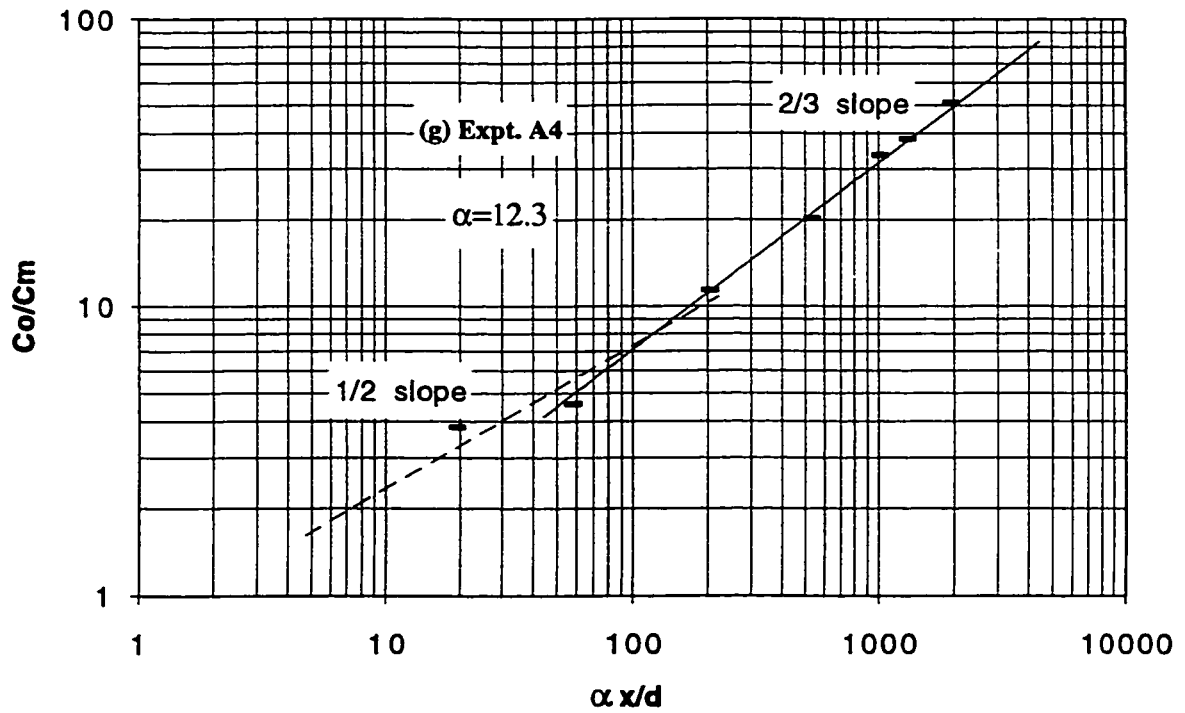
Fig. 3.26 (g-h) Variation of Minimum Dilution (C_o / C_m) with ($\alpha x/d$)
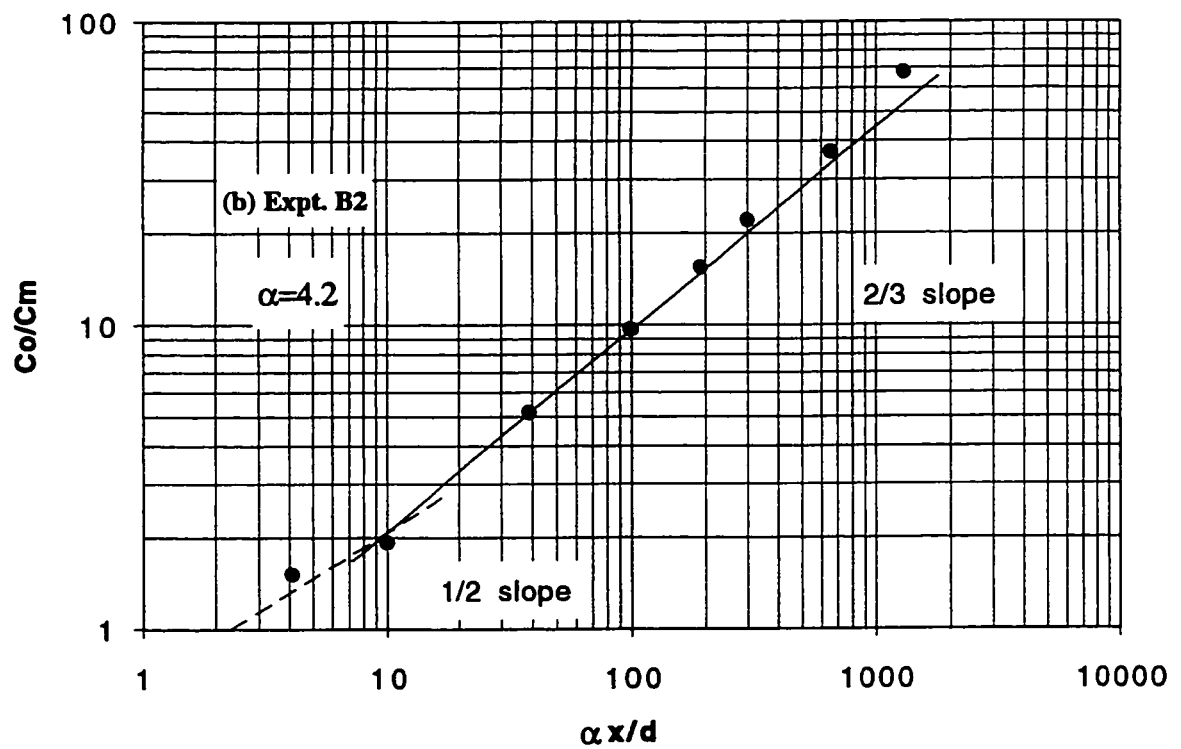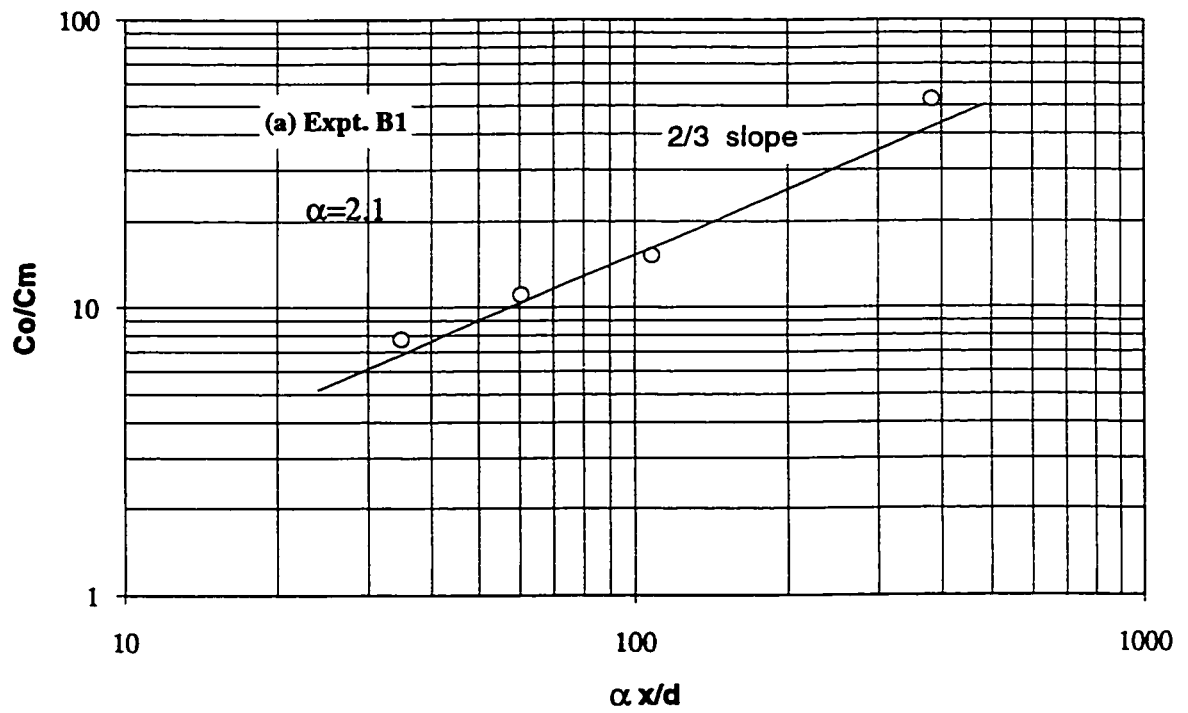for Several Values of α
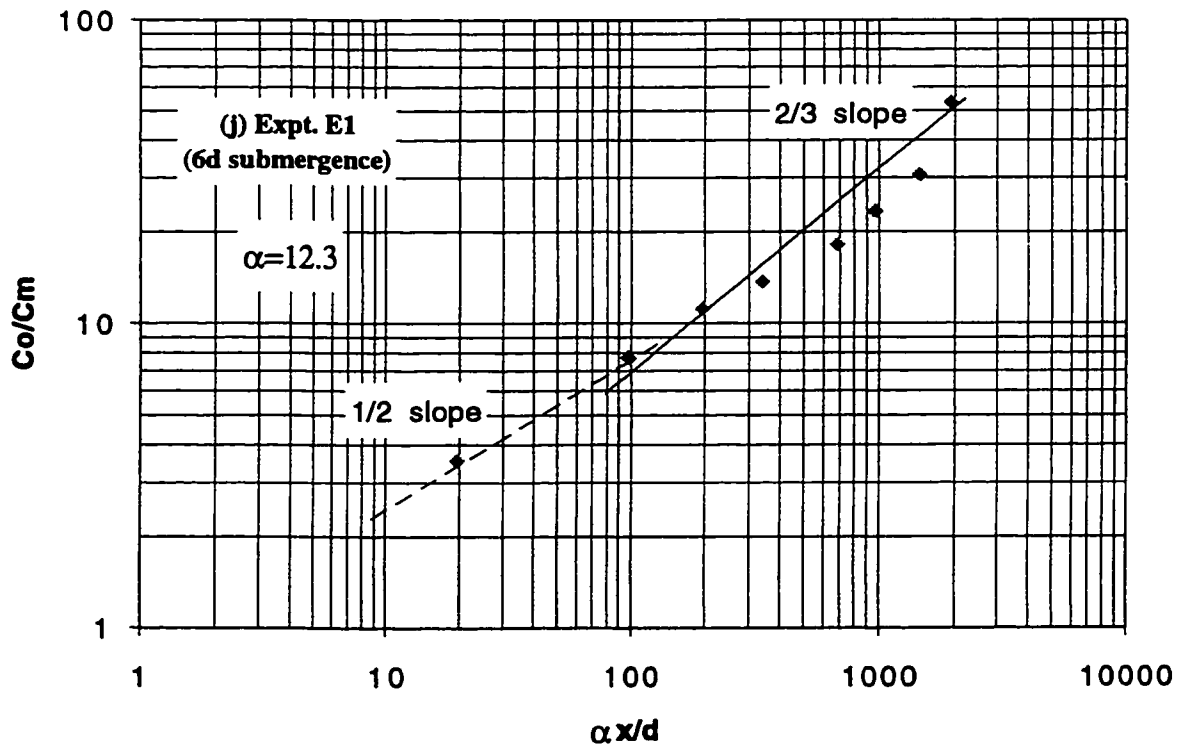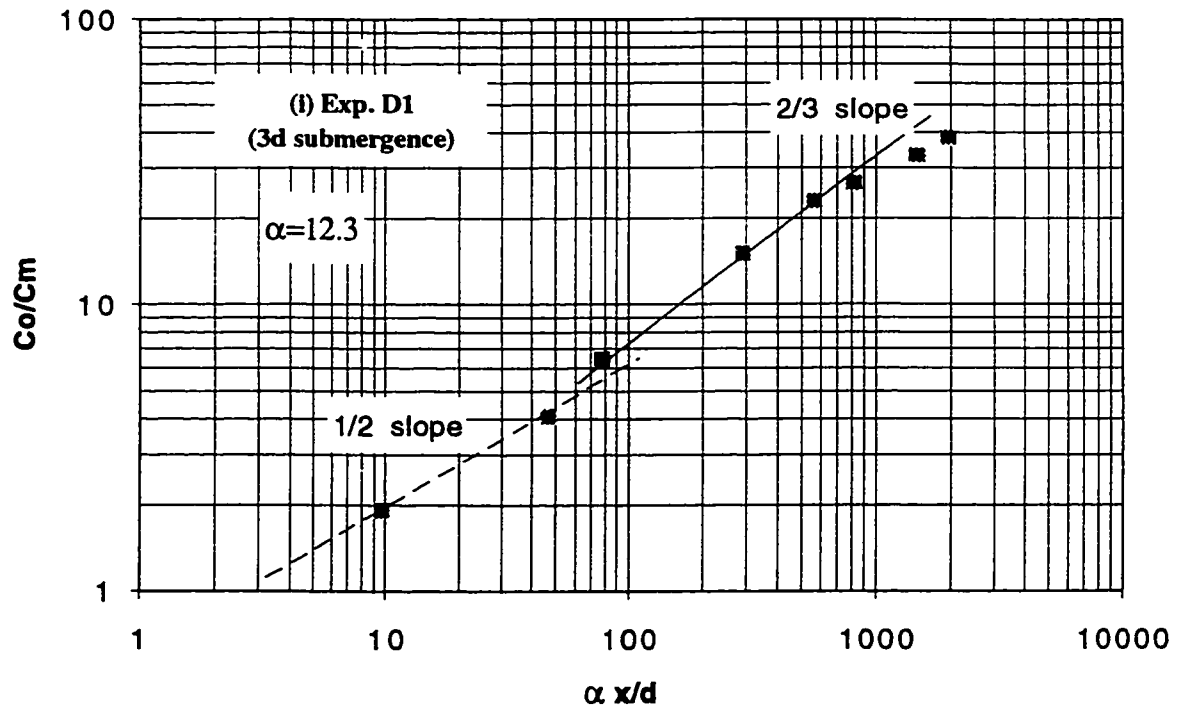
**Fig. 3.26 (i-j) Variation of Minimum Dilution (C_o/C_m) with ($\alpha x/d$)
for Several Values of α**

○	Uo/U=2.1,d=12.7mm
●	Uo/U=4.2,d=12.7mm
◆	Uo/U=6.8,d=12.7mm
■	Uo/U=6.8,d=12.7,(1d)
◇	Uo/U=6.8,d=6.35mm
▲	Uo/U=8.25,d=6.35mm
△	Uo/U=10.3, d=6.35mm
―	Uo/U=12.3,d=6.35mm
▣	Uo/U=12.3,d=6.35mm,(3d)
◈	Uo/U=12.3,d=6.35mm,(6d)
——	Eq. 3.7

Co/Cm
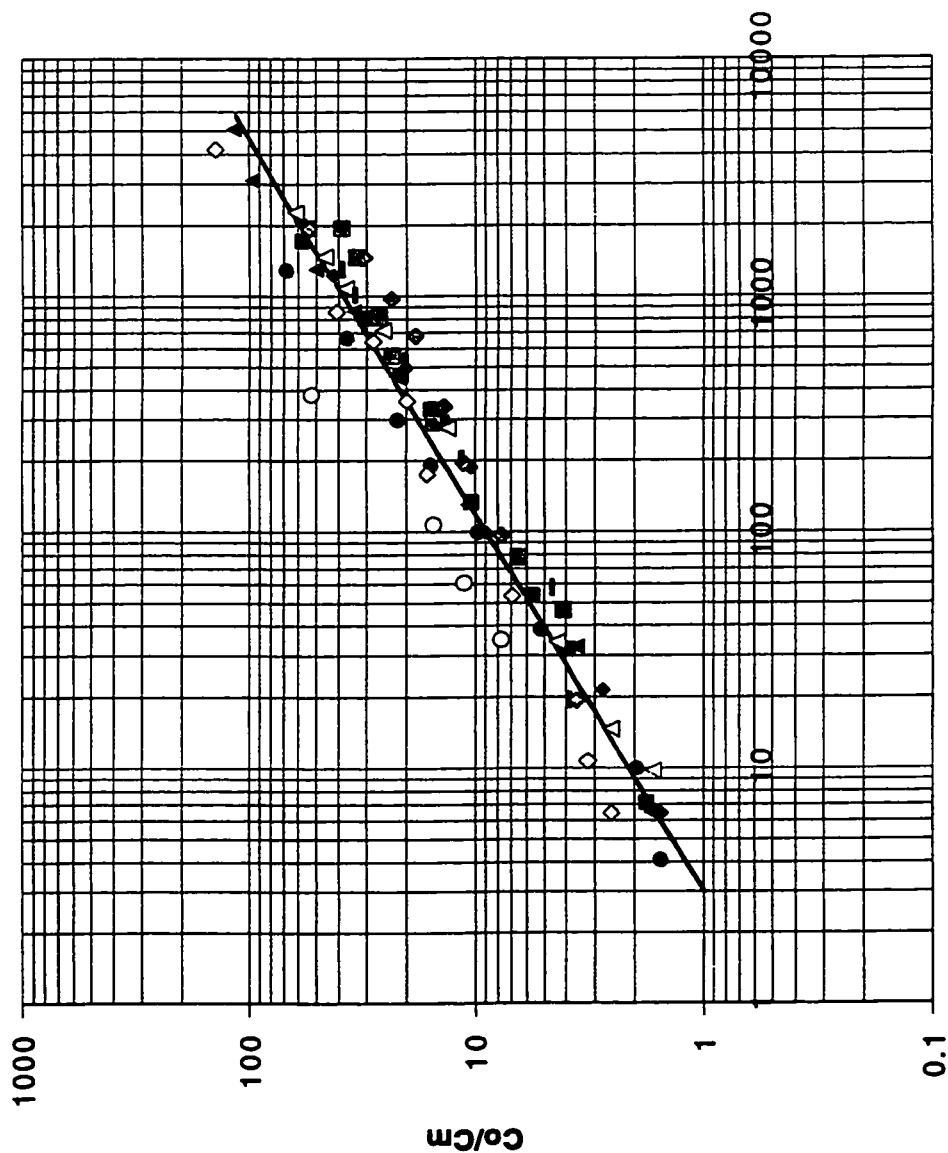
αx / d

Fig. 3.27 General Correlation for Minimum Dilution for Circular Surface Jets in Crossflows
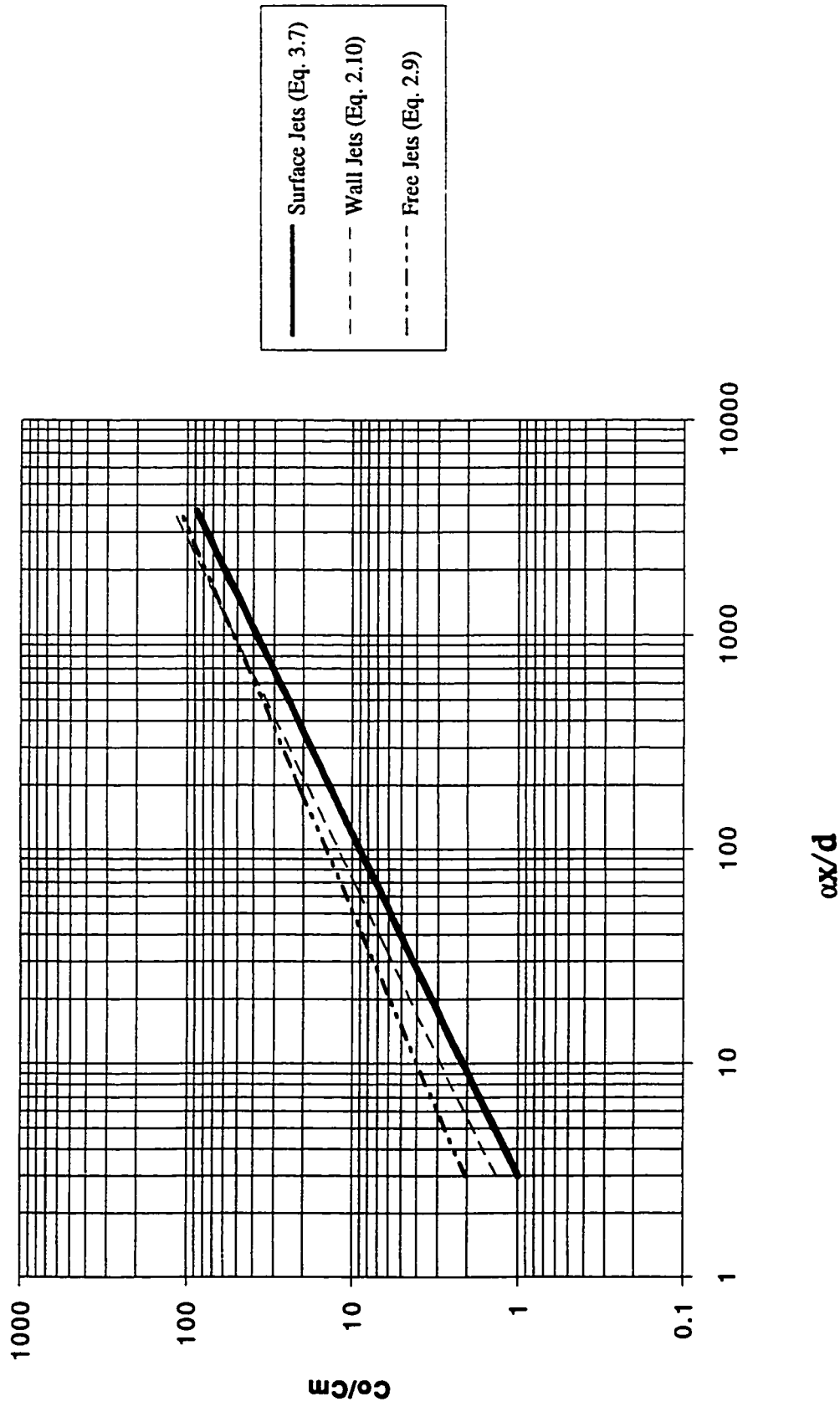
Fig. 3.28 Comparison of Minimum Dilution for Surface Jet, Wall Jet and
Free Jet in Crossflow
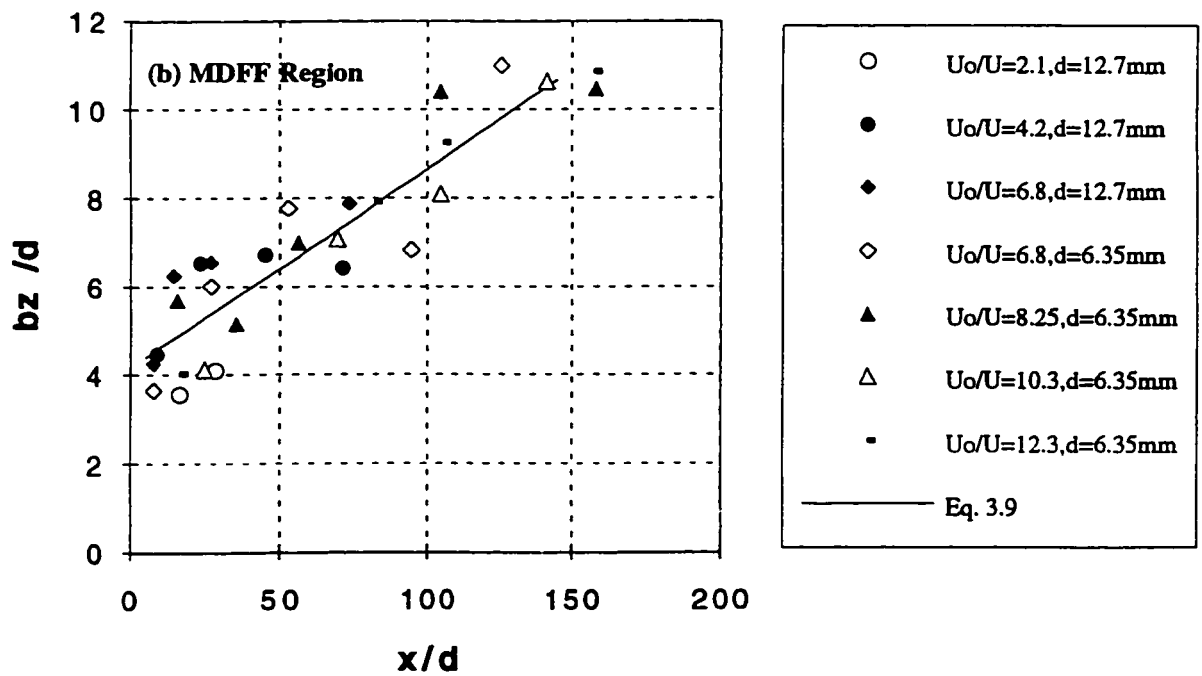
Fig. 3.29 (a-b) Growth of Jet Thickness

Legend:
○ Uo/U=2.1,d=12.7mm
● Uo/U=4.2,d=12.7mm
◆ Uo/U=6.8,d=12.7 mm
◇ Uo/U=6.8,d=6.35mm
◄ Uo/U=8.25,d=6.35mm
◁ Uo/U=10.3,d=6.35mm
▬ Uo/U=12.3,d=6.35mm
—— Eq. 3.10

Fig. 3.30a Growth of Jet Width

Fig. 3.30b Comparison of Jet Width for Surface Jet and Free Jet in Crossflow

127
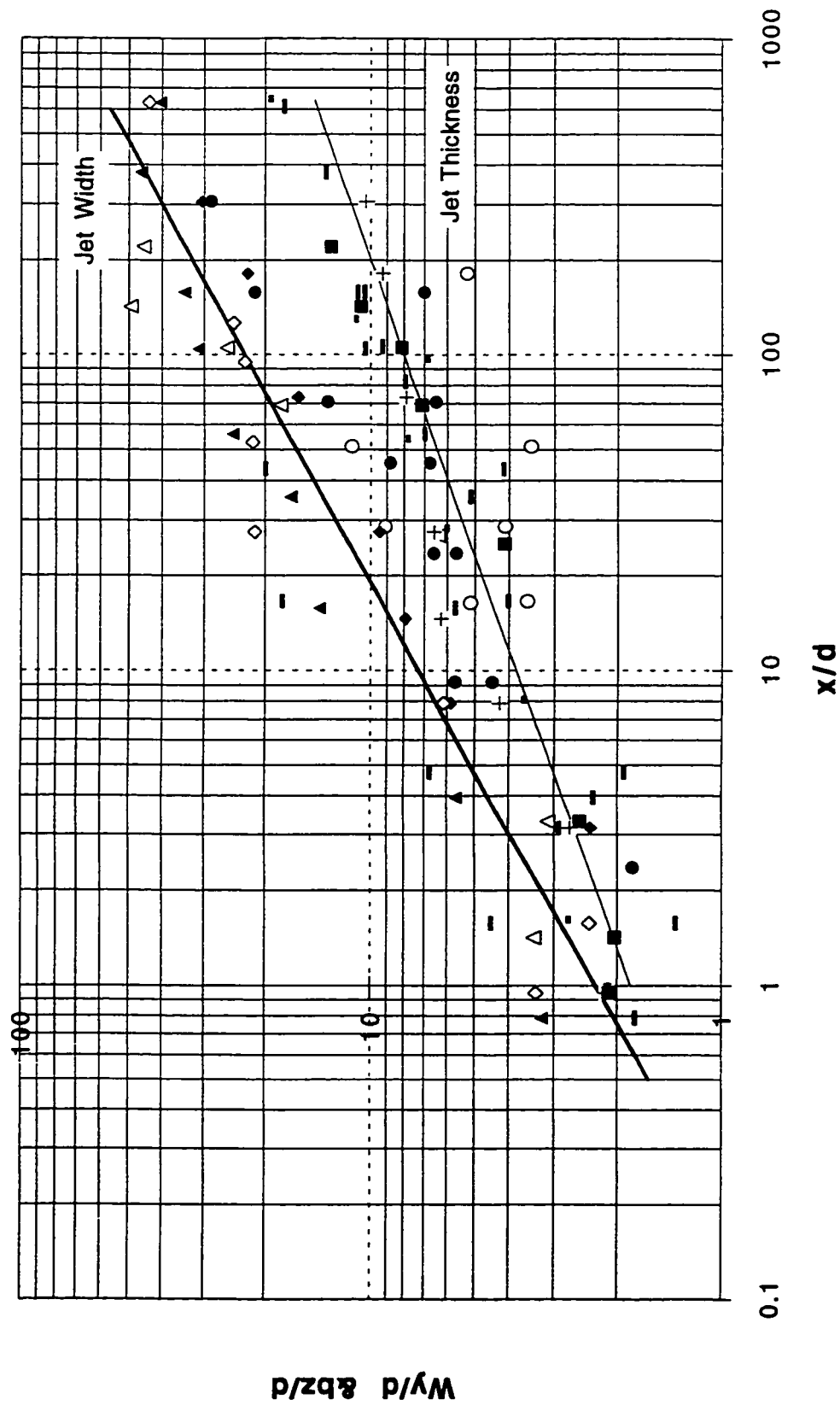
Fig. 3.31 Transverse and Vertical Growth for Surface Jets in Crossflows

128

Chapter 4

Dilution of Multiple Non-Buoyant Circular Jets in Crossflows*

4.1 Introduction

Turbulent jets in stagnant as well as coflowing surroundings have been studied both theoretically and experimentally for many years (see Abramovich 1963 and Rajaratnam 1976 for a list of references). But for jets issuing at right angles into a moving ambient, commonly referred to as jets in crossflows, the investigations have been generally empirical. The earlier studies were of the integral type (see Abramovich 1963 and Rajaratnam 1976) whereas the later studies used dimensional considerations along with simplified models (Wright ,1977). Using a length scale l_m equal to $\sqrt{(M_0 / \rho)} / U$ where M_0 is the momentum flux from the nozzle, ρ is the mass density of the fluid and U is the velocity of the crossflow, the region in which the distance y along the initial direction of the jet is smaller than l_m was called the momentum dominated near field (MDNF). In this MDNF, the crossflow simply pushes the jet downwind, with the jet diffusing essentially as in a stagnant environment. The region where y is larger than l_m was called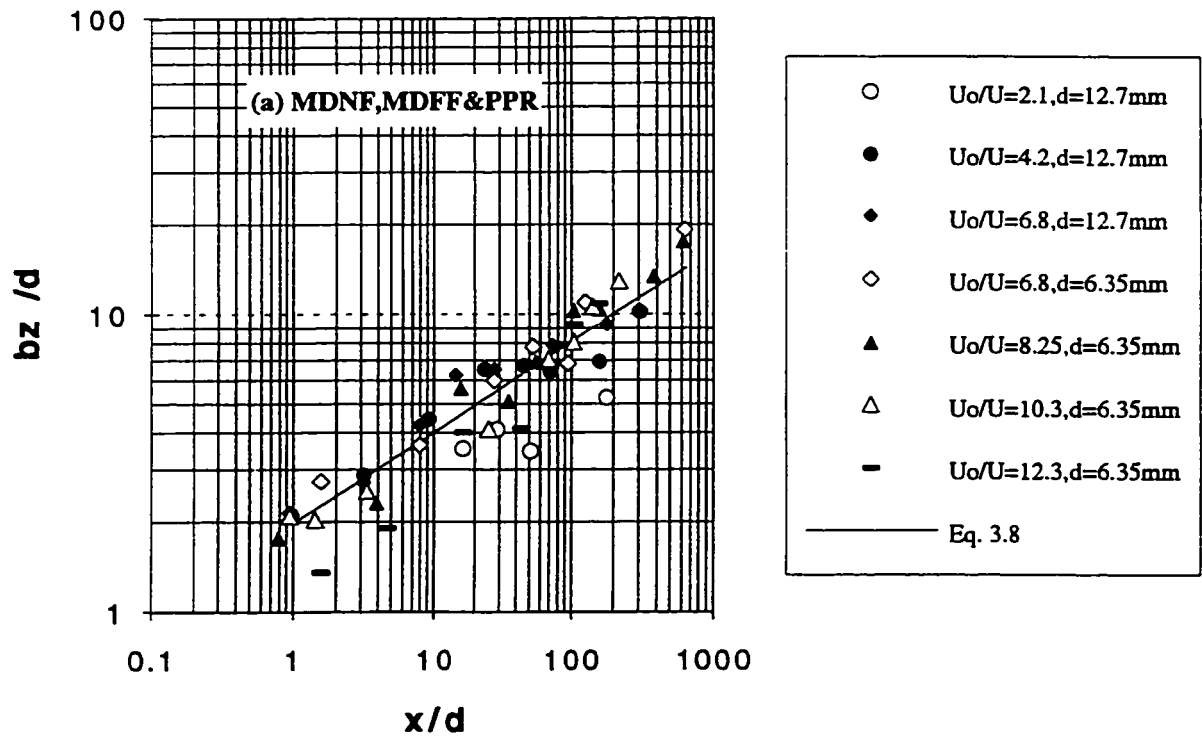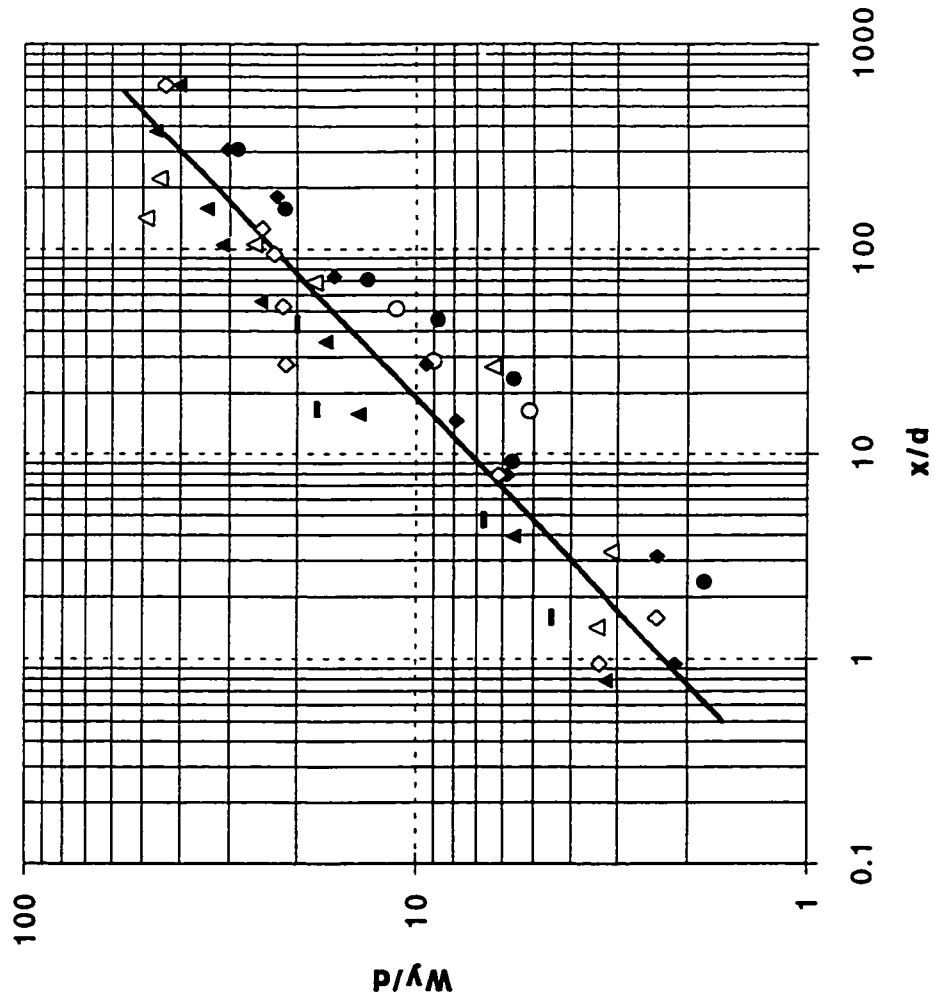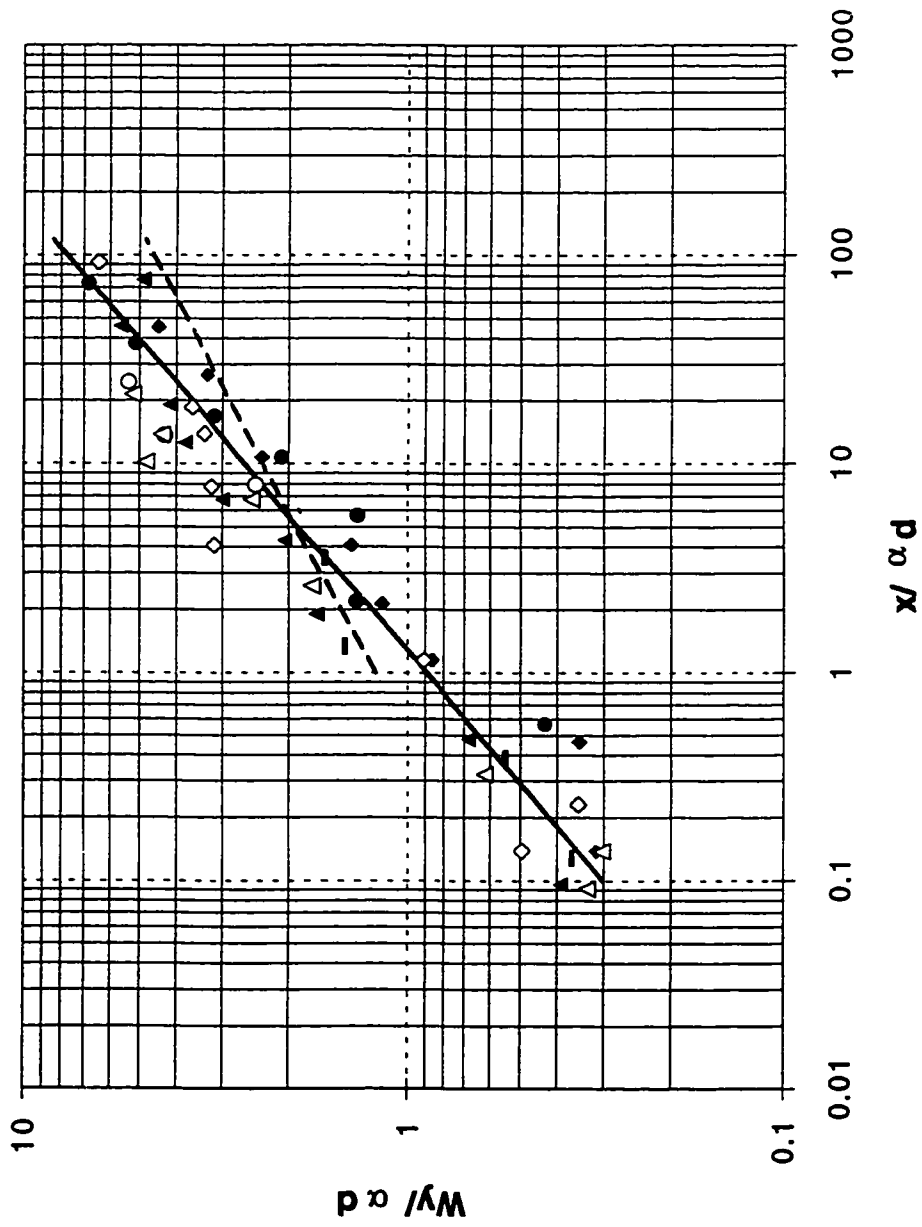 the momentum dominated far field (MDFF). In this region, the deflected jet is replaced by a series of momentum puffs issuing from a line source into the ambient fluid. From these considerations, it has been possible to predict theoretically the trajectory as well as the dilution of the deflected jets, at least partially (See Wright 1977). These two regions are followed by a passive plume region (PPR), in which the excess velocity in the deflected jet above that of the crossflow has disappeared. In this region, the mixing and dilution is due to the turbulence in the ambient flow. The transition from

---

* A paper based on the material in this chapter has been accepted for publication in the Journal of Environmental Engineering of the American Society of Civil Engineers.

129

the MDFF to the PPR was assumed (Rajaratnam and Langat 1995) to occur where the excess velocity in the jet above that of the crossflow falls to about 1% of (U_O-U) where U_O is the velocity of the jet at the nozzle.

The dilution produced by a circular jet discharging from the bed vertically into a channel flow (serving as the crossflow) in the mixing region, defined as the region in which significant dilution occurs because of jet mixing, was investigated by Hodgson and Rajaratnam (1992). It was found that for the minimum dilution, defined as the ratio of the concentration at the port C_O to the maximum concentration at a section C_m, to reach about 50, the mixing region had to be extended through the momentum dominated near and far fields to a part of the passive plume region. In this mixing region, using the concept of the MDNF and MDFF and experimental observations, $\alpha x/d$ was found to be a characteristic dimensionless distance (Hodgson and Rajaratnam, 1992) and the minimum dilution was given by the expression

$$\frac{C_o}{C_m} = 1.09(\frac{\alpha x}{d})^{0.56} \qquad (4.1)$$

where x is the downstream distance along the crossflow from the source of the jet of diameter of d and α is the ratio of the velocities of the jet to that of the crossflow. Empirical equations were also developed for the growth of the width and thickness of these jets. Rajaratnam and Langat (1995), presented a dimensionless plot of $\alpha x/d$ against α (see Fig. 3.9) showing the three separate regions (MDNF, MDFF, and PPR) for single jets in cross flows.

In some outfalls built in river beds for discharging effluents from larger plants in to the river as jets in crossflow, the outfall would have several jets. These jets would merge after traveling some distance as individual jets and further downstream, the effect of the individual jets might be lost. This study was performed to understand the characteristics of such cases of multiple jets in crossflow. The

crossflow was maintained deep so that the jets did not surface in the mixing region. Even though there is a considerable body of literature on multiport diffusers, most of these studies are concerned with either sewage outfalls in the ocean; thermal discharges in lakes or in coflowing streams (Fischer et al. 1979, Parr and Melville 1981, Adams 1982, Jirka 1982; Isaacson et al. 1983, Jirka and Akar 1991 and Roberts et al. 1989). Several ideas from these studies are used as guides in analyzing the experimental results obtained in this investigation. Several jet discharges with different α values were studied. The effect of spacing and the number of ports on the minimum dilution was also investigated. The results from this study are believed to be potentially useful in the design and analysis of outfalls in rivers.

4.2 Experimental Arrangement

The experiments were performed in a rectangular flume, 0.91 m wide, 0.77 m deep and 36.5 m long. Water was pumped to the flume from the laboratory sump and the flow was measured using a magnetic flow meter. The depth of flow D in the flume was controlled using a tailgate. The mean velocity in the flume was obtained from the measured discharge and the cross-sectional area of flow. The flow in the channel was fully developed at the location of the diffuser.

Identical jets with diameters of 7.93 mm and 4 mm were produced from the bed from a cylindrical reservoir, 206 mm in diameter and 310 mm long, placed under the flume. The length of the diffuser (L) defined as the distance between the centers of the outermost ports (see Fig.4.1 (a)), was kept constant and was approximately equal to 127 mm. The width of the flume was seven times the length of the diffuser and it was observed that the growth of the jets from the diffuser was not affected by the sidewalls of the flume. The diffuser was placed at a distance of about 22m downstream of the flume entrance. The number of the ports n was either 3 or 5. The spacing between the ports S was equal to either 8 d or 16 d. A 1/3 horse

power (250 watts)Jacuzzi pump raised the water from a 900 liter tank to a constant head tank placed about 3.5 m above the flume which provided the flow to the cylindrical reservoir feeding the ports. The total discharge (Q) through all the ports was measured with a calibrated Fischer rotameter. The jet velocity U_0 was obtained from the discharge Q and the total cross sectional area of the ports.

Rhodamine WT with a market concentration of 20% by weight and specific gravity of 1.19 was used as the tracer. The dye was mixed thoroughly in the 900 L tank with water pumped from the sump which also provided water for the crossflow. Fluid samples were obtained from the deflected jets by means of L-shaped sampling tubes with an internal diameter of 2.36 mm fixed to one of two rakes. Both rakes were mounted on a traverse which allowed movement in the transverse direction z (see Fig. 4.1 for a definition sketch). The first rake was vertical and housed 13 tubes with the spacing varying from 10 to 20 mm as shown in Fig. 4.2 This rake could be adjusted so that sampling could take place in the η direction simultaneously at distances close to the diffuser such that the tubes were perpendicular to the jet axis ξ. The axis of the deflected jets was determined through visual observations of jets using food dye. Figure 4.3 (a-d) shows typical jet trajectories, viewed from above. The second rake had up to 15 L-shaped tubes placed horizontally with a spacing varying from 20 to 40 mm. The tubes were set to withdraw the samples at the same level in the z axis simultaneously. This rake was used for sampling at sections relatively far from the nozzles where the jet axis ξ was almost parallel to the x axis and hence the η axis would coincide with the y axis.

The sampling tubes were connected to a siphoning system of vinyl tubes discharging the samples into 60 mL opaque plastic bottles positioned outside the flume. The sampling was done at approximately the same velocity as that at the sampling site. The concentration of the Rhodamine dye in the jet fluid was measured by a portable fluorometer (Turner model 10). The fluorometer was calibrated using

13 dye standard solutions over a range of 0.05 to 70 ppb. The calibration curve indicated that the fluorescence was a linear function of the tracer concentration. The initial concentration C_O at the nozzle ranged from about 30 to 50 ppb, with this relatively low concentration the specific gravity of the dye introduced could be considered equal to 1.0.

4.3 Experiments and Experimental Results

A total of eight experiments with almost 80 runs were conducted and the primary details of these experiments are shown in Table 4.1. Three series of experiments A, B and C were performed. The jet nozzles had two diameters of 4 mm and 7.93 mm. The velocity ratio α was varied over a practical range of 3.5 to 10. The number of ports n was equal to 3 or 5. The spacing S between the ports was given two values of 8d and 16d. The relative depth of the crossflow D/d was maintained in the range of 34 to 57 to ensure that the jets did not surface in the mixing region. The Reynolds number of the jets for all the experiments was greater than 4000 Concentrations were sampled at different downstream distances with different combinations of the velocity ratio α, number of ports n and jets spacing S.

Concentration field in the deflected jets was measured in the transverse direction z, in the η direction as well as in the vertical direction y at different stations along the jet axis ξ. Concentrations were sampled at up to 10 sections downstream of the diffuser for each of the conditions investigated and a total of about 8000 concentration measurements were made. The concentration measurements covered a distance of x/d=160 where x is the longitudinal distance downstream the diffuser. In terms of the transformed distance $\alpha x/d$, the measurements covered a range from 8 to 1500. The concentration at any point C was normalized by the concentration at the nozzle C_O.

4.3.1 Transverse Concentration Profiles

Typical transverse concentration profiles in the plane in which the maximum concentration occurs are plotted in Fig. 4.4 (a-f) for different sections downstream of the diffuser. For all the runs, the jets were not affected by the side walls of the flume. For stations closer to the ports, the three peaks may be noticed and for larger values of x, the individual peaks have disappeared. Fig.4.4 (c-d) shows corresponding results for $\alpha=8$ and $\alpha=10$. In Fig.4.4 (c-d), at large values of x, the concentration profiles show two peaks. It should be noted that the twin peaks profile occurred within the MDFF where bimodal concentrations are likely to occur because of the circulation caused by the component of the crossflow velocity perpendicular to the deflected jet. These bimodal distributions were observed in only a few experiments. Figures (4.5-4.12) show typical transverse concentration profiles in several horizontal planes at different longitudinal distances for different experiments. The concentration field in the jet is described even more clearly by plotting concentration contours at a number of sections. Typical concentration contours are shown in Fig. 4.13 (a-h), wherein concentration at any point C is normalized by the maximum concentration C_m at that section. It can be seen that generally the concentration field was unimodal and was nearly axisymmetric. For high velocity ratio of $\alpha=10$ in the MDFF (x=650mm), the concentration field was bimodal and there was a shift of the maximum concentration location from the mid plane to the vortex centers as shown Fig. 4.13 (e).

4.3.2 Vertical Concentration Profiles

Fig. 4.14 (a-h) show typical concentration profiles in the vertical planes passing through the point of maximum concentration for all the experiments. The effect of the bottom of the channel in restricting the growth of the jet in the vertical direction was noticed for small α ($\alpha=3.5$ & $\alpha=5$) where the concentration near the

bed reached a value of about 60% of the maximum concentration at the section in the PPR. On increasing the number of ports to 5, the effect of the bottom of the channel on the vertical growth of the jet was mostly noted for the case with $\alpha = 5$ (Experiment C1, Fig.4.14g). In this case, the jets became attached to the bed quite close to the diffuser at $x/\alpha d=5$.

4.3.3 Flow Regions

A study of all the concentration profiles indicated that the flow field of the multiple jets in a crossflow may be divided into three different regions which can be termed as zones I, II, III respectively as shown in Fig. 4.1. In zone I, each jet diffuses without any significant interference from its neighbors. From visual observations, it was found that the merging distance x_m of the jets depended on the velocity ratio α as well as on the relative spacing S/d between ports. As α increased the merging distance of the jets was found to decrease. Based on the dilution data, values for the dimensionless term $x_m/\alpha d$ were approximated. For the experiments in series A and C, $x_m/\alpha d$ was found to vary from 1.8 for $\alpha = 3.5$ to 0.22 for $\alpha=10$. As the spacing between the ports increased, the jets tended to merge further downstream and $x_m/\alpha d$ was found to vary from 5 to 2.5 for $\alpha = 5$ to 8. The experimental observations were described by the equation

$$\frac{x_m}{\alpha d} = 1.5[\frac{S}{\alpha d}]^{0.46} \qquad (4-2)$$

with the coefficient of determination equal to 0.96. Eq. 4.2 is plotted in Fig. 4.15a. It was found that zone I approximately occurred in the MDNF.

A transition zone (zone II) occurred where there was a partial merging of the jets. Figs. (4.5a, 4.6a, 4.10a) show typical concentration measurements in zone II. In zone III, the jets have merged completely. Except for cases where bimodal

135

concentration distributions were found, the concentration profile becomes approximately uniform across the whole length of the diffuser, at least in the transverse plane in which the maximum concentration for that section occurs. The distance x_{fm} at which the jets were fully merged was also dependent on the velocity ratio α as well as the spacing between the ports. As α increases the distance $(x_{fm}/\alpha d)$ decreases. The distance $(x_{fm}/\alpha d)$ varied approximately from 12.6 to 2.2 for $\alpha=3.5$ to 10 for the A series. On increasing the spacing between the ports (Series B), the distance $(x_{fm}/\alpha d)$ increased to 25 to 17 for $\alpha=5$ to 8 . The distance x_{fm} was approximately described by the following equation:

$$\frac{x_{fm}}{\alpha d} = 0.61[\frac{S}{\alpha d}]^{0.41} \qquad (4\text{-}3)$$

with a coefficient of determination equal to 0.92. Eq. (4-3) was plotted in Fig.4.15b. It was found that zone III occurred in the MDFF region.

4.4 Analysis of the Experimental Results

4.4.1 Minimum Dilution

The minimum dilution at any section is defined as the ratio of the concentration at the ports (C_0) to the maximum concentration at a section (C_m). Following the work of Hodgson and Rajaratnam (1992) for single jets in crossflow, the variation of the minimum dilution C_0/C_m with the dimensionless distance $\alpha x/d$ was studied for all the experiments. The measurements covered a range of $\alpha x/d$ from 8 to 1500. Fig. 4.16(a-c) show the variation of C_0/C_m with $\alpha x/d$ for all three series of experiments.

For the present study, very few data points were located in the MDNF compared to the MDFF, yet from regression analysis based on all the observations in the MDNF, the exponent in the power law relation for the minimum dilution was equal to 0.5 as shown in Fig. 4.17. For larger values of $\alpha x/d$ in the MDFF, the

variation of the minimum dilution with $\alpha x/d$ is affected to some extent by α for values of α equal to 3.5 and 5 where a dilution of 50 is obtained at a distance $\alpha x/d=1000$. As α assumes larger values, the minimum dilution tends to decrease with $\alpha x/d$ and C_o/C_m drops to 30 at $\alpha x/d=1000$ for $\alpha=10$ (Fig. 4.16a). The effect of α on the minimum dilution can also be noticed from the experiments in series B and C. In Fig. 4.16b, the minimum dilution decreases from about 80 at $\alpha x/d=1000$ to 55 when α was increased from 5 to 8. Similarly, it can be seen that in Fig.4.16c the minimum dilution decreases from about 40 at $\alpha x/d=1000$ to 25 when α was increased from 5 to 8. The dilution results for multiple jets were compared to the case of single jets discharging in crossflows (Hodgson and Rajaratnam 1992) by showing Eq. 4.1 in Fig. 4.16 (a-c) . For series A ($\alpha=3.5$ to 10, n=3, S=8d) It can be seen that for $\alpha x/d < 100$, the dilution produced by a single jet is generally the same as that produced by multiple jets. For $\alpha x/d>100$ and with the increase of α ($\alpha=8$ and 10), the dilution produced by a single jet is generally more than that of multiple jets. For experiment B1 where the spacing between the jets was increased (S/d=16) and with a relatively low velocity ratio ($\alpha=5$), the dilution at $\alpha x/d=400$ was more than that predicted by Eq.4.1 (Fig.4.16b). The deviation of the dilution data from Eq.4.1 for low α values was also noticed by Hodgson and Rajaratnam (1992). On increasing the number of ports (Experiments C1), the dilution produced by the multiple jets was generally less than that produced by the single jets. (Fig. 4.16c).

To study the effect of increasing the spacing on minimum dilution, the observations from experiments of series A are compared with that of series B for $\alpha=5$ and 8 in Fig. 4.18. The results indicate that there is generally an increase in dilution when the spacing between the ports increases for $\alpha x/d>100$. For $\alpha=5$, the dilution ratio was approximately 85 at a distance of $\alpha x/d=1000$ for S/d=16. This value is about 1.7 times greater than that for S/d=8. For $\alpha=8$ the dilution for S/d=16 was about 1.4 times greater than that of S/d=8. When the distance between the ports

was relatively small (S/d=8), the jets tended to entrain each other closer to the diffuser. The ambient diluting water was less entrained into the core of the merged jets and hence less dilution occurred. In the case of wider spacing (S/d=16), there was sufficient space between the ports and the merging of the jets was delayed and this allowed the individual jets to be distinct which resulted in more dilution.

Fig. 4.19 shows that the increase of the number of ports caused a decrease in dilution. The dilution for the case of 3 ports was about 1.4 times that for the case of 5 ports at $\alpha x/d=1000$. This effect was also shown by Davis et al (1978), where the increase of the number of ports for buoyant discharges in a stagnant ambient had resulted in lower dilution rate. This was due to the interference of the merging plumes on the entrainment mechanisms. The decrease of the available surface area upon merging leads to a decrease of the entrainment of each individual jet.

4.4.2 Similarity of Concentration Profiles

The transverse concentration profiles at the maximum concentration planes were tested for similarity. The transverse distance b_z measured from the centerline of the diffuser to the location where the concentration was equal to one half the maximum concentration C_m was used as the length scale and the maximum concentration C_m was used as the concentration scale. The transverse concentration profiles which were considered for similarity were in Zone III. Fig. 4.20 (a-h) shows the non-dimensional transverse concentration profiles for all the runs. A consolidated set is shown in Fig. 4.21 for all the experiments. It can be seen that the except for the bimodal sections concentration profiles are approximately similar at different sections for different test conditions.

The vertical concentration profiles were also tested for similarity by normalizing the concentration C at any point with C_m and the distance measured along the η direction by b* where the concentration was equal to one half the

maximum concentration C_m. Fig.4.22 (a-f) shows a typical set of dimensionless profiles for several sections. As mentioned earlier the effect of the bed on the jets spreading in the vertical direction was noticed on increasing the number of ports to 5 with a relatively small velocity ratio ($\alpha=5$) and hence the data from experiment C1 could not be examined for similarity. Fig. 4.23 shows a consolidated plot for all the runs except experiment C1. Fig.4.23 shows that the jets after merging were also similar in the vertical direction and they could be described well by the exponential equation

$$\frac{C}{C_m} = \exp[-0.693 * (\frac{\eta}{b_*})^2] \qquad (4\text{-}4)$$

4.4.3 Centerline Profiles

The location at which the maximum concentration occurred was used to define the jets center line position y_c. The centerline profile was expressed in terms of the downstream distance $x/\alpha d$. For experiments of series A, the entire data set was fitted by the equation

$$\frac{y_c}{\alpha d} = 1.10(\frac{x}{\alpha d})^{0.25} \qquad (4\text{-}5)$$

For series B where the spacing between the ports S/d was increased to 16, the trajectory of the jets was slightly higher than that for Series A ($S=8d$). The observations were fitted by the equation

$$\frac{y_c}{\alpha d} = 1.35(\frac{x}{\alpha d})^{0.21} \qquad (4\text{-}6)$$

139

The jet centerline profile for single jet in crossflows was described by Hodgson and Rajaratnam (1992) by the equation:

$$\frac{y_c}{\alpha d} = 1.46 (\frac{x}{\alpha d})^{0.46} \qquad (4\text{-}7)$$

The centerline profile data were examined as a function of the downstream distance for all the runs as shown in Fig. 4.22 except Experiment C1. A general equation for the centerline profile was found to be

$$\frac{y_c}{\alpha d} = 1.14 (\frac{x}{\alpha d})^{0.25} \qquad (4\text{-}8)$$

with a correlation coefficient of 0.89. Eq. 4.7 is compared with Eq. 4.8 in Fig.4.24. It can be seen that the merged trajectories are located below that of the single jet in crossflow. The same was noticed for merging buoyant discharges in coflowing streams (Cheng et al. 1992). From Fig. 4.24 it can be noticed that for Experiment C1 the interaction of the merged jets with the bottom of the channels resulted in the lowering of the jets.

4.4.4 Width and Thickness of Jets

The width of the jets (W_z) is defined as the distance measured along the z axis where the concentration on either side of the diffuser centerline is either 10% (W_{z10}) or 50% (W_{z50}) of the maximum concentration. The data for both the unimodal and bimodal distributions were examined and the width was expressed in terms of the length of the diffuser L and the downstream distance $x/\alpha d$ (Fig. 4.25 (a-b)).

The jet width (W_{z10}) for all the runs can be expressed by the equation:

$$\frac{(W_{z10} - L)}{\alpha d} = 1.61(\frac{x}{\alpha d})^{0.38} \qquad\qquad (4\text{-}9)$$

with a correlation coefficient of 0.93. An expression for the jet width W_{z50} where C/C_m is 50% can be expressed as:

$$\frac{(W_{z50} - L)}{\alpha d} = 1.02(\frac{x}{\alpha d})^{0.30} \qquad\qquad (4\text{-}10)$$

It should be noted that for Series C1, the width of the jets for distance $x/\alpha d$ up to 15 could not be represented by Eq. 4.10. This was due to the interaction of the bottom of the channel with the jets.

The thickness of the jets W_y is defined as the distance measured along the η and the y directions where the concentration on either side of the jets centerline is 50% of the maximum concentration. The jet thickness in terms of αd was related to the dimensionless distance $x/\alpha d$ by the equation

$$\frac{W_y}{\alpha d} = 0.89[\frac{x}{\alpha d}]^{0.43} \qquad\qquad (4\text{-}11)$$

with a correlation coefficient of 0.94. (Fig.4-26) . For experiment C1, due to the interference of the bed with the spreading of the jets as mentioned earlier, the thickness was determined as the distance measured from the bed to the point at the section where the concentration was 50% of the maximum concentration at that section. The thickness of a single jet discharged in crossflow was described by Hodgson and Rajaratnam (1992), using the following expressions:

$$\frac{W_y}{\alpha d} = 0.78[\frac{x}{\alpha d}]^{0.52} \quad x/\alpha d < 1 \qquad\qquad (4\text{-}12)$$

$$\frac{W_y}{\alpha d} = 0.78[\frac{x}{\alpha d}]^{0.37} \quad x/\alpha d > 1 \qquad (4\text{-}13)$$

On comparing the thickness of the single jet to that of the multiple jets , it was noticed that the thickness was larger for the case of multiple jets (Fig. 4.26). The thickness for multiple jets was approximately 1.8 times that for single jets in crossflow.

4.5 Summary and Conclusions

This paper presents the results of a laboratory study on the mixing characteristics of circular non-buoyant multiple jets discharged in relatively deep crossflows. The experiments were carried out with the velocity ratio (α) varying from 3.5 to 10. Three and five ports were used and the spacing (S) between the ports was varied from 8d to 16 d. The concentration measurements were carried out for a maximum relative distance of x/d=160. The concentration profiles in the vertical as well as the lateral directions in the planes of maximum concentration were found to be similar. A minimum dilution up to 80 was reached in the mixing region. It was found that the minimum dilution decreased with the increase of the velocity ratio α and the increase in the number of ports. Increase of the spacing between the ports resulted in a considerable enhancement of the dilution. The trajectory of the multiple jets was identified based on the maximum concentration location. Trajectory data indicated that discharges from multiple jets rose more slowly than that from a single jet. Finally, expressions describing the growth of the jets width and thickness were developed.

4.6 References

Abramovich, G. N. (1963). The Theory of Turbulent Jets. English Translation, M.I.T. Press, Cambridge, Mass., USA, 671p.

Adams, E.E. (1982). "Dilution for unidirectional diffusers." J. of the Hydr. Div., ASCE, 108 (HY3), 327-342.

Cheng, C. Wood, I.R., and Davidson, M.R. (1992)."Merging buoyant discharges in an ambient current." J. Hydr. Res., 30 (3), 361-372.

Davis, L. R., Shirazi, M.A., Siegel, D.L. (1978). "Measurement of buoyant jet entrainment from single and multiple sources." Journal of Heat Transfer, ASME, Vol. 100, 442-447.

Fischer , H. B. , List, J. E. , Koh , R. C. , Imberger, J., Brooks, N. H. (1979). Mixing in inland and coastal waters. Academic Press, Inc.

Hodgson, J. E. and Rajaratnam, N. (1992). "An experimental study of jet dilution in crossflows". Canadian Journal of Civil Engineering, 19 (5), 733-743.

Isaacson, M.S., Koh, R. C. Y and Brooks, N.H.(1983). "Plume dilution for diffusers with multiport risers. "J. Hydr. Engrg., 109 (2), 199-228.

Jirka, G.H. (1982). "Multiport diffusers for heat disposal : A summary." J. Hydr. Div., ASCE, 108 (12), 1425-1468.

Jirka, G.H., and Akar. (1991). "Hydrodynamic classification of submerged multiport diffuser discharges." J. Hydr. Engrg., ASCE, 117 (9), 1113-1128.

Langat, J. K. (1994). Dilution of circular wall jet in crossflow. Masters thesis, Univ. of Alberta, Edmonton, Alberta, Canada.

Parr. A. D. , Mellville.J.G. (1981). "Nearfield performance of river diffusers.", J. of Env. Engrg. ASCE, 107 (EE5), 995-1008.

Rajaratnam, N. (1976). Turbulent Jets. Elsevier Publishing Co., The Netherlands, 304p.

Rajaratnam, N. and Langat, J. K. (1995)." Mixing of circular turbulent wall jets in crossflows.", J. of Hydr. Engrg. ASCE, 121(10), 694-698.

Roberts, P.J.W. , Snyder,W.H. , Baumgartner, D. J. (1989)."Ocean outfalls. I Submerged wastefield formation." Journal of Hydraulic Engineering ASCE, Vol. 115, No. 1 pp 1-25.

Wright, S. J. (1977). "Effects of ambient crossflows and density stratification on the characteristic behavior of round turbulent buoyant jets". Report No. KH-R-36, W. M. Keck laboratory of Hydraulics and Water Resources. California Institute of Technology, California, USA, 254 p.

Table 4.1 Details of Experiments on Multiple Jets in Crossflows

Experiment No.	Diameter d(mm)	Number of Ports n	Spacing S	Depth of Flow D (mm)	Jet Velocity Uo (m/s)	Channel Velocity U (m/s)	$\alpha = Uo/U$	Jet Reynolds No. R=Uod/v
A1	7.93	3	8d	270	0.62	0.176	3.5	4908
A2	7.93	3	8d	270	0.90	0.18	5	7139
A3	7.93	3	8d	350	1.35	0.169	8	10709
A4	7.93	3	8d	450	1.69	0.169	10	13387
B1	4	3	16d	182	1.51	0.30	5	6050
B2	4	3	16d	182	2.41	0.30	8	9642
C1	4	5	8d	182	1.45	0.29	5	5785
C2	4	5	8d	182	1.83	0.23	8	7324

145
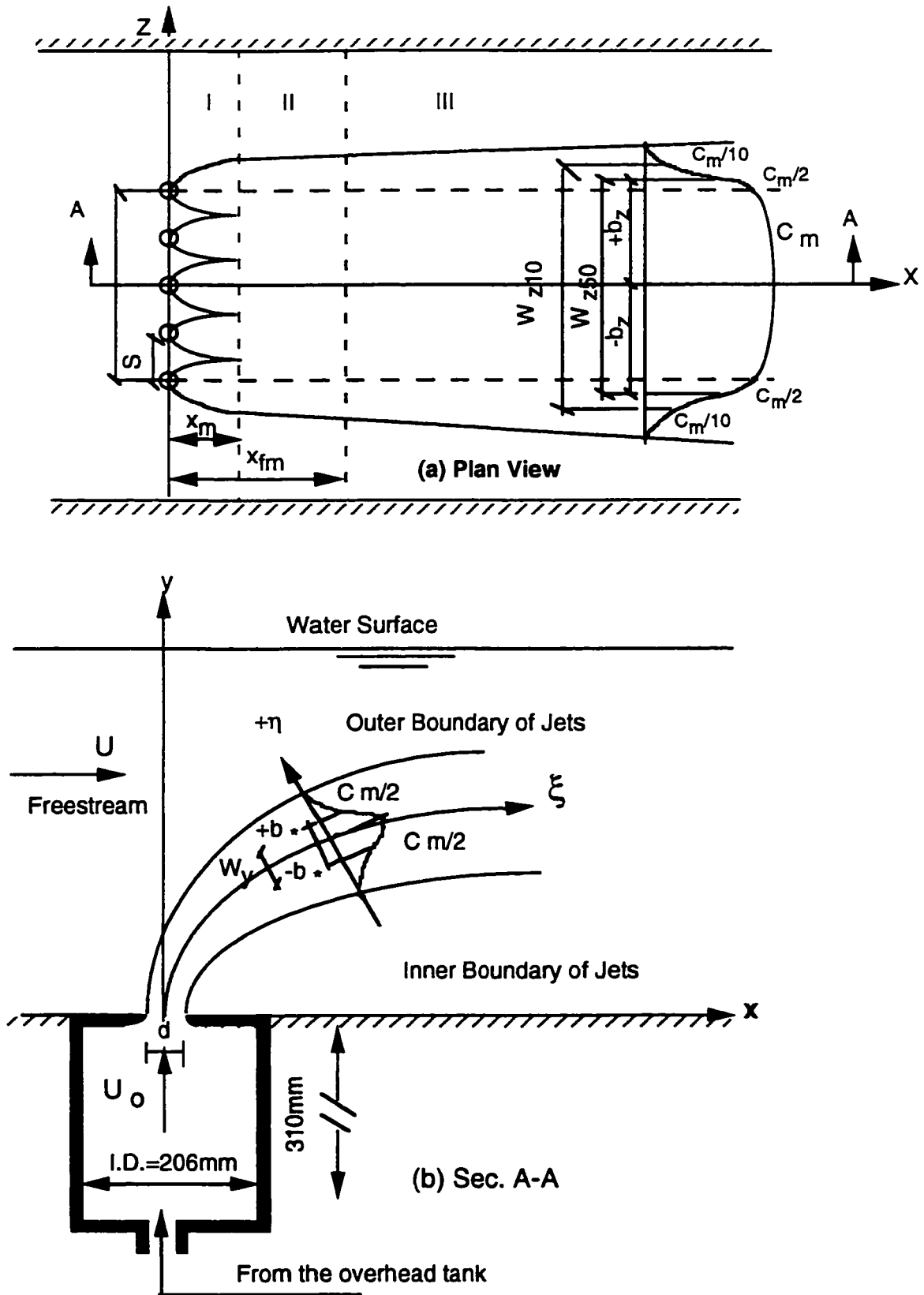
Fig. 4.1 (a-b) Definition Sketches of Multiple Jets in Crossflow
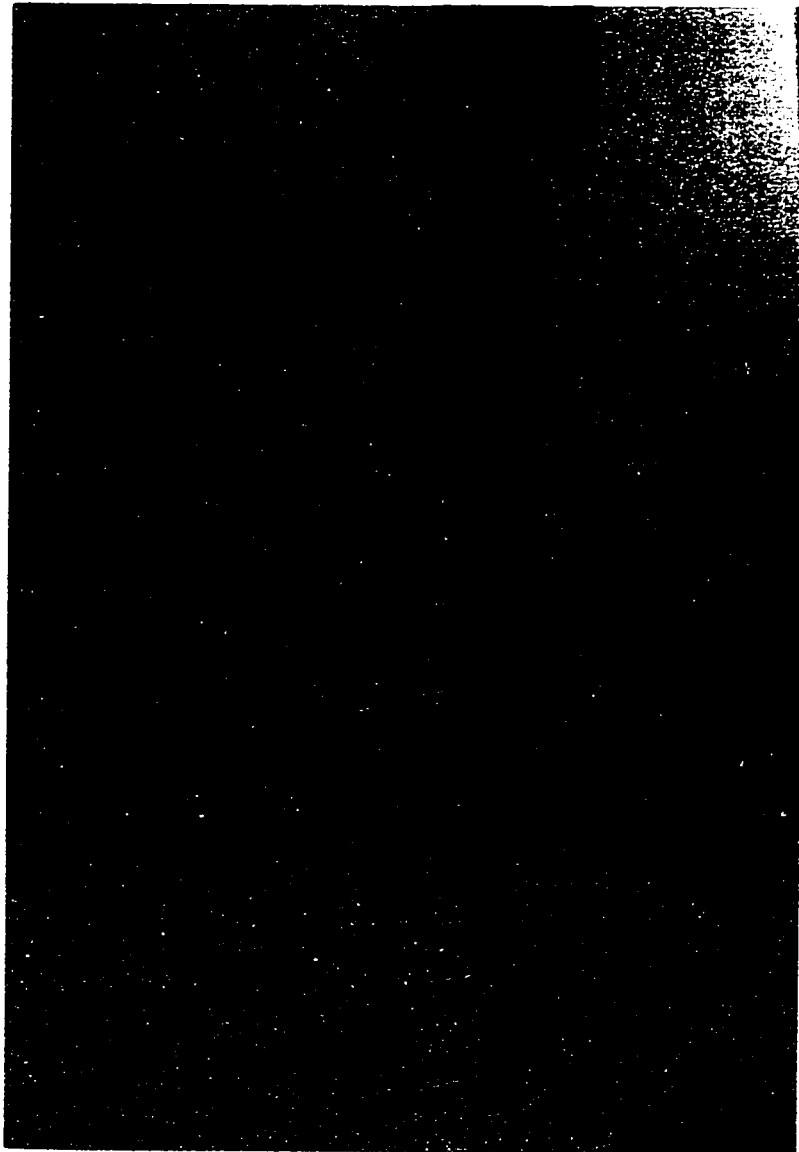
Fig. 4.2 Sampling Rake
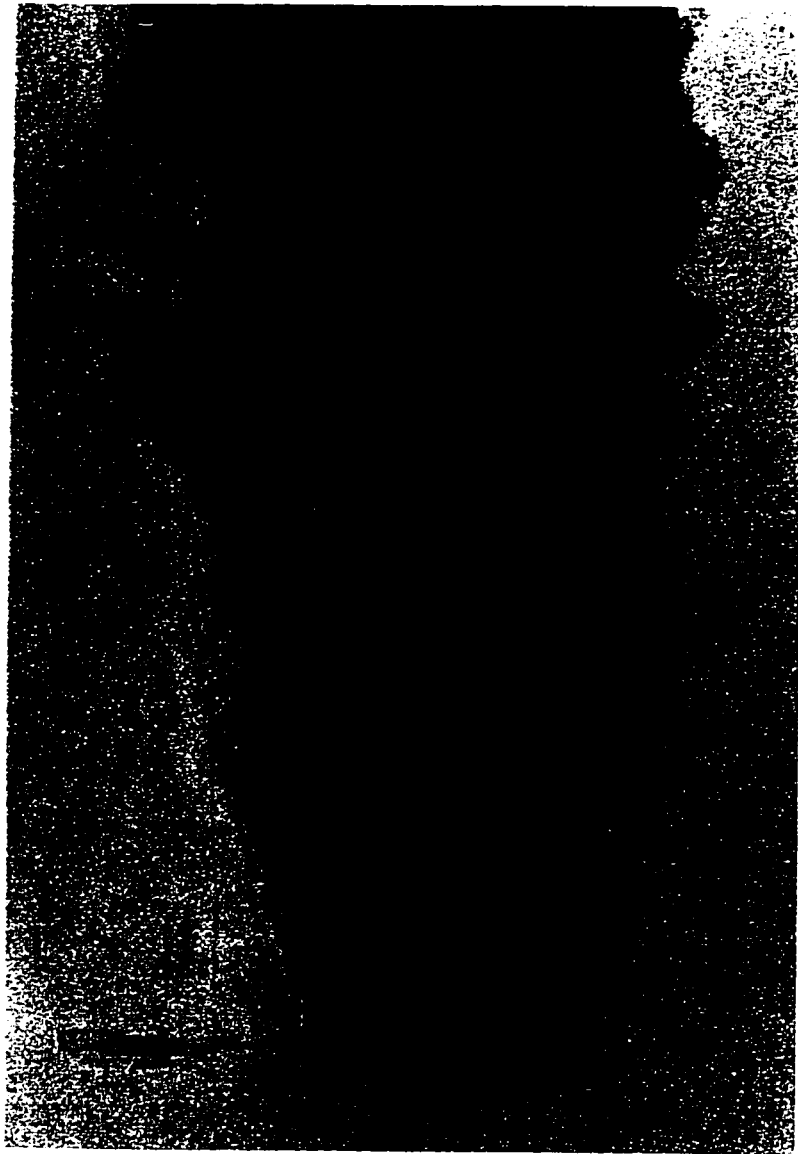
Fig. 4.3a Typical Plan View Photograph for Experiment (A4), Velocity Ratio $(U_0/U) = 10$

$S = 8d, \quad n = 3$
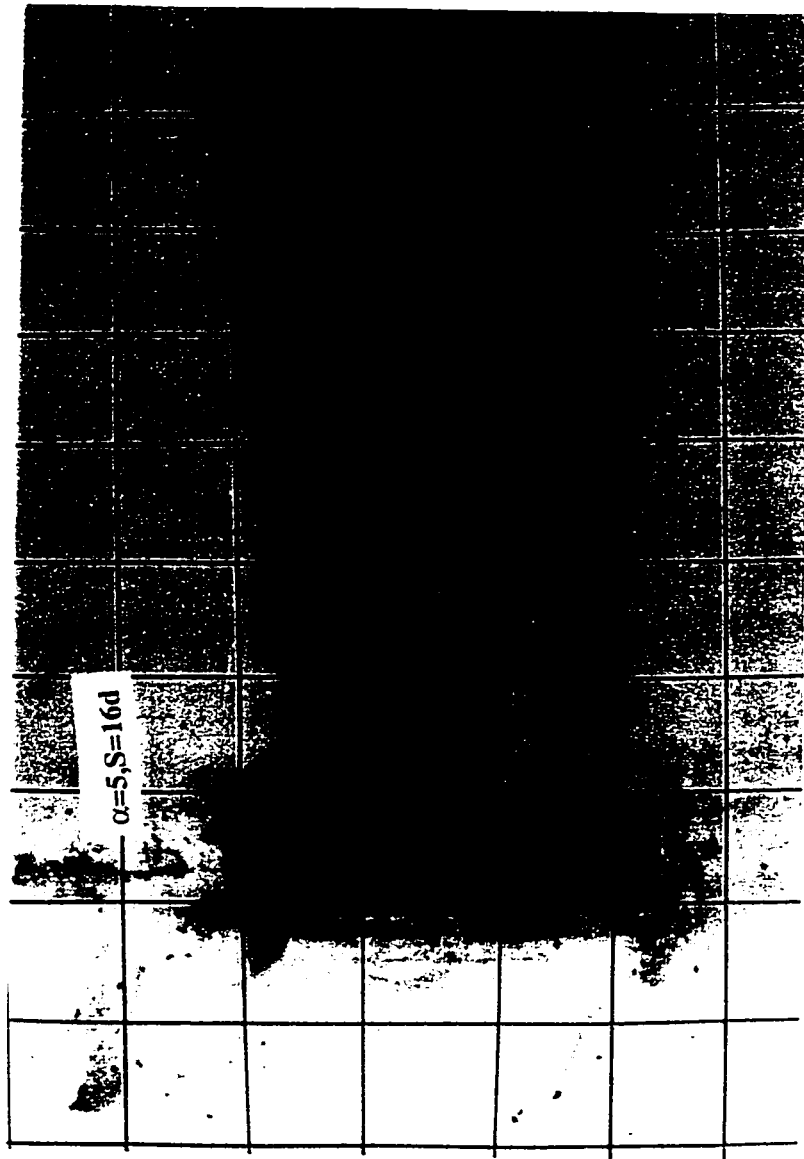
Fig. 4.3b Typical Plan View Photograph for Experiment (B1), Velocity Ratio (U_O/U) =5

S = 16d, n = 3 (grid size = 50 mm)

α=5,S=16d

149
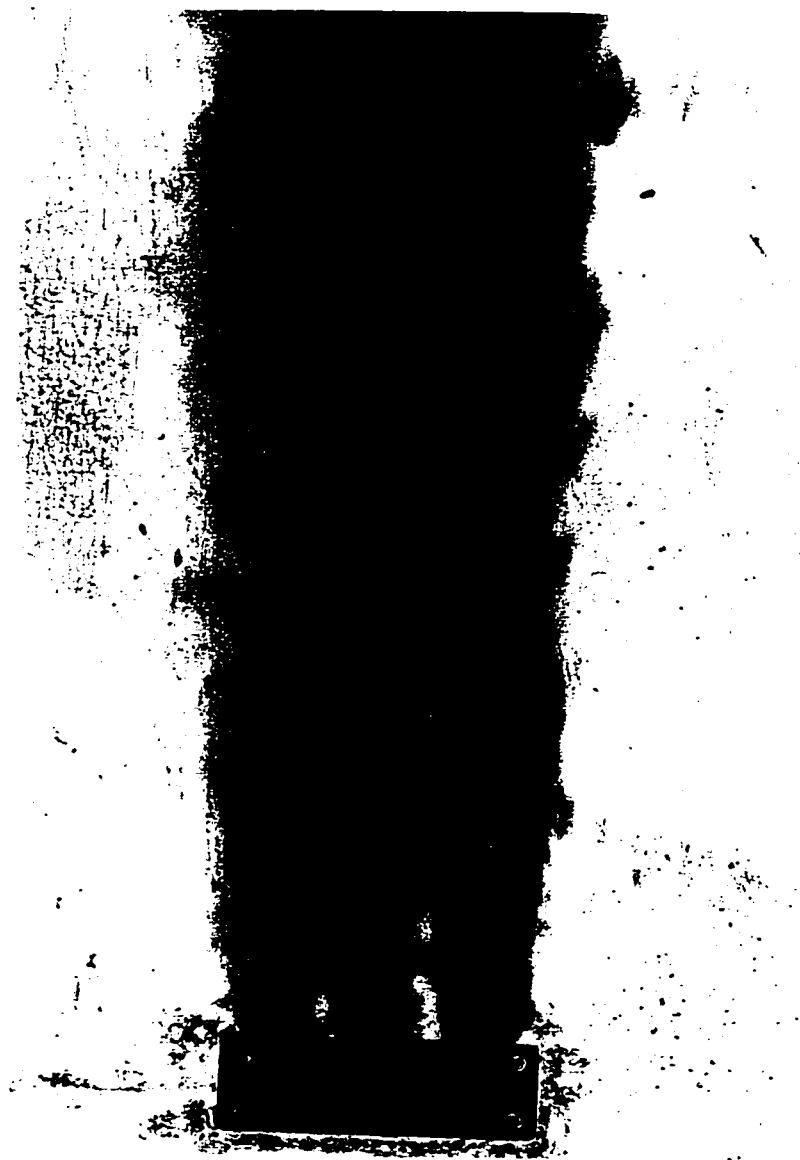
Fig. 4.3c Typical Plan View Photograph for Experiment (B2), Velocity Ratio $(U_0/U) = 8$

$S = 16d, \quad n = 3$
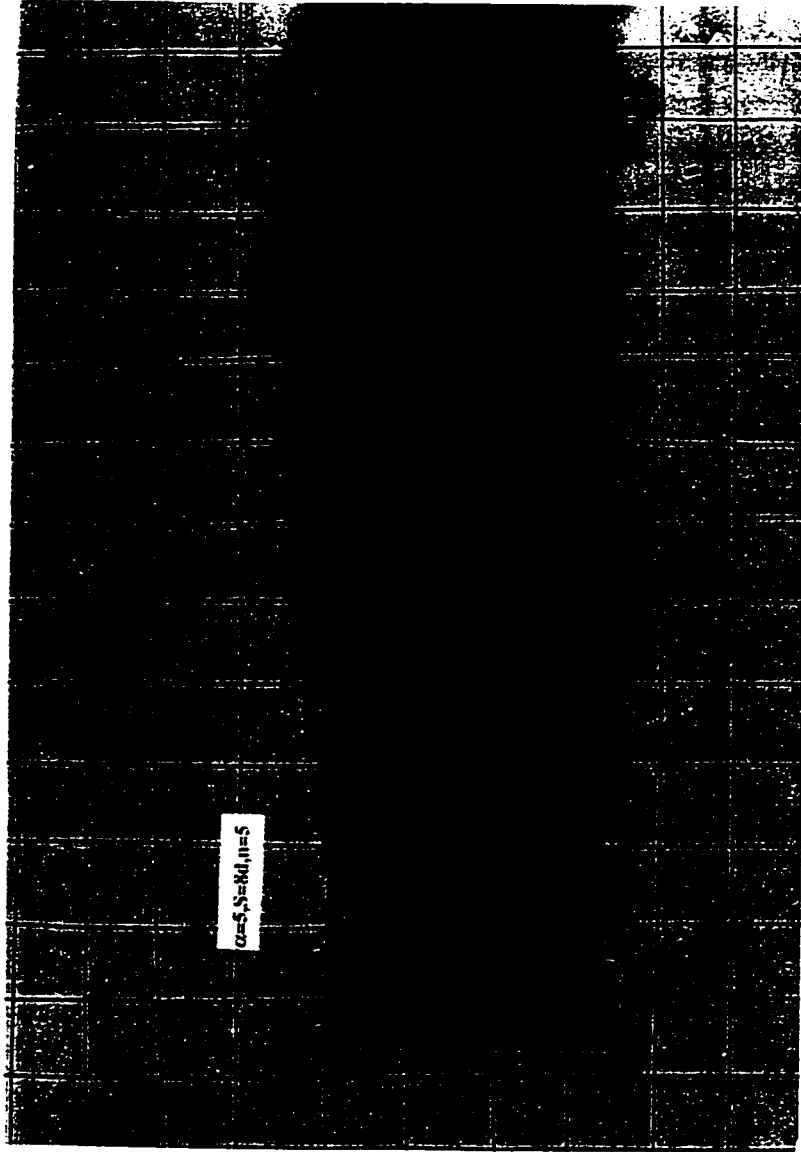
Fig. 4.3d Typical Plan View Photograph for Experiment (C1), Velocity $(U_0/U) = 5$

$S = 8d$, $n = 5$ (grid size = 50 mm)
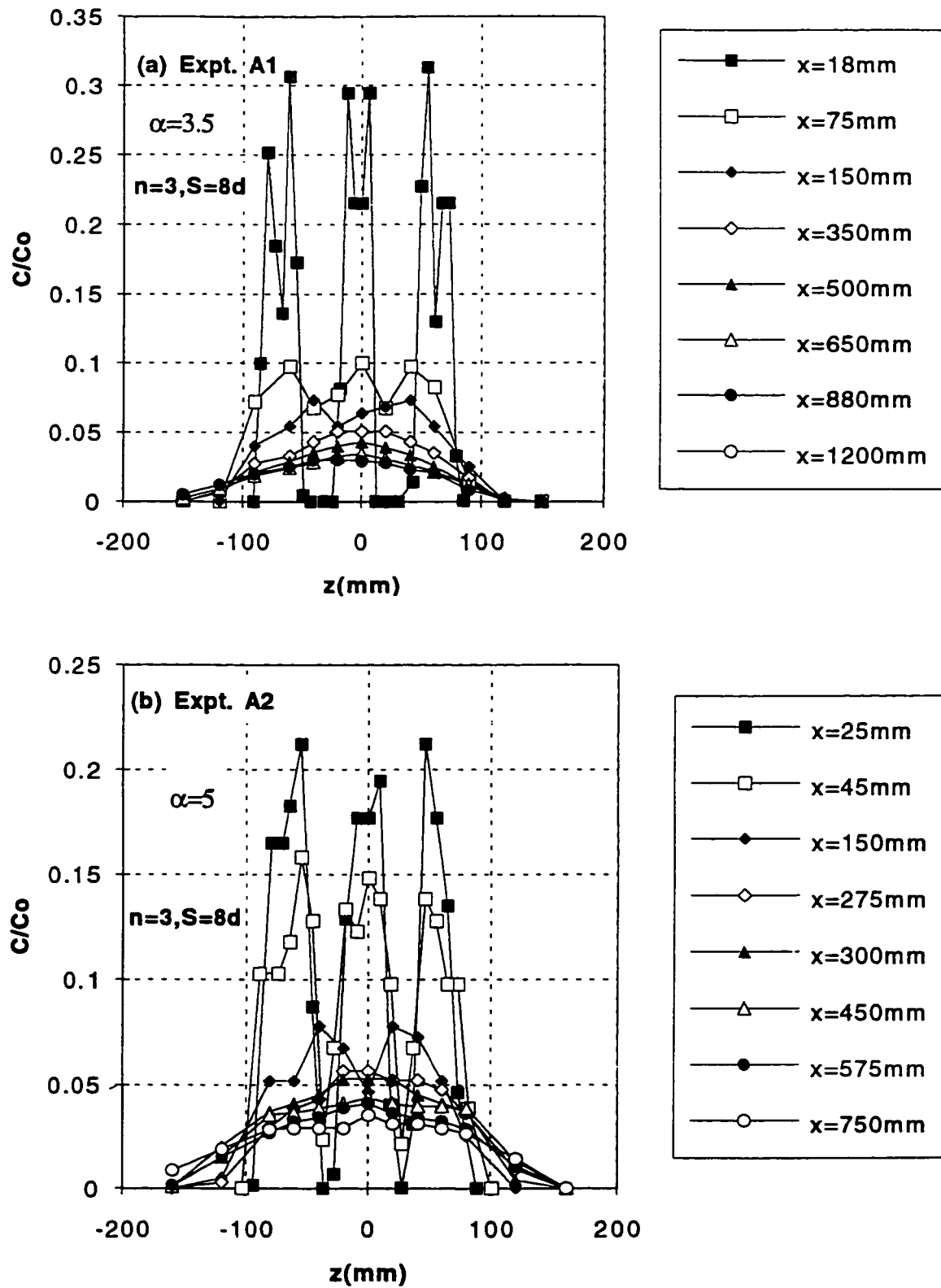
Fig. 4.4 (a-b) Typical Concentration Profiles for the Maximum Transverse Concentration Planes
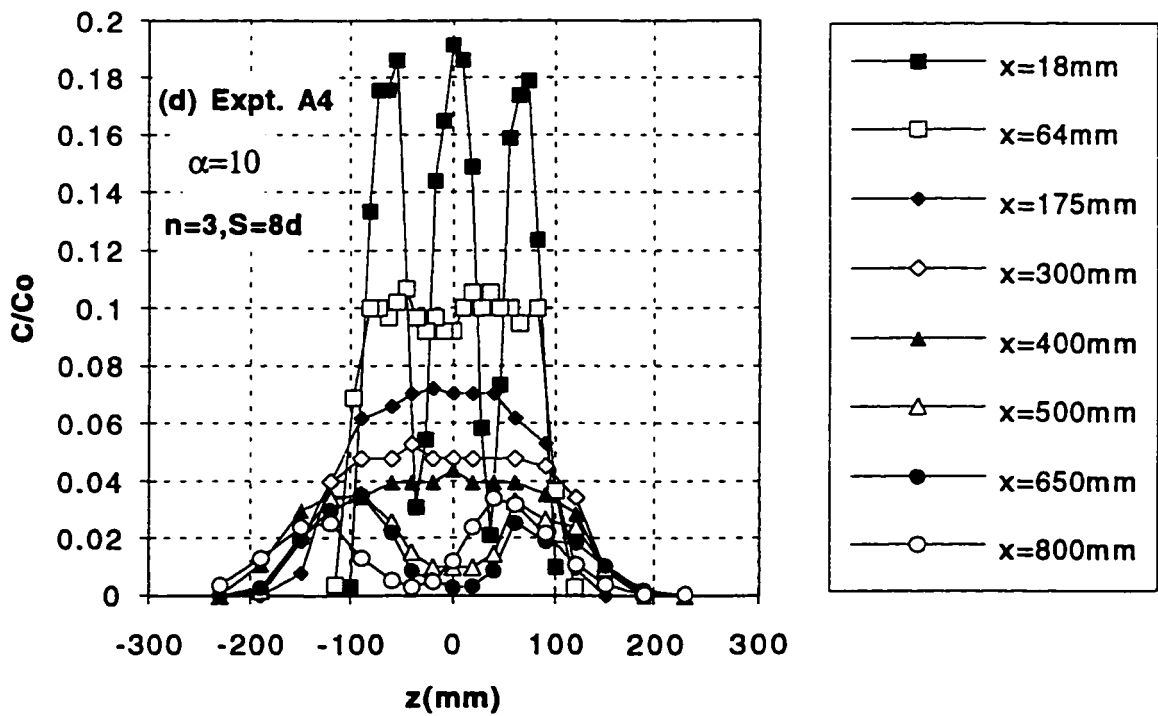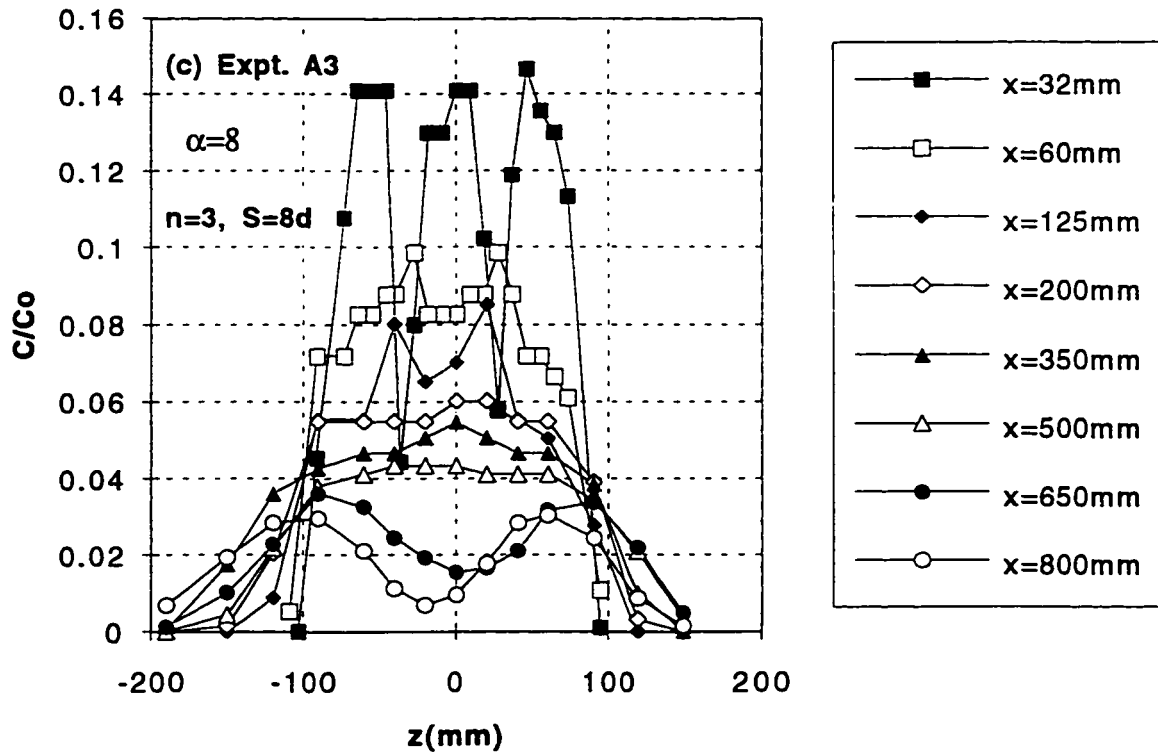
Fig. 4.4 (c-d) Typical Concentration Profiles for the Maximum Transverse
Concentration Planes
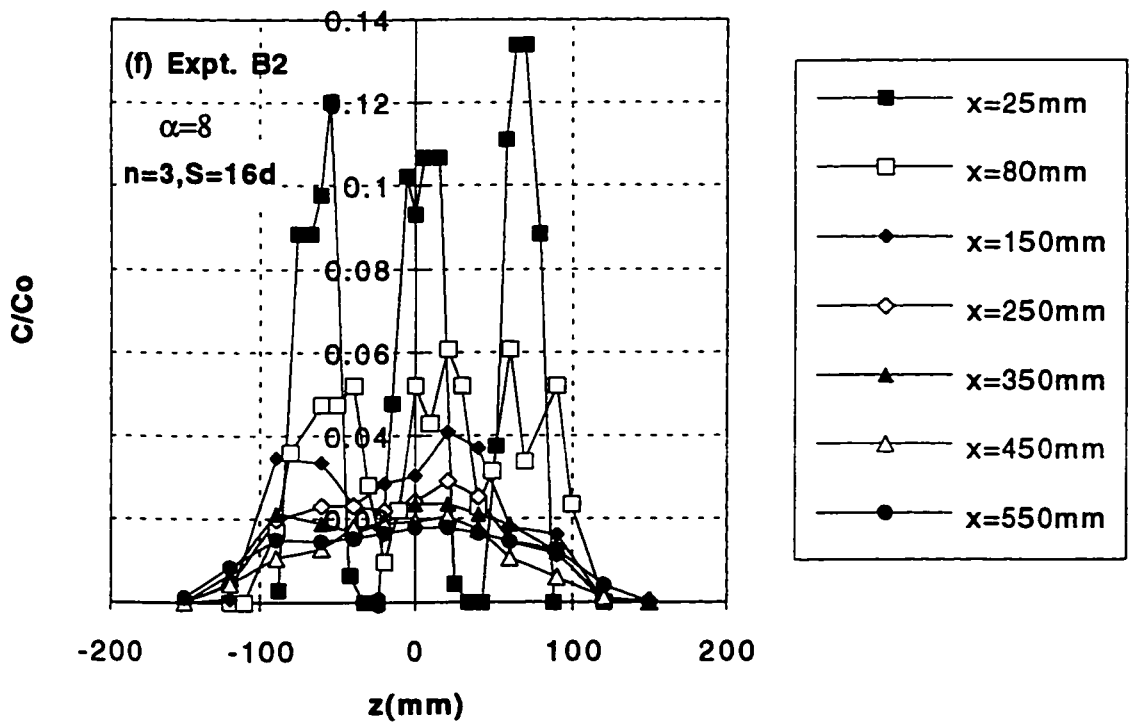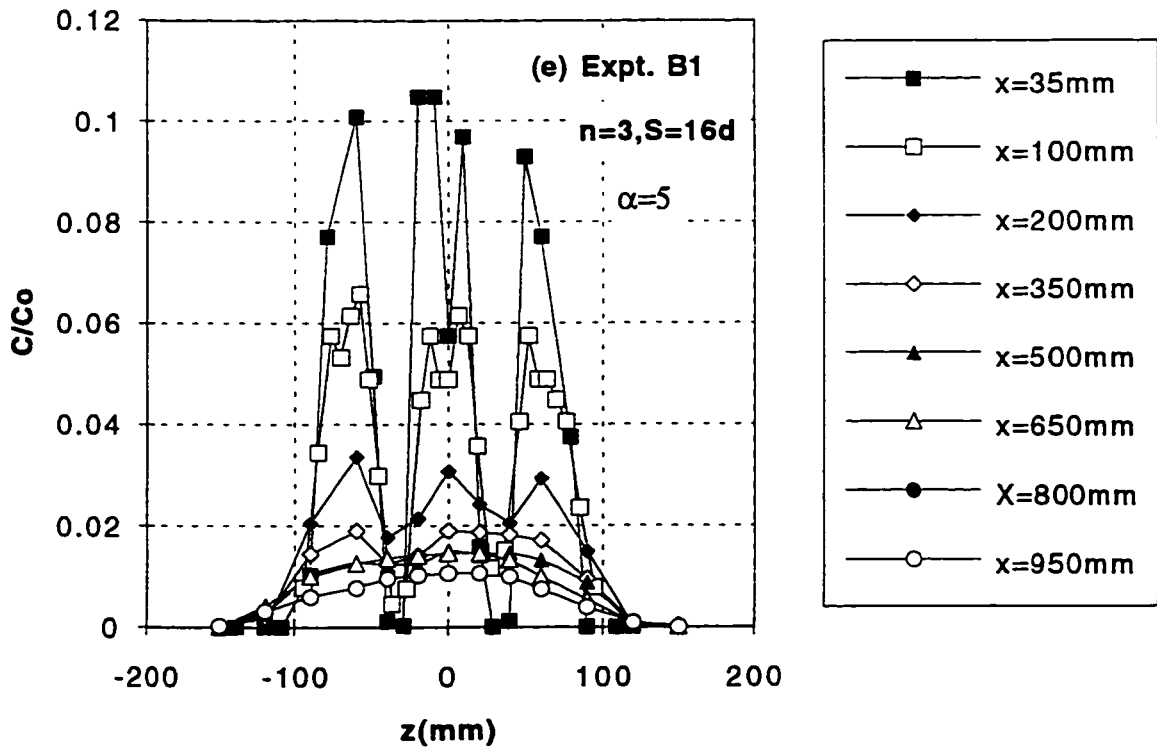
Fig. 4.4 (e-f) Typical Concentration Profiles for the Maximum Transverse
Concentration Planes

154
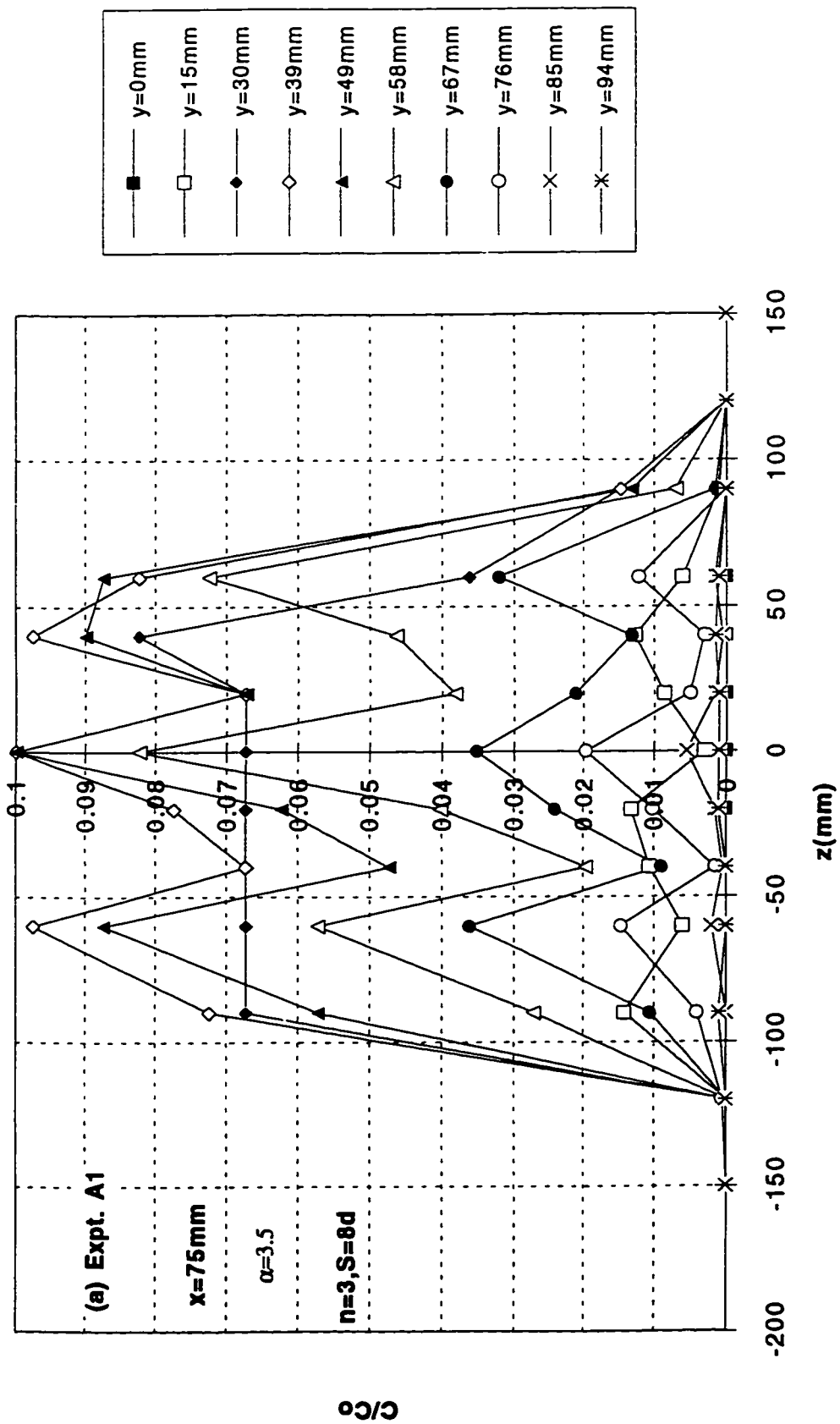
Fig. 4.5a Transverse Concentration Profiles at Different Levels for Expt. A1

(a) Expt. A1

x=75mm

α=3.5

n=3, S=8d

C/Co

z(mm)

Legend:
- y=0mm
- y=15mm
- y=30mm
- y=39mm
- y=49mm
- y=58mm
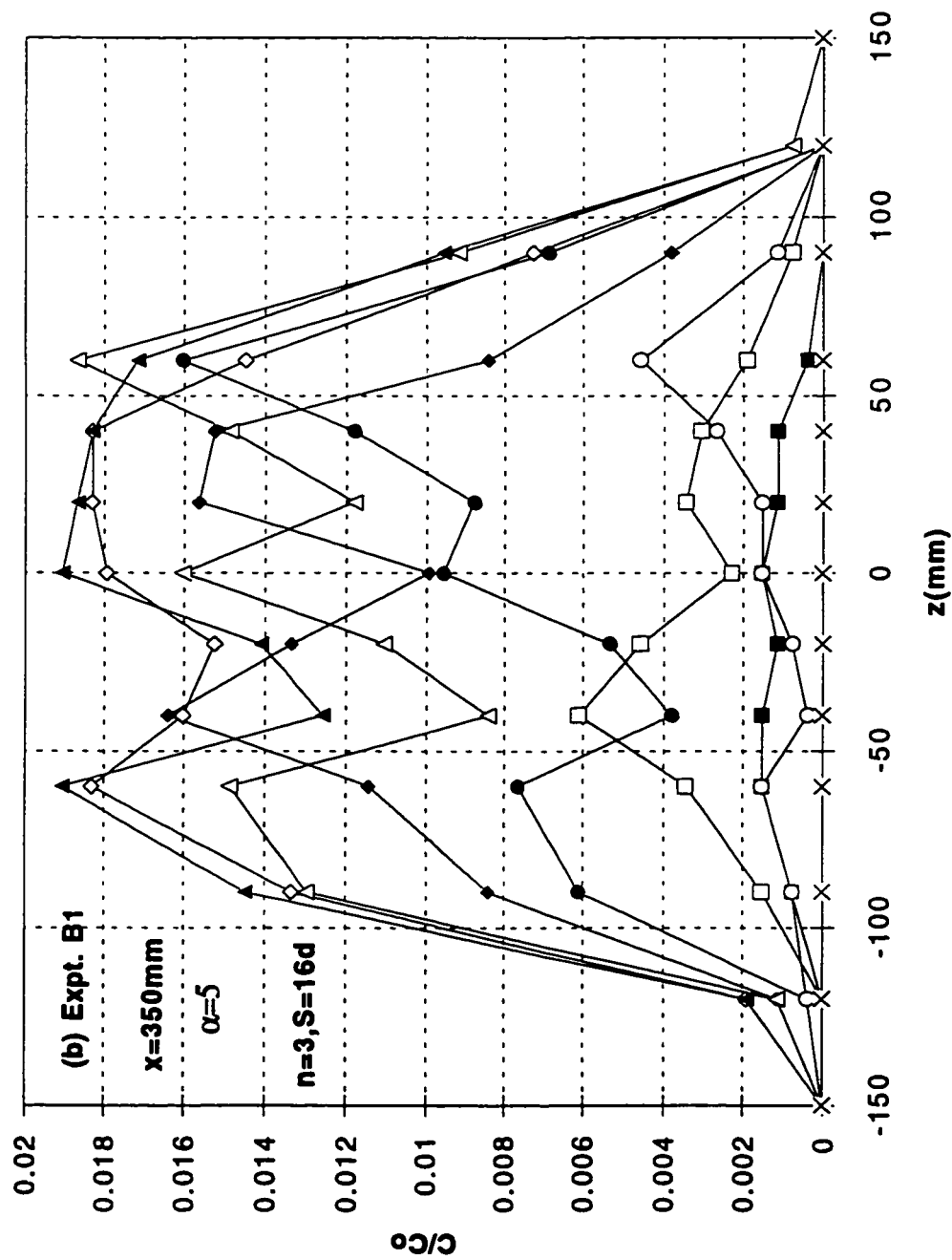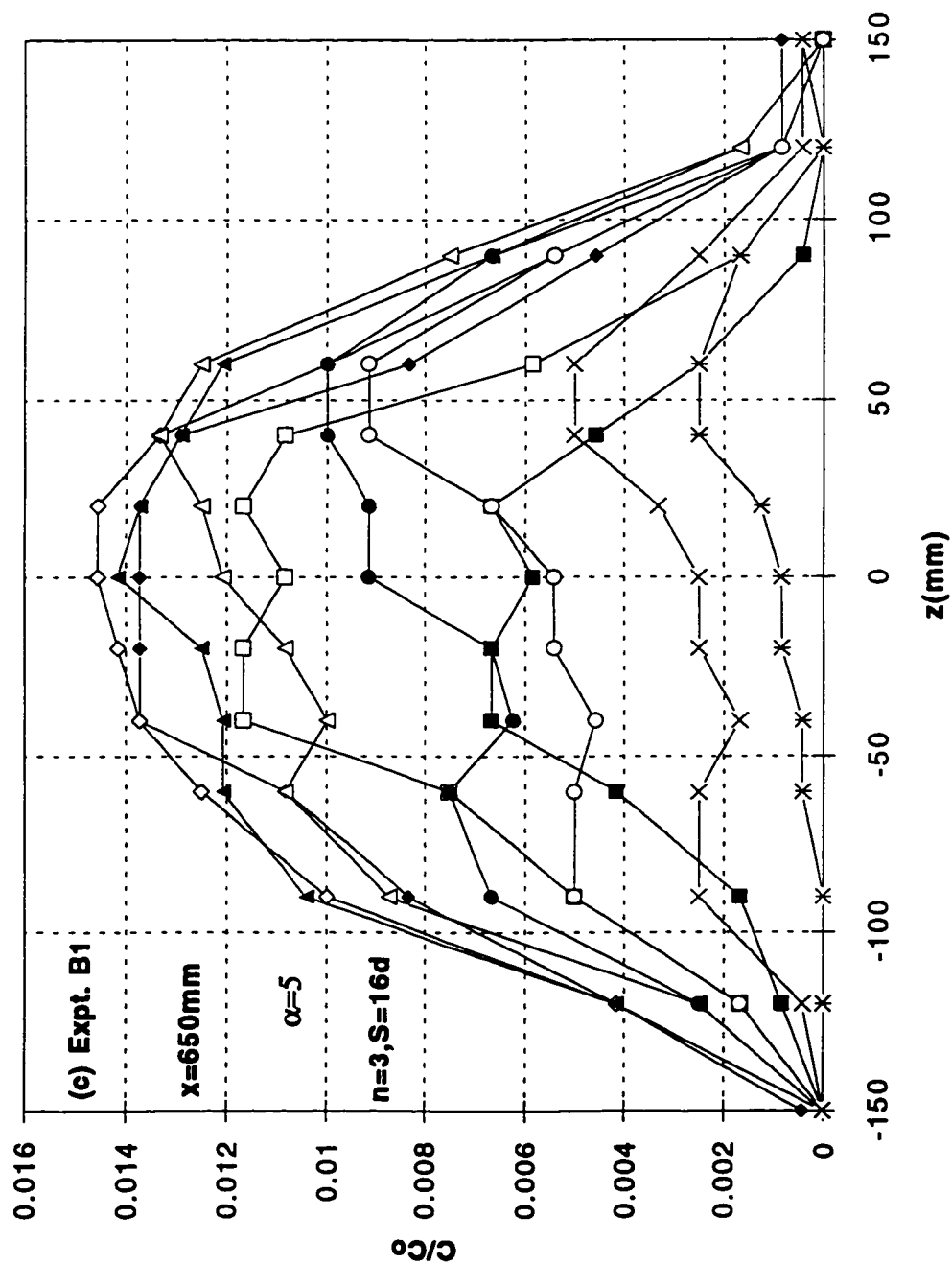- y=67mm
- y=76mm
- y=85mm
- y=94mm
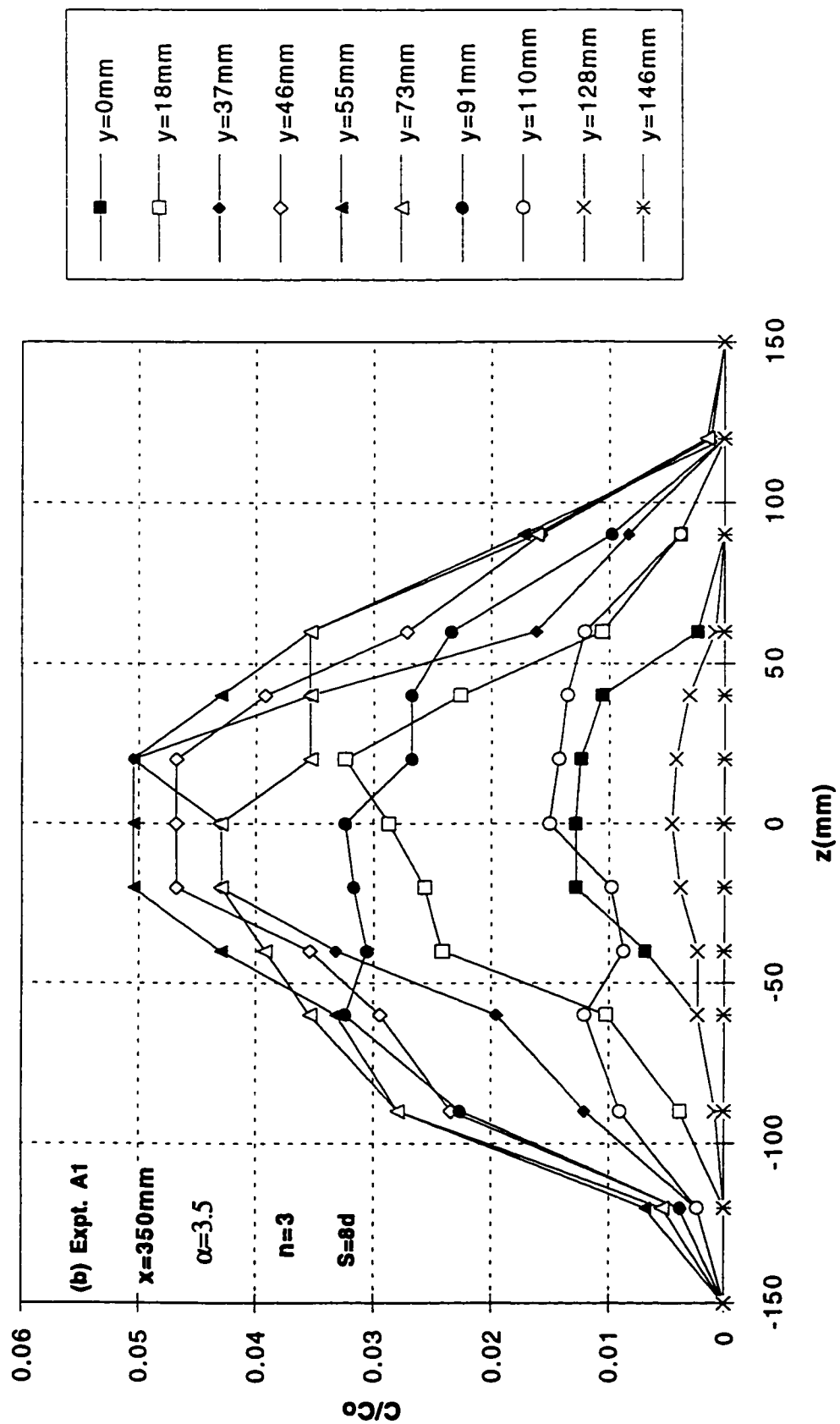
Fig. 4.5b Transverse Concentration Profiles at Different Levels for Expt. A1
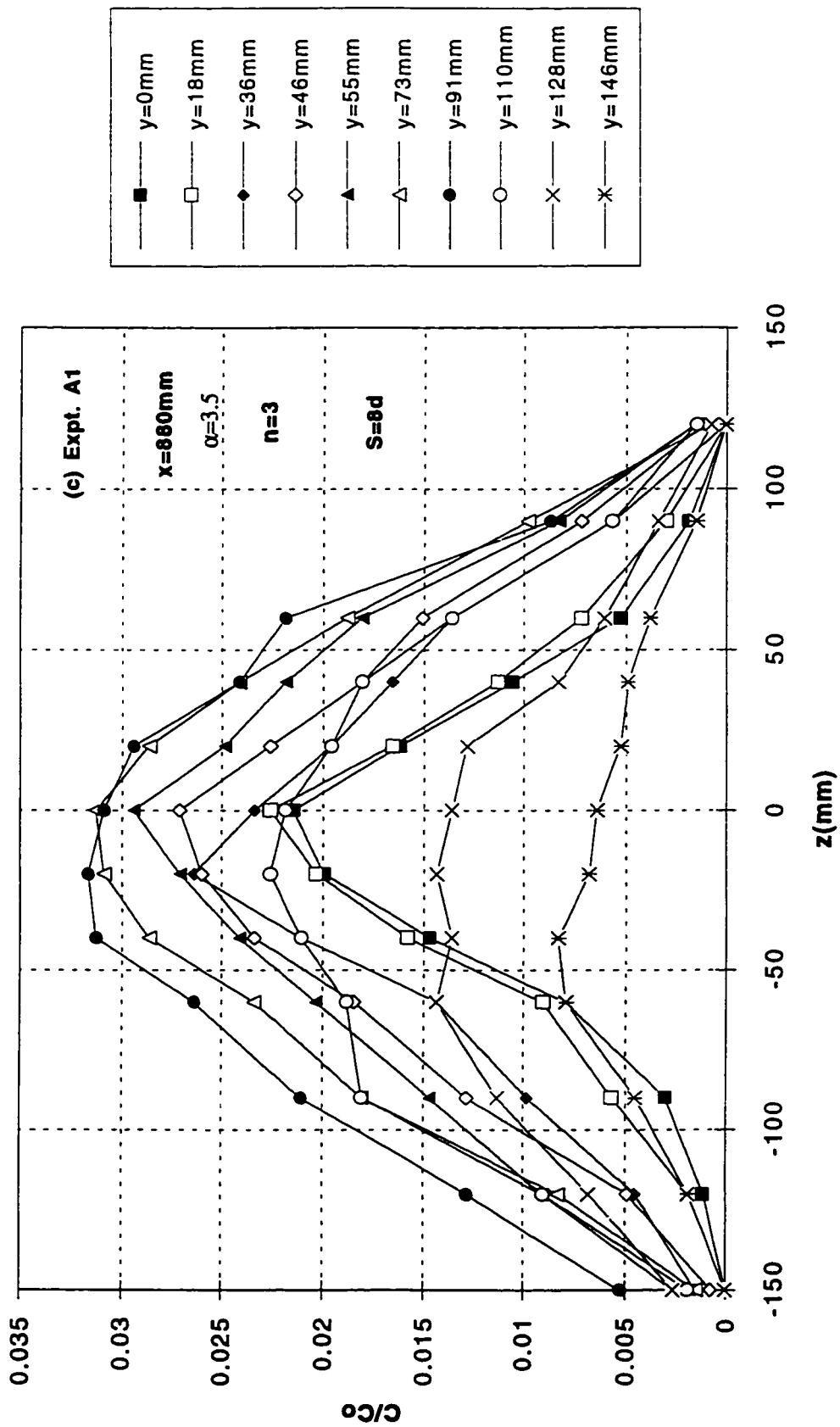
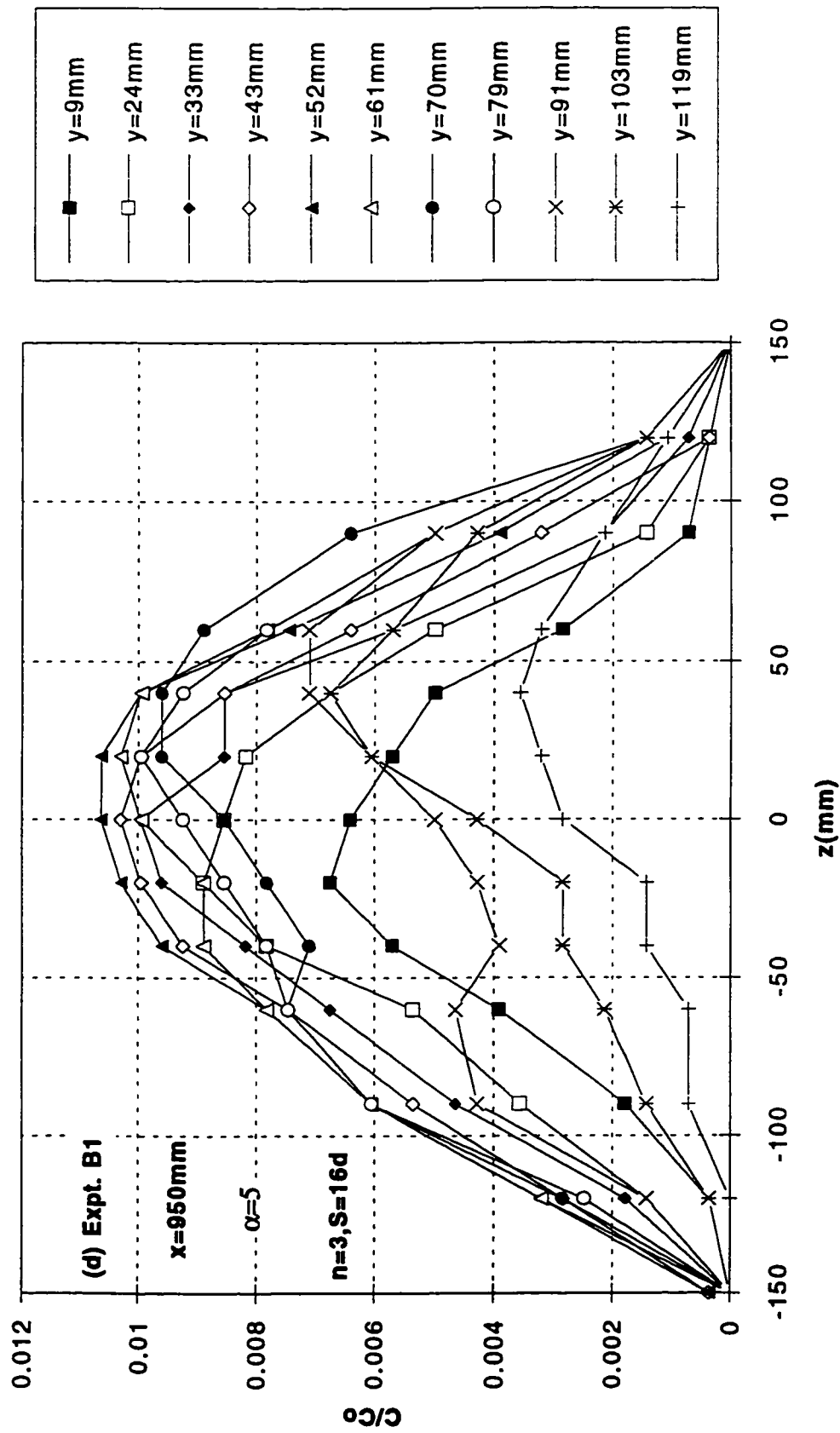Fig. 4.5c Transverse Concentration Profiles at Different Levels for Expt. A1

157
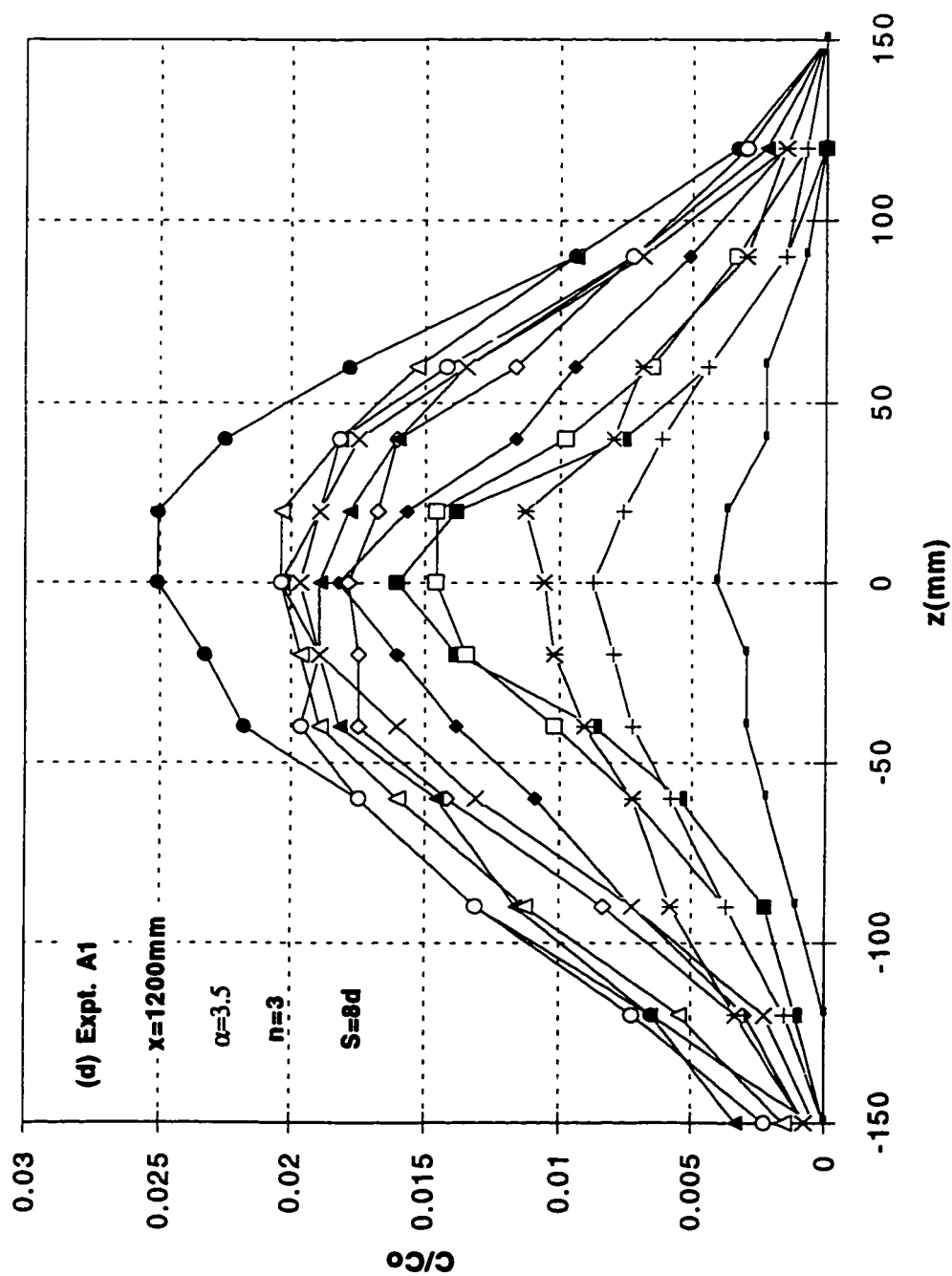
Fig. 4.5d Transverse Concentration Profiles at Different Levels for Expt. A1
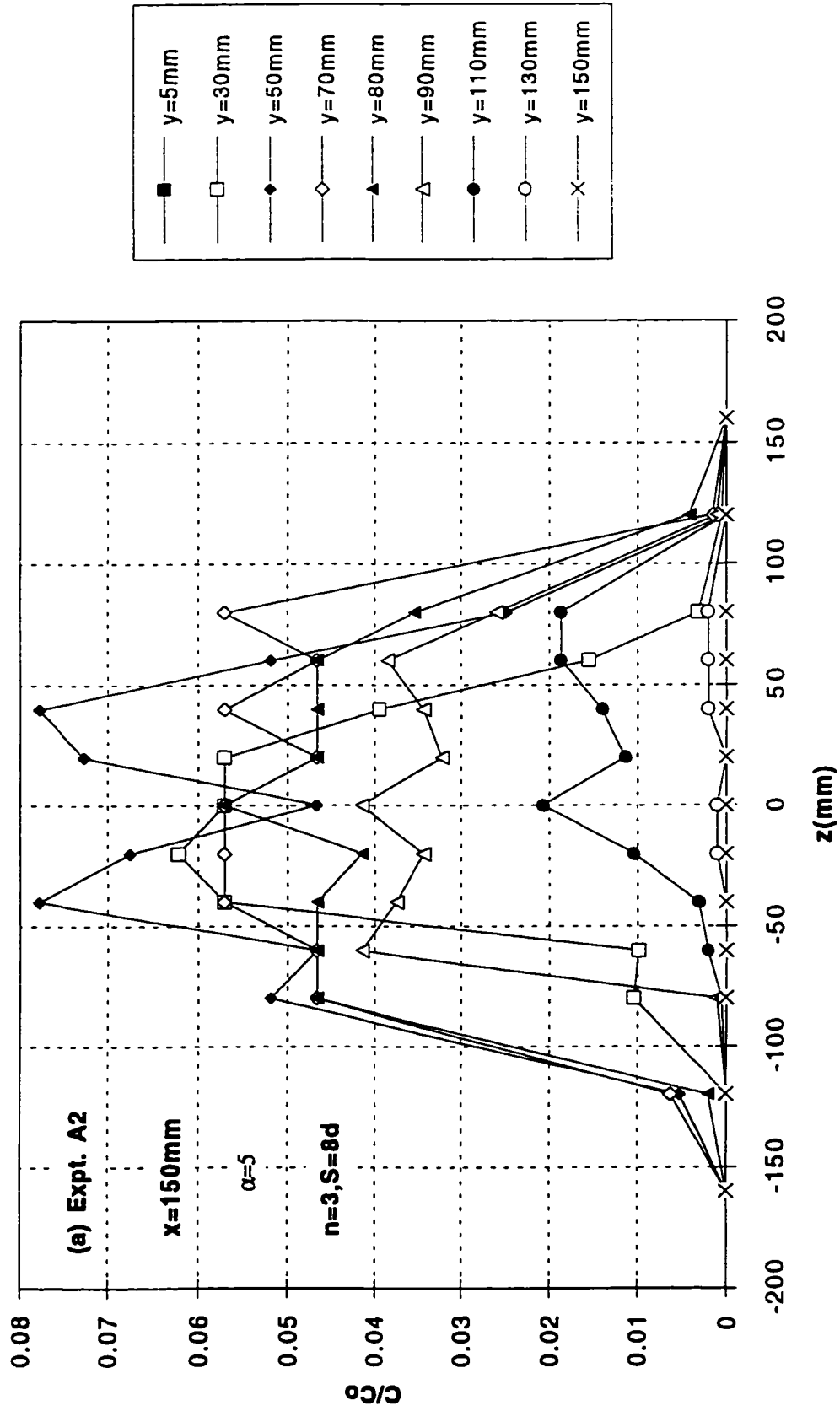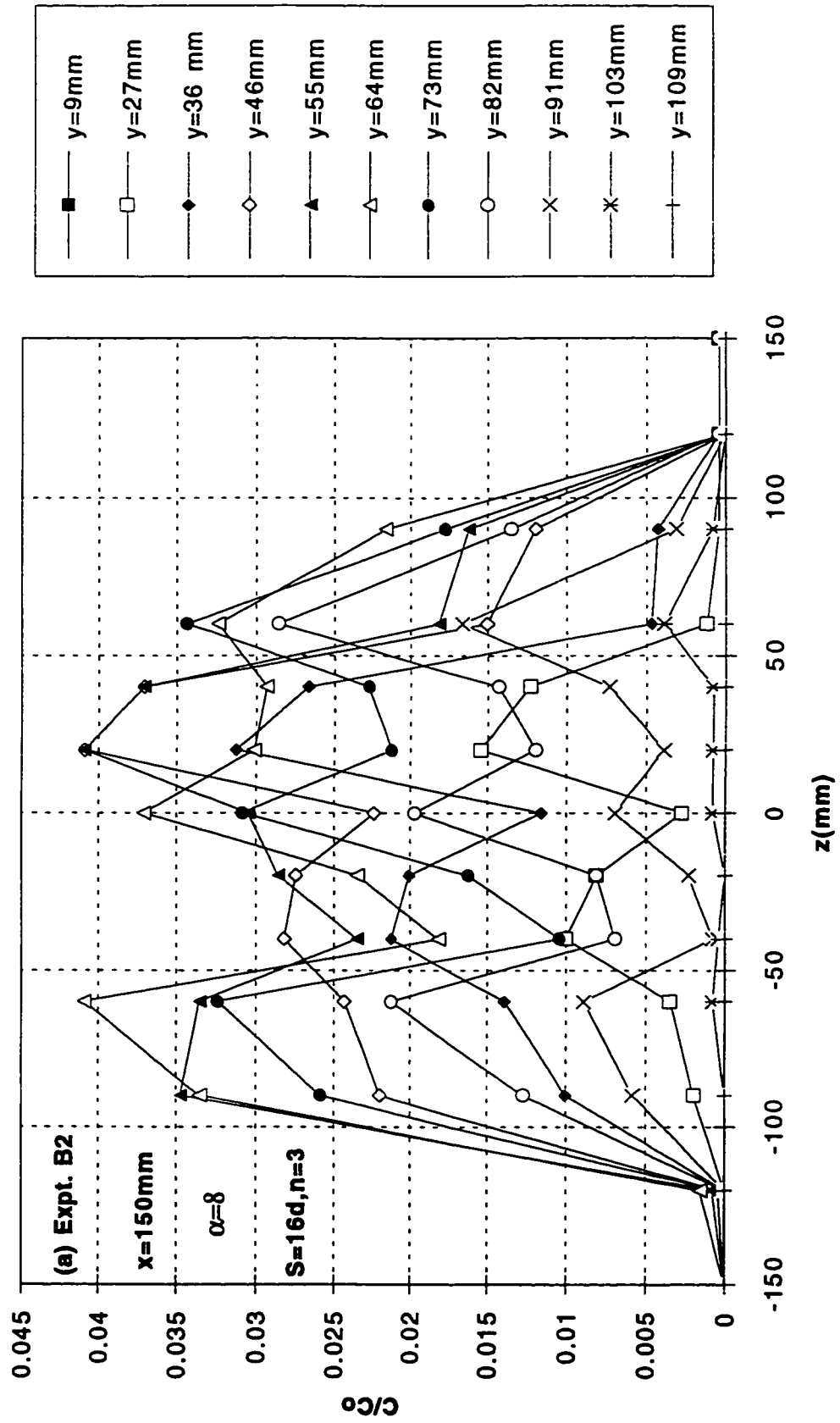
Fig. 4.6a Transverse Concentration Profiles at Different Levels for Expt. A2
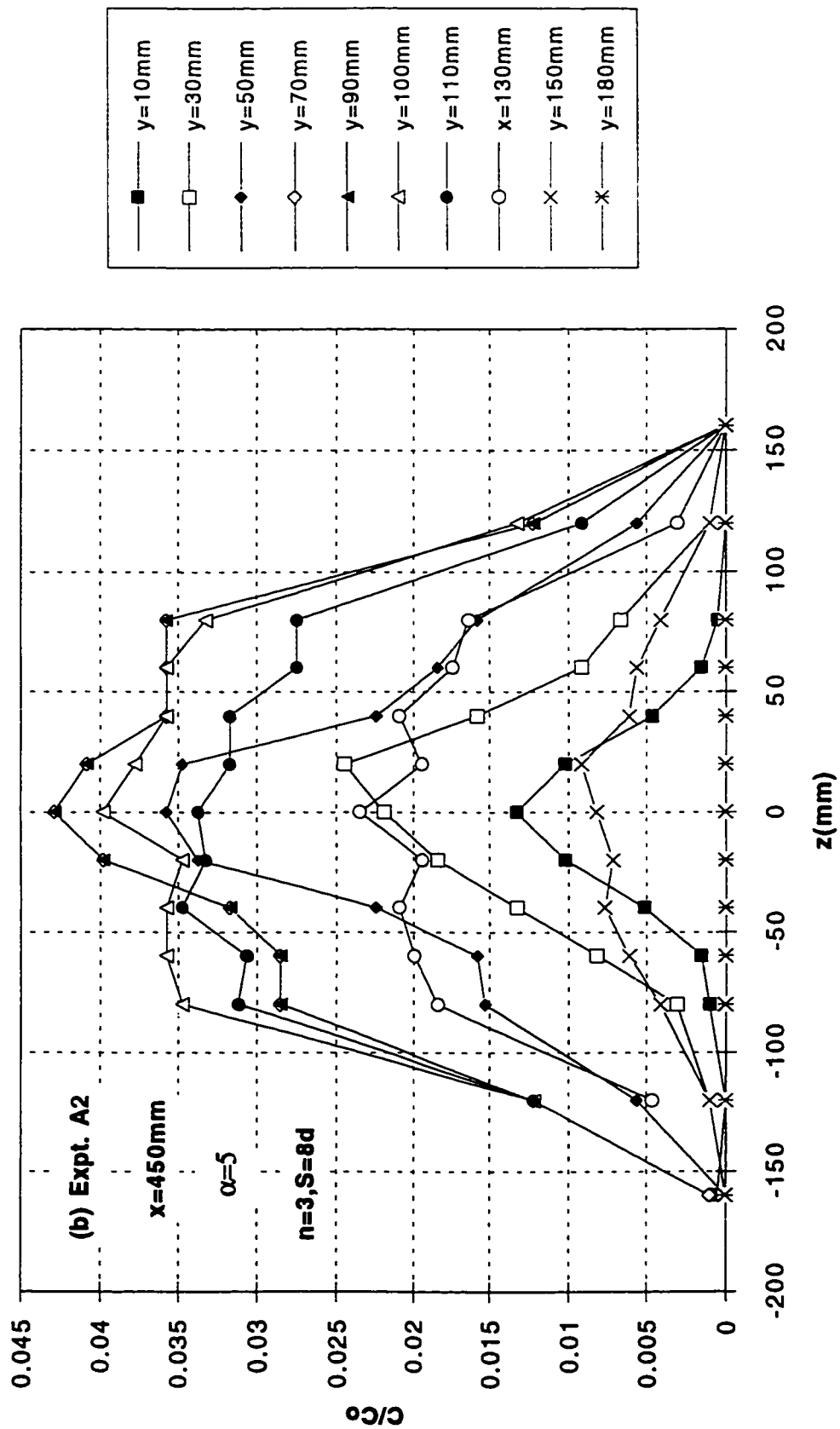
Fig. 4.6b Transverse Concentration Profiles at Different Levels for Expt. A2

(b) Expt. A2

x=450mm

α=5

n=3,S=8d
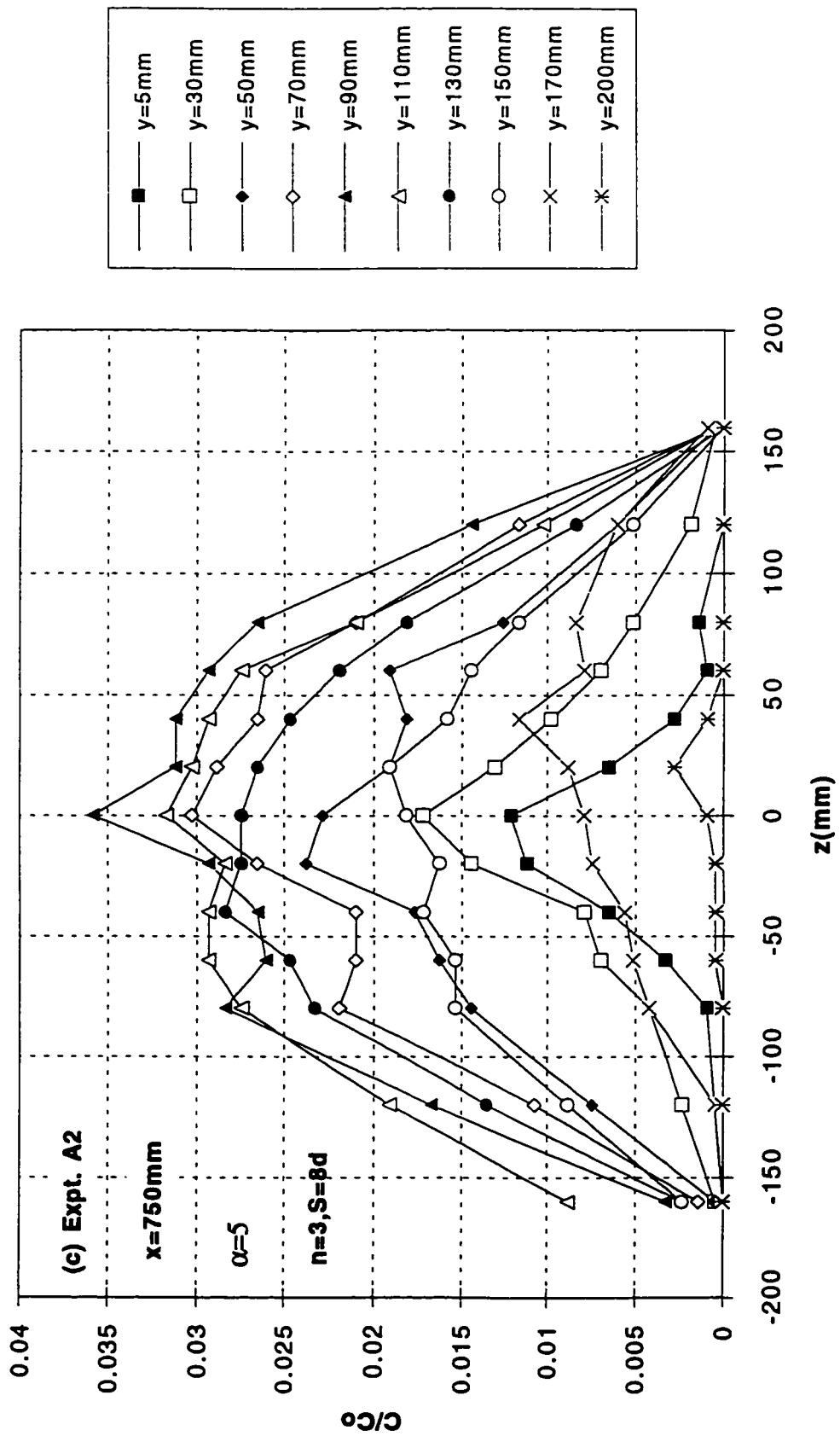
Fig. 4.6c Transverse Concentration Profiles at Different Levels for Expt. A2
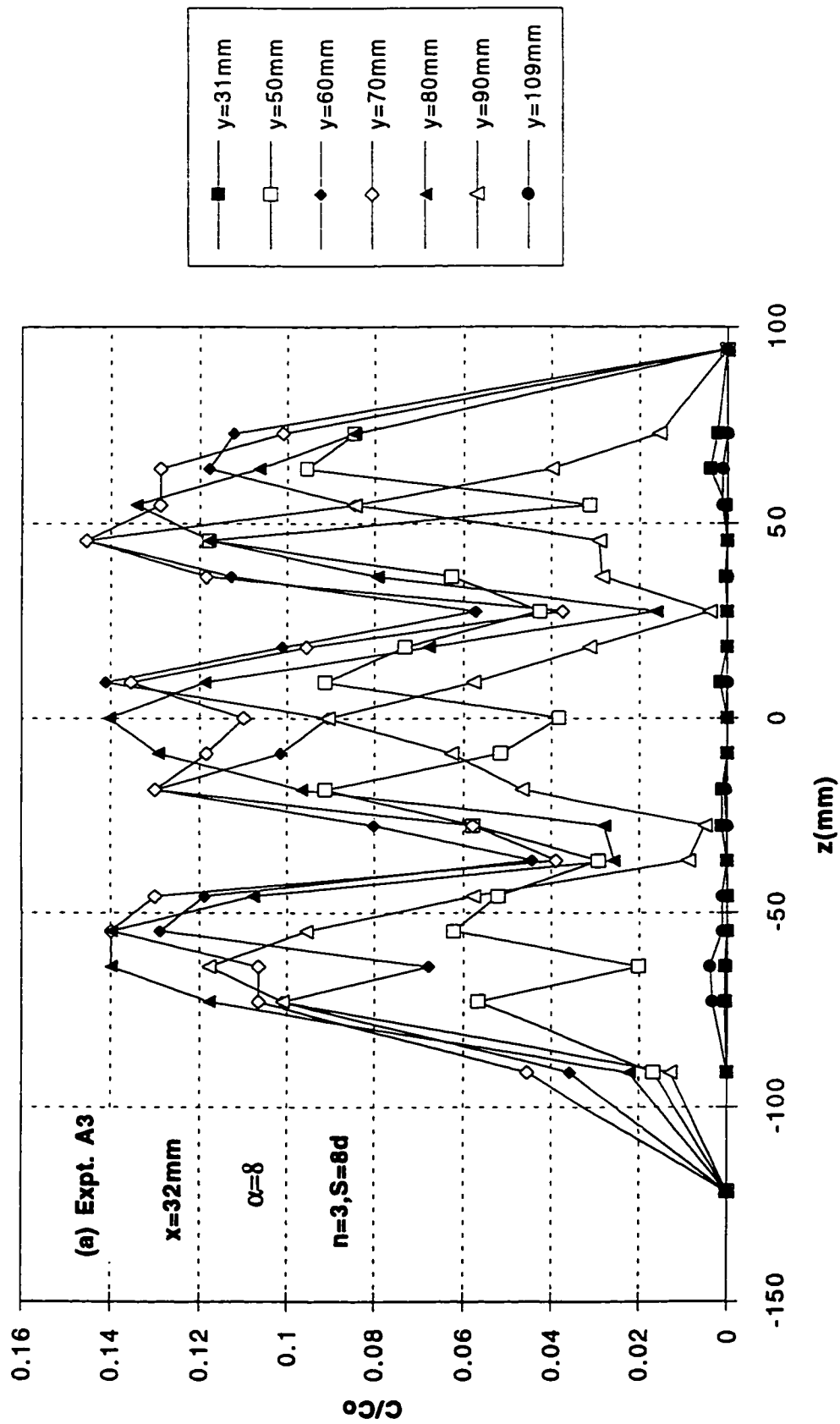
161

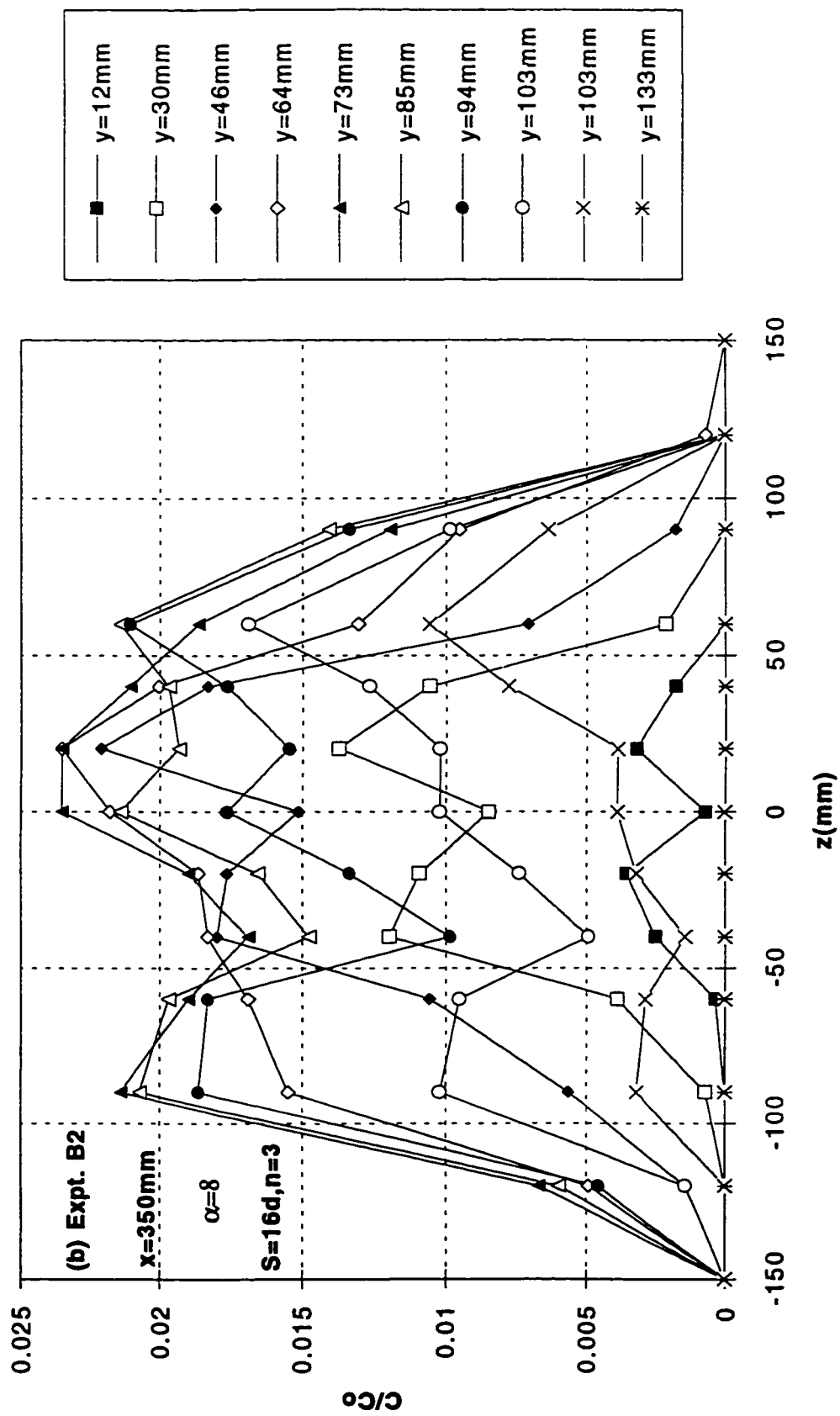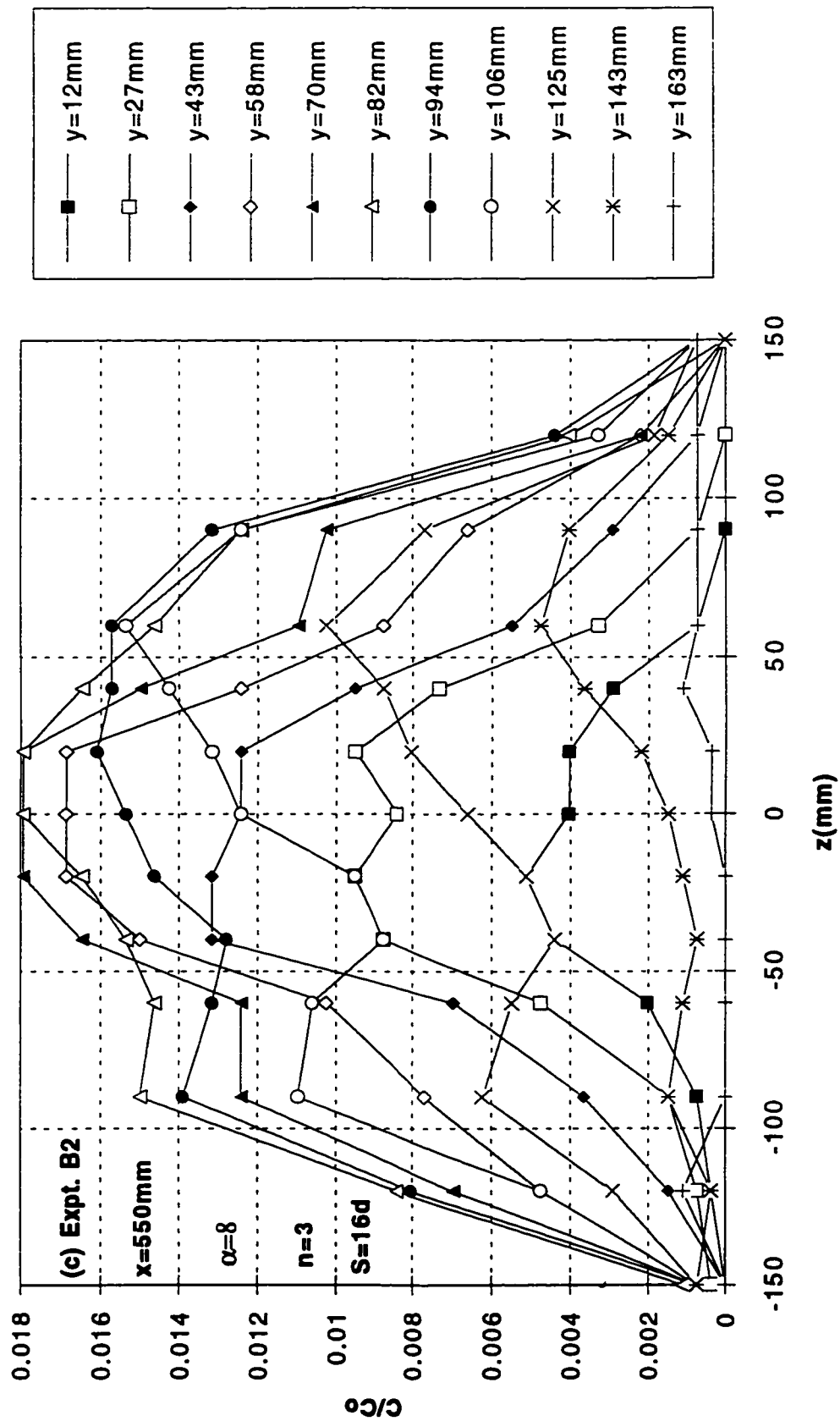Fig. 4.7a Transverse Concentration Profiles at Different Levels for Expt. A3
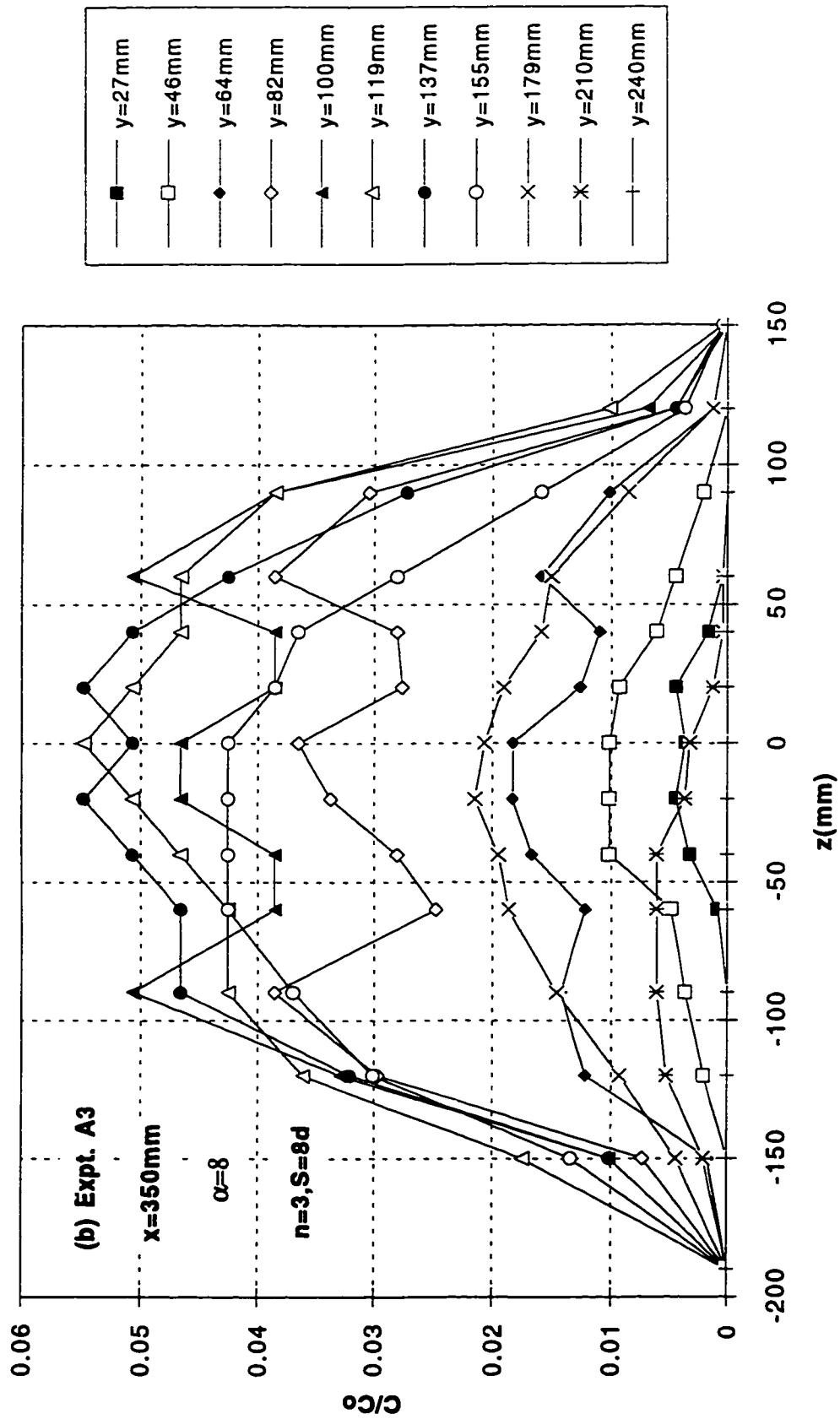
The chart legend shows:
- y=31mm (filled square)
- y=50mm (open square)
- y=60mm (filled diamond)
- y=70mm (open diamond)
- y=80mm (filled triangle)
- y=90mm (open triangle)
- y=109mm (filled circle)

Chart labels:
(a) Expt. A3
x=32mm
α=8
n=3, S=8d

Y-axis: C/Co (0 to 0.16)
X-axis: z(mm) (-150 to 100)

Fig. 4.7b Transverse Concentration Profiles at Different Levels for Expt. A3

Legend:
- y=27mm
- y=46mm
- y=64mm
- y=82mm
- y=100mm
- y=119mm
- y=137mm
- y=155mm
- y=179mm
- y=210mm
- y=240mm

(b) Expt. A3

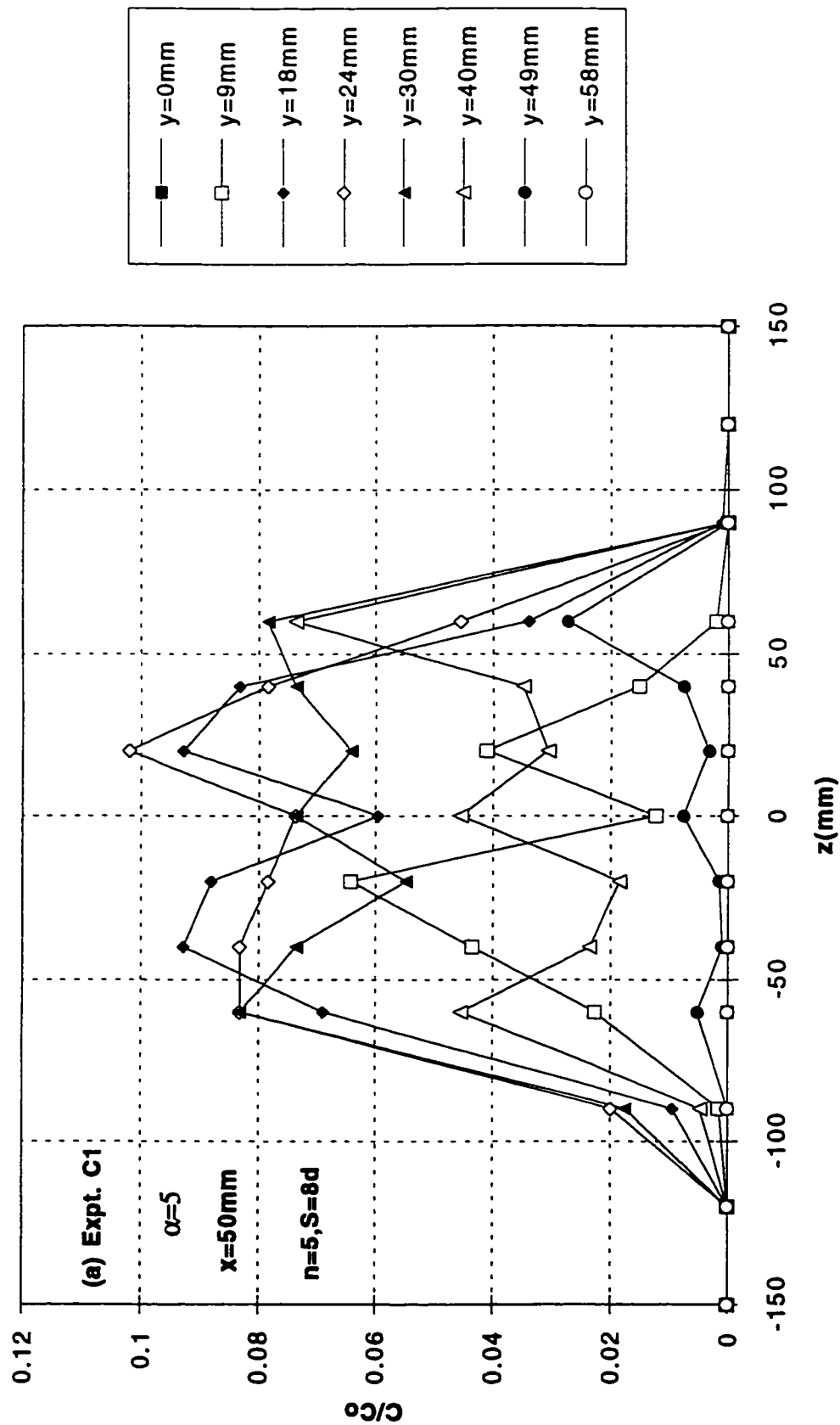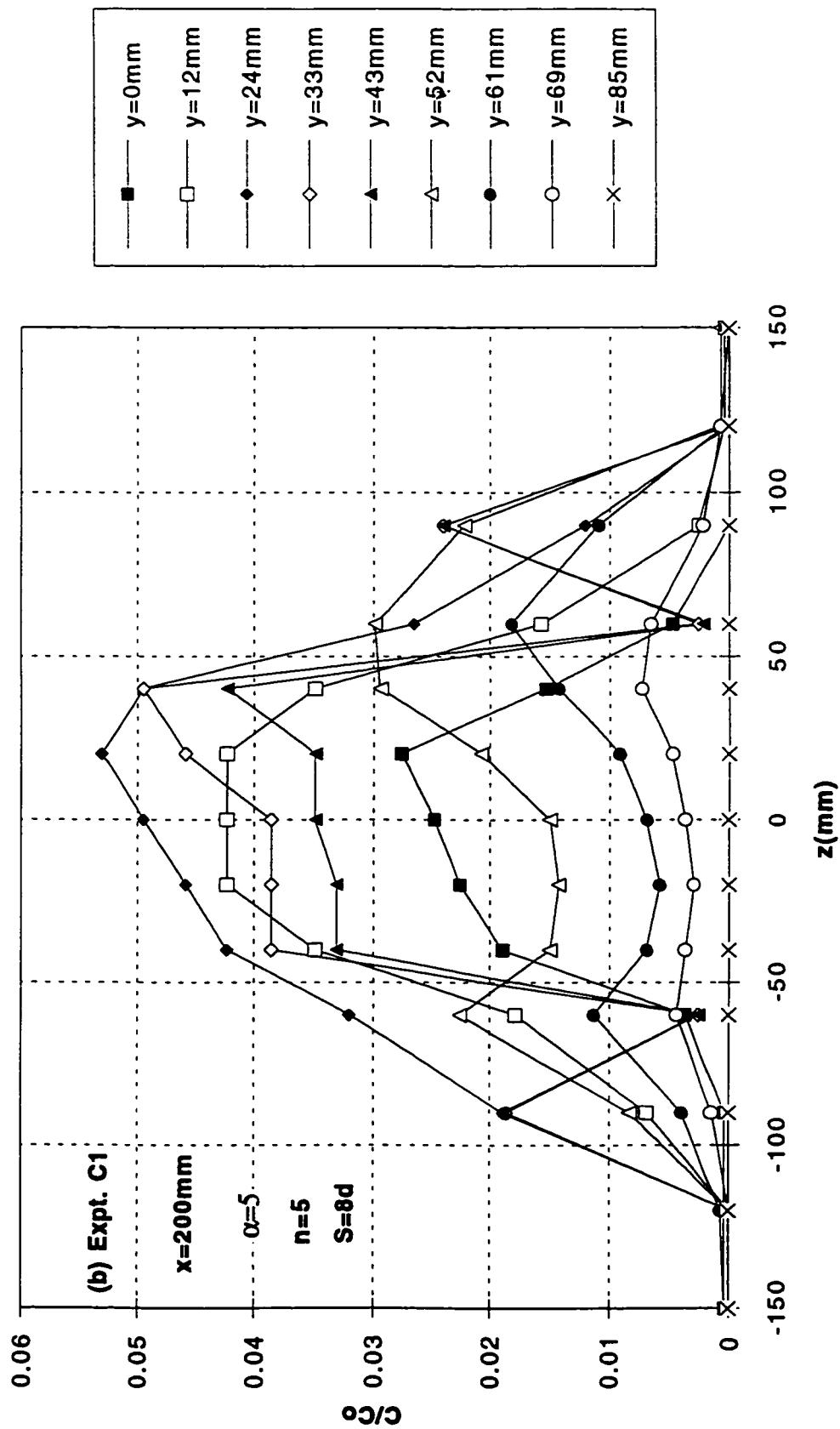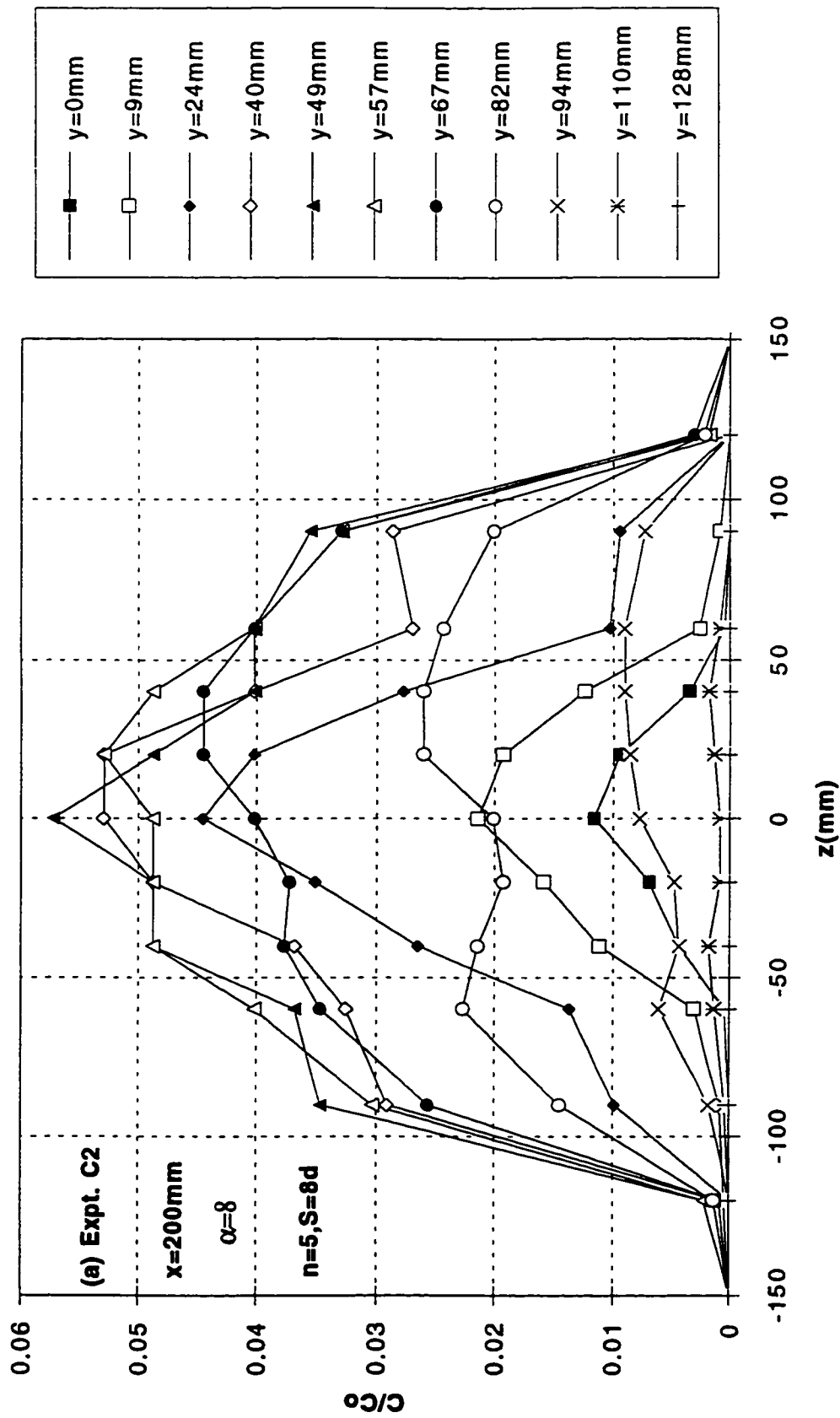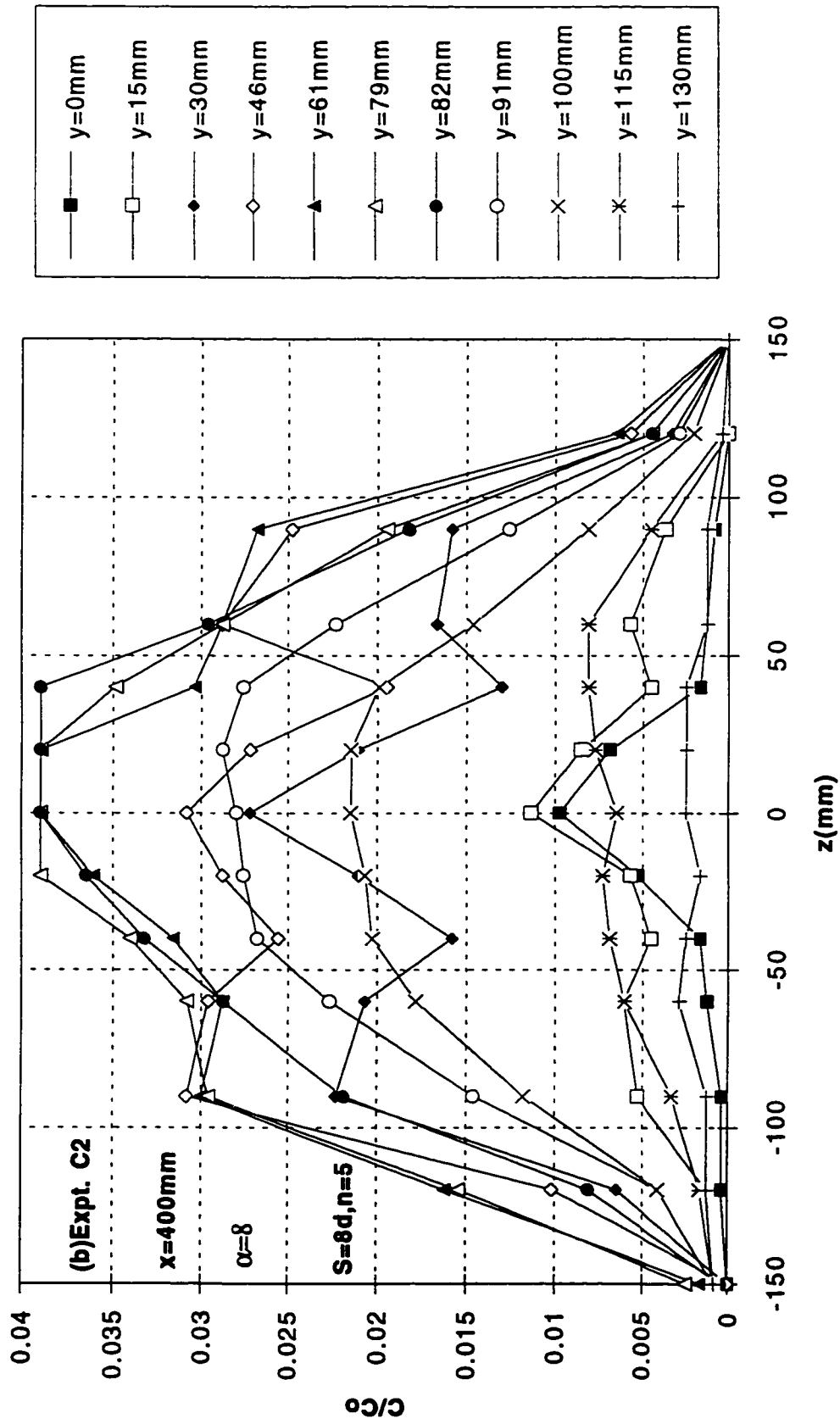x=350mm

$\alpha=8$

n=3, S=8d

y-axis: c/Co

x-axis: z(mm)
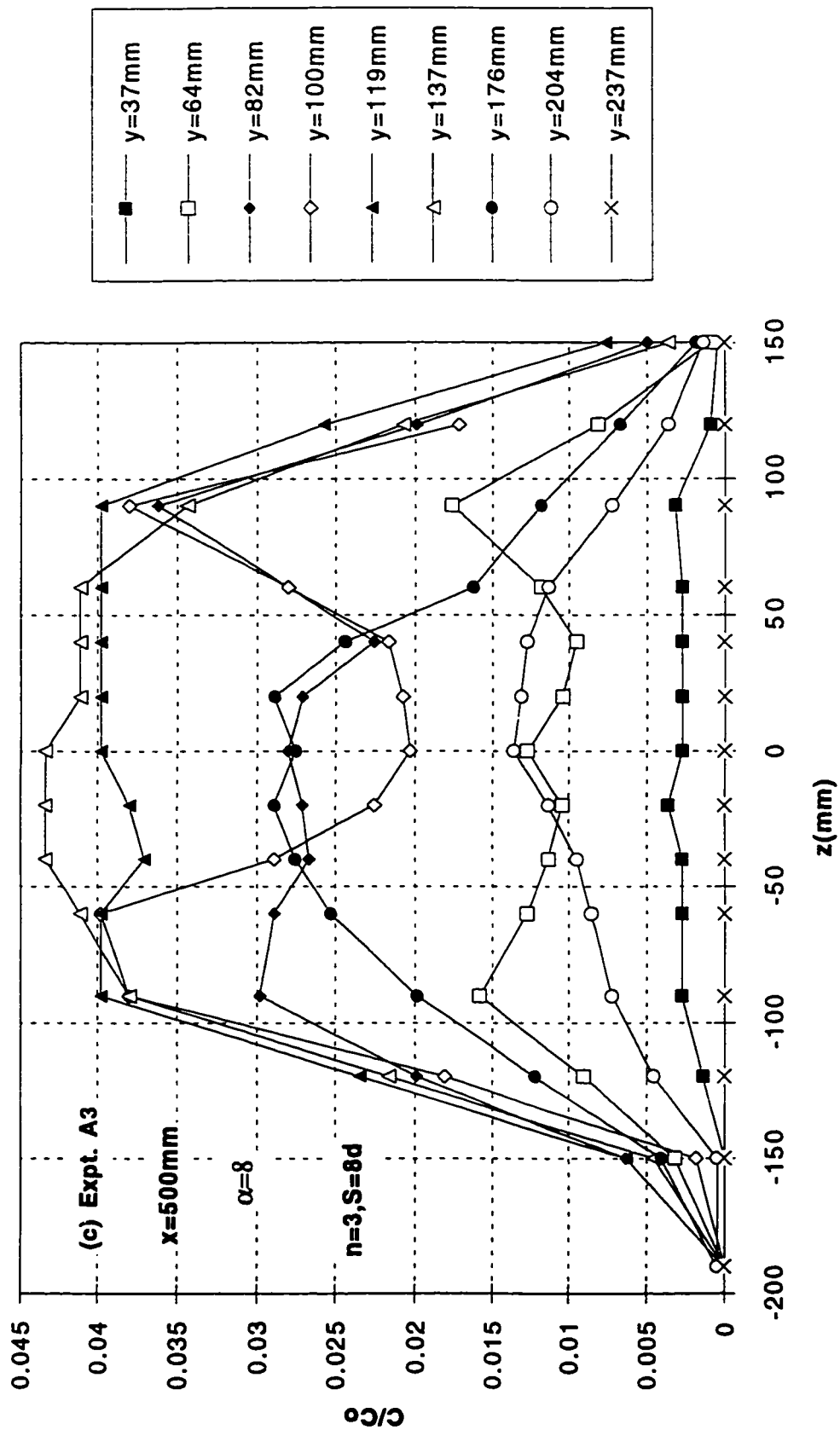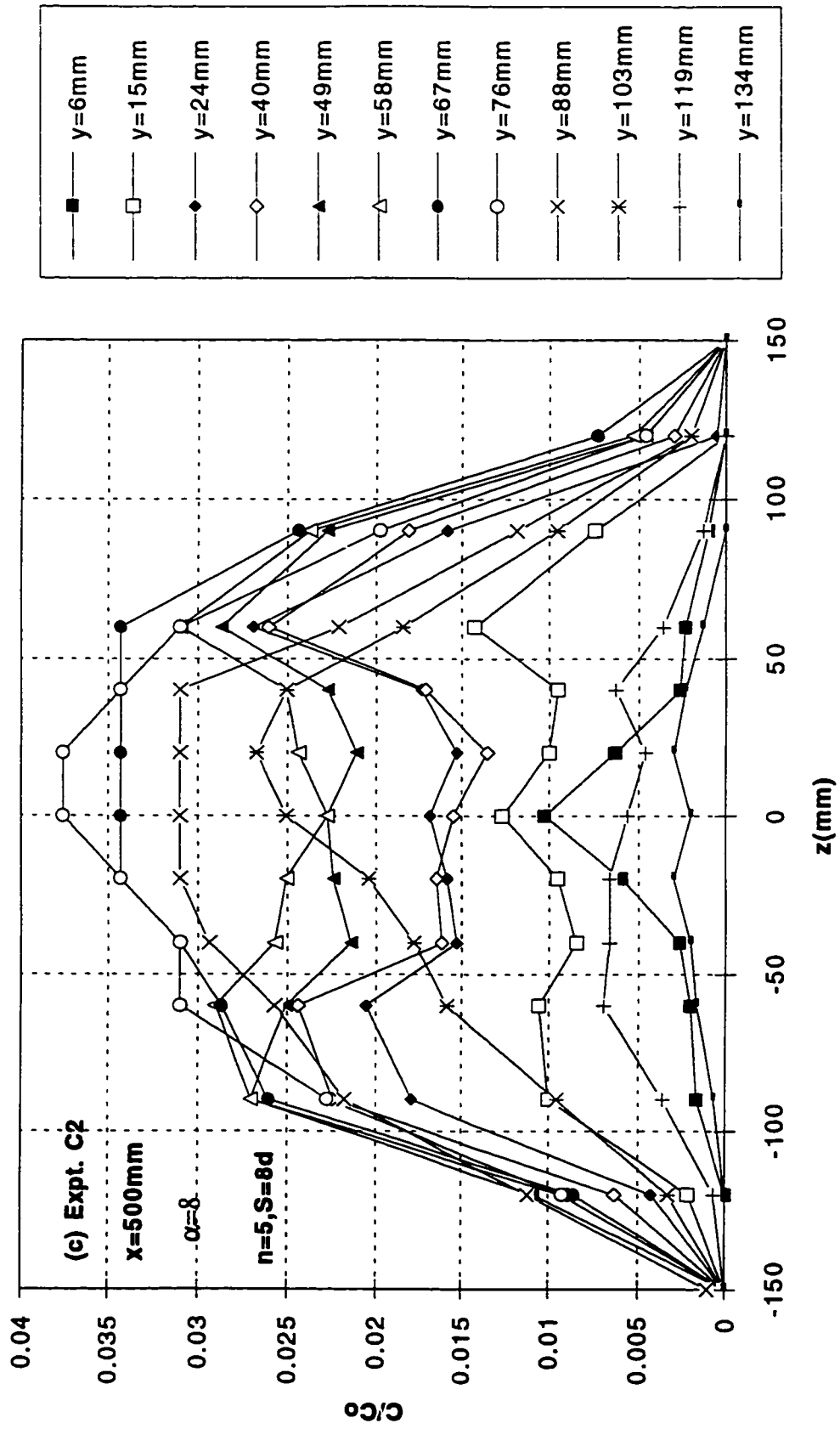
Fig. 4.7c Transverse Concentration Profiles at Different Levels for Expt. A3
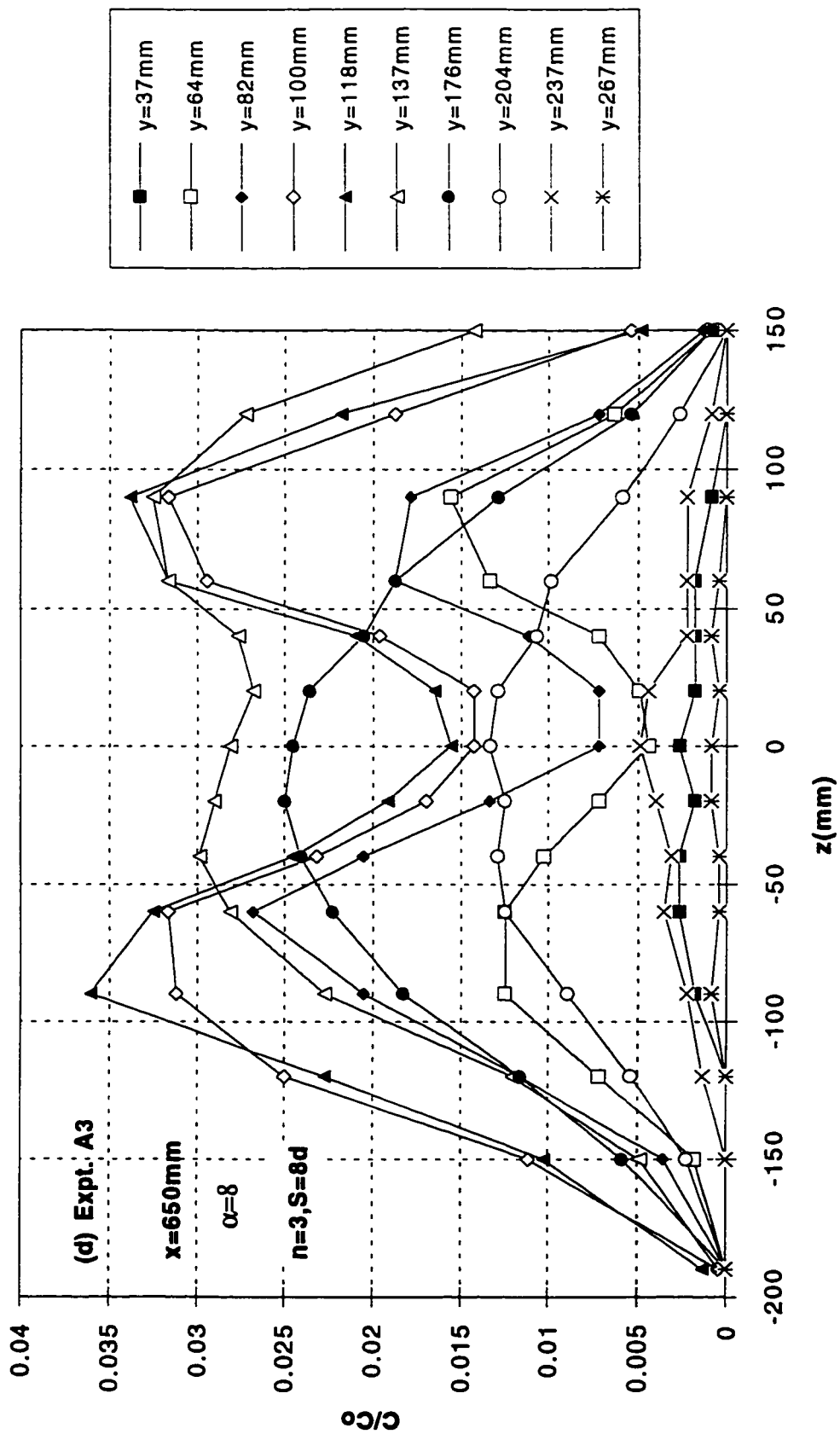
Fig. 4.7d Transverse Concentration Profiles at Different Levels for Expt. A3
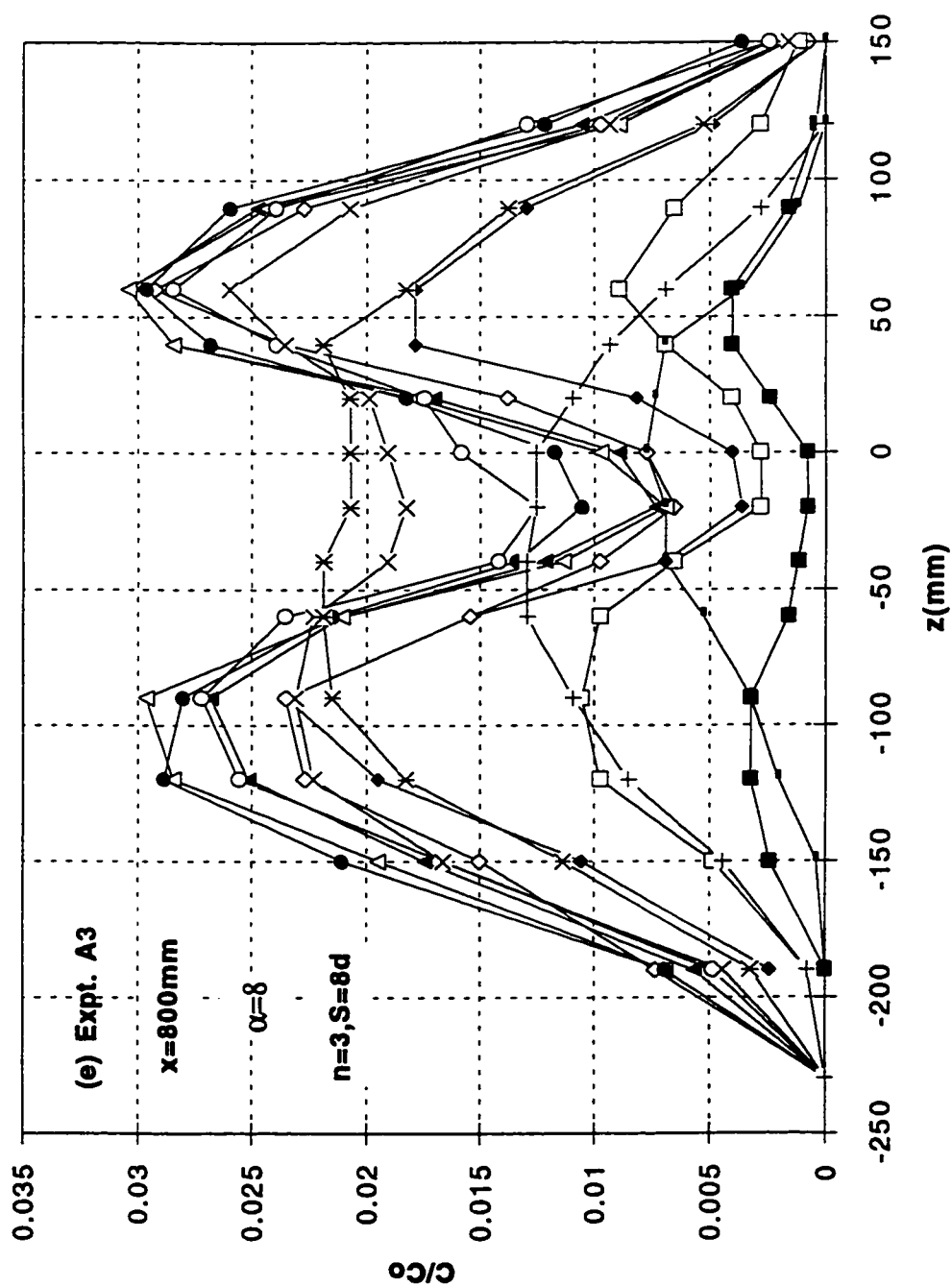
Fig. 4.7e Transverse Concentration Profiles at Different Levels for Expt. A3
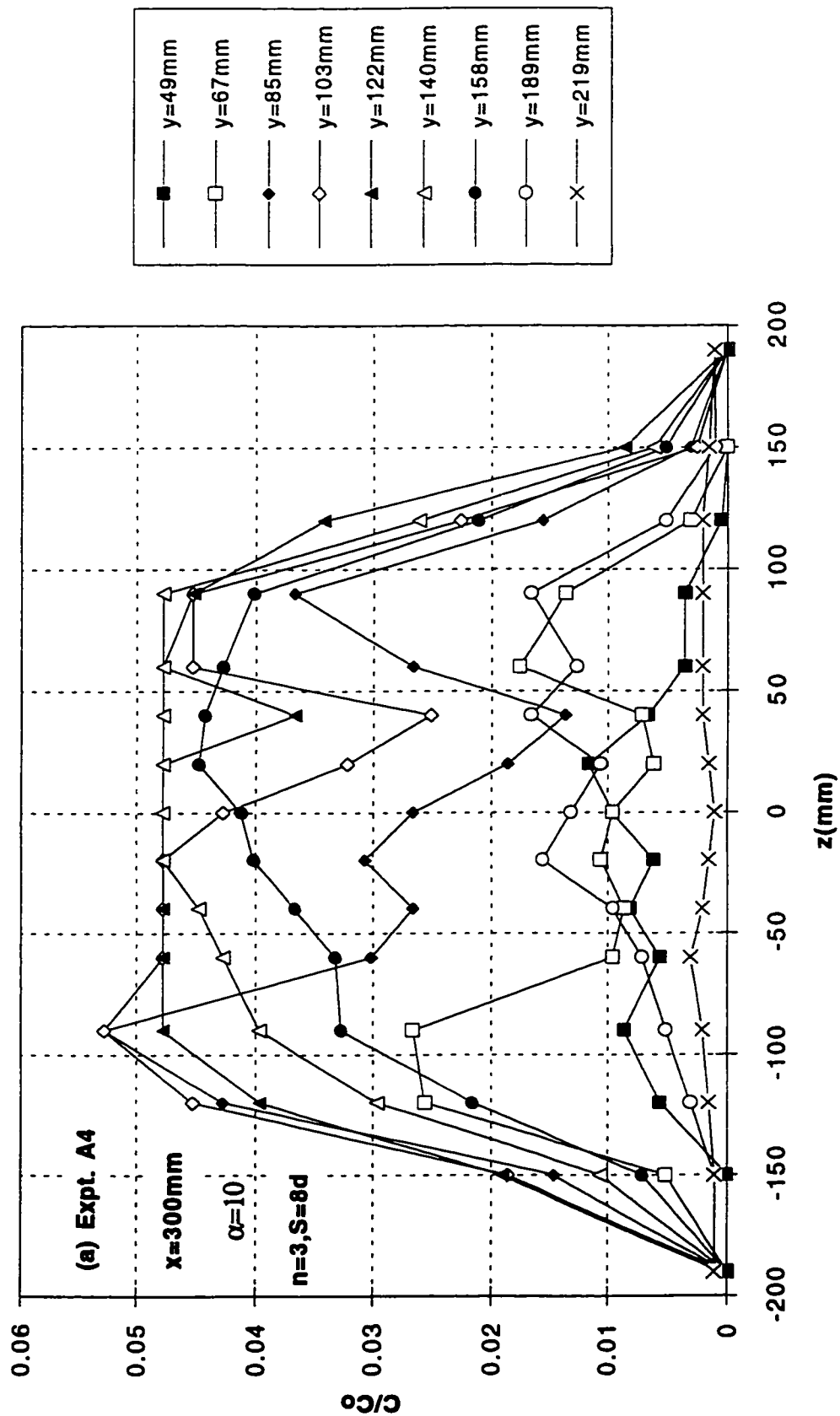
Legend:
- y=37mm
- y=64mm
- y=82mm
- y=91mm
- y=100mm
- y=110mm
- y=119mm
- y=137mm
- y=152mm
- y=192mm
- y=222mm
- y=268mm

(e) Expt. A3

x=800mm

α=8

n=3, S=8d

Fig. 4.8a Transverse Concentration Profiles at Different Levels for Expt. A4

The chart legend shows:
- y=49mm
- y=67mm
- y=85mm
- y=103mm
- y=122mm
- y=140mm
- y=158mm
- y=189mm
- y=219mm

Chart annotations:
(a) Expt. A4
x=300mm
$\alpha=10$
n=3,S=8d

Axes: c/Co (vertical), z(mm) (horizontal)

Fig. 4.8b Transverse Concentration Profiles at Different Levels for Expt. A4

The chart legend shows:
- y=49mm
- y=67mm
- y=85mm
- y=103mm
- y=122mm
- y=140mm
- y=158mm
- y=189mm
- y=219mm
- y=250mm

(b) Expt. A4

x=500mm

$\alpha=10$

n=3, S=8d

Axis labels: c/Co (vertical), z(mm) (horizontal)
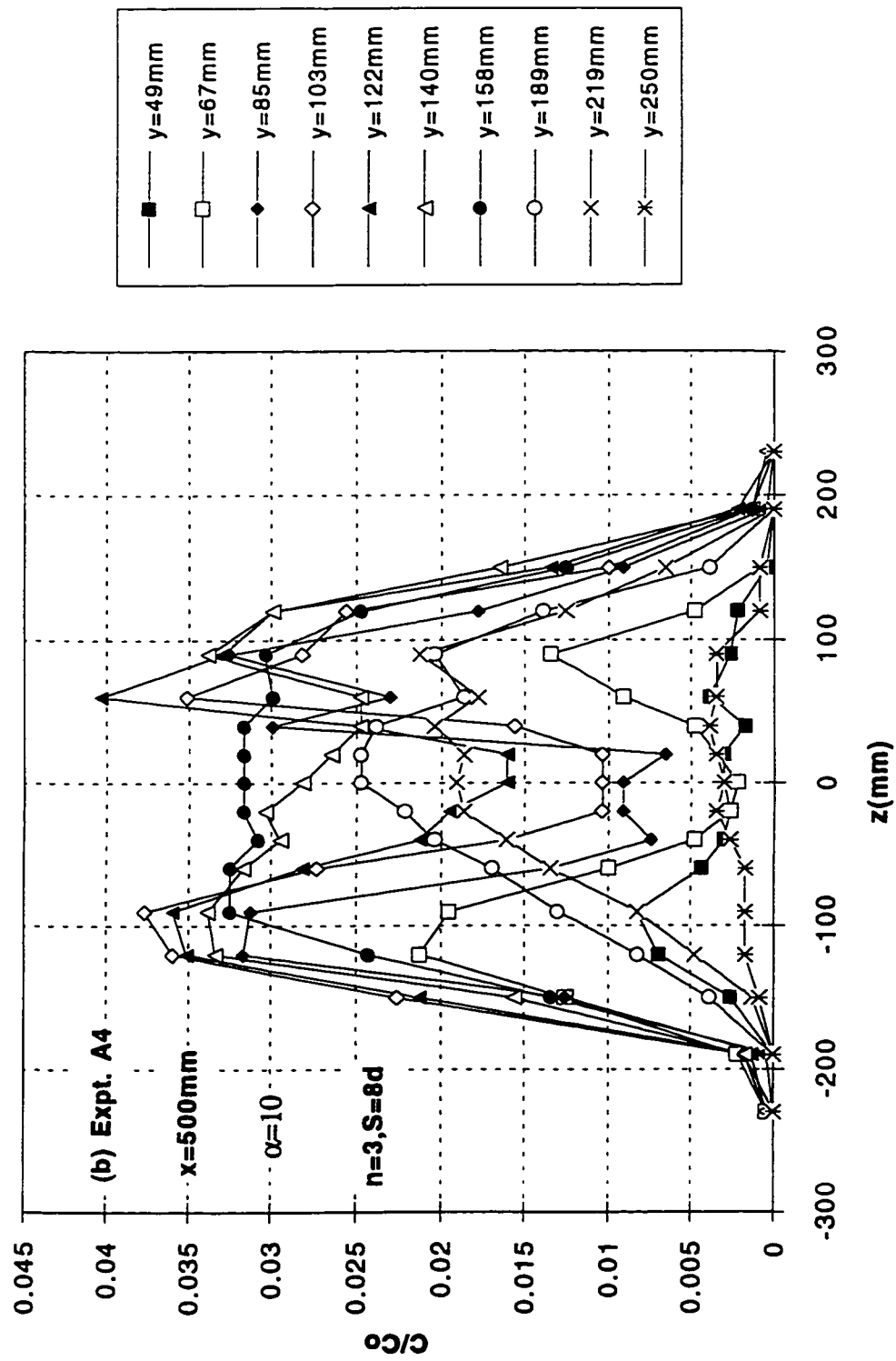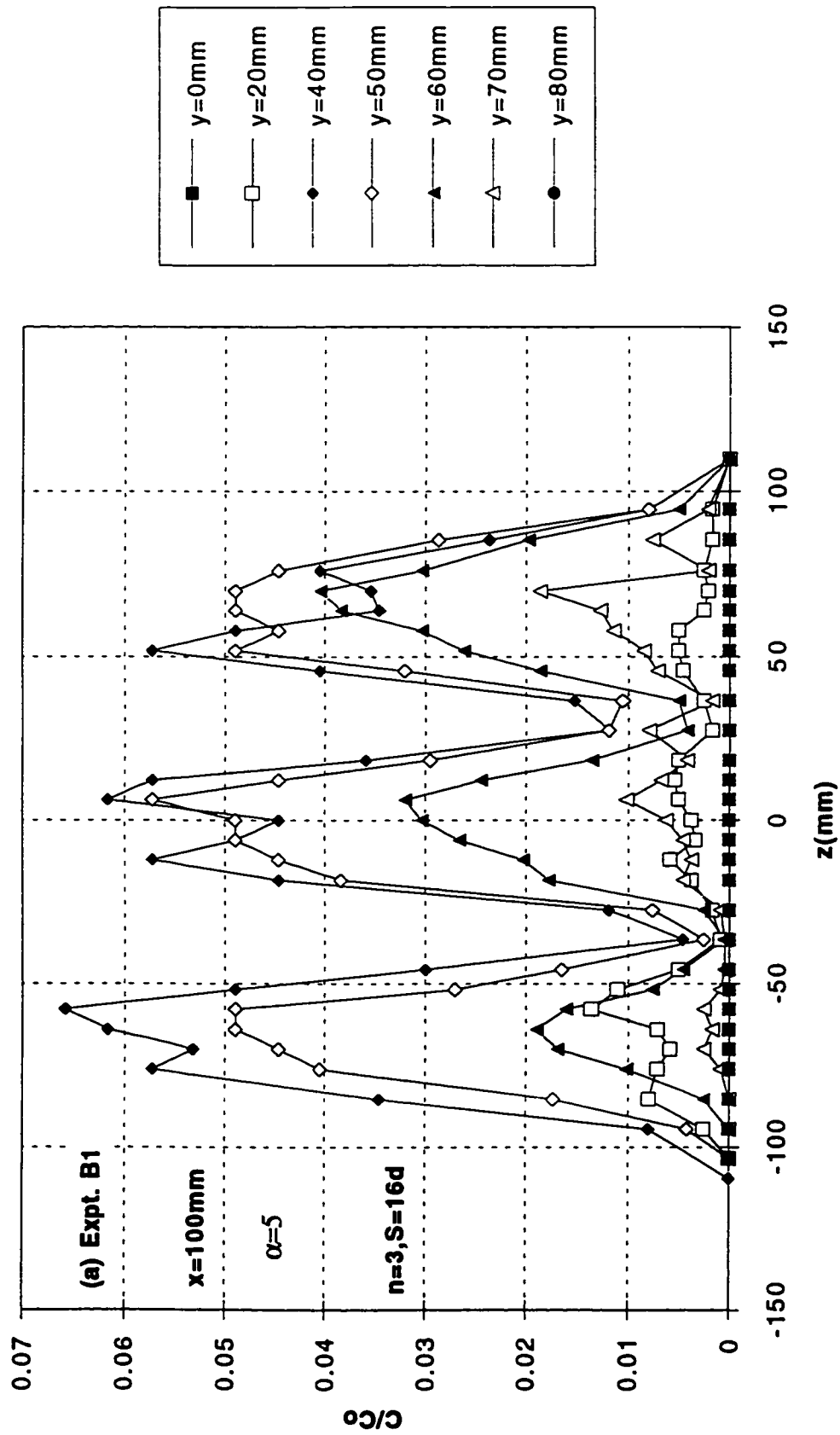
Fig. 4.9a Transverse Concentration Profiles at Different Levels for Expt. B1

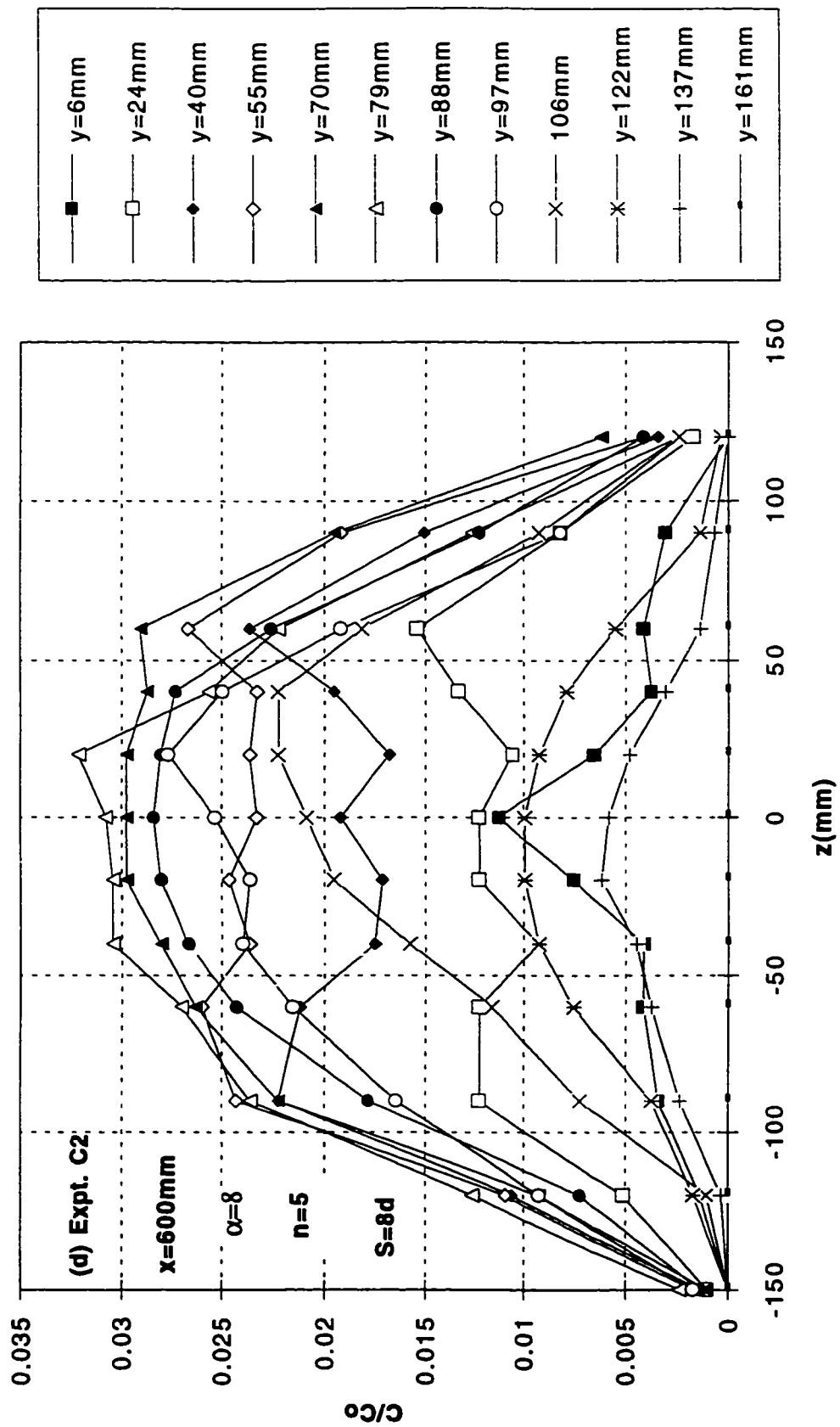Fig. 4.9b Transverse Concentration Profiles at Different Levels for Expt. B1

Fig. 4.9c Transverse Concentration Profiles at Different Levels for Expt. B1
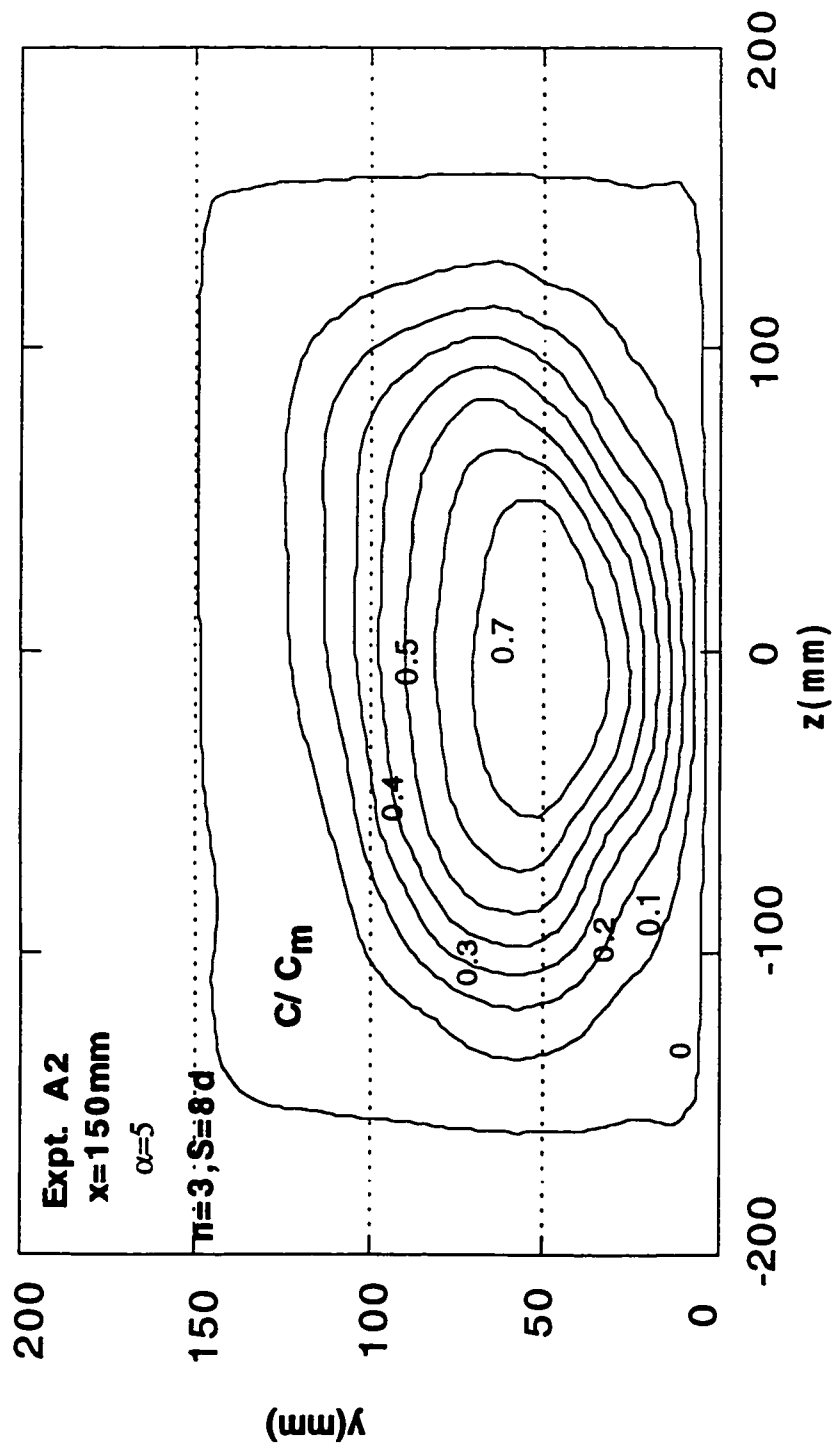
171

Fig. 4.9d Transverse Concentration Profiles at Different Levels for Expt. B1

Fig. 4.10a Transverse Concentration Profiles at Different Levels for Expt. B2

Fig. 4.10b Transverse Concentration Profiles at Different Levels for Expt. B2

Fig. 4.10c Transverse Concentration Profiles at Different Levels for Expt. B2

Fig. 4.11a Transverse Concentration Profiles at Different Levels for Expt. C1

Fig. 4.11b Transverse Concentration Profiles at Different Levels for Expt. C1

Fig. 4.12a Transverse Concentration Profiles at Different Levels for Expt. C2

Fig. 4.12b Transverse Concentration Profiles at Different Levels for Expt. C2

Legend:
- y=0mm
- y=15mm
- y=30mm
- y=46mm
- y=61mm
- y=79mm
- y=82mm
- y=91mm
- y=100mm
- y=115mm
- y=130mm

(b)Expt. C2

x=400mm

α=8

S=8d,n=5

z(mm)

c/Co

Fig. 4.12c Transverse Concentration Profiles at Different Levels for Expt. C2

Legend:
- y=6mm
- y=15mm
- y=24mm
- y=40mm
- y=49mm
- y=58mm
- y=67mm
- y=76mm
- y=88mm
- y=103mm
- y=119mm
- y=134mm

(c) Expt. C2

x=500mm

$\alpha=8$

n=5, S=8d

Axis labels: c/c_o (vertical), z(mm) (horizontal)

Fig. 4.12d Transverse Concentration Profiles at Different Levels for Expt. C2

Legend:
- y=6mm
- y=24mm
- y=40mm
- y=55mm
- y=70mm
- y=79mm
- y=88mm
- y=97mm
- 106mm
- y=122mm
- y=137mm
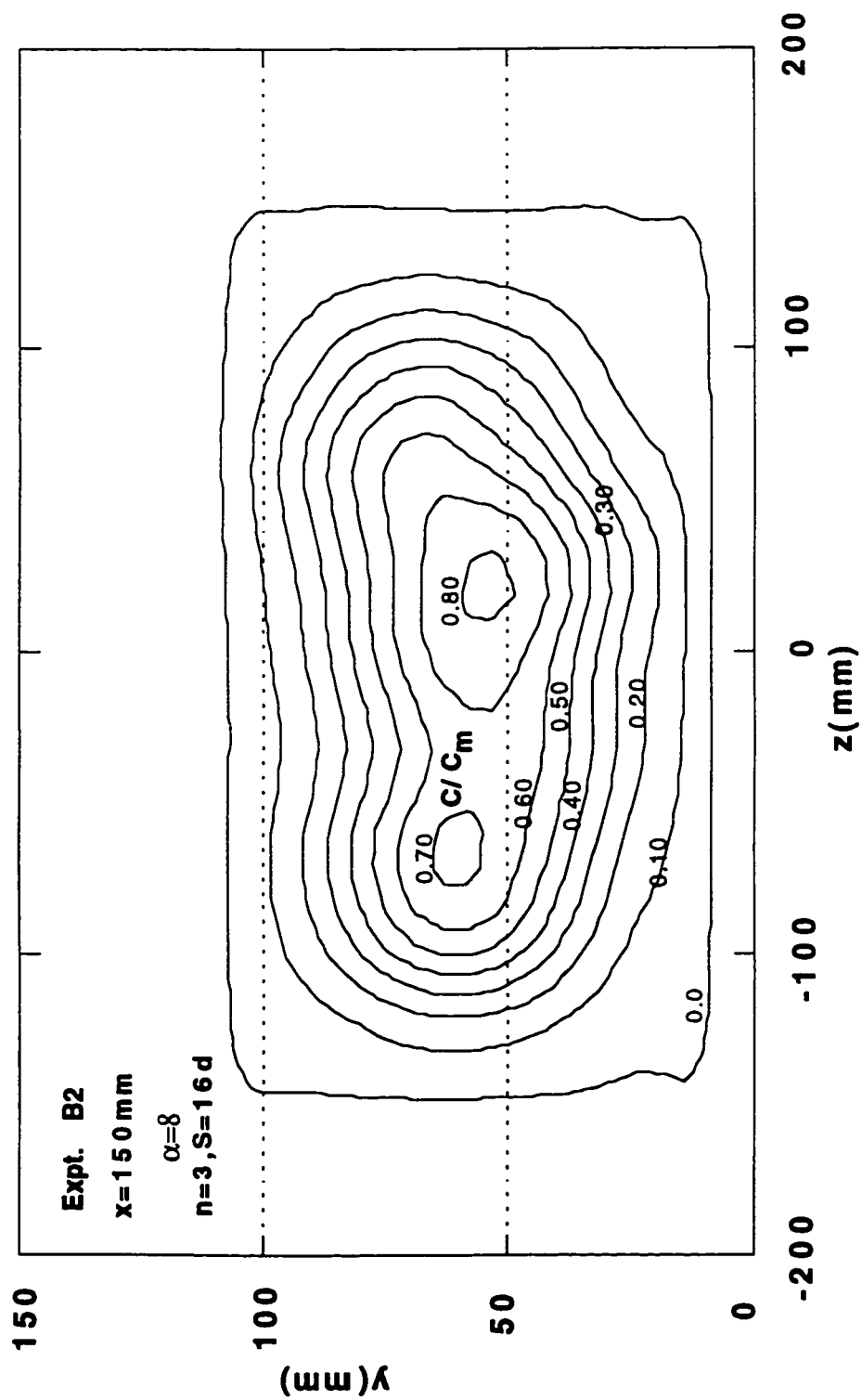- y=161mm

(d) Expt. C2

x=600mm

$\alpha=8$

n=5

S=8d

C/Co

z(mm)

Fig. 4.13a Typical Concentration Contours for Expt. A2
α=5, x=150mm
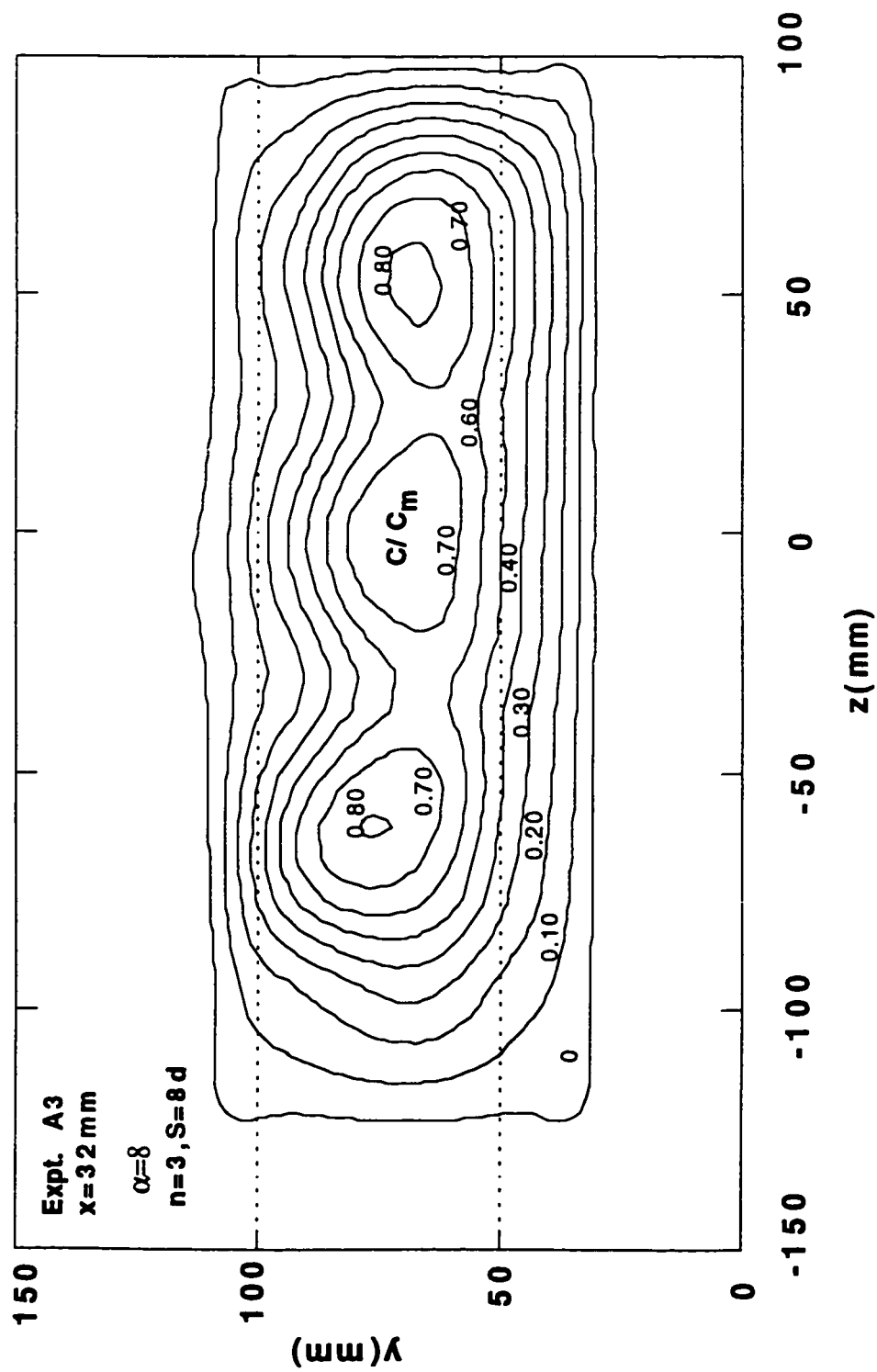
Fig. 4.13b Typical Concentration Contours for Expt. A3
$\alpha=8$, x=32mm

183
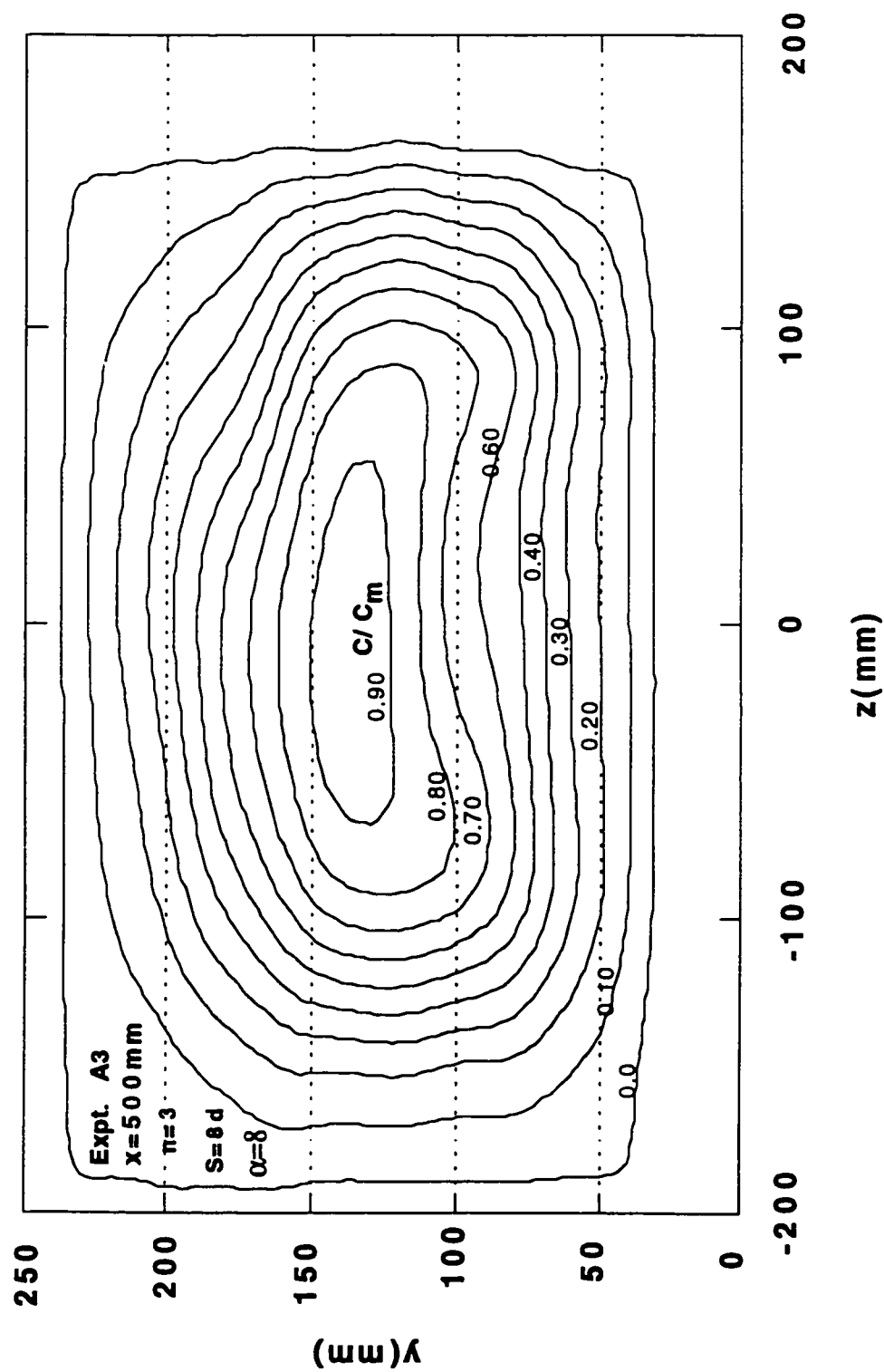
Fig. 4.13c Typical Concentration Contours for Expt. A3
$\alpha=8$, $x=500mm$
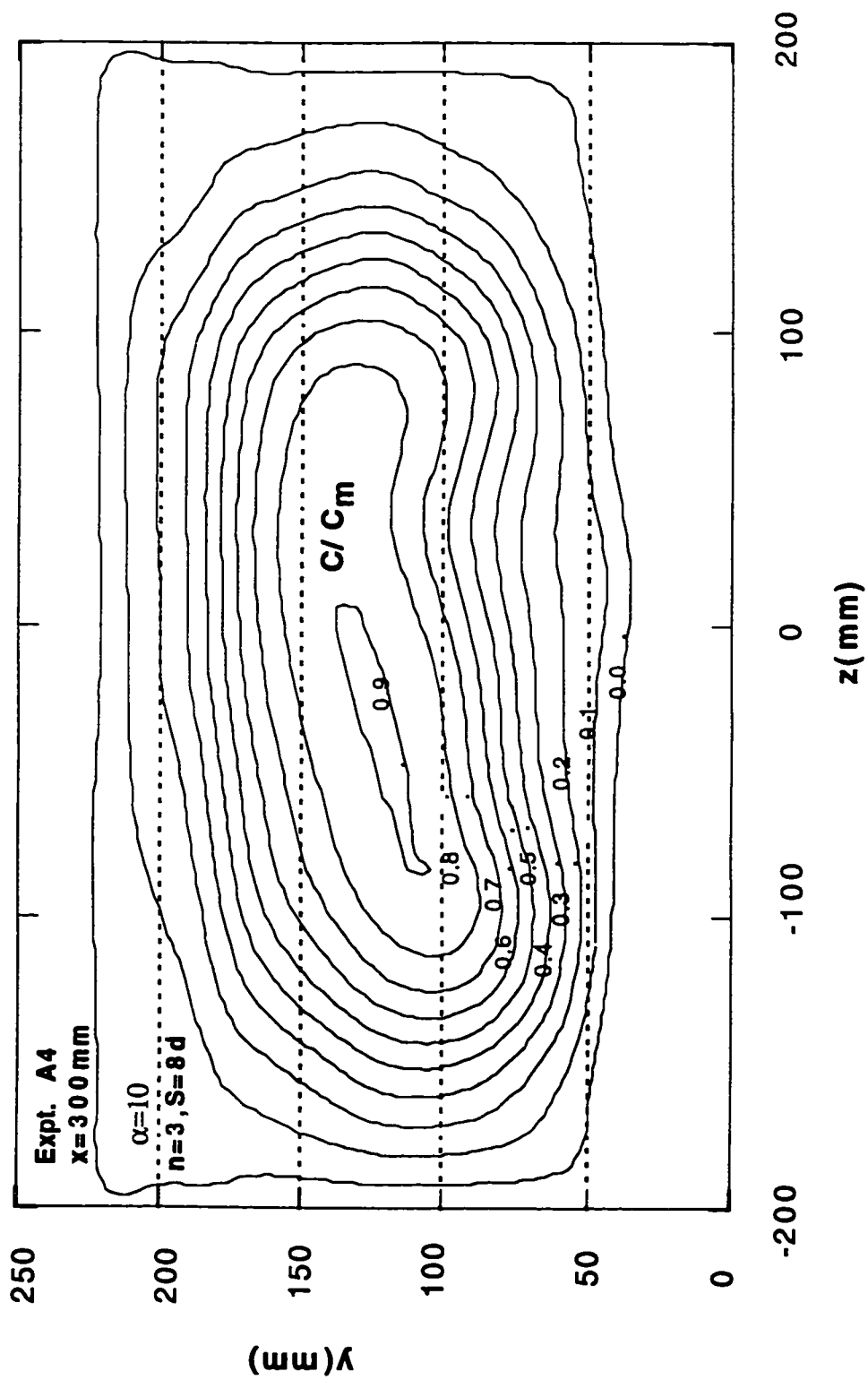
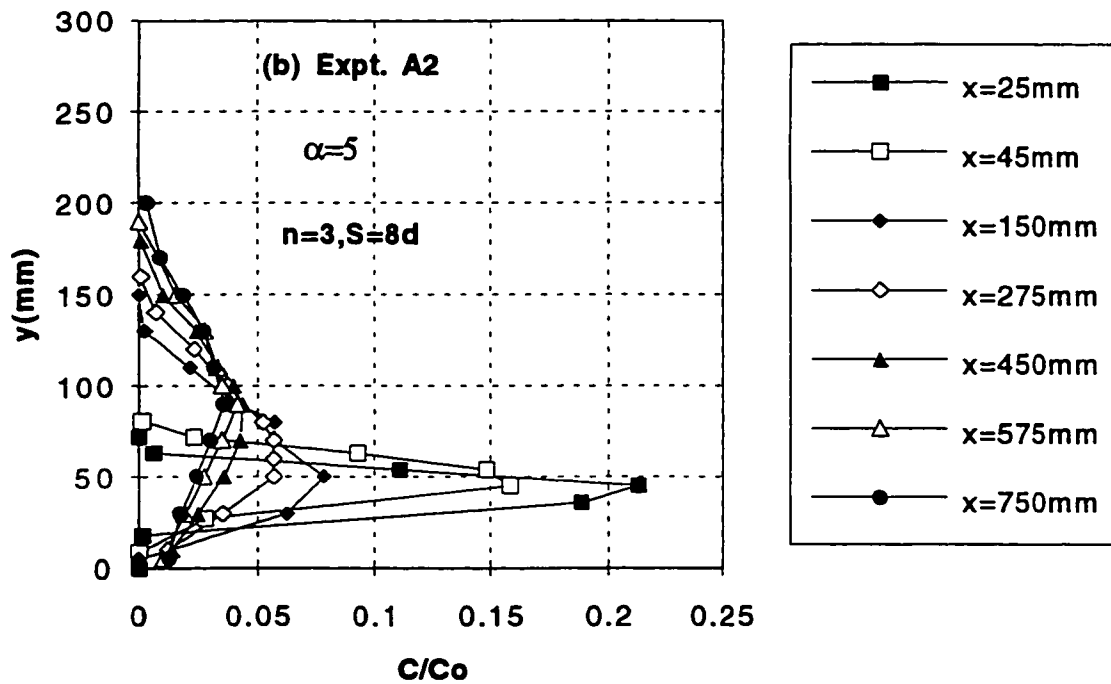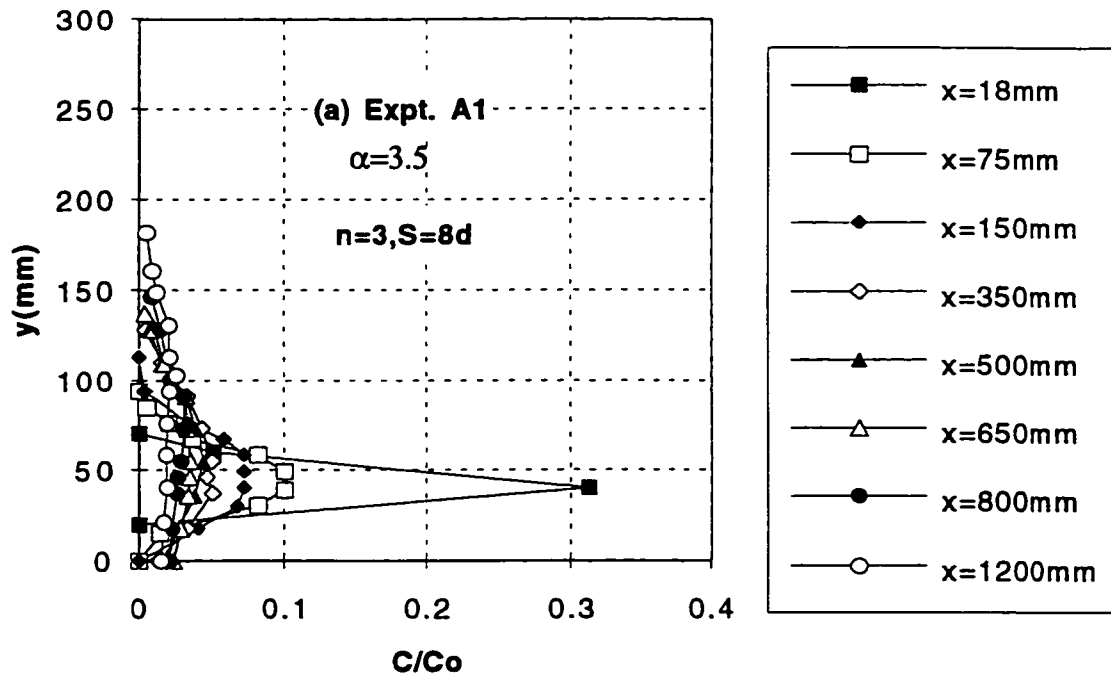Fig. 4.13d Typical Concentration Contours for Expt. A4
$\alpha=10$, x=300mm
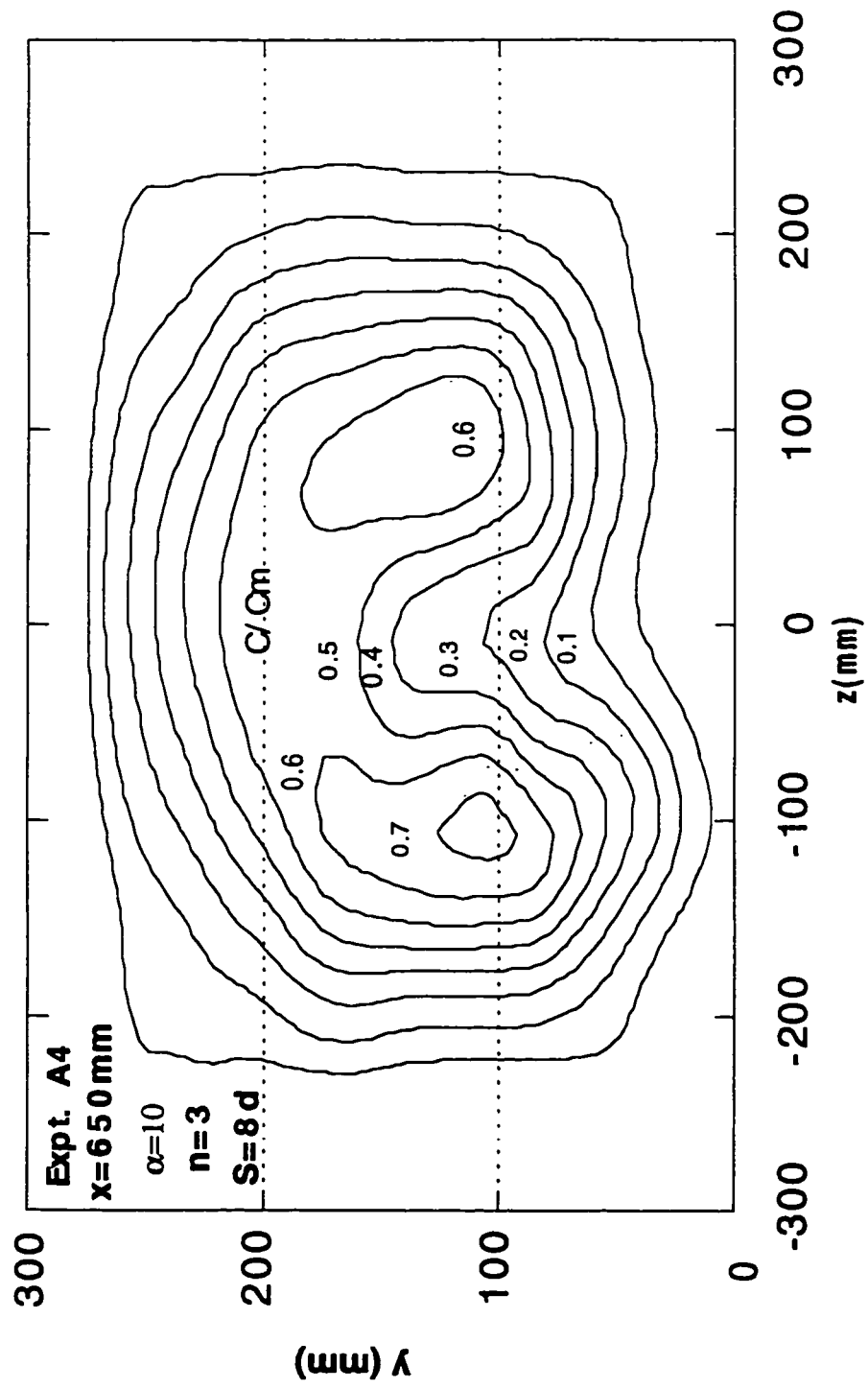
Fig. 4.13e Typical Concentration Contours for Expt. A4
α=10, x=650mm
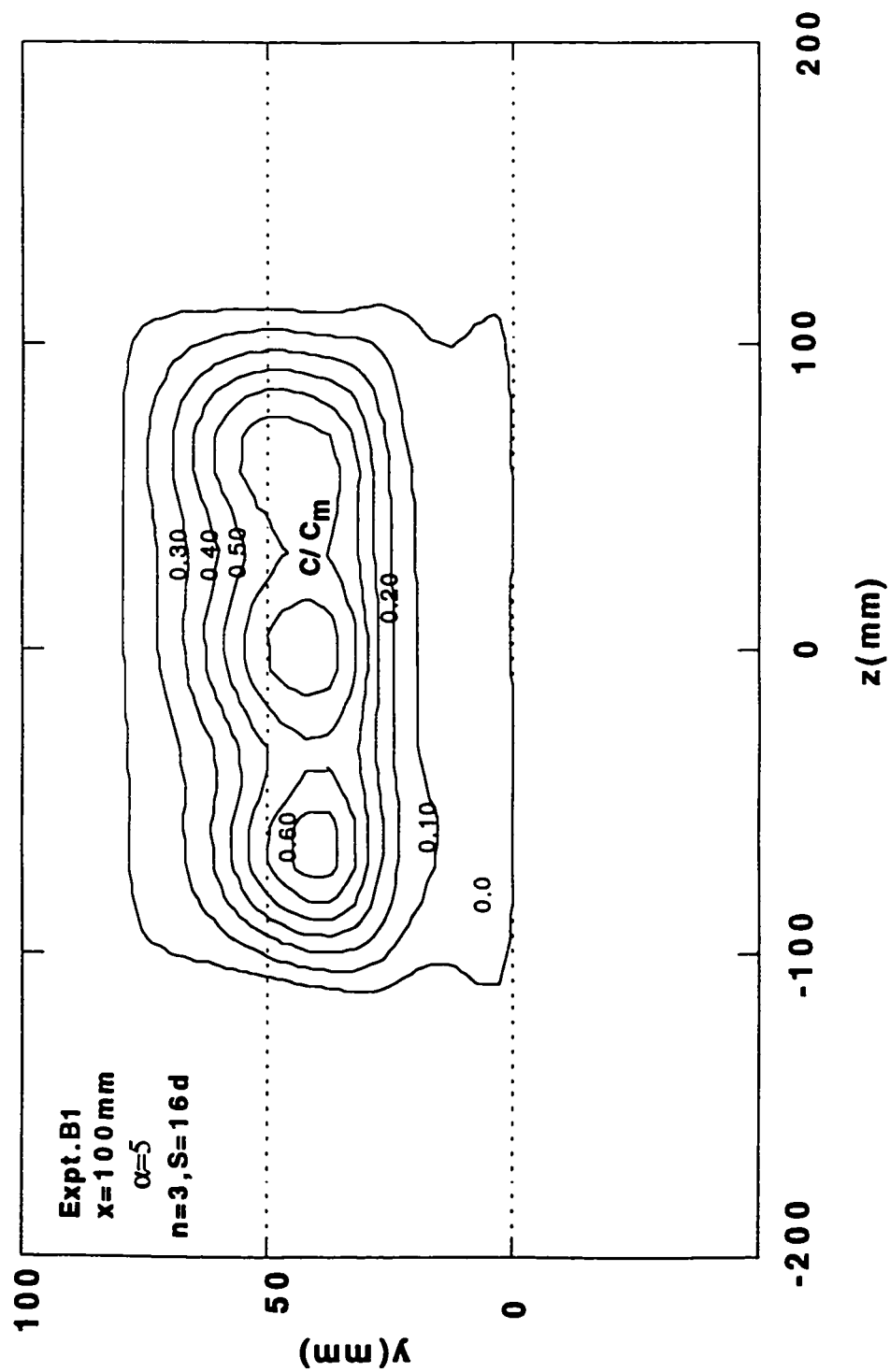
Fig. 4.13f Typical Concentration Contours for Expt. B1

α=5, x=100mm

Fig. 4.13g Typical Concentration Contours for Expt. B2
α=8, x=150mm
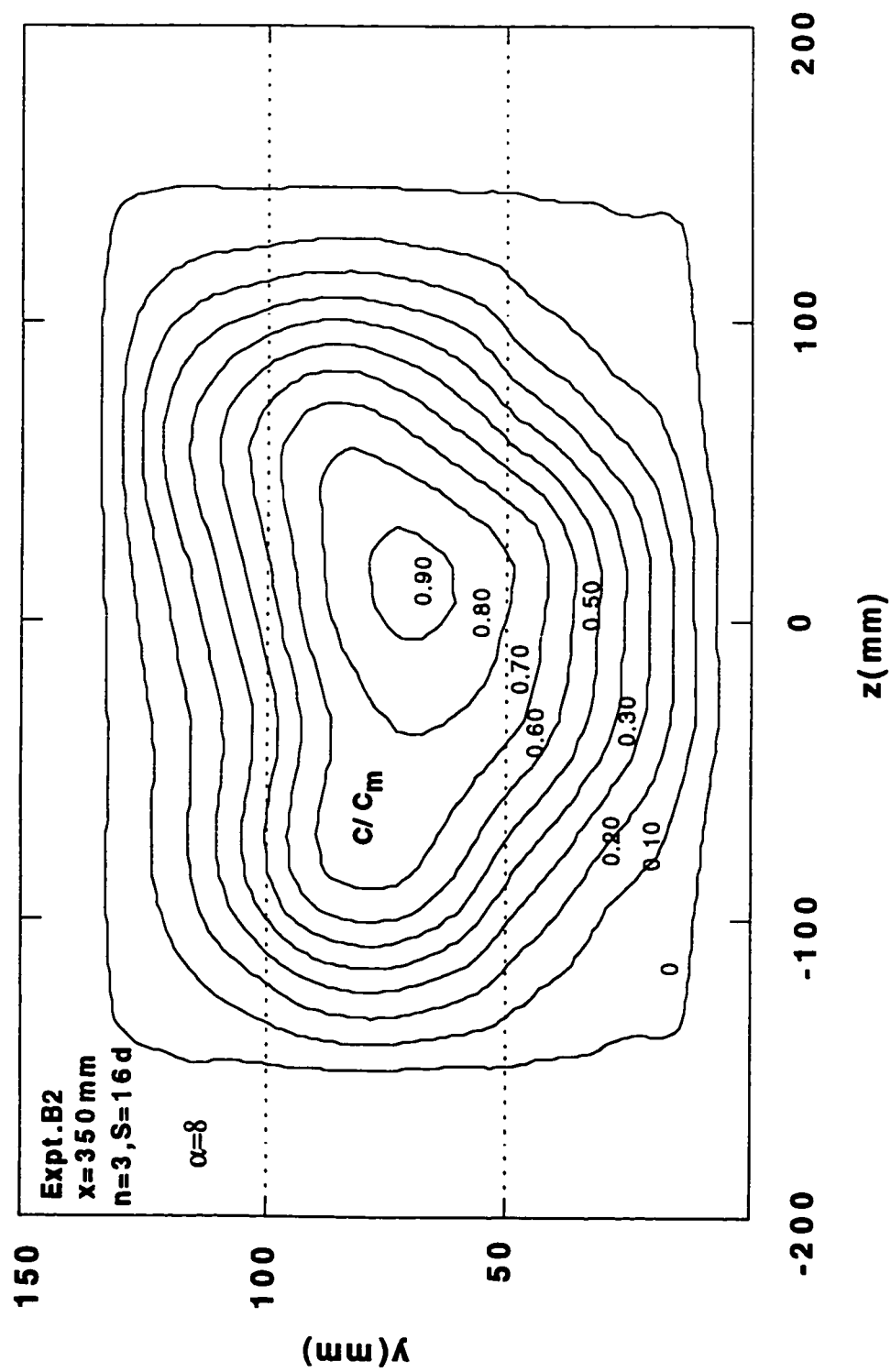
Fig. 4.13h Typical Concentration Contours for Expt. B2
$\alpha=8$, x=350mm

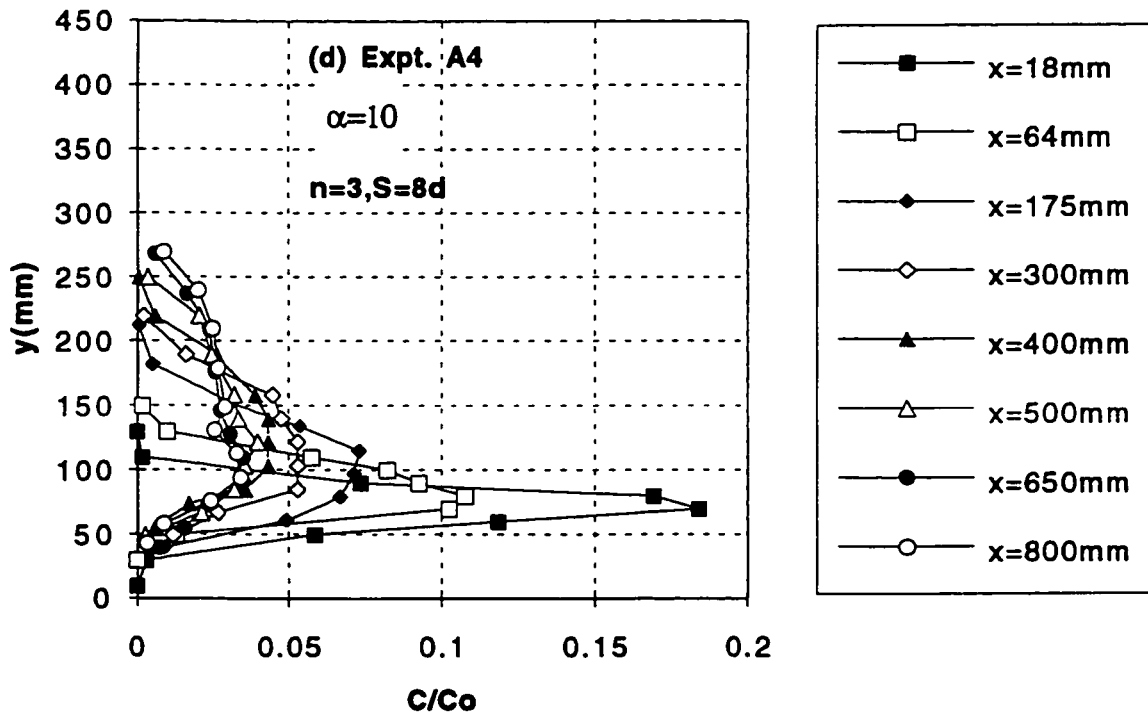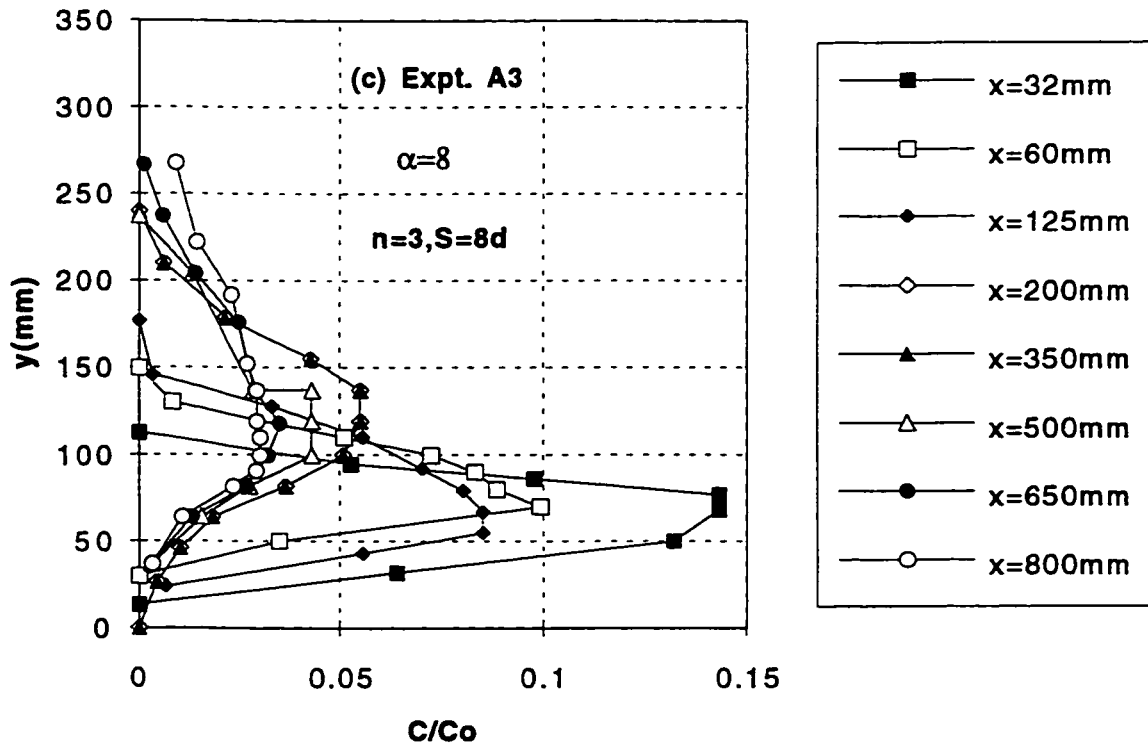**Fig. 4.14 (a-b) Vertical Concentration Profiles for Expt. A1 and Expt. A2**

190

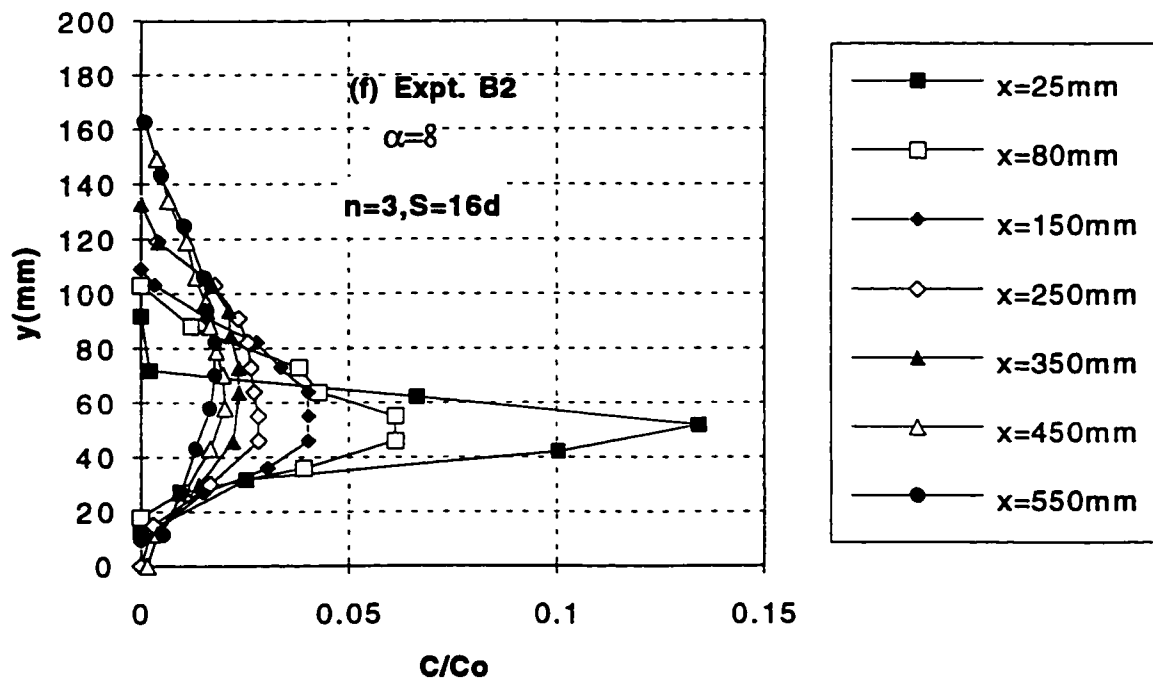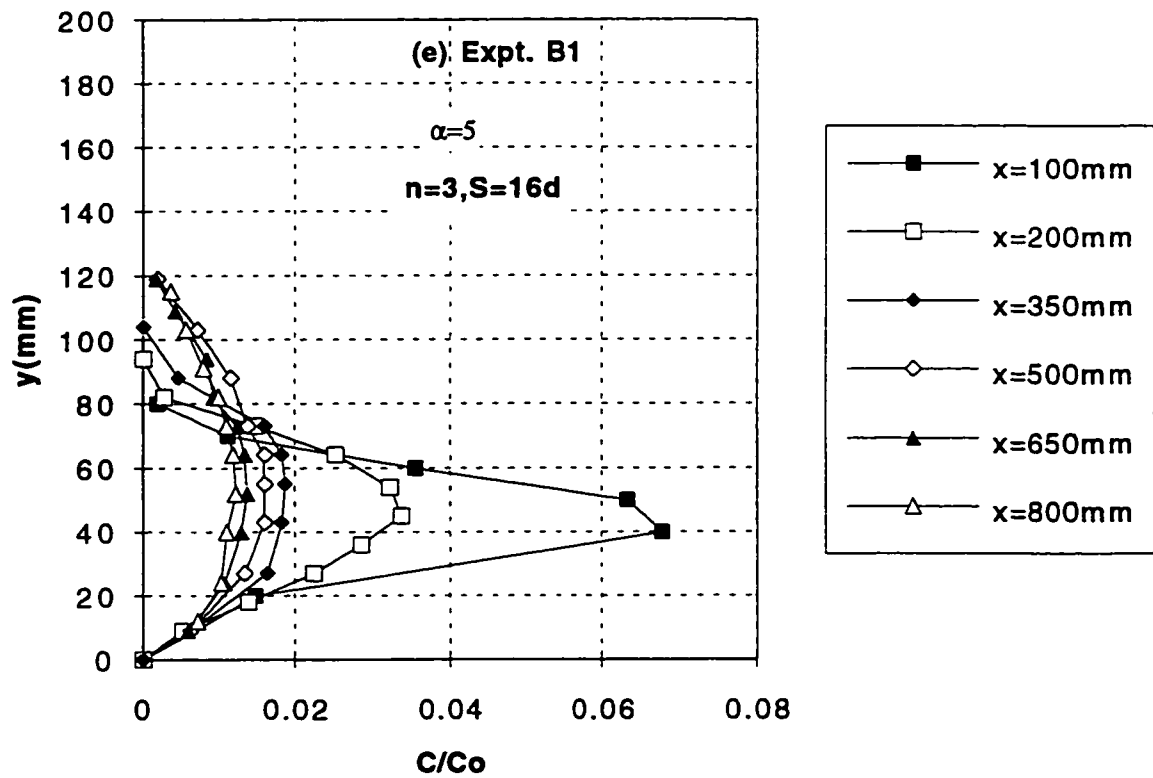**Fig. 4.14 (c-d) Vertical Concentration Profiles for Expt. A3 and Expt. A4**

Fig. 4.14 (e-f) Vertical Concentration Profiles for Expt. B1 and Expt. B2
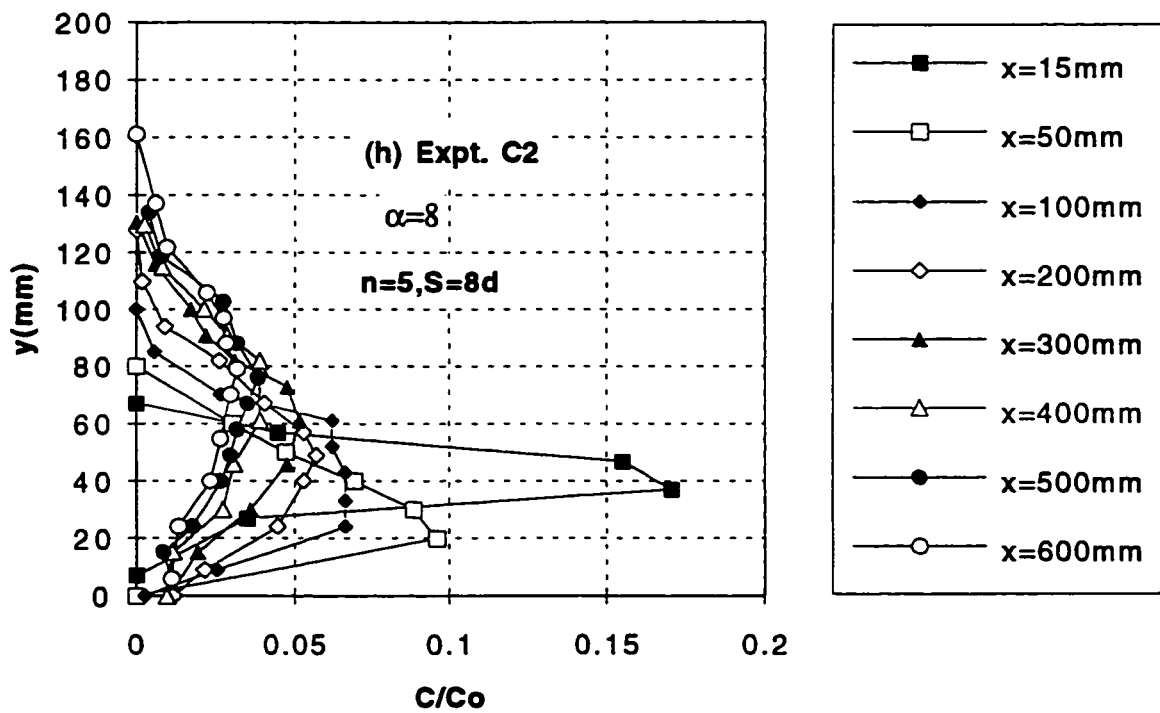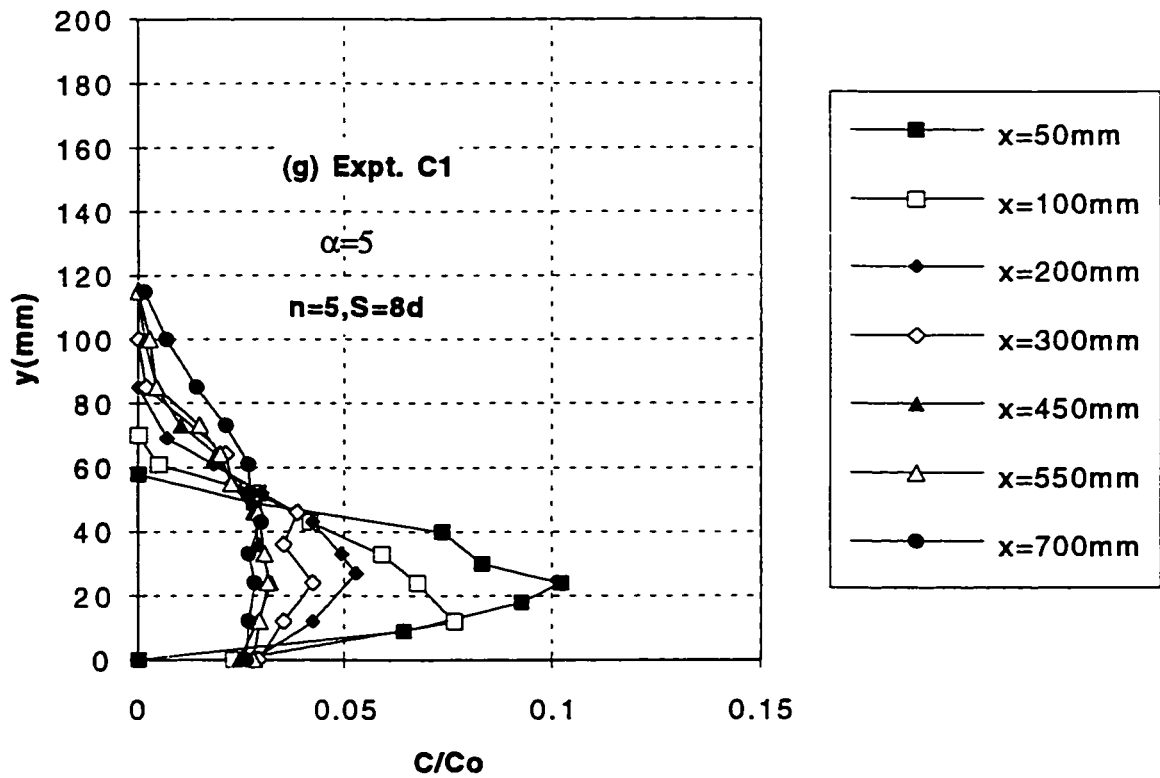
Fig. 4.14 (g-h) Vertical Concentration Profiles for Expt. C1 and Expt. C2
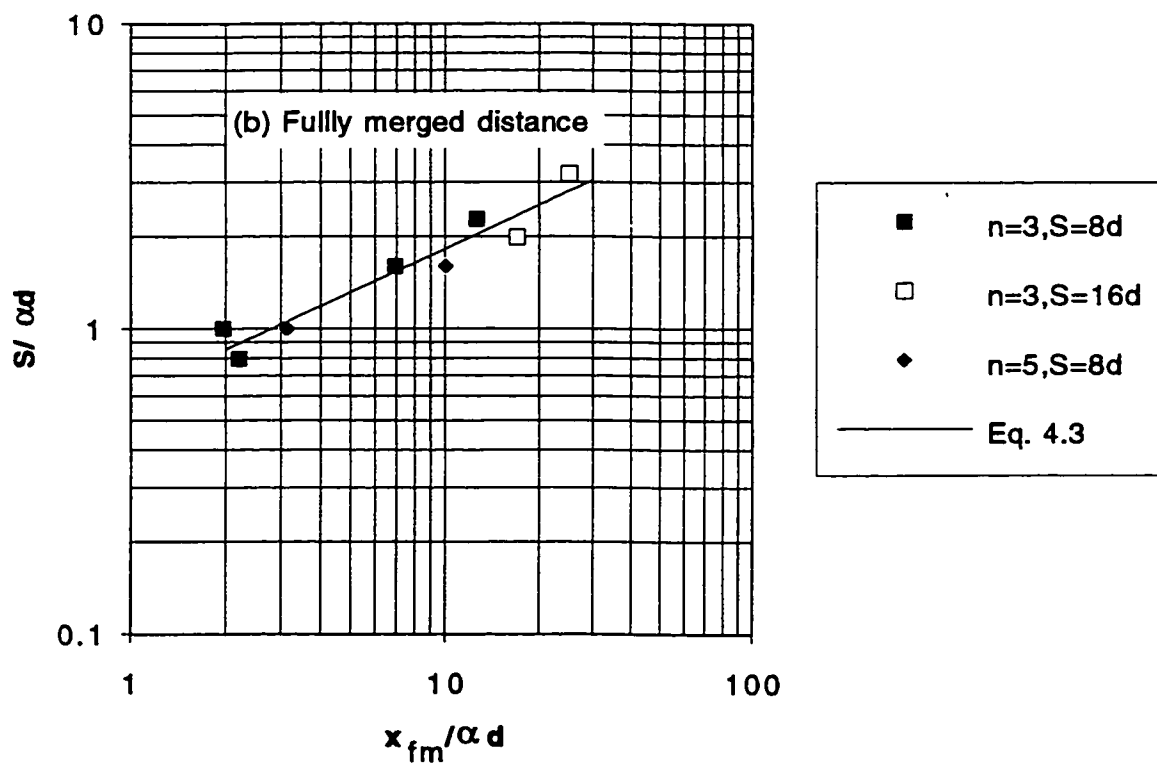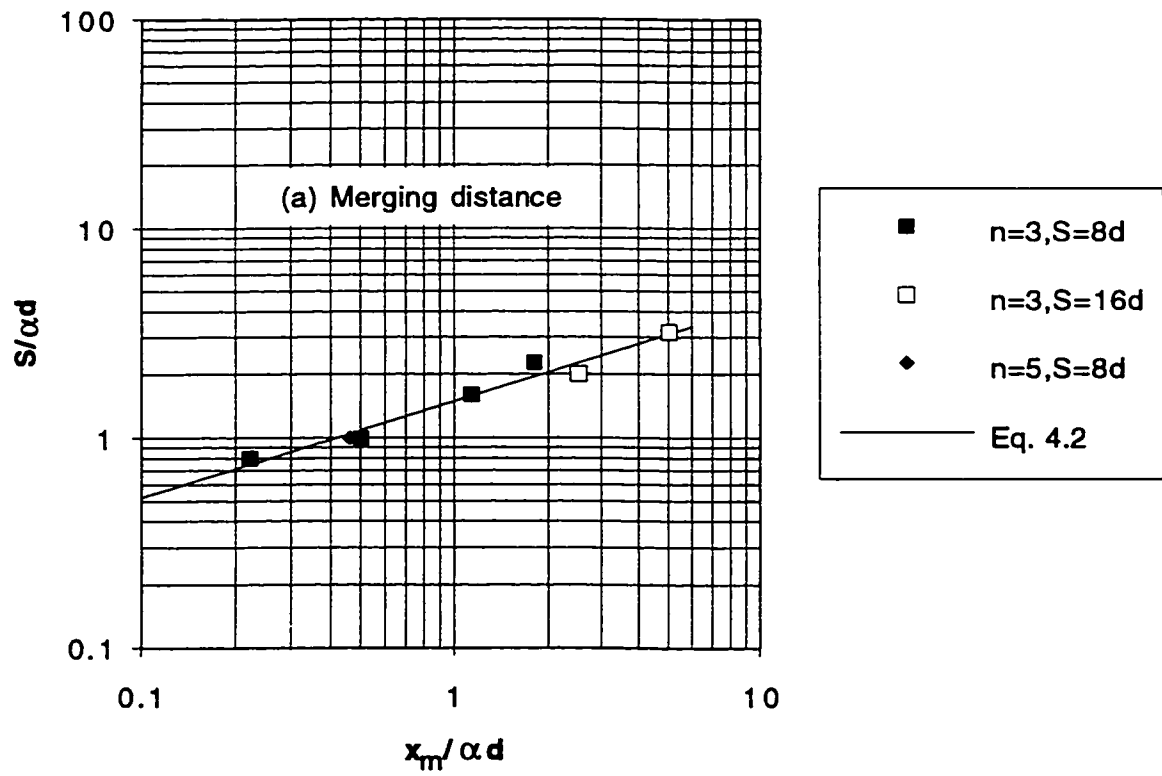
Fig. 4.15 (a-b) Merging Distances for Jets
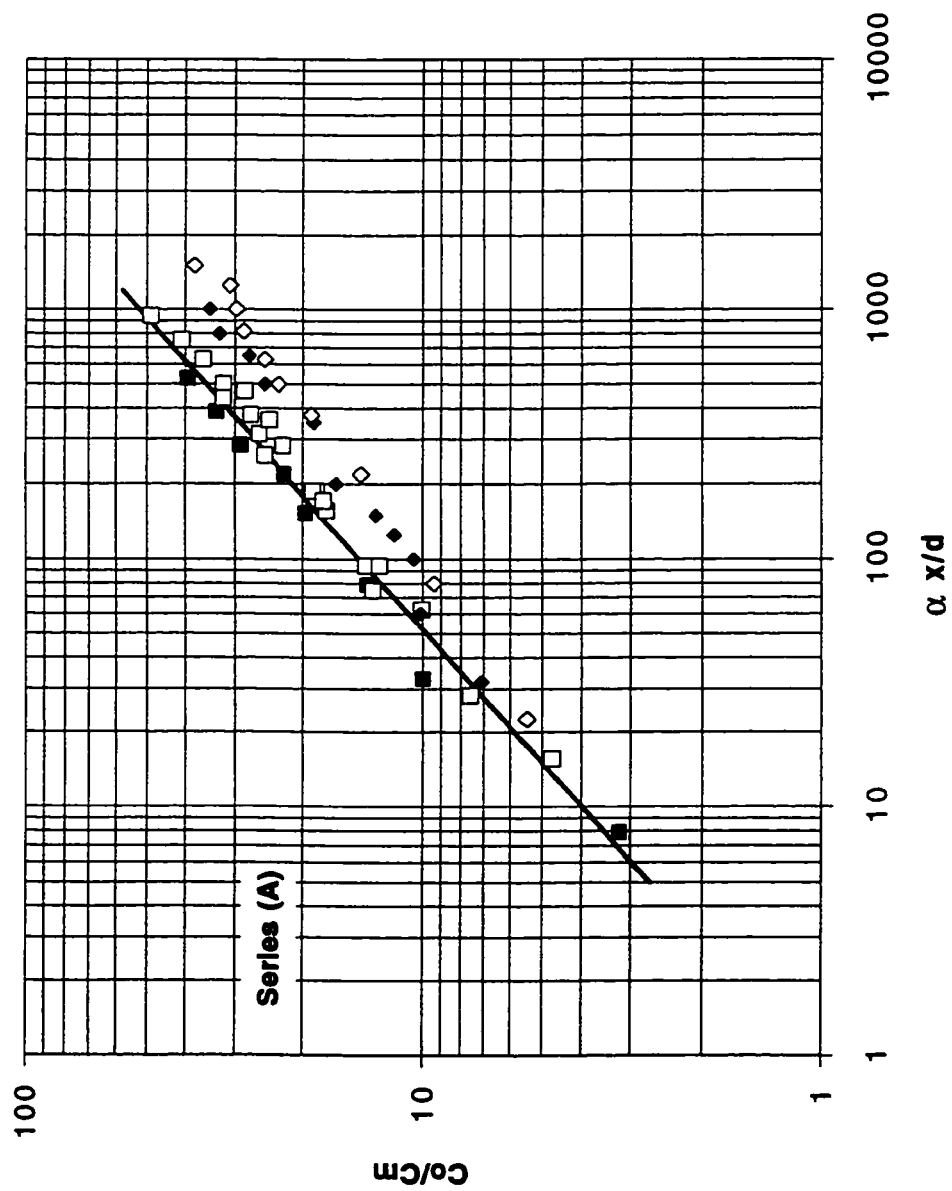
Fig. 4.16a Variation of Minimum Dilution (Co/Cm) with αx/d for Series A
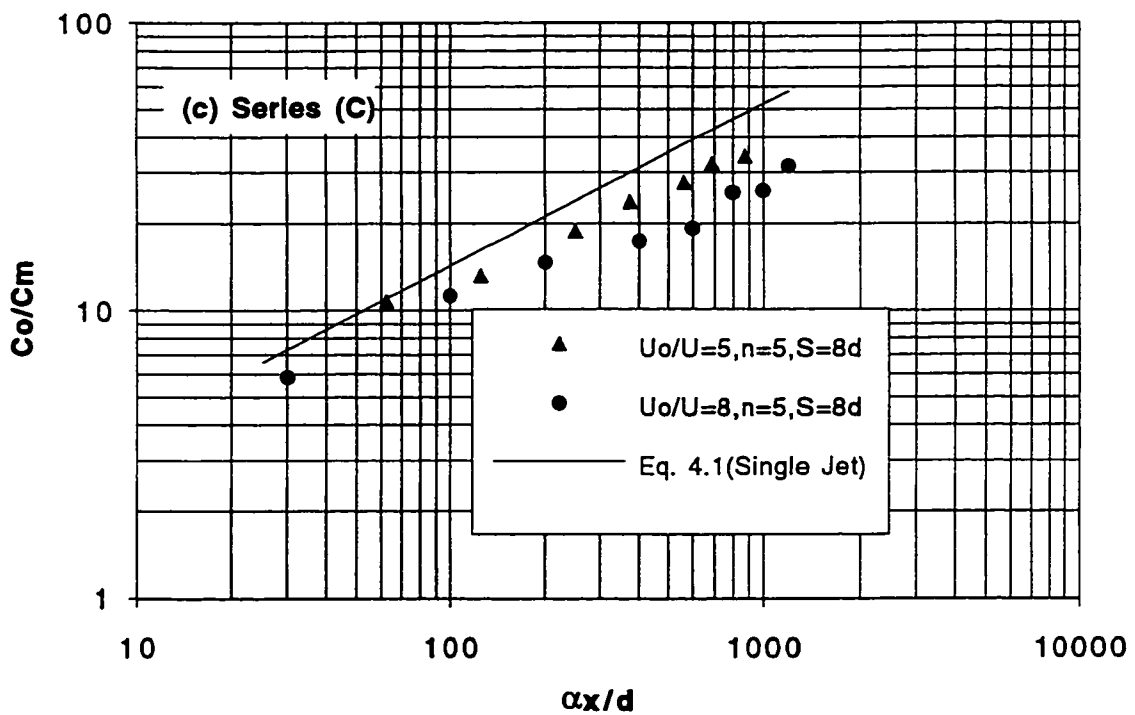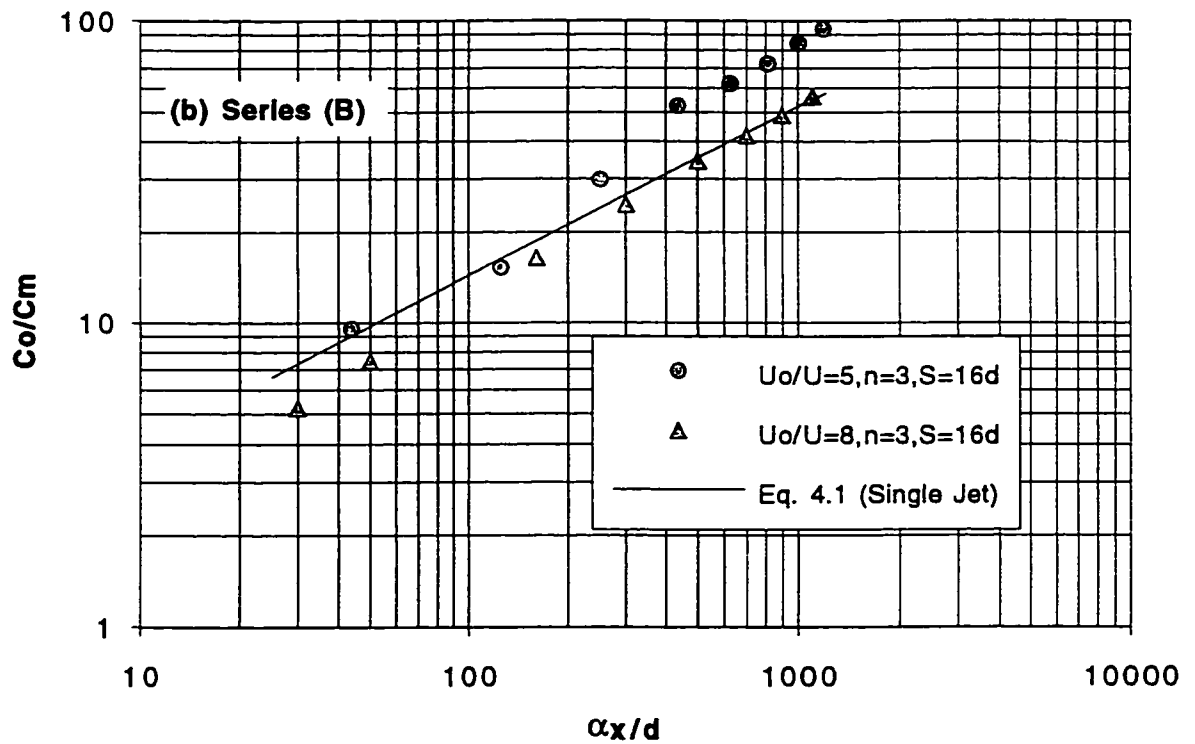
**Fig. 4.16 (b-c) Variation of Minimum Dilution (Co/Cm) with αx/d
for Series B and Series C**
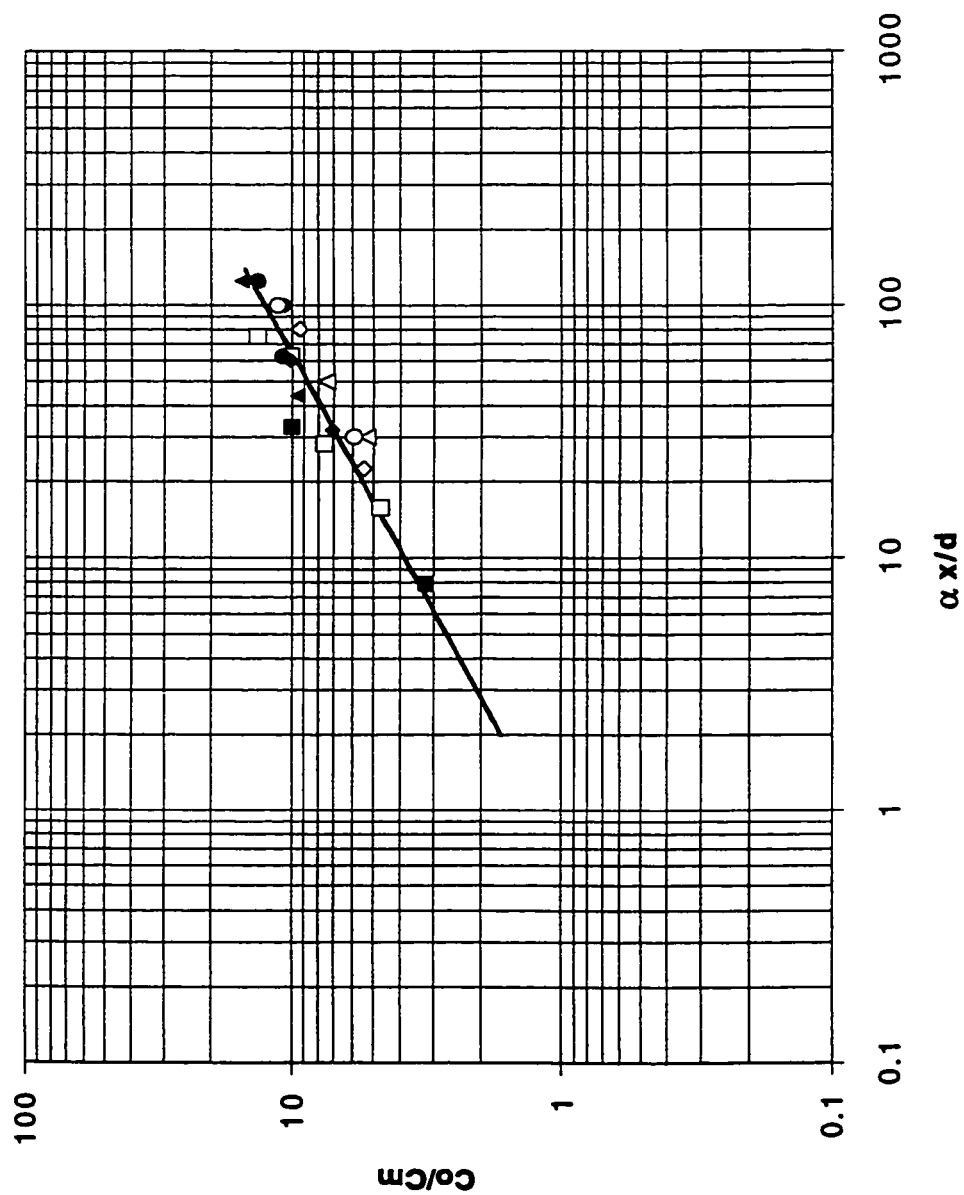
Fig. 4.17 Variation of Minimum Dilution in the MDNF Region
for all the Experiments

Legend:
- ■ Uo/U=3.5,n=3,S=8d
- □ Uo/U=5,n=3,S=8d
- ◆ Uo/U=8,n=3,S=8d
- ◇ Uo/U=10,n=3,S=8d
- ▲ Uo/U=5,n=3,S=16d
- △ Uo/U=8,n=3,S=16d
- ● Uo/U=5,n=5,S=8d
- ○ Uo/U=8,n=5,S=8d
- —— slope=1/2

x-axis: α x/d
y-axis: Co/Cm

197
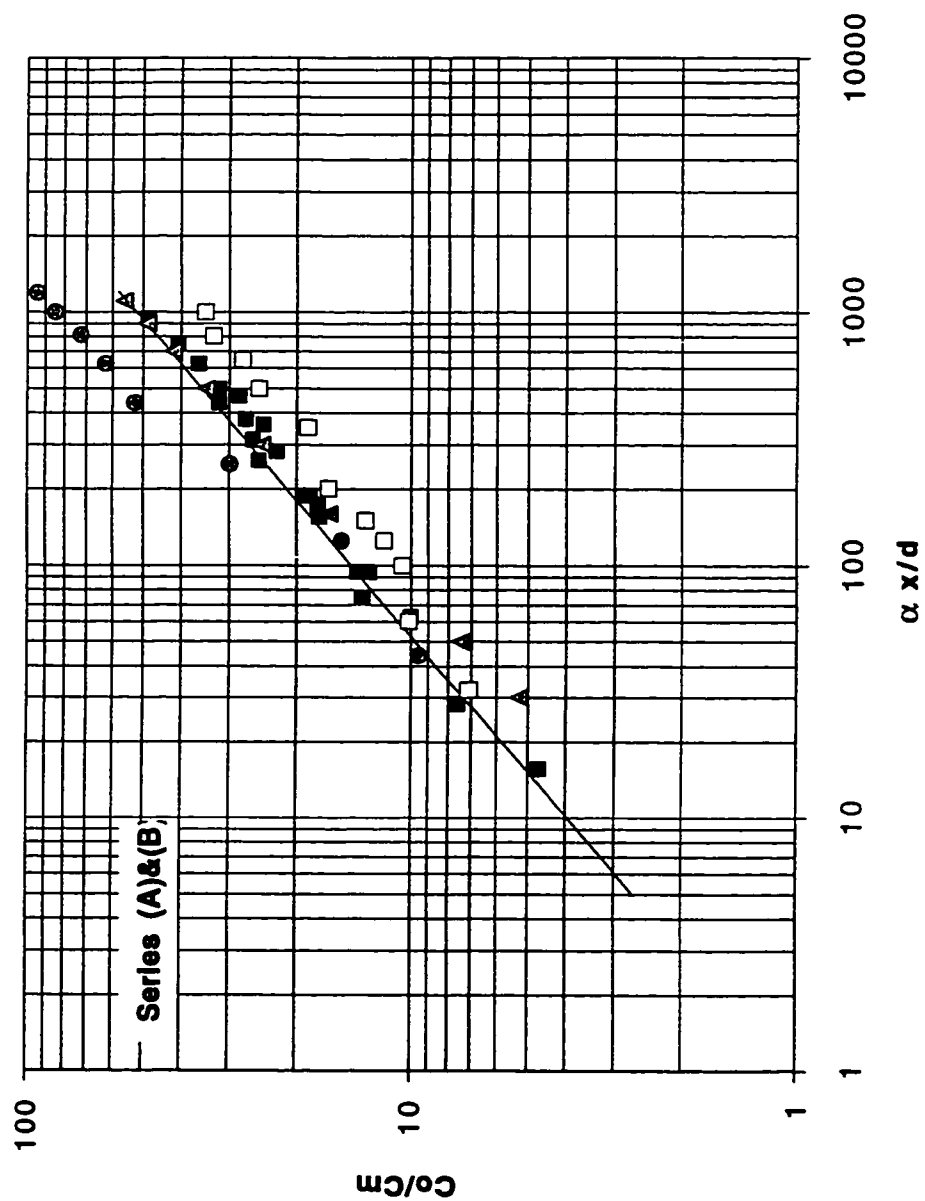
Fig. 4.18 Variation of Minimum Dilution with $\alpha x/d$ Showing the Effect of Changing the Spacing

198

Fig. 4.19 Variation of Minimum Dilution with $\alpha x/d$ Showing the
Effect of Changing the Number of Ports

(a) Expt. A1

α=3.5

n=3,S=8d

Legend:
- ■ x=150mm
- □ x=350mm
- ◆ x=500mm
- ◇ x=650mm
- ▲ x=880mm
- ● x=1200mm

(b) Expt. A2

α=5

n=3,S=8d

Legend:
- ■ x=275mm
- □ x=300mm
- ◆ x=450mm
- ◇ x=575mm
- ▲ x=750mm
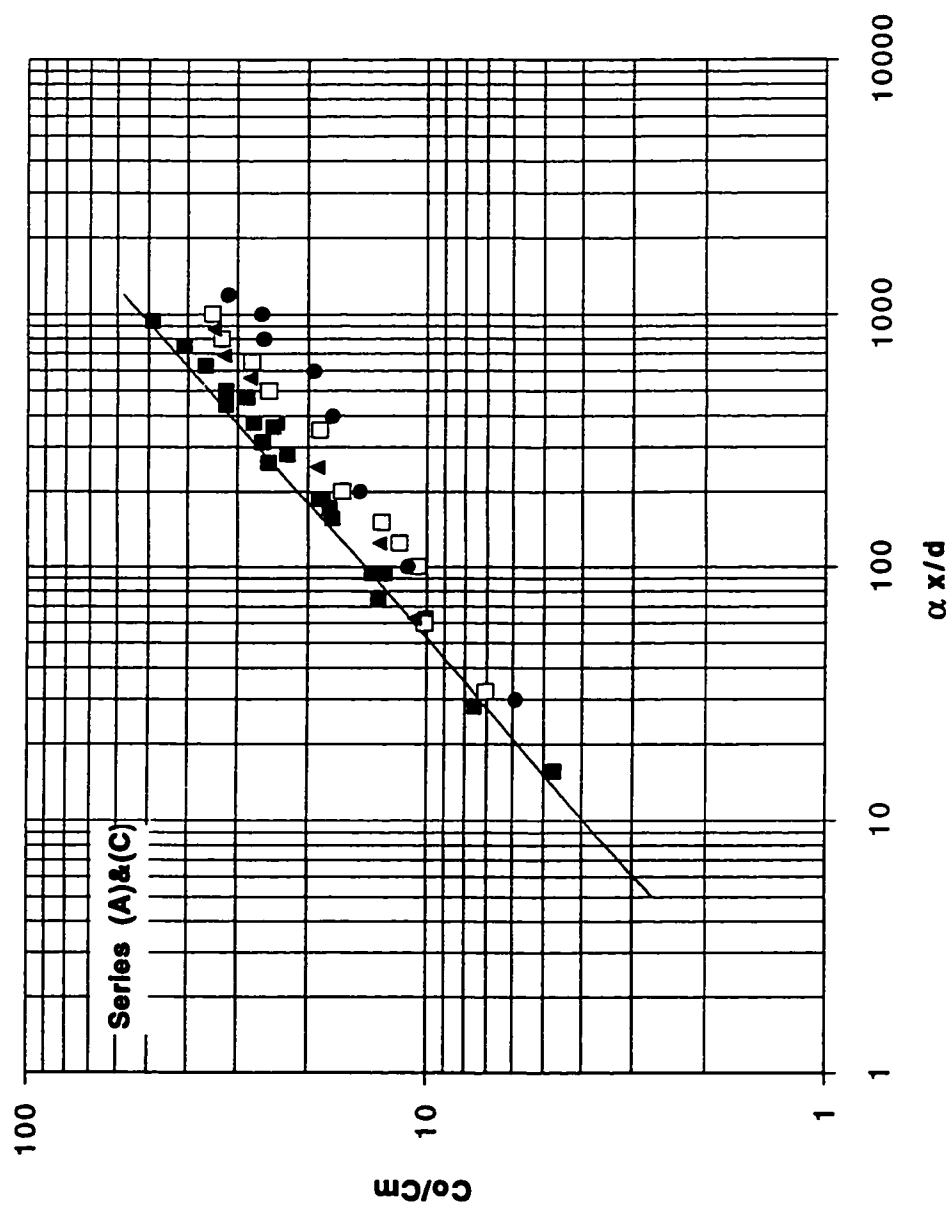
Fig. 4.20 (a-b) Similarity of Transverse Concentration Profiles for Expt. A1 and Expt. A2

Fig. 4.20 (c-d) Similarity of Transverse Concentration Profiles
for Expt. A3 and Expt. A4
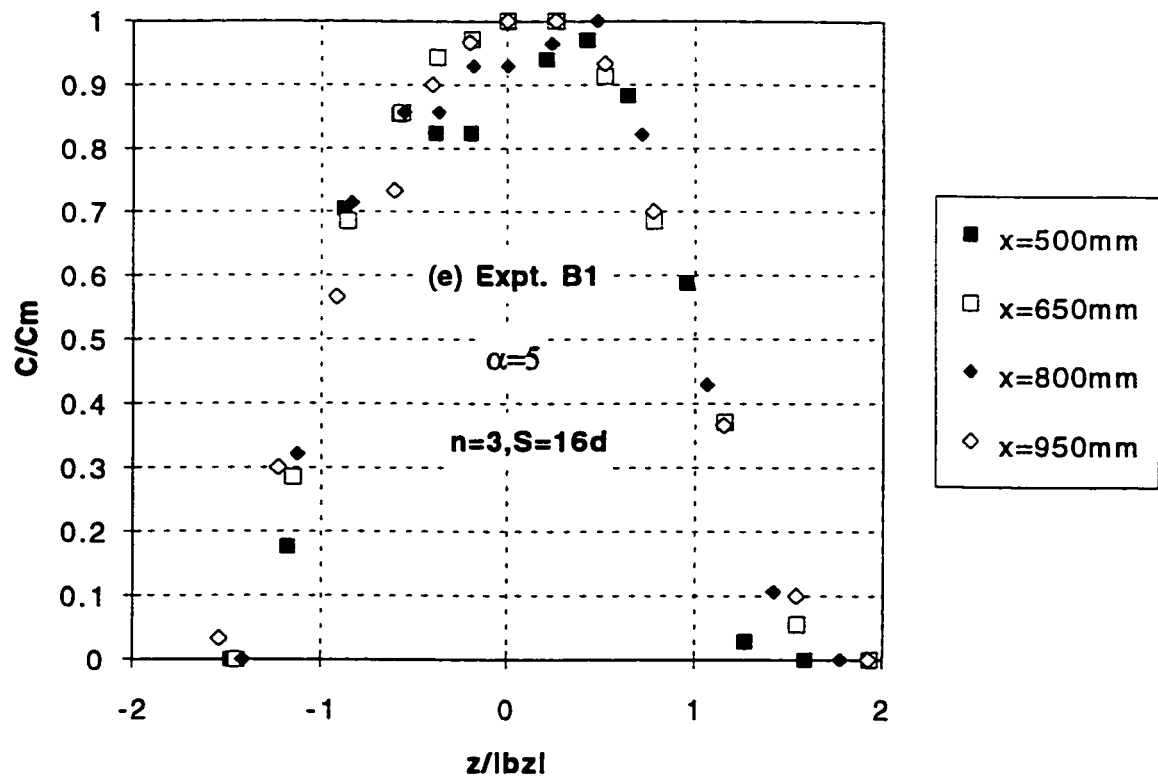
Fig. 4.20 (e-f) Similarity of Transverse Concentration Profiles for Expt. B1 and Expt. B2
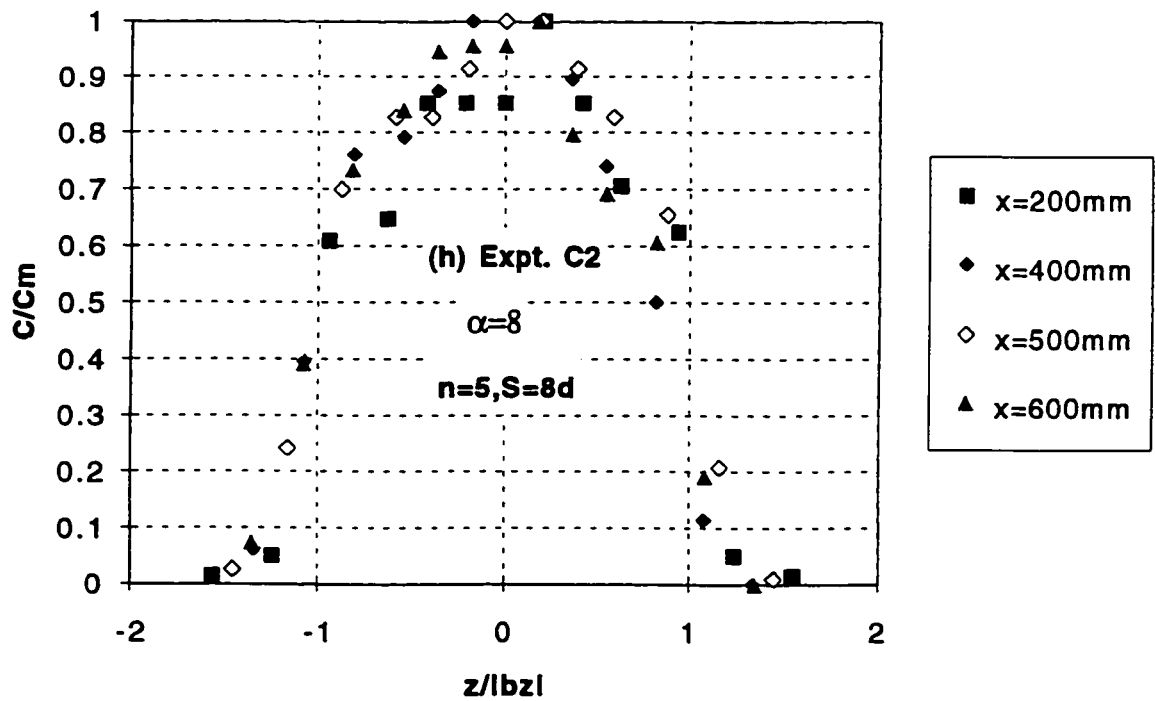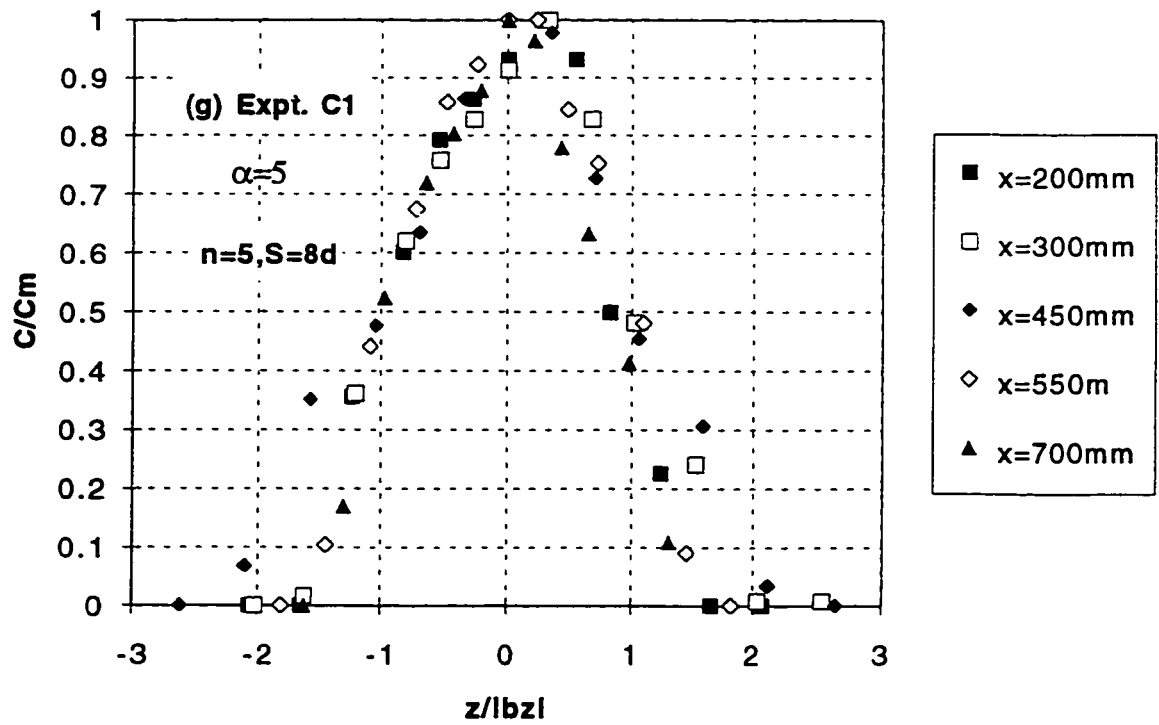
Fig. 4.20 (g-h) Similarity of Transverse Concentration Profiles
for Expt. C1 and Expt. C2
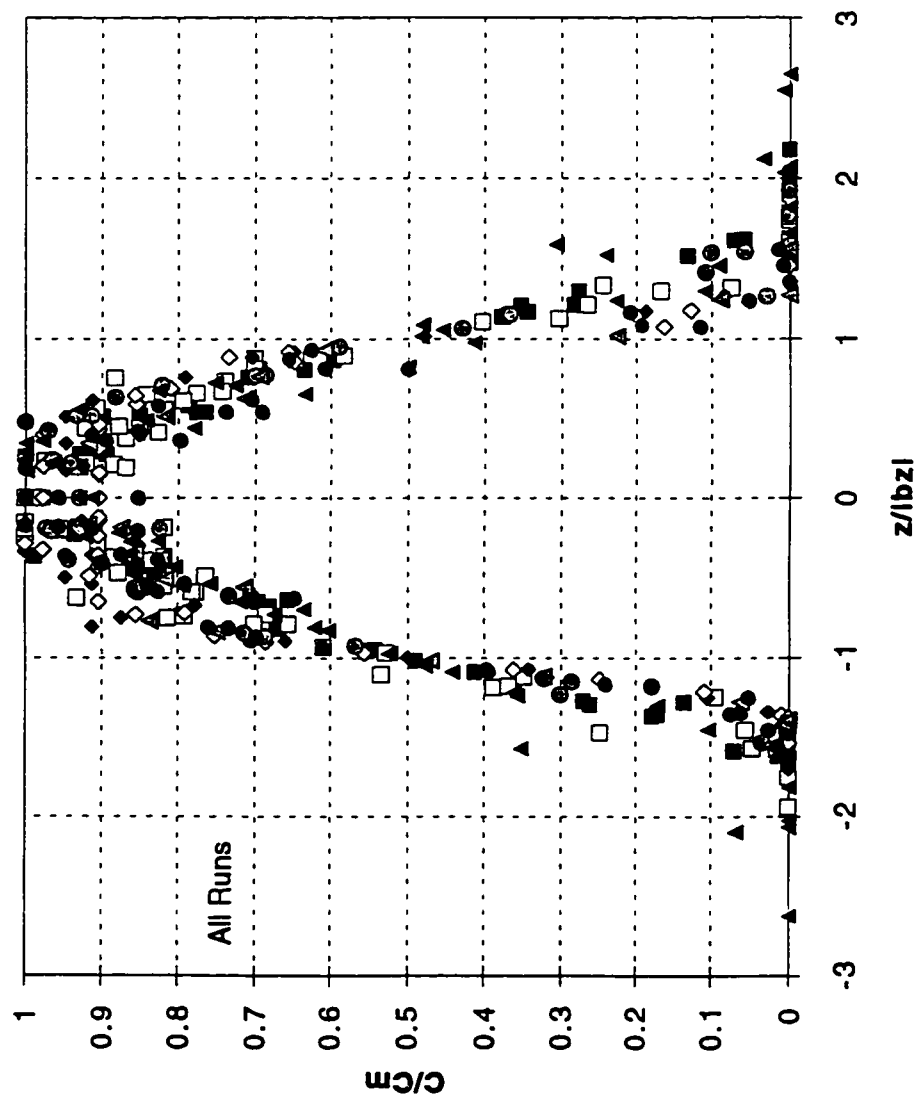
Fig. 4.21 Similarity of Transverse Concentration Profiles for all the Runs

Legend:
- ■ Uo/U=3.5,n=3,S=8d
- □ Uo/U=5,n=3,S=8d
- ◆ Uo/U=8,n=3,S=8d
- ◇ Uo/U=10,n=3,S=8d
- ◑ Uo/U=5,n=3,S=16d
- ▲ Uo/U=8,n=3,S=16d
- ▲ Uo/U=5,n=5,S=8d
- ● Uo/U=8,n=5,S=8d

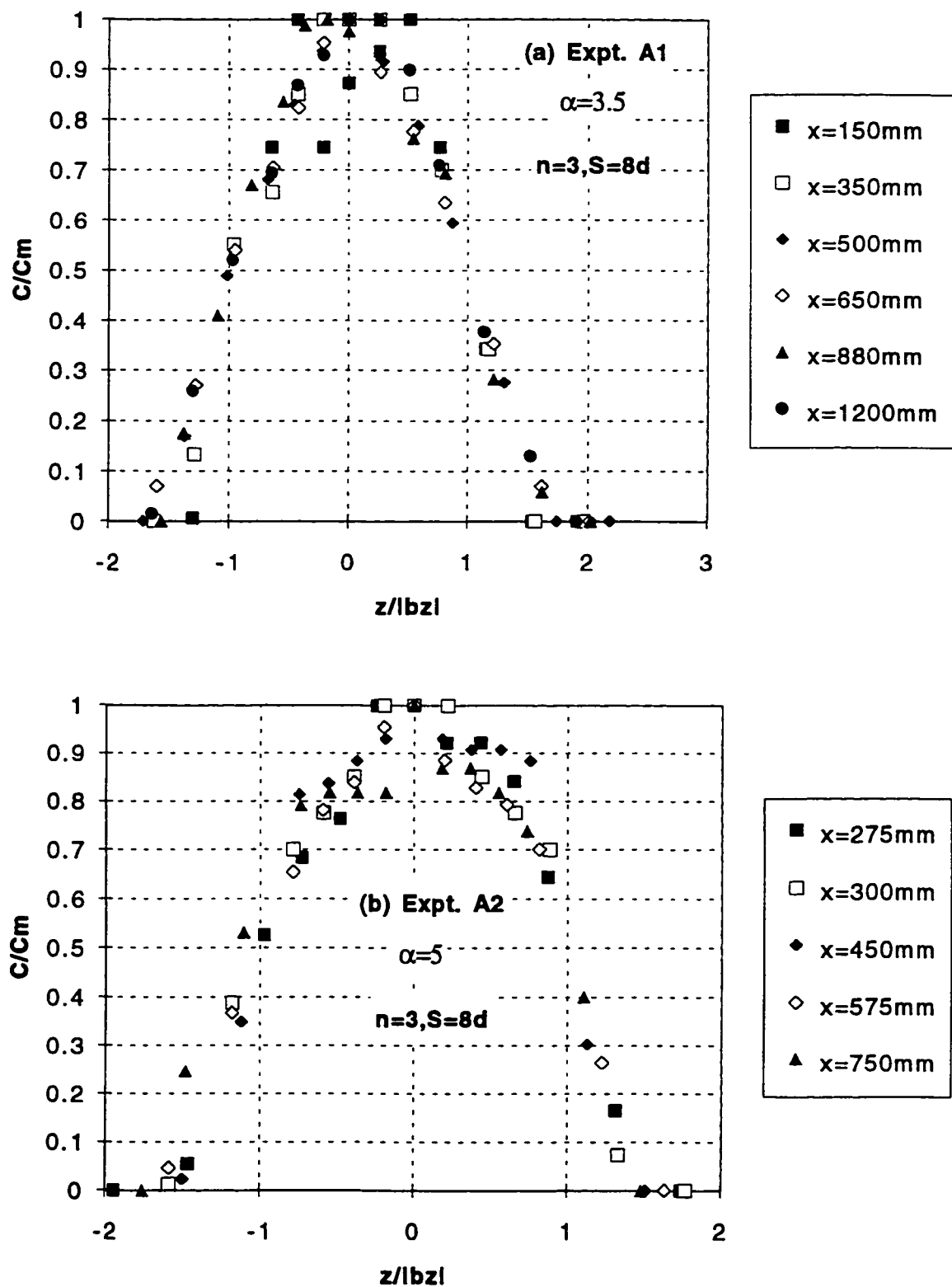All Runs
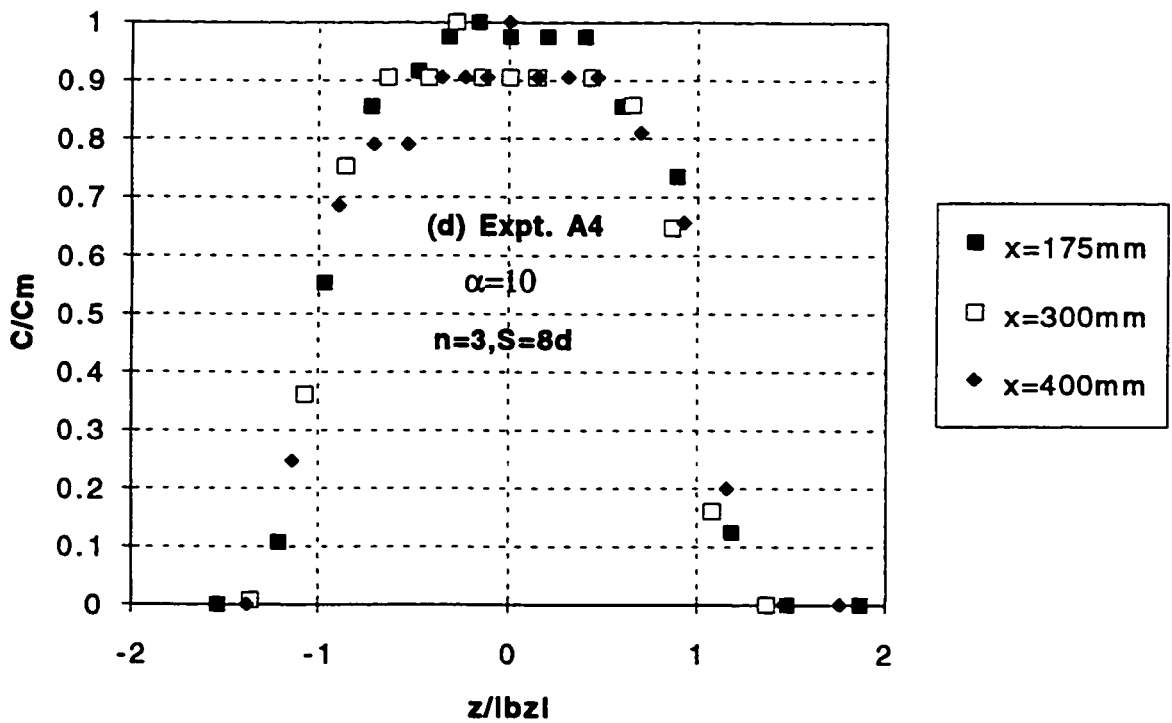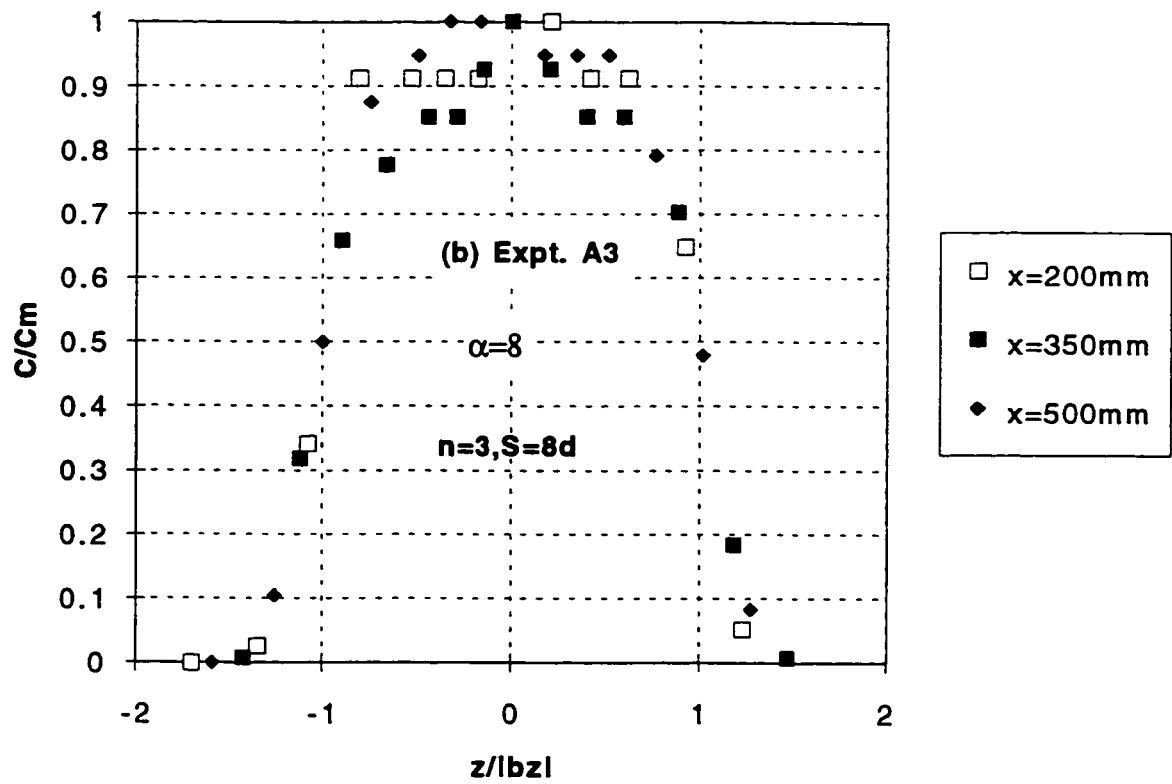
x-axis: z/|bz|

y-axis: c/cm
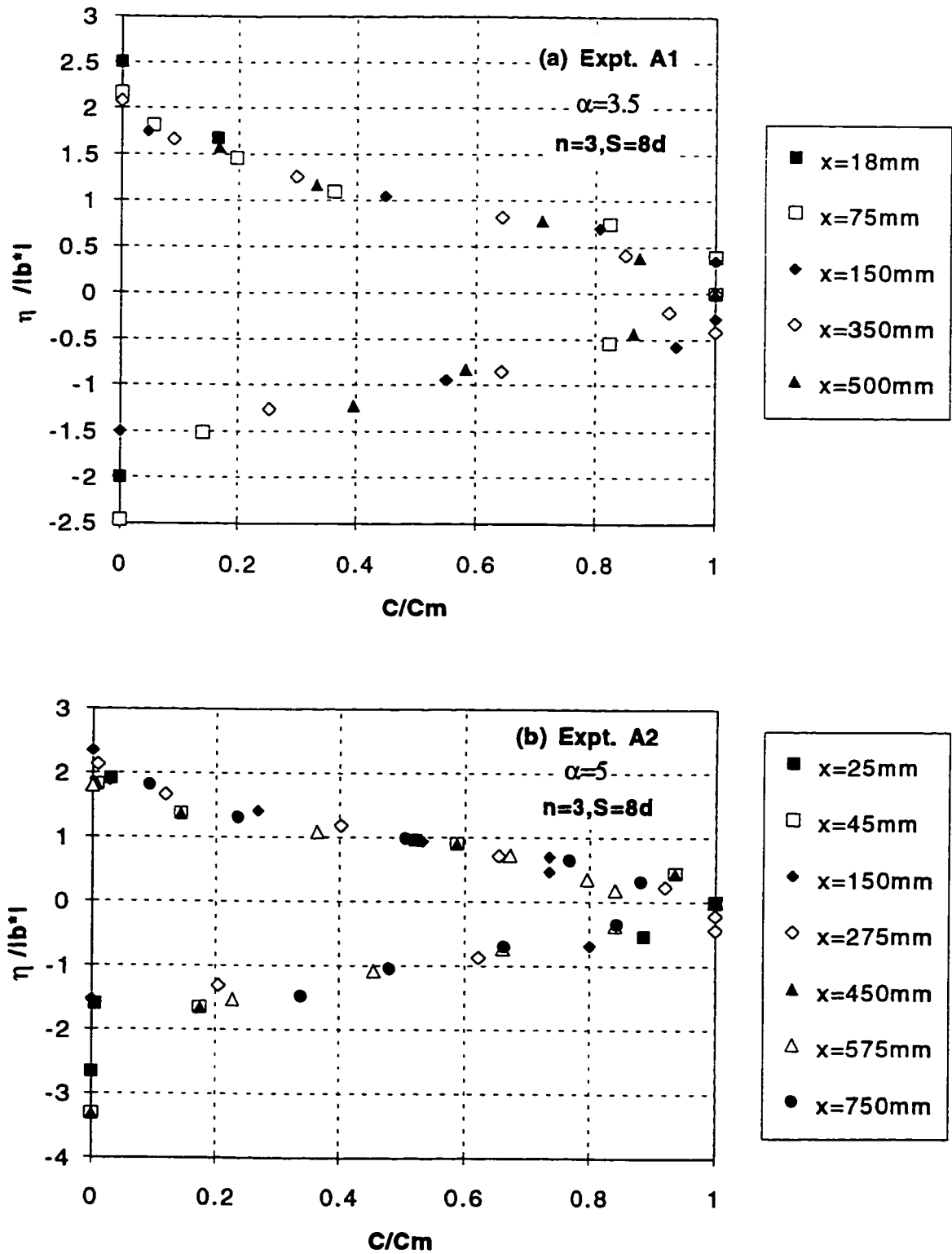
Fig. 4.22 (a-b) Similarity of Vertical Concentration Profiles for Expt. A1 and Expt. A2

205

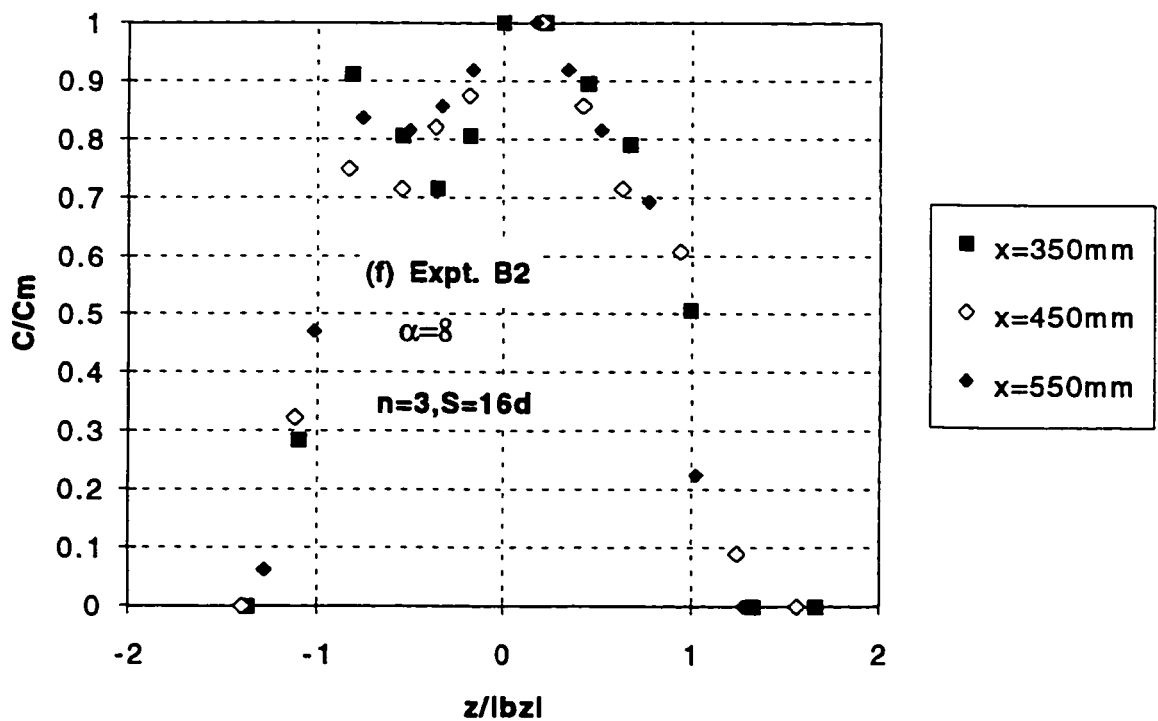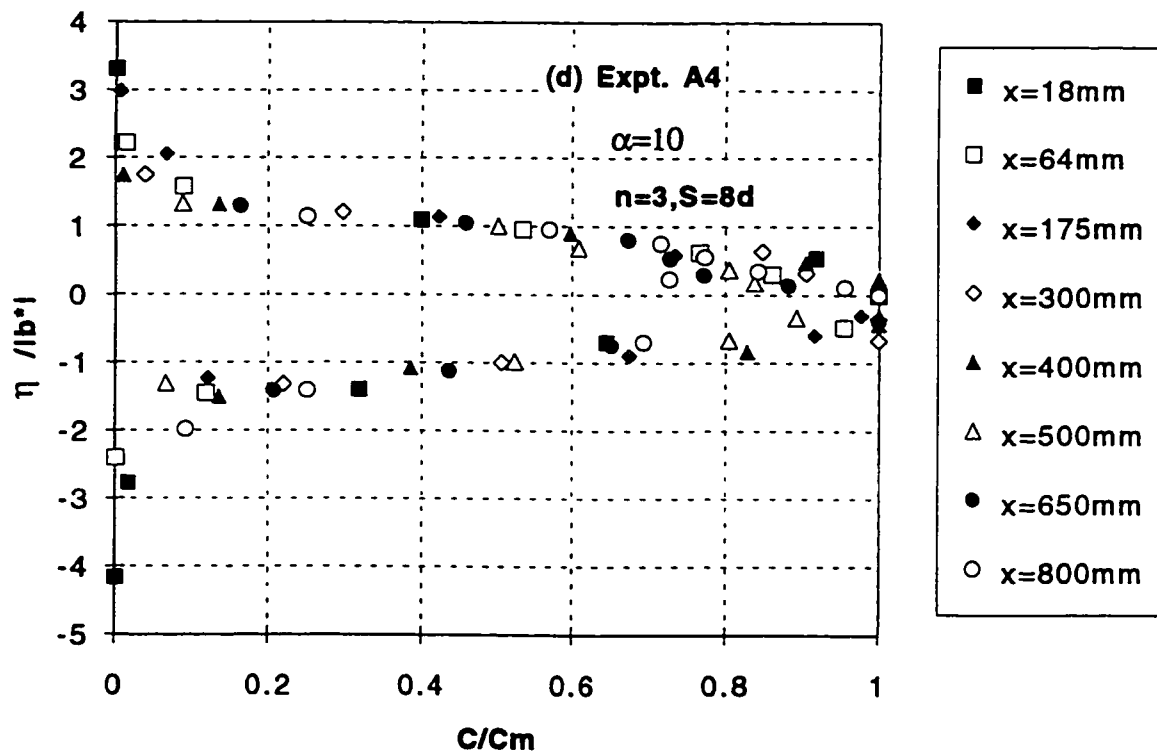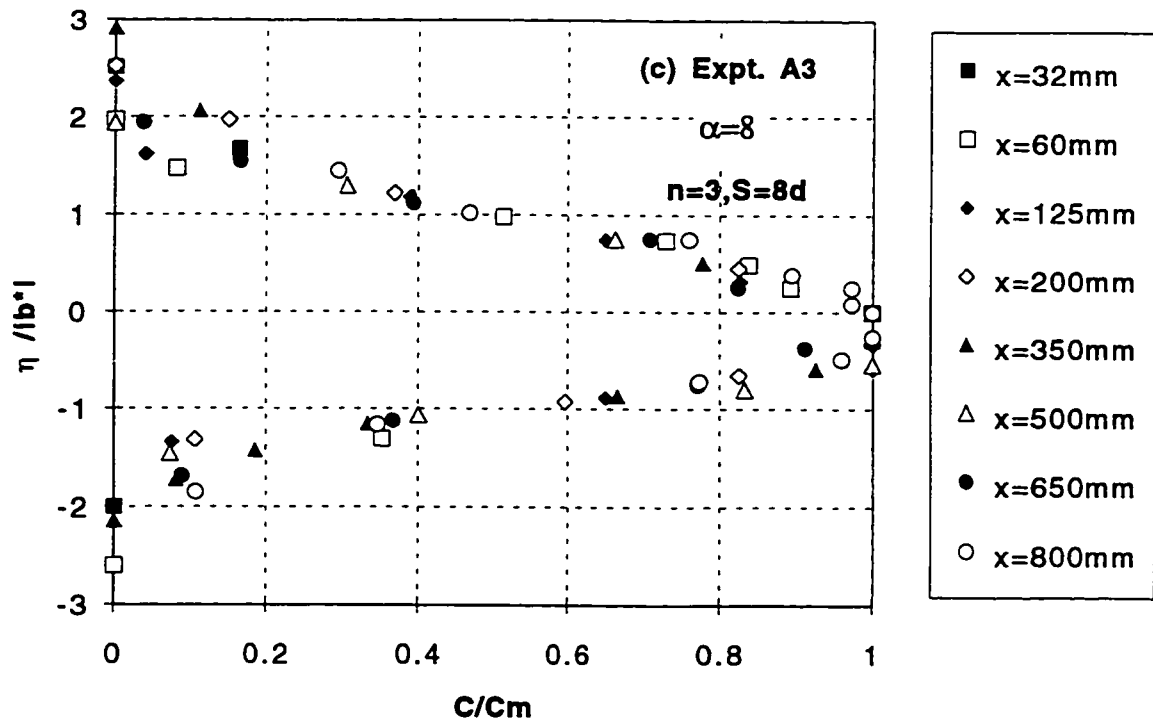Fig. 4.22 (c-d) Similarity of Vertical Concentration Profiles
for Expt. A3 and Expt. A4
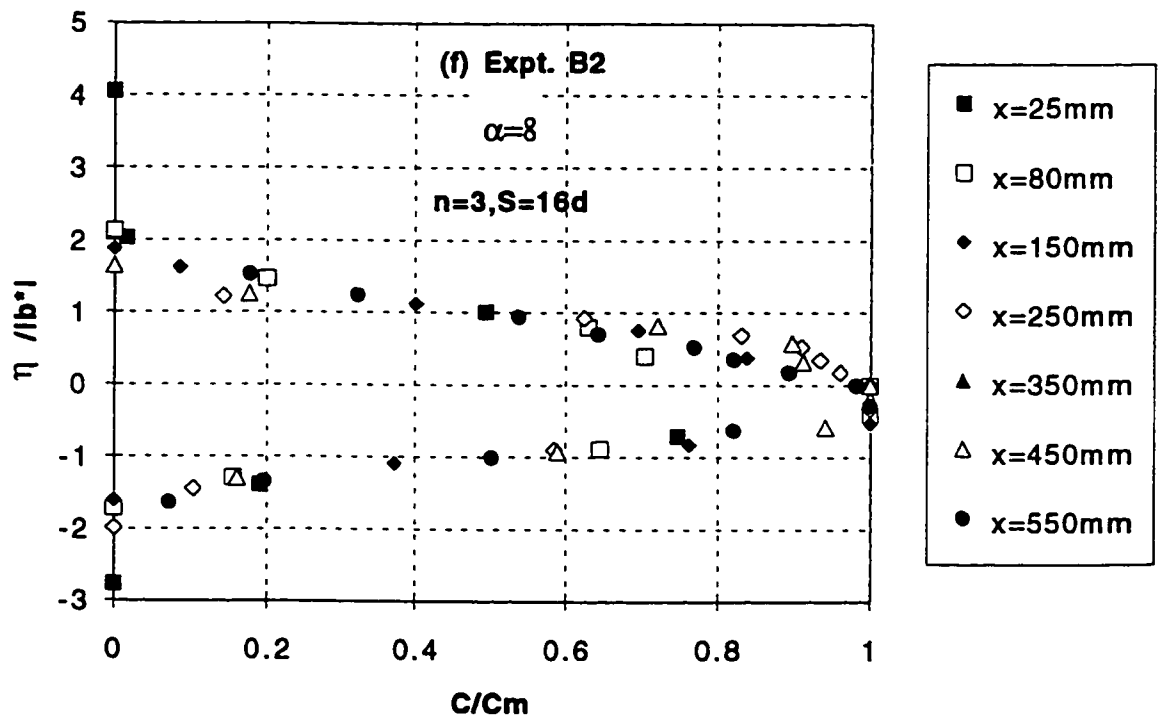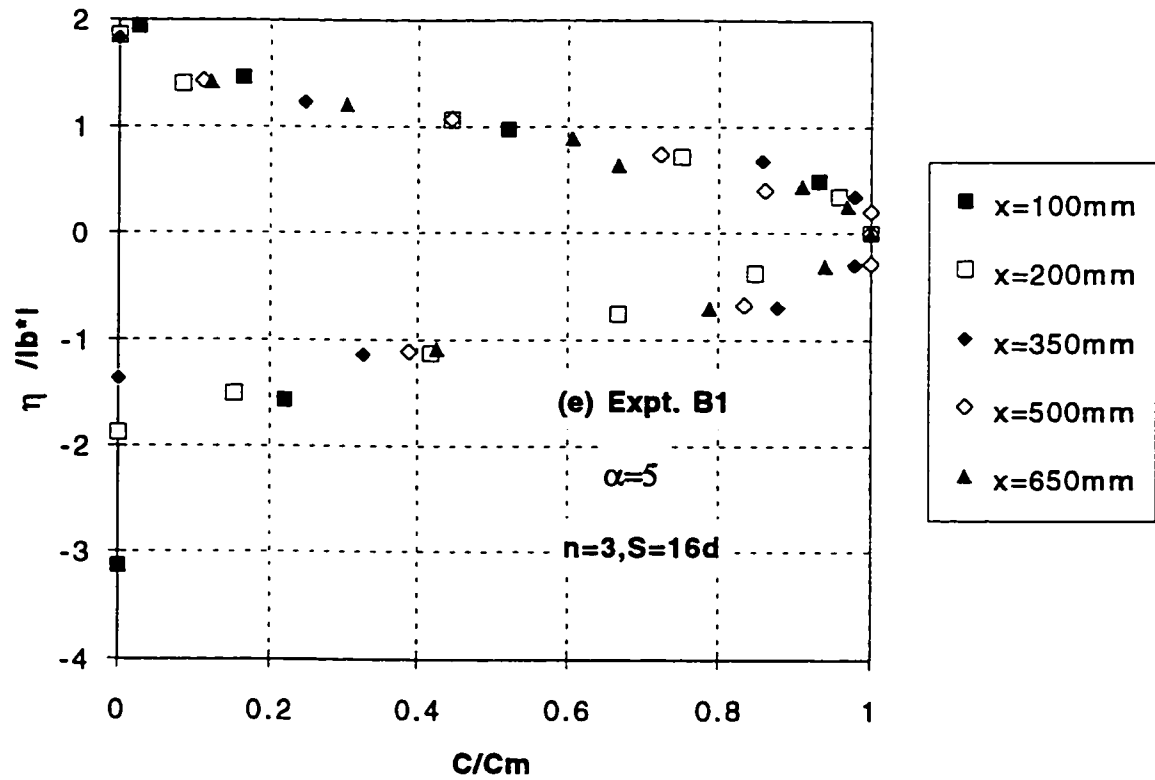
Fig. 4.22 (e-f) Similarity of Vertical Concentration Profiles
for Expt. B1 and Expt. B2
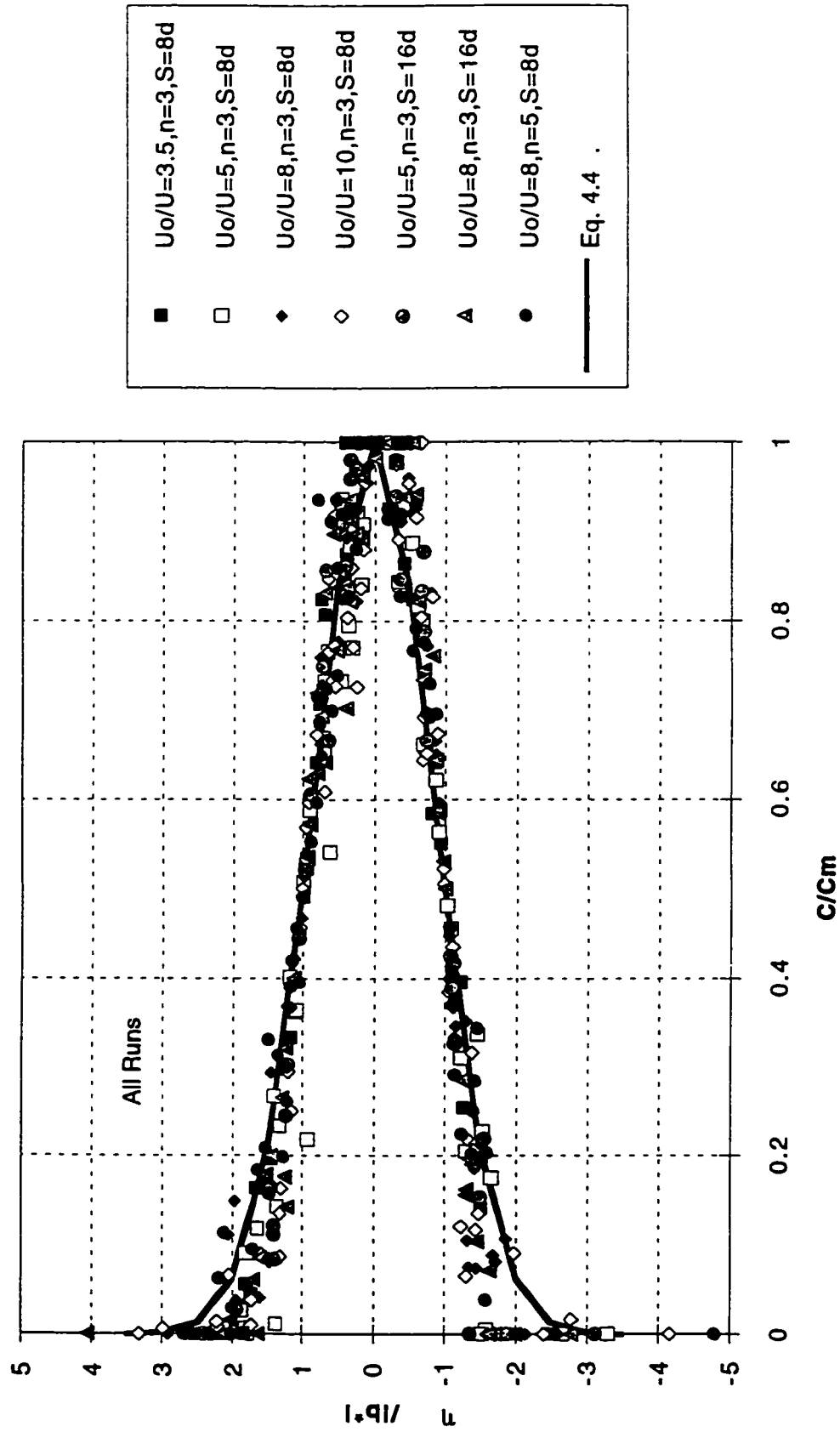
Fig. 4.23 Similarity of Vertical Concentration Profiles for all the Runs
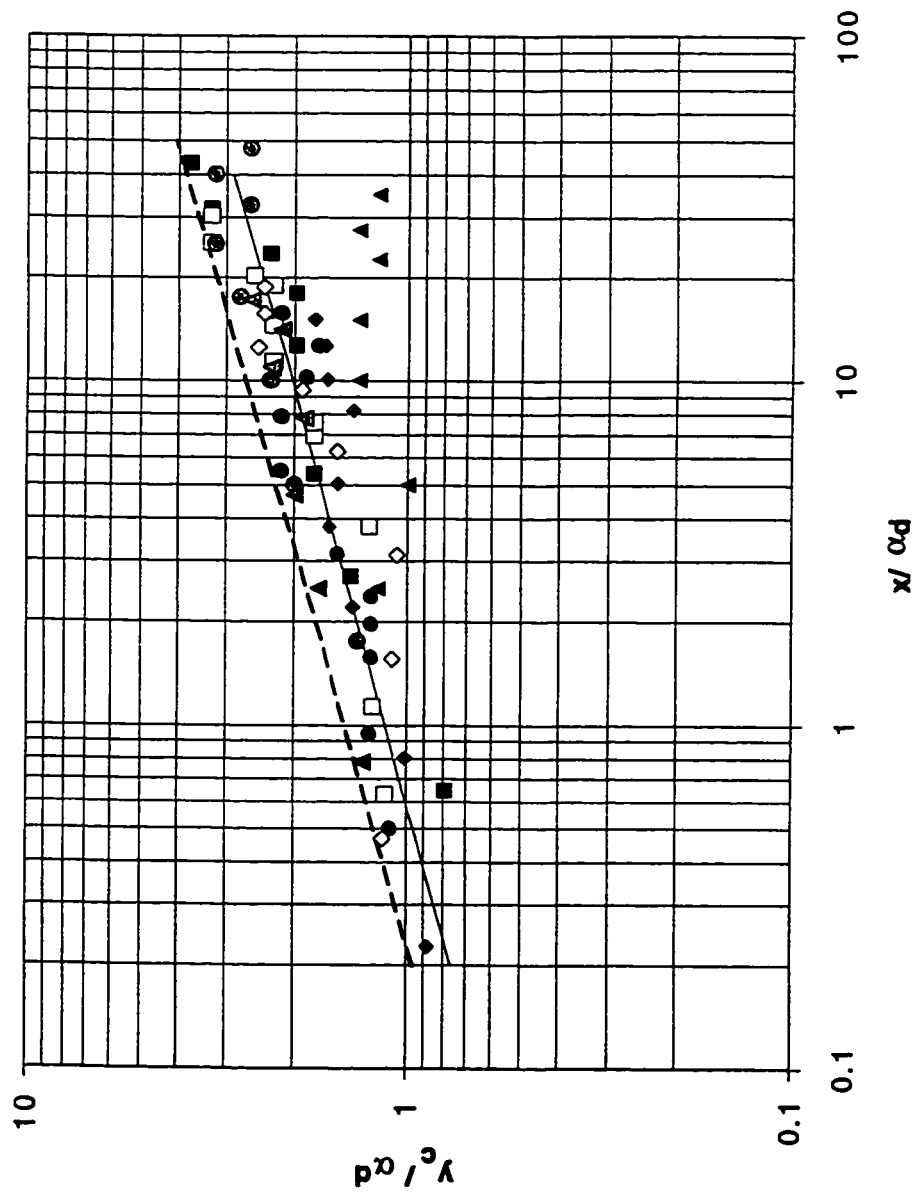
Fig. 4.24 Location of Concentration Centerline

Legend:
- ■ $U_0/U=3.5, n=3, S=8d$
- □ $U_0/U=5, n=3, S=8d$
- ◆ $U_0/U=10, n=3, S=8d$
- ◇ $U_0/U=8, n=5, S=8d$
- ⊛ $U_0/U=5, n=3, S=16D$
- △ $U_0/U=8, n=3, S=16d$
- ▲ $U_0/U=5, n=5, S=8d$
- ● $U_0/U=8, n=3, S=8d$
- – – – Eq. 4.7
- —— Eq. 4.8

x-axis: $x/\alpha d$

y-axis: $y_c/\alpha d$
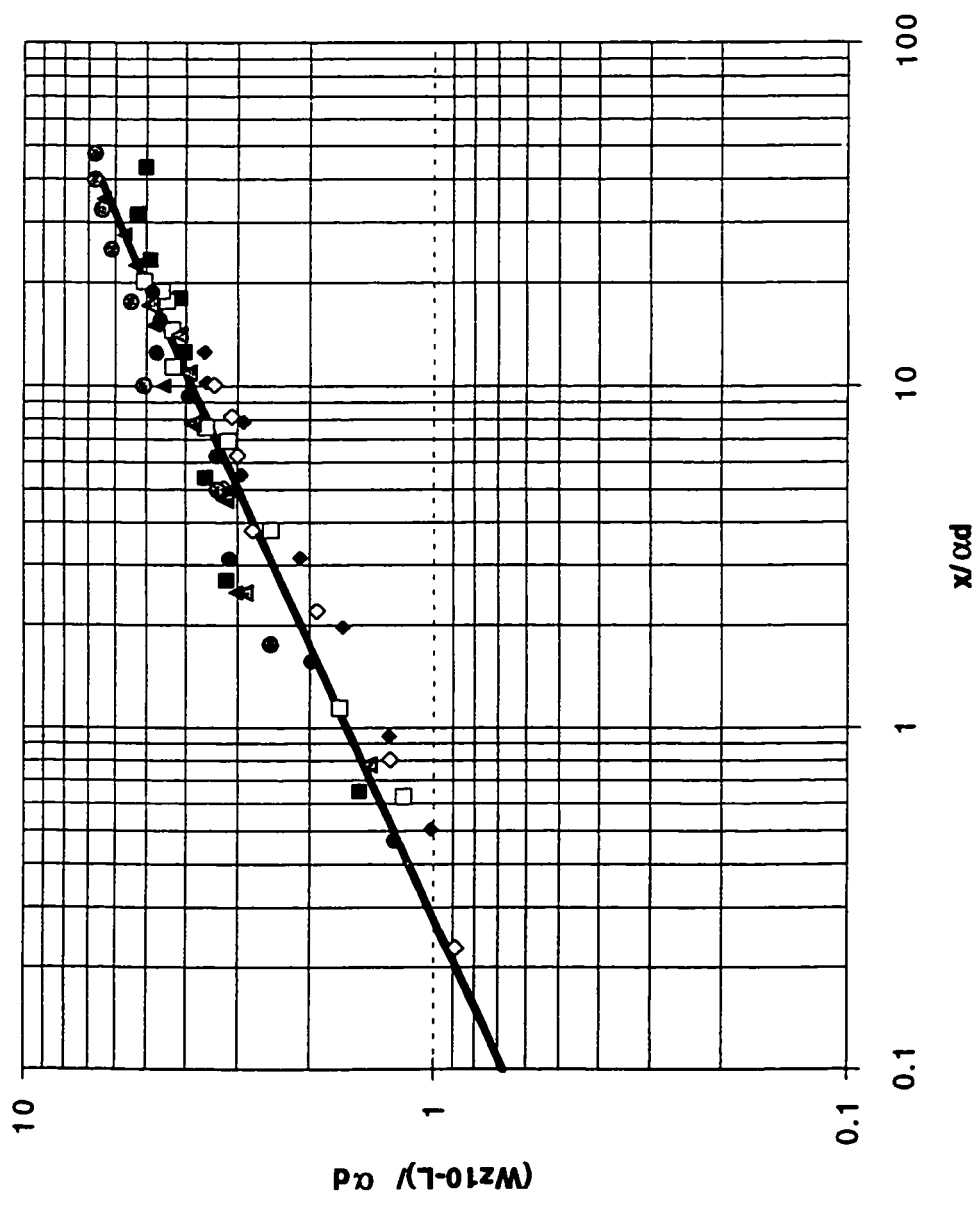
Fig. 4.25a Growth of Jet Width

Legend:
- ■ Uo/U=3.5,n=3,S=8d
- □ Uo/U=5,n=3,S=8d
- ◆ Uo/U=8,n=3,S=8d
- ◇ Uo/U=10,n=3,S=8d
- ⊕ Uo/U=5,n=3,S=16d
- △ Uo/U=8,n=3,S=16d
- ▲ Uo/U=5,n=5,S=8d
- ● Uo/U=8,n=5,S=8d
- —— Eq. 4.9

Y-axis: $(W_{z10}-L)/\alpha d$

X-axis: $x/\alpha d$
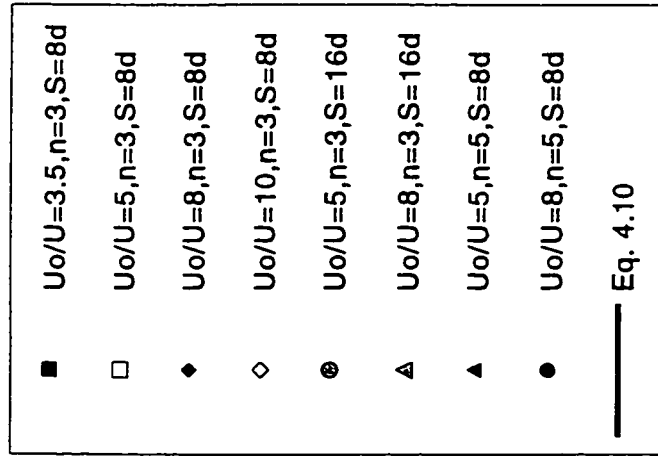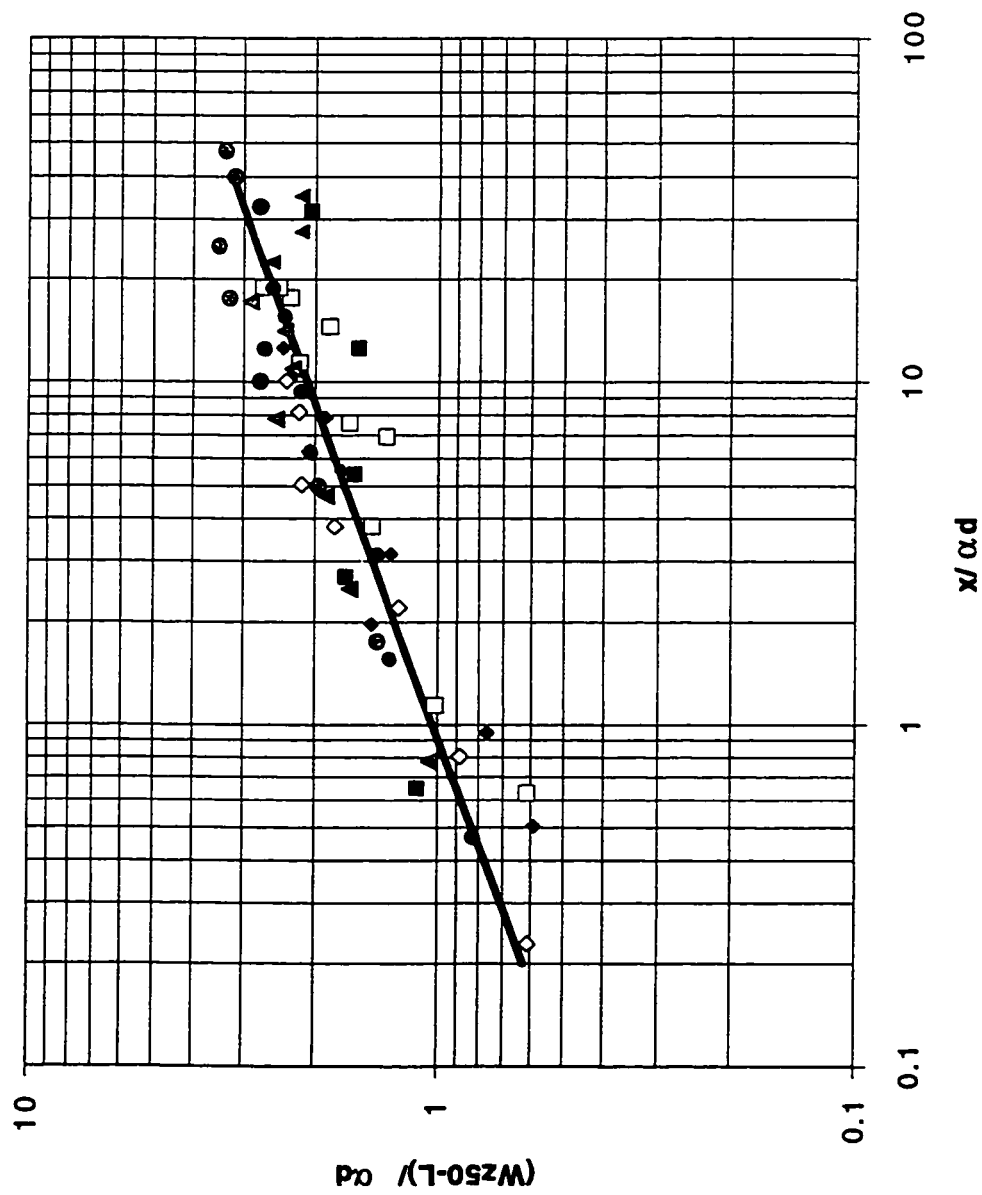
Fig. 4.25b Growth of Jet Width

211
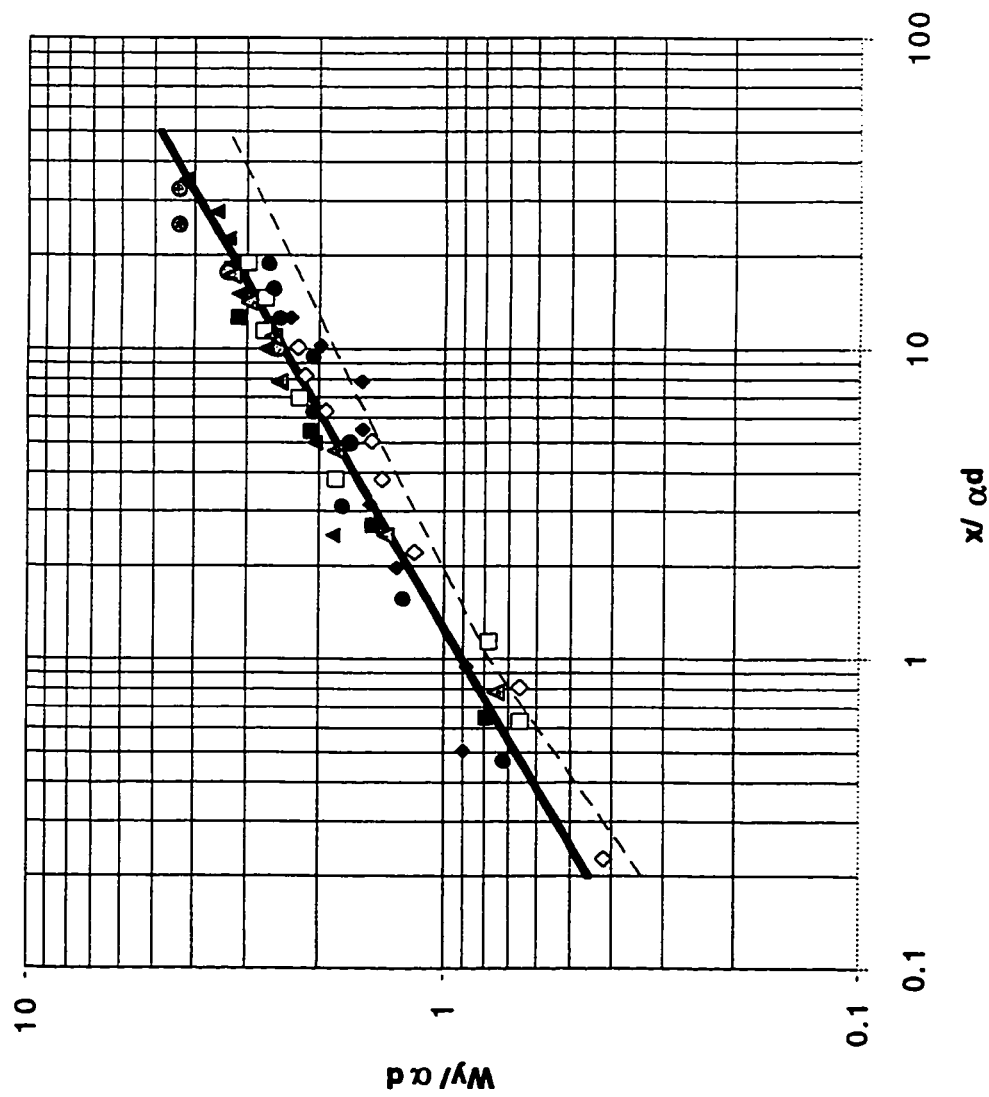
Fig. 4.26 Growth of Jet Thickness

Legend:

■ $U_o/U=3.5, n=3, S=8d$
□ $U_o/U=5, n=3, S=8d$
◆ $U_o/U=8, n=3, S=8d$
◇ $U_o/U=10, n=3, S=8d$
⊕ $U_o/U=5, n=3, S=16d$
△ $U_o/U=8, n=3, S=16d$
▲ $U_o/U=5, n=5, S=8d$
● $U_o/U=8, n=5, S=8d$

—— Eq. 4.11
– – – Eq. 4.12 & 4.13 (single jet)

Axis labels: $W_y/\alpha d$ (vertical), $x/\alpha d$ (horizontal)

Chapter 5

Mixing with Multiple Turbulent Jets

5.1 Introduction

In most water and wastewater treatment plants, rapid mixing is a part of chemical or biological water treatment processes. Rapid mixing should provide a complete homogenization of the added chemicals with the plant influent stream. This type of mixing is required in disinfection (chlorination) processes. Without rapid and initial mixing, localized reactions of high concentrations of chlorine might exist which is generally undesirable and may be costly. Mixing of liquids can be accomplished using conventional methods which include chambers equipped with mechanical mixing devices such as propellers or turbines, fixed blades in pipe lines, hydraulic jumps and others. In water treatment plants, it is most common to find that the treated water is transported in open channel flumes between unit processes where the chemicals may be added and mixed along the channel. In this study, turbulent jet mixing is used as an alternative to mechanical mixing. This was accomplished by installing a diffuser with a system of ports where jets can be discharged either perpendicular (crossflowing jets) or parallel (coflowing jets) to the flow. Jets in crossflows have been used previously to provide rapid mixing in pipes (Ger and Holley 1976; Chao and Stone 1979; Fitzgerald and Holley 1981). Benzina et al. (1974) have reported that the use of counterjet injection, combined with the effects of hydraulic blockage, could produce rapid and thorough mixing in open channels. The optimum mixing distance was defined as the distance to a section where the variation of the concentration over the cross-section was within some specified value.

This study investigates the viability of using turbulent jets in achieving rapid mixing. Several jets with different α values were studied. The effect of spacing and the number of ports on the optimum mixing distance and on the minimum dilution was investigated. The results from this study are believed to be useful in the design of an efficient mixing system which can be implemented by water treatment plants as an alternative to mechanical mixing.

5.2 Background

5.2.1 Jets in Crossflows

Jets in crossflows have been investigated earlier by Wright (1977) (refer to chapter 2). The flow in the deflected jet was divided into two main regions mainly the MDNF and the MDFF. These two regions were followed by the passive plume region (PPR) where the mixing and the resulting dilution is due to the turbulence in the ambient flow. The transition from the MDFF to the PPR was assumed (Rajaratnam and Langat 1995) to occur where the excess velocity in the jet above that of the crossflow velocity U falls to about 1% of (Uo-U) where Uo is the velocity of the jet at the nozzle.

The dilution produced by a circular jet in crossflows in the mixing region, defined as the region in which significant dilution occurs because of jet mixing, was investigated by Hodgson and Rajaratnam (1992). In this mixing region using the concept of the MDNF, MDFF and experimental observations, $\alpha x/d$ was found to be a characteristic dimensionless distance (Hodgson and Rajaratnam 1992) and the minimum dilution defined as C_0 / C_m was given by the expression :

$$\frac{C_o}{C_m} = 1.09(\frac{\alpha x}{d})^{0.56} \qquad (5\text{-}1)$$

where C_0 is the concentration at the nozzle; C_m is the maximum concentration at a section; x is the downstream distance along the crossflow ; d is the diameter of the nozzle producing the jet; and α is the ratio of the velocity of the jet to that of the crossflow.

As for multiple diffusers, it is possible that the minimum dilution would increase rapidly with the downstream distance. Mixing would be affected by the momentum fluxes and their interaction with the ambient current. This region can be referred to as the MDNF and the MDFF. Sometimes, this region is referred to as the initial mixing region (Roberts et al. 1989). Far from the diffusers, mixing due to the ambient turbulence dominates, resulting in a much slower rate of increase of dilution This region is referred to as the passive plume region.

5.2.2 General Considerations

When multiple jets are discharged into confined crossflows as in mixing open channel, the maximum value for the minimum dilution C_0/C_m attained would not exceed the value of the ratio of C_0 to $C_{infinity}$ (referred to as C_i) where C_i basically represents the concentration at a fully mixed section. In the presence of a background concentration (C_b) in the crossflow, and as the values of C_0/C_m are always with reference to this concentration, the maximum dilution value attained would not exceed the value of C_0 / C_i' where $C_i'=C_i-C_b$. The value of C_i can be determined from the mass balance equation:

$$C_i = \frac{C_o Q_o + C_b Q}{Q_o + Q} \qquad (5\text{-}2)$$

where Q_0 is the total discharge from the nozzle and Q is the ambient discharge. From Eq. 5.2, we can see that for a fully mixed section with $Q_o \ll Q$ and $C_b \ll C_0$

the value of C_o/C_i, depends mainly on the values of the ambient and the jet discharges so that :

$$\frac{C_o}{C_i} = \frac{Q}{Q_o} \qquad (5\text{-}3)$$

and hence at a fully mixed section

$$\frac{C_o}{C_m} * Q_r = 1 \qquad (5\text{-}4)$$

where $Q_r = Q_o/Q$.

5.3 Experimental Arrangement

The experiments were performed in a rectangular flume 1.20 m wide, 0.60 m deep and 18.5 m long. Wooden boards were placed in the channel so that the width of the channel was reduced to 0.60 m in the test section. A plan view of the experimental arrangement is shown in Fig. 5.1a. Water was supplied to the flume from the laboratory sump and the discharge was measured using an inline magnetic flowmeter. A tailgate was used to control the depth of flow. The mean velocity of the crossflow was obtained from the measured discharge and the cross-sectional area of the flow.

The injection system was placed at a distance of 10 m from the entrance (see Fig. 5.2). The system consisted of three vertical pipes which housed the jet nozzles which were flush with the pipe walls. The system was originally designed to accommodate 70 nozzles (see Fig.5.1(b)) . The nozzles were arranged in such a way that the flow of the jets can either be in the direction of flow (coflowing jets) or perpendicular to the flow (crossflowing jets). The middle pipe had three lines of

vertical diffusers, two would supply the crossflowing jets while the third produced the coflowing jets. Each of the two side pipes each had two lines of jets to supply both the crossflowing and the coflowing jets. Figure 5.3 shows the diffuser system as it was placed in the channel. The nozzles were 3.2 mm in diameter and the vertical distance between the nozzles was 12 d. The first nozzle from the bottom was placed at a distance of 12 d. A 1/3 horse (250 Watts) power Jacuzzi raised the water from a 900 L tank placed outside the flume to a constant head tank. This tank which was placed about 3.5 m above the flume provided the flow to the jet nozzles. The flow to the jet nozzle was measured using a (volumetrically calibrated) Fischer rotameter. The jet velocity was calculated from the measured flow rate and the diameter of the nozzles. During all the experiments, the operating jets were kept submerged so as to maintain a constant pizometric head at the nozzles. The number of the nozzles under operation were varied by plugging some of them using cork stoppers. Rhodamine WT with market concentration of 20% by weight and specific gravity of 1.19 was used as the tracer in this study. This dye was mixed thoroughly in a 900 L tank with water pumped from the same sump which provided the crossflow.

The sampling technique used was the same as that described in the previous chapters. A horizontal rake was used to sample the fluid at different elevations. Fig. 5.4 shows the position of the rake in the flume. The rake was set to withdraw samples at the same level in the y direction, starting from the bottom of the channel and moving vertically upward in the z direction. The concentration of the Rhodamine dye in the jet fluid was measured by Turner model 10-AU digital fluorometer as shown in Fig. 5.5. The fluorometer was calibrated to diluted standards over a range of 0.05 to 120 ppb. The background concentration of the water was continuously monitored and was not allowed to exceed 1/1000 of the initial concentration C_o.

5.4 Experiments and Experimental Results

The primary details of the experiments conducted are shown in Table 5.1. The diameter of the nozzles was equal to 3.2 mm. In experiments CC1 to CC3, both the coflowing and crossflowing jets were used. There were a total of 35 jets, of which 20 were crossflowing jets and the remaining 15 were coflowing jets with a constant spacing of 24 d. In experiments CC4 and CC5, the coflowing jets issuing from the vertical pipes adjacent to the side walls of the flume were closed and there were 20 crossflowing jets and 5 coflowing jets issuing from the central vertical pipe, with a constant spacing of 24 d. In the experiments CF1-CF7, all the coflowing jets were closed and only crossflowing jets were used, with spacing of 24 d in experiments CF1 to CF3 and 12 d in experiments CF4 to CF7. The velocity ratio α was varied from 8 to 16. The spacing between the ports was given two values of 12 d and 24 d. The number of ports n was varied from 20 to 36. The jet Reynolds number, defined as Ud/ν, where ν is the kinematic viscosity, was varied from about 2300 to 5000 and in this range of Reynolds number, the effect of viscosity on the behavior of the jets is believed to be negligible. The Reynolds number of the ambient flow ranged from 20000 to 40000.

A few comments concerning the way in which the parameters were varied are warranted. Generally, an increase in α values resulted from an increase in the jet discharge, when keeping the spacing between the ports and hence the depth of the flow constant. The change in the spacing between the ports from S=24 d (runs CF1-CF3) to S=12 d (runs CF4-CF6) was accompanied by a decrease in the flow depth. The α values were kept constant (8 to 16). The discharge per port was kept constant except for series CF4 where, at some sections, the discharge per port was increased and hence the ambient discharge had to be increased in order to maintain the same α (α=8). The increase in the number of ports n was accomplished while the spacing and the α values were kept constant.

5.4.1 Concentration Profiles

The concentration field downstream of the jets was measured in the transverse direction (y) and in the vertical direction (z) at different longitudinal sections. A total of about 4000 concentration measurements were made. The concentration measurements covered a distance of $x/d= 2000$. In terms of the transformed distance $\alpha x/d$, the measurements covered a range from 630 to 32050. The concentration (C) at any point was normalized by the concentration (C_i) at the section at which the dye becomes uniformly mixed. This concentration C_i for any run was calculated from Eq. 5.2.

As mentioned earlier (chapter 4), the flow field of the multiple jets in a crossflow may be divided into three different regions which were termed as zones I, II, III (MDNF, MDFF & PPR) respectively. The same notions may also be used for the present study, where it was found that the distance at which the jets merge was dependent on α. As α increased, merging between the jets occurred at shorter distances downstream of the diffuser. This was clearly shown from the visual observations using a food dye as shown in Fig. 5.6. In this study, more attention was given to the mixing occurring in the far field and the passive plume regions. Hence, most of the observations were made in zones II and III. The concentration distributions in the transverse direction (y-z plane) were investigated at different locations downstream of the nozzles. Figures (5.7 to 5.14) show typical transverse profiles in several horizontal planes from the bed and for several values of α and at different longitudinal distances.

For experiments series CC1 to CC3, 20 crossflowing and 15 coflowing jets were on. Typical concentration profiles are shown in Fig. 5.7. For series CC1 to CC3, Fig. 5.7 indicated that for some distance from the diffuser, the concentration field showed locations of smaller dilution downstream the nozzles producing the coflowing jets. This effect persisted even for distances as large as 3.5 m, especially

near the sidewalls. This is due to the presence of the coflowing jets on the two sides of the injection system, which can be almost considered as wall jets. For runs CC4 and CC5, (Fig.5.8), the coflowing jets on the side pipes were closed. Considering the concentration data for all the experiments in the CC series, it was noticed that the coflowing jets would not have a considerable effect on achieving rapid mixing. Hence, the main experiments were carried on using only the crossflowing jets (Series CF). Figures 5.9 to 5.14 show typical profiles for the transverse profiles for the cases of the crossflowing jets. On examining the concentration profiles, it can generally be noticed that as one gets closer to the diffuser, the jets seem to diffuse without any significant interference from its neighbors and concentration peaks can be identified (Fig. 5.9a, 5.12a). As one goes further along the channel, the concentration profiles seem to be more spreading in the transverse direction. Eventually the jets were completely merged and the concentration profiles were approximately uniform in the vertical direction and across the channel as shown in Figs. (5.10f, 5.13f, 5.14d, 5.14f). A study of the concentration profiles shows that for x greater than about 5m, the concentration field tends to become almost uniform. For some practical applications, it is useful to determine the distance after which the concentration at the section is 50% of the fully mixed concentration. From the concentration measurements for the CF series the maximum distance at which the value C/C_i reached 0.5 was estimated, in terms of the dimensionless distance, to be about 5000.

5.5 Analysis of Experimental Results

5.5.1 Mixing Distance

The degree of mixing in each section was defined using a normalized form of the standard deviation of the value C/C_i given as:

$$\sigma = \sqrt{\frac{\sum (\frac{C}{C_i} - \frac{\overline{C}}{C_i})^2}{N-1}}$$ (5-5)

where N is the number of observations and C is the average concentration at that section. A value of a zero standard deviation would indicate complete mixing. Theoretically σ would approach zero asymptotically. For practical purposes, adequate mixing may be assumed to occur when the standard deviation reaches a specified value. In this study this limit value was set equal to 5%. The distance required for this mixing to occur is termed as the "mixing distance" x_m. The standard deviation was calculated for each of the measured sections for all the experiments. Fig. 5.15 shows a plot of the variation of the standard deviation with the dimensionless longitudinal distance $\alpha x/d$. A general equation for the standard deviation was found to be:

$$\sigma = 108(\frac{\alpha x}{d})^{-0.76}$$ (5-6)

with a correlation coefficient of 0.93. From Fig. 5.15 it can be seen that the standard deviation σ was largest near the injection system where the concentration distribution was highly non-uniform. As the distance from the nozzles increases, the concentration profiles becomes progressively more uniform and the standard deviation would decrease to an asymptotic value of about 0.05% at $\alpha x/d = 25000$. Hence the mixing distance x_m is given by the expression:

$$x_m = 25000(d / \alpha)$$ (5-7)

221

It appears that the mixing distance x_m is independent of the configuration of jets, the spacing between the ports or on the number of ports, within the limits of the present experimental work.

5.5.2 Minimum Dilution

The minimum dilution at any section was defined as the ratio of the concentration at the ports (C_o) in terms of the maximum concentration (C_m) at that section. The maximum concentration (C_m) represents the maximum concentration at a section referred to the background concentration C_b, (i.e. if the maximum value at the section measured is C_{max} then C_m is equal to $C_{max}-C_b$). Following the work of Hodgson and Rajaratnam (1992) for single jets in crossflow, the variation of the minimum dilution C_o / C_m with the dimensionless distance $\alpha x/d$ was studied for all the experiments. Figures 5.16 to 5.18 show the variation of C_o/C_m with $\alpha x/d$ for all the CF series. For the experiments series CF, the maximum concentration normally occurred at the bed especially for lower values of α ($\alpha=8$). The maximum concentrations at the bed of the flume was about 10% higher than that above the bed.

The results showed that the dilution increases monotonically with distance for each value of α. As mentioned earlier, the dilution value at a fully mixed section would not exceed the value of C_o/C_i'. The values of C_o/C_i' for all the runs are plotted in Figs. 5.16 to 5.18. It Also can be noticed that the dilution increases with increase of α. It should be noted that for the same spacing and number of ports, the increase of α had to be always accompanied by the increase in the ratio of the jet discharges to the ambient discharges defined as Q_r ($Q_r=Q_o/Q$). The effect of this ratio on minimum dilution will be discussed later.

For series CC1, the minimum dilution decreases near the wall due to the presence of the coflowing jets as shown. Fig. 5.19. At the dimensionless distance

$\alpha x/d=9000$, the minimum dilution near the centerline of the flume was about 20% higher than that along the center line of the side coflowing jets.

To study the effect of increasing the spacing on minimum dilution, the data from experiments of series CF1 ($\alpha=8$, S=24 d) and CF3 ($\alpha=16$, S=24 d) were compared with that of experiments series CF4 ($\alpha=8$, S=12d) and CF6 ($\alpha=16$, S=12 d) respectively in Fig. 5.20. The results show that at the same α, dilution increases considerably with the increase of the spacing. For $\alpha=8$, at an approximate dimensionless distance $\alpha x/d=12500$, the dilution ratio at S=24 d was approximately 2 times higher than that for S=12d. As α increases to 16 the maximum dilution attained for S=24d was about 1.8 times higher than that at S=12 d. Again here, the decrease of spacing from S=24 d to S=12 d was accompanied by an increase in the Q_r value. To maintain a constant Q_r value, this would have required an increase in α for runs in series CF1 and CF3. For example if we take runs CF3 and CF6, α in the CF3 experiment would have to be increased to 27 in order to maintain the same Q_o/Q ratio ($Q_o/Q=0.015$) as the runs in series CF6. The effect of increasing the number of ports from 20 to 36 was studied by comparing the runs CF7 to CF6 in Fig. 5.21 . For the same α and the same Q_r value, the increase in the number of ports had no effect on the minimum dilution.

In order to check the validity of Eq. 5.4 , the ratio $C_o Q_r/C_m$ was calculated for all the experiments and the variation of this term was plotted against the dimensionless distance $\alpha x/d$ in Fig. 5.22 (a-b). It can be seen that the normalized dilution does not depend on the configuration of the diffuser, the spacing between the ports or the number of ports. The data in Fig. 5.22a shows that the normalized dilution had a value slightly less than 1. At the normalized distance of 25000, a value of about 0.92 can be taken as a limit for the normalized dilution in this study. The reason that the normalized dilution value was less than 1 is that the standard deviation of 0.05 was set as a limiting value to describe the uniformity of the

sections. Fig. 5.22a also indicates the extent of the scatter of the data, especially near the diffusers. This was mainly due to the fluctuation of the background concentration. The ratio C_b/C_i had a higher value near the nozzles (maximum of 8%), whereas the corresponding values at a larger distance were in the range of 3 to 4%. The observations were replotted on logarithmic scales in Fig. 5.22b. It can be seen that the data points at a distance $\alpha x/d$ less than 1000 followed a different slope compared to the results with $\alpha x/d > 1000$, which was expected as for larger distances the points are in the PPR.

5.5.3 Two Dimensional Equivalent Slot Diffuser Theory

The concept of the two dimensional slot diffuser has been discussed earlier (refer to chapter 2). Dimensional considerations led to the length scale L_m and the following results:

$$L_m = \frac{m_o}{U^2} \qquad (5\text{-}8)$$

where $m_o = M_o/L = qU_o/L$ and L represents the vertical length measured from the center of the ports along one line of discharge. The variable q, is defined as the discharge from one line of diffusers. For example, in the CF1 experiments L=305mm and q = $Q_o/4$ =2 L/min. In an attempt to use the same concept to analyze the data from this study, L_m was used as the length scale and Eq. 5.4 was modified so that:

$$\frac{C_o}{C_m} Q_r = f(\frac{x}{L_m}) \qquad (5\text{-}9)$$

Equation 5.9 is plotted in Fig. 5.23. The scatter in the data shows that Eq. 5.9 could not describe the data accurately and hence using the two dimensional equivalent concept can not be applied to this study. The reason for this is that in this study we have a finite length of diffusers and the jets were discharged in a confined environment where the boundaries (bed of the flume, walls and water surface) play a significant role in the mixing of the jets.

5. 6 Summary and Conclusions

In this study, laboratory experiments were carried out to investigate the effectiveness of multiple jets in producing rapid mixing in an open channel . The experiments were carried out with the velocity ratio α varying from 8 to 16. Two jet arrangements were considered. The first was a combination of coflowing and crossflowing jets and the second was just crossflowing jets, discharged into the ambient flow. Although both the two configurations were considered, main experiments were carried out for the jets in crossflow, as the effect of the first alternative on the mixing distance was found to be limited.

The number of ports for the crossflowing system was varied for 20 to 36 ports and the spacing between ports varied from 12d to 24d. The concentration measurements were carried out for distance x/d=2000. The approximate distance at which the concentration at any section is above the 50% of that of the fully mixed section, is estimated in terms of the non dimensionless distance $\alpha x/d$ to be equal to 5000. The standard deviation of the concentration distribution was used as a measure of the degree of mixing at each section. The dimensionless mixing distance $\alpha x_m/d$ at which the standard deviation reached a value of 5% was equal to 25000. For a fully mixed section, the dilution attained by the system was dependent on the ratio between the jet discharged and the ambient discharge. The results indicated that the mixing distance is independent on the spacing between the ports or on the number of

ports . Finally, the results of this study show that turbulent jets could be a successful alternative to mechanical methods for achieving rapid mixing .

5.7 References:

Benzina, A., S. Lin, and R. L. Wang (1974). "Counterjet and hydraulic blockage theory applications to mixing." Journal WPCF, Vol. 46, No. 12. pp 2719-2731.

Chao, J. L. and B. G. Stone (1979). "Initial mixing by jet injection blending." Journal AWWA, Vol. 71, pp 570-573.

Fitzgerald, S. D., Holley, E. R.(1981). "Jet injections for optimum mixing in pipe flow." Journal of the Hydraulics Division, ASCE, Vol.107, No. HY10, pp 1179-1195.

Ger., A. M. and Holley, E. R. (1976). "Comparison of single point injections in pipe flow." Journal of the Hydraulics Division, ASCE, Vol. 102, No. HY6, pp 731-746.

Hodgson, J. E. and Rajaratnam, N. (1992). "An experimental study of jet dilution in crossflows." Canadian Journal of Civil Engineering, Vol. 19, No.5, 733-743.

Rajaratnam, N. and Langat, J. K., (1995), " Mixing of circular turbulent wall jets in crossflows." J. of Hydr. Engrg. ASCE, Vol. 121, No. 10, pp 694-658.

Roberts, P.J.W., Snyder,W.H., Baumgartner, D.J. (1989). "Ocean Outfalls. I: Submerged Wastefield Formation." Journal of Hydr. Engrg. ASCE, Vol. 15, No. 1, pp 1-25.

Wright, S. J. (1977). "Effects of ambient crossflows and density stratification on the characteristic behavior of round turbulent buoyant jets". Report No. KH-R-36, W.M. Keck Laboratory of Hydraulics and Water Resources. California Institute of Technology, California, USA, 254 p.

Table 5.1 Details of Experiments of Coflowing and Crossflowing Multiple Jets

Exp. No.	Number of ports n	Spacing S	Depth of Flow D (mm)	Jets Discharges Q_o (L/min)	Ambient Discharges Q (L/s)	Jet Velocity U_o (m/s)	Channel Velocity U (m/s)	$\alpha = U_o/U$	Jet Reynolds No.
CC1	35	24d	388	12.5	20.62	0.722	0.09	8	2293
CC2	35	24d	388	15	17.51	0.902	0.0752	12	2865
CC3	35	24d	388	20	17.51	1.203	0.0752	16	3821
CC4	25	24d	388	12	19.61	1.010	0.0842	12	3209
CC5	25	24d	388	15	18.38	1.26	0.079	16	4012
CF1	20	24d	388	8	24.5	0.84	0.105	8	2674
CF2	20	24d	388	12	24.5	1.26	0.105	12	4012
CF3	20	24d	388	15	22.9	1.58	0.098	16	5015
CF4	20	12d	227	8	14.34	0.842	0.105	8	2674
	20	12d	227	15	26.89	1.57	0.197	8	5015
CF5	20	12d	227	12	14.34	1.26	0.105	12	4012
CF6	20	12d	227	15	13.36	1.57	0.098	16	5015
CF7	36	12d	388	17	14.27	0.99	0.062	16	3158
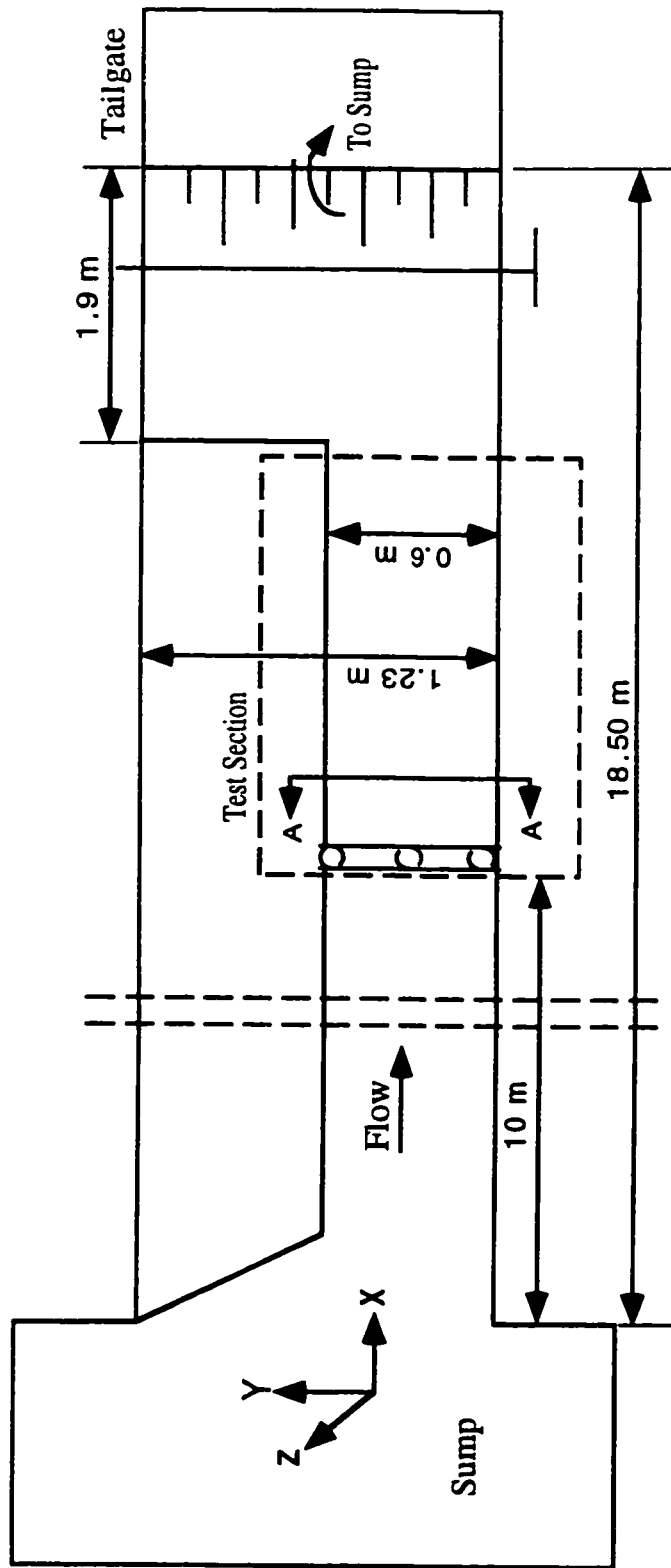
Fig. 5.1a Plan View of the Experimental Arrangement
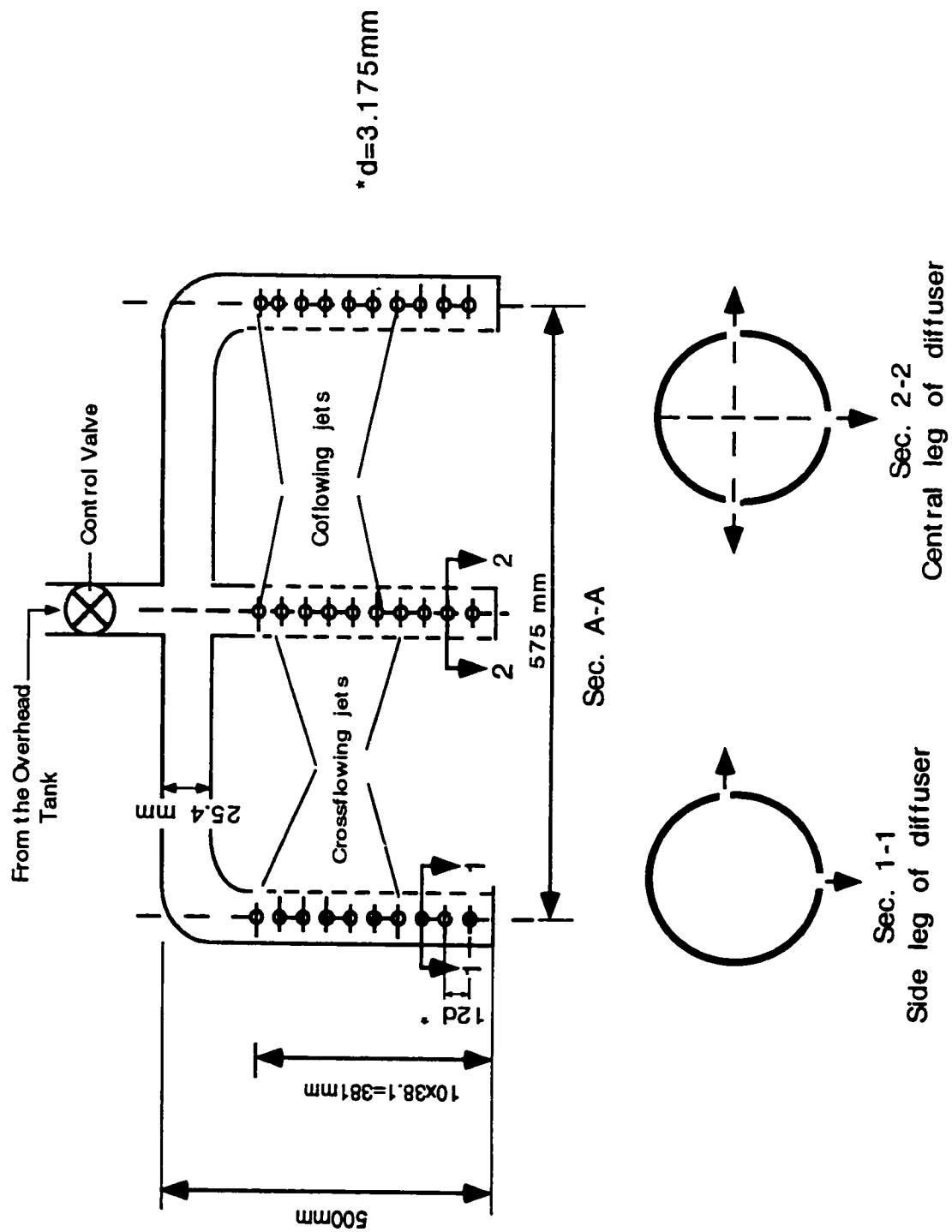
Fig. 5.1b Details of Diffuser

*d=3.175mm

From the Overhead Tank

Control Valve

Coflowing jets

Crossflowing jets

25.4 mm

575 mm

Sec. A-A

12d*

10x38.1=381mm

500mm

Sec. 2-2
Central leg of diffuser

Sec. 1-1
Side leg of diffuser

229
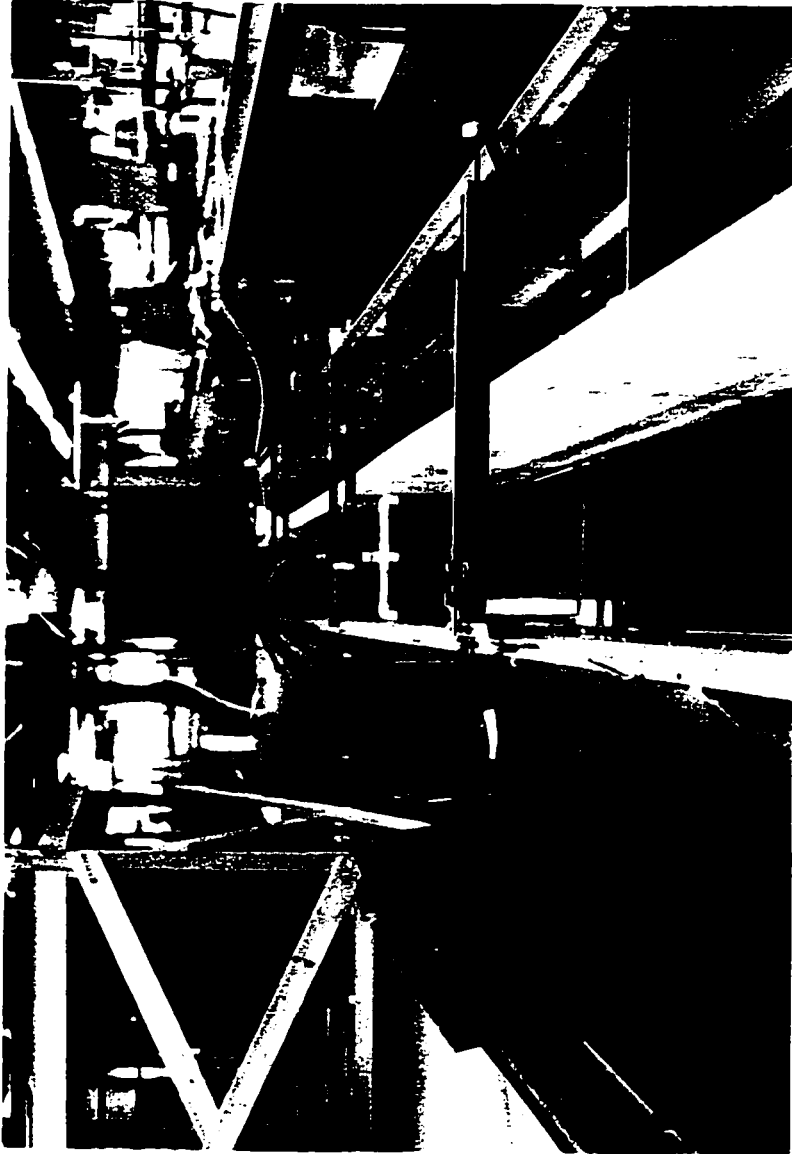
Fig. 5.2 Flume Arrangement
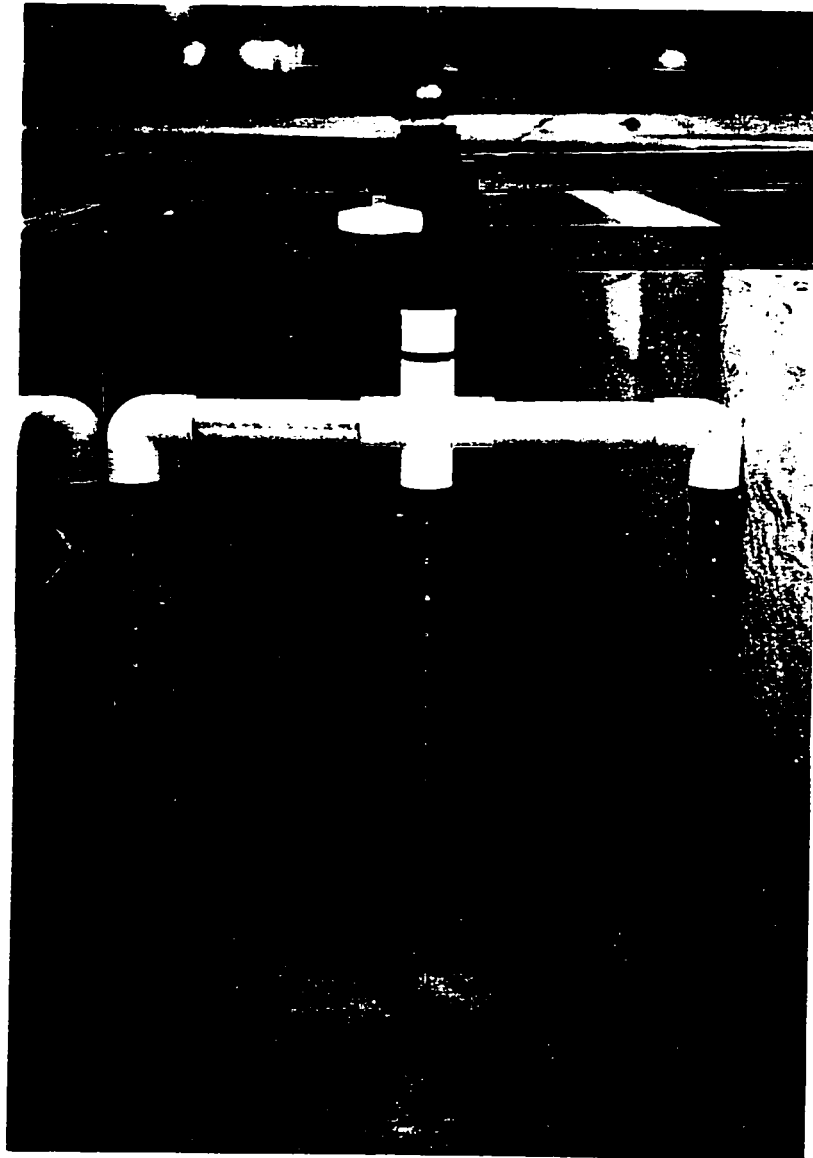
Fig. 5.3 Picture of Diffuser (Looking Upstream)

Fig. 5.4 Sampling Rake
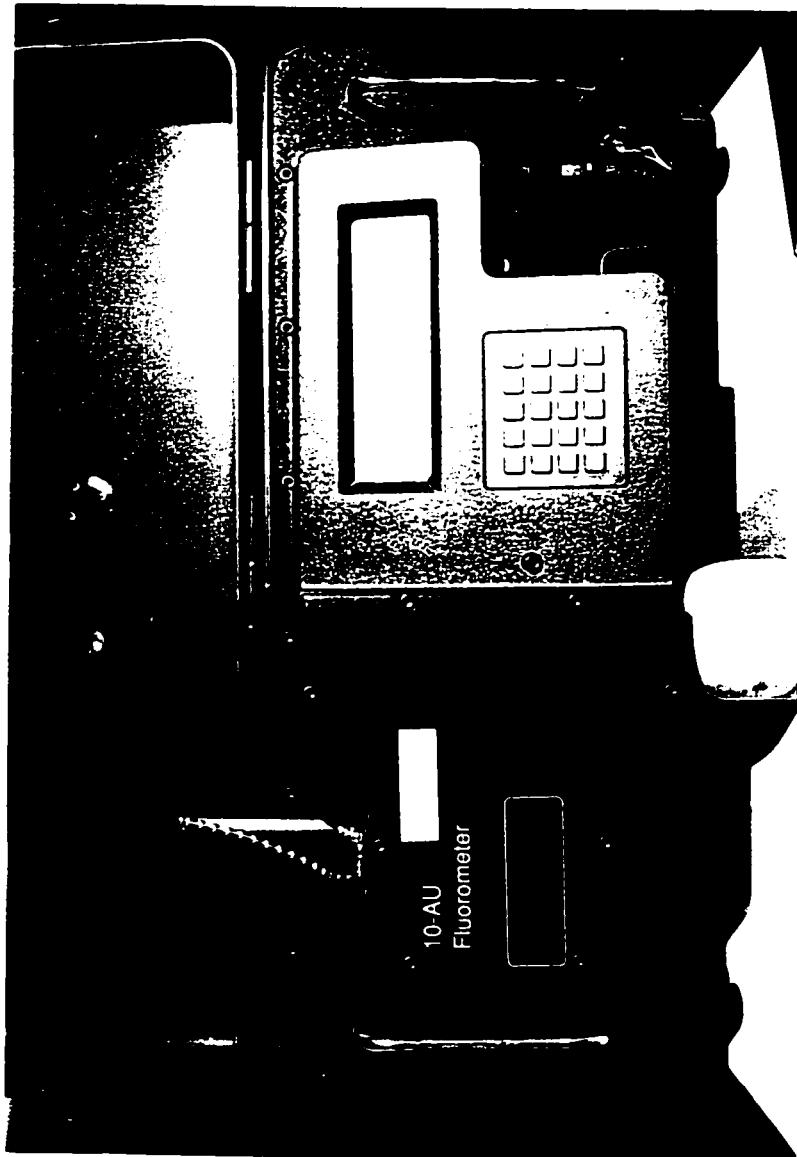
Fig. 5.5 Turner Model 10 - AU Digital Fluorometer

Fig. 5.6a Typical Plan View Photograph for Experiment (CC1), Velocity Ratio (U_0/U) = 8

$S = 24d$, $n = 35$

Fig. 5.6b Typical Plan View Photograph for Experiment (CF1), Velocity Ratio $(U_0/U) = 8$

$S = 24d$, $n = 20$

Fig. 5.6c Typical Plan View Photograph for Experiment (CF3), Velocity Ratio $(U_0/U) = 16$

$S = 24d$, $n = 20$

Fig. 5.6d Typical Plan View Photograph for Experiment (CF7), Velocity Ratio $(U_o/U) = 16$
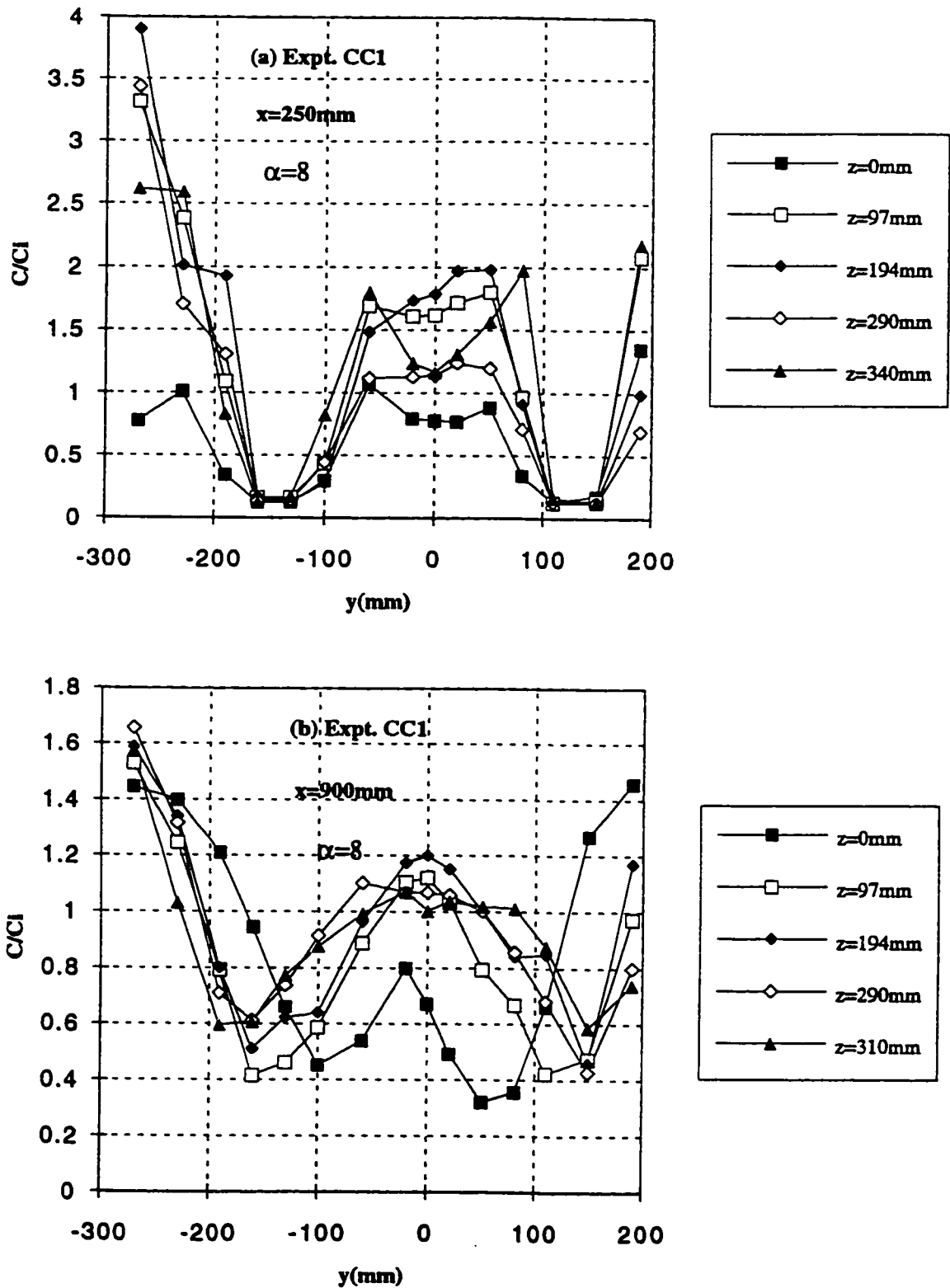
$S = 12d, \quad n = 36$

Fig. 5.7 (a-b) Typical Transverse Concentration Profiles at Different Levels
for Expt. CC1 - CC3

(c) Expt. CC1

x=1300mm

α=8

Legend:
- z=0mm
- z=97mm
- z=194mm
- z=290mm
- z=346mm

(d) Expt. CC1

x=1600mm

α=8

Legend:
- z=0mm
- z=97mm
- z=194mm
- z=290mm
- z=342mm
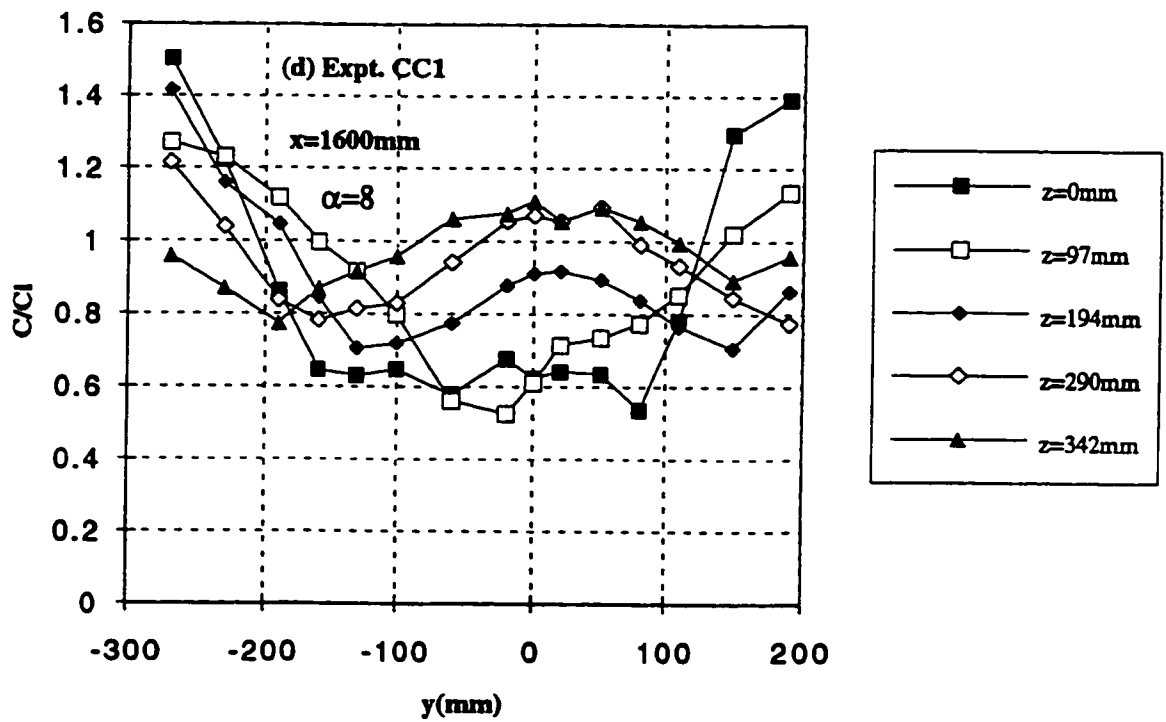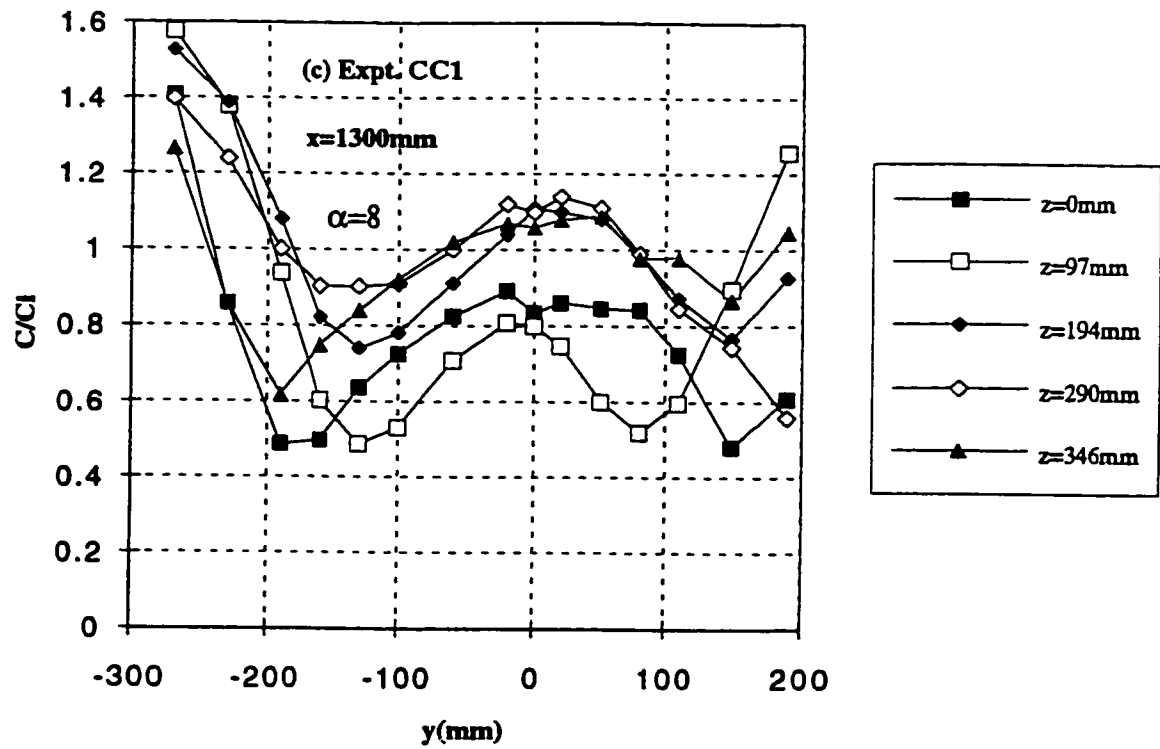
Fig. 5.7 (c-d) Typical Transverse Concentration Profiles at Different Levels for Expt. CC1 - CC3
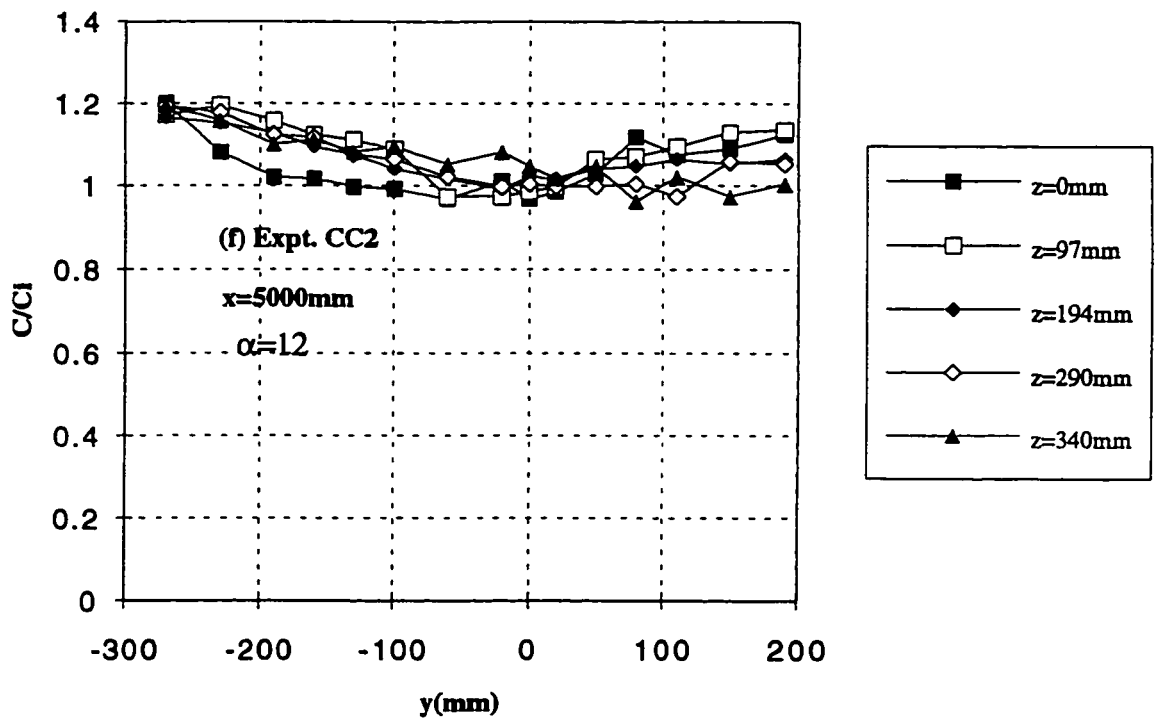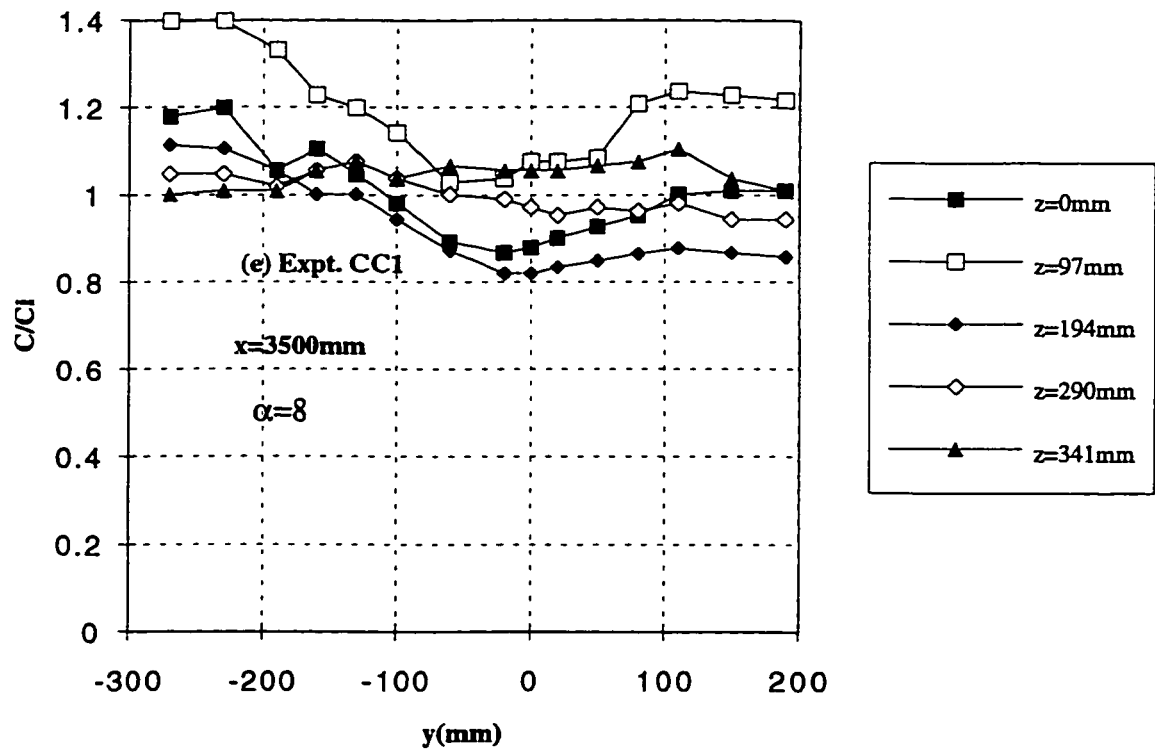
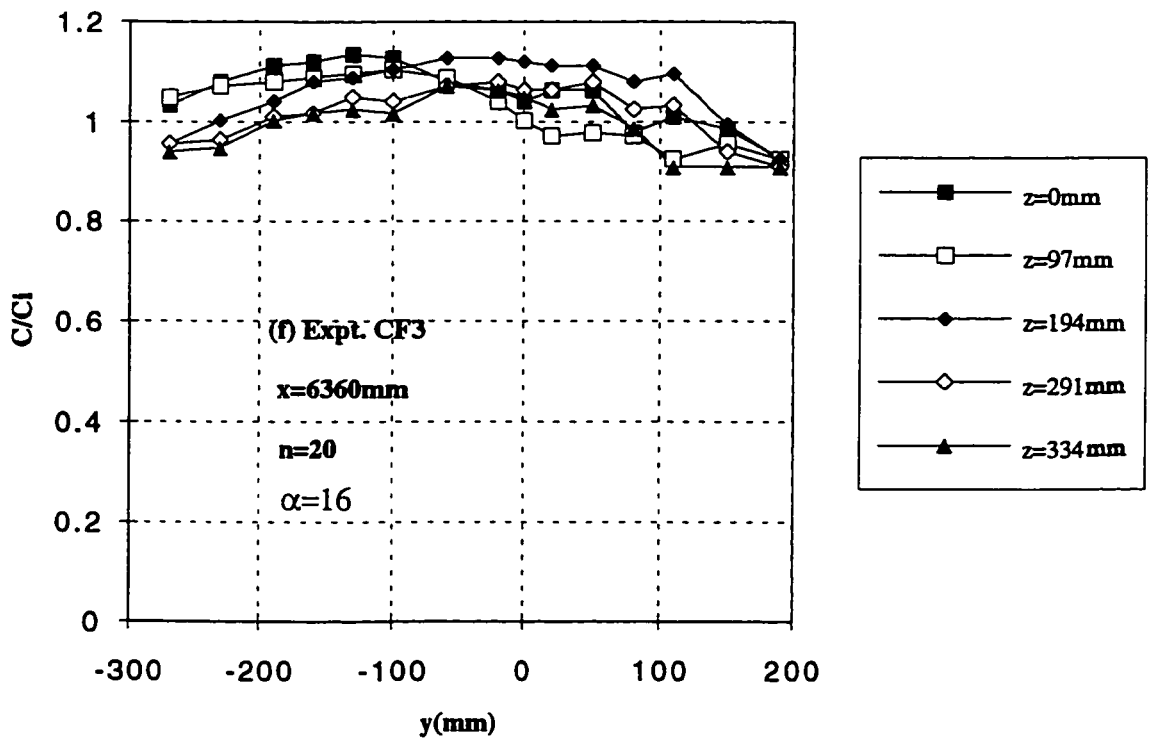**Fig. 5.7 (e-f) Typical Transverse Concentration Profiles at Different Levels for Expt. CC1 - CC3**
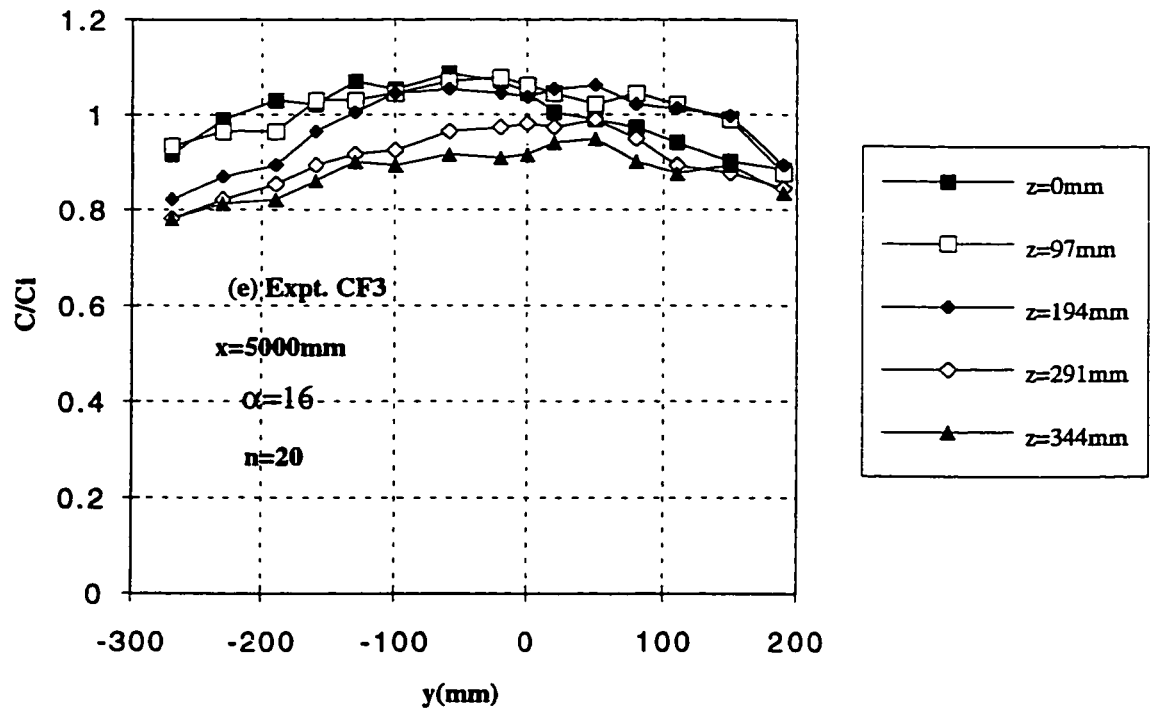
240
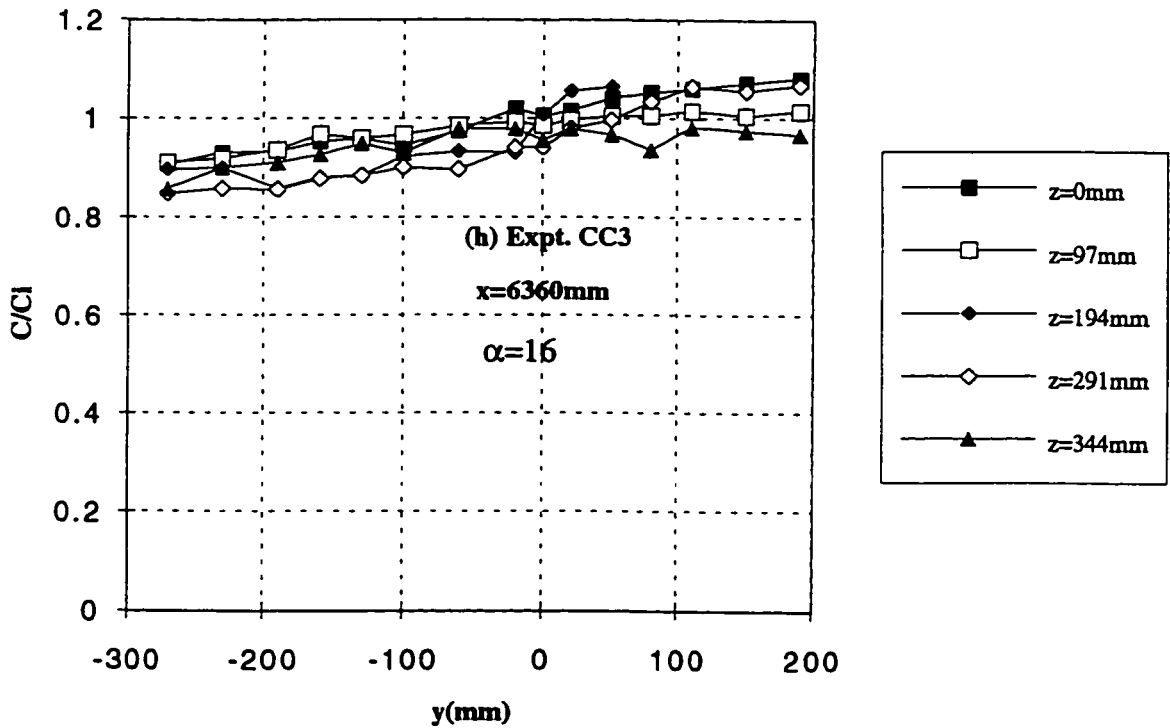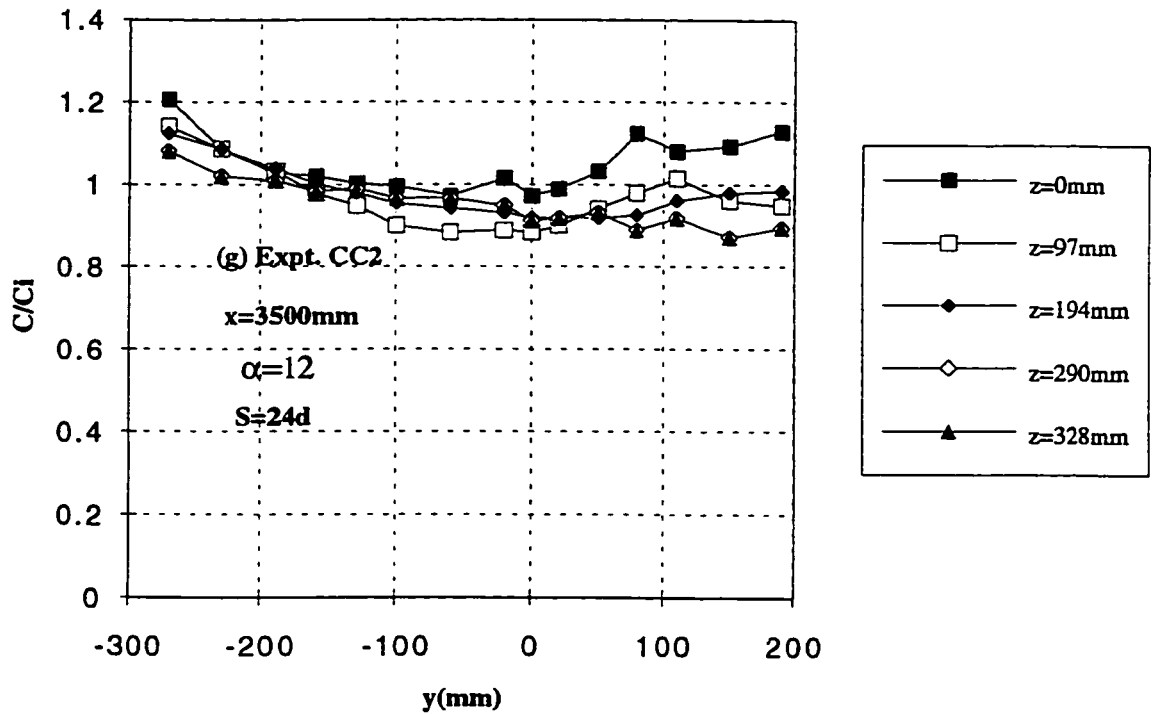
Fig. 5.7 (g-h) Typical Transverse Concentration Profiles at Different Levels
for Expt. CC1 - CC3
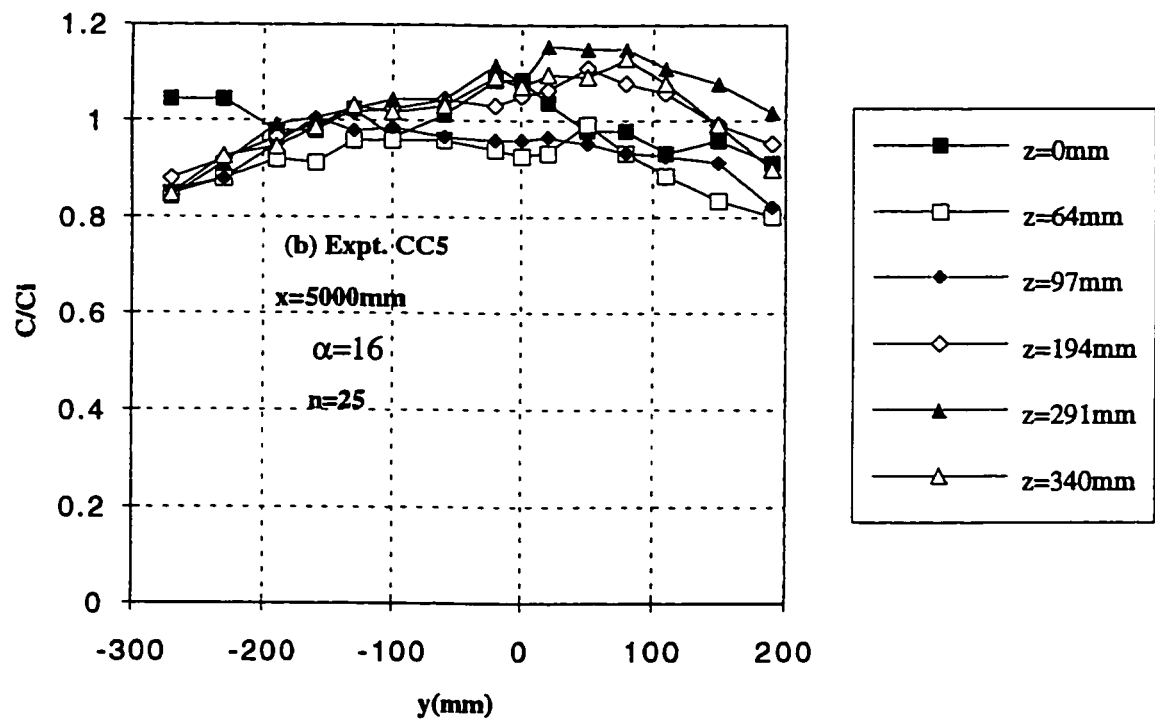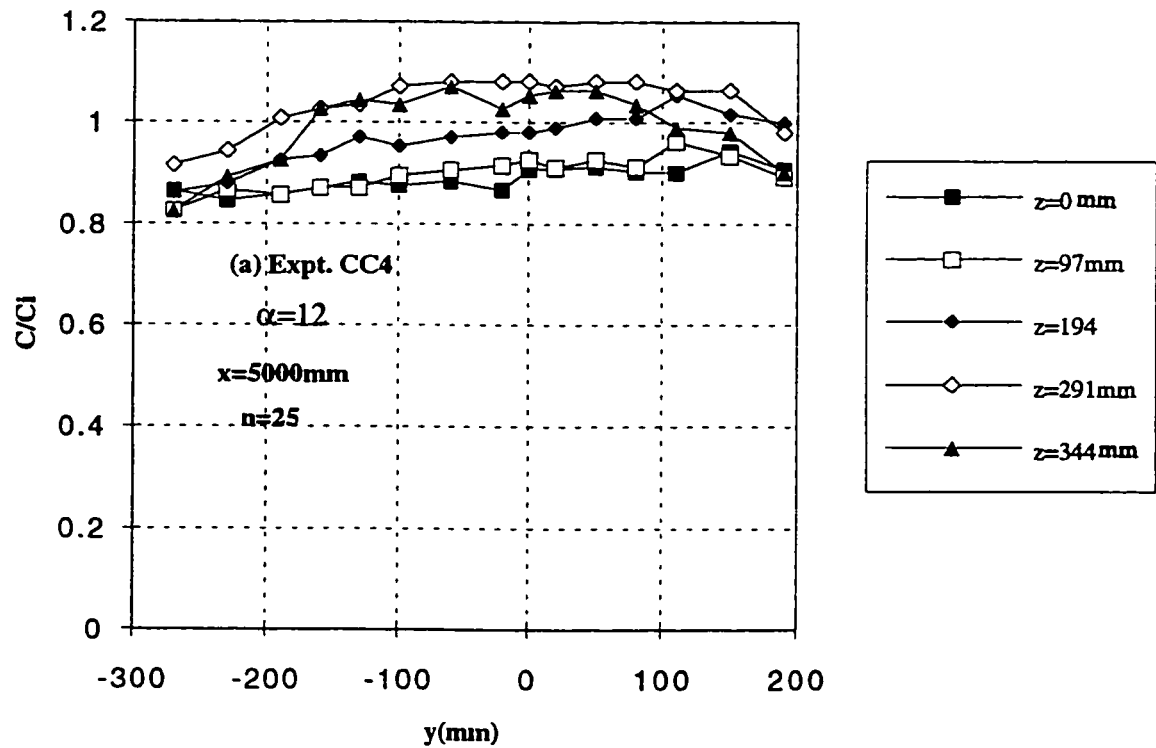
Fig. 5.8 (a-b) Typical Transverse Concentration Profiles at Different Levels for Expt. CC4 - CC5
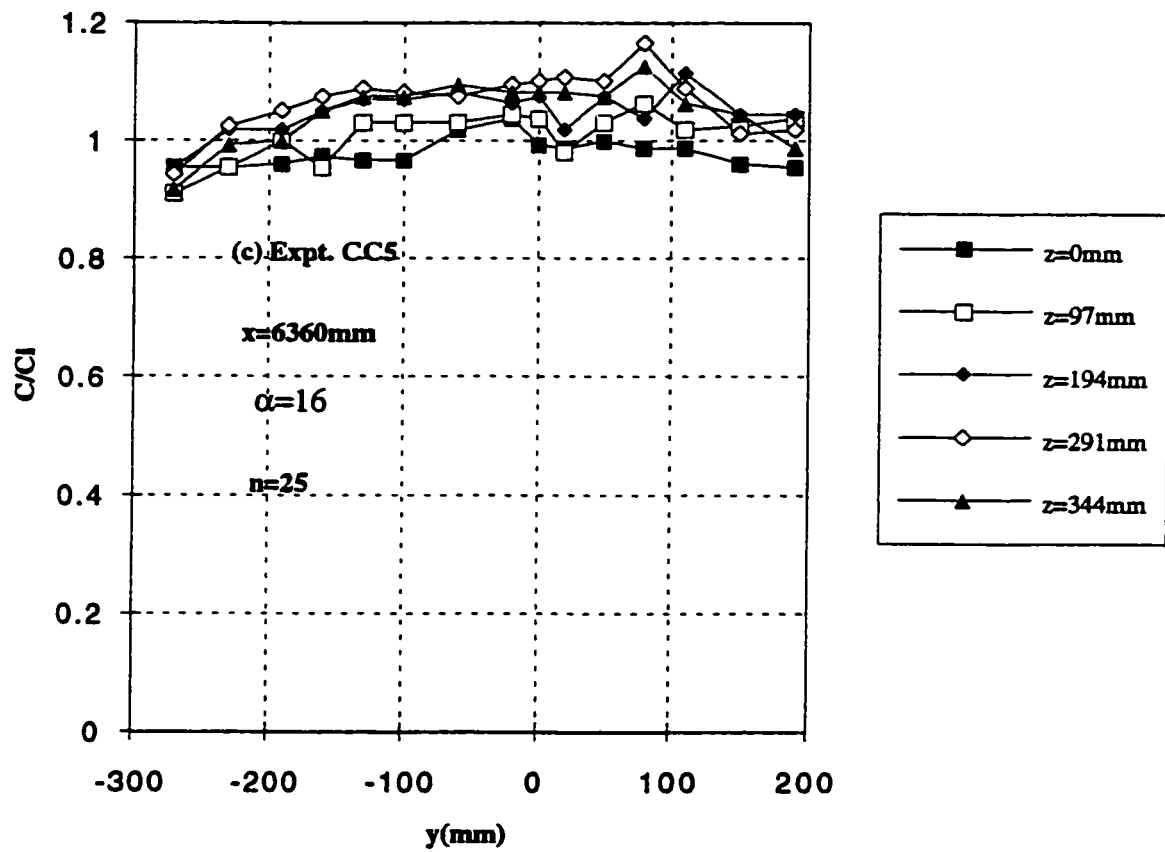
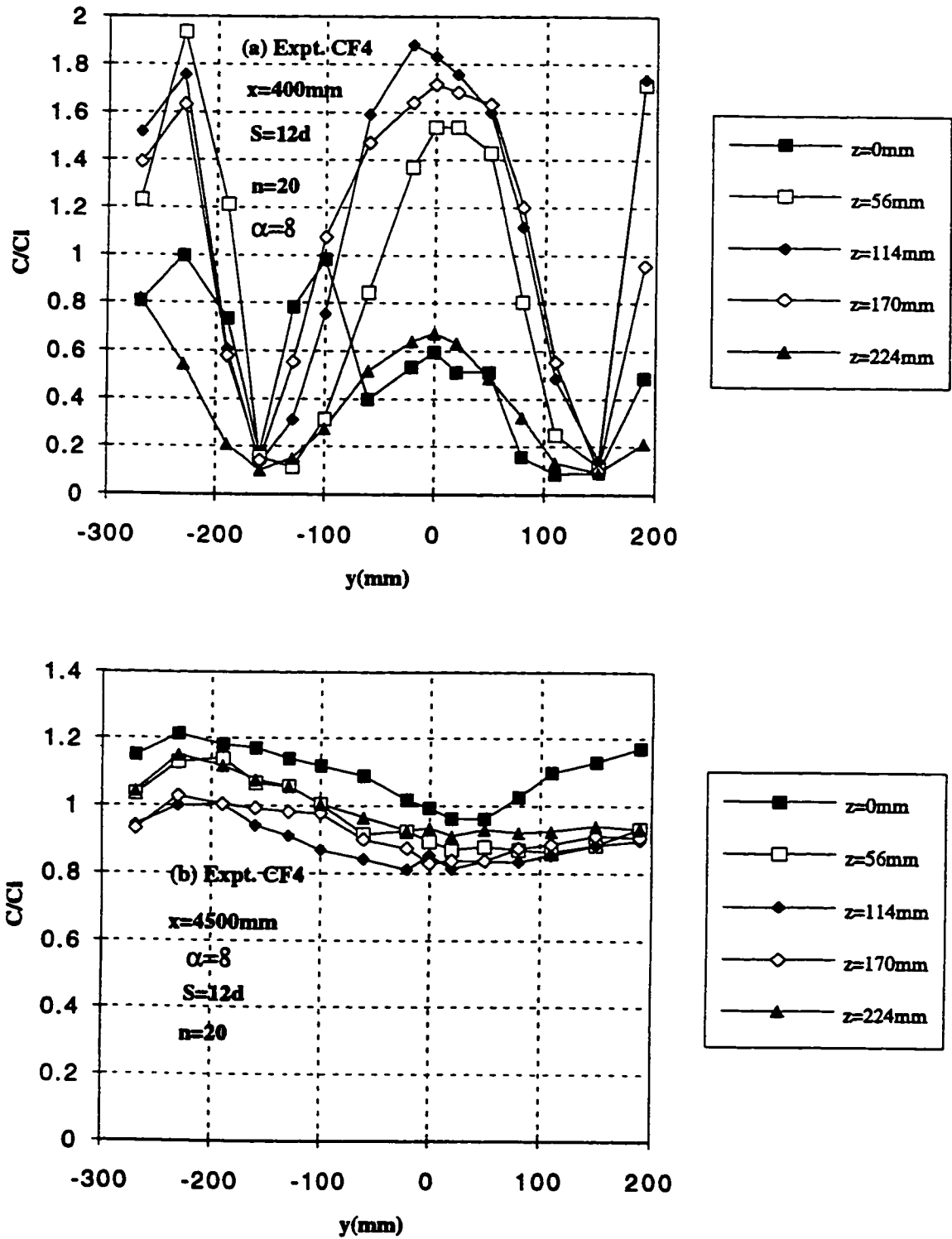Fig. 5.8c Typical Transverse Concentration Profiles at Different Levels
for Expt. CC4 - CC5
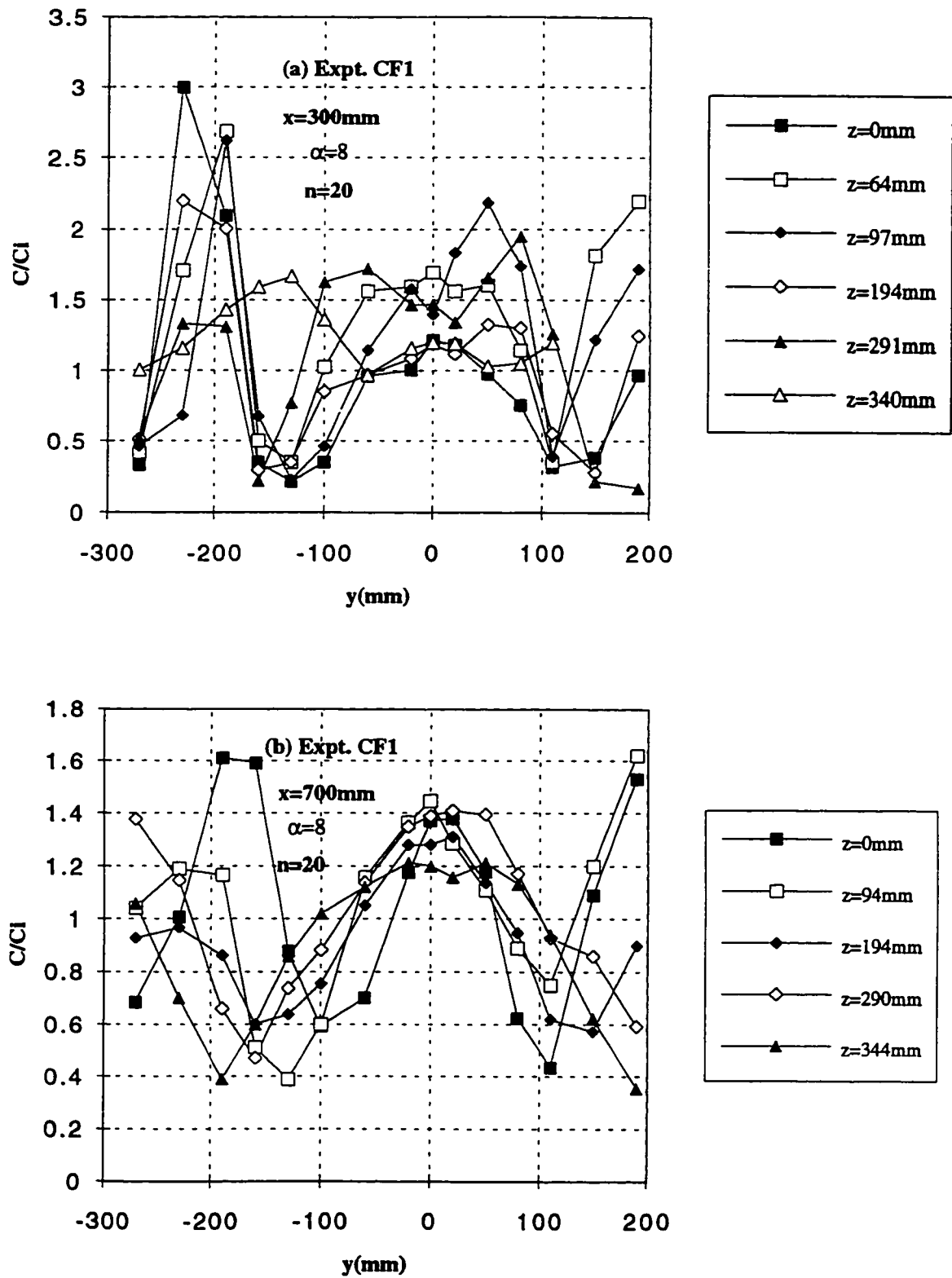
Fig. 5.9 (a-b) Typical Transverse Concentration Profiles at Different Levels
for Expt. CF1
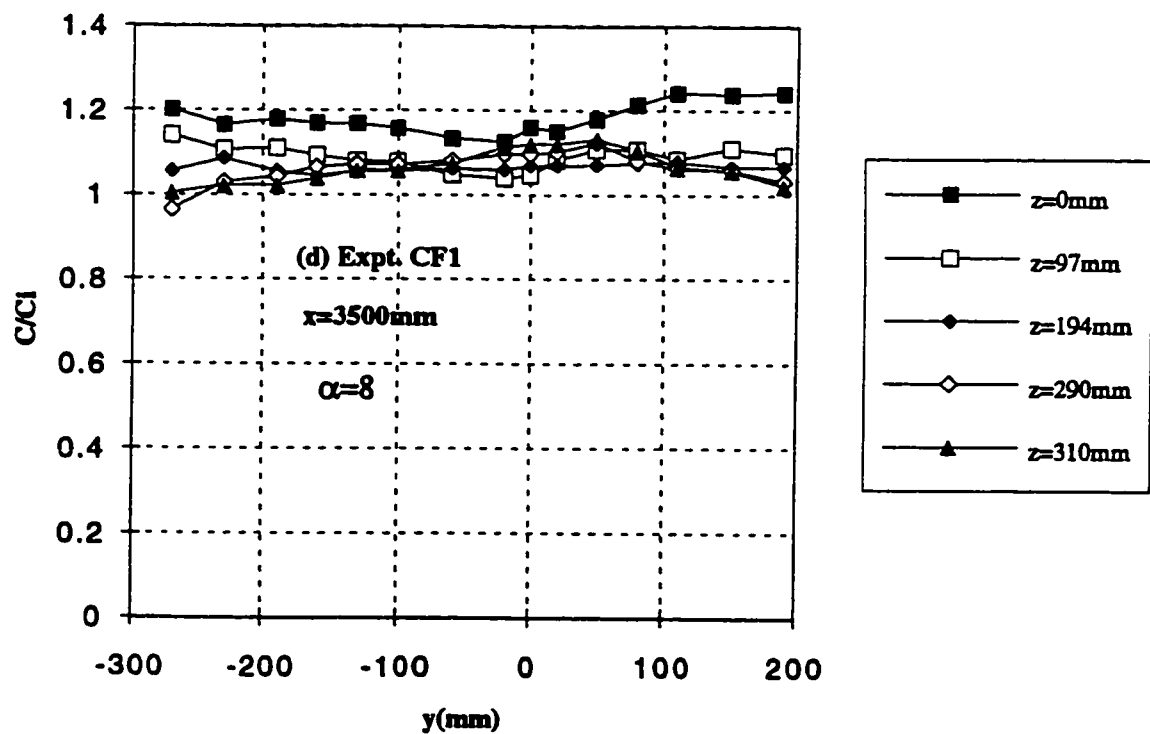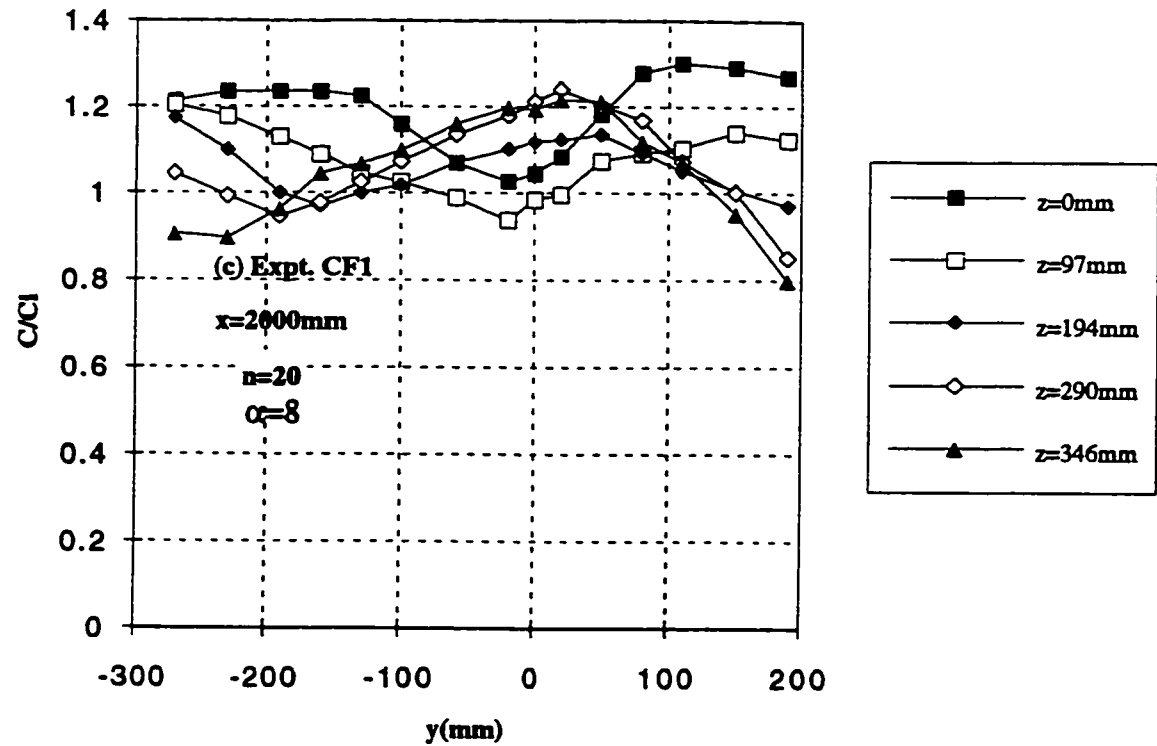
Fig. 5.9 (c-d) Typical Transverse Concentration Profiles at Different Levels
for Expt. CF1
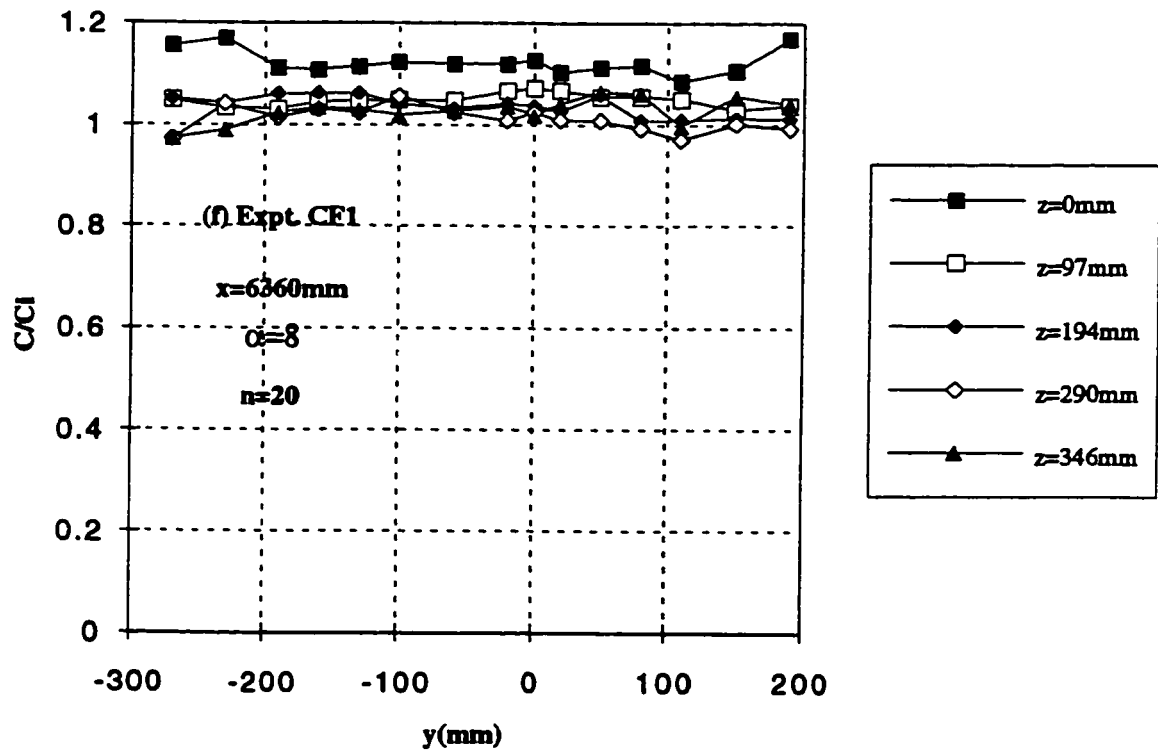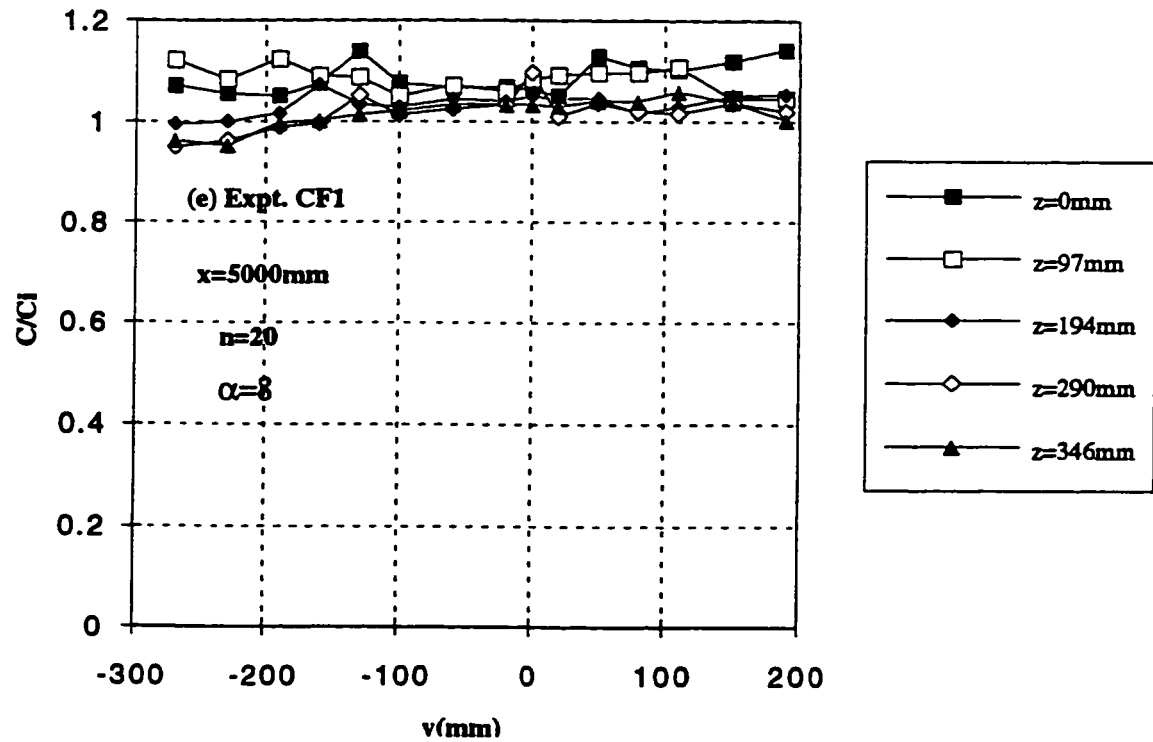
Fig. 5.9 (e-f) Typical Transverse Concentration Profiles at Different Levels
for Expt. CF1
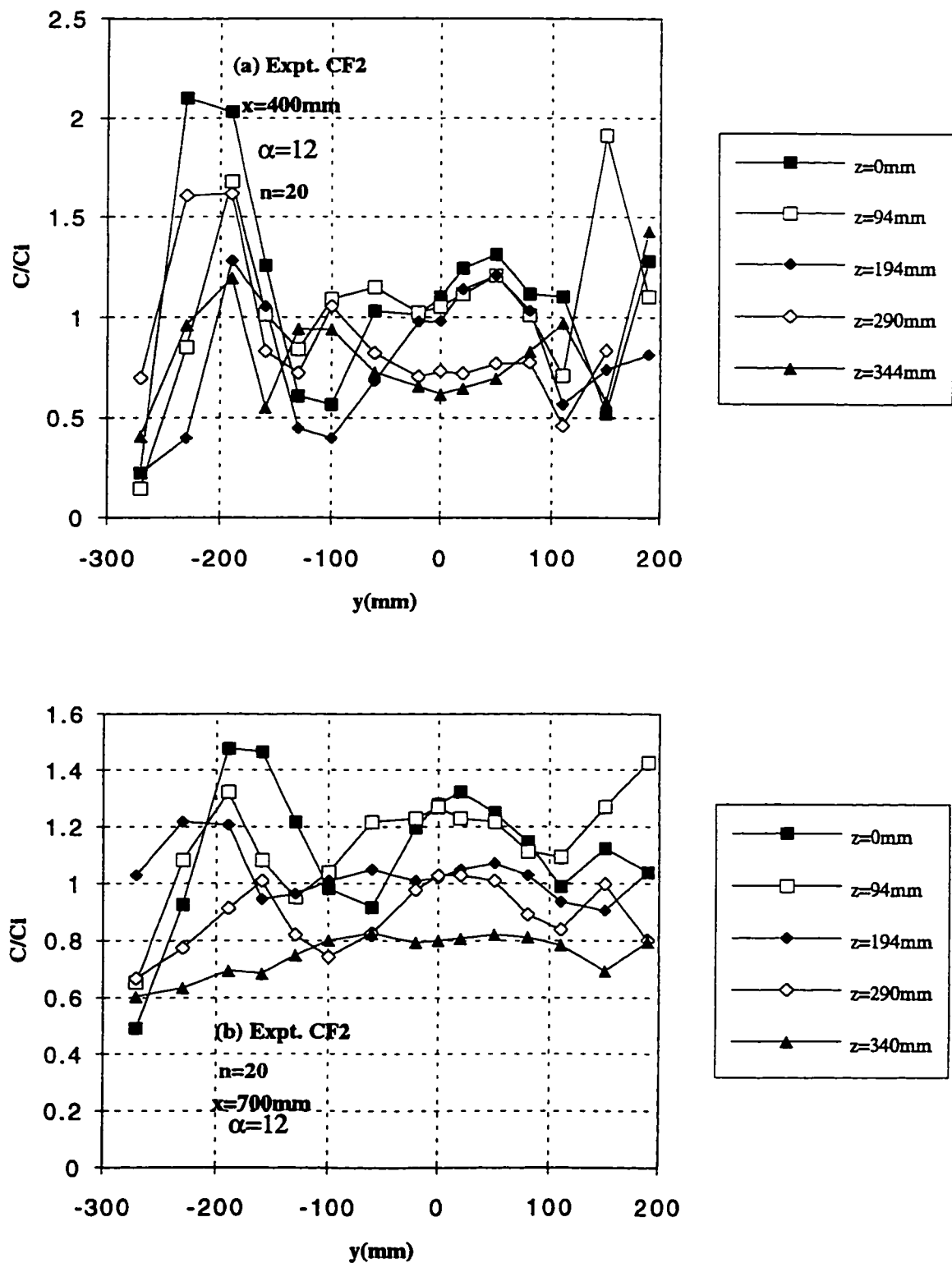
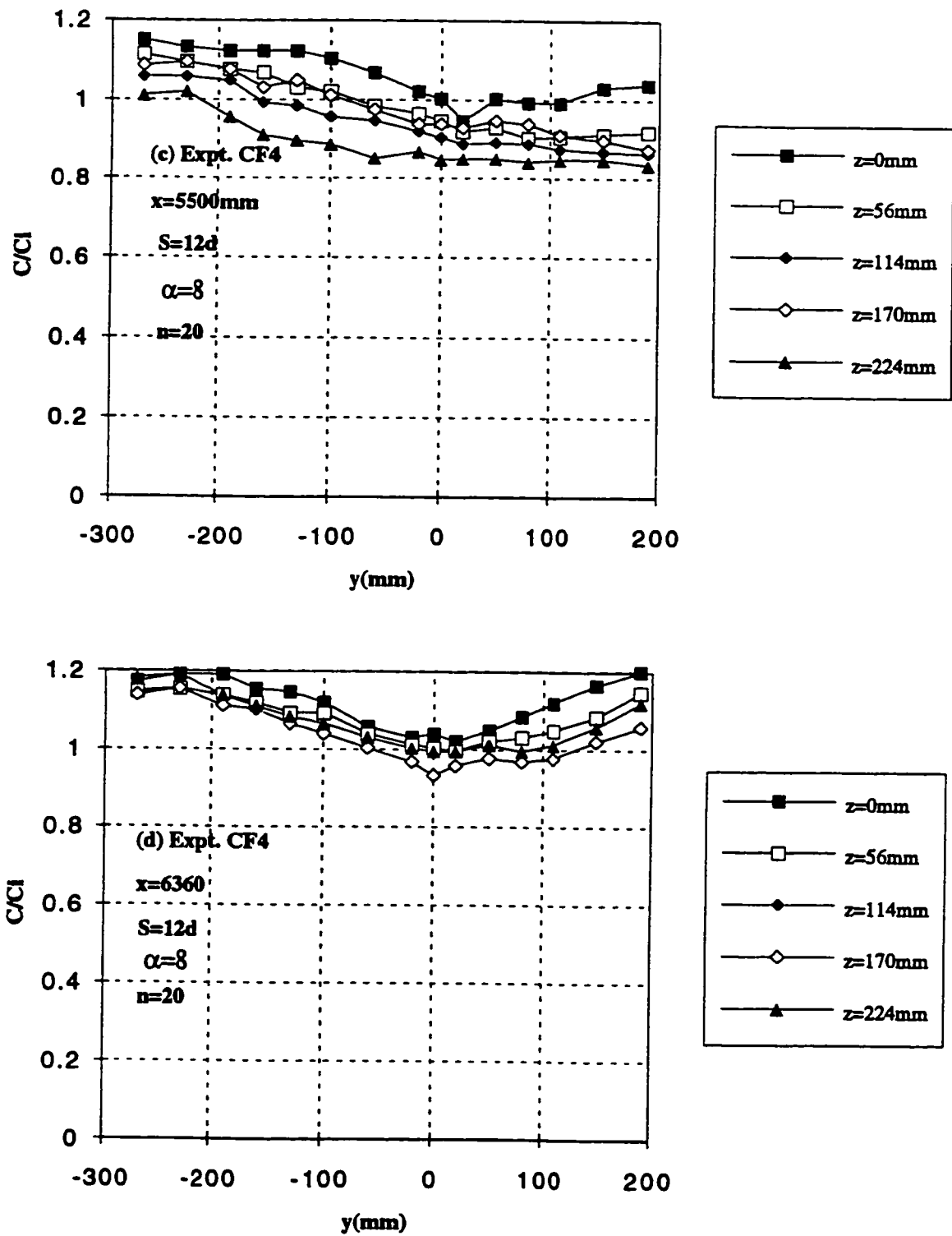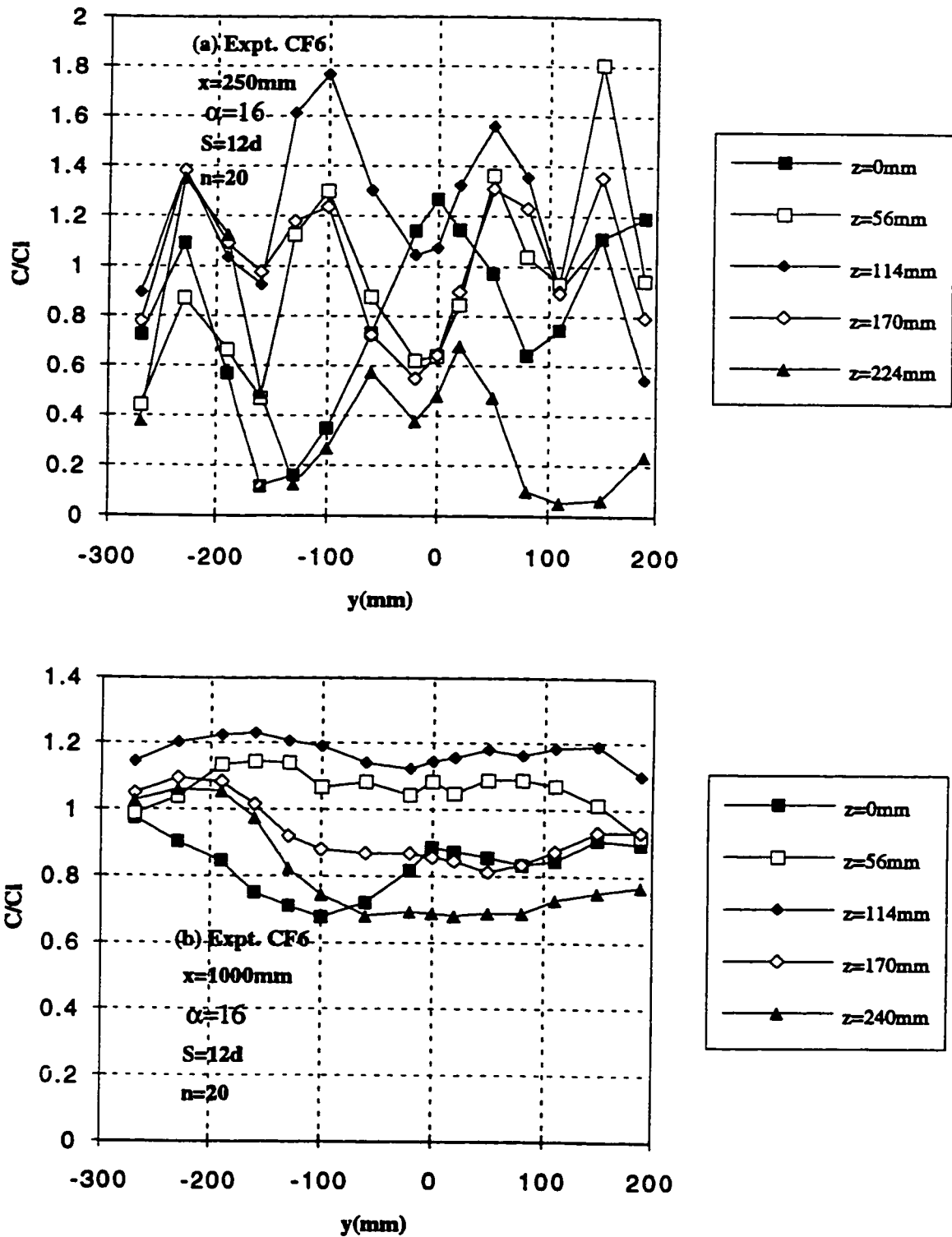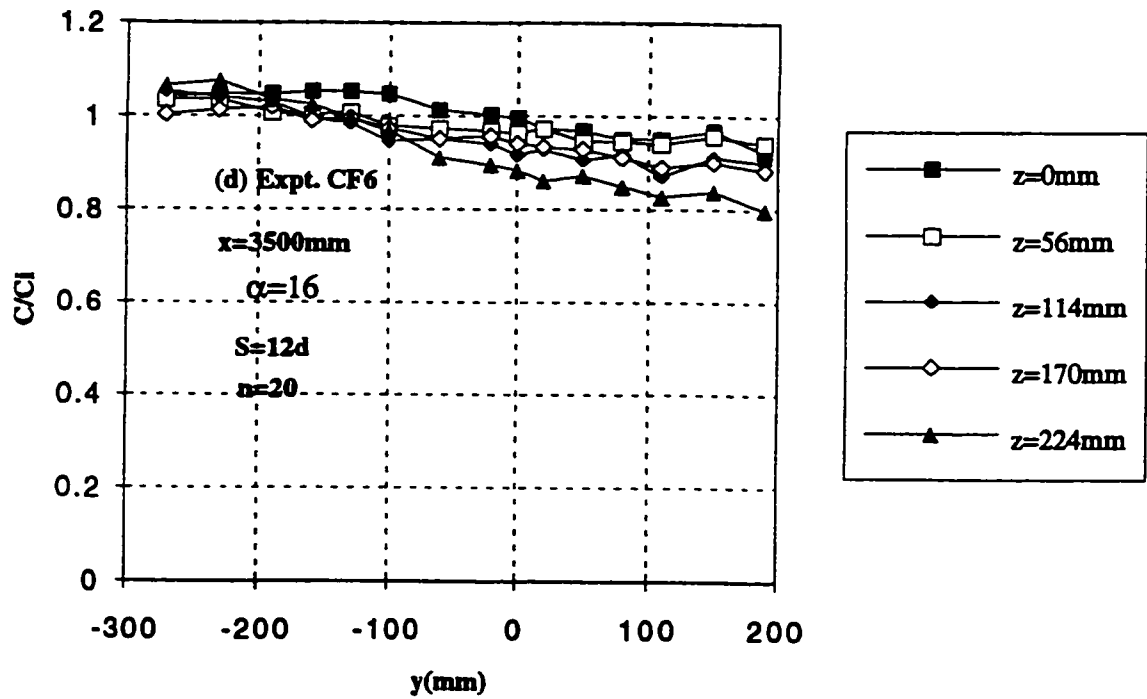Fig. 5.10 (a-b) Typical Transverse Concentration Profiles at Different Levels
for Expt. CF2
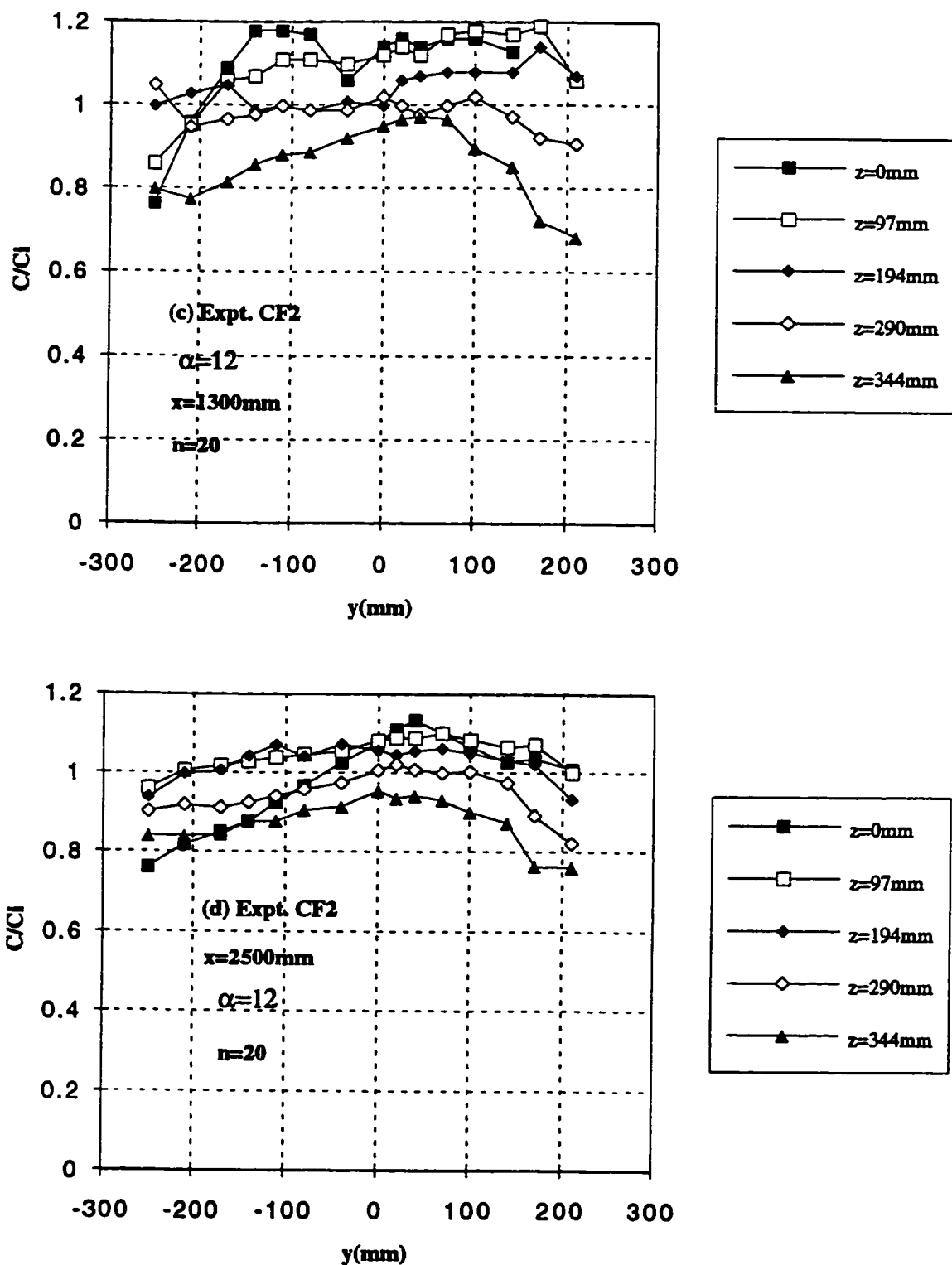
Fig. 5.10 (c-d) Typical Transverse Concentration Profiles at Different Levels for Expt. CF2
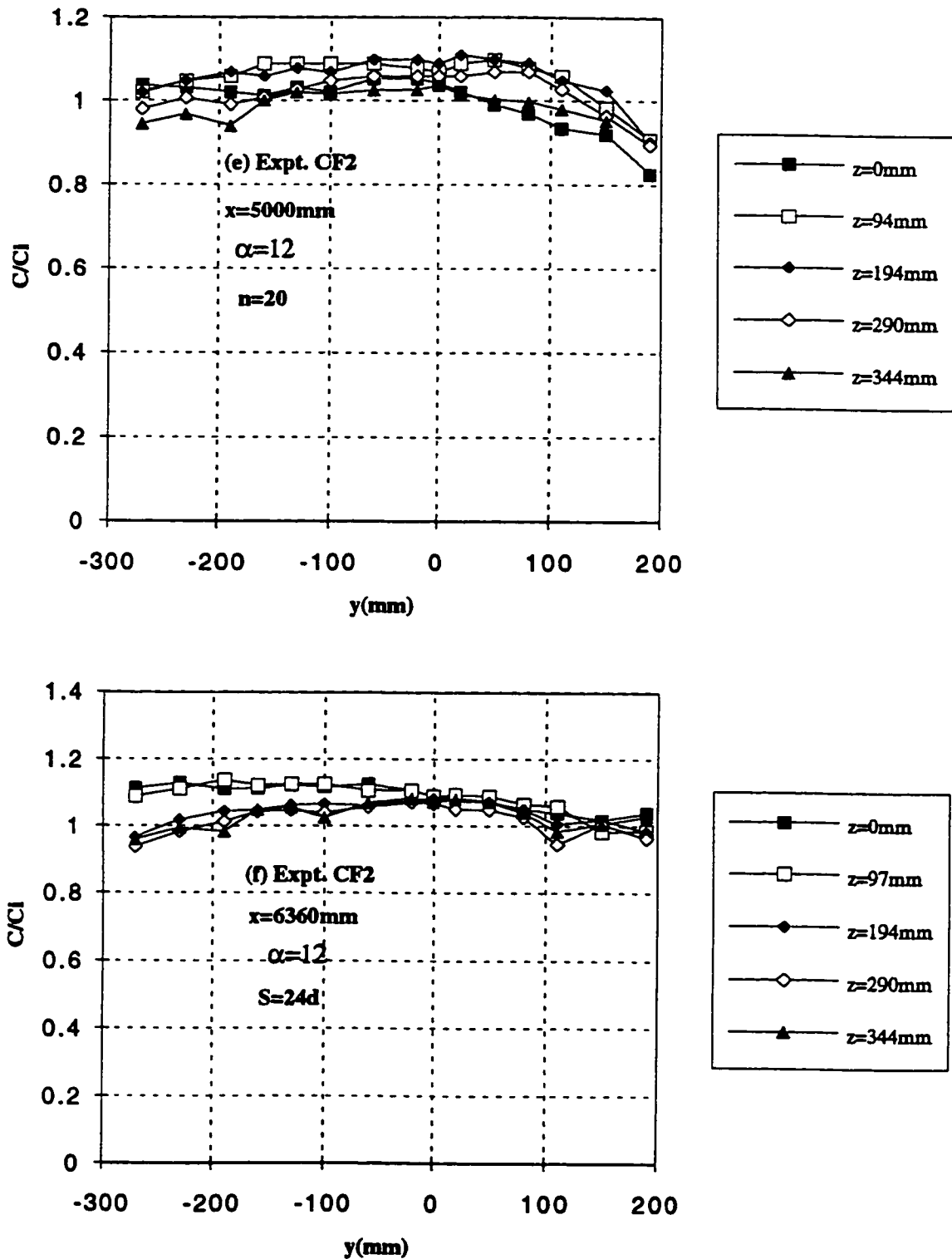
Fig. 5.10 (e-f) Typical Transverse Concentration Profiles at Different Levels for Expt. CF2
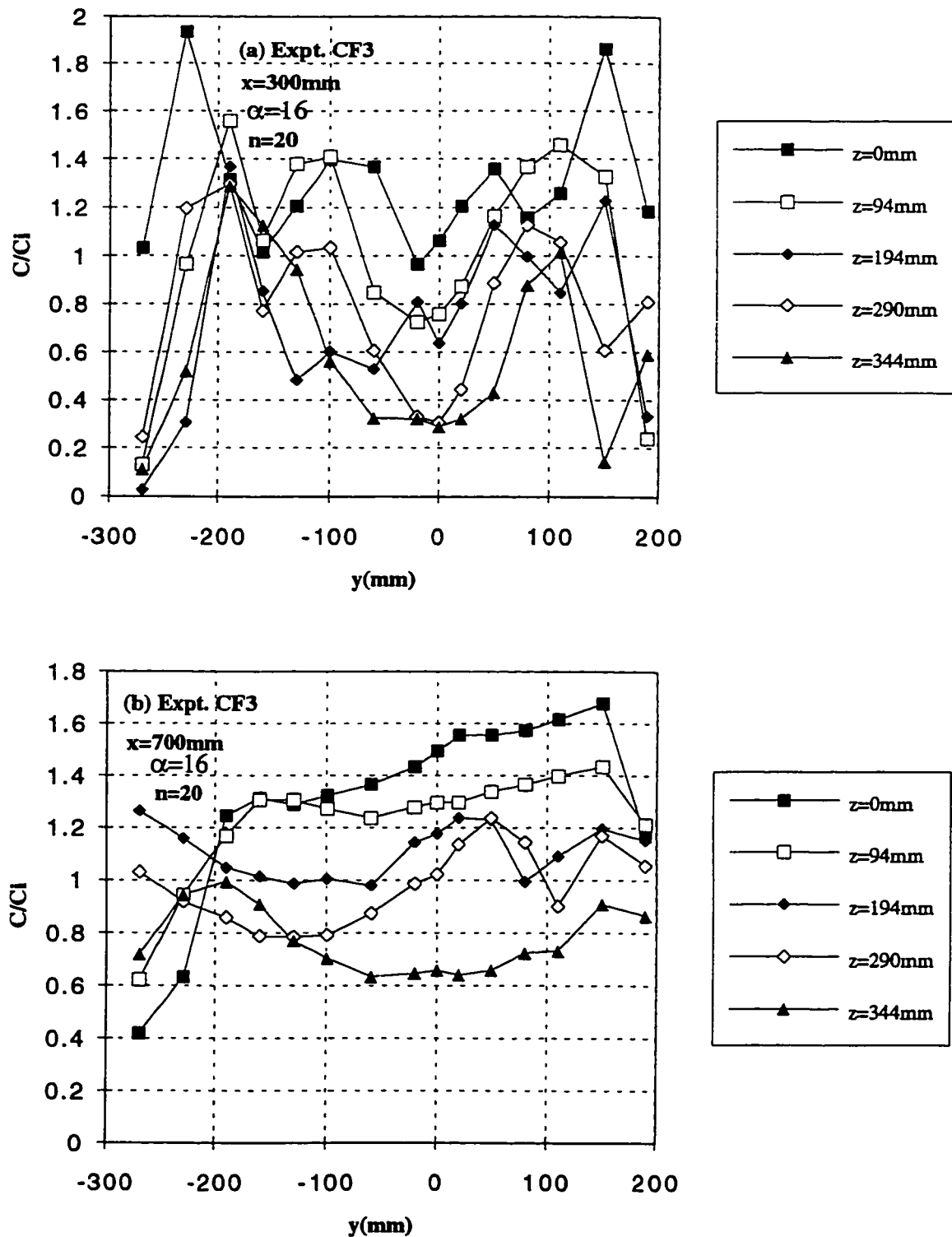
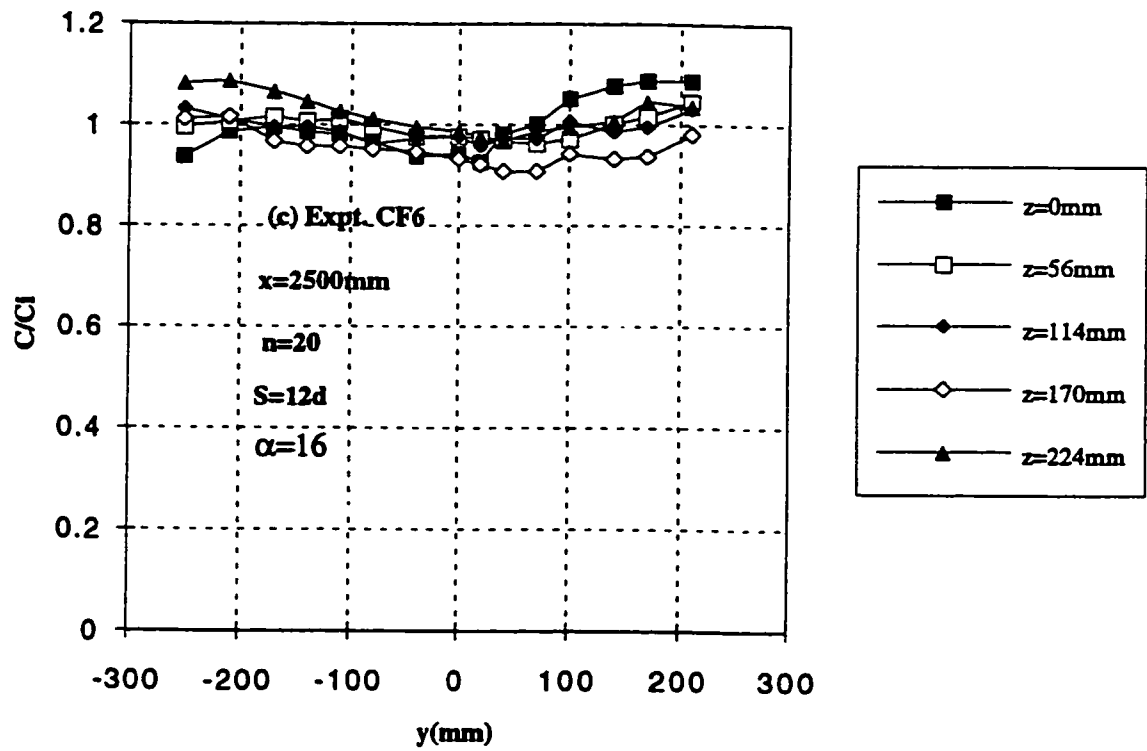**Fig. 5.11 (a-b) Typical Transverse Concentration Profiles at Different Levels for Expt. CF3**
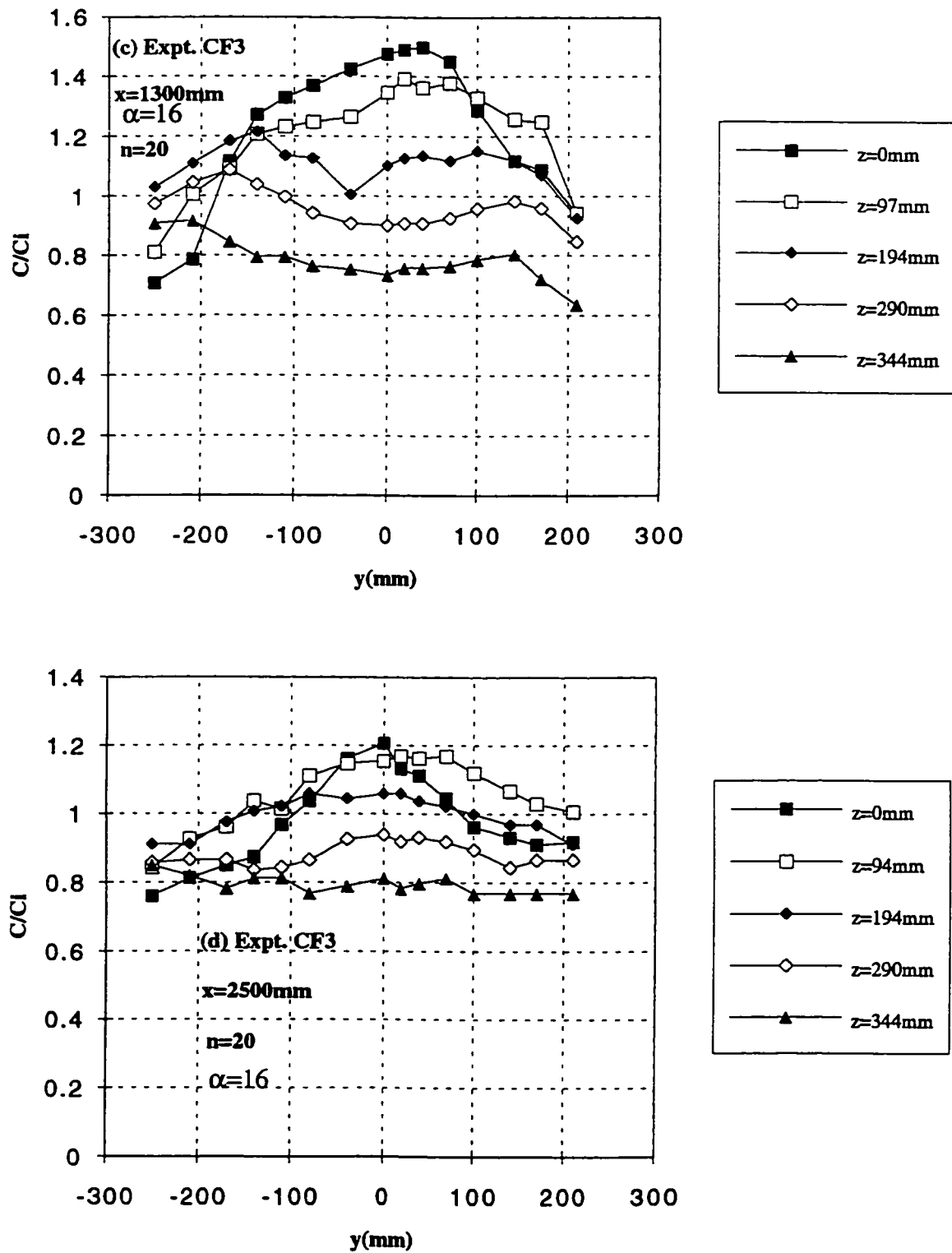
Fig. 5.11 (c-d) Typical Transverse Concentration Profiles at Different Levels for Expt. CF3

Fig. 5.11 (e-f) Typical Transverse Concentration Profiles at Different Levels
for Expt. CF3

Fig. 5.12 (a-b) Typical Transverse Concentration Profiles at Different Levels
for Expt. CF4

Fig. 5.12 (c-d) Typical Transverse Concentration Profiles at Different Levels for Expt. CF4
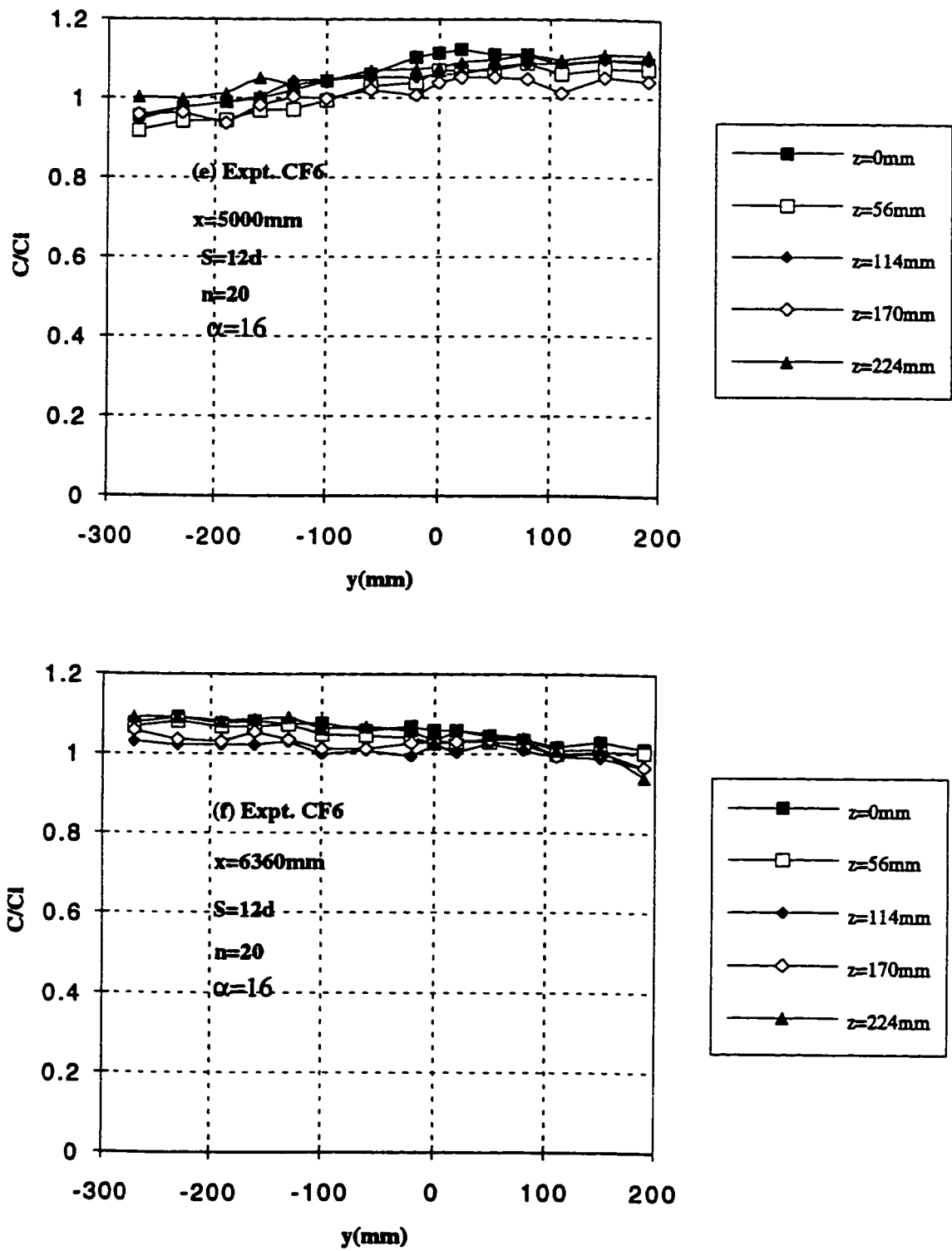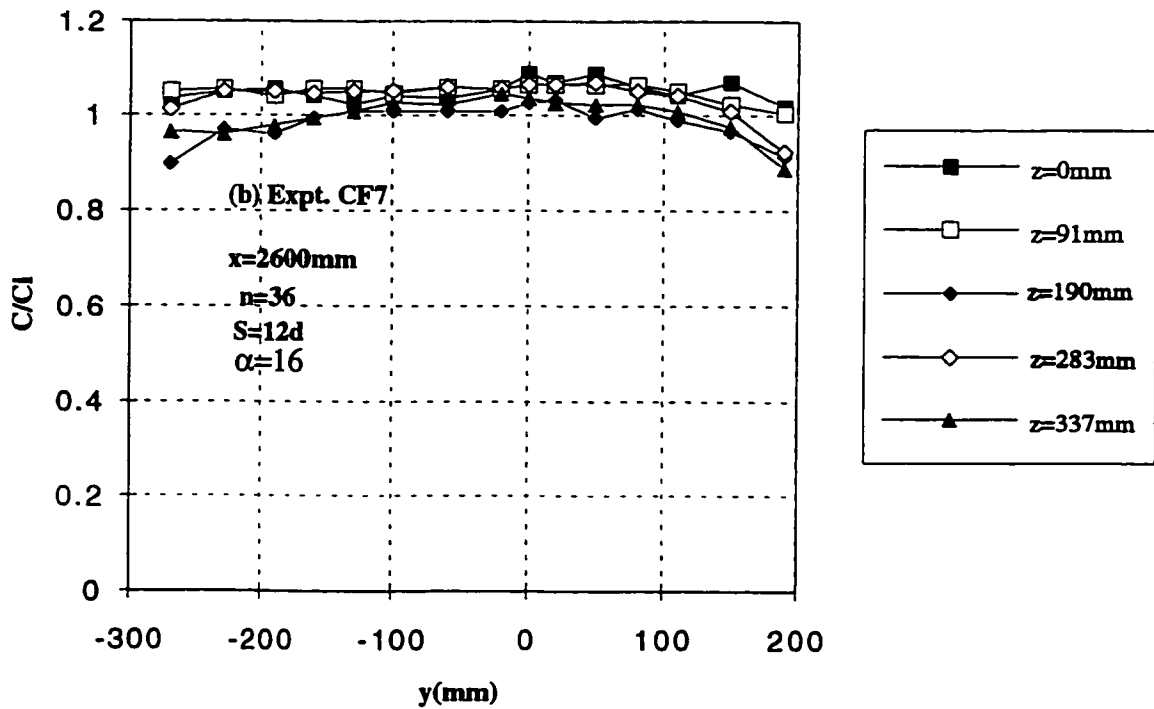
Fig. 5.13 (a-b) Typical Transverse Concentration Profiles at Different Levels
for Expt. CF6

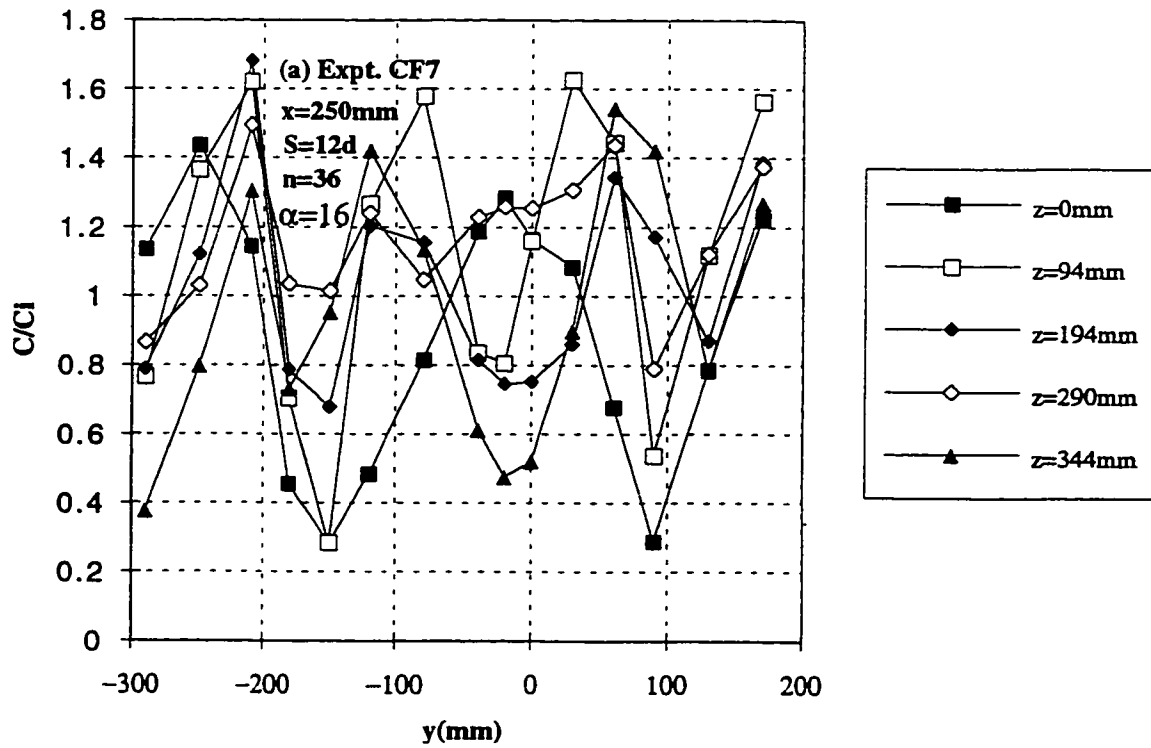Fig. 5.13 (c-d) Typical Transverse Concentration Profiles at Different Levels
for Expt. CF6

256

Fig. 5.13 (e-f) Typical Transverse Concentration Profiles at Different Levels
for Expt. CF6

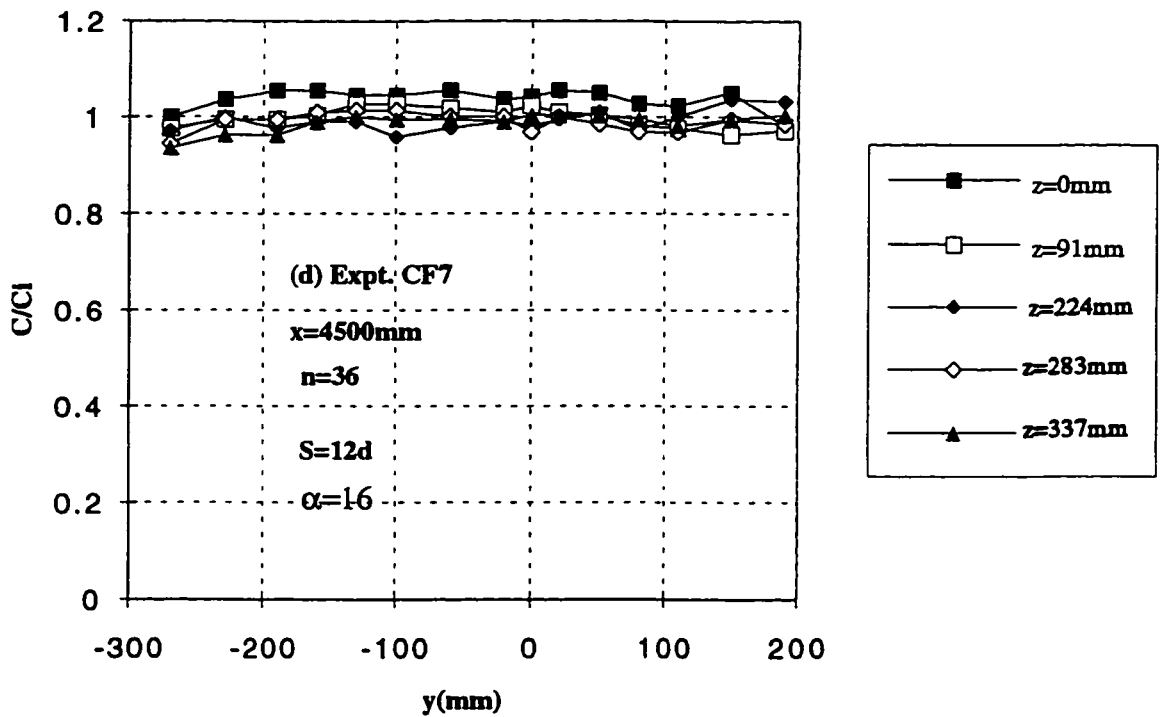**Fig. 5.14 (a-b) Typical Transverse Concentration Profiles at Different Levels for Expt. CF7**
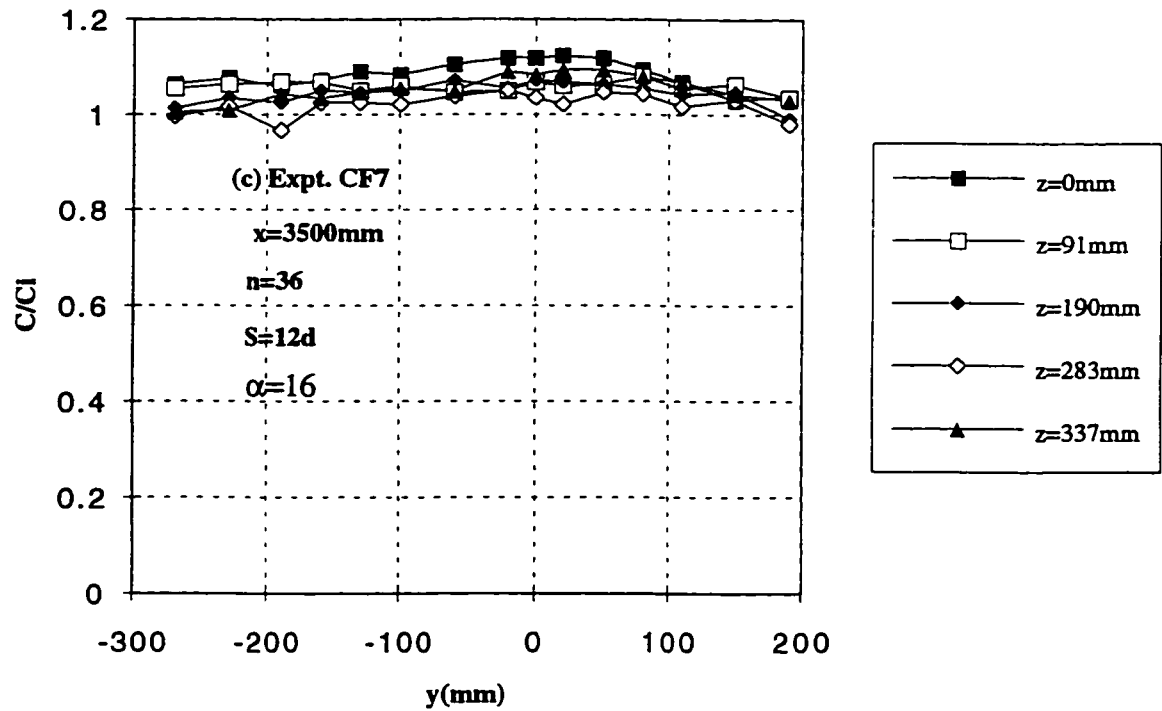
Fig. 5.14 (c-d) Typical Transverse Concentration Profiles at Different Levels for Expt. CF7
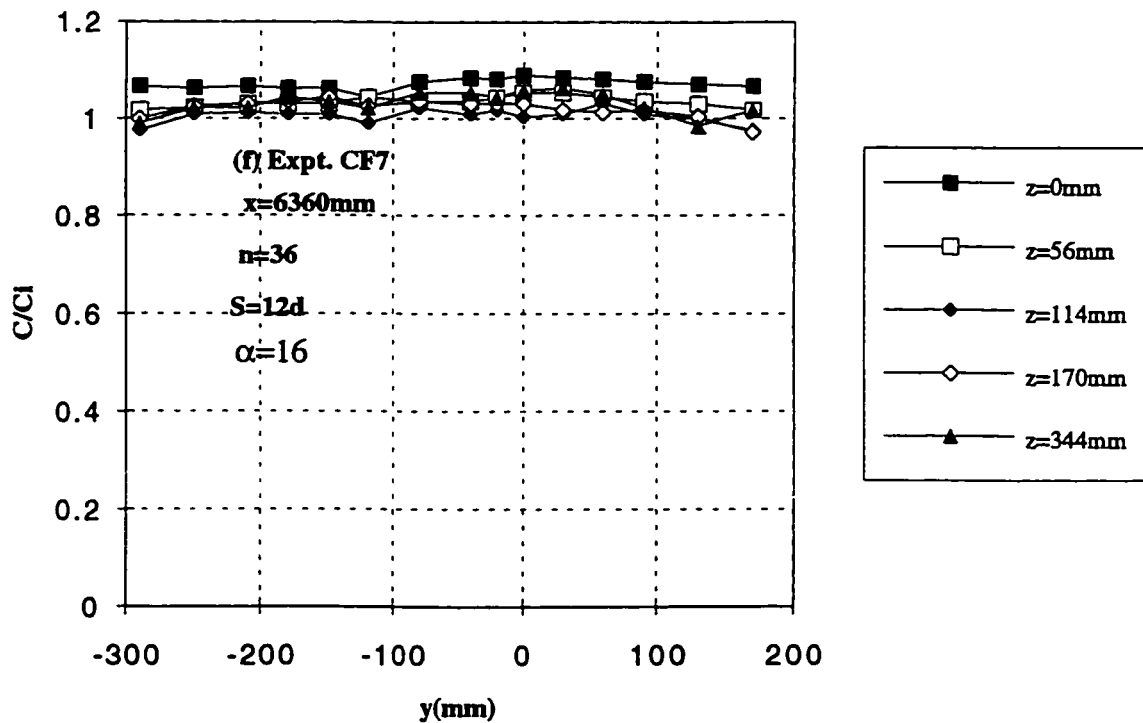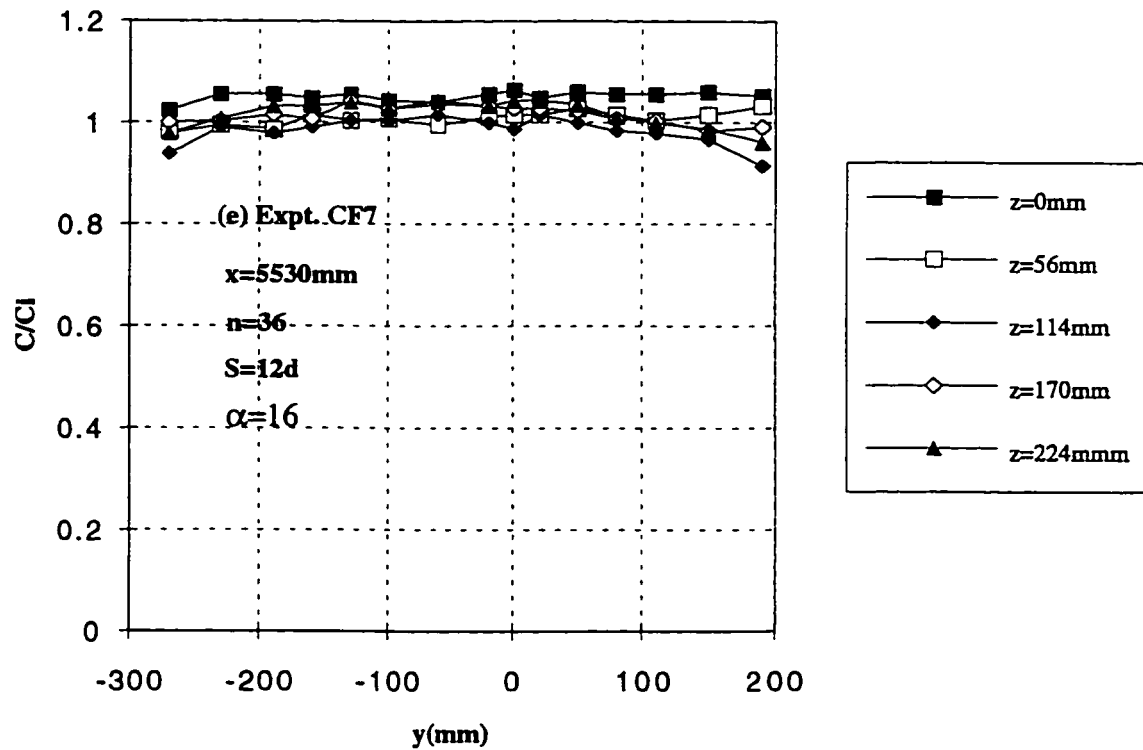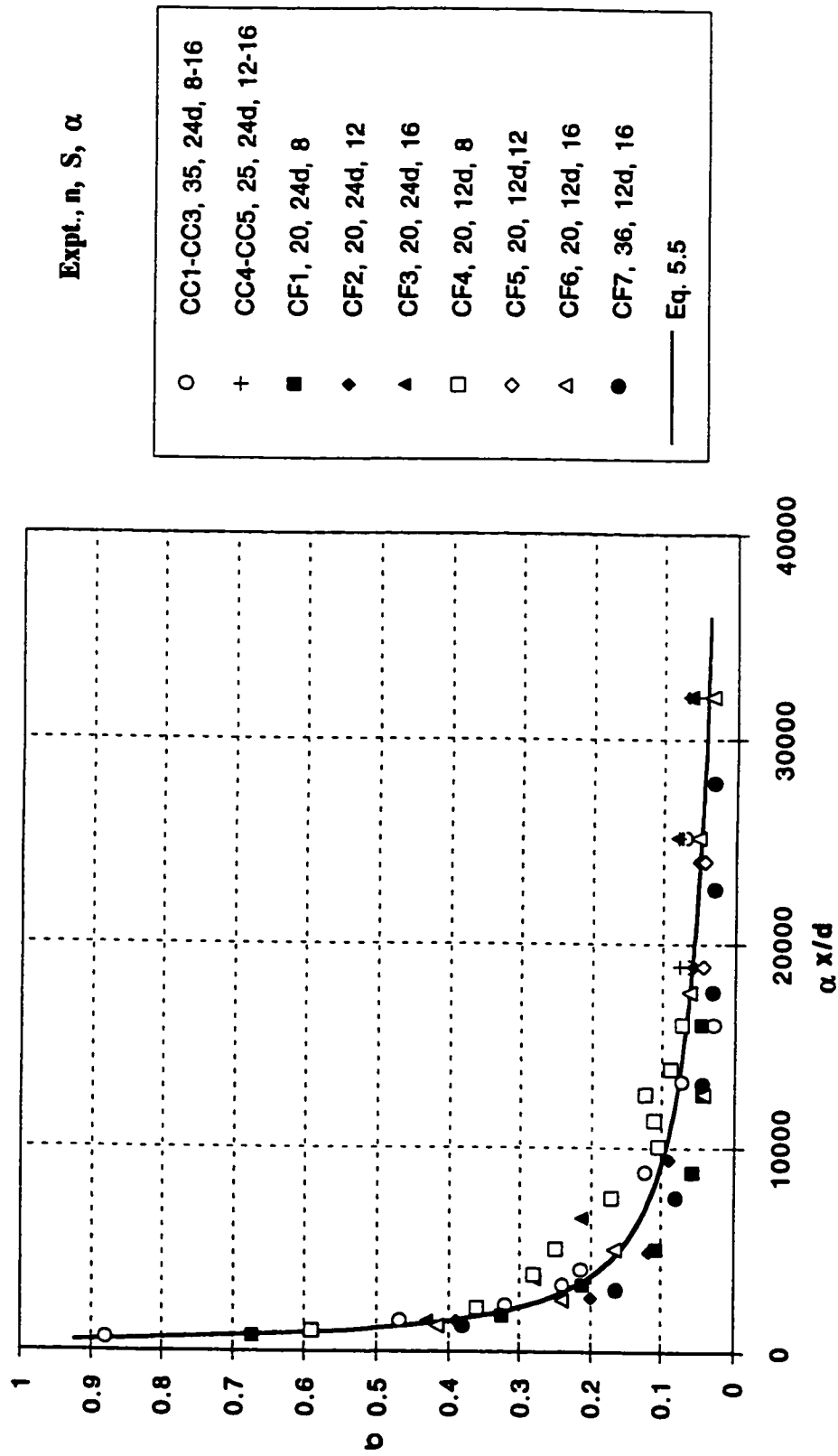
259

(e) Expt. CF7

x=5530mm

n=36

S=12d

α=16

Legend:
- z=0mm
- z=56mm
- z=114mm
- z=170mm
- z=224mmm

(f) Expt. CF7

x=6360mm

n=36

S=12d

α=16

Legend:
- z=0mm
- z=56mm
- z=114mm
- z=170mm
- z=344mm

Fig. 5.14 (e-f) Typical Transverse Concentration Profiles at Different Levels for Expt. CF7

260

Expt., n, S, α

○	CC1-CC3, 35, 24d, 8-16
+	CC4-CC5, 25, 24d, 12-16
■	CF1, 20, 24d, 8
◆	CF2, 20, 24d, 12
▲	CF3, 20, 24d, 16
□	CF4, 20, 12d, 8
◇	CF5, 20, 12d,12
△	CF6, 20, 12d, 16
●	CF7, 36, 12d, 16
——	Eq. 5.5

Fig. 5.15 Variation of the Standard Deviation with the Dimensionless Distance αx/d
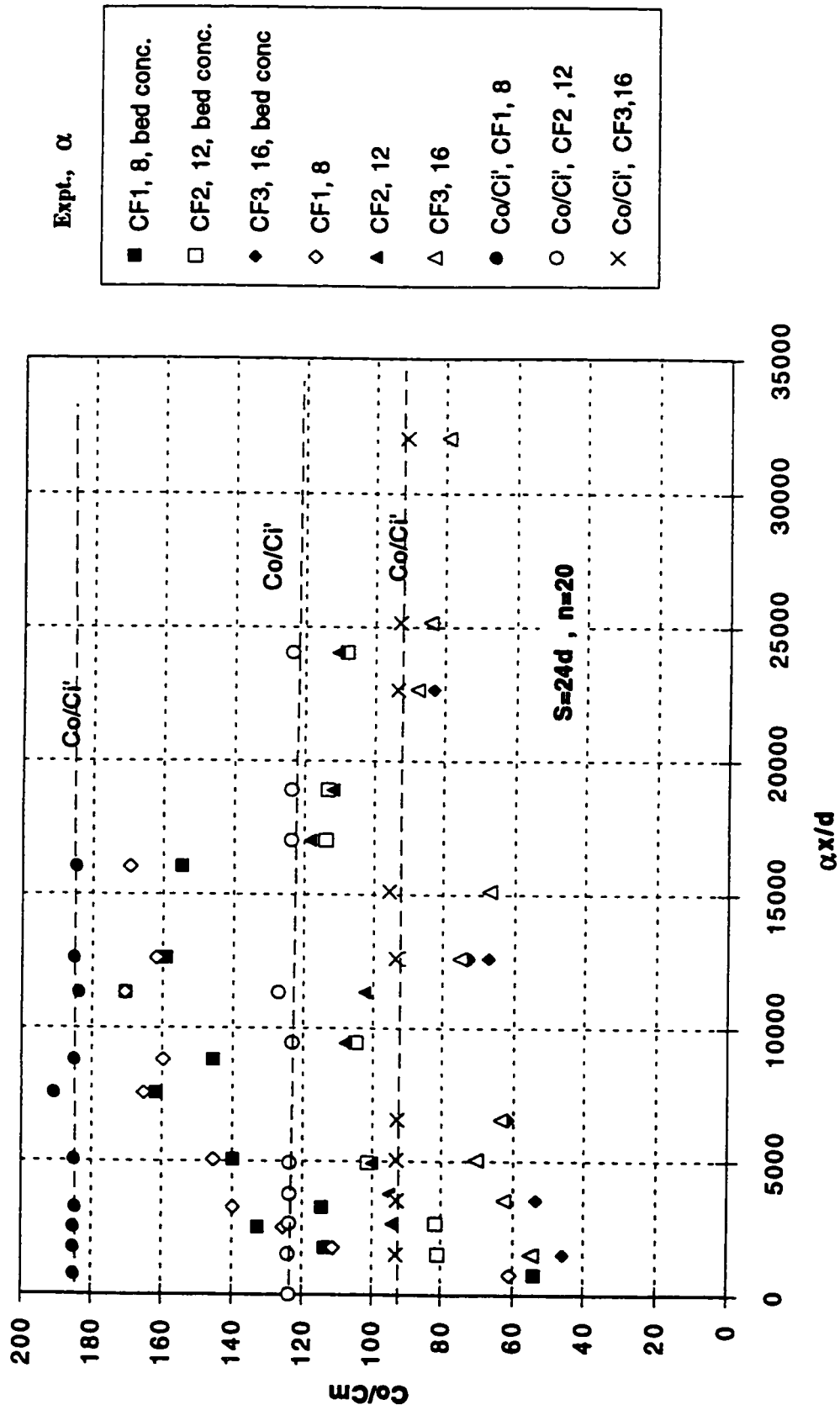
for all the Runs

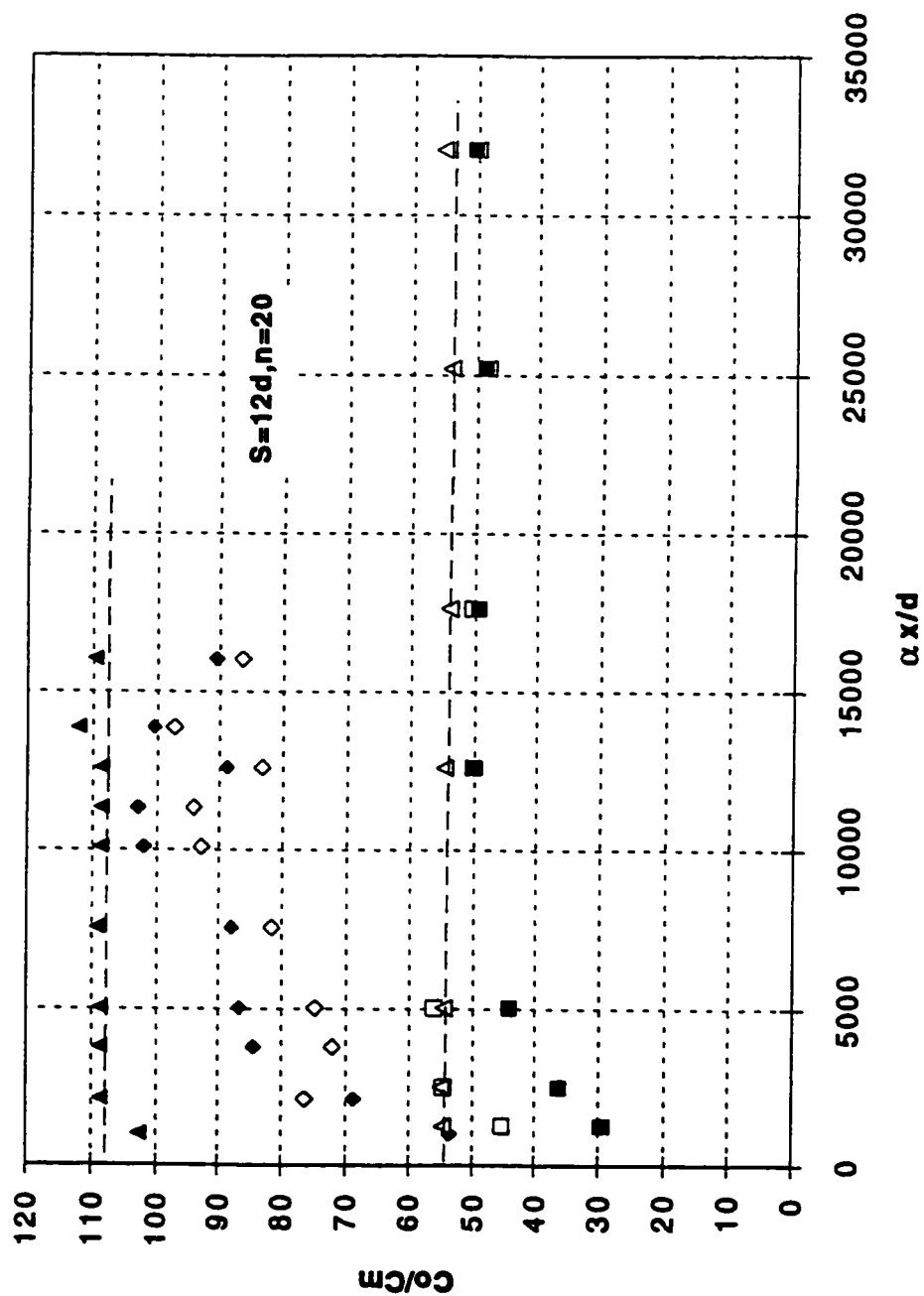Fig. 5.16 Variation of Minimum Dilution C_0 / C_m with $\alpha x/d$ for Experiments CF1-CF3

Fig. 5.17 Variation of Minimum Dilution (C_o/C_m) with $\alpha x/d$ for Experiments CF4 and CF6
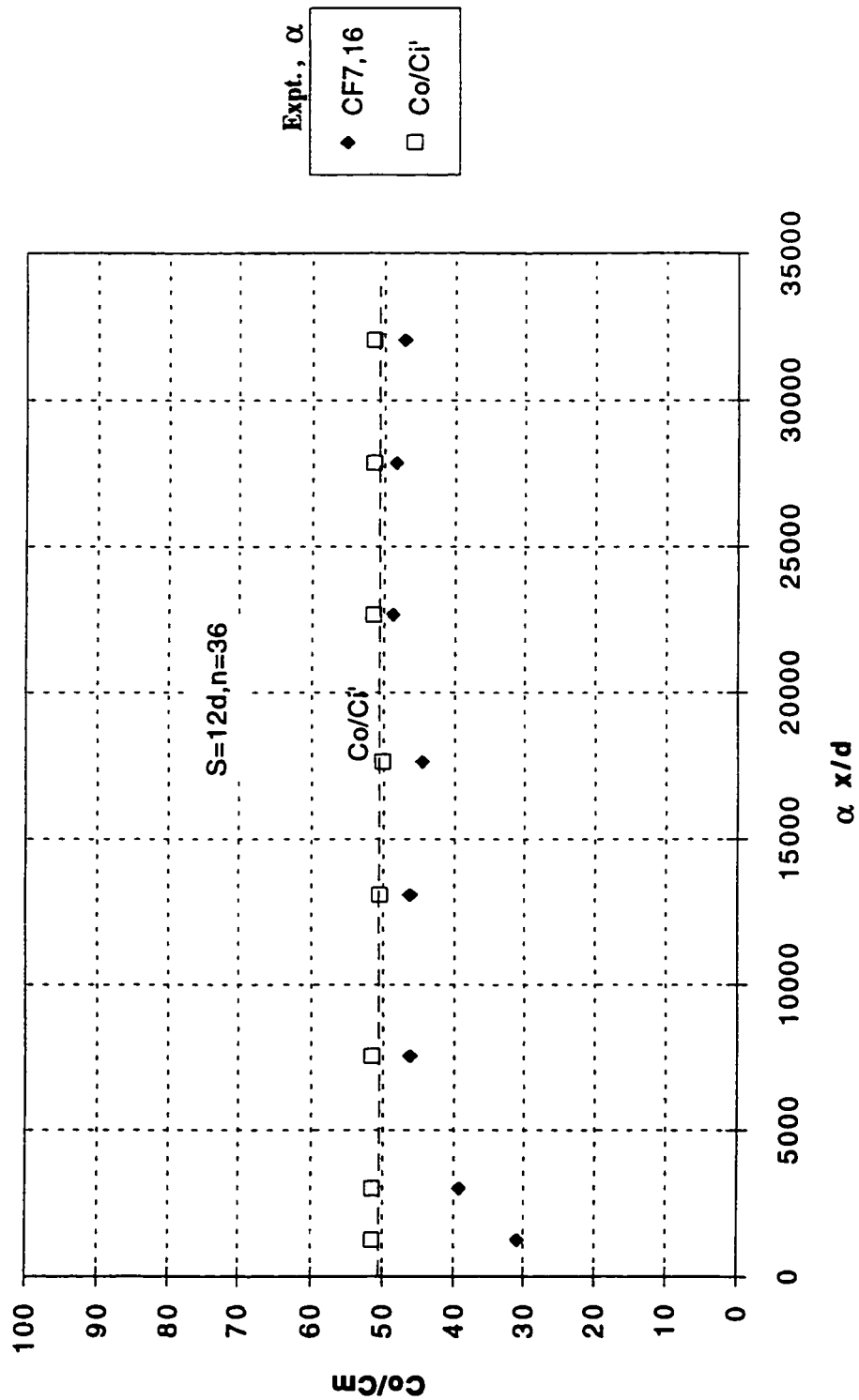
Fig. 5.18 Variation of Minimum Dilution (C_0/C_m) with $\alpha x/d$
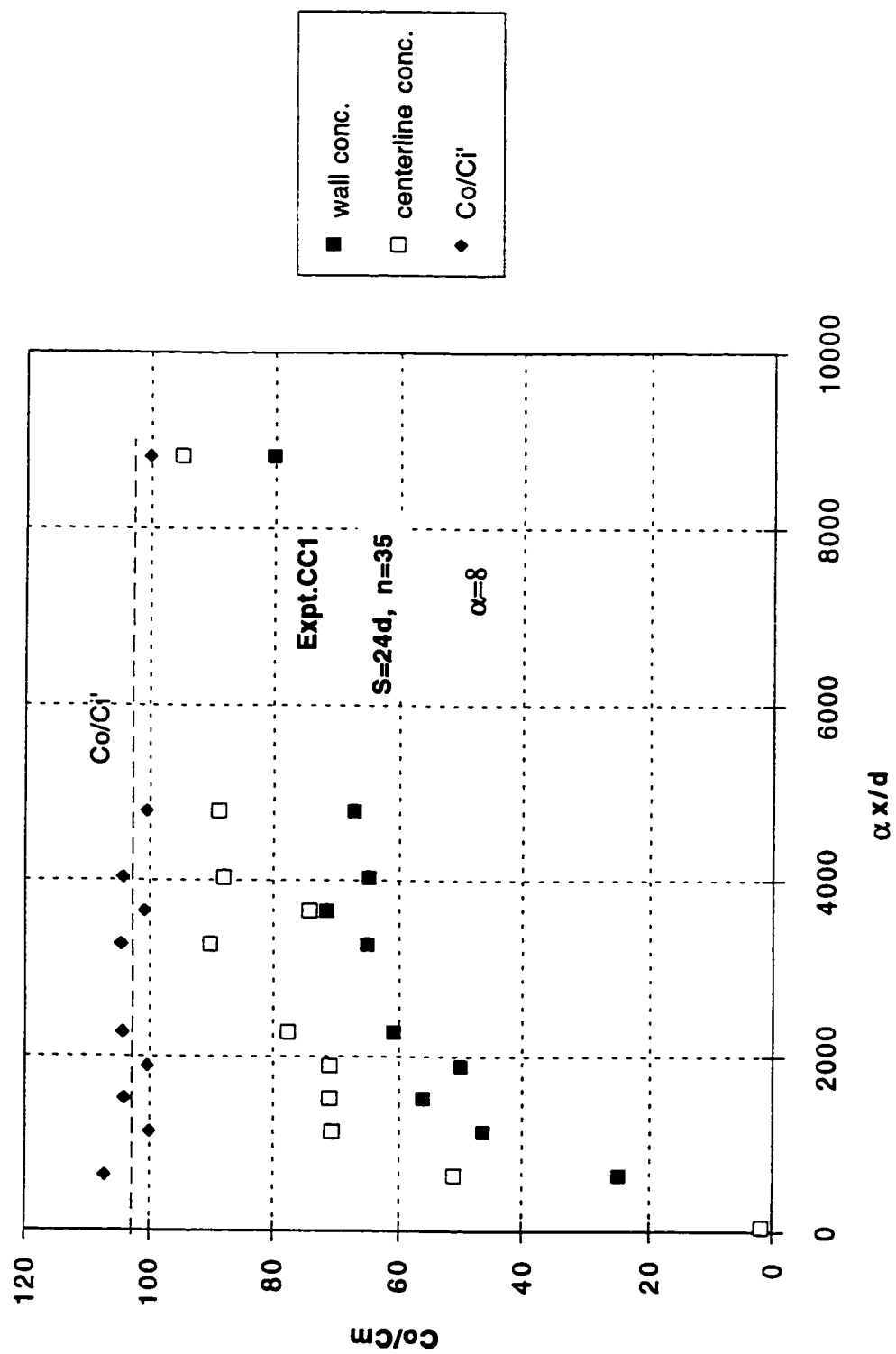
for Experiment CF7

Fig. 5.19 Variation of Minimum Dilution (C_0/C_m) with $\alpha x/d$ for Experiment CC1
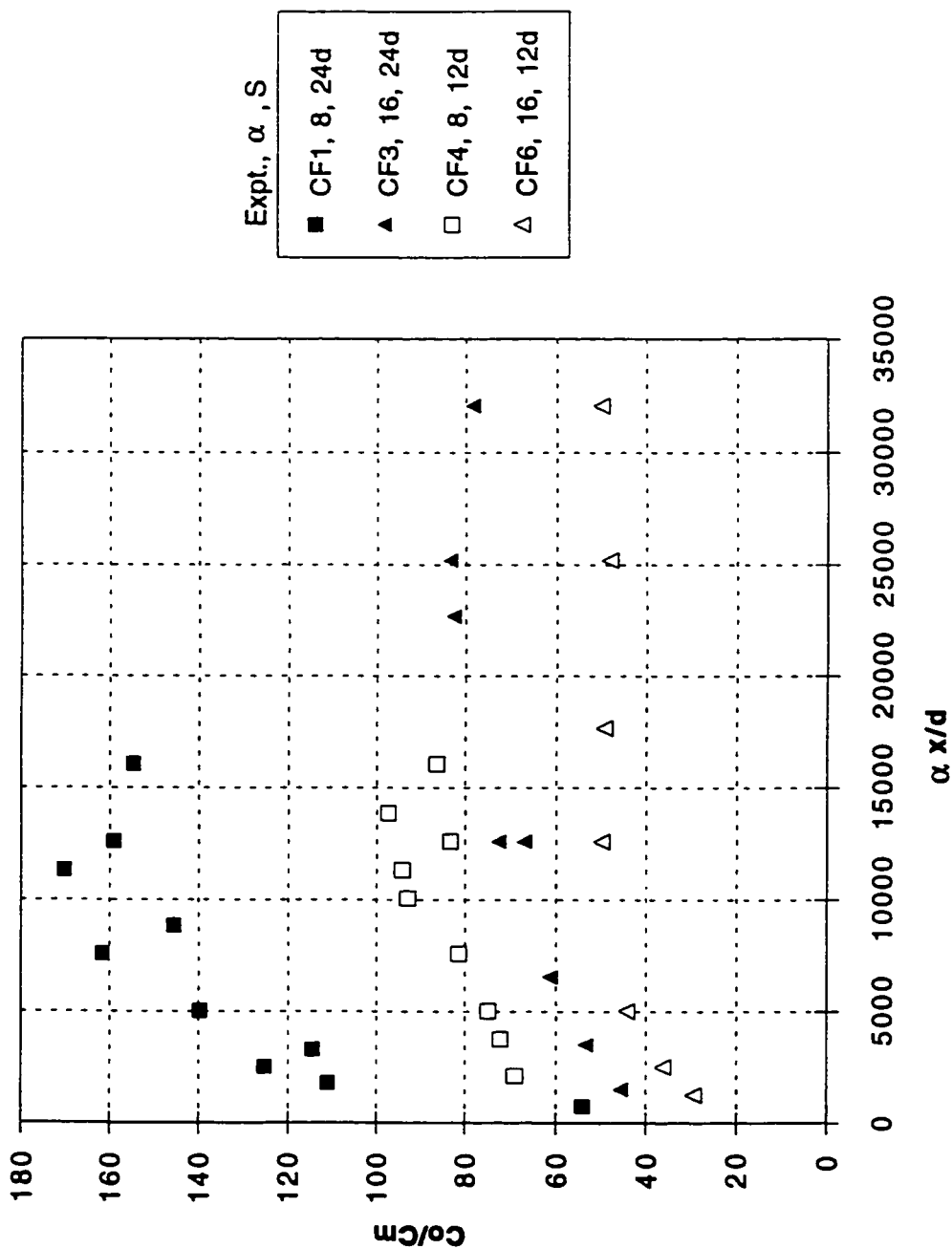
Fig. 5.20 Variation of Minimum Dilution (C_O/C_m) with $\alpha x/d$ Showing the Effect of Changing the Spacing
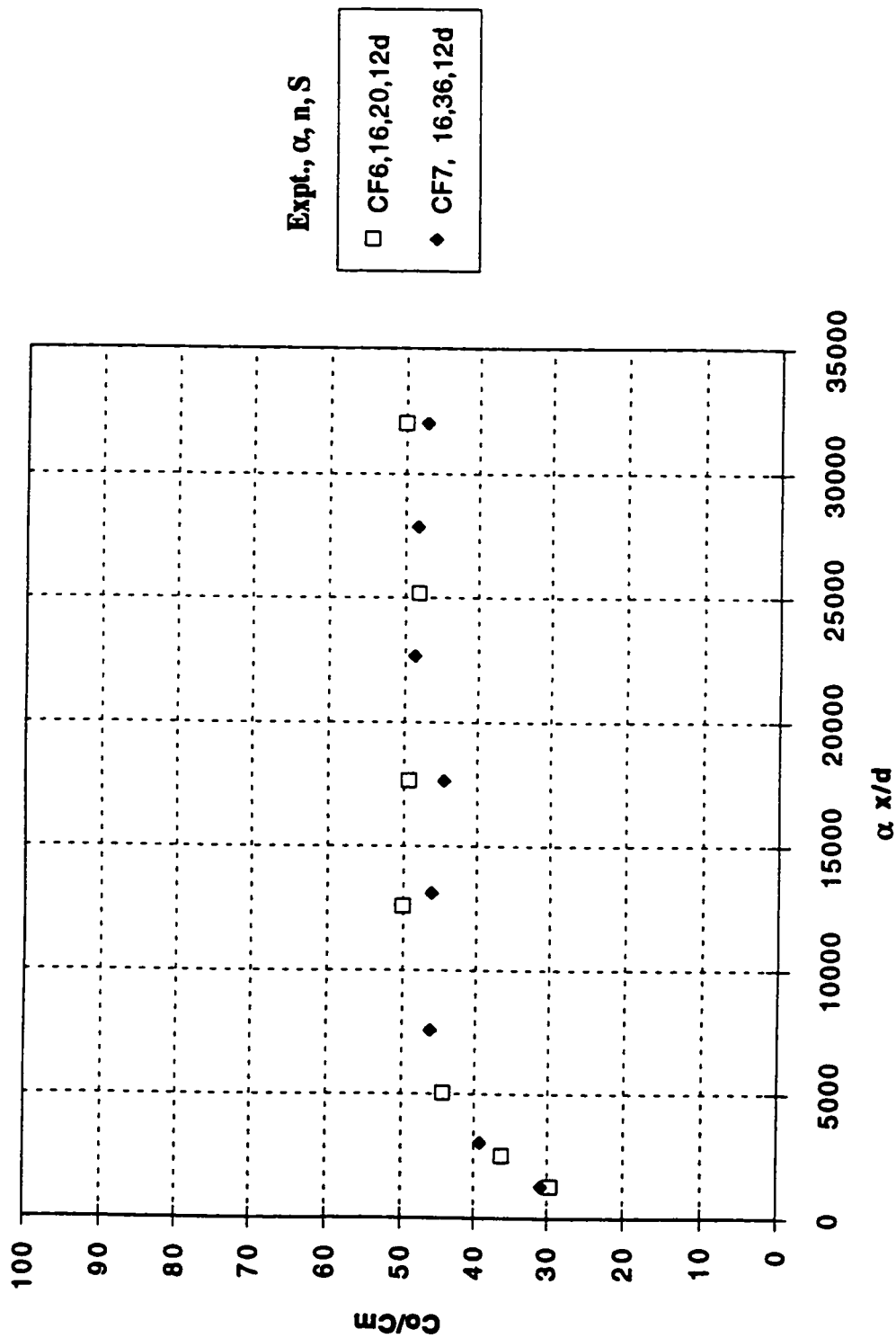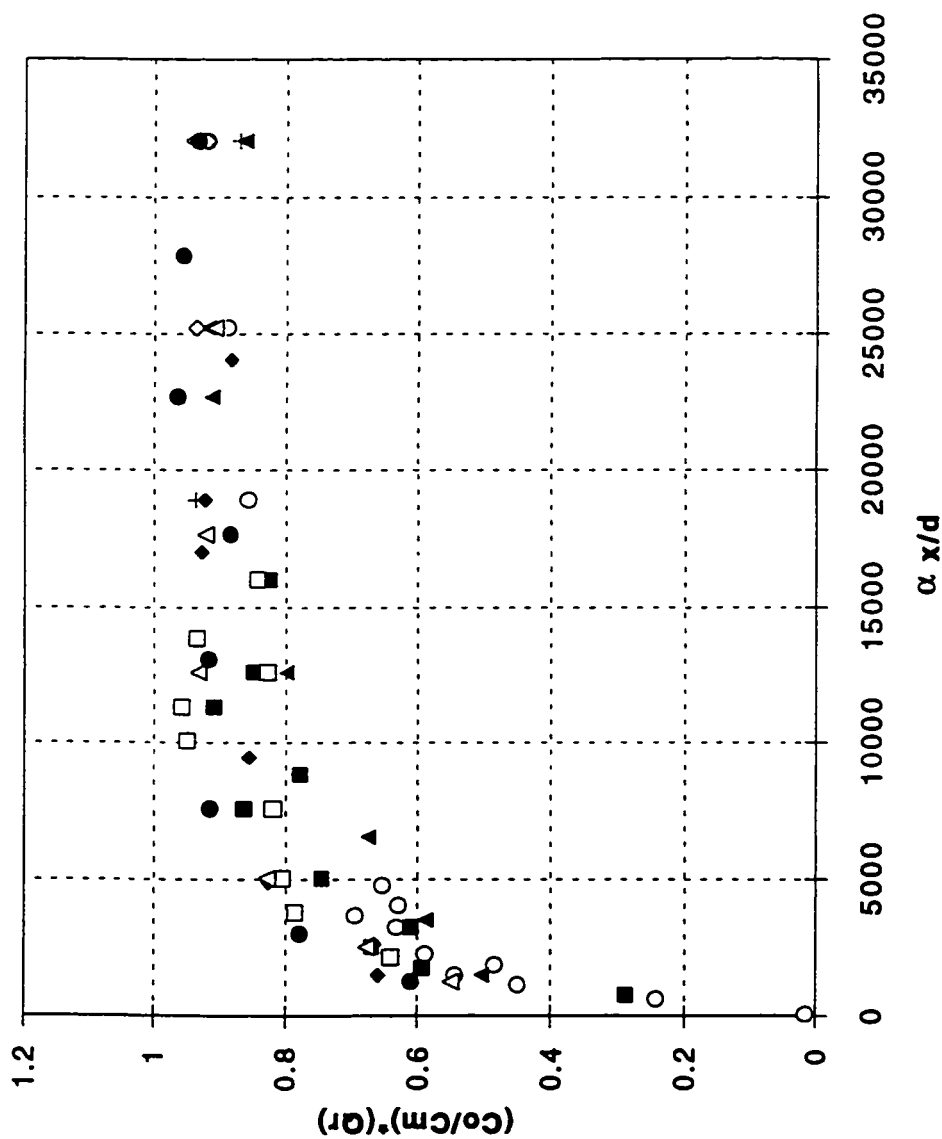
Fig. 5.21 Variation of Minimum Dilution (C_0/C_m) with $\alpha x/d$ Showing the Effect of Changing the Number of Ports

Fig. 5.22a Variation of $\dfrac{C_o}{C_m}Q_r$ with $\alpha x/d$ for all the Runs

Fig. 5.22b Variation of $\dfrac{C_o}{C_m} Q_r$ with $\alpha x/d$ for all the Runs

Legend:

Expt. , n, S, α

○ CC1-CC3, 35, 24d, 8-16

+ CC4-CC5,25, 24d,12-16

■ CF1, 20, 24d, 8.

◆ CF2, 20, 24d, 12

▲ CF3, 20, 24d, 16

□ CF4, 20,12d, 8

◇ CF5, 20, 12d, 12

△ CF6, 20, 12d, 16

● CF7, 36, 12d, 16

Y-axis: (Co/Cm)*(Qr)

X-axis: α x/d
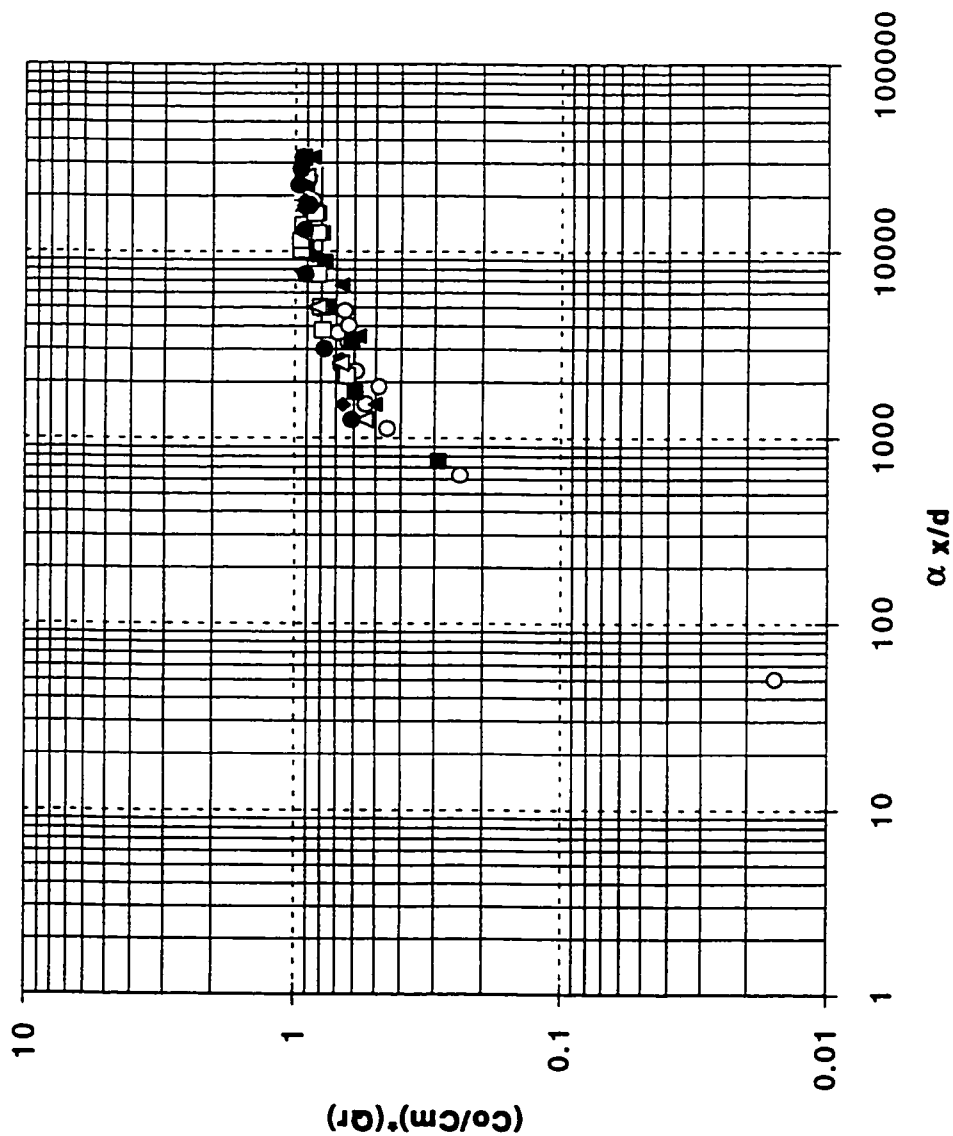
Fig. 5.23 Variation of $\dfrac{C_o}{C_m} Q_r$ with x/L_m for all the Runs

Chapter 6
Summary, discussion and conclusions

In the preceding three chapters, three studies have been presented on the dilution and the mixing of circular turbulent jets in moving ambients. In this chapter, a brief general discussion on each of these contributions as well as recommendations for future research work will be presented.
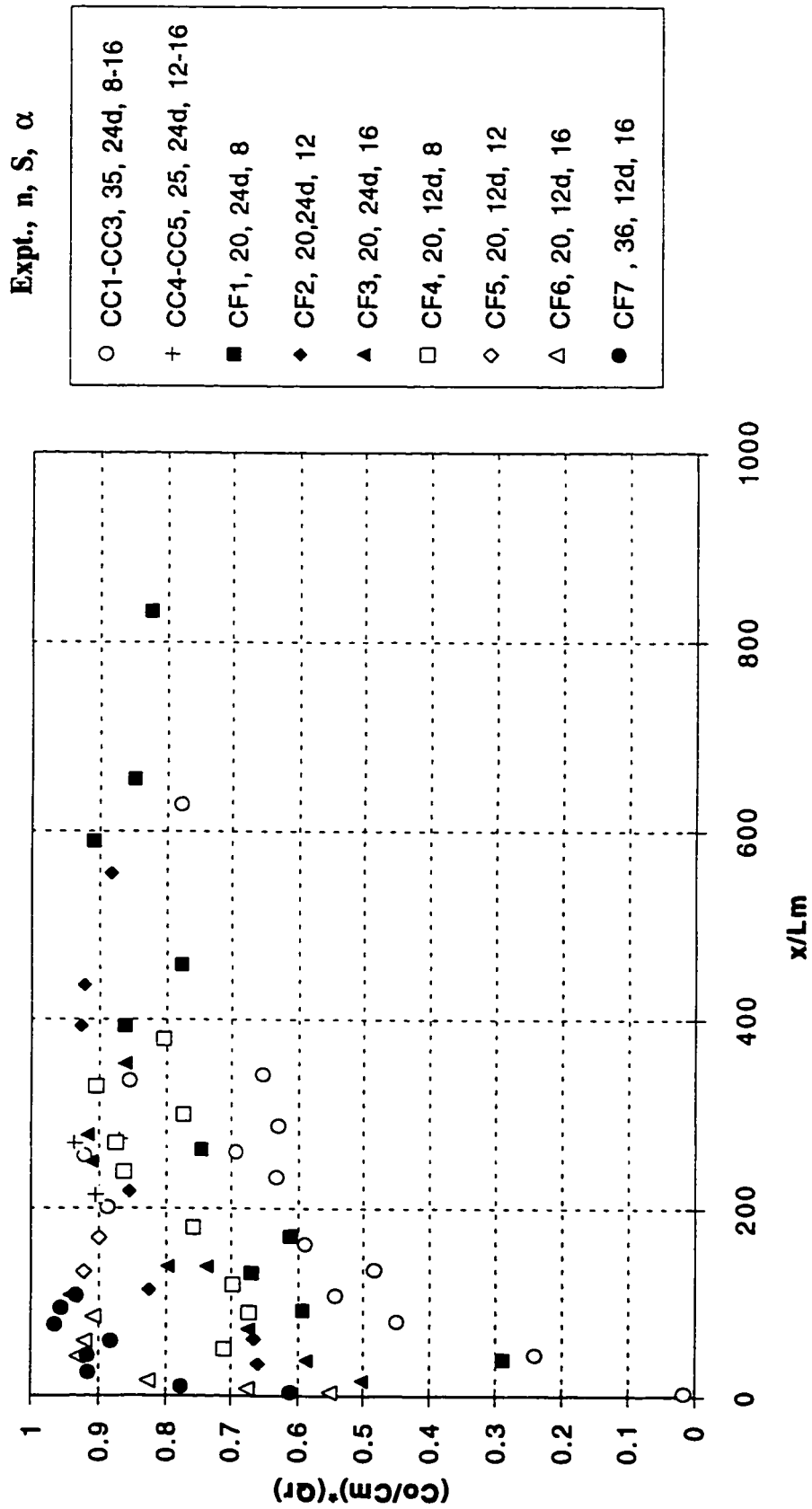
Chapter 3 presents the results of a laboratory study on the mixing characteristics of circular non-buoyant surface jets in relatively deep crossflows in an open channel. The mixing region is the zone in the vicinity of the outfall where significant dilution is produced by jet mixing. In this study, it was found that for the minimum dilution to reach a value of about 100, the mixing zone had to extend through the MDNF, MDFF into the PPR. In this mixing region, the concentration field was measured in considerable detail. The concentration field in the vertical as well as the transverse direction, in the planes of maximum concentration, was found to be similar. The variation of the minimum dilution C_o/C_m with the transformed distance $\alpha x/d$ was described by a relatively simple equation for the entire mixing region. Expressions were developed to describe the growth of the width and the thickness of surface jets in crossflows.

In this study, we have used the minimum dilution at any section as the measure of dilution and have used the minimum dilution of 100 to define the extent of the mixing region. If one is interested in average dilution at any section, the average dilution may be assumed to be twice that of the minimum dilution. Even though buoyant surface jets in crossflows are practically more important, this study would serve as a simpler case for future studies of the corresponding buoyant cases. Surface outfalls are generally economical to build and hence, it is important to be

271

able to evaluate their performance. Depending upon the stage of the river, a surface outfall could be submerged at higher stages or could act as a plunging jet for lower stages. In this study, some assessments have been provided for small submergence. For relatively large submergence, the flow can be treated as a free jet in crossflow. For a plunging jet, it is likely that relatively larger dilutions will occur, because of the jet impingement at the water surface. Further research to study the dilution characteristics of plunging jets is needed.

In chapter 4, an experimental study was performed to understand the mixing characteristics of circular non-buoyant multiple jets discharged in relatively deep crossflows. The experiments were carried out with the velocity ratio α varying from 3.5 to 10. Three and five ports were used and the spacing S between the ports was varied from 8 d to 16 d. The trajectory of the multiple jets was identified based on the maximum concentration location. Trajectory data indicated that multiple jets rose more slowly than single jets. It was found that the minimum dilution decreased with the increase of the velocity ratio α and with the increase in the number of ports. An increase of the spacing between the ports would lead to an increase in the minimum dilution. The vertical and transverse concentration profiles were found to be similar .

The results indicated that with multiple jets, dilution in the mixing region is generally reduced due to the presence of the neighboring jets. It appears that the spacing of 8 d is too close and that a spacing of 16 d appears to be satisfactory, in the range of the velocity ratios tested. This investigation should be considered as the first step in a systematic study of multiple jets in crossflow. If large length of diffusers are readily available, this study can be extended to cover much larger spacing with more ports. Also, this study was limited to the case of multiple jets discharged in deep crossflows. Further research is recommended to determine the effect of shallow receiving water on the dilution characteristics of multiple jets.
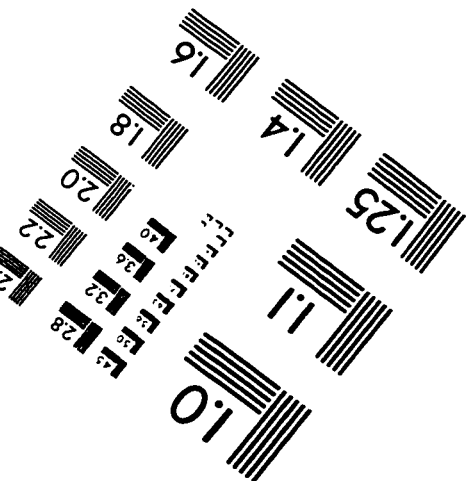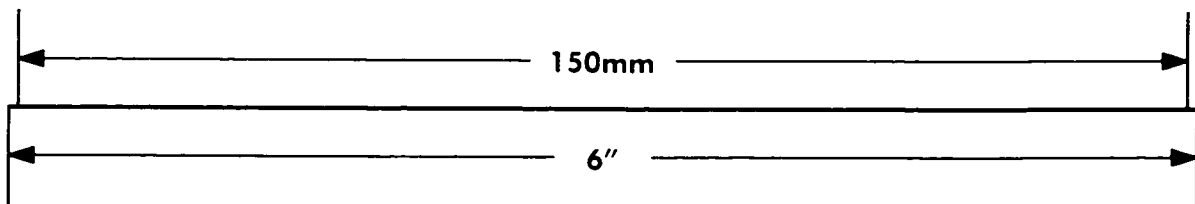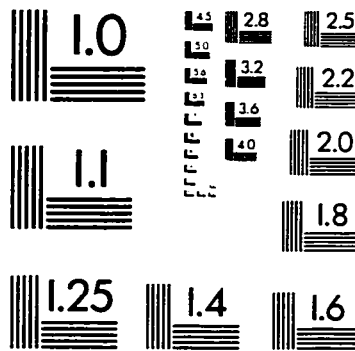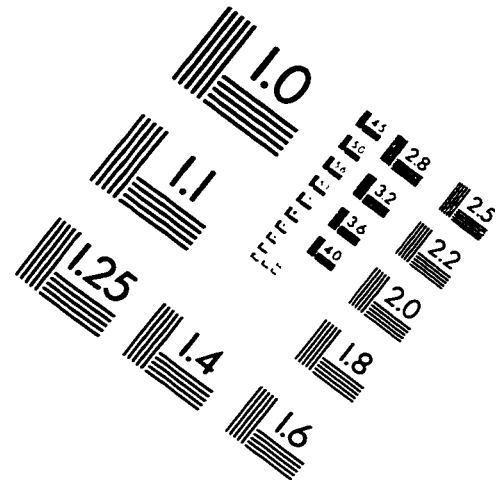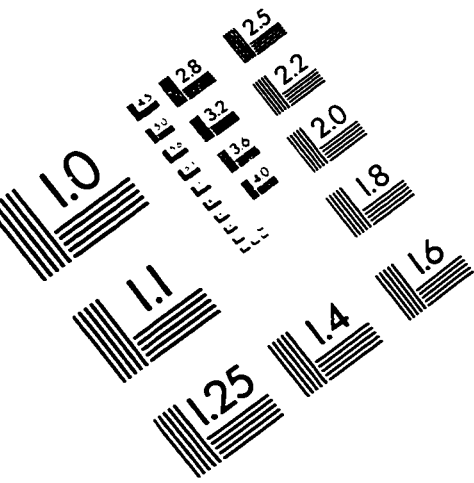
As for the application of the first and second study to large scale problems, field studies on jet mixing in the Lesser Slave River in Alberta (Hodgson and Rajaratnam 1992) agreed well with the laboratory dilution measurements. This would indeed be expected since the mixing and dilution is due to the jet interaction and not influenced by the turbulence in the river. So long as the jet is turbulent in the laboratory, in these type of studies, laboratory results could be applied with confidence to prototype situations.

The third contribution in chapter 5 deals with the mixing induced by multiple turbulent jets in a confined environment. A diffuser with a system of ports was installed in an open channel where jets could be discharged either perpendicular (jets in crossflows) or parallel (coflowing jets) to the flow. Several jet discharges with different α values were studied. The effect of the number of ports and the spacing between the ports on the dilution and the mixing distance was investigated. For practical purposes, adequate mixing could be assumed to have occurred when the standard deviation reaches a specified value. In this study this limit value was taken as 5%. The dimensionless distance $\alpha x_m/d$ at which this value was attained was equal to 25000. One of the interesting results of this study is that the standard deviation and the dilution attained by the system of injection proposed are independent on the spacing between the ports and on the number of ports.

The results of this study were based on a fixed set-up of three vertical diffusers placed in an open channel. To generalize the results, more work has to be done by examining other configurations. This can be accomplished by increasing the number of the vertical diffusers in the channel at different transverse spacings or by having a staggered arrangements of the jets.

All the analysis carried out in the three different contributions were based on a time averaged concentration data. To get a better understanding of the physics of the mixing processes, research work may have to be extended to obtain experimental data on the physics of turbulent processes in the problems considered in this thesis. This can only be accomplished by the fully three dimensional mapping of the tracer concentration filed using techniques like Laser-induced fluorescence (LIF). The results of such investigation could enhance our understanding of the mixing processes of contaminants in the environment. This would improve our ability to protect the quality of our water resources and promote wise and efficient use of the water in natural streams.

IMAGE EVALUATION
TEST TARGET (QA–3)

150mm

6"